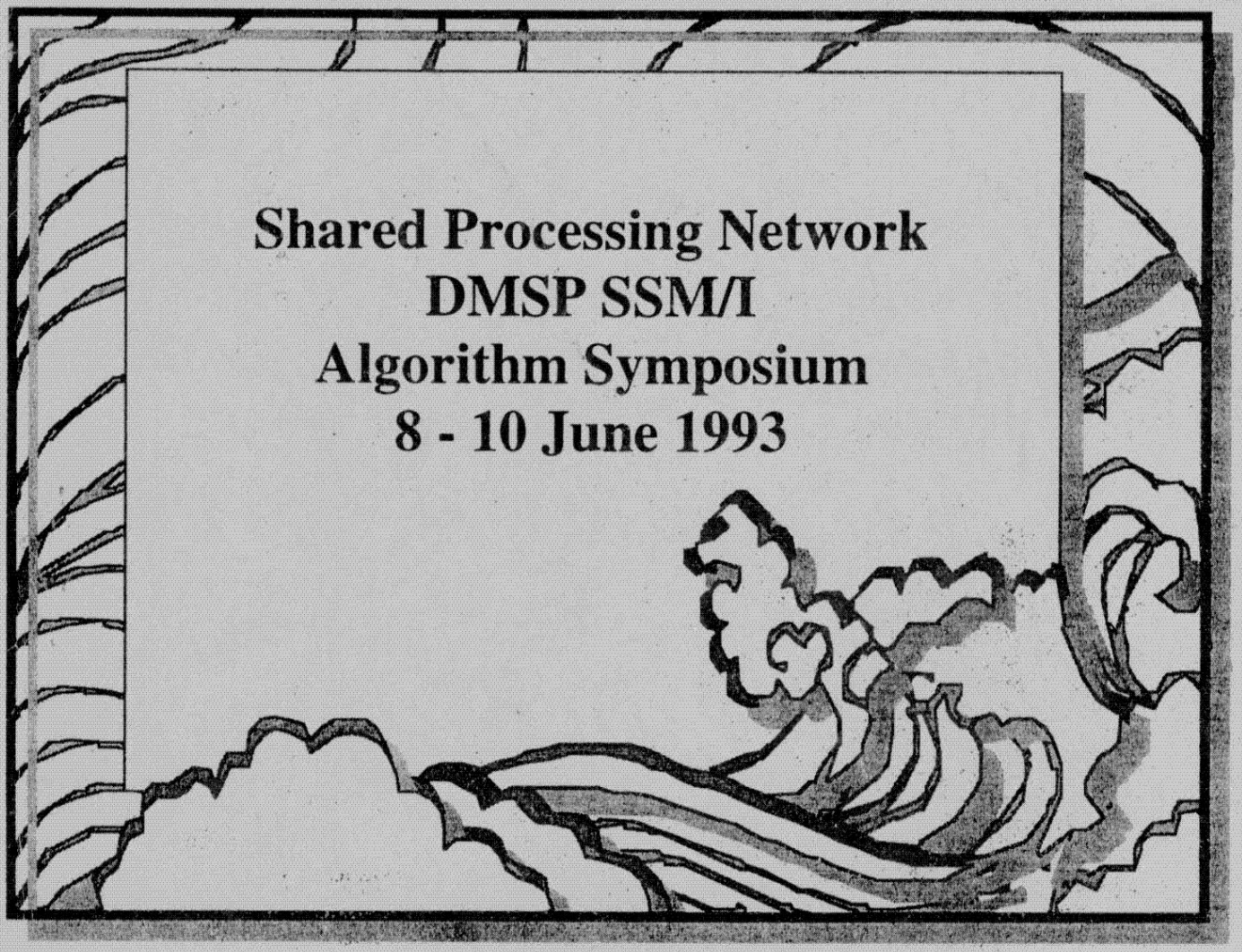


PROCEEDINGS



Please direct inquiries regarding this document to:

Dr. Marie C. Colton
Fleet Numerical Oceanography Center
Code 73
7 Grace Hopper Rd., Stop 1
Monterey, CA 93943



SHARED PROCESSING NETWORK
DMSP SPECIAL SENSOR MICROWAVE / IMAGER (SSM/I)
ALGORITHM SYMPOSIUM
8 - 10 JUNE 1993

Encl: (1) SPN SSM/I Algorithm Research Panel members
(2) Symposium agenda
(3) Symposium attendees
(4) Welcoming Remarks from CAPT Robert Plante, Commanding Officer, FLENUMOCEANCEN
(5) Status of the DMSP Satellites, LtCol Edwin Arrance, DMSP System Project Office
(6) SSM/I Operational Processing and Data Utilization at FNOC, AFGWC, and NOAA/NESDIS, Dr. Marie Colton, Capt Mike Farrar, Ms. Pam Taylor
(7) Sea Ice presentations
(8) Snow Cover presentations
(9) Land Parameters presentations
(10) Cloud Liquid Water, Column Water Vapor, and Surface Wind Speed presentations
(11) Precipitation presentations
(12) Future Directions presentations

Ref. (a) CNOC Letter, Ser5/324, 31 Aug 92.

1. In August, 1992, the Shared Processing Network (SPN) Operations Steering Committee established the SSM/I Algorithm Research Panel (ARP) as part of the SPN software change control infrastructure (Ref (a)). The impetus was to "organize a joint (Navy/Air Force/NOAA) forum to review, evaluate, and approve standard satellite data retrieval algorithms used to process satellite data into environmental products exchanged via SPN." In addition to considering their relative technical/scientific merits, the ARP was also charged with weighing the operational benefits and implementation costs of candidate algorithms.

2. Principle members of the ARP are technically informed representatives from each of the SPN centers and supporting research laboratories (FLENUMOCEANCEN, NRL, AFGWC, NOAA/NESDIS, NAVOCEANO). Each center has an SPN "Center of Expertise" designation indicating the satellite product(s) for which the center is primarily responsible; therefore, the SPN Center Coordinator is also a member of the panel. Contributing members from the user and academic community are invited to attend open scientific meetings at which they may present "mature" alternative algorithms or procedures for operational consideration. In the case of operationally imperative changes, the Science Chair of the Algorithm Research Panel will be made aware of the nature of the emergency and solicited for an immediate solution.

3. There have been three meetings of the SSM/I ARP since its August, 1992 inception. The inaugural meeting was held September 30, 1992 at the Naval Research Laboratory,

Washington, DC, with Dr. Jim Hollinger as the SSM/I ARP Chairman. The panel decided to hold an open SSM/I algorithm symposium to solicit new algorithms from the scientific community, and to host the symposium at the SPN Center of Expertise for microwave products, FLENUMOCEANCEN, Monterey, CA. Further, the need was recognized for a standardized data base of ground truth and SSM/I antenna temperatures with which to test candidate algorithms. NOAA/NESDIS began the effort to identify the data base contents, sources and format.

At the second meeting (16 Nov 92, DMSP System Project Office, El Segundo, CA), the membership of the ARP was expanded to include NASA, Army and NOAA/NGDC representation, adding valuable SSM/I algorithm development and archive expertise to the panel (Encl (1)). The dates for the open forum algorithm symposium were set for 8 - 10 June and a schedule was laid out for the Call for Abstracts, etc. The Call for Abstracts was mailed to all known individuals, agencies, or institutions who had previous experience with SSM/I algorithm development. Further, in an effort to be as open as possible, the invitation to participate was published in the Bulletin of the AMS (Jan.,1993), and posted to SCIENCENET and NASA Wetnet.

The third meeting of the ARP took place immediately following the SSM/I Symposium (10 June, Naval Postgraduate School, Monterey, CA). Mr. Poe (NRL) and Dr. Colton (FNOC) assumed the SSM/I ARP co-chairmanship from Dr. Hollinger (retired). The panel then summarized the Symposium proceedings, identified action items, and scheduled follow-up activities.

4. As authorized by Commander, Naval Oceanography Command (CNOC), FLENUMOCEANCEN hosted the first SPN SSM/I Algorithm Symposium, 8 - 10 June, 1993 at the Naval Postgraduate School. Colton (FNOC) chaired the meeting. The symposium agenda and attendance list are included (Encls. (2) and (3)). The format of the Symposium was two full days of presentations, with time in each session for open discussion and summary of presentations regarding the individual SSM/I environmental parameters. The morning of the third day was reserved for open discussion of all parameters and identification of possible immediate improvements to the processing software, and proposals for replacement of algorithms, if necessary. The minutes of the SPN SSM/I Algorithm Symposium are summarized in the following paragraphs.

5. INTRODUCTION. The opening presentations established the context of the Symposium to the algorithm developers by providing background information on the *operational* requirements of the SPN centers and the DMSP.

a. Welcoming remarks. CAPT Robert Plante (Commanding Officer, FLENUMOCEANCEN) discussed the mission and daily operations of FLENUMOCEANCEN, including acquisition and assimilation of the SSM/I data. He also reviewed the SPN partnership and the SPN Change Management Board (Encl (4)).

b. Status of the DMSP Satellites. LtCol Edwin Arrance (DMSP SPO) described the operational status of the five DMSP satellites currently on-orbit (Encl (5)), of which three (F8, F10, F11) carry an SSM/I. The SSM/I sensors on F10 and F11 are performing nominally; F8 has an inoperative 85GHz channel. Two of the four recorders on F8 have failed; F10 is in an elliptical, vice circular, orbit and three of the four on-board recorders

have failed; F11 is nominal. Spacecraft S11 (to be F12) is in storage at Vandenberg AFB awaiting launch call.

c. SSM/I Operational Processing and Data Utilization at FNOC, AFGWC, and NOAA/NESDIS. FNOC, AFGWC and NOAA/NESDIS have shared the responsibility for the disposition and distribution of SSM/I data since the launch of F8 in June, 1987 (Encl (6)). Colton discussed current satellite processing and development at FNOC, particularly operational SSM/I products. These products include SSM/I archive files, input files to NWP models, and imagery, graphics, or digital files to regional centers. Ongoing SSM/I development at FNOC enhances the above capabilities primarily through migration of the mainframe software to workstations, a platform which, among other attributes, has greater graphics and communications capabilities.

As required by the SPN agreement, FNOC transmits antenna temperature data records (TDR), brightness temperature and sensor calibration data records (SDR), environmental (geophysical) data records (EDR) and quality data records (QDR) to NOAA/NESDIS for archival on an orbit by orbit basis. On demand, the calibration coefficient files are also transmitted. For the six years prior to SPN operational capability (Jan, '93), FNOC copied the above SSM/I archive files to 6250 bpi tape and forwarded the tapes to NOAA/NESDIS, via NRL. As of September 30, 1993, NOAA/NESDIS will have a tape cartridge system installed with which to archive and distribute the incoming SPN files, and the 6250 bpi tape generation will stop.

SSM/I surface wind speed has been assimilated in the optimal interpolation scheme used by the Navy Operational Global Atmospheric Prediction System (NOGAPS) since October, 1990. Current NOGAPS modeling efforts are now focussed on assimilation of the SSM/I total precipitable water parameter. Ice concentration files are used daily to initialize the Primary Ice Prediction System at NRL, produce Postscript graphics of polar regions for the Navy/NOAA Joint Ice Center, and generate ice edge information for the Optimum Thermal Interpolation System at FNOC. SDR and EDR files from the West Pacific and Indian Oceans are transmitted on an orbit basis to the Joint Typhoon Warning Center (JTWC) at Guam, thereby expanding JTWC SSM/I coverage from their own DMSP line of sight capability to their entire area of responsibility.

CAPT Mike Farrar next provided information about the DMSP data flow at AFGWC, Air Force users of DMSP microwave data and the future of satellite processing at AFGWC. DMSP data are received from the DMSP spacecraft at one of several downlink sites worldwide and relayed via communications satellite (DOMSAT) to the ground station at AFGWC. The data are ingested at Site III (see viewgraph), where they are decrypted and decommutated. Full resolution OLS and SSM/I data are sent to the Satellite Data Handling System (SDHS), where they are used for operational weather support. OLS data at 3.0 nm resolution and all of the mission sensor data are sent to the Cloud Depiction and Forecast System (CDFS), also known as System 5, a Unisys 1100 mainframe computer. Here the OLS data are mapped into the Satellite Global Database (SGDB) and ingested by the Real-time Nephanalysis (RTNEPH) cloud model for use as imagery by various customers.

The DMSP mission sensor data, of which the SSM/I data are a subset, are separated into so-called PREPFILES, which include raw sensor and ephemeris data. Some of these data are transmitted to customers, such as the SESS sensor data (SSIES and SSJ/4) to the

Air Force Space Forecast Center and SSM/I to NOAA/NESDIS. Data from the microwave sensors SSM/I (imager), SSM/T (temperature sounder) and SSM/T-2 (humidity sounder) are processed to produce SDR and EDR files to support various users (see list in viewgraphs).

CAPT Farrar discussed the future of satellite processing in terms of Navy-Air Force cooperation (NAVAF), DMSP Block 5D-3 (SSMIS), and AFGWC computer upgrades. NAVAF is the program for cooperation between the Navy and Air Force to reduce duplication in many areas of weather support between the two services. One such area is satellite processing, where AFGWC will become the Primary DOD METSAT Center. Under this plan, DOD satellite processing will be consolidated at AFGWC beginning with the SSMIS and Block 5D-3 (ca. 1997). AFGWC will then transmit any data that FNOC requires for their operational use. A new distributed processing network of workstations has been purchased by the DMSP SPO for the Aerospace Corporation for use at AFGWC in the Cal/Val of all the new Block 5D-3 sensors, including SSMIS. In these future plans, two major upgrades will affect satellite processing at AFGWC: SDHS-Upgrade (SDHSU) and CDFS2. Phase 1 of SDHSU, scheduled in 1995, will provide for and upgrade the ingest center, Site III. CDFS2 will provide for an upgrade to the mainframe computer, but this is not scheduled until 1997/98.

The operations and research users and developers of SSM/I products at NOAA/NESDIS were described by Ms. Pam Taylor. In an operational mode, NOAA/NESDIS uses the FNOC SSM/I data record files and the AFGWC raw sensor and ephemeris data (PREPFILES mentioned by Capt Farrar) transmitted via SPN. The processed data record files are used to produce a permanent archive on data cartridge and to populate an intermediate, 1/8 deg mesh, polar stereographic data base of 30 orbits per spacecraft. The database is available in near real-time to NOAA users, and extractions from the data base are used to produce "Master Maps" of environmental parameters. By Oct '94, the database will be expanded from 30 orbits to one years' data available on line. The PREPFILES are used to match the SSM/I radiances for consistency with those of the temperature and humidity sounders at the surface.

NOAA/NESDIS researchers are developing systems that will aid the study and improvement of SSM/I algorithms: the Candidate Algorithm System (CAS) and the Climate Product System (CPS). The Candidate Algorithm System (see flowchart viewgraph) will use FNOC SDR files as input to proposed new algorithms (as many as 20). The EDR files produced from the new algorithms will be compared to the FNOC EDR files to evaluate differences among the environmental parameters computed by the differing algorithms. Results from the intercomparisons will be forwarded to the SSM/I ARP for action. The SSM/I Climate Product System will generate longer-term statistics on SSM/I parameters suitable for use in climatology studies. Current plans call for daily, pentad and monthly statistics from the SPN EDR and CAS algorithms; of initial interest are the Total Precipitable Water (TPW) and rain rate parameters.

The National Hurricane Center (NHC), National Meteorological Center (NMC) and the National Weather Service (NWS) all use SSM/I data. NHC utilizes the 85GHz channel to see through the cirrus shield of many storms and track the low-level cyclone center. They also use the rain rate and ocean surface wind speeds to characterize storms and identify high-sea and storm force winds. NMC combines the SSM/I rain rate values

with GOES imagery to identify precipitating clouds. The NMC atmospheric model ingests wind speed, and they are assessing snow, sea ice, total precipitable water, and cloud liquid water for input to their variational assimilation scheme. The NWS Office of Hydrology uses the SSM/I snow depth to supplement the AVHRR imagery in their weekly snowpack product. NOAA/NESDIS also forwards the archived SPN products to many users; eg., WETNET, NASA Pathfinder, Canadian Atmospheric Environment Service.

d. Symposium Objectives and Guidelines. With the operational missions of the SPN centers clarified, Colton and Poe (NRL) advised the attendees of the objectives of the Symposium, given that the task of the ARP was to compile a list of possible improvements to the SSM/I operational code, with the necessary steps for implementation of each option. Therefore, the *primary objective* was the identification and assessment of existing, "mature", passive microwave algorithms for SSM/I geophysical parameters. Although the presentations described some of the most well known algorithms, the audience was requested to identify others with which they were familiar. The algorithm developers were asked to supply concrete information regarding their algorithms, and a questionnaire with appropriate questions regarding algorithm attributes was supplied (these questionnaires appear with the presentation material in this document). In addition, forms for submitting action items and documenting issues of concern regarding any aspect of an algorithm or process were supplied.

A *second objective* of the Symposium was the definition or identification of independent test data sets or methods with which to objectively compare algorithms. For example, there are currently several sources of SSM/I archive data, with small differences in geolocation of scene stations and calibration of brightness temperatures. Therefore, intercomparison of algorithms should start with the same SSM/I data set, and should include the "validated" DMSP Cal/Val algorithms as a benchmark from which to develop recommended changes. Finally, the *third objective* was to establish the connection between the algorithm developers and SPN operational centers via the Algorithm Research Panel. The results, experiences and timelines of similar algorithm research boards were solicited.

6. SESSION 1: SEA ICE. (Mr. Jeff Hawkins, NRL, Chair).

The SSM/I sea ice algorithm continues the long standing passive microwave efforts to map global sea ice conditions. Initial algorithms benefitted from the nearly 20 years of Nimbus Electronically Scanning Microwave Radiometer and Seasat Scanning Multichannel Microwave Radiometer experience, but still searched for "surface truth" to fine tune SSM/I algorithms. The talks included here summarize four major efforts to enhance SSM/I sea ice products. Particular emphasis has been placed on reducing anomalous values due to "weather effects", better handling of new/young ice in the total sea ice concentration, and multiyear ice in general.

Dr. Irene Rubenstein outlined improvements incorporated by her group at the Institute for Space and Terrestrial Science on the original SSM/I "Cal/Val" algorithm (operational at FNOC). The algorithm accuracy is enhanced by including decision making rules that allow input of signatures and atmospheric correction of each pixel. The regional/seasonal values are used as first guess input and additional calculations are

performed before the final output of the total and FY-MY ice concentrations. The parameters derived using these coefficients are tested by comparing the observed brightness temperatures with the expected (e.g., scatterplot) values. Different modules of the retrieval procedure are called in to recalculate these parameters in order to minimize the differences. The modules contain ice free ocean roughness and simplified atmospheric retrieval algorithms.

Dr. Per Gloersen (NASA Goddard Space Flight Center-GSFC) summarized the work done with Dr. Don Cavalieri to form the latest version of the "NASA Team" sea ice algorithm. Two independent variables, the polarization and spectral gradient ratio, are used to calculate the total multiyear (MY) ice concentrations. A third ratio involving the 19 and 22 GHz channels augments the weather filter. Validation efforts revealed a total sea ice concentration accuracy within 7%, while the MY ice values were within 12%. Recent modifications permit mapping of new and young ice types in seasonal ice zones and significantly reduce earlier biases in low concentration domains. This is especially important since seasonal ice zones may be covered with up to 30% new and young ice, which in turn radically change the fluxes of heat and moisture in the region.

Dr. Joey Comiso (NASA-GSFC) presented results from his bootstrap technique that is based on multichannel cluster analysis. Open water, FY and MY ice serve as the "tie points" for determining the fraction of each within a given footprint. One of the main obstacles is the presence of new ice in the marginal ice zone where errors of up to 20% may occur. This problem has been minimized by applying the algorithm with regional tie points. The different regions are identified using an unsupervised cluster analysis and a neural network that makes use of all channels including 85 GHz. Otherwise, average errors of 7% or better can be obtained.

Ms. Florence Fetterer (NRL-SSC) detailed the recent effort to take advantage of the ERS-1 SAR's superior spatial resolution. Multiyear ice concentrations from collocated SSM/I and ERS-1 Synthetic Aperture Radar (SAR) data sets in the Beaufort Sea during winter were compared. The MY concentrations from the SAR were used to create local "tie points" for enhanced algorithms. For instance, the NASA Team algorithm estimated the MY concentration as 20% lower than estimated by SAR for one case study. This difference was reduced to 2-8% using SAR assisted tie points. Since the accuracy estimates from SAR remain unvalidated (recent work has shown the SAR algorithm may be overestimating MY concentration), it is inadviseable to force agreement between SAR and SSM/I values without further study. Further research efforts with a larger data base are ongoin, and hold promise in upgrading existing SSM/I algorithms through data fusion.

7. SESSION 2: SNOW COVER (Dr. Christopher Neale, Utah State Univ., Chair).

The four papers presented in this session described the development of two new regional algorithms, one alternate global algorithm, and validation data sets for snow cover products. For reference, recall that the current DMSP cal/val snow products are classification of dry, wet or refrozen snow types, and snow depth in mm, computed from a linear calibration of the vertical polarized 37GHz brightness temperature.

Dr. Norm Grody (NOAA/NESDIS) presented a global algorithm for the

determination of areal snow extent. The physical basis for the algorithm is the positive difference (22V > 85V), or "scattering signature", between the 22 and 85GHz, vertical polarized (V) antenna temperatures due to microwave scattering materials such as snow, atmospheric ice particles, desert sand and some ice surfaces. The algorithm employs the line, 22V = 257K and linear relationships between the 22V and 85V antenna temperatures to discriminate between snow cover and precipitation. The 19GHz polarization difference (19V - 19H) separates desert sand from precipitation over land, where H indicates the horizontal polarized channel. A 19V - 37V threshold difference is used to distinguish frozen ground from snow as observed in the Tibetan Plateau. Finally, the anomalous, nonscattering regions (22V < 85V) observed in Greenland and Antarctica are labelled as "substratified ice" (snow over stratified ice) and then correctly shown as snow covered by applying additional tests on the magnitudes of the 22V and 85V temperatures.

The global algorithm is used to produce experimental snow cover maps at NOAA/NESDIS for hydrological applications and numerical model initialization. Comparisons with surface data and visible satellite imagery suggests that the microwave product is capable of identifying significant snowfall (> 1 in). However, since the algorithm uses the 22V instead of the 19V channel, wet ground or melting snow can be misclassified as precipitation, and snow over vegetation is problematic. Grody noted that these issues, and hopefully, a snow depth algorithm, will be considered in future investigations. Current work includes the conversion of the algorithm to use brightness temperatures instead of antenna temperatures, thereby removing sensitivity of the algorithm to antenna pattern corrections among the SSM/I sensors.

The first of two regional snow products was presented by Dr. Anne Walker (and Dr. B.E. Goodison; Canadian Climate Centre), who described the development and testing of a snow water equivalent (SWE) passive microwave algorithm for the open prairie region of western Canada. This work is part of the Cryospheric System for Global Change Monitoring in Canada; therefore, the algorithm will gradually be extended to other landscape regions in Canada (and implicitly any region of similar terrain and vegetation).

Comparisons between the SSM/I derived SWE (SWE (mm) = -20.7 - 49.27(37V - 19V)/18.0) and ground snow survey measurements have shown that the regional patterns of snow distribution from both data sources agree very well, generally within 10mm of each other. One problem area identified during the validation process was the discrimination of wet snow from snow free areas (SWE = 0). Since liquid water within the snow pack reduces the 37V - 19V to near-zero values, the 37GHz polarization difference is checked when SWE = 0 to detect and label the presence of water.

Access to SSM/I data in near real-time via the Civilian Navy/NOAA Oceanographic Data Distribution System (CNODDS) has provided the Canadian Climate Centre with the capability to generate and validate snow products within hours after data acquisition. These maps are distributed by fax machine to several water resource agencies for their use in monitoring snow conditions, planning for ground surveys, and preparing run-off forecasts.

The results from a second set of regional analyses were presented by Dr. David Kilham (and Dr. Eric Barrett, Remote Sensing Unit, Univ. Bristol, United Kingdom). The parameters examined were SSM/I snow products in the UK, ice products in the East Greenland Sea and rain rate over the Sahara and Australian deserts.

The key issues involved in snow cover monitoring over the UK were the scale of the UK drainage basins as compared to the SSM/I footprint, types of snow and transience of snow events in the UK. The scale of the UK necessitated deconvolution/remapping of the SSM/I antenna temperatures using the actual antenna pattern in order to obtain maximum spatial resolution of the low frequency (surface) channels. The snow depth calibration curves were found to vary by region and the snow distribution patterns were improved by monitoring changes in the 19, 37 and 85GHz polarization differences, as well as the magnitude of the 37H - 85H frequency difference.

Using data sets from the East Greenland Sea, the Bristol team compared the output of the NASA Team, Comiso, DMSP Cal/Val and York Univ. sea ice algorithms. The conclusions were that the algorithms provided different types/densities of information and were more successful in different contexts (ice edge, ice concentration, etc.) so that it was not possible to declare any one of the algorithms as clearly superior to the rest.

Finally, the analysis of rain over desert surfaces indicated that the addition of a horizontal polarization frequency difference (37H - 85H > 0) was able to discriminate between no rain/rain over sand and bare soil surfaces.

Applications of these and other improved SSM/I techniques and algorithms will soon be made by the Royal Navy both globally and regionally, the latter in relation to data obtained directly from DMSP satellites by the new UK Ministry of Defence DMSP reception facility now under construction and expected to become operational before the end of 1993.

Validation and intercomparison of algorithms, such as those described above, is often hindered by the difficulty of compiling conventional data sets on a common grid and concurrent with SSM/I measurements. Under the auspices of the SSM/I Products Working Team (part of the NASA Earth Observing System Pathfinder effort), the National Snow and Ice Data Center (NSIDC) is producing a standard environment with which to validate algorithm output for snow covered regions. Dr. Richard Armstrong (and Dr. Molly Hardman, NSIDC) described the environment which includes an interpolation/gridding scheme (Equal Area SSM/I Earth Grid, EASE-Grid) for collocation of SSM/I brightness temperatures, algorithm output and conventional data. Once on this common grid, digital image subtraction techniques are used to make comparisons between the satellite data and conventional observations.

NSIDC has compiled a validation data set of surface station measurements for the northern hemisphere winter of 1988-1989 using specific data from the United States, Canada, and the former Soviet Union, as well as data from WMO for the remaining regions. These data will be used to test the Grody, Goodison, DMSP Cal/Val and Nagler (Univ. of Innsbruck, Austria) snow cover and depth algorithms. Preliminary results, including time-series images of mean, maximum,and minimum differences between the validation data and algorithm output, are expected in autumn, 1993. The global EASE-Grid data sets for the period of July, 1987 to November, 1988 will be available in about one year from the NASA SSM/I Pathfinder group.

8. SESSION 3: LAND PARAMETERS (Dr. Christopher Neale, Utah State Univ., Chair).

Three papers were presented in this session concerning overland parameters (other

than snow). Dr. Christopher Neale described two approaches, empirical and physical, for retrieving surface moisture using the SSM/I. The empirical approach, used in the development of the Cal/Val surface moisture algorithms, represents surface moisture by an Antecedent Precipitation Index (API). The physically-based retrieval obtains the surface soil volumetric water content and percentage of standing water within a footprint through the inversion of the Land Surface Radiative Transfer Model developed at Utah State University.

Dr. Neale described some of the problems involved in retrieving surface moisture with the SSM/I namely, the short wavelengths of the SSM/I which result in small penetration depths, the decrease in sensitivity to surface moisture caused by overlying vegetation, the heterogenous nature of the surface within the large SSM/I footprint sizes and, the inclusion of water bodies such as lakes and reservoirs within the SSM/I footprint which contaminate the signature. He pointed out that for the Cal/Val algorithms to work properly, a dynamic database must be implemented to keep track of the vegetation density and surface type (moisture included) within a grid cell, so that the proper empirical algorithm is applied for the particular vegetation density class in the region. He showed results from applying the empirical surface moisture algorithms to a time series of SSM/I data over the U.S. central plains retrieving surface moisture resulting from storms in the region.

The physically-based retrievals offer a new approach to directly obtain soil surface volumetric water content and physical temperature. However, further testing of the method is required and the procedure needs to be ported to a fast computer workstation to test it for entire images.

Dr. Richard Savage presented the land surface type classification scheme developed at Hughes Aircraft Co. Like the Cal/Val algorithms, this method is also statistically based however it uses principal component analysis to extract information regarding surface types and their different microwave properties. The basis for the classifier was a two year set of manually classified SSM/I observations on which a discriminant analysis was performed to reduce the seven SSM/I brightness temperatures to three discriminant scores. A lookup table translates the discriminant score into one of twenty-three surface types, classified in the three major categories of ocean, land, and "unknown" (points outside the discriminant bounds).

The last presentation in the session was by Lt. Col. Charles Holliday, who described the use of the SSM/I at AFGWC for tropical cyclone and regional tactical analyses. LtCol Holliday used dramatic imagery to demonstrate how the unique capabilities of the DMSP sensors were applied to military operations during Desert Shield, Desert Storm and Operation Restore Hope. Particularly noteworthy were the new software innovations at the DoD operational centers and tactical sites that allow coregistered, multispectral display of the OLS and SSM/I imagery.

9. SESSION 4: CLOUD LIQUID WATER, COLUMN WATER VAPOR AND SURFACE WIND SPEED (Mr. John Alishouse, NOAA/NESDIS, Chair).

Discussions of the atmospheric parameters were somewhat synergistic since a central issue was "crosstalk" between the water vapor and liquid water parameters, and their effects

on the estimation of the surface wind. Two new algorithms for cloud liquid water (Petty, Simmer) and one new surface wind algorithm (Stogryn) were presented. Other candidate algorithms, such as the Wentz algorithms used in some of the NASA Pathfinder efforts, were also described in the presentations.

Dr. Grant Petty (Purdue Univ.) summarized his evaluations of all known over-ocean cloud liquid water (CLW) algorithms for the SSM/I, and specified the characteristics of his two 37 and 85 GHz CLW algorithms. Both algorithms are logarithmic functions of either the 37 or 85 GHz polarization differences, normalized for wind speed and water vapor. Cloud temperature, or a surrogate based on sea surface temperature, is also required by the algorithm. The 85GHz algorithm is used for marine stratocumulus, when there is neither excessive water vapor nor significant precipitation. Petty recommends using the 37GHz algorithm when there is very high liquid water content; dense, spatially inhomogeneous clouds, and/or light precipitation.

For the CLW algorithm intercomparisons, Petty established evaluation criteria, including the ability of the algorithm to correctly retrieve zero CLW in the absence of clouds and the correct magnitude of CLW in the presence of clouds. In addition, the sensitivity of each algorithm to crosstalk from other sources was examined using an analytical radiative transfer model. The intercomparisons showed the Cal/Val algorithm exhibited significant crosstalk between water vapor and cloud liquid water, producing an overestimate of up to 0.2 kg/m^2 in a moist tropical atmosphere. Petty's own algorithm and that of Wentz showed no such crosstalk, however, the Wentz algorithm had higher rms deviations from zero in the cloud free data.

Petty continued his presentation with a similar evaluation of nine column water vapor algorithms (precipitable water, PW), including his own two statistical, and one physical, algorithms. The statistical algorithms were expressed as linear combinations of the 19V, 22V and 37H natural logarithms. The 19GHz polarization difference is used as a precipitation screen.

The algorithm intercomparison included computation of rms differences from a derivative of the Cal/Val raob-SSM/I matchup data, where the matchup criteria were revised to exclude land contamination and eliminate cases where the raob station was not in the SSM/I swath. SSM/I pixels used in the comparisons were within 50 Km of the raob station. Additional comparison criteria were the linearity of the predicted values, presence of systematic biases and theoretical crosstalk sensitivity. Most of the other algorithms exhibited biases between the measured and predicted values which could be removed by fitting cubic polynomials to the residuals. With the biases removed, the rms differences between the SSM/I estimates and raob water vapor measurements ranged from 2.63 kg/m^2 for the Cal/Val algorithm to 3.15 kg/m^2 for the Wentz algorithm. Petty reported an rms difference of 2.58 kg/m^2 from his algorithm, but cautioned that the training and validation data sets used to derived his algorithm were not independent; therefore, further validation was required. However, his new algorithm was less susceptible to liquid water crosstalk than the Cal/Val algorithm.

Dr. Clemens Simmer (Univ. Kiel, Germany) described the derivation and validation of their over-ocean CLW algorithm. The algorithm was developed with simulated brightness temperatures from a radiative transfer model and approximately 3000 radiosonde ascents acquired during Mar - Oct, 1979, over the North Atlantic. If successful, this

method would allow easier development and validation of CLW algorithms since radiosonde data are far more readily available than radiometer data. Liquid water content was estimated using a parameterization based on the temperature and humidity vertical profiles, since the radiosondes do not directly measure liquid water. Applying multiple regression, two, four and seven channel algorithms were derived which express liquid water as linear combinations of the natural logarithms of each channel.

The algorithms were validated using ship-based upward looking radiometer data acquired in the North Sea during the International Cirrus Experiment, 1989. The rms differences of the three algorithms were about 0.03 kg/m^2 , with the 22V/37V combination having the smallest rms and bias values (0.0248 kg/m^2 , -0.004 kg/m^2 when CLW = 0). The rms and bias values increase when there is partial or complete cloud coverage within a pixel.

Maps of monthly CLW for several years were plotted using SSM/I measurements in the Atlantic Ocean. Significant interannual variability in CLW was observed in all regions of the Atlantic. The interannual variability was not a sufficient explanation of the differences observed between the SSM/I estimates and monthly estimates from a climatological model.

Dr. Chuck Norris (Scripps Inst. of Oceanography) addressed the relative performance of three precipitable water vapor algorithms: Cal/Val (Alishouse), Wentz, and Schussel and Emery. The Cal/Val global algorithm is a nonlinear combination of the 19V, 22V, $(22V)^2$, and 37V brightness temperatures resulting from regression analyses between matched SSM/I observations and radiosonde profiles. The Wentz algorithm uses an iterative solution of a parameterized radiative transfer equation to simultaneously solve for precipitable water, water vapor and wind speed. Schussel and Emery derive a semilogarithmic algorithm based on regression analyses between precipitable water and simulated 22V, 37V and 85V brightness temperatures from an atmospheric radiative transfer model.

To test the algorithms, Norris compiled a larger set of radiosonde and SSM/I matchups than was used in the original cal/val effort. The data set included more equatorial (moist) observations and limited quality control was applied to the observations in order to maximize the size of the data set. Overall, the three algorithms produced PW values which were consistent with each other and radiosondes (correlation coefficients of greater than 0.96). Still, each algorithm exhibited attributes which can affect subsequent analyses. The Cal/Val algorithm overestimates PW at very low values (< 10 kg/m^2) and saturates at high values (>50 kg/m^2), with a good fit in the midrange. Some of this behavior is due to underrepresentation of tropical radiosondes in the training data set. The linearity of the Wentz algorithm is greater than the Cal/Val algorithm (0.95 v. 0.89) but the scatter about the line is also greater (rms of 5.1 kg/m^2 v. 4.9 kg/m^2). The Schlussel and Emery algorithm appears to underestimate PW over the range of observed values (slope of the best-fit line was 0.87 and rms of residuals was 6.2 kg/m^2).

Instead of comparing the output of multiple algorithms with data from a single sensor, Dr. Jorge Geaga and Dr. Don Rudy (Aerospace Corp.) examined the consistency of the Cal/Val wind speed and cloud water algorithms with data from two sensors, F8 and F11. This effort was a precursor to the F8 Tilt experiment (described in Session 6). The objective, which was satisfied, was to verify that the F10 and F11 data could be used as

"ground truth" for coincident F8 data, as F8 moved through different pitch angles during the Tilt experiment.

Comparisons of the lower five channel brightness temperatures and the derived wind speed and cloud water values were performed, using temporally coincident (within 30 min, June 26-27, 1992) and spatially overlapping (25 - 50N; 198 - 210E) F8 and F11 data. The 19V, 19H, 37V and 37H brightness temperature distributions as a function of latitidue were similar, except for a 0.8K positive shift in the F11 19V brightness temperatures. Due to water vapor absorption, the 22V brightness temperatures exhibited greater variability especially above 40N in this test case.

The F8/F11 cloud water and wind speed distributions were also consistent. Ranging from 0 to about 35 m/s (no cap applied to the algorithm), most of the wind speed values were below 10 m/s with a peak at approximately 6 m/s. The cloud water values peaked at 0.1 kg/m^2 over the range 0 - 0.9 kg/m^2 although the full range of values occurred only above 40N. Also noted was the nearly linear correlation between cloud water and wind speed in this region of high water content.

Continuing with efforts directed at future requirements, Neale (Utah State Univ.) provided an update on the activities of the NASA/NOAA "Pathfinder" program. Part of the "Mission to Planet Earth" concept, a Pathfinder Science Working Group (SWG) exists for each of the major satellite sensors flying today: GOES, AVHRR, TOVS, and SSM/I. The overall function of each group is to provide high quality, standard format sensor data to the science community for research toward future sensors and applications. The groups also provide advice on technical issues, data distribution, products and algorithms.

The SSM/I Pathfinder SWG (Neale, Chair) was formed in March, 1993 and has met twice (April 20-21, 1993, Tallahassee; Oct 21-22, 1993, Annapolis). The members of the group, researchers and program administrators from NASA/NOAA/university/private enterprises, formed subcommittees to expedite decision making in several key areas: 1) operations, data access and services, 2) ocean parameters, 3) precipitation algorithms, 4) snow and ice products, and 5) over land parameters.

The first requirement addressed by the SSM/I SWG was the distribution and content of the SSM/I Pathfinder data sets. A decision was made that the initial release would be F8 data from the period Aug 1, 1987 to Nov 30, 1988. Based on the scientific needs of the research community, four levels of SSM/I data and products were proposed: 1) full resolution antenna temperatures, 2) full resolution brightness temperatures (using the Wentz antenna pattern correction scheme), 3) full temporal resolution data products using recommended algorithms, and 4) temporally averaged data both at full resolution and on standard grids. The full resolution data sets will be distributed from NASA/MSFC on 8mm data cartridges in Hierarchial Data Format (HDF); the gridded data will be distributed from NOAA/NSIDC in HDF on CD-ROM.

Processing algorithms for the SSM/I geophysical products were evaluated by each of the subcommittees. As with the operational concerns of the SPN SSM/I Algorithm Research Panel, the Pathfinder groups hoped to find consensus algorithms which were "mature" and well-validated. The Ocean Parameters subcommittee (Wentz, Remote Sensing Systems, Chair) considered five wind speed (Bates; Goodberlet, Swift and Wilkerson; Schuessel and Luthardt; Smith; and Wentz), three water vapor (Alishouse et al., Petty and Katsaros, Wentz) and two cloud water (Wentz and Petty-Katsaros) algorithms.

The Wentz algorithms were recommended for water vapor and cloud water. The choice of wind speed algorithm was delayed pending further comparison of the Wentz and Goodberlet (Cal/Val) algorithms (see next presentation). [*Subsequent to the Symposium, the Pathfinder SSM/I SWG selected the Wentz wind speed algorithm.*]

The Precipitation subcommittee (Petty, Purdue Univ., Chair) elected to use the Adler et al. (NASA/GSFC) instantaneous rainrate algorithm for the benchmark data set until the final results of the WetNet Precipitation Intercomparison Project-2 were available. Given the relative immaturity of the existing rainrate algorithms, the subcommittee also considered alternative products such as a rain/no rain flag and monthly rain averages on a regular grid.

The Snow and Ice subcommittee (Armstrong, NOAA/NSIDC, Chair) identified the three algorithms discussed here in Session 1 as candidates for the Pathfinder benchmark data. NRL was assigned the task of conducting an intercomparison study in cooperation with the Navy/NOAA Joint Ice Center (Suitland, MD). Snow edge and extent algorithms are well documented and the subject of comparison studies by the Land parameters subcommittee. At this time, no single snow water equivalent algorithm could be recommended since all such algorithms are currently site-specific.

The Land parameters subcommittee (Neale, Chair) is evaluating surface type classifications schemes (Hughes, Neale et al. (Cal/Val), and Grody), surface moisture (Neale), and surface temperature (McFarland et al., Cal/Val) algorithms. Other vegetative type products were considered, such as fraction of cover (biomass), seasonal inundatation and microwave vegetative index. The final algorithm recommendations from this subcommittee are pending completion of these evaluations.

Reporting on a study for the Ocean Parameters Pathfinder subcommittee, Petty presented results of a comparison between the Wentz and Goodberlet (Cal/Val) wind speed algorithms. The comparison statistics were generated from a quality controlled subset of the buoy/SSMI matchup data set developed by Goodberlet for the original Cal/Val algorithm. Petty found that the Goodberlet algorithm exhibited superior rms errors (1.75 m/s) relative to Wentz (1.95 m/s), but it also exhibited a significant water vapor-dependent bias. By applying a correction which is quadratic in the SSM/I water vapor, most of the water vapor bias was removed and the rms error reduced to 1.56 m/s.

The matchup data set did not include wind speeds much above 20 m/s, therefore the relative accuracies of the algorithms at high wind speeds could not be determined. However, the algorithms do diverge at higher wind speeds, with a projected difference of 4 m/s in the vicinity of 30 m/s.

Both algorithms degrade in the presence of precipitation and/or heavy liquid water, and corrections for this rain bias would be of little value. Petty noted that the screens used in the Goodberlet algorithm to identify precipitation contaminated pixels do not satisfactorily discriminate between brightness temperature effects due to rain and those due to combinations of high water vapor content and high wind speed. Therefore, the Goodberlet algorithm could be improved by developing new precipitation flags which are referenced to SSM/I derived liquid water values rather than thresholded brightness temperatures.

Dr. Alex Stogryn (Aerojet Electronic Systems Div.) presented a new, neural network approach to the development of the SSM/I surface wind speed algorithm. Using

brightness temperatures from the lower four channels, and the Goodberlet SSM/I buoy matchup data, two fully connected, feed forward neural networks with two neurodes in the hidden layer were developed. The input vector elements are the four brightness temperatures at 19V, 22V, 37V and 37H, and the neurodes are tests for clear or cloudy conditions using polarization and frequency differences or brightness temperature magnitudes. Based on the outcome of these tests, weights and coefficients for either a clear or cloudy network are used, and the output is the wind speed computed from the hyperbolic tangent of the weighted sum of the brightness temperatures. No wind speeds are computed for pixels which do not satisfy either test; i.e., those pixels with significant liquid water contamination. The networks were developed using 1600 clear and 238 cloudy data points from the buoy/SSMI matchup data. Stogryn provided the deceptively simple computer logic and network coefficients for others to evaluate.

For the clear sky network, Stogryn's own tests resulted in rms errors of 1.41 m/s with a bias of 0.1 m/s. The corresponding statistics were 1.98 m/s and 0.3 m/s for the Goodberlet algorithm and 1.68 m/s, 0.0 m/s for the Wentz algorithm. The second cloudy network yielded an rms error of 2.39 m/s with a bias of 0.2 m/s, more than a factor of two better in both numbers than the alternate algorithms.

10. SESSION 5: PRECIPITATION (Mr. Gene Poe, NRL, Chair).

Two largely empirical algorithms for rain rate were presented by Dr. Norm Grody (NOAA/NESDIS). One represents an improvement over that published in the JGR in 1991 and is based on the scattering effects of rain at 85 GHz. The second algorithm, applicable to ocean only, is based on the retrieval of liquid water at 19 GHz. The coefficients of the retrieval algorithms are determined by ground-based radar data from sites in the United States, Japan, and the United Kingdom. Comparisons were presented of these algorithms and the current SSM/I Cal/Val rain rate algorithm and indicated that the Cal/Val algorithm significantly underestimates the rainfall rate. Additional coincident radar and SSM/I data are being collected to obtain a more globally representative rainfall data base for further evaluations.

Dr. George Huffman (NASA/GSFC) presented the Goddard Scattering Algorithm (GSCAT). The algorithm uses all SSM/I channels in an empirical fashion to eliminate areas of non-precipitation. Cold surfaces (e.g. snow or frozen ground) are given a preliminary identification of ambiguous due to similar signatures with rainfall. The rainfall rate is retrieved using the 85 GHz (horizontal polarization) in an algorithm where coefficients vary with surface type. Removal of the ambiguous identifications is done by comparing neighborhood signatures. Validation of the algorithm has been performed using the Global Precipitation Climatology Centre rain gauges (monthly 2.5° x 2.5° grids over land) for July 87 to June 88. The primary difficulty that arose in the investigation was the inability to detect the presence of warm rain over land.

Dr. Steve Goodman described the difficulty of obtaining an SSM/I rainfall algorithm that is acceptable to both global change scientists (Pathfinder) and operational users. The problem stems in part from insufficient data to conduct independent validation and inter-comparisons. Two inter-comparison projects were described–the WMO (AIPS) and the NASA WETNET–which provide a forum for detailed inter-comparison of

algorithm performance. Goodman presented results which showed that the current SSM/I Cal/Val rain rate algorithm underestimates rainfall rate. He suggested the source of the problem may be traced to the limited range of rain rate used in the development of the SSM/I Cal/Val coefficients. The need for larger dynamic range of rainfall rates was stressed.

Dr. Simon Chang (NRL) presented a comparison of SSM/I total rainfall (4 hours) based on the original Cal/Val algorithm for Hurricane Hugo in South Carolina with rainfall data obtained from an objective analysis of a network of rain gauges over Georgia, North and South Carolina. The SSM/I derived and rain gauge rainfalls agreed surprisingly well. In addition SSM/I marine windspeed were compared with buoy observations and an objectively analyzed wind field for Hurricane Florence.

Mr. Roland Nagle (CSC, Monterey) presented the diagnosed rainfall rate as determined by a numerical model that uses a modified Petty-Katsaros rainfall algorithm. The initial rainfall areas were remapped to later positions and put into animated sequences of 24-hour forecasts of SSM/I rain rate and net water vapor content. Several examples were presented which showed good agreement between the forecasted SSM/I rain rate patterns and verification patterns.

Dr. David Kilham presented a number of inter-comparisons of SSM/I rain rate algorithms currently being examined in the WetNet Precipitation Intercomparison Project-1 (PIP-1). The results presented involved relative comparisons of algorithm performances on a global, climatological basis. Presented in color on global maps number of interesting qualitative differences were readily apparent among the 16 algorithms selected. The performance of several algorithms could be associated with surface type or area for which they were calibrated. These preliminary results suggest that the single best rain rate algorithm may be a combination of several algorithms. Future investigations (PIP-2) will emphasize quantitative case studies of the algorithm performances. Final results of the PIP-1 algorithm studies will be presented at the next WetNet meeting (20-21 Sept, Logan, Utah).

11. SESSION 6: FUTURE DIRECTIONS (Dr. Marie Colton, FNOC, Chair).

Four more SSM/I sensors of the current design exist for the DMSP Block 5D-2 program. The presentations in this session described work aimed at sensors for the follow-on DMSP programs, Blocks 5D-3 and Block 6, scheduled and proposed for ca. 1997 and beyond.

A goal of the Block 6 program is the elimination of the interorbit gap at the equator; i.e., contiguous swaths. Dr. Samuel Gasster (Aerospace Corp.) explained how contiguousness can be accomplished by increasing either the orbital altitude above 833 km, the earth incidence angle (EIA) beyond 53.1°, or a combination of both. Increased orbital altitude introduces several systems concerns, including an increase in the natural radiation budget and the need for a large sensor aperture to maintain resolution. On the other hand microwave remote sensing phenomenology at high incidence angles is relatively unknown and existing models for predicting environmental parameters are likely to be inappropriate. Furthermore, the atmospheric path length at 69°, for example, is nearly doubled.

The F8 Tilt Experiment was proposed by Aerospace Corp. in response to trade

studies performed for the microwave imager during Phase I of the DMSP Block 6 concept studies. The plan was twofold: first, to acquire high incidence angle data from tower based radiometers (accomplished by NRL in December, 1991 and June, 1992 from the North Sea tower), and second, to acquire high incidence angle data from a spaceborne radiometer. F8 was chosen for the test since there was less operational impact, due to the failed Operational Line Scanner system in 1990 and the already degraded SSM/I (no 85 GHz channel).

Gasster described the test and analyses plans for the Tilt experiment which involved reprogramming the attitude control flight software at Sixth Operations Command and the geolocation ground processing software at FNOC. Data acquisition personnel at both FNOC and AFGWC were involved in the exercise. [*Executed mostly as planned, F8 was pitched from its nominal 53.1° ,to 69° , 64.5° , 60° , 57° , and back to 53.1° during the period June 25 to July 12, 1993. F10 and F11 data were also saved for intercomparison at F8 coincident times and locations. Analyses are now underway to assess the impact of the higher incidence angles on the measured brightness temperatures and geophysical retrievals.*]

Kreiss (Aerojet Electronic Systems Div.) presented the final paper of the Symposium on the Block 5D-3 SSMIS (Special Sensor Microwave Imager/Sounder) which combines the three current microwave sensors (SSM/I, temperature sounder, SSM/T-1; humidity sounder, SSM/T-2) into one instrument. For the most part, the retrieval algorithms currently incorporated in the SSMIS ground processing software take advantage of the heritage of the comprehensive DMSP SSM/I Cal/Val program, but enhancements have been made. First, the sea ice algorithm has been updated by AES/York University (see Session 1). Second, the work of Spencer and Grody has been used to construct a rain flag algorithm that takes advantage of the higher spatial resolution of the dual polarized 91.65 GHz data and channel comparisons at the lower frequencies to remove ambiguities over cold or snow covered surfaces. In addition, the information content of the higher resolution 150 and 183 GHz humidity sounding channels has been included in the rain flag. Third, the most recent correction to the SSM/I Cal/Val ocean wind speed algorithm has been included to improve retrievals under adverse weather conditions. Fourth, the work of Kunzi and Chang has been incorporated in the development of the snow water equivalent algorithm. Finally, the sea ice edge and snow pack boundary algorithms employ the efficient edge detection Sobel operators.

12. PLENARY SESSION.

a. General.

The half-day plenary session allowed the Symposium participants to reflect on individual presentations and isssues in a less structured setting. The objective was to find "middle ground" in the algorithm development process and transfer accepted improvements to operations for immediate action. Each attendee was supplied with an "Issues and Concerns" worksheet on which to elaborate his or her ideas (see eg., Encl (7), Sea Ice). The Session Chairs lead the discussions of the individual environmental parameters.

Short-, near-, and long-term improvements were identified as: validation and incremental improvements to the current Cal/Val algorithms, possible wholescale replacement of algorithms, and single or multisensor data fusion algorithms. An acceptable sequence of development was first, regional algorithms, then global algorithms with some

problem areas, finally global algorithms with no restrictions. Of course, there will always be "hot spots" for which unique, regional algorithms will be preferred.

Accomplishment of the short-term, incremental improvements to the algorithms would be easier with better access to near real-time data for validation The NOAA/NESDIS online archive and CNODDS were mentioned for data access. *Users requiring near real-time SSM/I data can request CNODDS support via online data or data cartridge from NOAA/Ocean Applications Group, Monterey, CA.. Similarly, Ms. Pam Taylor of NOAA/NESDIS can be contacted for information on the NESDIS online archive.*

Near term improvements (algorithm replacements) require a standard test set of SSM/I antenna and brightness temperatures and environmental parameters, eventually to include conventional data. The Pathfinder data set is a start in this direction, if the environmental data records are expanded to include output from the Cal/Val algorithms. Dr. Jim Dodge (NASA HQ) felt that at least part of the 18 month data set could have simultaneous runs from the Pathfinder and Cal/Val algorithms. Lt Col Arrance (DMSP SPO) submitted an Action Item for the Algorithm Research Panel to evaluate how a standard data set could be created and to estimate its cost and time for generation.

Recognizing the limitations of the SSM/I frequencies, the longer-term data fusion approach to new algorithms appeared to be the most desireable to many people. For example, Dr. Ron Isaacs (AER) mentioned in an Issue writeup that the atmospheric moisture parameters (cloud liquid water, water vapor and rain) are sources of error for determination of the surface SSM/I parameters (surface wind, snow, ice); variable backgrounds, especially snow and ice, are sources of error for automated cloud analyses schemes using OLS visible data; and cloud and variable background emissivity are sources of error for SSM/T-2 water vapor profile retrievals. Therefore, a unified approach to algorithm development is necessary. As a start, the OLS visible data could be used to determine if there are clouds in the SSM/I field of view before attempting to retrieve cloud liquid water.

Dr. Richard Savage also noted that the DMSP data are too fragmented, with the primary OLS sensor and all Mission Sensor data processed as separate streams. He pointed out that the separate processing was a constraint imposed by the original ground processing computers and that migration to distributed workstations, as is now happening at the central sites, could allow data fusion methods to be used. Regardless of the newer computer technology, a significant redesign of the ground processing software, supported by the DMSP System Project Office, would have to occur for combined OLS and SSM/I algorithms to be implemented for operational use.

b. Sea Ice

The current operational algorithm produces some extraneous values due to weather contamination. Spurious sea ice can thus occur in open water that is difficult for an automated process to identify and discard. New methods are needed to perfect the weather filtering function needed for an operational algorithm. This is especially true for products that are assimilated in an automated mode, such as ice concentration in the Polar Ice Prediction System (PIPS) forecast model. Sea ice is also produced in regions that are not possible for given time frames, but this can be remedied by externally specifying and updating sea ice geographic limits.

Summer melt problems are common to all algorithms and extreme care must be taken by users during this time frame. Additional work needs to be done to "highlight" when this condition is prevalent with something akin to a "melt flag".

Concentration values in excess of 100% often occur during the winter months and sometimes imply addition information about surface conditions. Studies with coincident SAR and altimeter data could assist in extracting additional sea ice properties from SSM/I data sets. Multi-sensor data sets should take on a high priority given the present budgetary climate and the high cost of polar field studies. Taking advantage of each sensor's strong suit can often lead to improved algorithm performance. This approach is more feasible in several thrusts due to new long term, digital, coincident satellite data sets.

c. Snow parameters.

Global and regional snow parameter algorithms were presented. Global classification of snow cover in the form of dry, wet or refrozen snow is presently conducted under the Cal/Val land surface classification scheme. The differences shown at the meeting between Dr. Norm Grody's results on (global) areal snow extent and the Cal/Val snow cover was due to the fact that the comparison only included the dry snow classification. Dr. Norm Grody has studied many of the "anomalous" snow signatures found in different parts of the world to reclassify the erroneous pixels. The regional snow algorithms were shown to be effective products when used in the appropriate context.

d. Land parameters.

The two land surface classification schemes, namely Cal/Val and Hughes, are presently being compared within the realm of the NASA WetNet program and the NASA/NOAA SSM/I Pathfinder activities. The existing Cal/Val surface moisture algorithm will not work properly until it is used in conjunction with a *dynamic* database in the current ground processing system.

e. Cloud liquid water, column water vapor, and surface wind speed.

The Cal/Val over-ocean cloud liquid water algorithm is based on limited data and may overestimate the presence of clouds, especially in the presence of higher humidity values. This is the serious problem which Petty describes as "crosstalk" between CLW and water vapor. The negative CLW values that are observed with the Cal/Val algorithm are not a serious problem and can be considered as "noise" that could be eliminated by simply setting the negative value to zero, or an artificial value which indicates "probably clear". The absolute calibration of any CLW algorithm is problematic; i.e.,exact zero values computed under cloud free conditions. A two stage algorithm which first determines the presence of clouds, then computes liquid water content (excluding rain) might work.

As known for sometime, the Cal/Val water vapor algorithm underestimates (saturates) at high water vapor values, overestimates at low values, and displays "crosstalk" behavior between CLW and water vapor (see Alishouse et al. in the Cal/Val Vol. II). One possible short-term solution is the use of logarithmic regression variables; i.e., log(280 -

T_B). Another possible short-term solution is to use a two stage regression that uses a cubic polynomial of the initial estimate to arrive at the final estimate of column water vapor. The problem is the size of the independent test data set that can be reasonably compiled and matched with SSM/I data for deriving coefficients and demonstrating improvements, given current resources.

The Cal/Val surface wind speed algorithm significantly overestimates wind speed in the tropics and displays appreciable correlation with atmospheric water vapor. Several short-term options for fixing these problems exist. The original Cal/Val buoy/SSM/I data set underrepresented tropical windspeeds, therefore, the larger tropical wind speed errors are not surprising. Recomputing the regression coefficients with a data set containing more tropical data could alleviate both the overestimation problem and water vapor dependence. Simple application of Petty's "22V water vapor correction" to the computed wind speed might remove most of the water vapor correlation. The adjusted algorithm should be compared with alternative algorithms (Wentz, Stogryn) prior to installation.

f. Precipitation.

The papers presented in the precipitation session reveal the myriad of difficulties that arise when attempting to retrieve rainfall rate from passive microwave radiometric measurements and, in particular, from the SSM/I. The horizontal resolution of the SSM/I beams usually do not match the spatial scales of rainfall and thus introduce obvious beam-fill problems. These problems are compounded when one includes the non-linear relationship between rainfall rate and measured brightness temperature.

Furthermore, the relationships between the absorption and emission of liquid hydrometeors, the multiple scattering produced by precipitation size ice particles, and the rainfall rate are complex and poorly understood components of the radiative transfer problem. Complex convective systems represent physical processes distinct from stratiform rain systems and must be treated differently. Surface emission contributions must be taken into account for the rainfall retrieval problem so that land background is treated separately from water or ice surfaces.

In addition, the validation of candidate algorithms must, of course, have a sufficient range of accurate "ground-truth" to go along with coincident SSM/I data. The observed underestimation of rain rate by the Cal/Val algorithm is likely due to and insufficient range of rain rate in the training data. Radar data, calibrated in terms of a network of rain gauges, have usually constituted the major source of "ground-truth" with a typically resulting accuracy of a factor of 2. Despite these (and other) problems, significant improvements in SSM/I rainfall rate algorithms are being achieved as evidenced by the papers presented in the symposium.

13. RESULTS OF SYMPOSIUM AND SUBSEQUENT ARP MEETING.

a. ARP Recommendations.

The Algorithm Research Panel met after the close of the Symposium to assign short-term actions, identified during the Symposium, which could significantly improve the

operational SSM/I products in a six month to one year timeframe. Recommending adjustments to the DMSP Cal/Val algorithms should not be construed as parochialism, rather, simple changes could be used effectively while further intercomparison studies are completed on new algorithms. Furthermore, any significant digression from multiple regression algorithms in the environmental processing paradigm could require redesign of the ground processing software. This type of change would be accomplished more efficiently after the centers have completed their near-term goal of rehosting the SSM/I operations to a workstation environment.

Sea Ice. Jeff Hawkins will investigate the possibility of imposing monthly geographic limits on the possible appearance of sea ice. The results and recommendations will be documented in a report to the ARP.

Snow parameters. Pam Taylor and Norm Grody will investigate the differences that occur between the DMSP snow depth/extent maps (available in near real-time via Shared Processing Network) and those determined by NOAA (also online). These comparisons will be coordinated with Chris Neale to make sure the NOAA algorithm includes the refrozen snow category.

Land parameters. Chris Neale will report the results of the WetNet comparison study between his (Cal/Val) surface type classification scheme, and that of Hughes Aircraft Co., due at the 20 September Wetnet meeting.

Column Water Vapor. John Alishouse will investigate possible modifications to the present algorithm by: 1) developing an algorithm using logarithmic variables, 2) implementing a second stage of regression by using the initial algorithm retrieval as a predictor for the final retrieval, or 3) developing an algorithm which uses the 22V brightness temperature raised to a power greater than two. In the interest of time, algorithms will be developed from the present Cal/Val database, but should be evaluated against each other on independent data. The compilation, matching, and editing of a suitably sized independent data set may require more time and resources than are available.

Surface Wind Speed. Marie Colton and Jim Cornelius will investigate the feasibility of obtaining commercially or from FNOC, a global data set of buoy/ SSM/I/raob matchup data which contains more tropical information. These data would be used to generate new regression coefficents for the existing Cal/Val algorithm. Due to the potential significant improvement identified by Alex Stogryn for neural networks, Gene Poe will investigate the possibility of having Stogryn generate a new set of coefficients with an expanded, global data set. The final performance evaluation will include an examination of the dependence of the windspeed residuals as a function of water vapor, and the generation, if needed, of new quality flags. The results and recommendations will be documented in a report to the ARP.

Cloud Liquid Water. The CLW retrievals seem to be of lower priority than other SSM/I parameters. However, data sets from upward looking radiometers for ASTEX and TOGA-COARE will soon be available. The proposed action is to assemble a data set from the ASTEX and TOGA-COARE projects and explore algorithms with a more physical basis that can distinguish betwen the presence and absence of water clouds. These algorithms may need "tuning" or "scaling", accomplished empirically from the data set. This revision will require more than a six month to one year effort.

Precipitation. The Algorithm Research Panel acknowledged that the Wetnet

Precipitation Intercomparison Projects would establish the best "community" rain rate algorithm, and that pending these results, no extensive algorithm intercomparisons would be undertaken by the ARP.

However, Pam Taylor and Norm Grody will generate a new set of regression coefficients for the current rain rate algorithm using a coincident set of radar/rain gauge/SSMI data that contain a large range of rain rates. The performance of this algorithm change will be determined using an independent, hopefully global, data set. For completeness, the current DMSP rain rate algorithm as well as the NOAA precipitation algorithm will be included in the evaluation of the proposed algorithm change. (It is important that proper weighting be given to the higher rain rates during the regression of the new coefficients to offset the preponderance of low rain rates). In addition, Taylor and Grody will make a comparison of the performance of the current rain flag with that used at NOAA in response to the concern about ambiguities arising from dry or refrozen snow. The results and recommendations for changes will be documented in a report.

Miscellaneous. Chris Neale will investigate the possibility of having the Pathfinder data set include DMSP Cal/Val products for selected timeframes, to facilitate future comparisons between the Pathfinder and DMSP SSM/I products. The integration of the DMSP SSM/I data into the Pathfinder data set must follow the completion of the above action items.

Marie Colton will prepare a report containing all changes that have occurred in the current SSM/I algorithms since the publication of the final DMSP SSM/I Cal/Val report, Vol. II in May, 1991.

b. Timeline.

The findings and recommendations of the Algorithm Research Panel will be forwarded for approval, via the SPN Operations Working Group, to the SPN Steering Committee in time for their November meeting.

The ARP will meet again to discuss directions from the SPN Steering Committee and progress on action items in December at the DMSP Mission Sensor Working Group meeting (at the NOAA/National Hurricane Center, Coral Gables).

SHARED PROCESSING NETWORK
SSM/I ALGORITHM RESEARCH PANEL
MEMBERSHIP ADDRESS LIST

Mr. John Alishouse
NOAA/NESDIS
World Weather Building
E/RA 14 Room 810
Camp Springs, MD 20233
Phone: (301) 763-8136
FAX: (301) 763-8108

Lt Col Edwin Arrance
USAF SMC/CIA
P.O. Box 92960
Los Angeles, CA 90009-2960
Phone: (310) 336-4090 DSN 833
FAX: (310) 336-4364

Ms. Barbara Banks
NOAA
Federal Building 4
Room 2039
Suitland, MD 20746
Phone: (301) 763-4310
FAX: (301) 763-1724

CDR Leslie Burgess
SPAWAR 165-2
5 Crystal Park, Room 301
2451 Crystal Drive
Arlington, VA 23201
Phone: (703) 602-3187
FAX: (703) 602-1535

Dr. James Cogan
US Army Atm. Sciences Lab.
AMSRL-BE-W
White Sands Missile Range, NM 88002-5501
Phone: (505) 678-2094 DSN 258
FAX: (505) 678-3385

Dr. Marie C. Colton (co-chair)
Fleet Numerical Oceanography Center
Code 73
Airport Rd, Bldg 702
Monterey, CA 93943
Phone: (408) 656-4623 DSN 878
FAX: (408) 656-4489

Mr. James Cornelius
Fleet Numerical Oceanography Center
Code 73, Satellite Div. Head
Airport Rd
Monterey, CA 93943
Phone: (408) 656-4398 DSN 878
FAX: (408) 656-4489

Dr. James Dodge
NASA HQ, Code SED
Earth Science & Applications Div.
Independence Ave
Washington, DC 20546
Phone: (202) 358-0763
FAX: (202) 358-3098

Encl(1)

SHARED PROCESSING NETWORK
SSM/I ALGORITHM RESEARCH PANEL
MEMBERSHIP ADDRESS LIST

CAPT Michael Farrar
AFGWC/SYS
106 Peacekeeper Drive
Offutt AFB, NE 68113-4039
Phone: (402) 294-7437 DSN 271
FAX: (402) 294-3505

Ms. Florence Fetterer
NRL Stennis Space Center
Code 321
Bay St. Louis, MS 39529-5004
Phone: (601) 688-5456 DSN 485
FAX: (601) 688-4149

Lt Col Charles Holliday
AFGWC
DOA Suite 2N3
106 Peacekeeper Dr.
Offutt AFB, NE 68113-4039
Phone: (402) 294-5451 DSN 271
FAX: (402) 294-3505

Dr. James P. Hollinger (retired)
NRL
Code 7211
Washington, DC 20375-5320
Phone: (202) 767-3398 DSN 297
FAX: (202) 767-9194

Dr. Herb Kroehl
NOAA/NGDC
E/GC2
325 Broadway
Boulder, CO 80303
Phone: (303) 497-6121
FAX: (303) 497-6513

Mr. Rob Mairs
NOAA/NESDIS
E/SP1
Federal Bldg 4, Room 301
Camp Springs, MD 20233
Phone: (301) 763-5687
FAX: (301) 763-1724

CAPT Jeff Malan
AFGWC
DOX
106 Peacekeeper Dr.
Offutt AFB, NE 68113-4039
Phone: (402) 294-5984 DSN 271
FAX: (402) 294-3505

Dr. Paul Moersdorf
COMNAVOCEANCOM
Code N5B
Stennis Space Center, MS 39529-5000
Phone: (601) 688-4129 DSN 485
FAX: (601) 688-5791

Mr. Gene Poe (co-chairman)
NRL
Code 7211
Washington, DC 20375-5320
Phone: (202) 767-3398 DSN 297
FAX: (202) 767-9194

Encl(1)

SHARED PROCESSING NETWORK
SSM/I ALGORITHM RESEARCH PANEL
MEMBERSHIP ADDRESS LIST

LCDR C. W. Green
COMNAVOCEANCOM
Code N533
Stennis Space Center, MS 39529-5000

Phone: (601) 688-4047 DSN 485
FAX: (601) 688-5791

MAJ Peter Rice
HQ AWS
DOO
Scott AFB, IL 62225-5206

Phone: (618) 256-4110
FAX: (618) 256-2417

Ms. Pam Taylor
NOAA/NESDIS SIB
E/RA23
Federal Bldg. 4, Room 3210A
Suitland, MD 20233

Phone: (301) 763-4380
FAX: (301) 420-0932

Encl(1)

SPN SSM/I Algorithm Symposium Agenda

[8 June 1993]

0830 Welcoming Remarks and Meeting Objectives, CAPT Plante, Commanding Officer, FNOC
0840 DMSP SSM/I System Status, Lt Col E. Arrance, DMSP System Project Office
0845 SSM/I Operational Processing and Data Utilization at FNOC, AFGWC, and NOAA/NESDIS, Colton (FNOC), Farrar (AFGWC), and Taylor (NOAA/NESDIS)
0915 Symposium Guidelines (Colton/Poe)

SESSION I: SEA ICE (Jeff Hawkins, NRL, Chair)
0925 "The York Univ. Passive Microwave Sea Ice Algorithm," I. Rubinstein (Inst. for Space and Terrestrial Science), A. Stogryn, G. Poe and W. Kreiss (Aerojet Elec. Sys. Div).
0945 "NASA Team Sea Ice Algorithm for the DMSP SSM/I," D. Cavalieri and P. Gloerson, NASA/GSFC.
1005 Coffee Break
1025 "The Bootstrap Technique for Deriving Geophysical Sea Ice Parameters from Multichannel Passive Microwave Data," J. Comiso, NASA/GSFC.
CANCELLED "NORCEX 85H Ice Concentration Algorithm for SSM/I," K. Kloster, O. M. Johannesen, and S. Sandven, Nansen Env. Remote Sensing Center, Norway.
1045 "SAR for Validating and Improving SSM/I Sea Ice Estimates," F. Fetterer, NRL/Stennis Space Center.
1105 Session 1 Summary
1130 Lunch

SESSION 2: SNOW COVER (Chris Neale, Utah State, Chair)
1300 "Global Snow Cover and Identification using SSM/I Measurements," N. Grody and A. Basist, NOAA/NESDIS.
1320 "Development and Operational Application of a Canadian Snow Water Equivalent Algorithm using SSM/I Data," A.E. Walker and B.E. Goodison, Canadian Climate Centre.
1340 "Validation Data Sets for SSM/I Derived Snow Cover Products," R. Armstrong and M. Hardman, Univ. Colo./CIRES.
1400 "Improvements to SSM/I Techniques and Algorithms in Areas of Sand, Sea Ice, Snow and Frozen Ground," E. Barrett, Kelly, R.J., Kilham, D.A., and D.R. Kniveton, Univ. Bristol, C. Durbin (Royal Navy) and J. C. Scott (U.K. Defence Res. Agency.
1420 Session 2 Summary
1440 Coffee Break

SESSION 3: LAND PARAMETERS (Chris Neale)
1500 "Soil Moisture Retrievals with SSM/I: Empirical and Physical Based Approaches," C. N. Neale and G. Vassiliades, Utah State Univ.
1530 "SSM/I Scene Classification," R. Savage, Hughes Aircraft Co.
1550 "AFGWC SSM/I Applications: Wet Desert and Thunderstorm Discrimination during Desert Storm, and Tropical Cyclone Analyses," C. Holliday, Air Force Global Weather Central.
1620 Session 3 Summary

1700 - 1900 ***No-host Icebreaker*** *(Hermann Hall, LaNovia room)*

Encl (2)

[9 June 1993]

SESSION 4: CLOUD LIQUID WATER, COLUMN WATER VAPOR AND SURFACE WIND SPEED (J. Alishouse, NOAA/NESDIS)

0830 "SSM/I Algorithms for the Estimation of Column Cloud Water and Water Vapor," G. Petty, Purdue Univ.
0850 "Interannual Variation of Cloud Liquid Water Content derived from SSM/I Observations," U. Hargens, C. Simmer, E. Ruprecht, Inst. fur Meereskunde, Univ. Kiel, Germany.
0910 "Intercomparison of SSM/I Integrated Water Vapor Algorithms," C. Norris, Scripps Inst. of Oceanography.
0930 "Consistency of Retrieved Wind Speed and Cloud Water from Coincident F8/F11 Data," J. Geaga and D. Rudy, Aerospace Corp.
0950 Coffee Break
1010 "Status Report of NASA/NOAA SSM/I Pathfinder Effort," C. Neale, SSM/I Pathfinder Chair, Utah State Univ.
1030 "A Comparison of SSM/I Algorithms for the Estimation of Surface Winds," G. Petty, Purdue Univ.
1045 "SSM/I Wind Speed Retrieval using Neural Networks," A. Stogryn, Aerojet Corp.
1110 Session 4 Summary
1140 Lunch

SESSION 5: PRECIPITATION (G. Poe, NRL)

1300 "Global Rain Rate Retrievals using SSM/I Scattering and Emission Algorithms," R. Ferraro, N. Grody, G. Marks, and S. Kusselson, NOAA/NESDIS.
1320 "Precipitation Estimation from SSM/I Data with Goddard Scattering Algorithm," G. E. Huffman and R. F. Adler, NASA/GSFC.
1340 "An Intercomparison of the Navy Cal/Val and SSM/I Pathfinder Precipitation Algorithms," S. Goodman, F. LaFontaine,NASA/MSFC; G. Huffman and R. Adler, GSFC.
1400 "Some Evaluations of SSM/I Retrieved Fields in Tropical and Extra-Tropical Cyclones," S. Chang, R. Alliss, and G. Sandlin, NRL/Washington, D.C.
1420 "On the use of SSM/I data in the Short-Term Prediction of Maritime Precipitation," R. Nagle, Computer Sciences Corp.
1440 Coffee Break
1500 "Global Rainfall Monitoring: the WetNet Precipitation Intercomparison Project (PIP-1), Results and Reflections," E. C. Barrett, C. Kidd, D. Kniveton (Univ. Bristol) M. Goodman and B. Motta (NASA/MSFC).
1530 Session 5 Summary

SESSION 6: FUTURE DIRECTIONS (Colton, FNOC)

1550 "F8 High Incidence Angle TILT Experiment," S. Gasster, Aerospace Corp.
1610 "The SSMIS Imaging Algorithms," W. Kreiss, G. Poe, and A. Stogryn, Aerojet Elec. Sys. Div.
1630 Session 6 Summary

[10 June 1993]

PLENARY SESSION

0830 Summarization statement of meeting/issues/actions pertinent to all parameters. Guidelines for discussions. (Colton/Poe)

Development of recommendations/open discussion of:
0845 Sea ice algorithms (Hawkins)

0930 Snow/land parameters

1015 Coffee break

1030 Atmosphere/ocean parameters

1115 Conclusions

Encl (2)

GOVERNMENT ATTENDEES

Mr. John Alishouse
NOAA/NESDIS
E/RA 14 Rm 810
Camp Springs, MD
20233
(301) 763-8136

Ms. Cheryl Bertoia
NOAA/Joint Ice Center
4301 Suitland Rd
Washington, DC
20395
(301) 763-5973

Ms. Pim Chavasant
FNOC Code 70A
7 Grace Hopper Rd
Stop 1
Monterey, CA
93943
(408) 656-4444

Mr. Jim Cornelius
FNOC Code 73
7 Grace Hopper Rd
Stop 1
Monterey, CA
93943
(408) 656-4398

Dr. Jim Dodge
NASA HQ
2 Independence Sq.
Washington, DC
20546
(202) 358-0763

Ms. Florence Fetterer
NRL
Code 7240
StennisSpace Ctr, MS
39520
(601) 688-5456

LCDR C.W. Green
COMNAVOCEANCOM
1020 Balch Blvd
Stennis Space Ctr, MS
39529
(601) 688-4047

Mr. Jeffrey Hawkins
NRL
Systems Support Br
Monterey, CA
93943-5006
(408) 656-4753

LtCol Edwin Arrance
SMC/CIA
Suite 1467-D9
Los Angeles AFB, CA
90009-2960
(310) 336-4090

Dr. Bruce Brasnett
Can. Climate Ctr
2121 N. Service Rd.
Dorval, CANADA
H9P1J3
(514) 421-4665

Dr. Marie Colton
FNOC Code 73
7 Grace Hopper Rd
Stop 1
Monterey, CA
93943
(408) 656-4623

Dr. Chris Crosiar
NRL
Sys Support Branch
Monterey, CA
93943-5005
(408) 656-4726

LCDR Chris Durbin
DNOM(RA)
Lacon House
Theobalds Rd
London, WC1X8R4
UNITED KINGDOM
071-430-6734

Dr. Per Gloersen
NASA/GSFC
Code 971
Greenbelt, MD
20771
(301) 286-6362

Dr. Norm Grody
NOAA
E/RA 12
Washington, DC
20233
(301) 763-8042

LtCol Charles Holliday
AFGWC
Code DOA
Offutt AFB, NE
68113-5000
(402) 294-9756

Ms. Barbara Banks
NOAA/NESDIS/IPD
FB#4 Rm 2045
Suitland, MD
20746
(301) 763-4310

Dr. Simon Chang
NRL
Code 7220
Washington, DC
20375
(202) 767-2436

Dr. Josefino Comiso
NASA GSFC
Code 971
Greenbelt, MD
20771
(301) 256-9135

Dr. John Derber
NOAA/NWS
W/NMC 213
Washington, DC
20233
(301) 763-8005

Capt Michael Farrar
AFGWC
Code SYSS
Offutt AFB, NE
68113-5000
(402) 294-7437

Dr. Steve Goodman
NASA MSFC
ES/42
Huntsville, AL
35812
(205) 544-1683

Dr. David Halpern
Jet Propulsion Lab.
4800 Oak Grove Dr.
Pasadena, CA
91109
(818) 354-5327

Dr. George Huffman
NASA GSFC
Code 912
Greenbelt, MD
20771
(301) 286-9875

Encl(3)

GOVERNMENT ATTENDEES

Dr. Edward Josberger
U.S. Geological Survey
Univ. of Puget Sound
Tacoma, WA
98335
(206) 593-6516

Dr. Rangaro Madala
NRL
Code 7225
Washington, DC
20375
(202) 767-2226

Mr. Brian Moore
AFGWC/SYSM
MBB 39
Offutt AFB, NE
68113-4039
(402) 294-5504

Dr. Vincent Noble
Naval Research Lab
Code 7203
Washington, DC
20375-5000
(202) 767-2330

Maj Peter Rice
HQ AWS
Code DOO
Scott AFB, IL
62225-5206
(618)256-4110

Dr. Phil Schwartz
Naval Res. Lab.
Code 7220
Washington, D. C.
20375-5000
(202) 767-3391

Dr. Anne E. Walker
Can. Climate Ctr.
4905 Dufferin St.
Downsview, ONTARIO
CANADA M3H 514
(416) 739-4357

Dr. Herb Kroehl
NOAA/NGDC
325 Broadway
Boulder, CO
80303
(303) 497-6121

Mr. Doug May
NRL
Code 7240
StennisSpaceCtr, MS
39529
(601) 688-4845

Maj. Steve Musto
Onizuka AFB
SMC/OD4
Sunnyvale, CA
98089-1234
(408) 752-6310

Mr. Gene Poe
NRL
Code 7211
Washington, DC
20375-5320
(202) 767-3398

Mr. Kim Richardson
NRL
Sys. Support Br.
Monterey, CA
93943-5006
(408) 656-4771

Ms. Pam Taylor
NOAA/NESDIS SIB
E/RA 23 FOB#4
Suitland, MD
20233
(301) 763-4380

Dr. Godelieve DeBlonde
Atmos. Env. Service
2121 TransCanadian
Hway.
Dorval P.Q. H9P1J3
CANADA
(514) 421-4749

Mr. Tom Lee
NRL
Sys. Support Br.
Monterey, CA
93943-5006
(408) 656-4797

Dr. Andrew Milman
NASA/MSFC
AMK ES/43
Huntsville, AL
35812
(205) 544-1439

LCDR Cynthia Nelson
OFCM Suite 900
6010 Executive Bldg
Rockville, MD
20852
(301) 443-8704

Dr. Peter Ranelli
COMSPAWARSYSCOM
PMW 165
Washington, DC
20363-5100
(703) 602-3187

Mr. John Ruggiero
NAVSPASYSGRP
SMC/CIN
Los Angeles AFB, CA
90009-2960
(310) 336-4410

LCDR R. Tompkins
NAVSPASYSGRP
SMC/CIN
Los Angeles AFB, CA
90009-2960
(310) 336-4340

UNIVERSITY ATTENDEES

Dr. Richard Armstrong
Univ. of Colorado
CIRES/NSIDC CB 449
Boulder,CO
80309
(303) 492-5171

Dr. Eric Barrett
Univ. of Bristol / RSU
Dept of Geography
Bristol,BS8 1SS
UNITED KINGDOM
011-44-202-303-745

Dr. Peter Flatau
UCSD/CSI
Mail Code 0221
La Jolla,CA
92903
(619) 534-1025

Dr. Newell Garfield
NPS
Code OC/GF
Monterey,CA
93943
(408) 656-3226

Dr. Molly Hardman
Univ. Colorado
NSIDC/Box 449
Boulder,CO
80309
(303) 492-3895

Dr. Siri Khalsa
Univ. of Colorado
Aerospace & Eng. Sci.
Boulder,CO
80309-0429
(303) 492-1445

Dr. David Kilham
Univ of Bristol
Remote Sensing Unit
Bristol,BS8 1SS
United Kingdom
011-44-272-303745

Dr. Kjell Kloster
Univ. Bergen / NERSC
Edvard Griegsvei 3a
SOLHEIMSVIK,N-5037
NORWAY
011-47-5-297288

Dr. Ken Knowles
Univ. Colorado
NSIDC/Box 449
Boulder,CO
80309
(303) 492-0644

Dr. Christopher Neale
Utah State Univ.
Agric/Irrig Eng.
Logan,UT
84322-4105
(801)750-3689

Dr. Charles Norris
UC San Deigo
Scripps Inst. of Ocean.
San Diego,CA
92093-0224
(619) 530-0341

Dr. Grant Petty
Purdue Univ.
Earth & Atm. Sci.
West Lafayette,IN
47907-1397
(317) 494-2544

Dr. Greg Sharfen
Nat. Snow&Ice Data Ctr
Univ. Colorado / CIRES
Boulder,CO
80309-0449
(303) 492-6197

Dr. Clemens Simmer
Inst. for Meereskunde
an der Univ. Kiel
Dusternbrooker Weg 20
D-2300 Kiel1,
GERMANY
011-49-431-597-3875

Dr. Ron Weaver
Univ. Colorado
NSIDC/Box 449
Boulder,CO
80309
(303) 492-3895

Ms. Annette Schloss
Univ. New Hampshire
Morse Hall
Durham, NH
03884
(603) 862-1956

Encl(3)

CORPORATE ATTENDEES

Mr. Don Boucher
The Aerospace Co.
P.O. Box 92957
Los Angeles,CA
90009
(310) 336-8837

Mr. Mike Davis
Lockheed Missiles&Space
1111 LockheedWay O64-14
Sunnyvale,CA
94089
(408) 742-5799

Dr. James Ehrisman
Atlantis Sci. Sys. Grp.
1827 Woodward. Dr.
Ottawa,ONTARIO
CANADA K2C 0P9
(613) 727-1087

Dr. Samuel Gasster
The Aerospace Co.
P.O. Box 92957 M4/927
Los Angeles,CA
90009
(310) 336-60005

Dr. Jorge Geaga
The Aerospace Co.
P.O. Box 92957 M4/927
Los Angeles,CA
90009
(310) 336-6311

Dr. Morton Glass
Phillips Laboratory
PL/GPAS
Hanscom AFB,MA
01731
(617) 277-2946

Dr. Kenneth Hardy
Lockheed Missile&Space
3251 Hanover St.
Palo Alto,CA
94304-1191
(415) 424-2825

Dr. Ronald Isaacs
AER, Inc.
840 Memorial Dr.
Cambridge,MA
02139
(617) 547-6207

Dr. Duc Kieu
Aerojet Electrosystems
1100 W. Hollyville
Azusa,CA
91702-0296
(818) 812-8161

Dr. William Kreiss
Aerojet Electrosystems
1100 W. Hollyville
Azusa,CA
91702-0296
(818) 812-2095

Dr. Doug Moore
S M Sys. Res. Corp.
4201 Northview Dr.
Bowie,MD
20716
(301) 763-3211

Mr. Roland Nagle
Computer Sci. Corp.
7 Grace Hopper Rd.
Monterey,CA
93943
(408) 656-4715

Mr. Adrian Ritchie
Hughes STX
Code ES/44
NASA/MSFC,AL
35812
(205) 544-8850

Dr. Irene Rubenstein
EOL/ISTS
4850 Keele St
North York,Ontario
CANADA M3J 3K1
(416) 665-5410

Dr. Richard Savage
Hughes Aircraft Co.
16800 E.CentreTechPkway
Aurora,CO
80011
(303) 344-6176

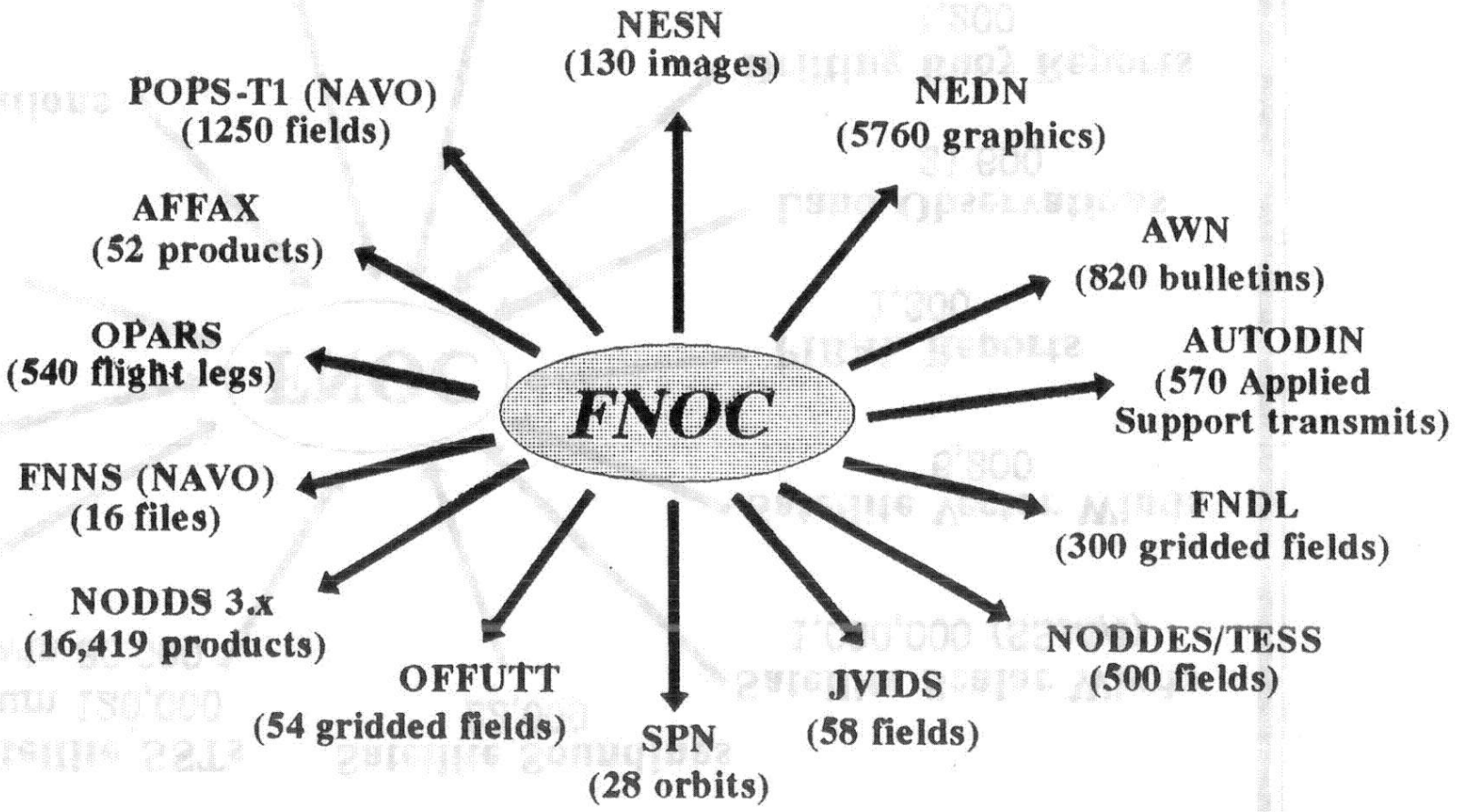
Ms. Julia Sheldon
Aerojet Electrosystems
1100 W. Hollyville
Azusa,CA
91702-0296
(818) 812-1624

Dr. Alex Stogryn
Aerojet Electrosystems
1100 W. Hollyville
Azusa,CA
91702-0296
(818) 812-1154

Dr. Frank Wentz
Remote Sensing Systems
1101 College Ave
Santa Rosa,CA
95404
(707) 545-2904

Encl(3)

A TYPICAL DAY IN THE OFFICE . . .

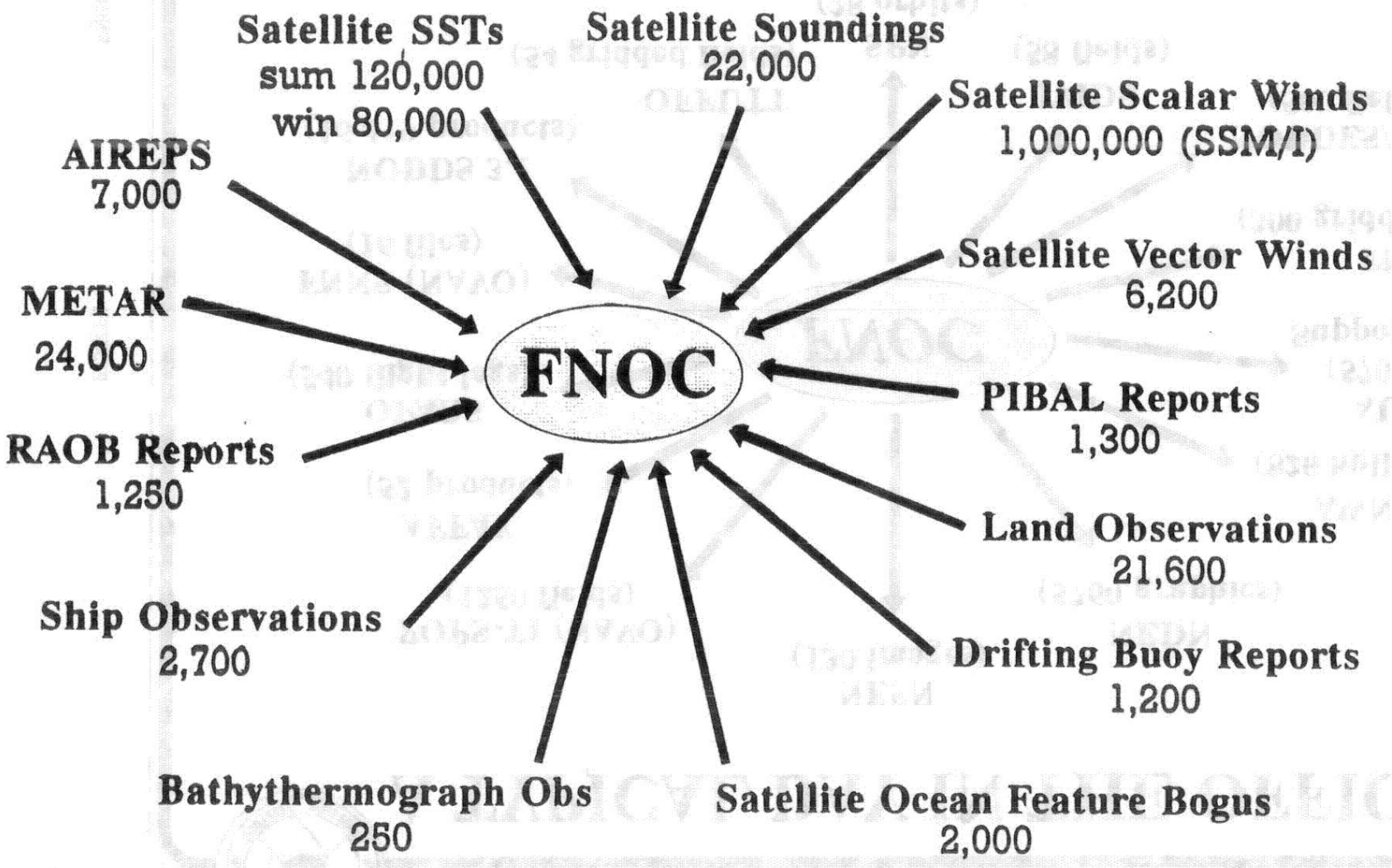


26,497 PRODUCTS SENT EACH DAY, 1/3.3 SEC.

PLANTE

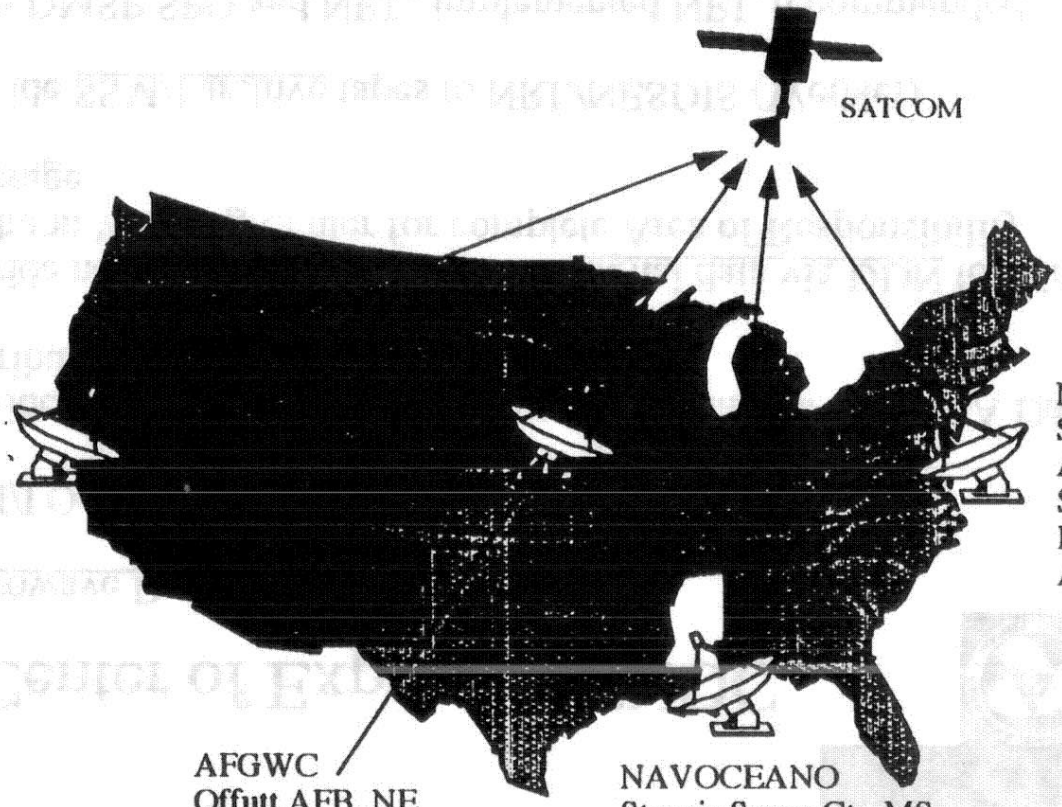
ENCL (4)

24 HOUR DATA SOURCES



1.2 MILLION OBS RECEIVED EACH DAY, 13.8/SEC

Shared Processing Network Overview



SPN Center of Expertise: FNOC

Microwave Data and Products

SSM/I Operational Processing since 1987 (F8, F10, F11)

Provide near real-time SSM/I data to (Civilian) Navy/NOAA Data Distribution System (CNODDS)

Provide near real-time SSM/I stored digital data via DDN to Joint Typhoon Warning Center for complete Area of Responsibility coverage

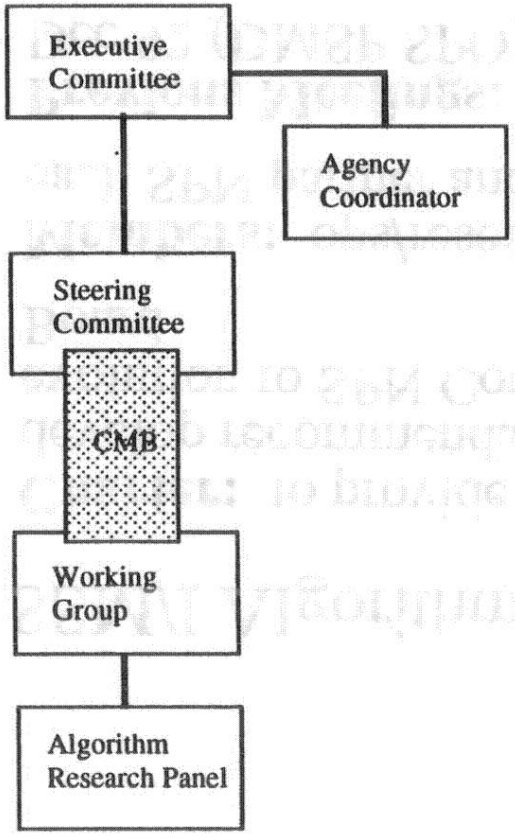
Provide SSM/I archive tapes to NRL/NESDIS (WetNet)

With DMSP SPO and NRL, implemented NRL recommended Cal/Val algorithms (completed May '91)

Implemented SSM/I software configuration management for benchmark algorithms and software

Since Jan '92, provide near real-time SSM/I data to SPN

SPN Change Management Board



Controlled Evolution of SSM/I Software

Configuration Management Plan

Establish Algorithm Research Panel

Resource Management / Funding Mechanism(s)

Algorithm Research Panel

Met 30 Sep 92 (NRL) and 17 Dec 92 (DMSP SPO)

Essentials: updated algs and test data sets

SPN SSM/I Algorithm Symposium: 8-10 June 93

SSM/I Algorithm Research Panel

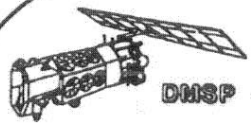
Charter: to provide technical guidance and develop recommendations for SSM/I software evolution to SPN Configuration Management Board

Members: ops/research representatives from each SPN partner and NASA

Previous Meetings: 30 Sep 92 (NRL) and 17 Dec 92 (DMSP SPO)

ACTIONS: update algorithms via open forum process and compile test data sets

Next meeting: 10 June 93 after symposium

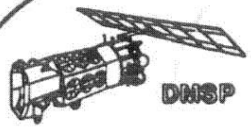


SATELLITE / SENSOR OPERATIONAL STATUS

CIEC
JUNE 3,1992

ARRANCE

ENCL (5)



F - 6

LOCAL ASCENDING NODE TIME 0613

STATUS: NON OPERATIONAL

- **128 Months on-orbit (Dec 82-Jun 93) Rev 54,200**
- **X & Y - Gyros failed, PDT-2 failed**
- **SADLAG 0 Degrees**

SCP1: (Bad memory) Precision Mode

SCP2: Master in 2-gyro Basic

OLS: Scanner failed/T channel inoperative/PR4 inoperative

SENSORS: All off except SSJ/4 (operative but unpowered)



F - 8

LOCAL ASCENDING NODE TIME 0619

STATUS: OPERATIONAL/SADLAG +75 deg

- 72 months on-orbit (Jun 87- JUN 93) Rev 30,600

SCP1: Controlling Attitude in Precision Mode (bad memory at 6800# to 6FFF#

SCP2: Master in Monitor Mode (swapped 8K Boards and bad memory at 2800 # to 2FFF# and 4000# to 47FF#)

OLS:
- OLS Scanner Inoperative
- PR1 and PR2 Failed
- Receives Lunar Location Data from Spacecraft

SENSORS: SSI/ES-failed, SSM/I (85 GHZ V& H unusable), SSJ/4, SSB/X-M, SSM/T



F - 9

LOCAL ASCENDING NODE TIME 0829

STATUS: NON-OPERATIONAL/ SADLAG - 82 Degrees

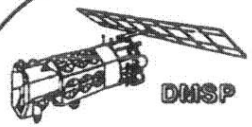
- 62 months on-orbit (Feb 88-Jun 93) Rev 27,600

SCP1: Controlling Attitude in Precision Mode

SCP2: Master in Monitor Mode

OLS:
- OLS Scanner in test status
- Receives Lunar Location Data from S/C
- T Channel Sensitivity is decreasing
- PR4 Noisy and Unacceptable for Data Recovery

SENSORS:
- SSI/ES - failed
- SSM/T (Channel 1 AGC Noisy, Ch 5, 6, and 7 shifting levels)
- SSK(off), SSJ/4, SSB/X-M



F - 10

LOCAL ASCENDING NODE TIME 2117

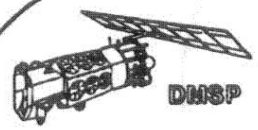
STATUS: OPERATIONAL/SADLAG -65 deg
- 30 months on-orbit (Dec 90- Jun 93) Rev 13,000
- Elliptical Orbit (apogee minus perigee 62 mi)

SCP1: Controlling Attitude in Precision Mode(swapped 8K boards)

SCP2: Master in Monitor Mode

OLS:
- Receives Lunar Location Data from S/C
- T Channel left segment override
- PR2 and PR4 failed, PR1 used for limited fine, HRD on backup postamp

SENSORS: SSI/ES, SSMI, SSJ/4, SSB/X-2,SSM/T all nominal



F - 11

LOCAL ASCENDING NODE TIME 1730

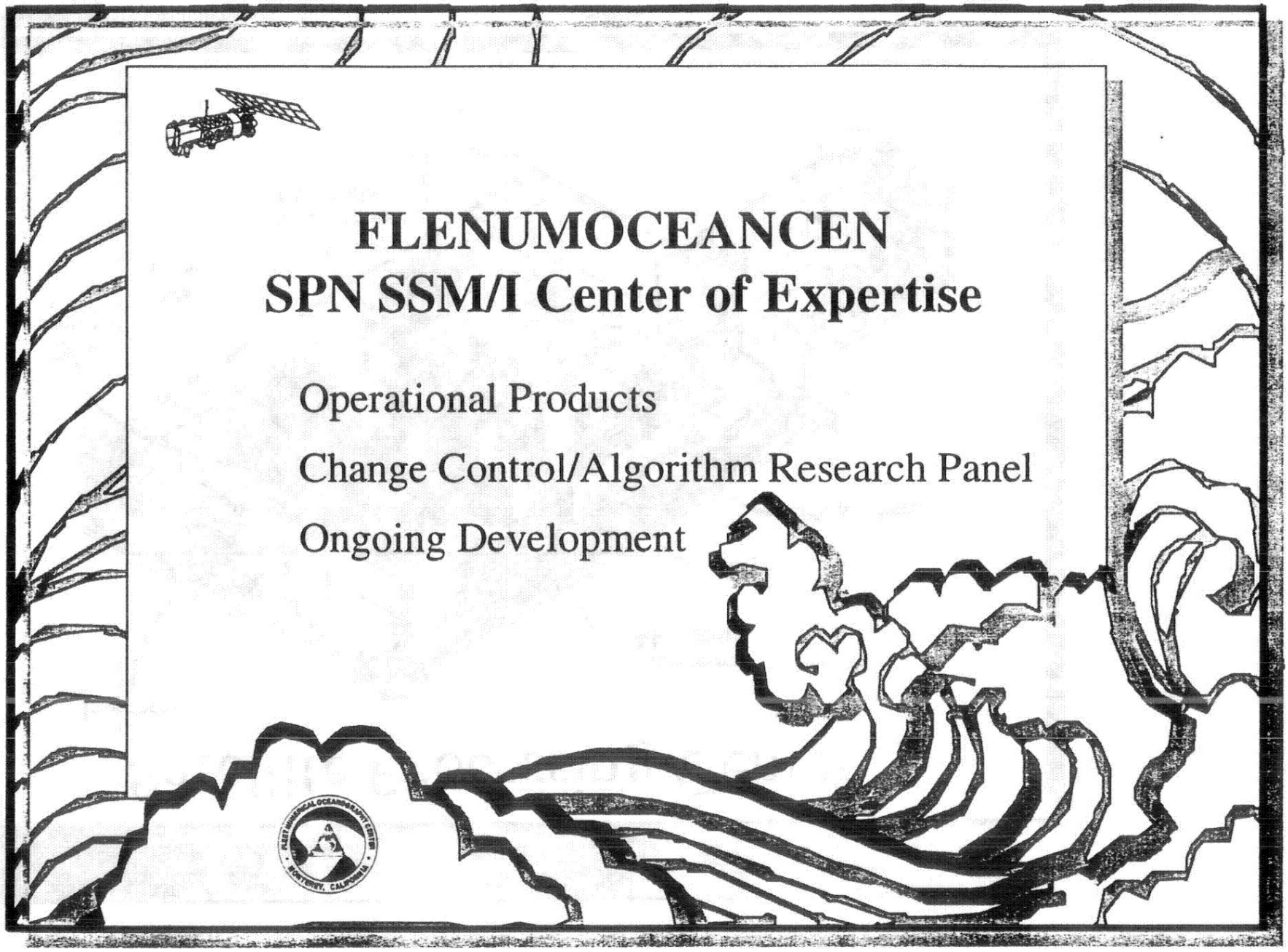
STATUS: OPERATIONAL/SADLAG -65 Degrees
- 19 months on-orbit (Nov 91-JUN 93) Rev 7,700

SCP1: Controlling Attitude in Precision Mode

SCP2: Master in Monitor Mode

OLS:
- Receives Lunar Location Data from S/C

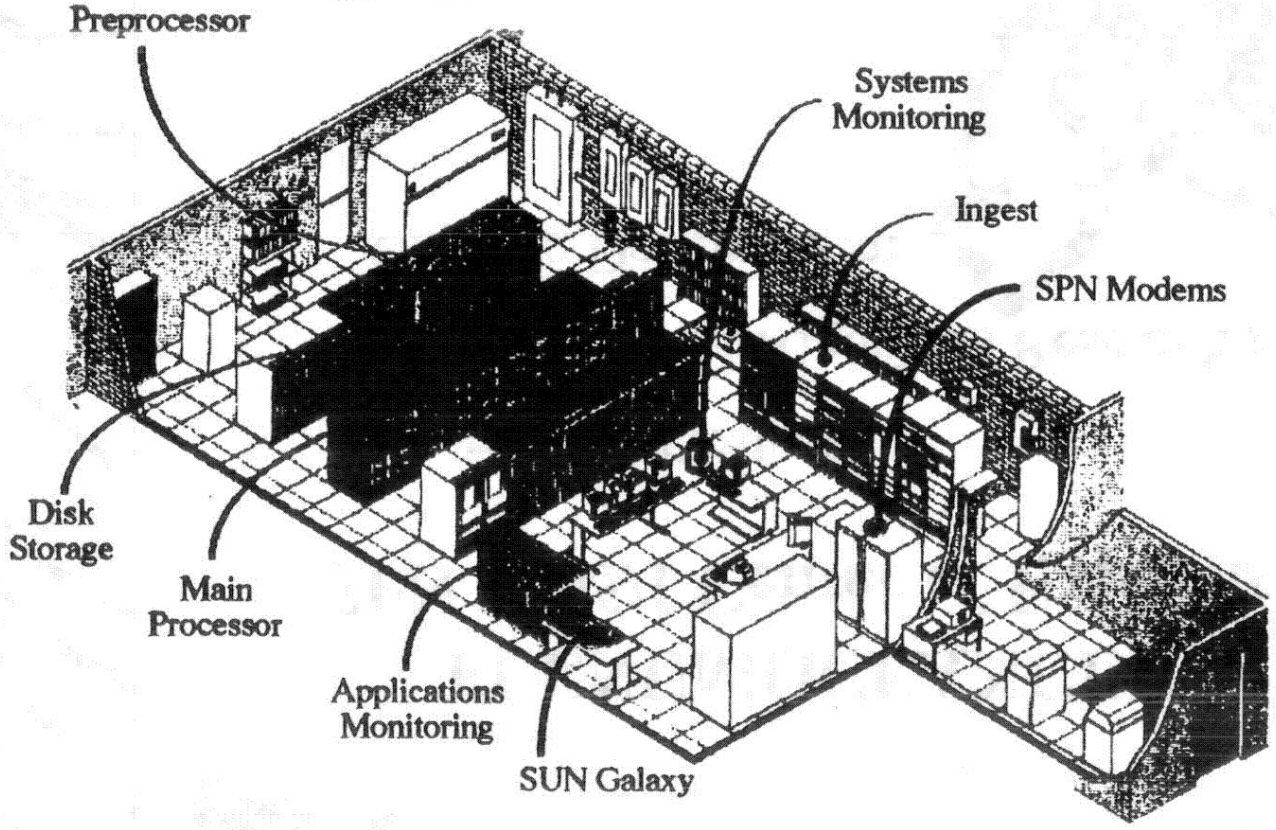
SENSORS: SSI/ES, SSMI, SSJ/4, SSB/X-2,SSM/T-1,SSM/T-2
All are nominal



COLTON

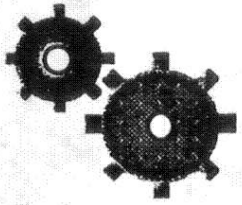
ENCL (6)

Satellite Processing Center



Operational SSM/I Products

Satellite Processing Computer



SPN DEF files

NOGAPS surface wind ingest

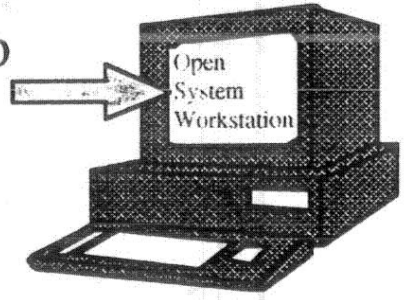
NEDS imagery

Tape archive (with Cyber) / Status

Glimpse of the Future

Digital data transfers to Guam MISTIC

Postscript graphic of ice concentration to NPOC




CLOUD WATER CONTENT
Dsc: MISTIC DB Image
HEMI:N BOX:1

FNOC SSMI ICE CONCENTRATION



Bering Sea

4-15-93 F11 04Z



Ongoing Development

Conversion to Workstation via OASIS

NAVAF Co-op dictates data ingest

Data output to relational DBMS

93-96

BUFR encoder/decoder for data exchange

WMO standard / DDN transmits

93-94

SSM/I data to NODDS

Compression routines

Gridded analyses

93-94

Block 5D3 SSMI/S TQM activities

Ground Processing Sys ECP: Change of Platform

93-96

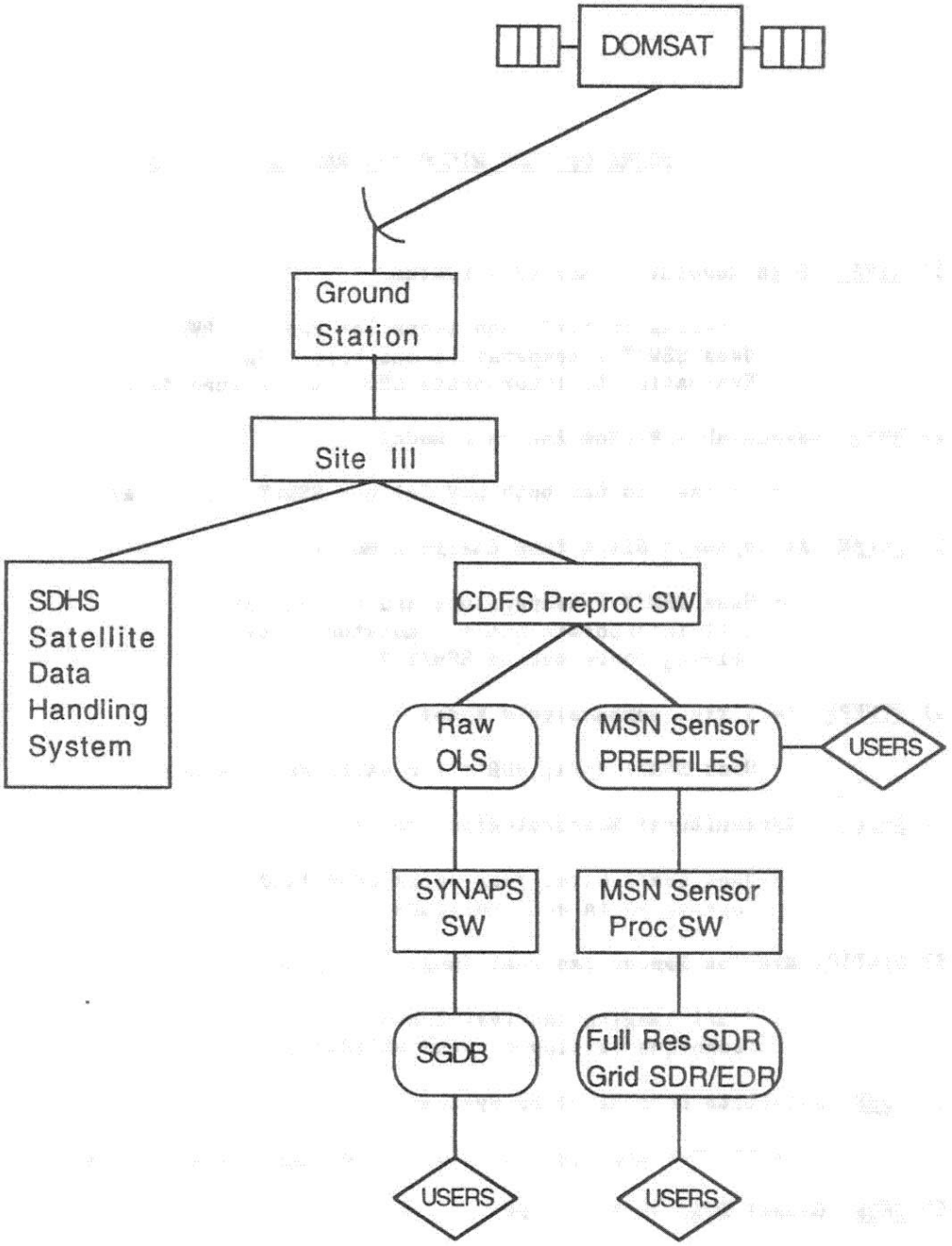
Block 6 F8 Tilt Experiment (TEX)

High incidence angle for contiguous coverage at equator

Two week experiment: No earlier than 24 Jun 93

93-94

DMSP Data flow at AFGWC



USERS OF DMSP MICROWAVE RADIOMETER DATA

1) HIRAS: **High Resolution Analysis System**

- Provides initial conditions for GSM and RWM
- Uses SSM/T-1 temperature and height data
- Evaluation to incorporate SSM/T-2 moisture data

2) RWAM: **Relocatable Window Analysis Model**

- Planned to use both SSM/T-1 and SSM/T-2 profiles

3) ASPAM: **Atmospheric Slant Path Analysis Model**

- Uses SSM/T-1 temperature and height data
- Will incorporate SSM/T-2 moisture data
- Driving force behind SSM/T-2

4) RTNEPH: **Real Time Nephanalysis Model**

- Uses SSM/I data; SDR's for earth skin temperature

5) AGRMET: **Agricultural Meteorological Model**

- Uses SSM/I data; rain rates over land
- Interested in soil moisture

6) MISTIC: **Mission Sensor Tactical Imaging Computer**

- SSM/I imaging and fast EDR's
- Technique development and validation

7) SDHS: **Satellite Data Handling System**

- SSM/T-1 and SSM/I displays to enhance weather forecasts

8) GEON: **Global ETAC OL-A Network**

- Satellite transmission of databases to Asheville, NC

9) SSM/T-2 CAL/VAL: **SSM/T-2 calibration and validation study**

- Process real time SSM/T-2 for data collection
- Process other data sets required for validation

10) Tropical Forecast: **Tropical Storm fixing**

- Uses SSM/I data; rain rates and surface wind speed

11) Shared Processing: **Near real time transmission to FNOC and NOAA NESDIS**

- Raw data (prepfiles) SSM/I, SSM/T-1,and SSM/T-2

Future of Satellite Processing at AFGWC

1. NAVAF Cooperation
   - Designate AFGWC Primary DOD METSAT Center
   - Consolidate Satellite Processing at AFGWC
   - Effort will begin by Block 5D-3 timeframe

2. SSMIS
   - Cal/Val by AFGWC and Aerospace
   - Conducted on Dist. Proc. Workstation environment

3. Satellite Processing Hardware Upgrades
   - SDHSU - New SDHS, upgrade to Site III
   - CDFS2 - New satellite processing environment

SSM/I SYMPOSIUM - JUNE 8, 1993

NOAA/NESDIS SSM/I DATA PROCESSING:

1. OPERATIONS
2. RESEARCH
3. USERS

P. TAYLOR

TAYLOR

ENCL(6)

NOAA/NESDIS SSM/I DATA PROCESSING

1. OPERATIONS:

- o Receive SSM/I Data & Products via Shared Processing Network (SPN)
  - o Orbital Transmissions of F-10 and F-11
  - o Temperature Data Records (TDRs) Ta's
  - o Sensor Data Records (SDRs) Tb's
  - o Environmental Data Records (EDRs)

- o Archived in DEF Format

- o Unpacked to Intermediate Data Base - 30 Orbits per S/C
  - o 30 orbits per spacecraft
  - o Near Real Time Availability to Users via CEMSCS
  - o Master Map - Polar Sterographic Projection 1/8th Mesh
  - o Operational Active Archive in place By Oct '94 - 1 yr of data available on-line.
- o Orbital SSM/I Prepfiles from AFGWC to match SSM/T1 and T2 data
  - o Earth located counts with calibration parameters
  - o Calculated with Hughes software
  - o Allowed for early evaluation of SSM/I data until available via SPN

TAYL

ENCL(6)

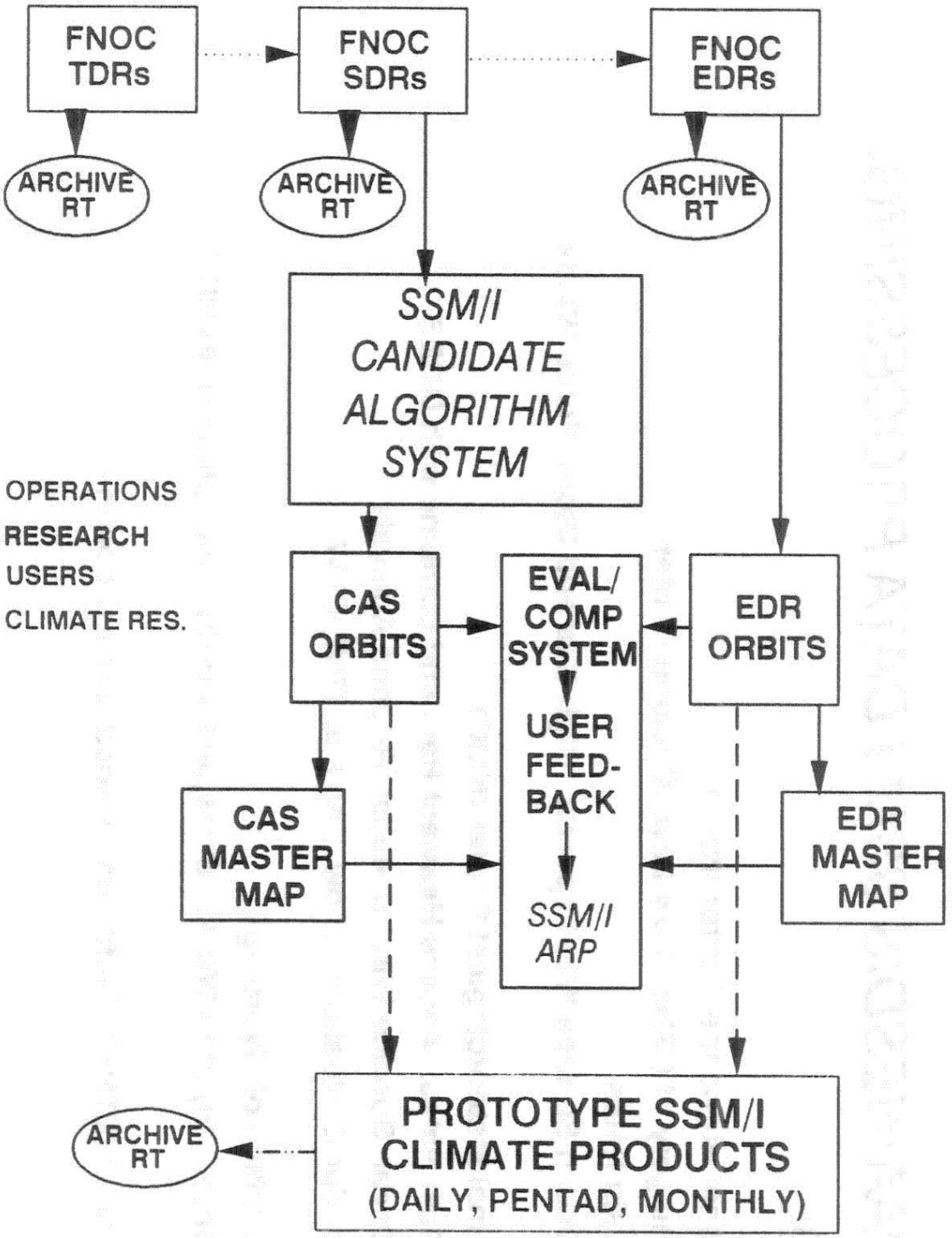
NOAA/NESDIS SSM/I DATA PROCESSING

2. RESEARCH:

- o Develop SSM/I Candidate Algorithm System (CAS)
  - o Test/Evaluate 20 different algorithms/products
  - o Generate Orbitally from FNOC SDRs
  - o Compare Orbitally to FNOC EDRs
  - o Provide Evaluation Feedback to SSM/I ARP

- o Develop Prototype SSM/I Climate Product System (CPS)
  - o Generate Daily, Pentad, and Monthly from EDRs and CAS products
  - o Initial Products: TPW and Rain Rate
  - o Design allows for additional climate products
  - o Design allows for data reprocessing
  - o Design allows for possible future operational implementation

NOAA/NESDIS
SSM/I DATA/PRODUCT OPERATIONS AND R&D



NOAA/NESDIS SSM/I DATA PROCESSING

3. USERS:

- o National Hurricane Center (NHC)
  - o Imagery - 85GHz: Low-Level Cyclone Center
  - o Rain Rates
  - o Ocean Surface Wind Speeds: High-Sea and Storm Force Winds
- o National Meteorological Center (NMC)
  - o Rain Rates: Assess Heaviest Rain and combine with GOES
  - o Ocean Surface Wind Speeds: Routine Analysis
  - o Under Evaluation: Snow, Sea Ice, TPW, CLW
- o NWS Office of Hydrology
  - o Snow: Input to Weekly Snowpack product (supplement AVHRR)
- o Archive, WETNET, Pathfinder, Canadians, Europeans.....

Session 1

Sea Ice

(Jeff Hawkins, NRL, Chair)

Session 1

Sea Ice

(Jeff Hawkins, NRL, Chair)

The York University Passive Microwave Sea Ice Algorithm

Irene Rubenstein
Inst. for Space and Terrestrial Science
North York, Ontario, Canada, M3J 3K1

Alex Stogryn, Gene Poe and William Kreiss
Aerojet Electronic Systems Div., Gencorp
Azusa, CA

The description and performance of an algorithm used operationally with SSM/I data at the Institute for Space and Terrestrial Science (ISTS) and the Canadian Meterological Center (CMC) for forecasting sea ice conditions and as input to Numerical Weather Prediction is presented in this paper. The algorithm contains elements of traditionally used algorithms (e.g., SSM/I Cal/Val algorithm) augmented with decision rules developed using empirical/statistical variability in the brightness temperatures induced by the weather or seasonal changes and is being implemented in the SSMIS ground software.

The strong contrast in the emissivity of sea ice covered surfaces and the ice free ocean permits the development of relatively simple sea ice retrieval algorithms. All currently used algorithms retrieve the extent and percentage area of the pixel covered first year or old ice or a mixture of both. Brightness temperatures from areas identified as containing mainly first year or old ice are used as signatures. The use of cluster diagrams for channels used in the algorithms provides not only the signature brightness temperatures, but can also be used to estimate the uncertainty due to the variability in the signatures. The seasonal and regional variability in the signatures is reflected in the algorithms by using several sets of coefficients. The use of lookup tables of seasonal coefficients improves the algorithm CPU efficiency. These algorithms provide useful sea ice information on a global spatial scale and as a weekly or a monthly climatological indicator.

The algorithm accuracy is enhanced by including decision making rules that allow input of signatures and atmospheric correction of each pixel. The regional/seasonal values are used as first guress input and additional calculations are performed before the final output of the total ice concentration and the concentrations of various ice types. The parameters derived using these coefficients are tested by comparing the observed brightness temperatures with the expected (e.g., scatterplot) values. Different modules of the retrieval procedure are called in to recalculate these parameters in order to minimize these differences. These modules contain ice free ocean roughness and simplified atmospheric retrieval algorithms.

This algorithm has been tested using data obtained during numerous sea ice research campaigns. We will present the results of its performance for several scenarios.

The use of currently available high speed personal computers and workstations reduce the CPU time used by this more complex algorithm. Thus, it is expected that the algorithm performance can be further enhanced by additional modules containing training routines.



I S T S

INSTITUTE FOR SPACE AND TERRESTRIAL SCIENCE

INSTITUT DE SCIENCE TERRESTRE ET SPATIALE

Passive Microwave Sea Ice Algorithm for SSM/I and SSM/IS

Irene G. Rubinstein
Institute for Space and Terrestrial Science
4850 Keele St., North York,
Ontario, Canada, M3J 3K1
and
Alex Stogryn, Gene Poe and William Kreiss
Aerojet Electronic Systems Division GenCorp.
Azusa, CA

June 8, 1993

4850 Keele St.
North York, Ontario
M3J 3K1

Tel: 416-665-3311
Fax: 416-665-2032
Internet: inquiries@ists.ca

Abstract

The description and performance of an algorithm used operationally with SSM/I data at the Institute for Space and Terrestrial Science (ISTS) and the Canadian Meteorological Center (CMC) is presented in this paper. Substantial portions of this algorithm were developed under subcontract to Aerojet Electronic Systems Division, the prime contractor for the SSM/IS system. The SSM/IS is under development for the U.S. Department of Defense as a replacement for the SSM/I. The algorithm contains elements of tradionally used algorithms (e.g. SSM/I Cal/Val algorithm) augmented with decision rules developed using empirical/statistical variability in the brightness temperatures induced by the weather or seasonal changes and is being implemented in the SSM/IS ground software.

The strong contrast in the emissivity of sea ice covered surfaces and the ice free ocean permits the development of relatively simple sea ice retrieval algorithms. All currently used algorithms retrieve the extent and the percentage area of the pixel covered with sea ice. In addition, sea ice covered is classified as containing first year or old ice or mixture of both. Brightness temperatures from areas identified as containing mainly first year or old ice are used as signature input. The seasonal and regional variability in the signatures is reflected in the algorithm by including coefficients corresponding to different seasonal/weather ice surface conditions. These algorithms provide reliable sea ice information on a global spatial scale and as a weekly or a monthly climatological indicator.

The algorithm accuracy is enhanced by including decision making rules that allow input of signatures and atmospheric correction of each pixel. The regional/seasonal values are used as first guess input and additional calculations are performed before the final outputof the total ice concentration and the concentrations of various ice types. The retrieved parameters are evaluated for the accuracy by comparing the observed brightness temperatures with the expected (e.g. scatterplot) values. Different modules of the retrieval routine are called in to recalculate these parameters in order to minimize these differences. These modules contain ice free ocean roughness and simplified atmospheric retrieval algorithms.

The algorithm has been tested using data obtained during numerous ice research campaigns. We will present the results of its performance for several scenarios.

The use of currently available high speed personal computers and work stations reduce the CPU time used by this more complex algorithm. Thus, it is expected that the algorithm performance can be further enhanced by additional modules containing training routines for user specified ice condition scenarios.

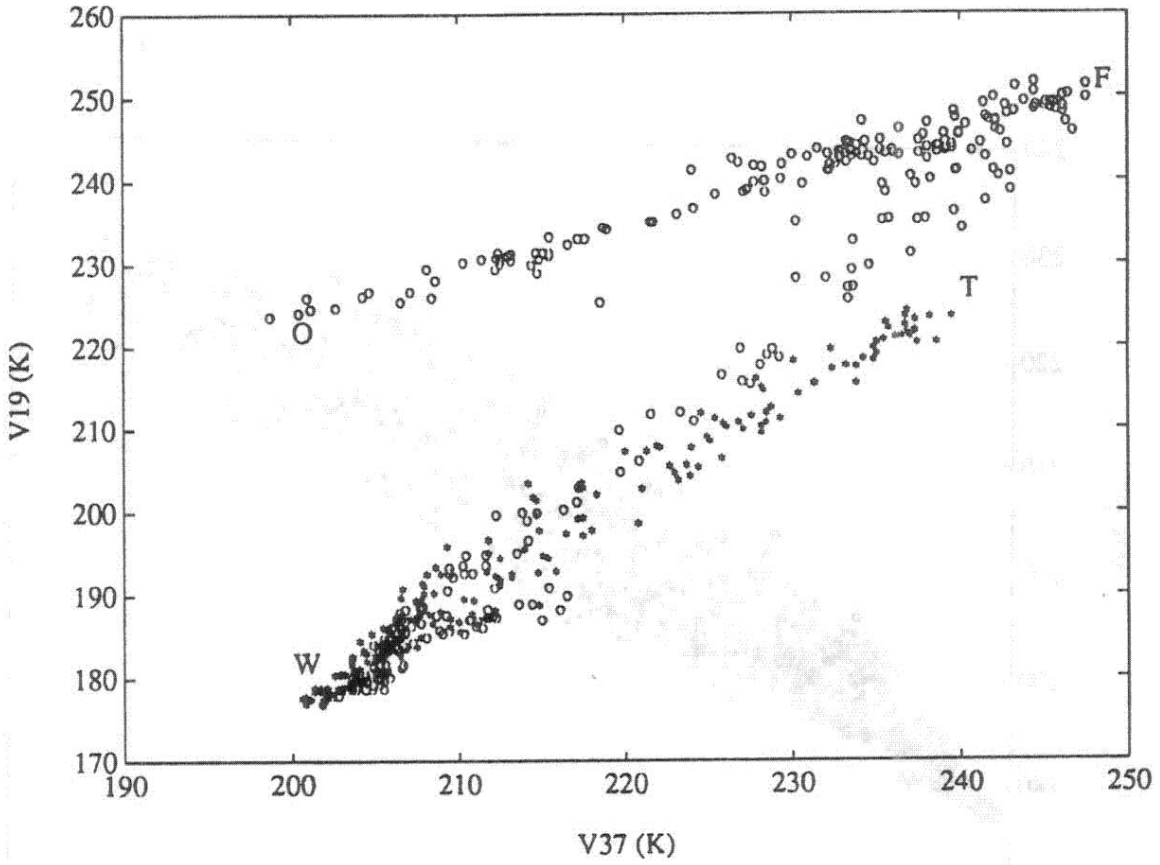


Figure 1: Signature Scatterplot

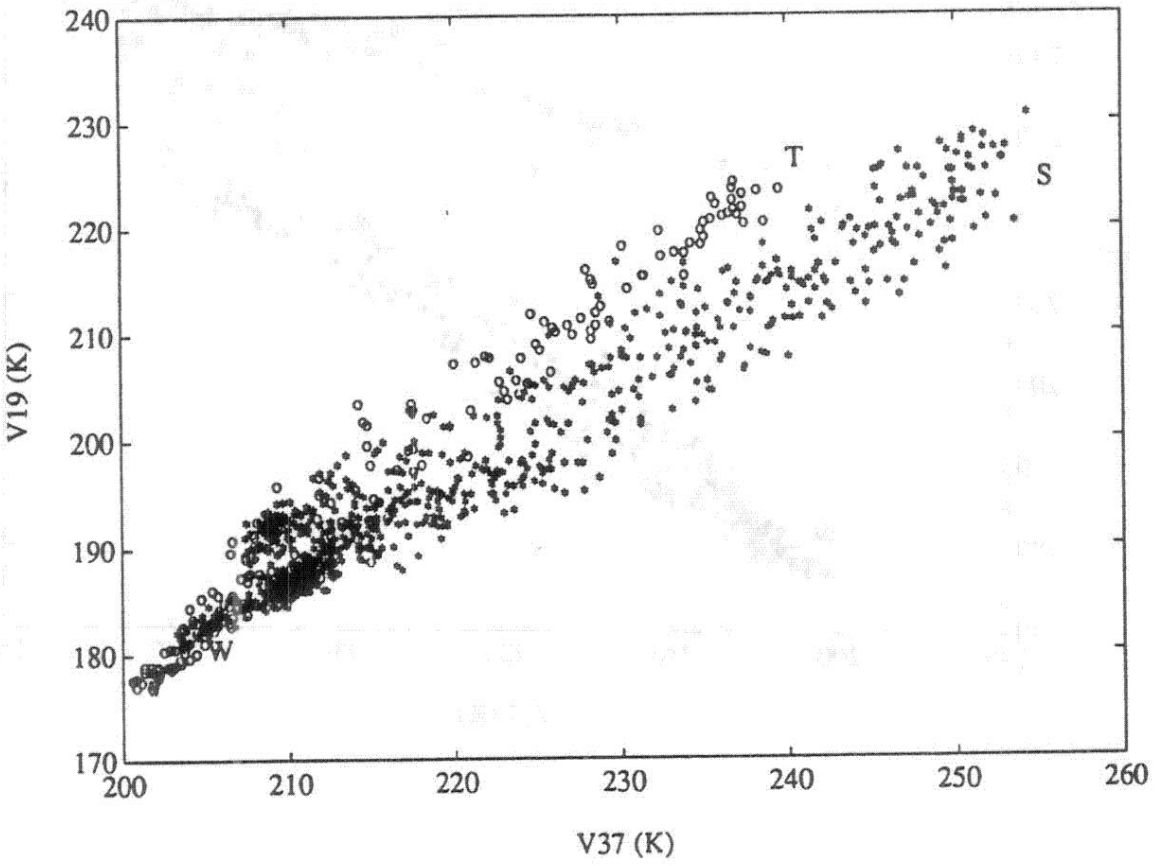


Figure 2: Storm and new ice signatures

4

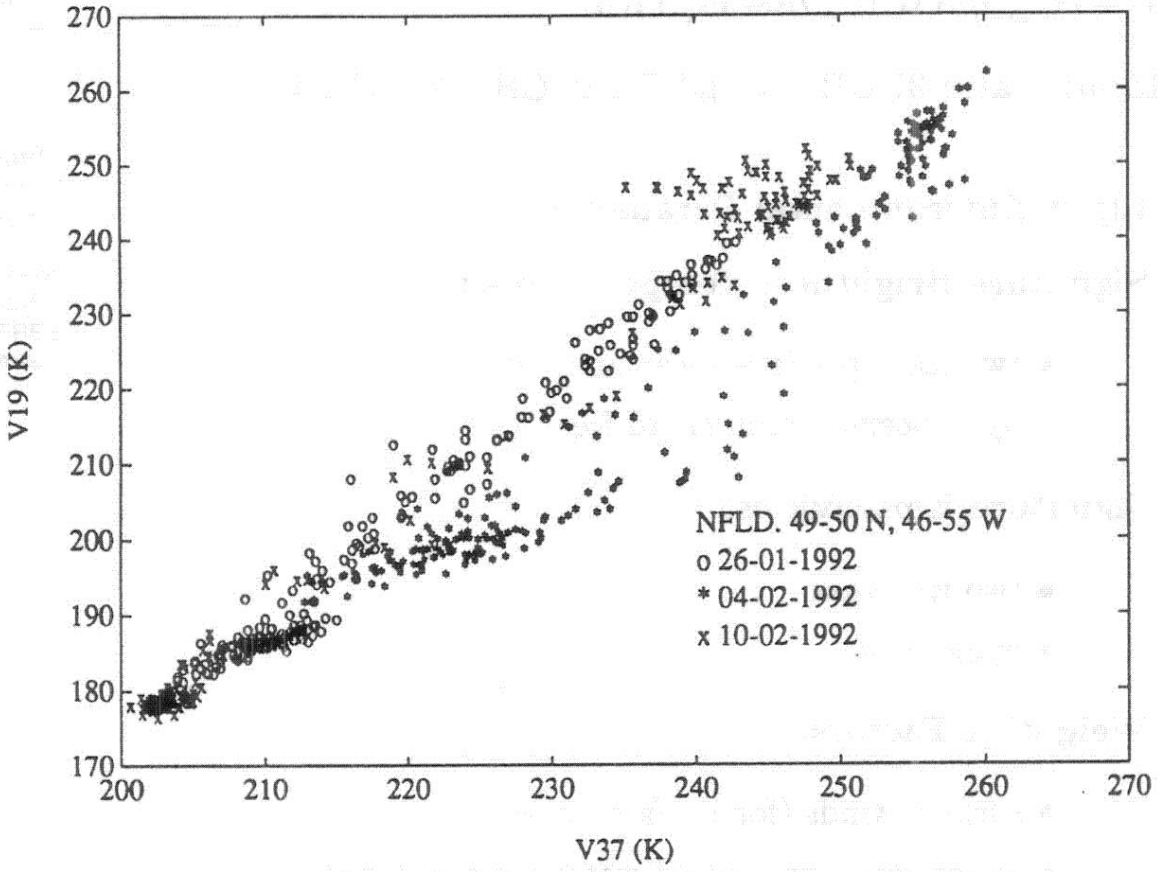


Figure 3: Snow cover influence on first-year ice brightness temperatures



INSTITUTE FOR SPACE AND TERRESTRIAL SCIENCE

INSTITUT DE SCIENCE TERRESTRE ET SPATIALE

1 Algorithm Description

Input Data: 37 GHz (V and H); 19 GHz (V and H)

Input Environmental Parameters

Signature Brightness Temperatures :

- two ice types (first-year and old
- open ocean (calm, cloud free)

Signature Emissivities:

- two ice types
- open ocean

Weighting Factors:

- surface winds (for ice free ocean)
- water vapor and liquid water (atmosphere)

Criteria for Flagging:

- snow cover influence
- deviation in atmospheric conditions from climatological values
- precipitation induced changes
- "new" ice presence
- errors induced by the footprint size differences

Rules for correcting errors caused by the above listed factors.

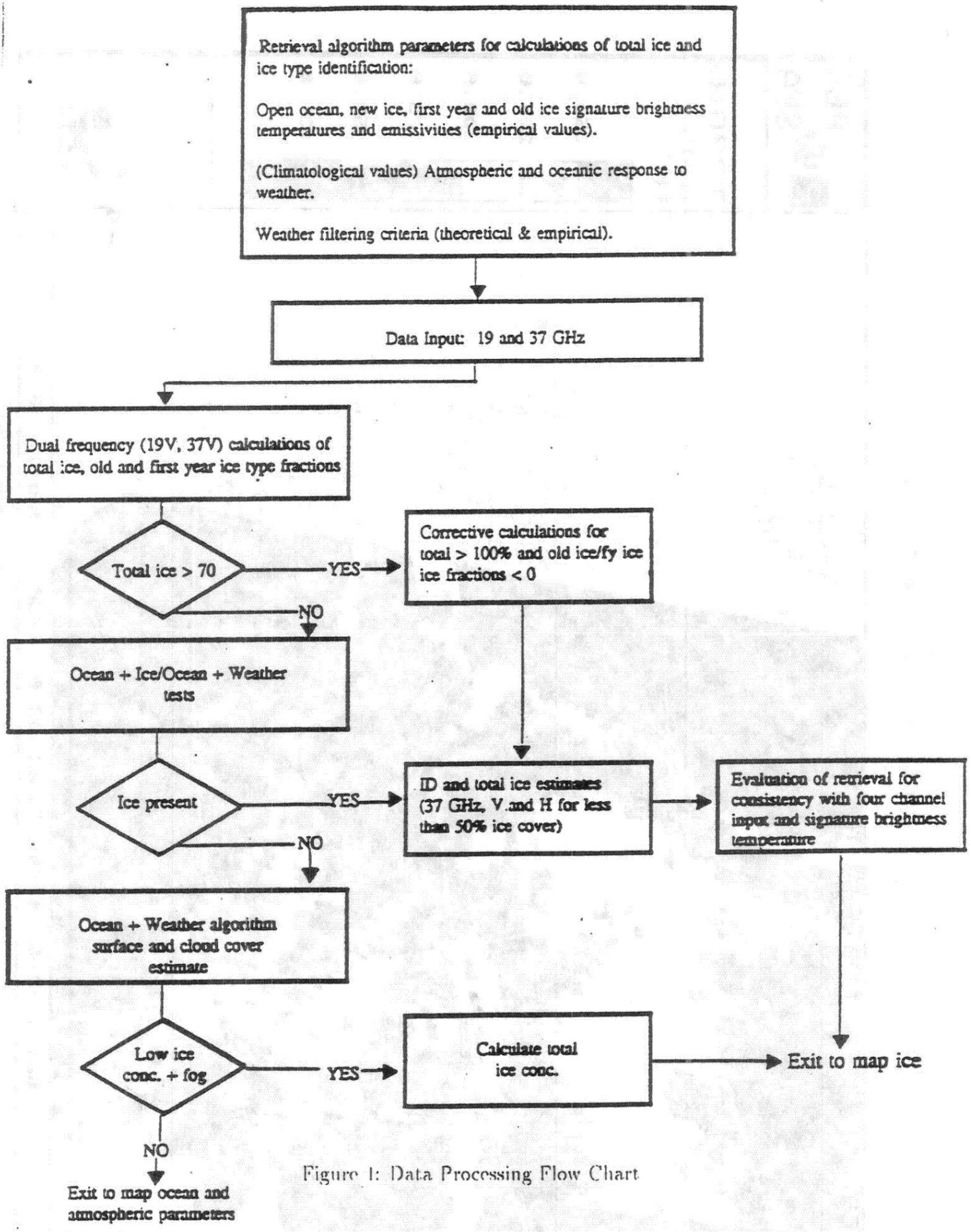
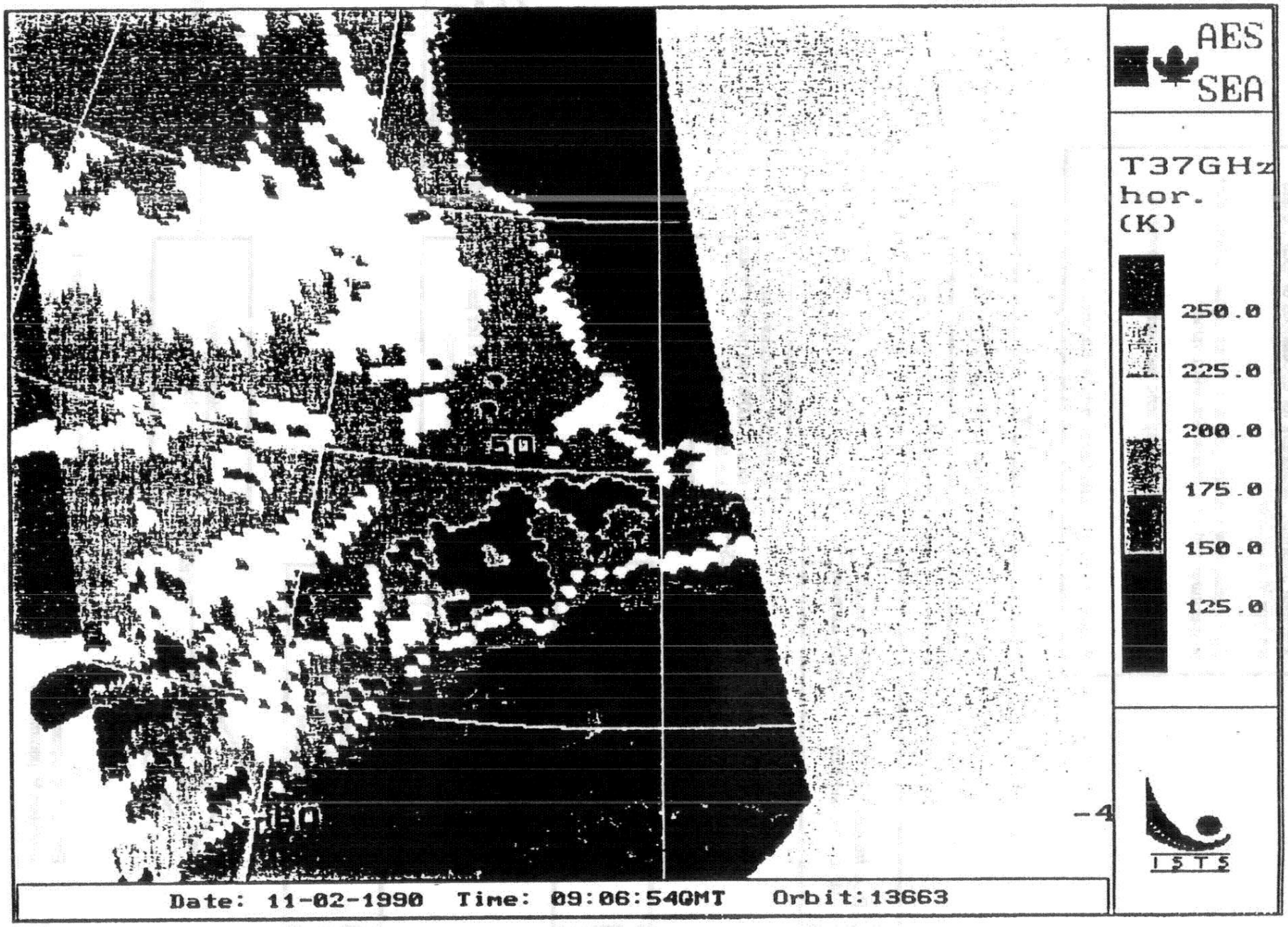


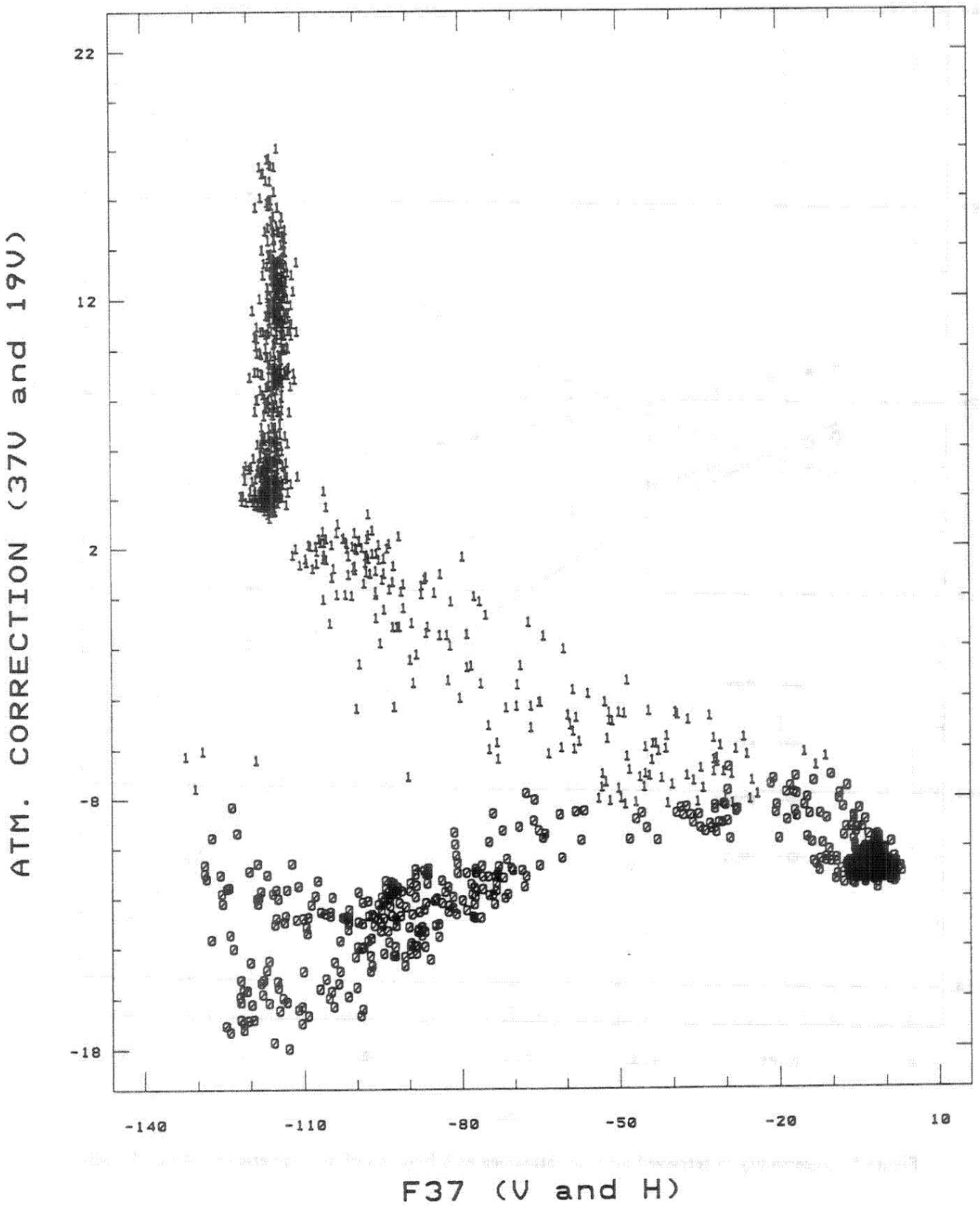
Figure 1: Data Processing Flow Chart

7

WEATHER EFFECTS



WEATHER CORRECTION FUNCTIONS



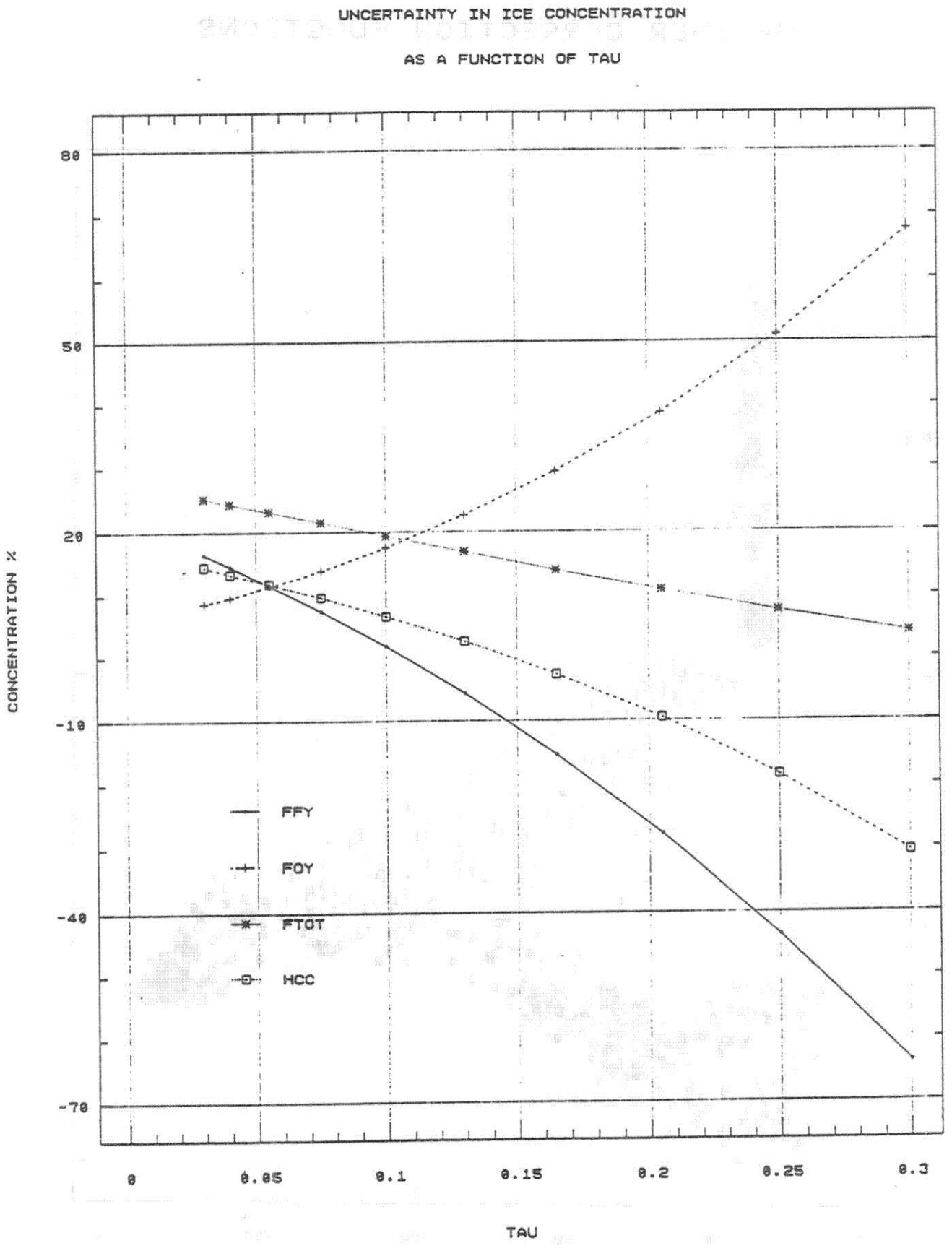


Figure 5: Uncertainty in retrieved ice concentrations as a function of atmospheric opacity at 37 GHz

§ STABILITY TESTS

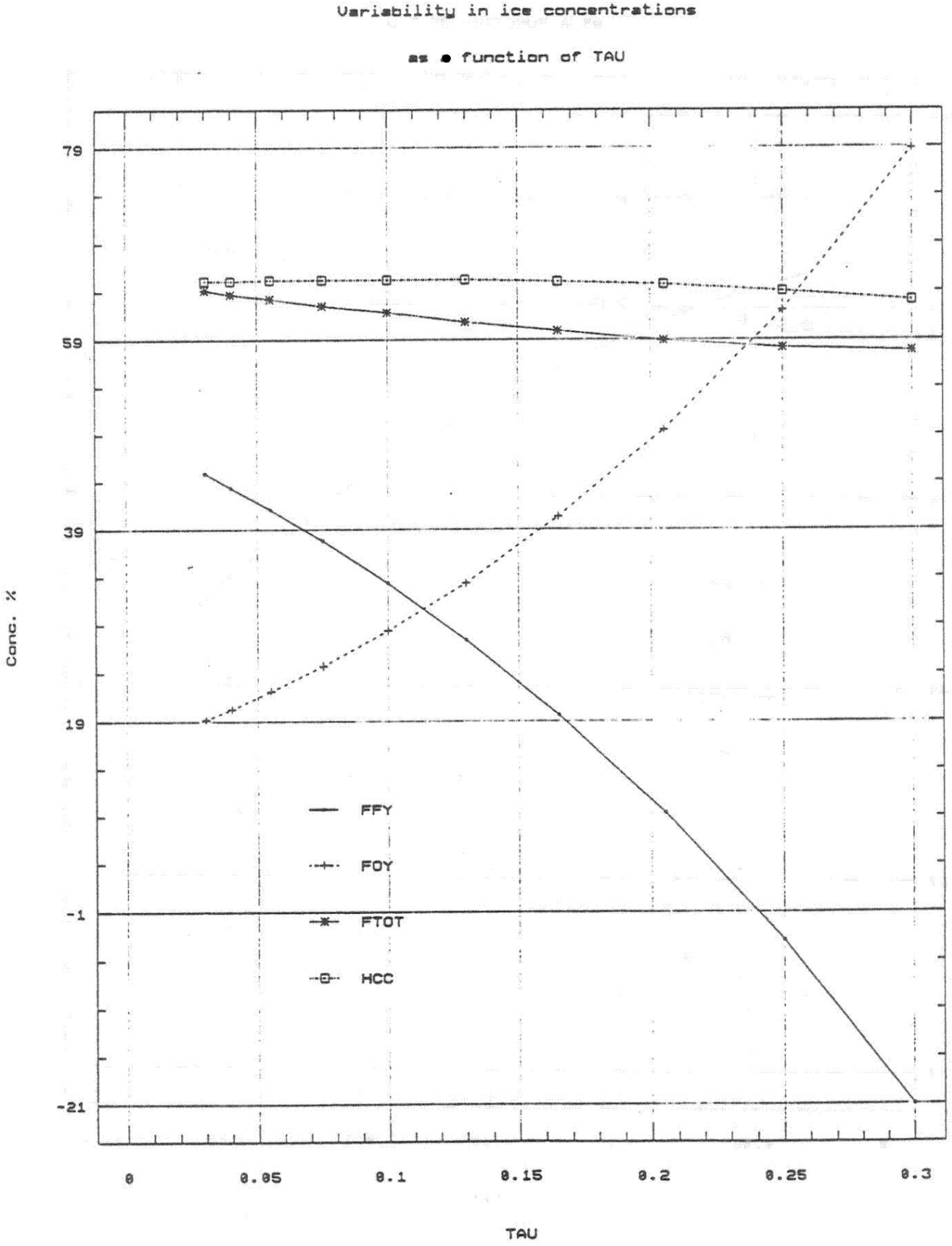


Figure 7: Uncertainty in retrieved ice concentrations as a function of atmospheric opacity

11

STABILITY TESTS

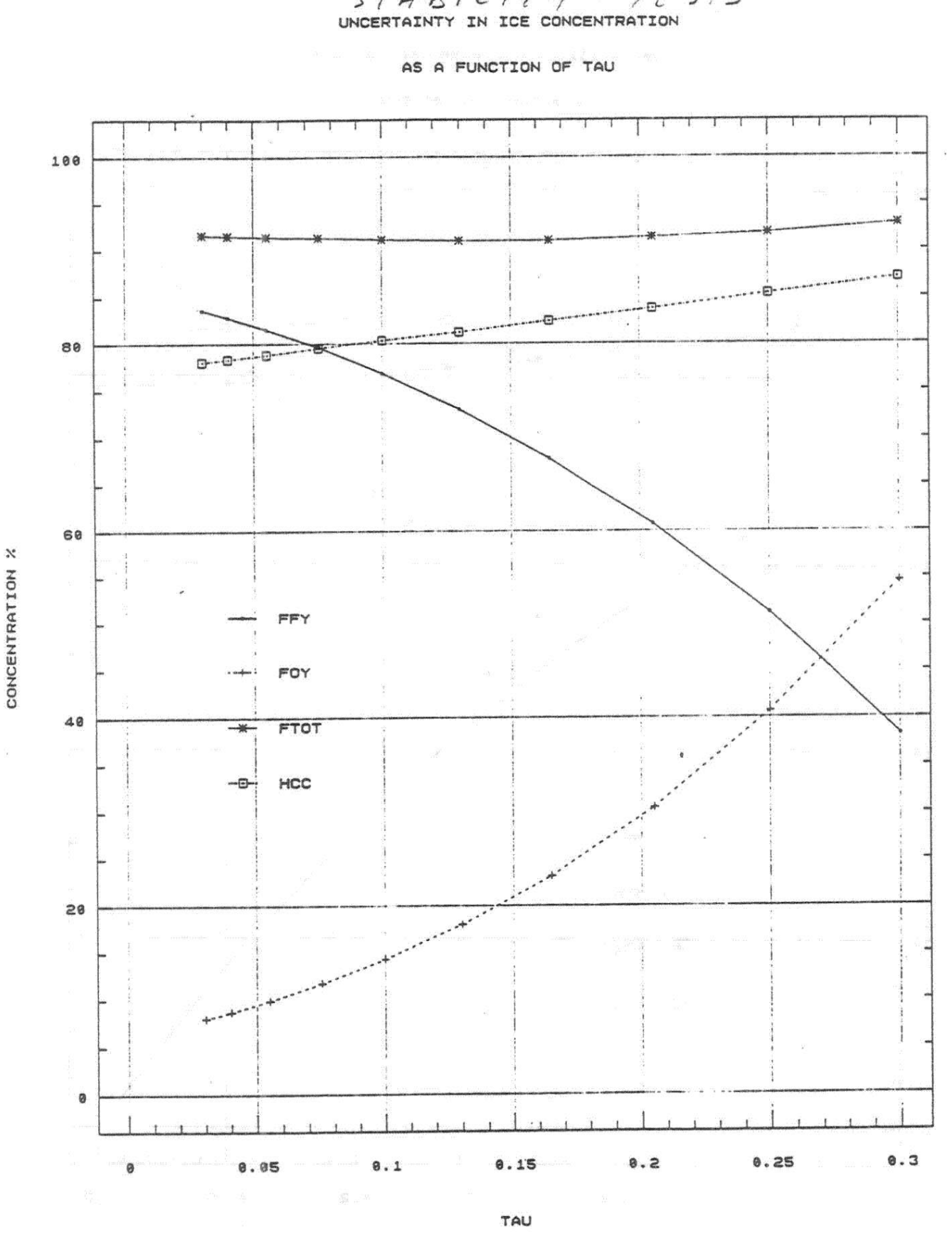


Figure 8: Uncertainty in retrieved ice concentrations as a function of atmospheric opacity

12

STABILITY TESTS

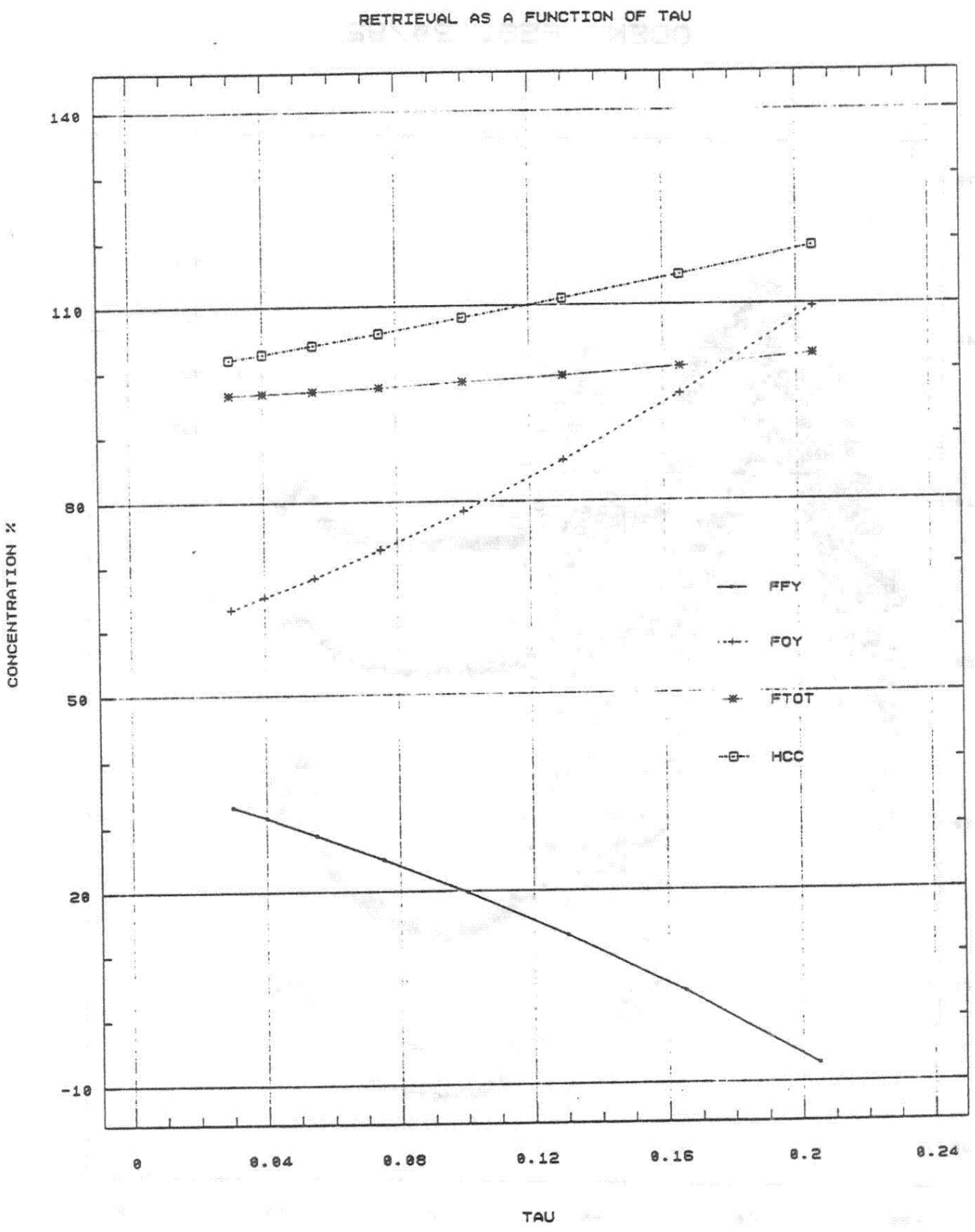
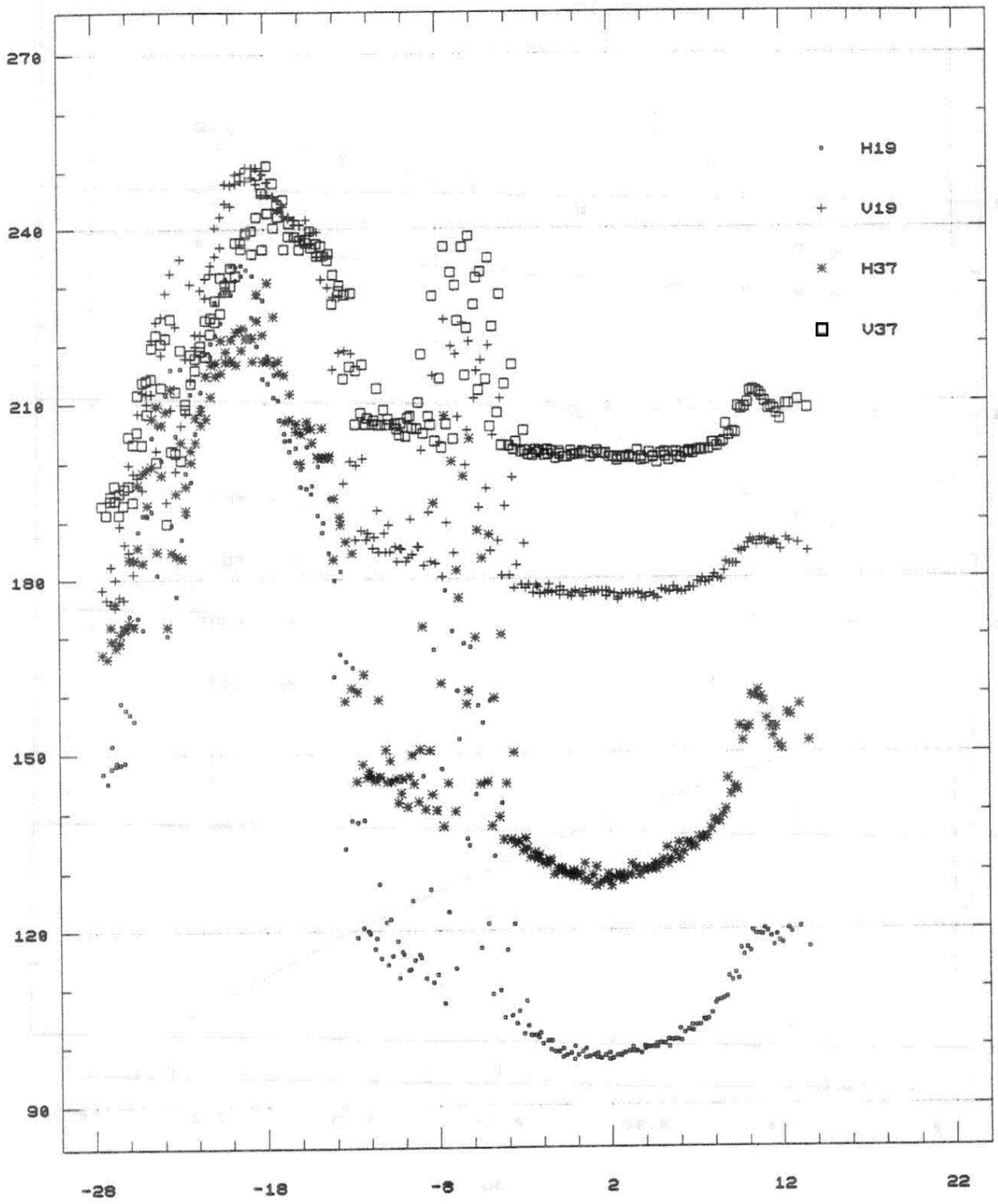


Figure 6: Uncertainty in retrieved ice concentrations as a function of atmospheric opacity

NEW ICE SIGNATURE TESTS

ODEN FEB. 20/92





INSTITUTE FOR SPACE AND TERRESTRIAL SCIENCE

INSTITUT DE SCIENCE TERRESTRE ET SPATIALE

2 Validation and Application

Near-real time testing for the following regions:

- Gulf of Bothnia 1988
- Greenland Sea 1989, 1990, 1991, 1993
- Weddell Sea 1989, 1991, 1992
- Beaufort Sea 1988, 1990, 1991
- Labrador 1988, 1990, 1991
- Newfoundland Waters 1988, 1989, 1990, 1991, 1992

Marginal Ice Zone Research Campaigns:

- Labrador Ice Margin Experiment, January to April 1989
- Canadian Atlantic Storm Project II, January to April 1992

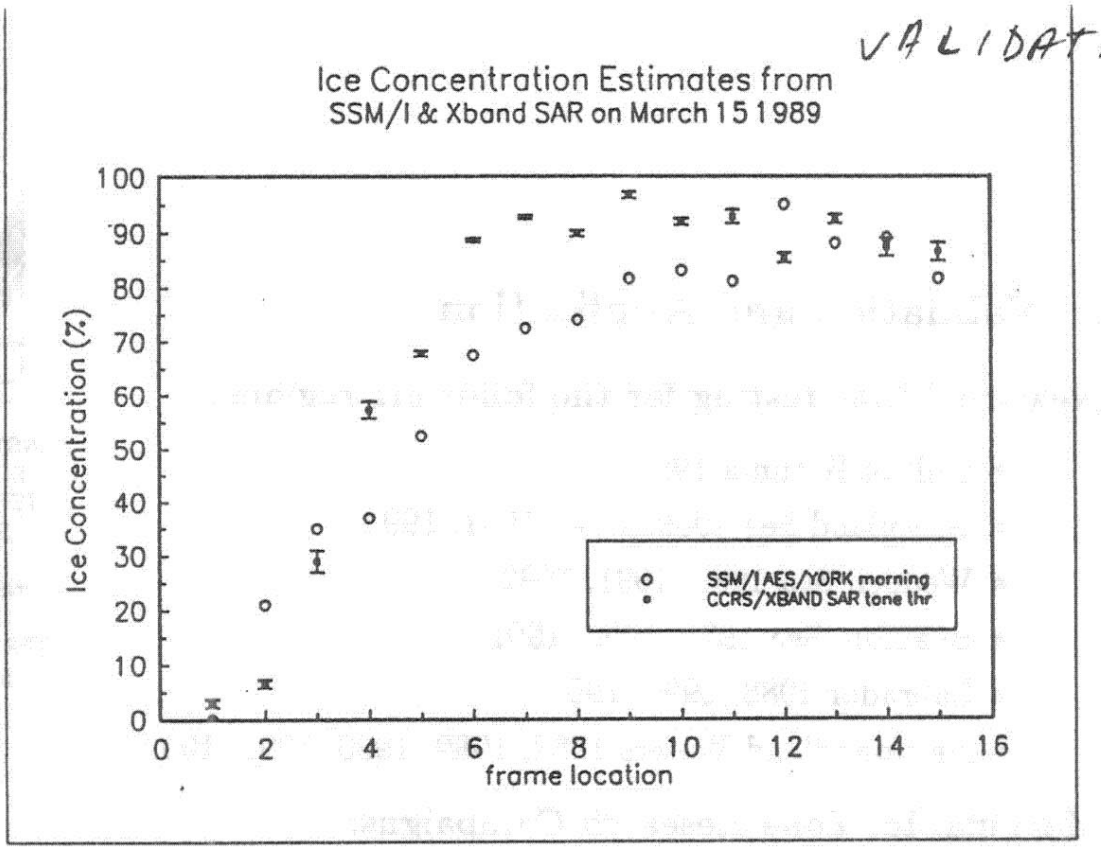
Operational Use at:

- Canadian Meteorological Centre (CMC) -global and regional (Sea ice, ocean surface winds and precipitation over ocean data retrieved from SSM/I data at CMC are available to all (federal) weather centres and the ice forecasing across Canada)
- Several Canadian Comp. (Ice Centre and Ice R/D arrangements) are providing near real time navigational support to ships in Weddell Sea, Greenland Sea and other regions.
- DNMI, Oslo, Norway (1992)
- NHL-Sinteff, Norway (during research campaigns)

Utilization in Numerical Models

- Numerical Weather Prediction Model (CMC)
- Regional Ice Forecasting Model (Research stage, Ice Centre, AES, Canada)
- Ice Edge Forcasting Model (Research stage, CCORE, Memorial University, NFLD, Canada)

VALIDATION



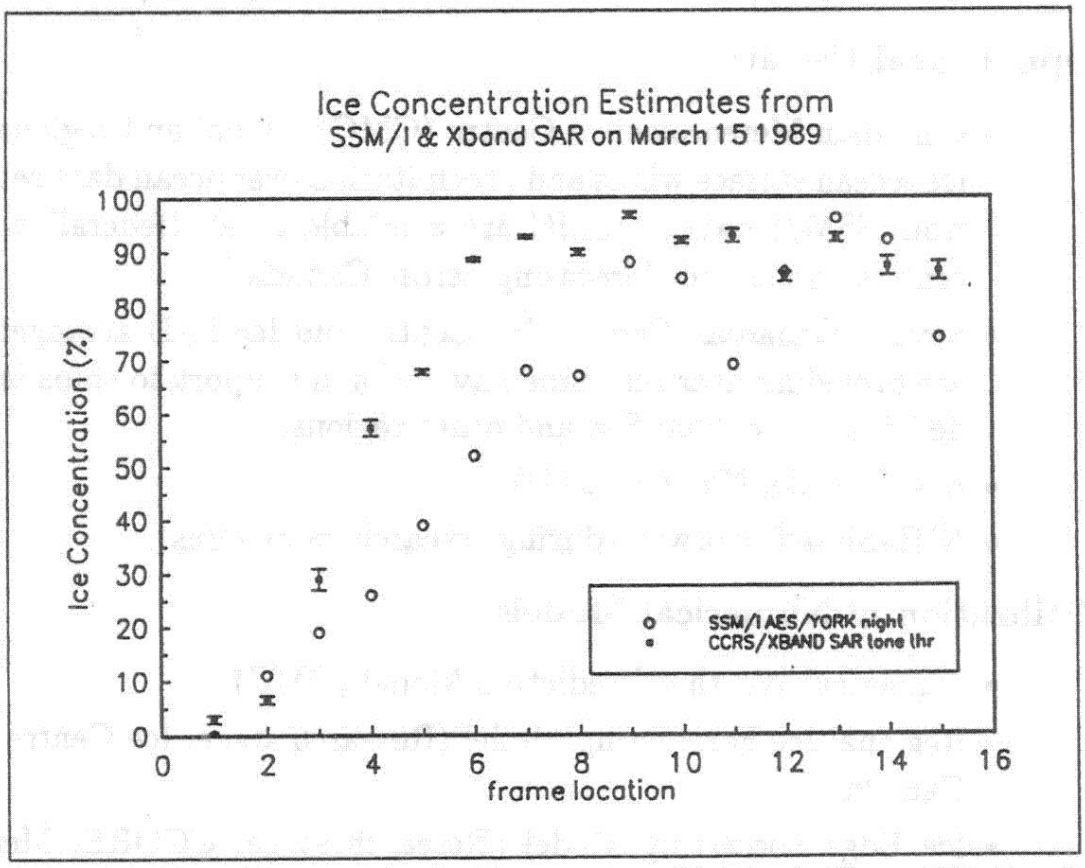
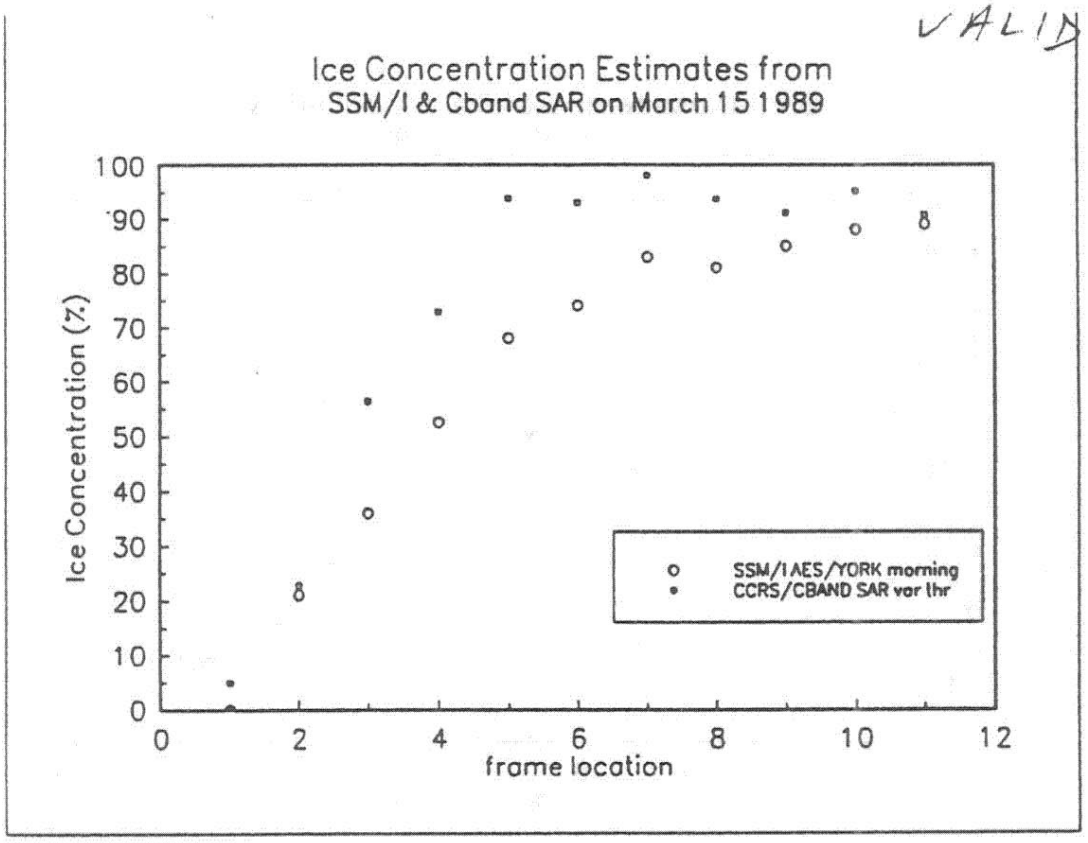


Figure 17: Comparison of Retrieved Sea Ice Concentrations with X-band airborne SAR. Two different techniques for SAR imagery interpretation were used

16

VALIDATION



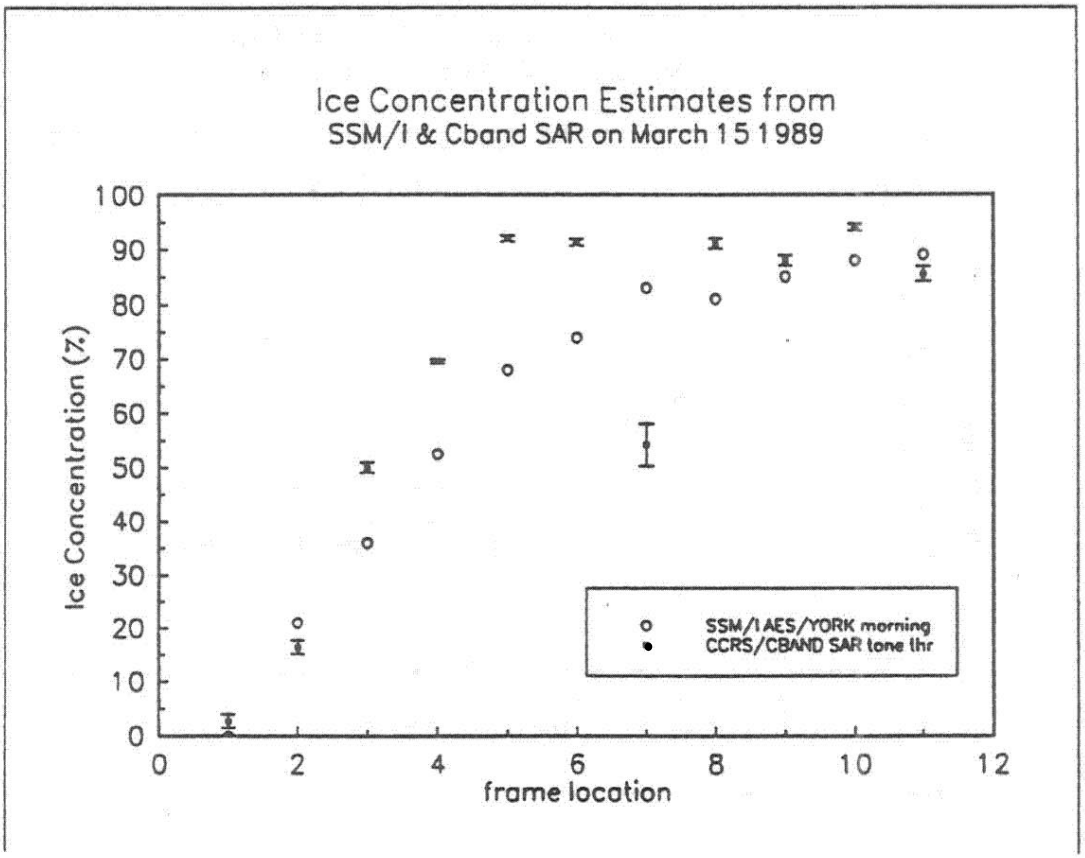
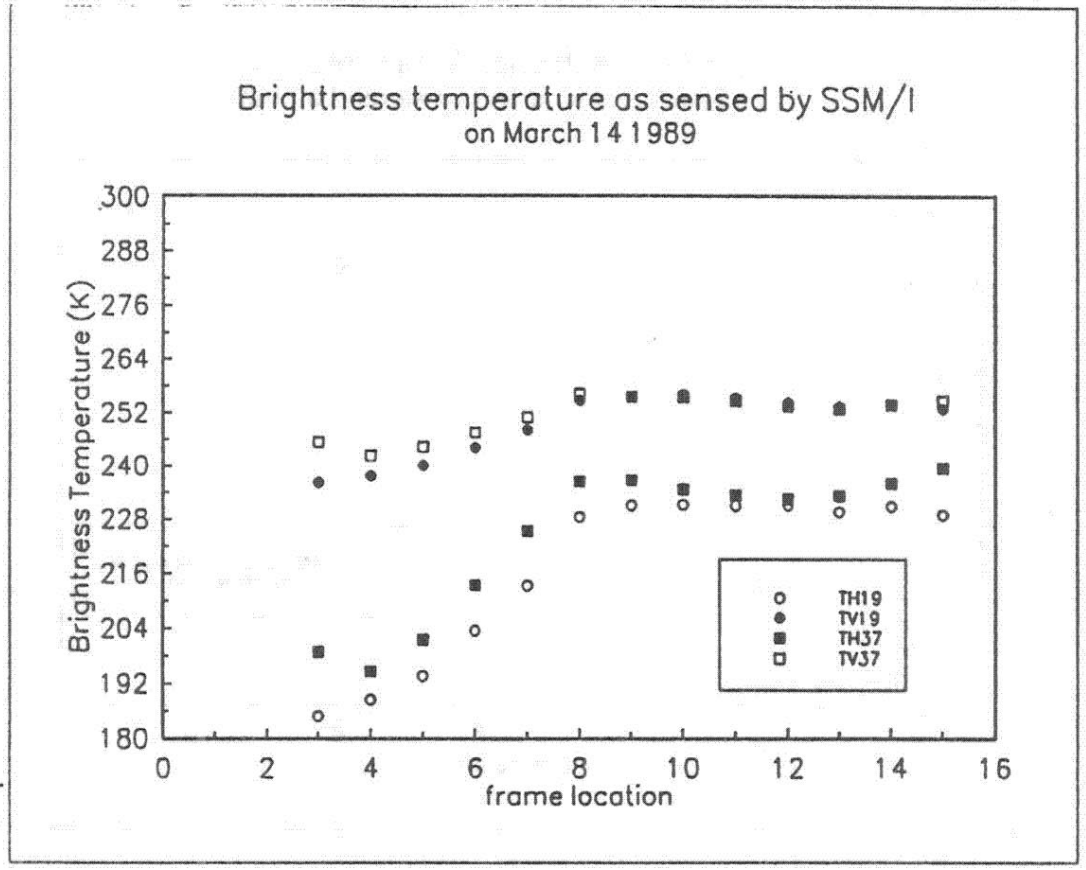


Figure 15: Comparison of Retrieved Sea Ice Concentrations with C-band airborne SAR. Two different techniques for SAR imagery interpretation were used



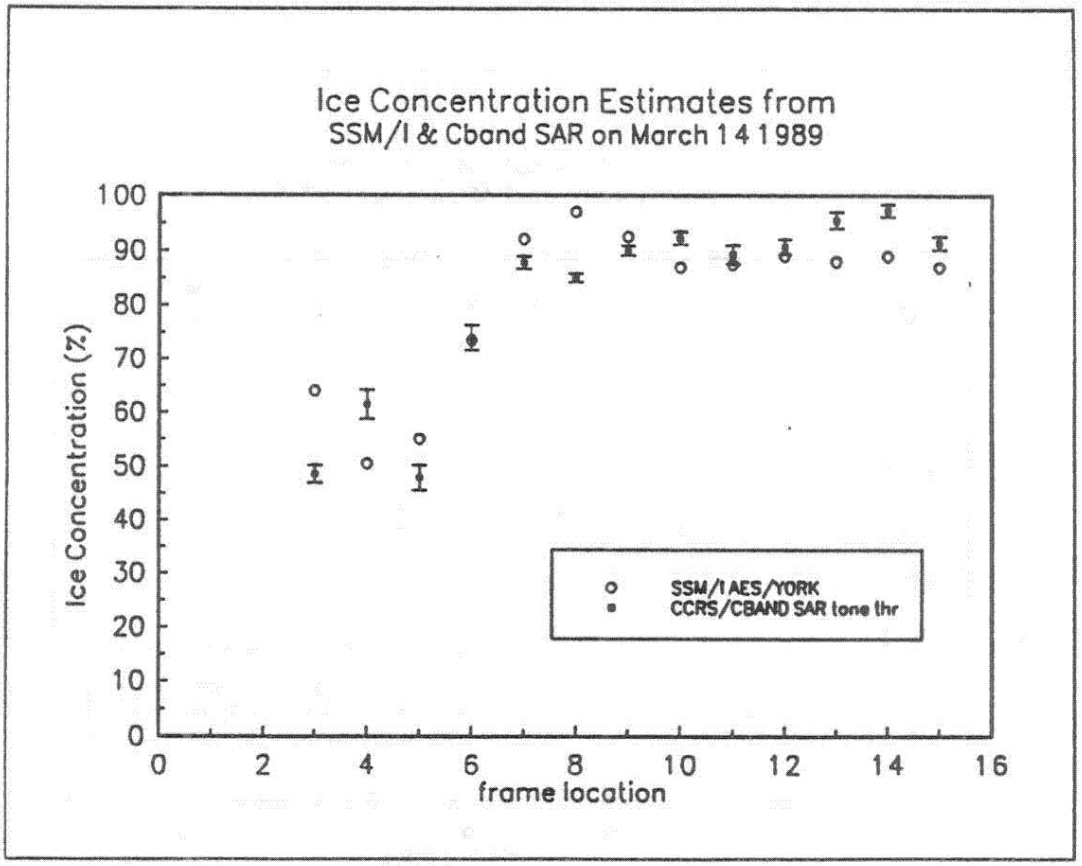
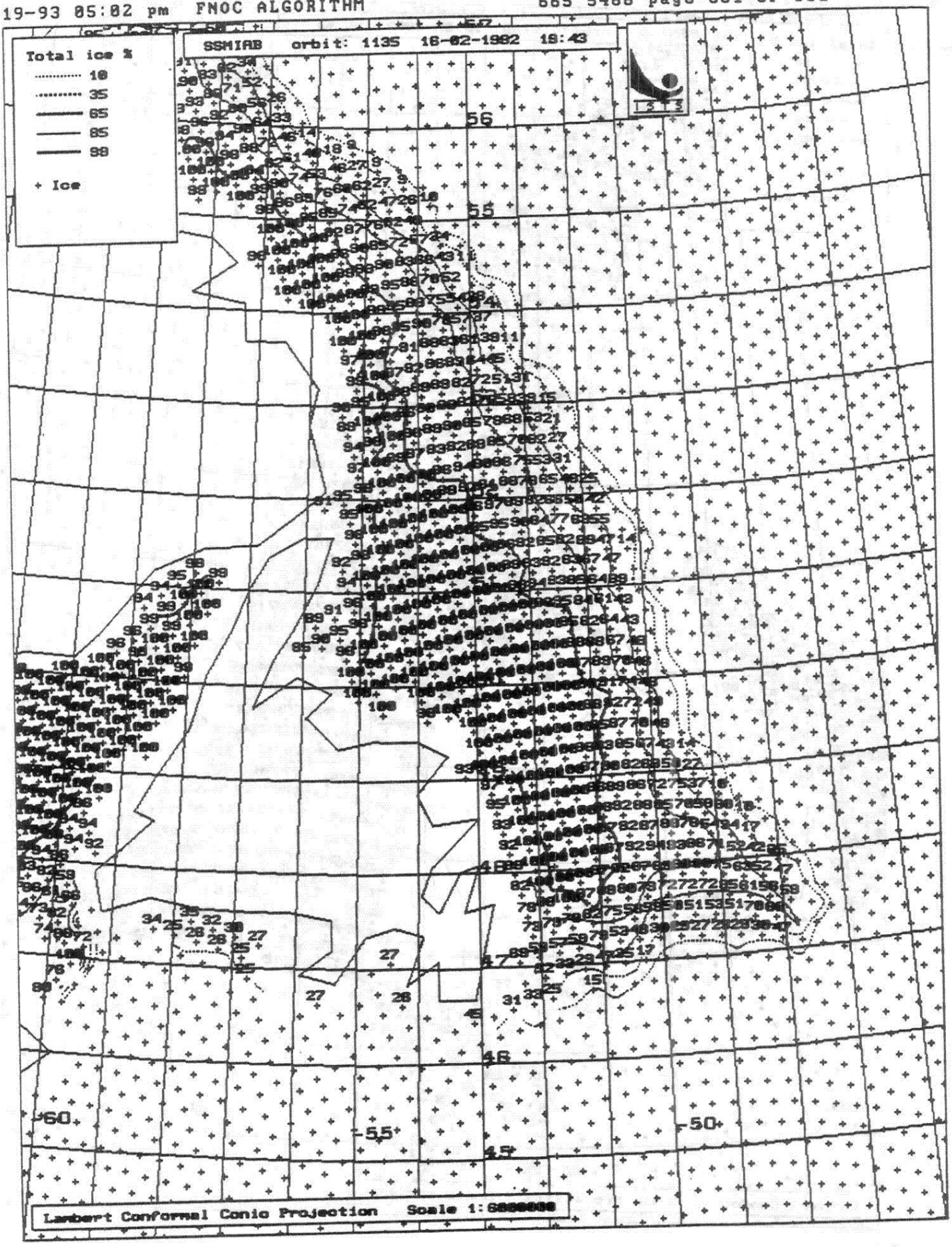
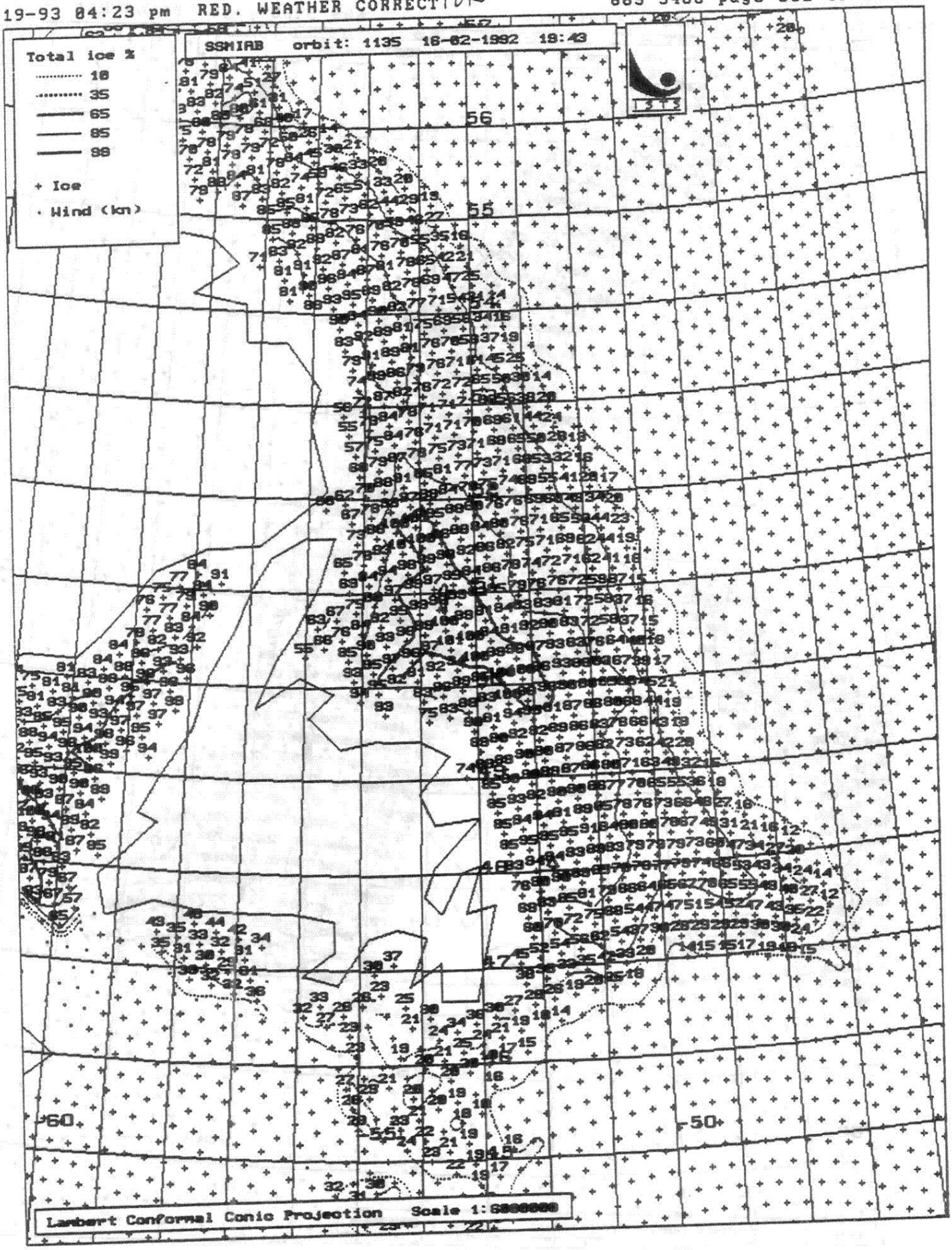
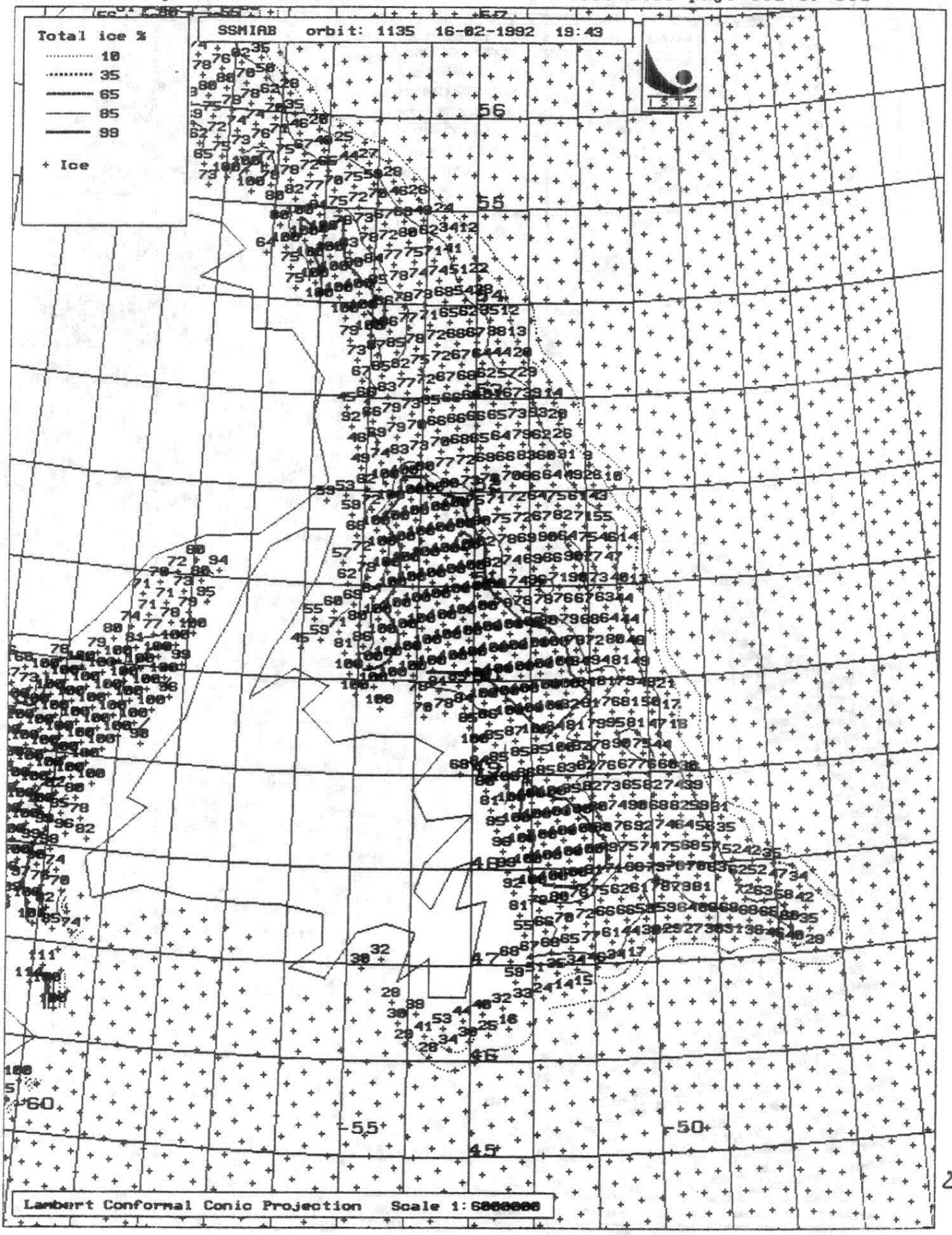


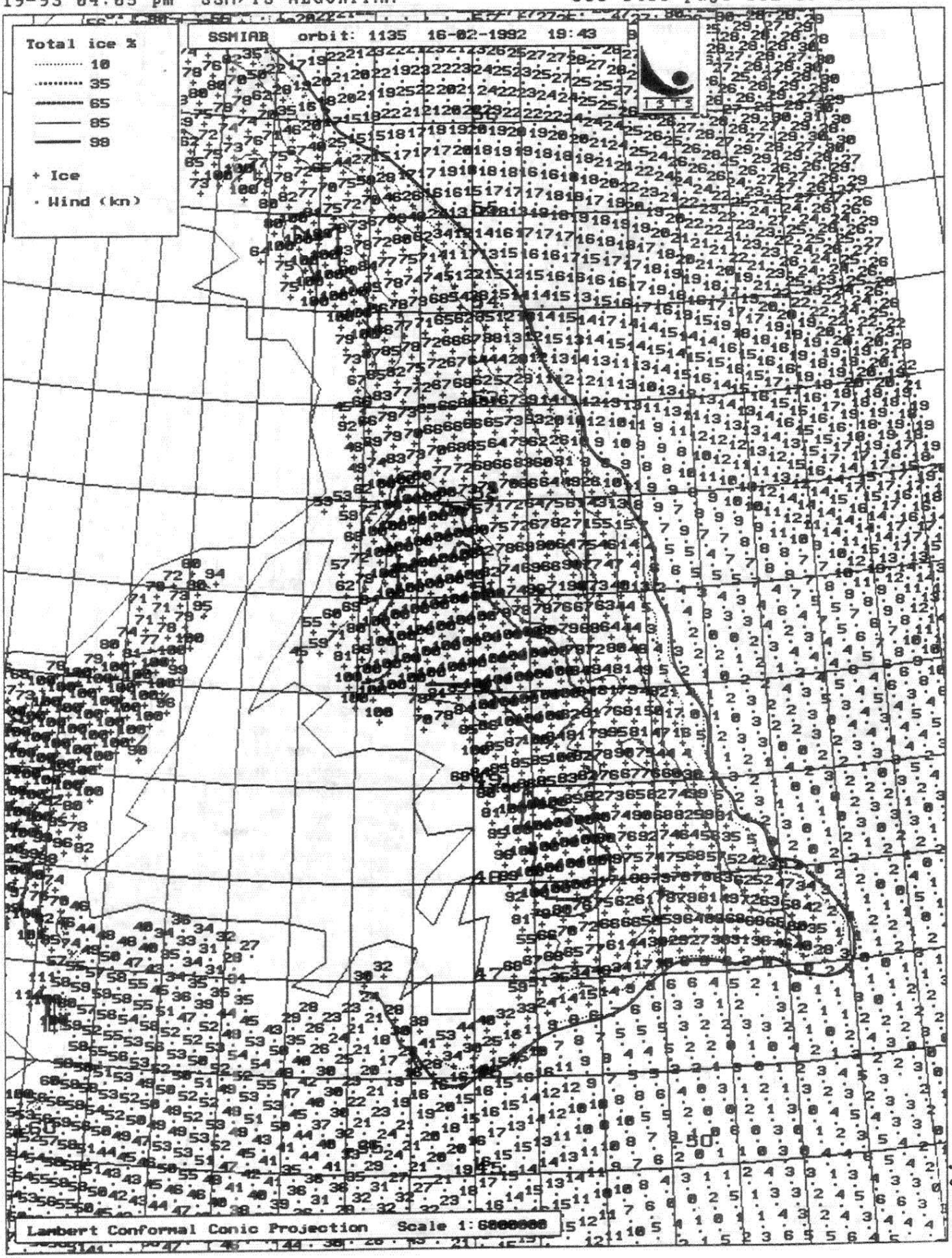
Figure 16: Comparison of Retrieved Sea Ice Concentrations with C-band airborne SAR.

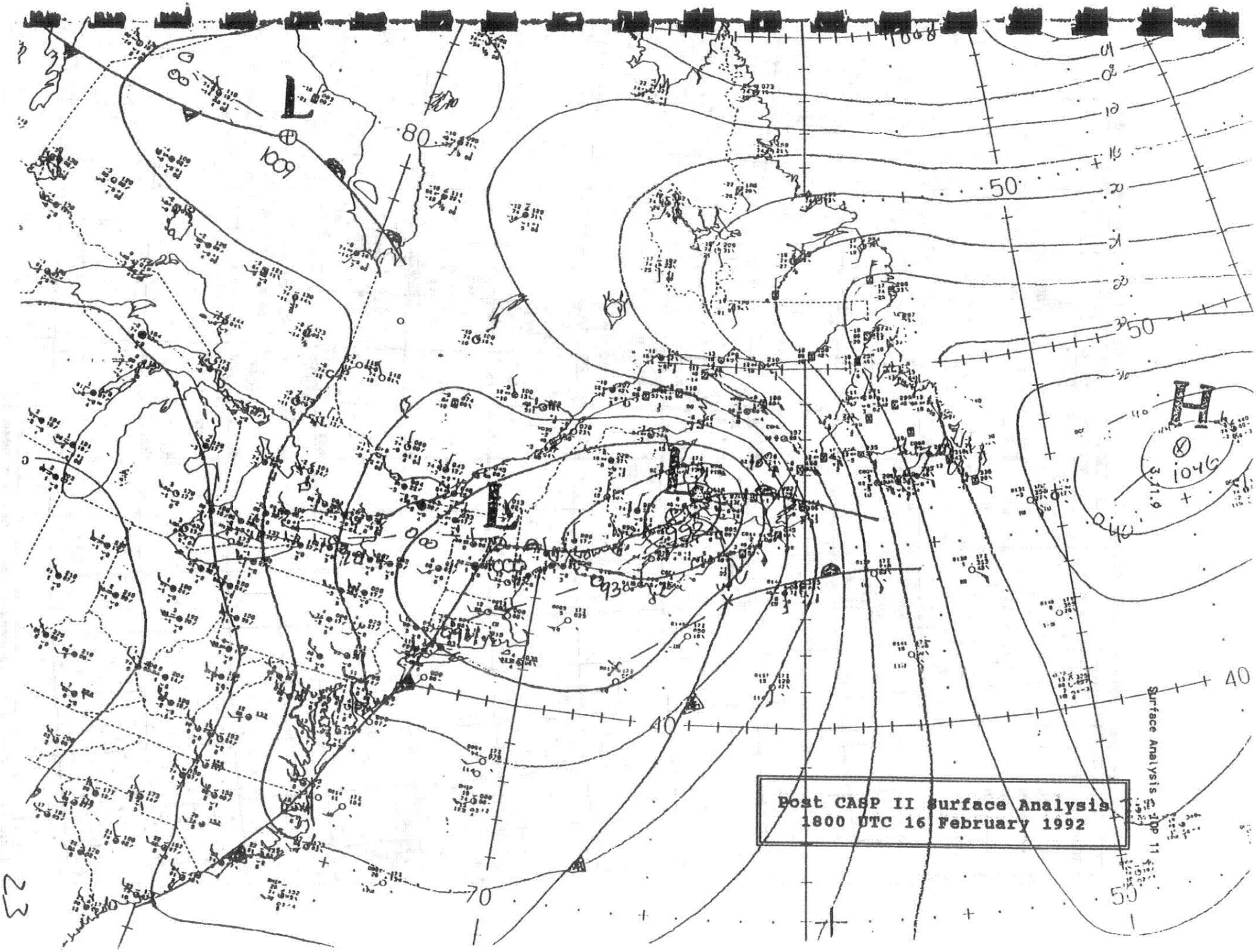

Total ice %
10
35
65
85
98
+ Ice
SSMIAB orbit: 1135 18-02-1982 19:43
Lambert Conformal Conic Projection Scale 1:6000000

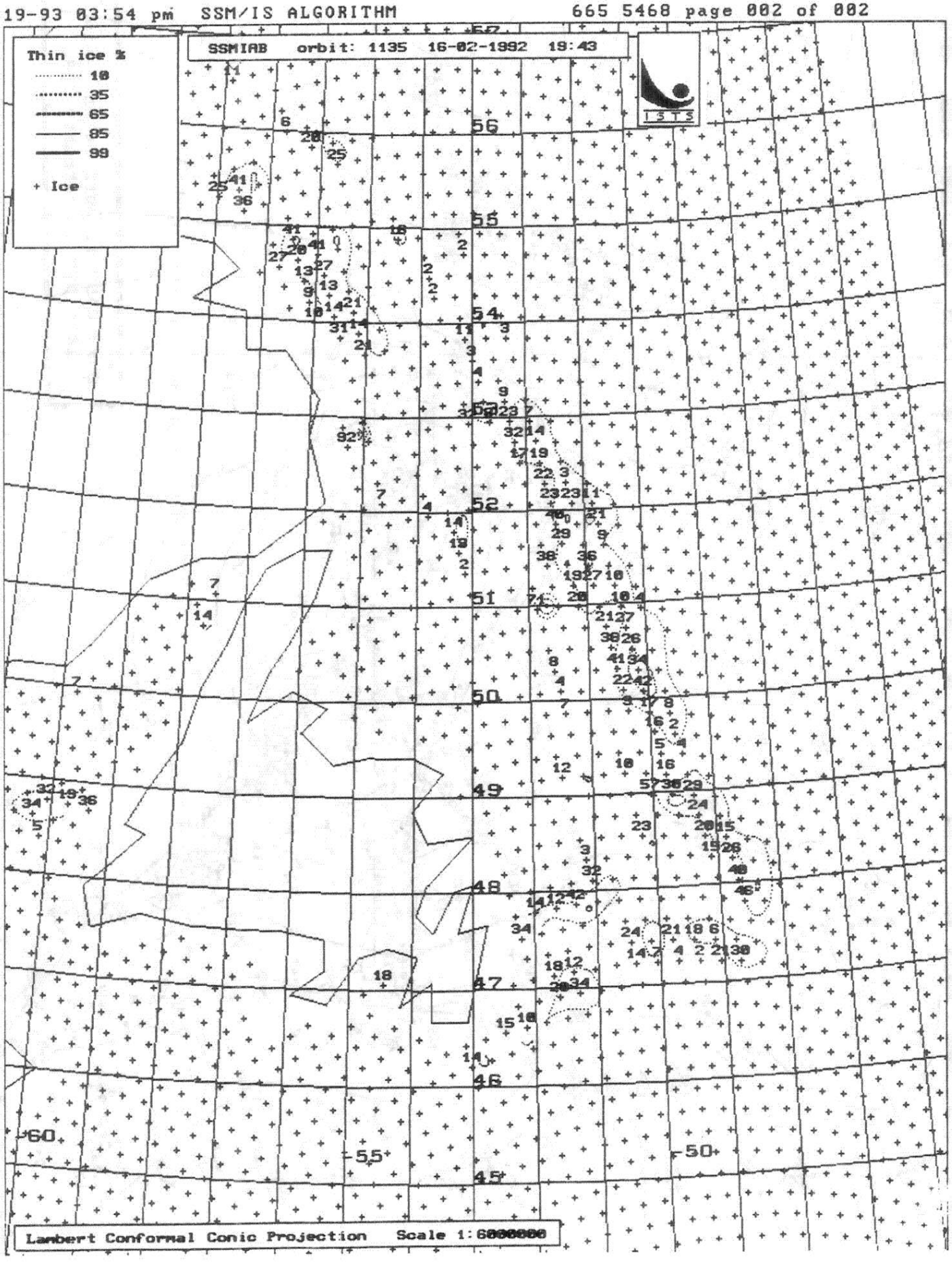
EXAMPLE OF


NASA
Total ice %
10
35
65
85
98
+ Ice
· Wind (kn)
SSMIAB orbit: 1135 18-02-1992 19:43
Lambert Conformal Conic Projection Scale 1:6000000

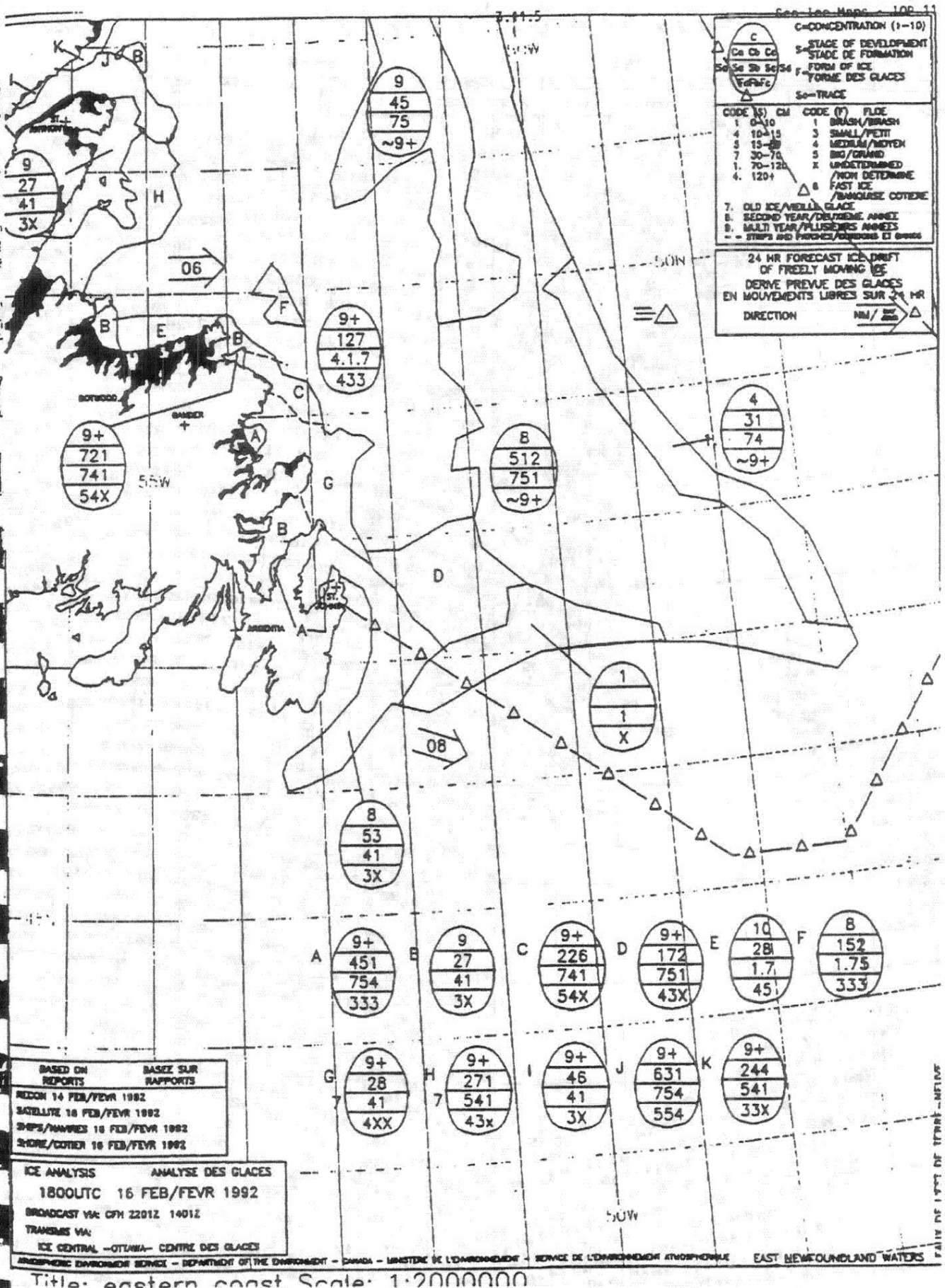

Total ice %
10
35
65
85
98
+ Ice
SSMIAB orbit: 1135 16-02-1992 19:43
56
55
54
-60
-55
-50
45
Lambert Conformal Conic Projection Scale 1:6000000


Total ice %
10
35
65
85
98
+ Ice
· Wind (kn)
SSMIAB orbit: 1135 16-02-1992 19:43
I S T S
Lambert Conformal Conic Projection Scale 1:6000000


L
1009
L
H
1046
Post CASP II Surface Analysis
1800 UTC 16 February 1992
Surface Analysis - Flight 11


Thin ice %
10
35
65
85
99
Ice
SSMIAB orbit: 1135 16-02-1992 19:43
I S T S
Lambert Conformal Conic Projection Scale 1:6000000

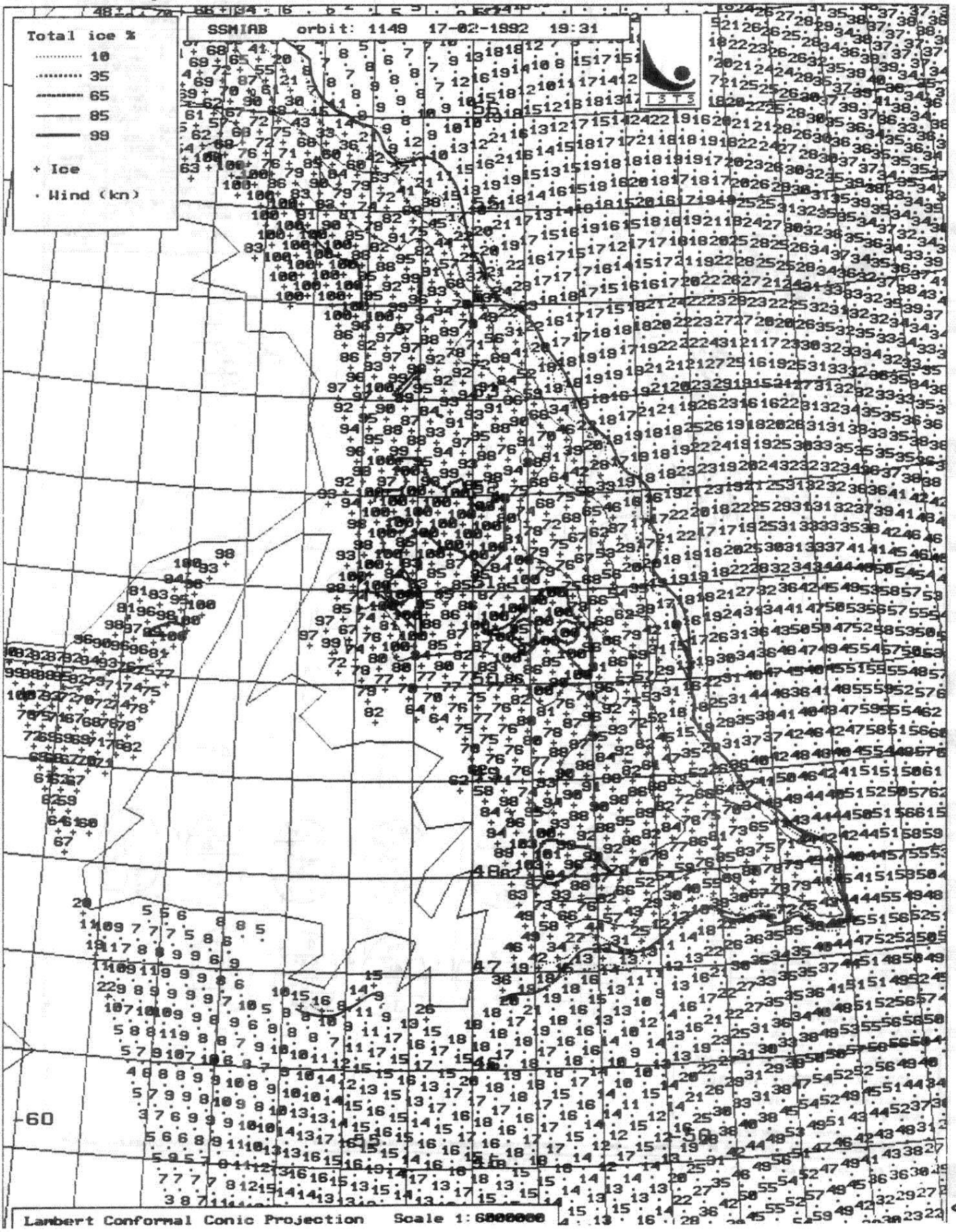
MAPS W0827C WIS-EAST NEWFOUNDLAND ICE ANALYSIS
Printed Sun Feb 16 22:03:44 UTC 1992

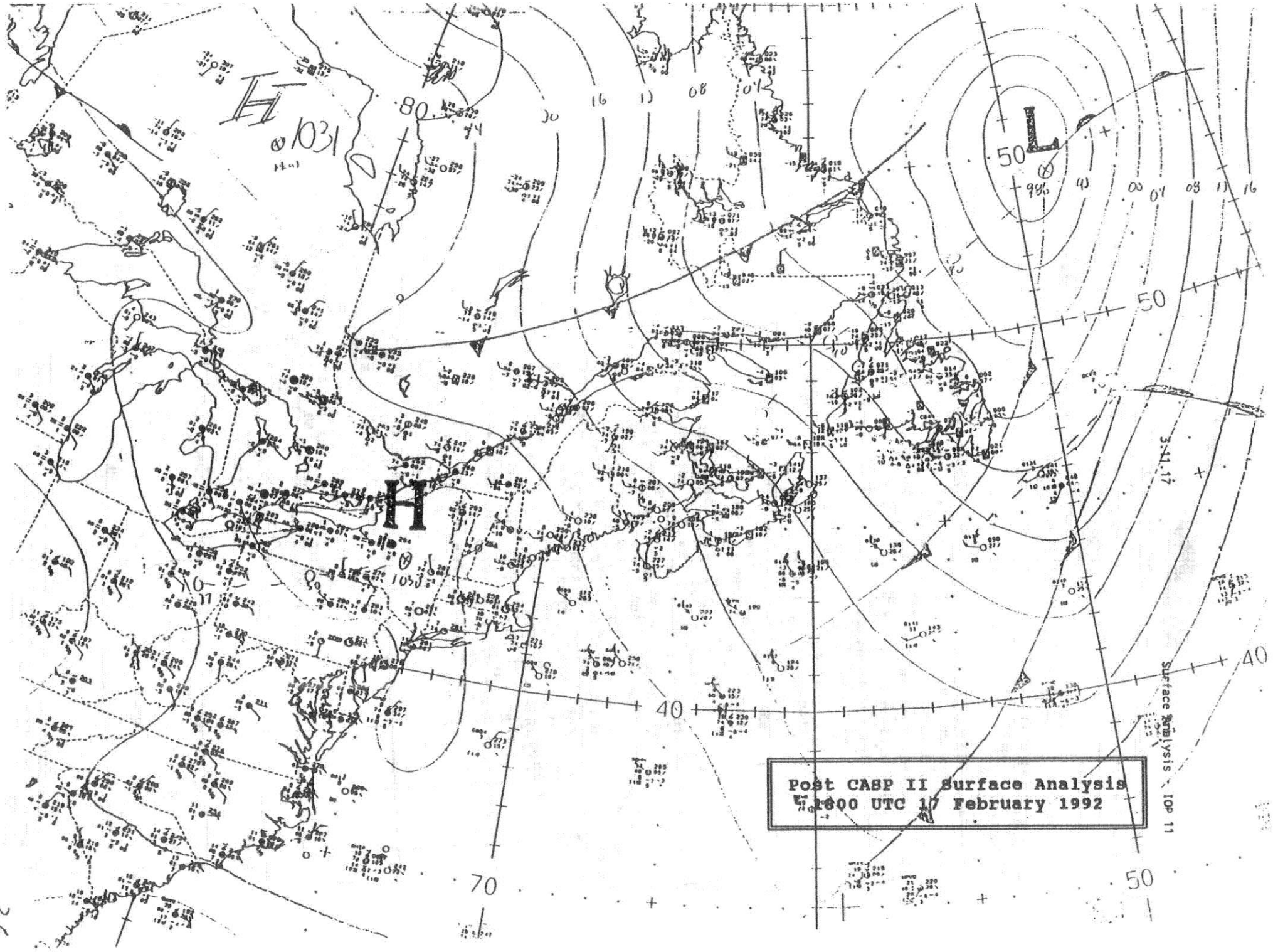


Title: eastern coast Scale: 1:2000000

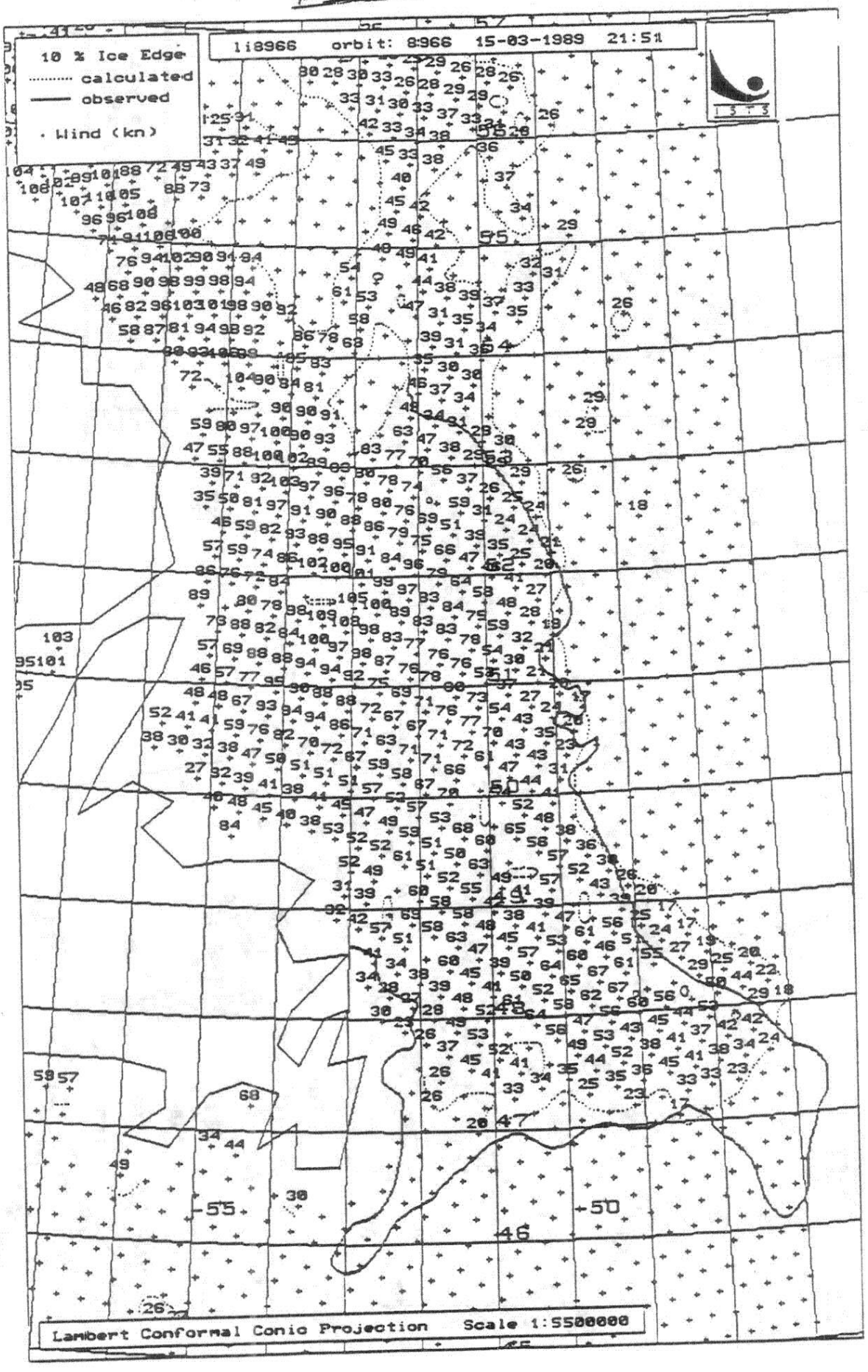
EXAMPLE OF SYNERGETIC USE OF ALGORITHM

05-19-93 04:05 pm SSM/IS ALGORITHM 665 5468 page 001 of 002

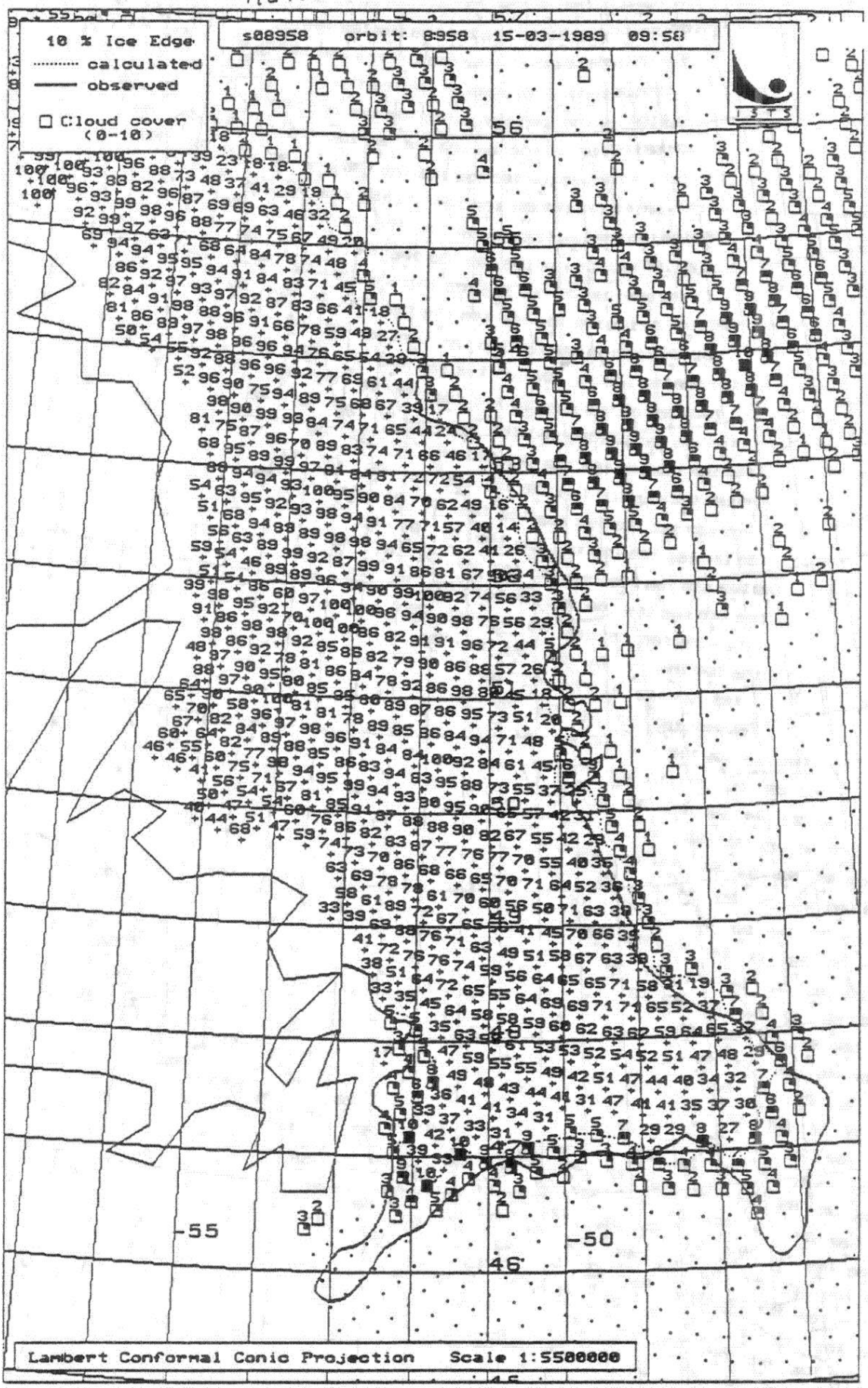


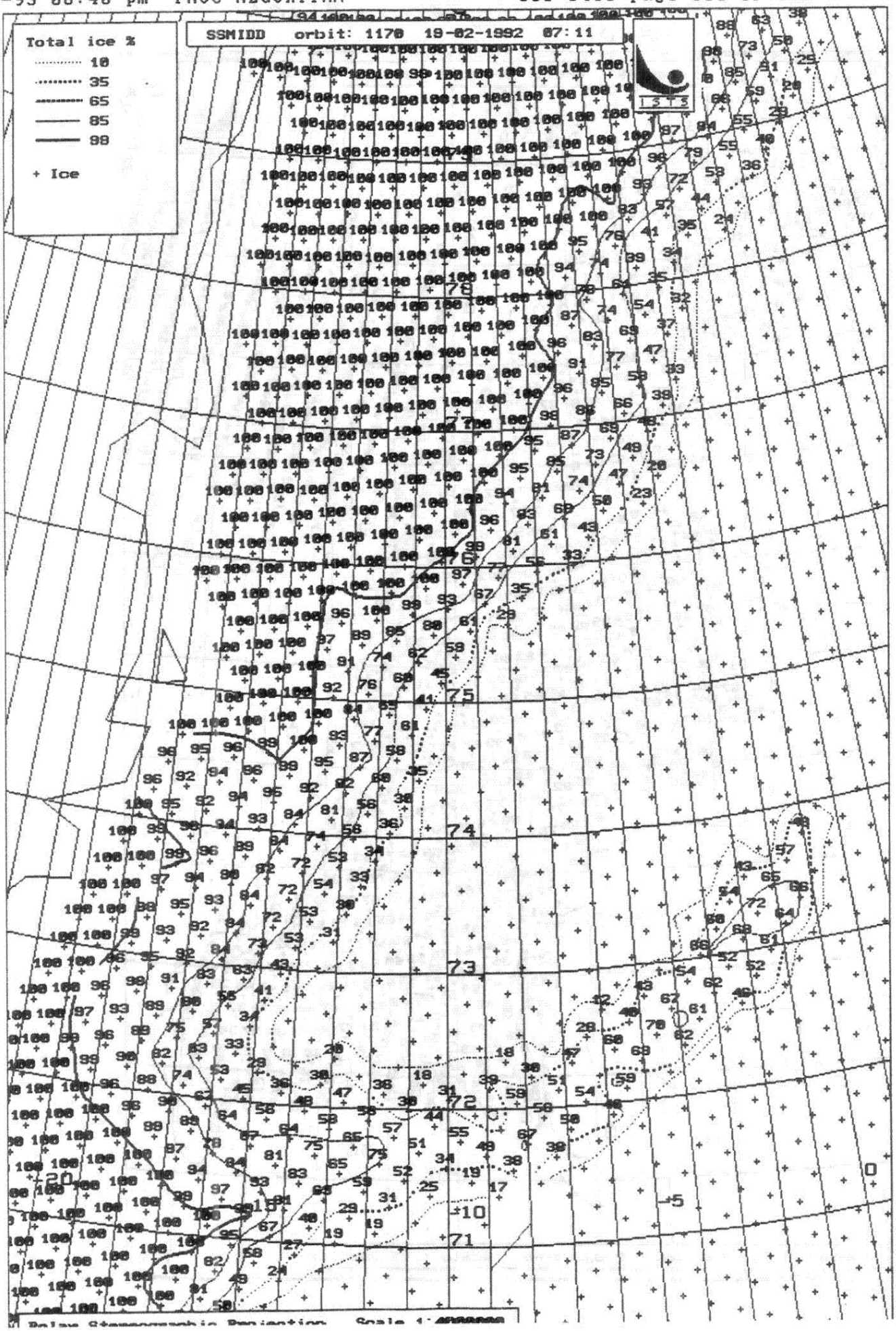

H
1031
L
998
H
1031
Post CASP II Surface Analysis
1600 UTC 17 February 1992
3-11-17
Surface Analysis - IOP 11
80
70
50
40
50
40
50

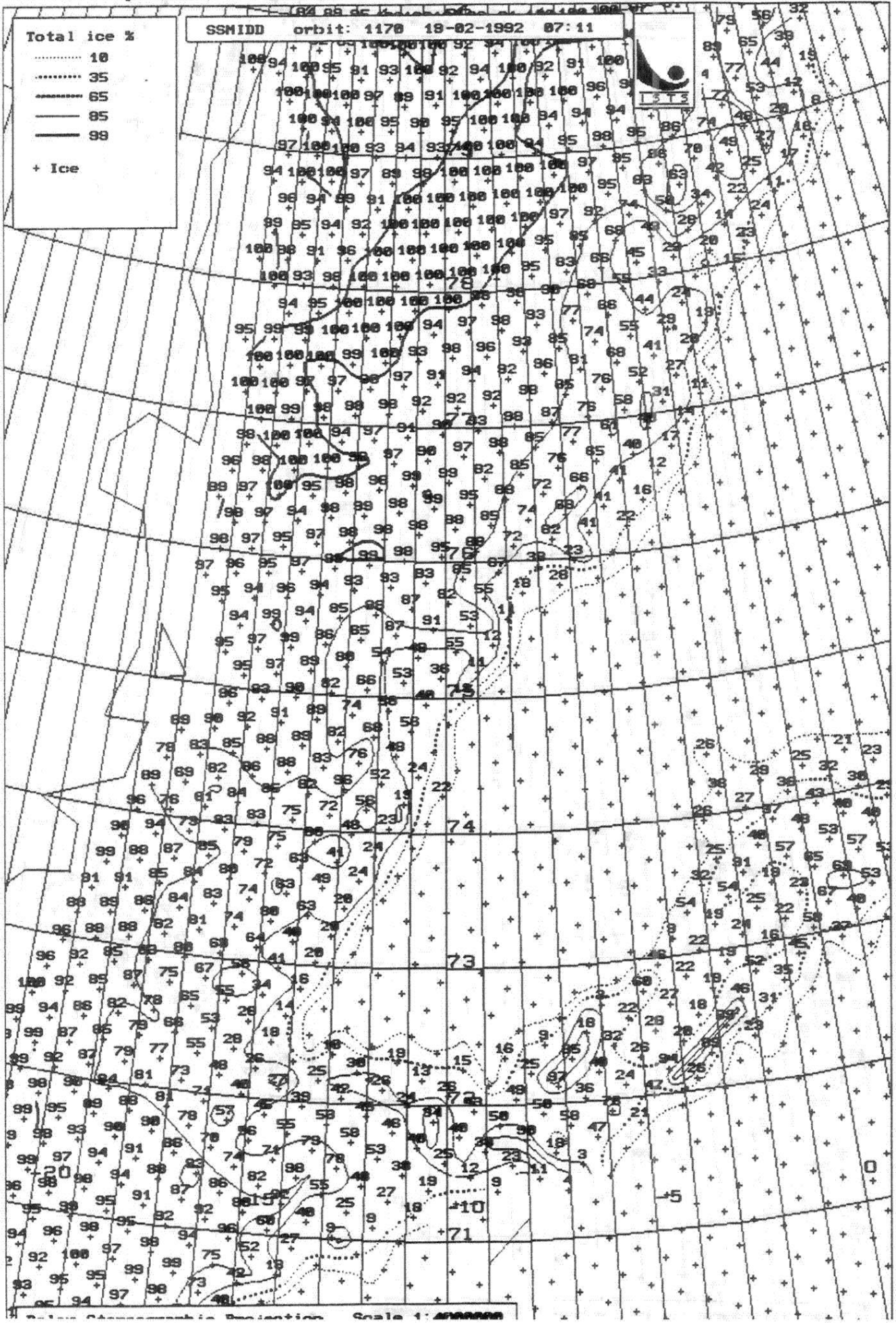
EXAMPLE OF REDUCED WEATHER CORRECTIONS

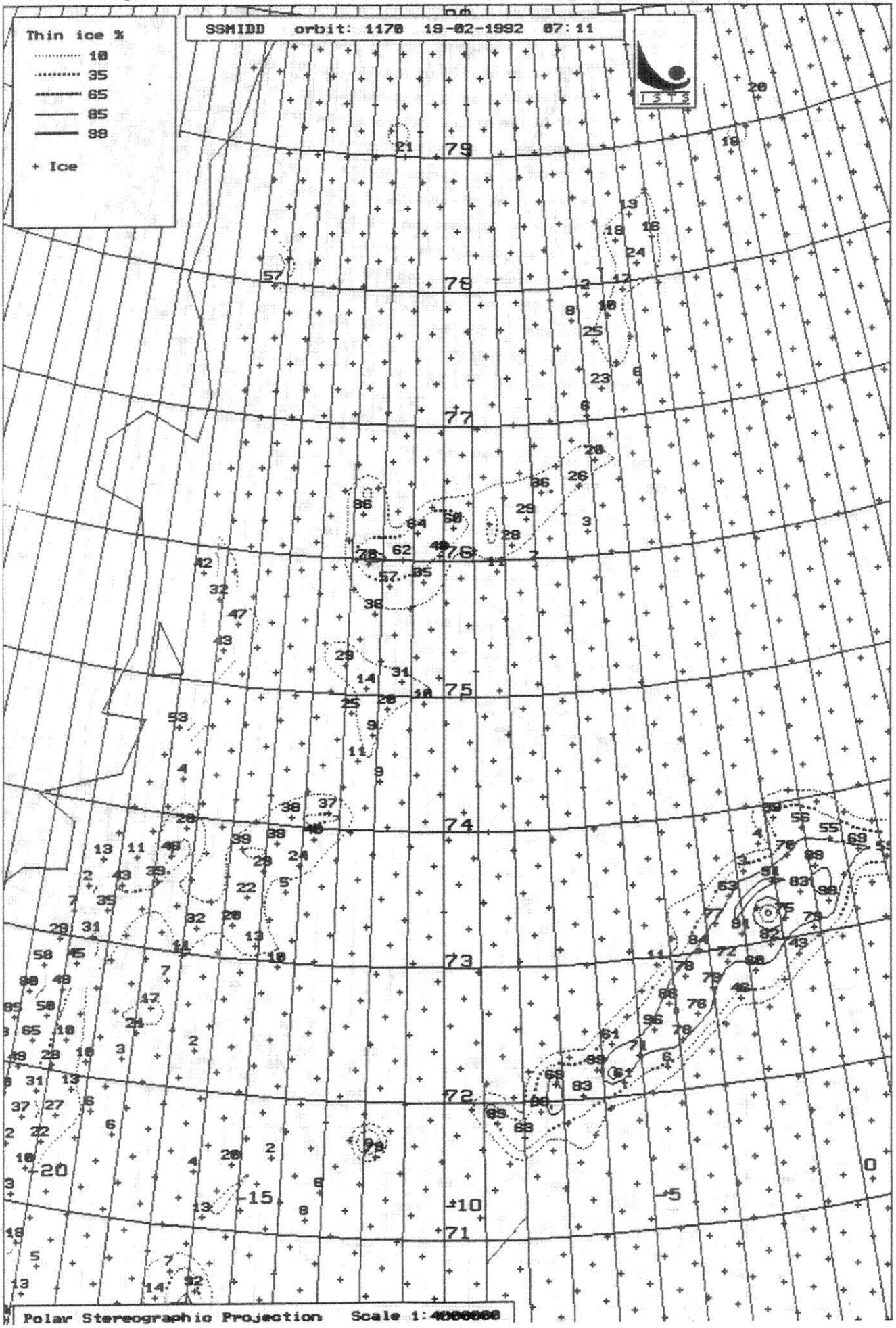


AERO VALIDATION



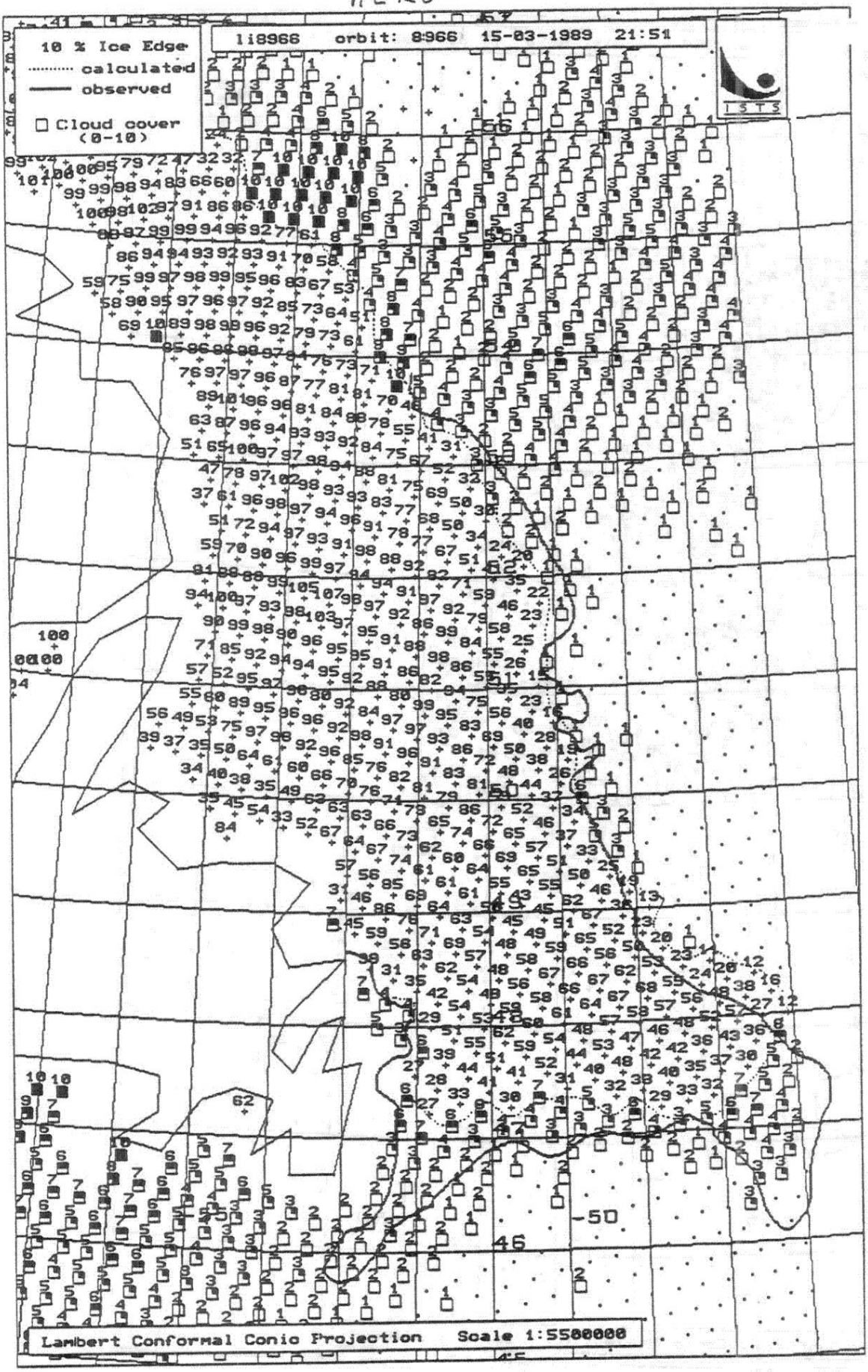

Total ice %
10
35
65
85
98
+ Ice
SSMIDD orbit: 1170 19-02-1992 07:11


Total ice %
10
35
65
85
99
+ Ice
SSMIDD orbit: 1170 19-02-1992 07:11
I S T S

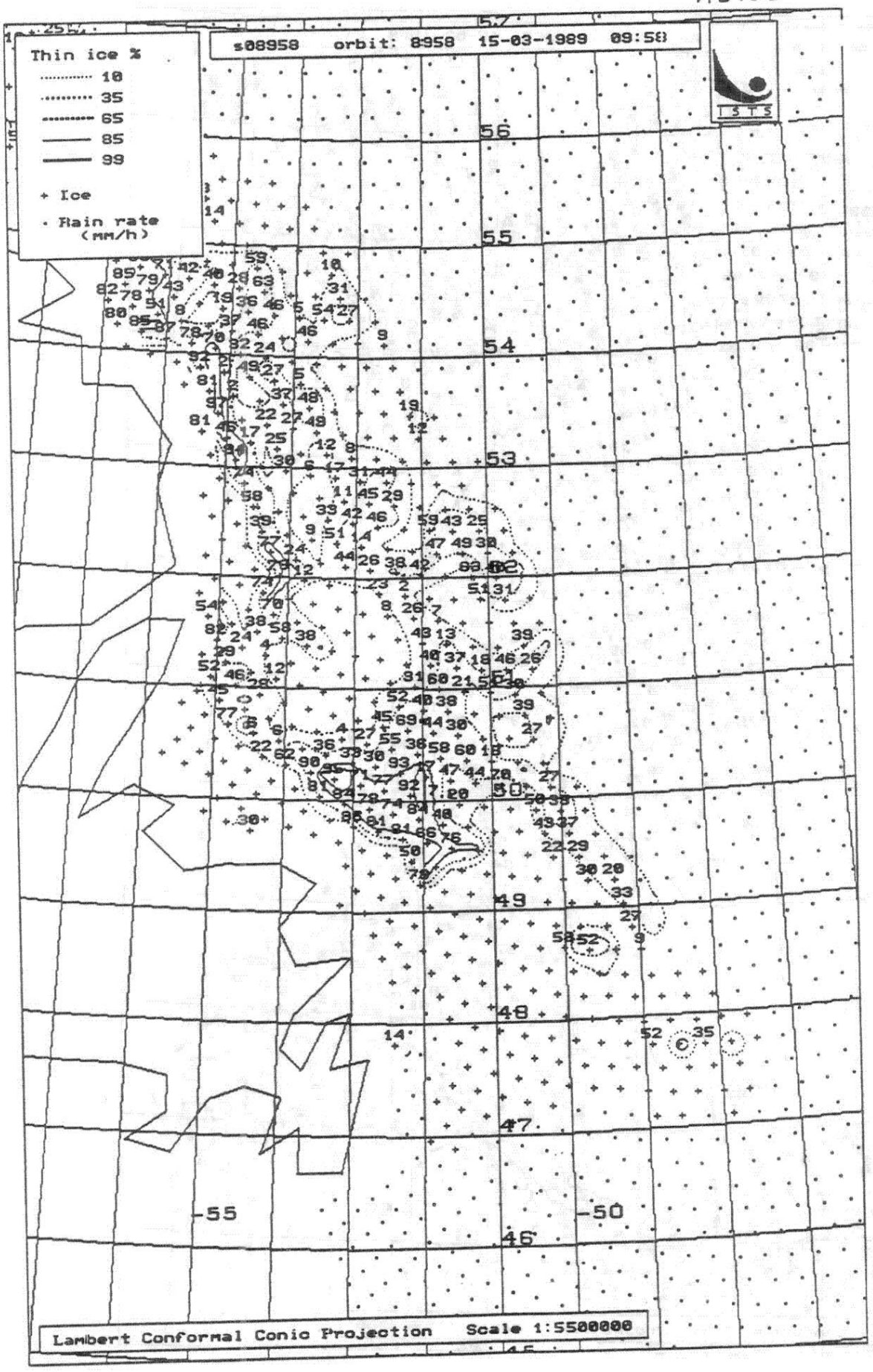

Thin ice %
10
35
65
85
98
+ Ice
SSMIDD orbit: 1170 19-02-1992 07:11
Polar Stereographic Projection Scale 1:

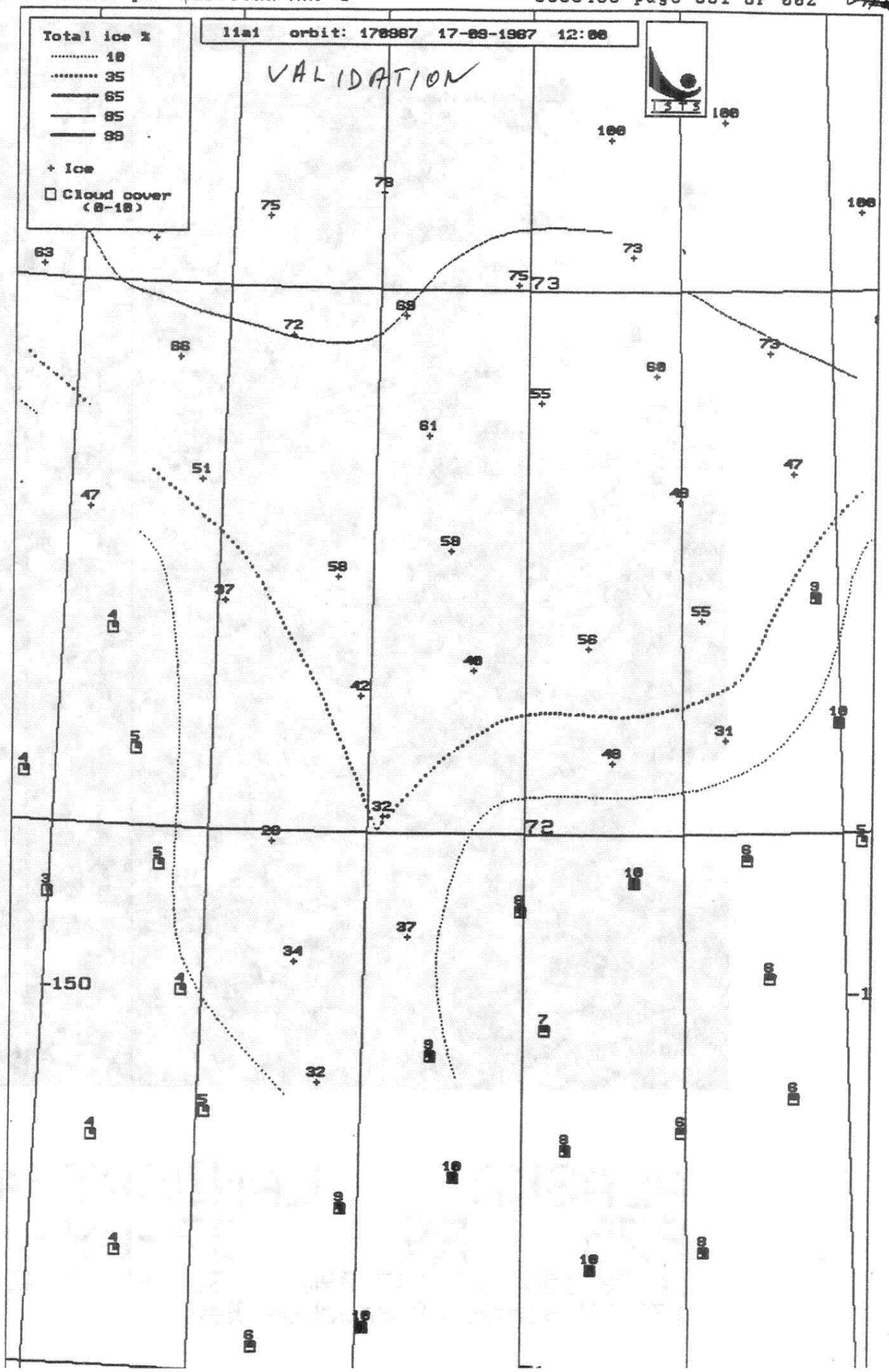
VALIDATION EXAMPLE OF SYNERGETIC USE OF ICE AND CLOUDS ALGORITHMS

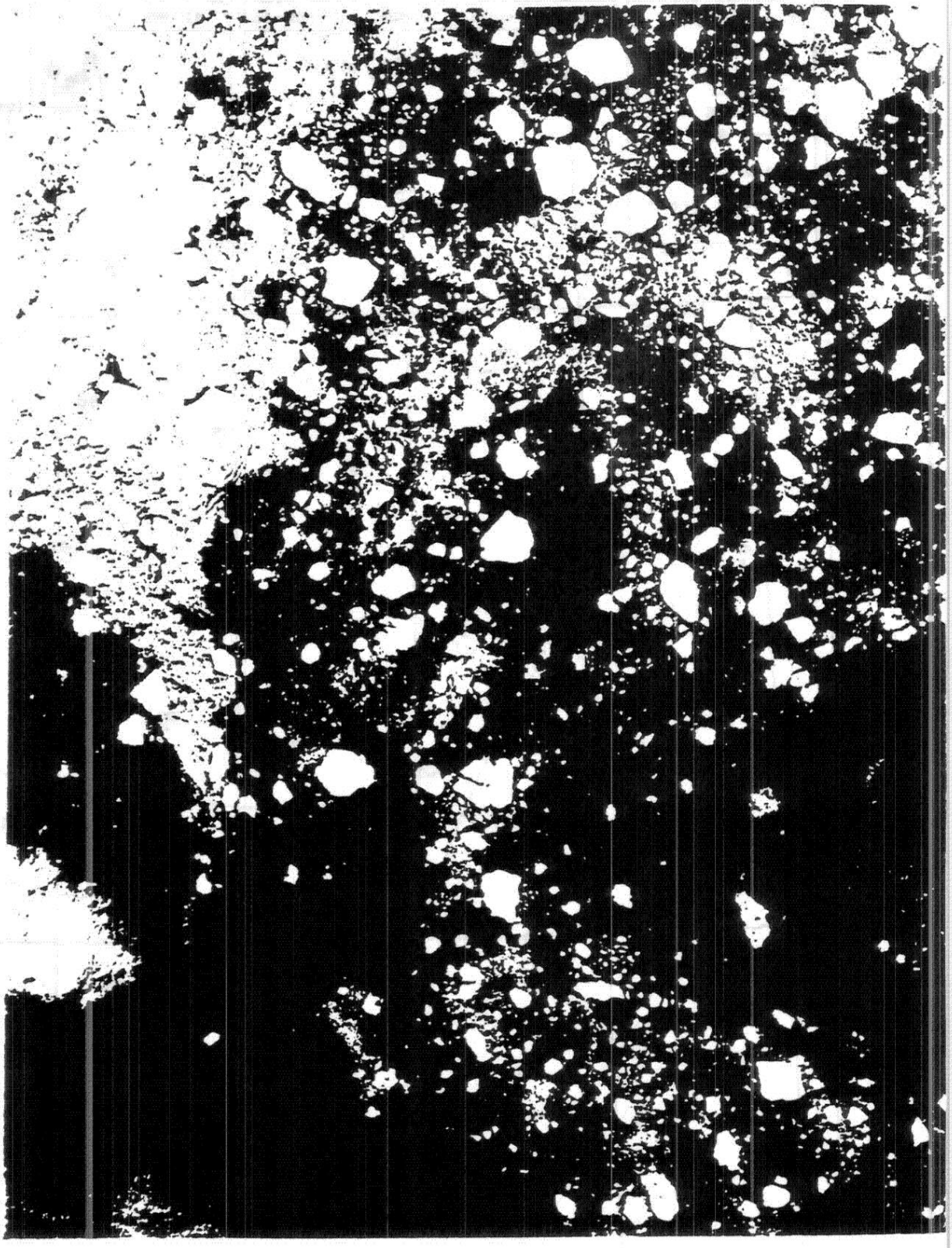
AERO



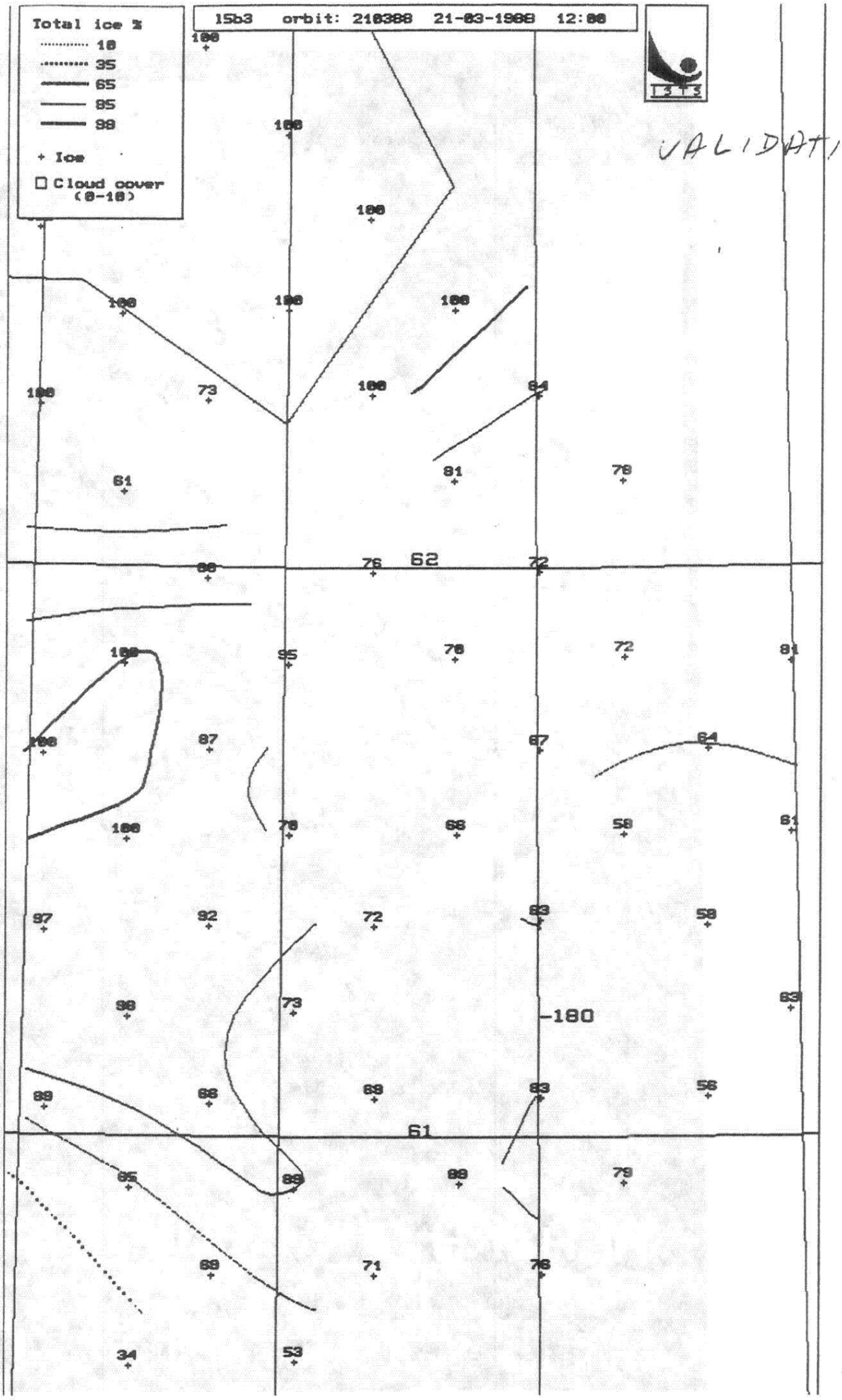
AERO


Thin ice %
10
35
65
85
99
Ice
Rain rate (mm/h)
s08958 orbit: 8958 15-03-1989 09:58
TSTS
56
55
54
53
49
48
47
46
-55
-50
Lambert Conformal Conic Projection Scale 1:5500000


Total ice %
10
35
65
85
98
+ Ice
Cloud cover (0-10)
11a1 orbit: 170987 17-09-1987 12:00
VALIDATION
-150



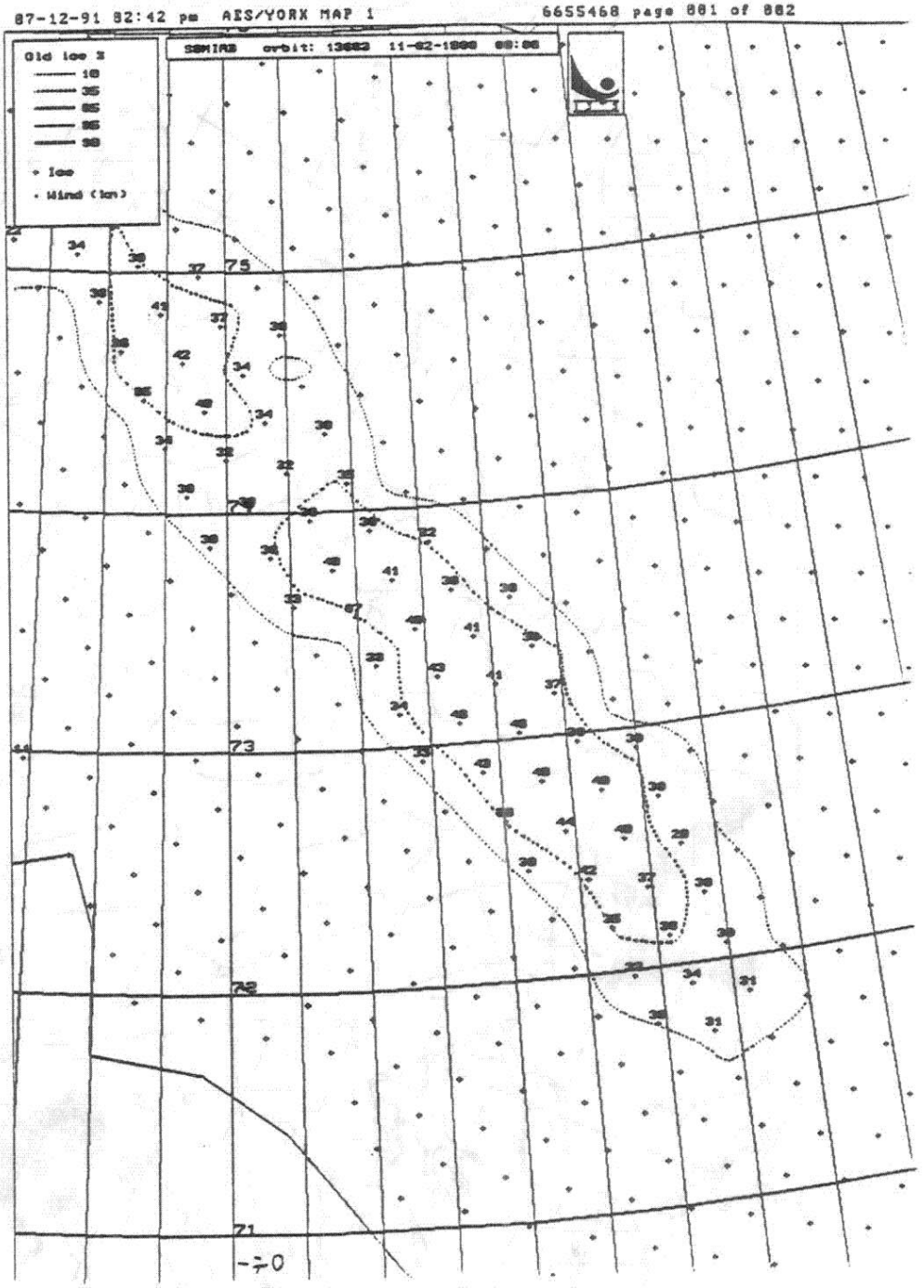
ALASKA LANDSAT-4
P75 R9 87-09-17
LA 72.15N LO 147.09W SUN EL 19 AZ 170
170 KM North of Prudhoe Bay Lin5

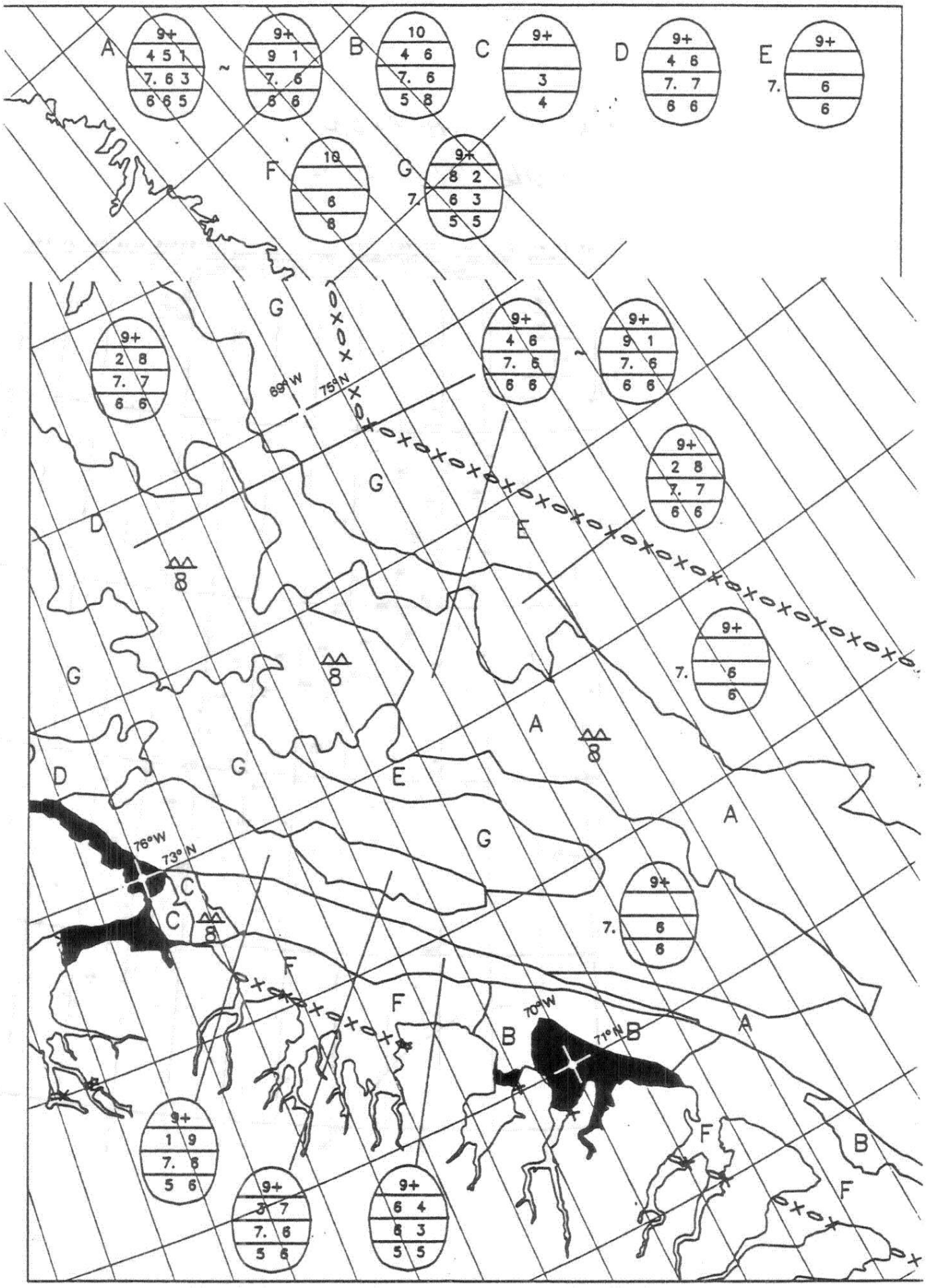

Total ice %
10
35
65
85
98
+ Ice
Cloud cover (0-10)
15b3 orbit: 218388 21-03-1988 12:00
-180

VALIDATION


ALASKA LANDSAT-5
P89 R17 88-03-21
LA 61.47N LO 179.05E SUN EL 27 AZ 156
60 miles south of Keniut, USSR Inv.W

VALIDATION
FOR OLD ICE





2. Ice Analysis - Baffin Bay
Analyse des Glaces - Baie de Baffin

January 28 and February 10/11, 1990/le 28 Janvier et le

APPLICATION

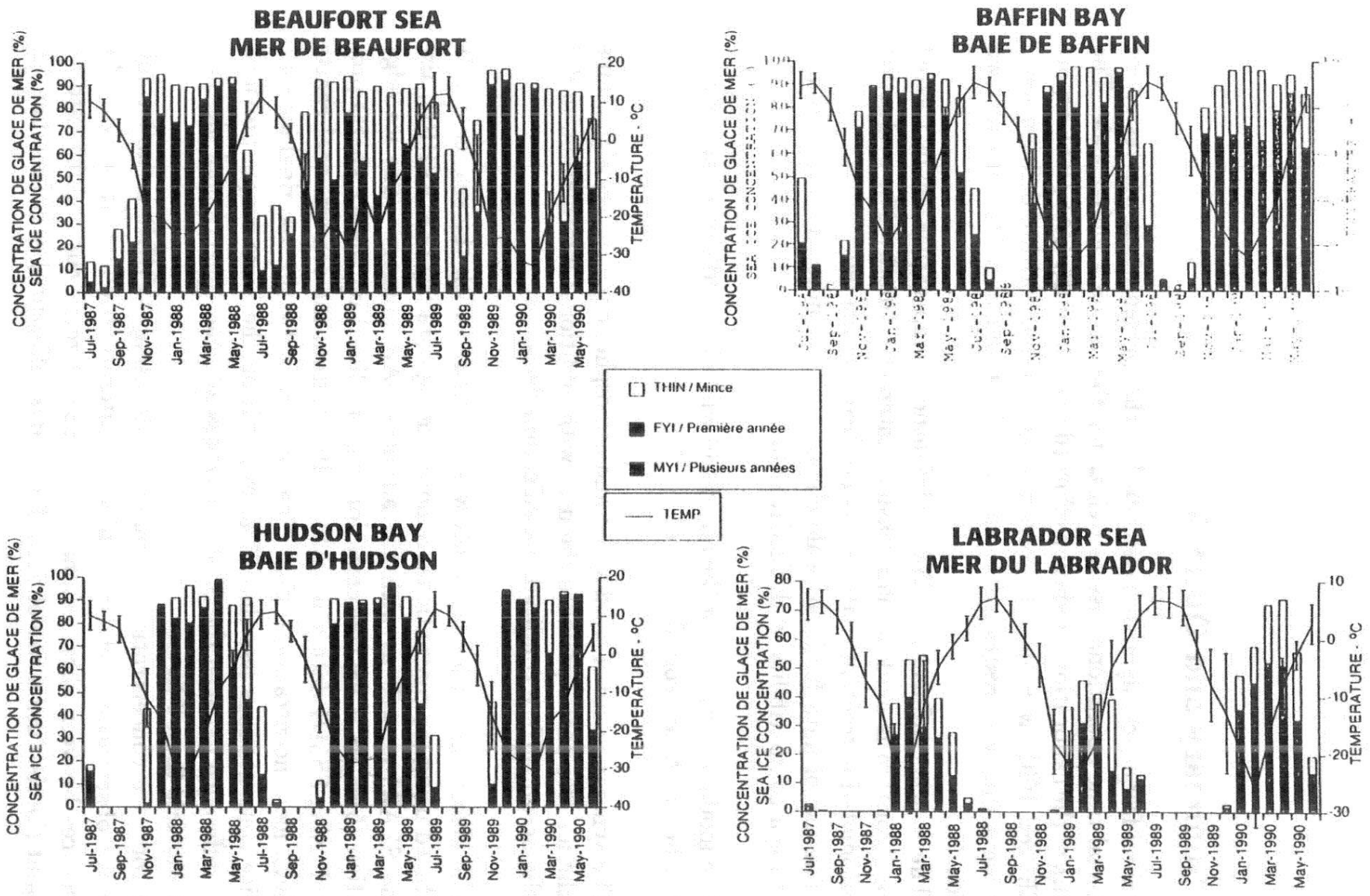


Figure 7.2 Monthly values of sea ice concentration by category and the monthly temperature and standard deviation .
Figure 7.2 Valeur mensuelle des concentrations de glace de mer par catégorie, température du mois et écart-type.

3 Summary and Outlook

The dual frequency algorithm described in this presentation was tested for near-real time operational use as well as for the use on a global scale. The results of the calibration validation effort (described in the CAL/VAL report (Hollinger, 1991) were used to correct some of the algorithm deficiencies. The algorithm was restricted to the use of 19 and 37 GHz data for two reasons:
(1) The weather influence on 85 GHz brightness temperature can be treated if the algorithm is used in man/mashine interactive mode. The evaluation of automated correction routines has not been completed.
(2) The use of data for large scale climatological studies imposes requirement for a compatibility with SSMR data.

The modular structure of the algorithm will allow addition of newer routines when tests are completed.

The synergetic use of wind speed and atmospheric parameter algorithms for the ice free pixels provides the user with additional information, useful for the ocean surface condition classification decisions.

The algorithm sea ice retrievals were compared with the sea ice charts produced using (a) conventional remote sensing data (NOAA AVHRR, airborne SLAR) as well as with the airborne SAR imagery. The ice edge location (5 or 10 % ice concentration contour lines) on the ice charts produced using SSM/I data was within ± 10 km from the conventional charts for high ice concentration region. The comparison for the marginal ice zone (i.e ice concentations less that 65%, were within the same range, provided time difference between the SSM/I overpass and the conventional observation was less than 3 hours.
The total ice concentration estimates made using AVHRR or active microwave observations rely on subjective interpretation of imagery. The differences between these estimates and SSM/I retrievals (taking into an account the resolution size of SSM/I and time difference) were less than 12.

The captains of "Polarstern", "N. Palmer" and Canadian Coast Guard have used the ice charts faxed to them from ISTS (or from companies designated by Dr. R. Ramseier (AES) to provide near-real time service) to navigate during severe weather conditions.

The use of the SSM/I sea ice information on a global scale as an input to the numerical weather prediction and climatological models is undergoing evaluation at the Canadian Meteorological Center and at the University of Waterloo (Dr. E. LeDrew).

The future research (regional, operational application) goals are:

- To use in the retieval algorithms modules containing external regional environmental information (from data sources other than SSM/I).
- To include atmospheric and/or ice surface condition information that could be derived from higher frequency channels.

4 Acknowledgments.

This work was made possible by funding from the following :

Ice Branch, AES, Canada Translation of SMMR algorithm to SSM/I application (AES/Ph.D algorithm); Cal./Validation 1987-1989; Operational testing for Canadian Waters (1989-1990); partial support for data acquisition (navigational application evaluation during "Polarstern" cruises).

Canadian Meteorological Centre Development of the Satellite Image Display Software tools; Validation .

Aerojet Electronic System GenCorp.(1989-1991) Partial support for: validation and Development of the algorithm modules ; data acquisition during research and operational testing campaigns.

Institute for Space and Terrestial Science, project #9-97605, 1988-1992 The author would like to thank Mr. A. Davies (meteorology) and ARM consulting staff (programming) for their assistance, and Dr. R.O Ramseier (Ice Branch, AES, Canada) for providing an opportunity to become involved in this research project.

NASA Team Sea Ice Algorithm for the DMSP SSM/I

Donald J. Cavalieri and Per Gloersen
Oceans and Ice Branch/Code 971
Laboratory for Hydrospheric Processes
NASA Goddard Space Flight Center
Greenbelt, Maryland 20771

ABSTRACT

The NASA Team sea ice algorithm for the SSM/I is functionally the same as the Nimbus 7 SMMR algorithm described by Cavalieri et al. (1984) and Gloersen and Cavalieri (1986). The three SSM/I channels used in the algorithm are the 19 GHz H and V channels and the 37 GHz V channel. The two independent variables used in the algorithm are the polarization (PR) and the spectral gradient ratio (GR). PR is defined by [TB(19V)-TB(19H)]/[TB(19V)+TB(19H)] and GR by [TB(37V)-TB(19V)]/[TB(37V)+TB(19V)] where TB is the observed brightness temperature at the indicated channel. These radiance ratios are independent of physical temperature changes, at least to first order. From these two parameters, first-year and multiyear ice concentrations are calculated for the Arctic. The total ice concentration is the sum of the first-year and multiyear concentrations. Only the total ice concentration is mapped in the Antarctic, since the radiometric distinction between first-year and multiyear ice is lost.

The SSM/I algorithm uses two weather filters to reduce spurious ice concentrations caused by weather-related effects such as wind-roughened seas, cloud-liquid water, and atmospheric water vapor over the ocean. The first weather filter sets the total ice concentration to 0% for those SSM/I grid cells with GR greater than 0.05. A third ratio, used as the second filter, is defined by GW = [TB(22V)-TB(19V)]/[TB(22V)+TB(19V)]. Total ice concentration is set to 0%, if GW is greater than 0.045 (Cavalieri et al.,1993a).

In 1987, NASA sponsored a sea ice validation program to provide the polar research community with a measure of the accuracy of the sea ice concentrations derived from the SSM/I calibrated radiances with the NASA algorithm (Cavalieri et al., 1992). For total ice concentration under winter conditions, SSM/I-Landsat MSS comparisons gave a mean difference of -3.6%±6.6%, indicating that the SSM/I ice concentrations are slightly lower relative to Landsat. Results from NASA and Navy aircraft underflights also show that the SSM/I ice concentrations are lower (-2.4%±2.4%) relative to the aircraft measurements. This compares well with the SSM/I-Landsat comparisons which gave -2.1%±3.1% for the same region. From aircraft high-resolution radiometer and SAR images, SSM/I multiyear ice concentrations were found to be about 12%±11% greater than the aircraft-derived values. Finally, a recent modification of the NASA Team algorithm allows mapping of new and young ice types in seasonal sea ice zones (Cavalieri, 1993b). This modification also substantially reduces the low ice concentration bias typically found in areas of thin ice.

NASA Team Sea Ice Algorithm for the DMSP SSM/I

Donald J. Cavalieri and Per Gloersen
Oceans and Ice Branch/Code 971
Laboratory for Hydrospheric Processes
NASA Goddard Space Flight Center
Greenbelt, Maryland 20771

ABSTRACT REFERENCES

Cavalieri, D. J., P. Gloersen and W. J. Campbell, Determination of sea ice parameters with the Nimbus 7 SMMR, J. Geophys. Res., 89, 5355-5369, 1984.

Gloersen P. and D. J. Cavalieri, Reduction of Weather Effects in the Calculation of Sea Ice Concentration from Microwave Radiances, J. Geophys. Res., 91, 3913-3919, 1986.

Cavalieri, D. J., J. Crawford, M. Drinkwater, W. J. Emery, D. T. Eppler, L. D. Farmer, M. Goodberlet, R. Jentz, A. Milman, C. Morris, R. Onstott, A. Schweiger, R. Shuchman, K. Steffen, C. T. Swift, C. Wackerman and R. L. Weaver, NASA Sea Ice Validation Program for the DMSP SSM/I: Final Report, NASA Technical Memorandum 104559, National Aeronautics and Space Administration, Washington, D. C., pp. 126, 1992.

Cavalieri, D. J., K. St. Germain, and C. T. Swift, Reduction of weather effects in the calculation of sea ice concentration from the DMSP SSM/I, in preparation, 1993a.

Cavalieri, D. J., A Passive Microwave Technique for Mapping New, Young, and First-Year Sea Ice Types in Seasonal Sea Ice Zones, J. Geophys. Res., submitted, 1993b.

SPN SSM/I ALGORITHM SYMPOSIUM
Algorithm Questionnaire

"NASA TEAM SEA ICE"
Per Gloersen, respondent

Please provide the following essential information about your algorithm(s).

* ALGORITHM DESCRIPTION

- Type (statistical, physical, other) — *An "interpolation" algorithm*

- Input required / Output produced

  Input: 19 GHz (h-pol and v-pol); 37 GHz (v-pol)
  Output: Total ice concentrations; Multiyear ice type concentrations

- Auxiliary sensor/data base requirements — *None*

- Major limitations / approximations — *How universal are the "tie points"? (some validation results are published)*

- Computer resource requirements — *Very modest; e. g. , a personal computer A single pass algorithm - no interations or decision trees*

* ALGORITHM PERFORMANCE

- Development / test data sets (regional / global / seasonal)

(See reports by Cavalieri, et al., e.g., "NASA Sea Ice Validation Program for the DMSP SSM/I: Final Report", NASA Tech. Memo. 104559, pp. 126, Jan, 1992; papers by Steffan et al., Cavalieri, et al., AGU Monograph "Microwave Remote Sensing of Sea Ice")

- Ground truth (accuracy / limitations)

(See above documents)

- Major assumptions of evaluation

There are no assumptions required for intercomparison of this algorithm with others; however, the absolute validation of any one algorithm is difficult given the veracity of comparison data sets

* ALGORITHM PERFORMANCE (continued)

- Strengths / weaknesses

*The algorithm is **global**. Accuracy is poorer in perimeter seas. **Regional** accuracy can be improved with regional tie points, perhaps enhancing operational utitlity, but regional tiepoints within a hemisphere are unacceptable for climate studies.*

* ALGORITHM MATURITY

- Operational useage

The Naval Polar Oceanography Center has implemented the NASA Team algorithm

- Refinement / additional development

*Thin ice aspects need development (see **regional** comments above)*

- Availability

Algorithm is available upon request.

NASA TEAM SEA ICE ALGORITHM FOR THE DMSP SSM/I

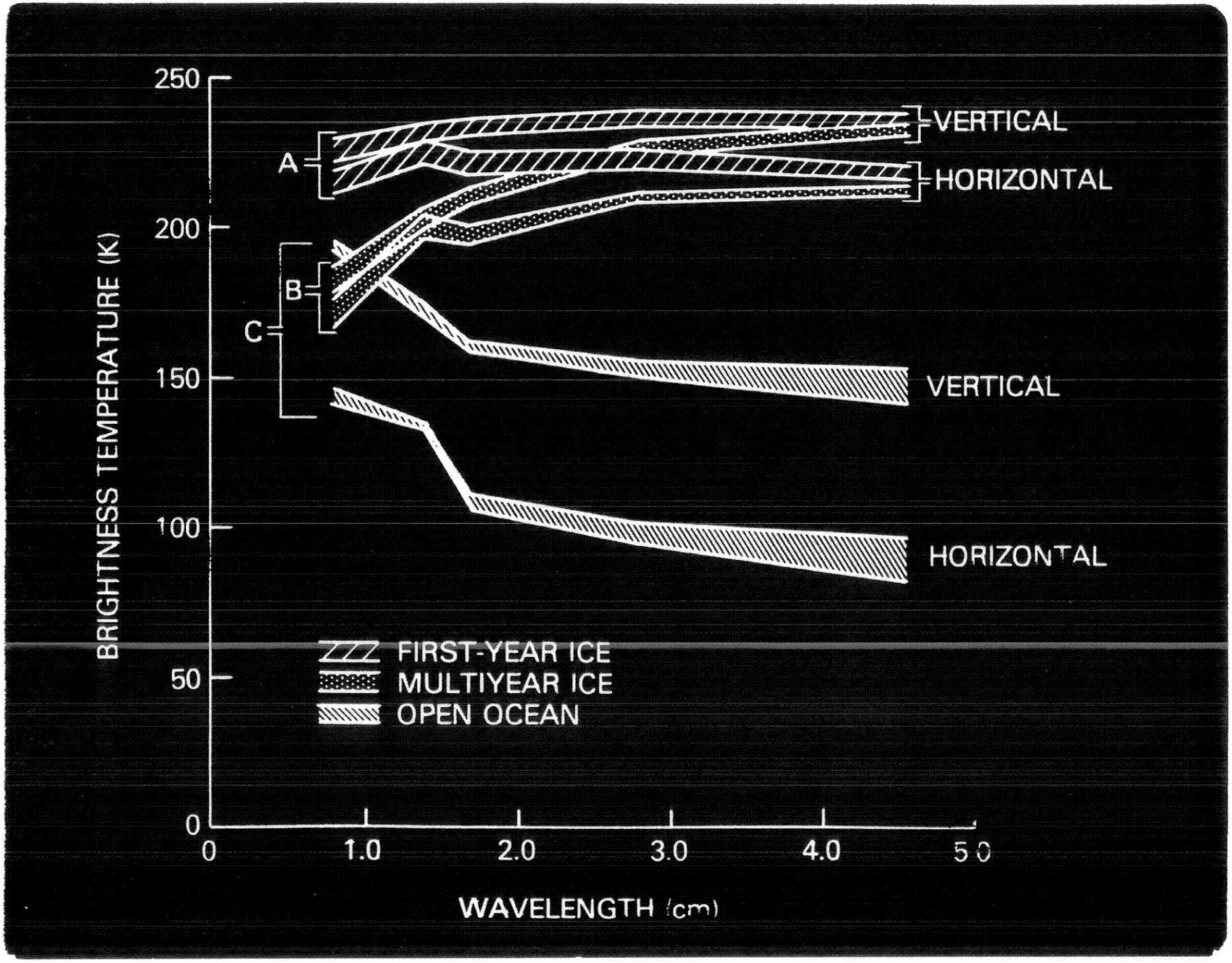
DONALD J. CAVALIERI AND PER GLOERSEN

OCEANS AND ICE BRANCH/CODE 971

LABORATORY FOR HYDROSPHERIC PROCESSES

NASA GODDARD SPACE FLIGHT CENTER

GREENBELT, MD 20771


250
200
150
100
50
0
BRIGHTNESS TEMPERATURE (K)
A
B
C
VERTICAL
HORIZONTAL
VERTICAL
HORIZONTAL
FIRST-YEAR ICE
MULTIYEAR ICE
OPEN OCEAN
0
1.0
2.0
3.0
4.0
5.0
WAVELENGTH (cm)

Basic Equations

$$TB = (TB_W)(1 - C_F - C_M) + (TB_F)(C_F - C_M) + (TB_F)(C_F) + (TB_M)(C_M)$$

$$PR = \frac{TB_{1.55V} - TB_{1.55H}}{TB_{1.55V} + TB_{1.55H}}$$

$$GR = \frac{TB_{0.81V} - TB_{1.55H}}{TB_{0.81V} + TB_{1.55H}}$$

Solution

$$C_M = \frac{[M_0 + M_1 \cdot PR + M_2 \cdot GR + M_3(PR)(GR)]}{[D_0 + D_1 \cdot PR + D_2 \cdot GR + D_3(PR)(GR)]}$$

$$C_F = \frac{[F_0 + F_1 \cdot PR + F_2 \cdot GR + F_3(PR)(GR)]}{[D_0 + D_1 \cdot PR + D_2 \cdot GR + D_3(PR)(GR)]}$$

$$C_{TOT} = C_F + C_M$$

Table 4.1. NASA DMSP SSM/I Sea Ice Algorithm Tie-points and the Coefficients Used in the Calculation of Sea Ice Concentrations

Northern Hemisphere

Channel	OW	FYice	MYice
19.4H	100.8	242.8	203.9
19.4V	177.1	258.2	223.2
37.0V	201.7	252.8	186.3

a_0 = 3286.56	a_1 = -20764.9	a_2 = 23893.1	a_3 = 47944.5
b_0 = -790.321	b_1 = 13825.8	b_2 = -33104.7	b_3 = -47720.8
c_0 = 2032.20	c_1 = 9241.50	c_2 = -5655.62	c_3 = -12864.9

Southern Hemisphere

Channel	OW	Ice Type A	Ice Type B
19.4H	100.3	237.8	193.7
19.4V	176.6	249.8	221.6
37.0V	200.5	243.3	190.3

a_0 = 3055.00	a_1 = -18592.6	a_2 = 20906.9	a_3 = 42554.5
b_0 = -782.750	b_1 = 13453.5	b_2 = -33098.3	b_3 = -47334.6
c_0 = 2078.00	c_1 = 7423.28	c_2 = -3376.76	c_3 = -8722.03

In addition to constraining the solutions to concentrations between 0% and 100%, the algorithm also sets the total ice concentration to 0% for those SSM/I grid cells with GR greater than 0.05. This serves to reduce spurious ice concentrations caused by weather-related effects at polar latitudes. Wind-roughened seas, cloud-liquid water, and atmospheric water vapor all contribute to these spurious concentrations over the open ocean. This so-called weather filter also eliminates ice concentrations below 15%. This is not considered a serious limitation, since the ice edge has been defined previously for satellite passive-microwave imagery as the 15% ice concentration contour (e.g., Zwally et al., 1983, and Parkinson et al., 1987). Furthermore, a comparison of aircraft-determined ice-edge positions with SSM/I ice concentrations shows that the location of the ice-edge position is accurately determined by the 15% ice-concentration contour (see Chapter 7).

4.2 SSM/I Tie-points

The monthly-mean sea ice concentrations illustrated in Color Plates 1 and 2 were calculated using the tie-points in Table 4.1. The selection of these tie-points was based on an analysis of SSM/I TBs, PR-GR distributions, and histograms of sea ice concentrations, and on comparisons with near simultaneous measurements from the Nimbus-7 SMMR during July and August 1987 (see Preface). The two sets of SSM/I tie-points (one for the northern hemisphere and one for the southern hemisphere) represent a "global" set designed for mapping global ice concentrations. While

National Aeronautics and Space Administration

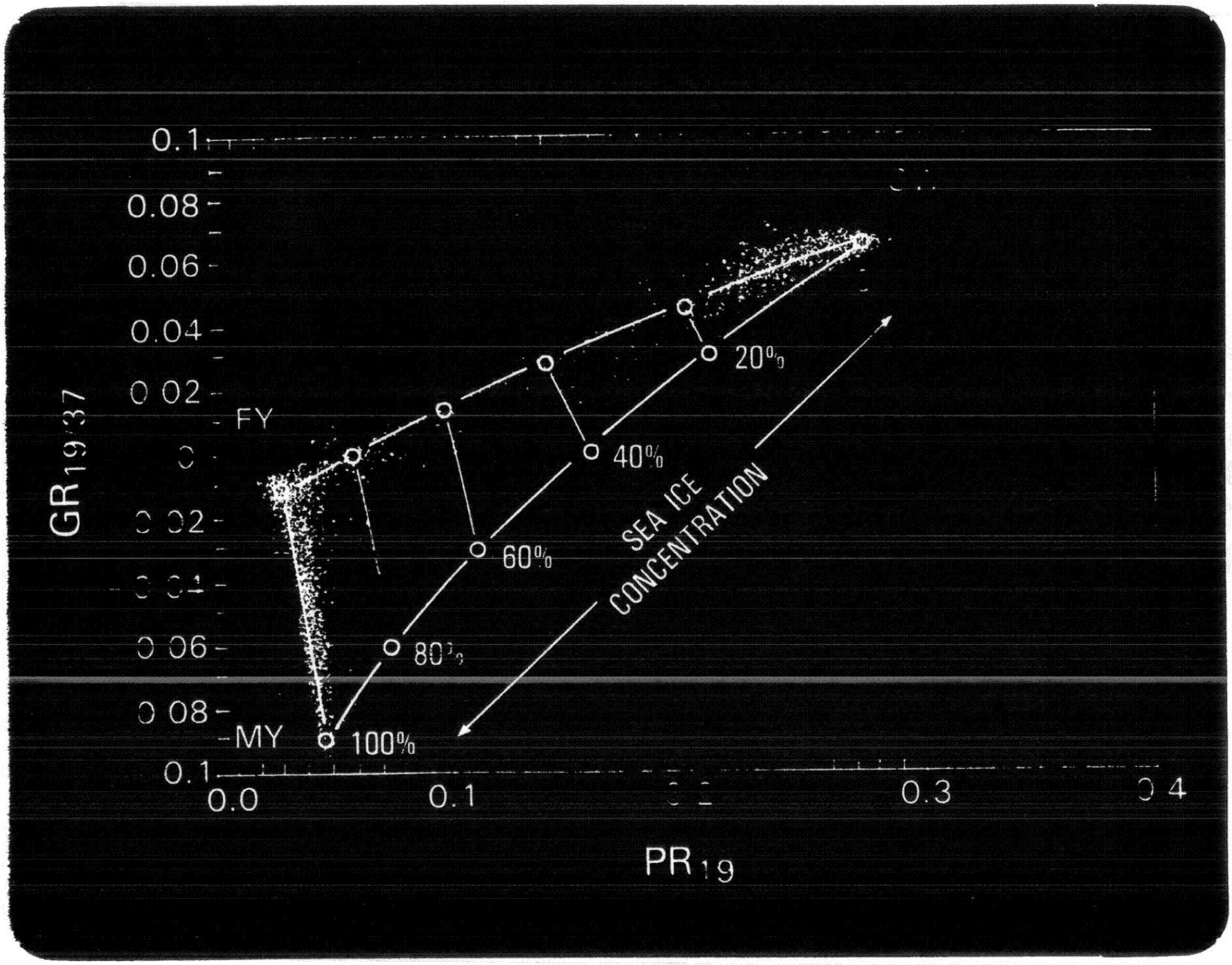

0.1
0.08
0.06
0.04
0 02
0 02
0 06
0 08
GR19 37
FY
MY
20%
40%
60%
80%
100%
SEA ICE
CONCENTRATION
0.0
0.1
0.3
PR19

Table 2.3.4. Quantitative Estimates of Algorithm* Accuracy Based on Comparisons With Other Sources of Ice-Concentration Measurements

REGION	MONTH	SENSOR	MEAN DIFF. ±1 SD	REF. DATA SET	REF.
Total Ice Concentration					
Bering Sea	Feb	SMMR	±5% (Thick FY)	Ship reports	(1)
Baffin Bay	Mar-May	SMMR	-3.5%	Landsat MSS	(2)
Baffin Bay	Jun	SMMR	-10%	Landsat MSS	(2)
Beaufort Sea	Oct	SMMR	-1.5%±2.6%	Landsat MSS	(3)
Weddell Sea	Oct	SMMR	0.3%±7.6%	SIR-B	(4)
Beaufort & Chukchi Seas	Sep-Nov	SSMI	0.6%±7.4%	Landsat MSS	(5)
Beaufort Sea	Mar	SSMI	-2.1%±3.1%	Landsat MSS	(5)
Bering Sea	Mar	SSMI	-9.4%±6.1%++	Landsat MSS	(5)
Greenland Sea	Sep	SSMI	-3.7%±1.4%	Landsat MSS	(5)
Weddell Sea	Nov	SSMI	-1.1%±3.1%	Landsat MSS	(5)
Summary		SSMI	-3.6%±6.6%	Landsat MSS	(5)
Amundsen Sea	Dec	SSMI	1.3%±3.6%	Landsat MSS	(5)
Beaufort & Chukchi Seas	Mar	SSMI	-2.4%±2.4%	NADC/ERIM SAR & NOARL	(6)
				KRMS	(6)
Multiyear Ice concentration					
Beaufort & Chukchi Seas	Mar	SSMI	5%±4% 12%±11%**	*NADC/ ERIMSAR & NOARL KRMS	(6)
Beaufort Sea	Mar	AMMR	-6.0%±14%	JPL C-band SAR	(6)

(1) Cavalieri et al. (1986)
(2) Steffen and Maslanik (1988)
(3) Steffen, unpubl. data (1990)
(4) Martin et al. (1987)
(5) Steffen and Schweiger (1991)
(6) Cavalieri et al. (1991)

*The algorithm has been used with SMMR, SSMI, and AMMR data
++Including new ice
.*Excluding data from 1 of the 4 flights which gave anomalously large and unexplained biases.
**Including data from all 4 flights.

Table 10.1. Summary Results From the DMSP SSM/I Sea Ice Validation

Sea Ice Parameter:		
Ice-edge location (AMMR/SSMI):		15% SSM/I concentration contour is within 25 km of initial ice band; 38% concentration is within 25 km of main ice pack.
Total sea ice concentration		Global TP
	Landsat/SSMI:	
	All Winter Cases:	Mean -3.6% S.D. 6.6%
	Aircraft/SSMI:	
	All March data:	Mean -2.4% S.D. 2.4%
Multiyear sea ice concentration		
	Aircraft/SSMI:	
	All March data:	Mean +12.0% S.D. 11.0%

SUMMARY OF ALGORITHM ATTRIBUTES

- PR AND GR ARE NORMALIZED PRINCIPAL COMPONENTS
- ALGORITHM OUTPUT IS INDEPENDENT OF PHYSICAL TEMPERATURE TO FIRST ORDER
- ALGORITHM OUTPUT
  - N.H. TOTAL AND MULTIYEAR SEA ICE CONCENTRATIONS
  - S.H. TOTAL SEA ICE CONCENTRATION
- PROVIDES A CONTINUOUS TIME-SERIES WITH THE ALMOST 9 YEARS OF SMMR DATA
- DEMONSTRATED ALGORITHM ACCURACY
  - TOTAL ICE CONCENTRATION ± 6.6%
  - MULTIYEAR ICE CONCENTRATION ± 11.0%
- SSM/I WEATHER FILTER
- SEASONAL SEA ICE ZONE ALGORITHM PROVIDES:
  - REDUCED ICE CONTRATION BIAS
  - MAPPING OF NEW, YOUNG AND FIRST YEAR ICE

(8 pp)

ISSUES AND CONCERNS
SPN SSM/I Algorithm Symposium

Date: 6.8.93

Author(s): Gloersen

1. What is the problem? Provide subject, scope and illustration if necessary.

A number sea ice and snow cover algorithms presented do not explicitly solve for, or eliminate the physical temperature variable. The snow cover algorithms generally have been applied only in local areas, where it might be argued that the spatial variation in physical temperature might be acceptably small over a sufficiently small time interval. But what happens over a long time interval or large spatial scale? A similar defense and question applies to the sea ice algorithms referred to. To illustrate the latter, Figure 1 shows some brightness temperatures at 18V and 37V calculated for eight different physical temperatures 5°C apart and for first-year (FY) and multiyear (MY) sea ice, and for a 50-50 mixture of FY & MY. The 35°C temperature span is typical of the spatial variation over the Arctic and Antarctic sea ice surface temperatures during their respective winters, and of the temporal variation over the course of a year. In the bootstrap algorithm,

2. How did we get here? What do we know about the problem? How long has it existed? What brought the problem into being? What are the effects of the problems we see now or in the future?

for instance, this represents about a ±12 % error (See Fig 1). The experimental realization of this situation is shown in Fig. 2, a single-day collection of 18V & 37V T_B's from SSM/I from the entire sea ice canopy surrounding Antarctica in mid-July (not the coldest part of austral winter), & perhaps indicating similar temperature variations.

ISSUES AND CONCERNS
SPN SSM/I Algorithm Symposium

3. Where do we want to come out? Specify goal in terms of complete, acceptable or compromise solution(s). What are the criteria for an acceptable solution?

"Global" algorithms (i.e with spatial and temporal coverage) demands taking into account physical temp variations at the very least.

4. Which is the best solution? Consider drawbacks and implementation.

Using radiance (brightness temperature) ratios takes out the dependence on physical temperature to at least first order. The "NASA Team" algorithm accomplishes this with polarization (PR) and spectral gradient ratio (GR) parameters. The data shown in Fig. 2 have been plotted in PR-GR space in Figure 3. Now the point scatter can be more confidently interpreted as ice concentration (and type) variation since the physical temp variations have been ratioed out.

For snow-cover, the GR-parameter would remove part of the global and temporal variations observed. The spatial and temporal variation of snow grain size does remain as an equally serious concern, however.

5. Agreement and plan for action:

SSMI Algorithm Symposium: June 8-10, 1993 at Monterey, California

The Bootstrap Technique for Deriving Geophysical Sea Ice Parameters from Multichannel Passive Microwave Data

Joey C. Comiso
Laboratory for Hydrospheric Processes, NASA/GSFC, Greenbelt, MD

ABSTRACT

Sea ice concentration and ice type are two of the basic parameters over the polar oceans which can be derived from multichannel passive microwave data. Because of coarse resolution, a mixing formalism has to be implemented to determine ice concentration and the areal coverage of the different ice types. However, since the multichannel data are basically two dimensional, a mixing formalism that includes ice classification is effective only if there are at the most three dominant surface types within the satellite footprint. The bootstrap technique makes use of characteristics of the SSMI data as a basis for deriving ice concentration and ice type. It takes advantage of the fact that vast areas within the ice pack have nearly 100% ice cover, as confirmed by aircraft and helicopter flights, ship observations, and fine resolution satellite data. Multichannel cluster analysis indicates that data in consolidated ice region behave in a predictable fashion. The signature of open water can also be uniquely identified. The algorithm incorporates this information in a radiative transfer equation to determine ice concentration, without making assumptions about ice type. Some ambiguities in this formulation exist due to the presence of new ice which is difficult to discriminate from mixtures of thicker ice types and open water. The problem is that the radiative signature of new ice, which forms in open water under very cold environment, evolves from that of open water to that of thick ice as form, structure, and thickness changes. Another source of error is flooding, wetness, and spatial and temporal variations in snow cover and surface characteristics. Also, some channels are sensitive to atmospheric effects which cause further uncertainties especially during adverse weather conditions. The ambiguities have been evaluated and results indicate average errors of about 7% in consolidated ice regions to about 20% in the marginal ice zone and other very active regions. The latter is high because of inappropriate emissivity used in the algorithm for new ice which cannot be discriminated from mixtures of thick ice and open water. This error has been minimized by applying an ice classification algorithm on a regional basis, assuming that there are only three dominant surface types in each region. The different regions are identified using an unsupervised cluster analysis (and a neural network) that makes use of all channels including the 85 GHz channel. This method calculates both ice concentration and ice type fractions in each region. Comparison of results with in-situ and other SSMI validation data will be presented.

SPN SSM/I ALGORITHM SYMPOSIUM
Algorithm Questionnaire

"Bootstrap Sea Ice Algorithm"
Joey Comiso, respondent

Please provide the following essential information about your algorithm(s).

* ALGORITHM DESCRIPTION

- Type (statistical, physical, other) *Statistical and physical*

- Input required / Output produced

Input: Brightness Temperatures from 19 GHz (v- and h-pol); 37 GHz (v- and h-pol);

Output: Total ice concentrations; Multiyear ice type concentrations and regimes

- Auxiliary sensor/data base requirements *None*

- Major limitations / approximations

Due to the spatial resolution of the SSM/I footprint, it is not possible to discriminate open water and new ice areas within the inner ice pack

- Computer resource requirements *Workstation*

* ALGORITHM PERFORMANCE

- Development / test data sets (regional / global / seasonal)

Bootstrapped from global data. Further testing used regional in-situ data. (See Comiso and Sullivan, "Satellite microwave and in-situ observations of the Weddell Sea ice cover and marginal ice zone," J. Geophys. Res., 91, pp. 9663-9681, 1986)

- Ground truth (accuracy / limitations)

Several cruises to the Antarctic, the Arctic and flight programs in the Arctic

- Major assumptions of evaluation

"Consolidated cluster" of 19 GHz v. 37 GHz brightness temperatures is approximately near 100% ice cover

* ALGORITHM PERFORMANCE (continued)

- Strengths / weaknesses

The algorithm accounts for most of the spatial changes in surface emissivities, including snow ans flooding.

* ALGORITHM MATURITY

- Operational useage

Archived and distributed worldwide on CD-ROM by the NOAA Snow and Ice Data Center (Boulder, CO). Used in several scientific publications.

- Refinement / additional development

Use of neural net for ice type classification

- Availability

Algorithm is available upon request.

ISSUES AND CONCERNS
SPN SSM/I Algorithm Symposium

Date: 6/10/93

Author(s): Joey Comiso

1. What is the problem? Provide subject, scope and illustration if necessary.

a Summer Ice - emissivities of sea ice drastically change during the spring/summer period.

b. New Ice - emissivity intermediate between fluid ice and ~~flow~~ open water

c. Flooding - as much as 30% in some areas emissivity for some channels can drastically change.

2. How did we get here? What do we know about the problem? How long has it existed? What brought the problem into being? What are the effects of the problems we see now or in the future?

a) Problem is old but solution is poor due mainly to lack of validation data. With SAR - product can be improved to remove bias but rms error is still large

b) Problem is old. Solution difficult because of small features compared to satellite footprints.

c) Problem not well quantified. Discovered in recent cruises.

Tony Gross

ISSUES AND CONCERNS
SPN SSM/I Algorithm Symposium

3. Where do we want to come out? Specify goal in terms of complete, acceptable or compromise solution(s). What are the criteria for an acceptable solution?

a) Want good quantification of Summer Ice
- very important for climate studies & navigation. Solution should be consistent w/ SAR results.

b) Need to assess accuracy for heat flux studies & Salinization statics

c) Results should be consistent w/ in situ observations

4. Which is the best solution? Consider drawbacks and implementation.

a) Local algorithms & correlation analysis w/ SAR data

b) local algorithms - use of ancillary data

c) local algorithms — MIZ vs Inner Zone

5. Agreement and plan for action:

Use SAR retrievals to readjust tie points for local algorithms of all cases — a), b) & c).

The Bootstrap Technique for Deriving Geophysical Sea Ice Parameters from SSM/I Data

Joey Comiso/NASA GSFC

OUTLINE OF TALK:

1. **Introduction**
   Background; Why bootstrap?

2. **Physical and Electrical Properties of Sea Ice**
   Thickness, Salinity, Snow Cover, Wetness

3. **Theoretical Studies**
   Frequency Dependence, Polarization Dependence
   Roughness and Flooding Effects

4. **Phenomenological Analysis**
   Cluster analysis - 2D&3D, Isoclass,
   Time Series/Summer Ice, Regional Effects

5. **The Bootstrap Technique**
   Radiative transfer/mixing formulation
   Arctic/Antarctic techniques
   Filter for Atmospheric Effects

6. **Validation and Error Analysis**
   Northern and Southern Hemispheres
   Marginal Zone/Summer Ice

7. **Conclusions**

BACKGROUND

- Satellite PM data available since 1972. ESMR, SMMR, and SSMI in CD ROM/Atlases
- Passive Microwave provides comprehensive spatial and temporal coverage.
- Data is suitable for mapping large scale features of the ice cover.
- Coarse Resolution - cannot resolve leads, ridges, most icebergs.
- Main Product: Ice concentration, type, and extent.

WHY BOOTSTRAP?

- Theoretical inversion technique cannot be implemented effectively because sea ice is too complex to model accurately.

- Even with a good model, retriving sea ice parameters is not simple because of large spatial and temporal variations of sea ice emissivities and atmospheric effects. Also, calibration of satellite data is not perfect.

- The multichannel brightness temperature of sea ice cover show consistent patterns which can be readily implemented in a bootstrap phenomenological formulation. Interpretation of such patterns have been found to be consistent with aircraft and ship observations.

PHYSICAL BASIS OF SURFACE TYPES:

- o age/thickness (e.g., new, young and first year ice)
- o age/salinity (e.g., first year and multiyear ice)
- o roughness - rafted, ridged
- o snow cover (fine, granular, thick)
- o Wetness (on snow, on snow/ice interface)

RADIATIVE TRANSFER BASIS OF SURFACE TYPES:

- o emission: lossy for new, young and first year ice

  transparent for multiyear ice
- o scattering: high for granular or thick snow cover

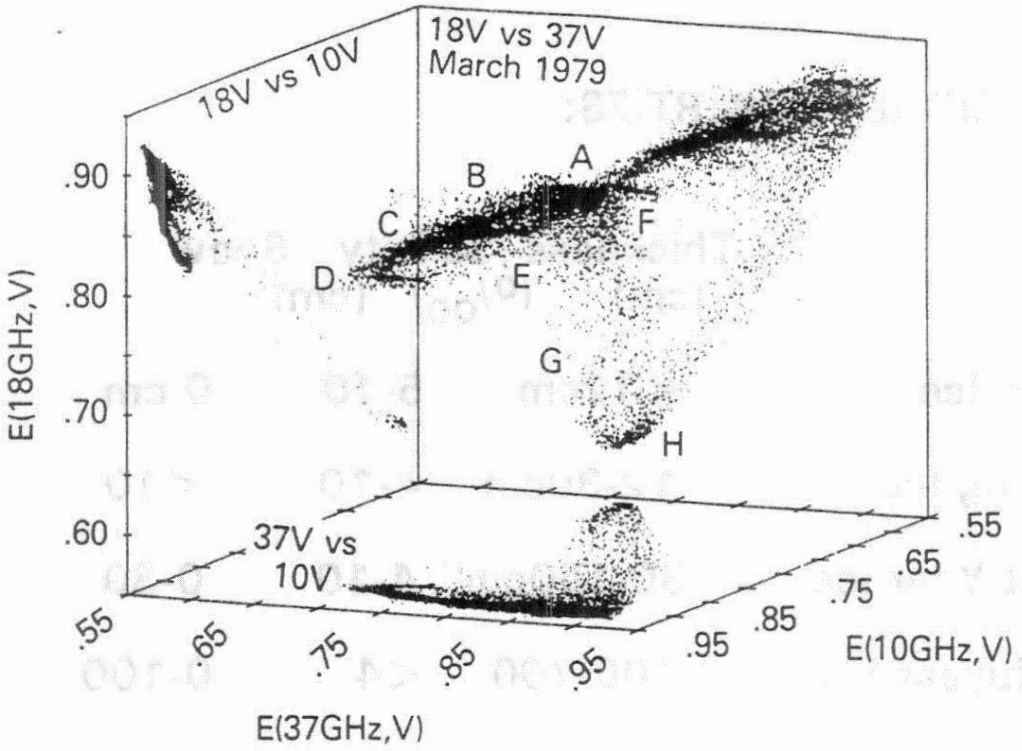
  high for multiyear ice

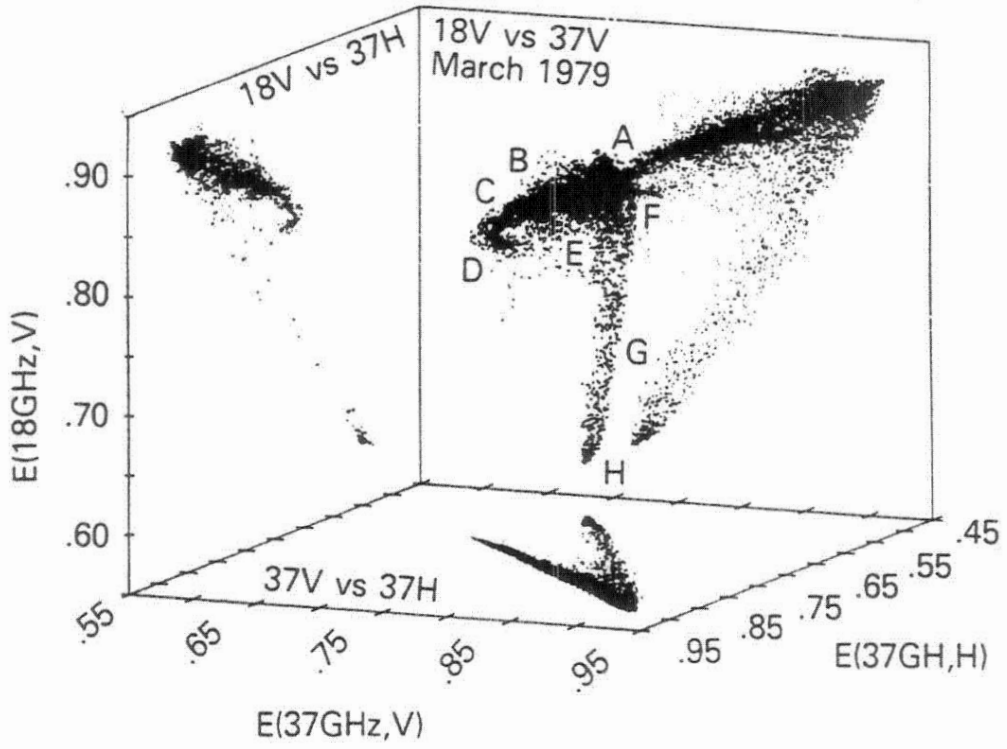
  high for snow ice/ice lenses at the interface
- o frequency, polarization, and atmospheric dependence

PHYSICAL PROPERTIES:

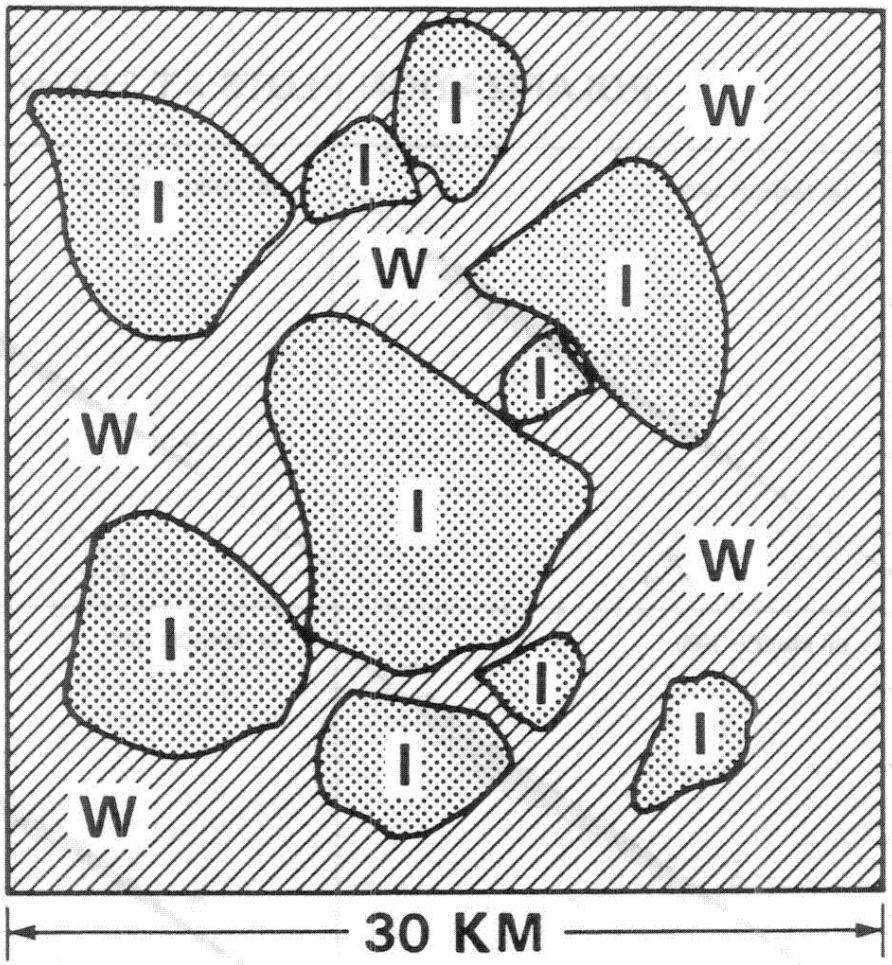
	Thickness (cm)	Salinity ($^{o}/_{oo}$)	Snow (cm)
New Ice	<12cm	5-10	0 cm
Young Ice	12-30cm	4-10	<10
First Year Ice	30-150cm	4-10	0-30
Multiyear Ice	100-700	<4	0-100

3-D characteristics of ice clusters





Bootstrap Technique for 2 surface types - ice & water



$$T_B = C_W (\varepsilon_W T_W + T_{AW}) + C_I (\varepsilon_I T_I + T_{AI})$$

$$C_W + C_I = 1$$

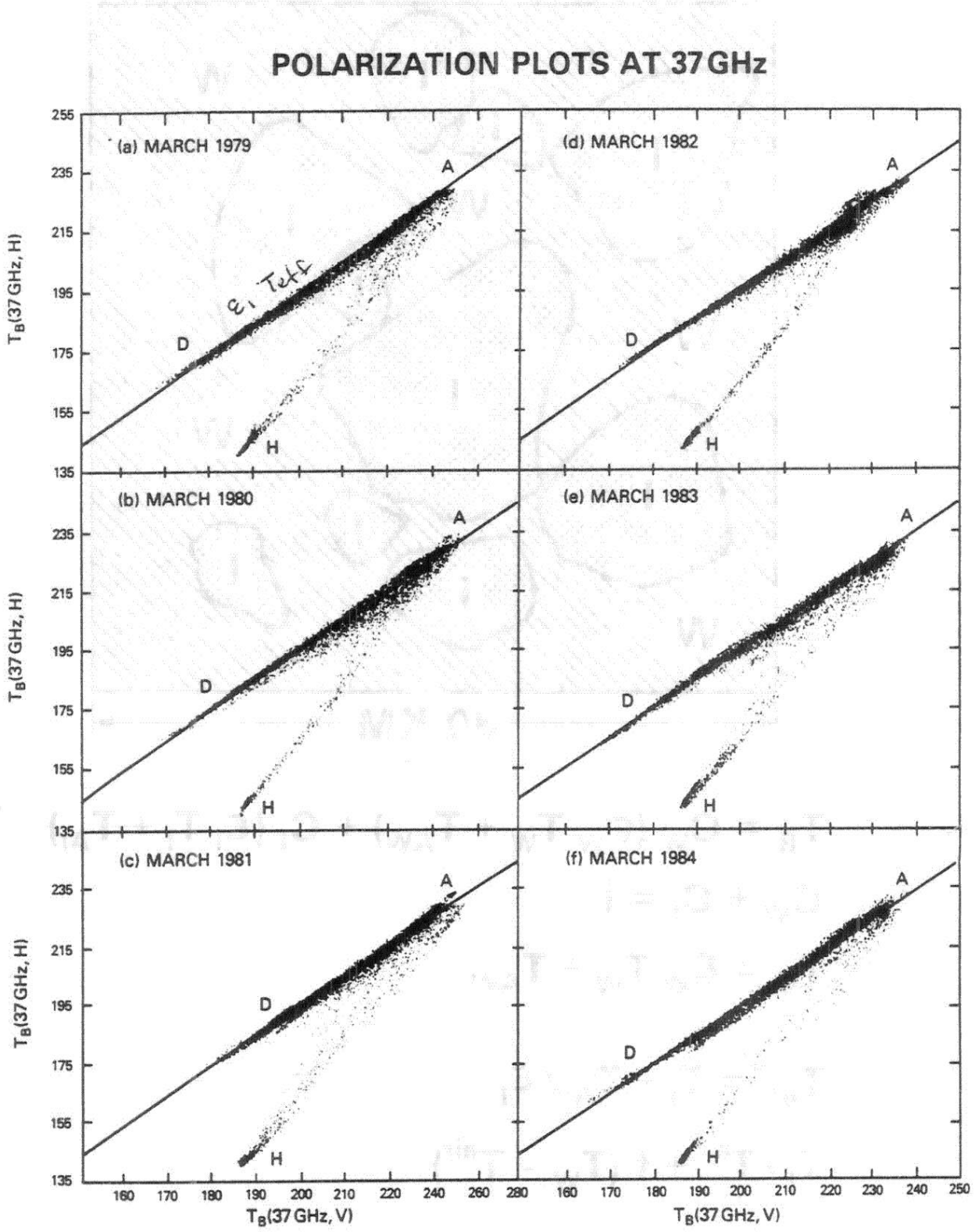
$$T_O = \varepsilon_W T_W + T_{AW}$$

$$T_{eff} = T_I + T_{AI} / \varepsilon_I$$

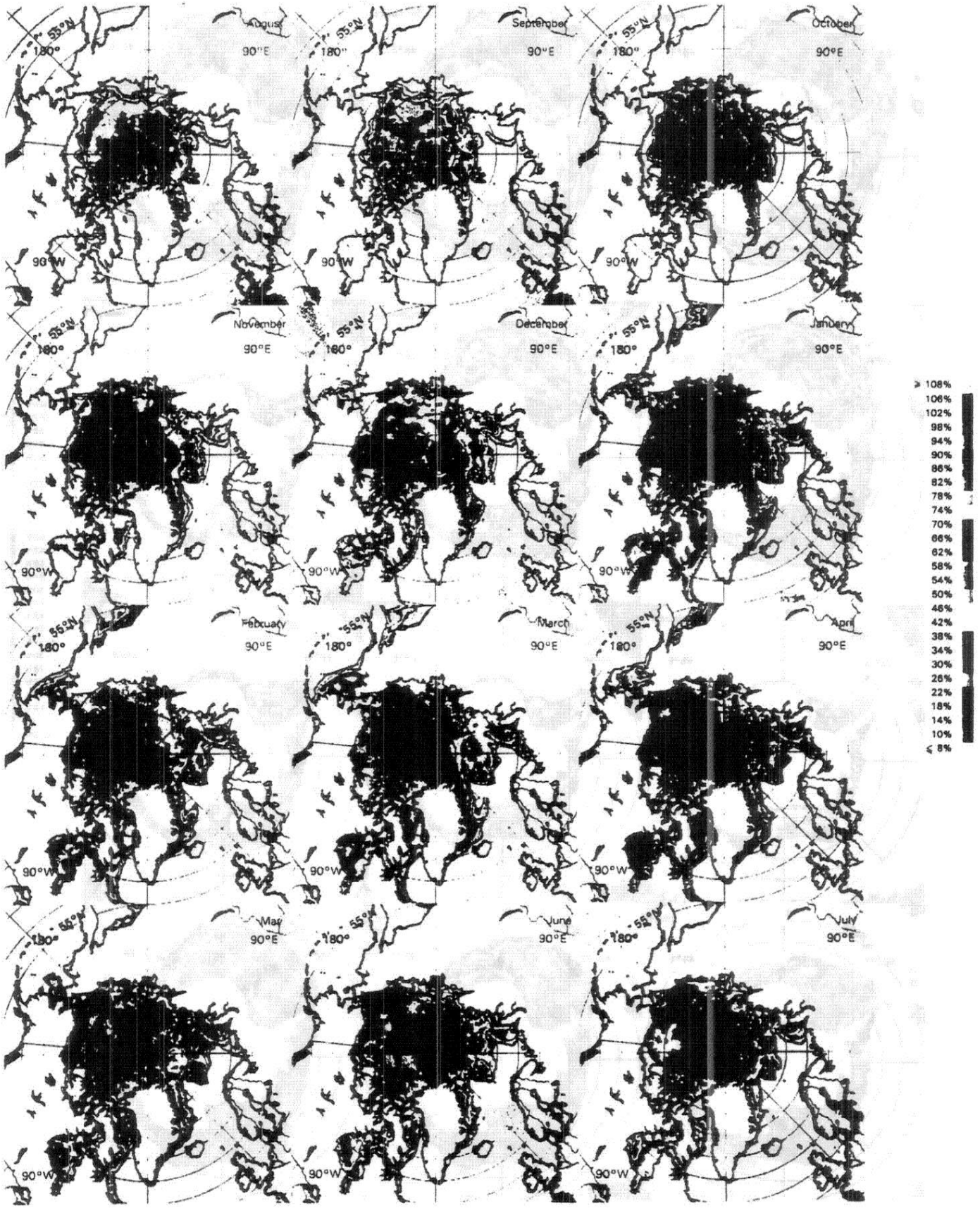
$$T_I = T^{air} + f (T_W - T^{air})$$

$$C_I = \frac{T_B - T_O}{\varepsilon_I T_{eff} - T_O}$$

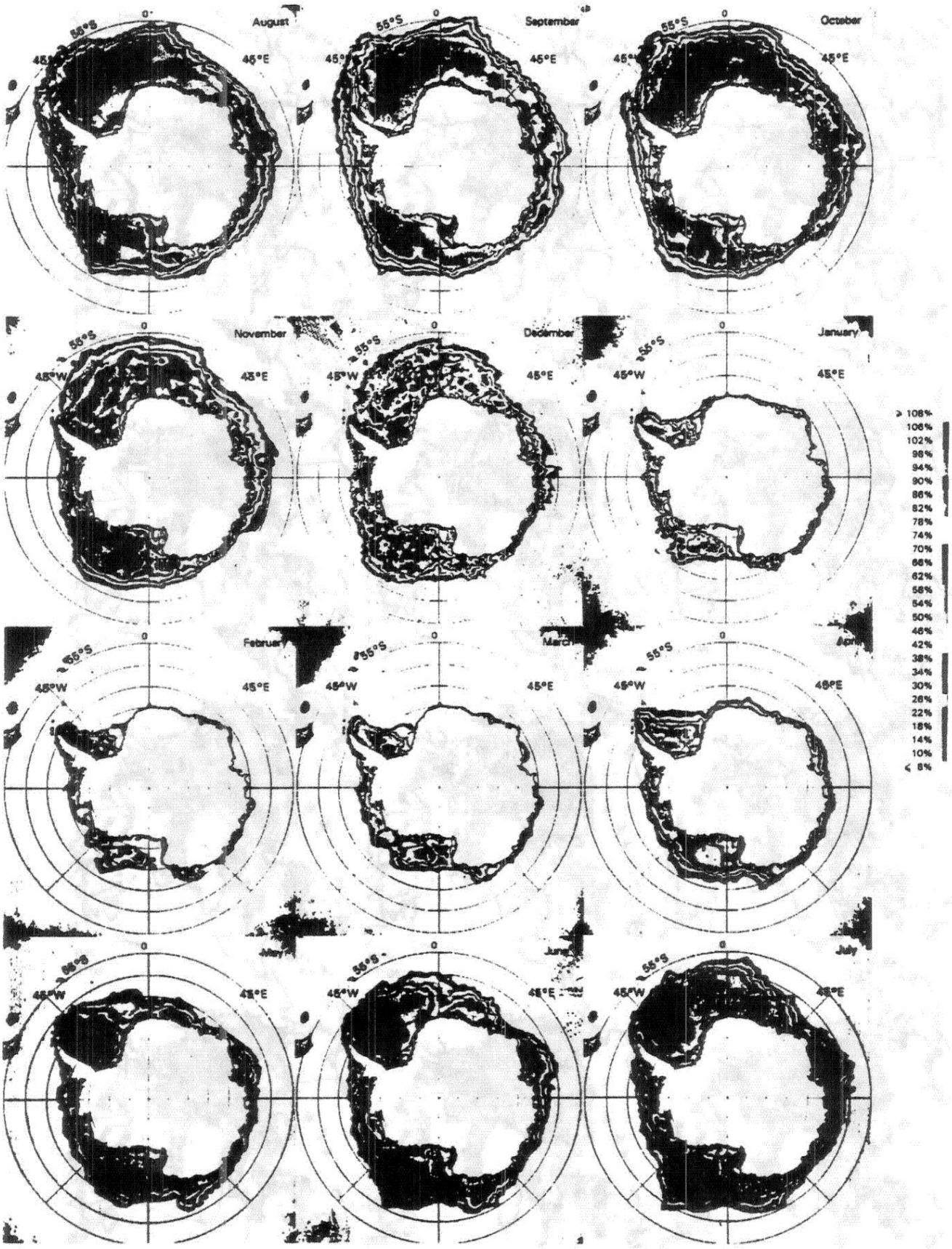
consistency check - several years of data

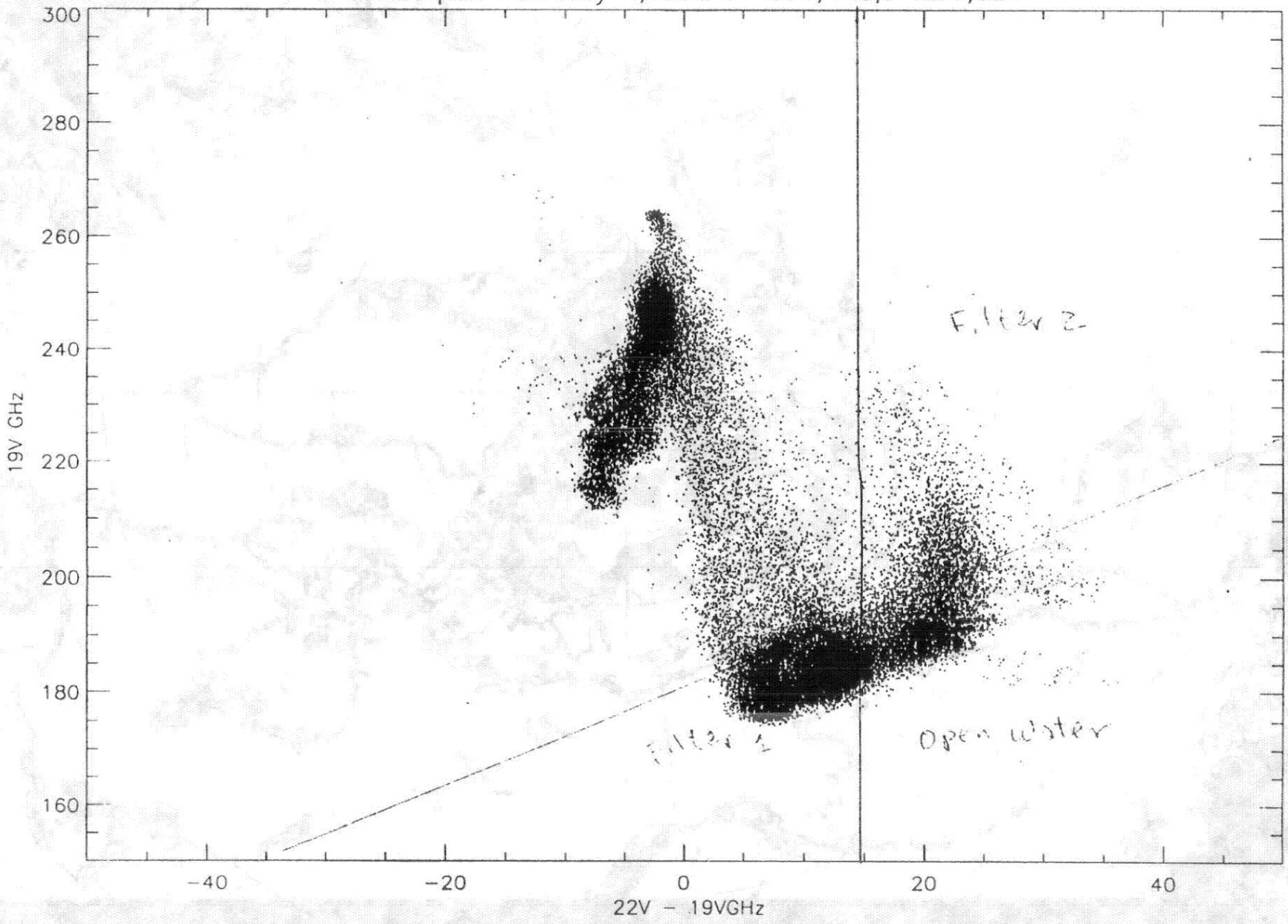


Arctic Sea Ice
August 1987–July 1988



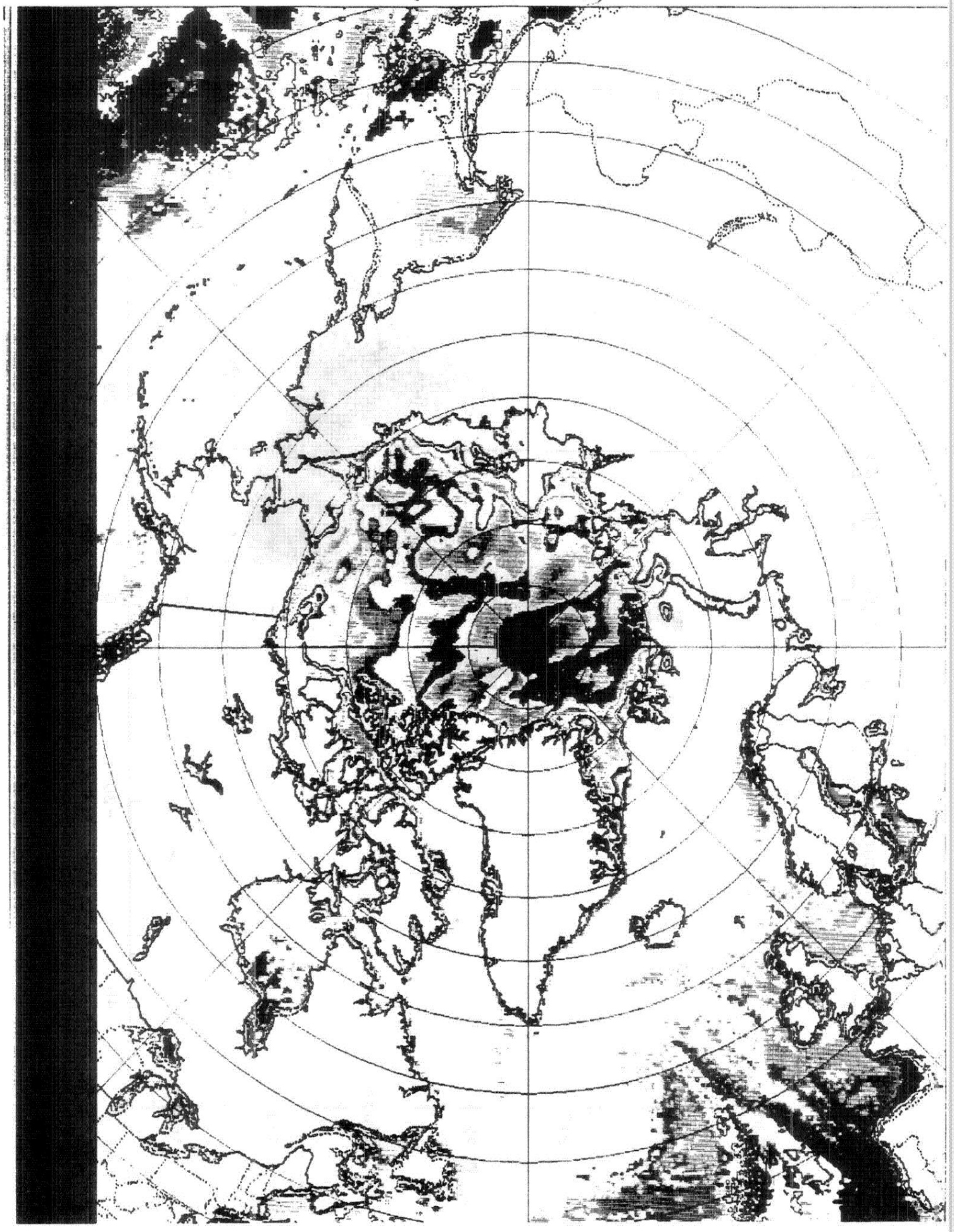
Antarctic Sea Ice
August 1987–July 1988



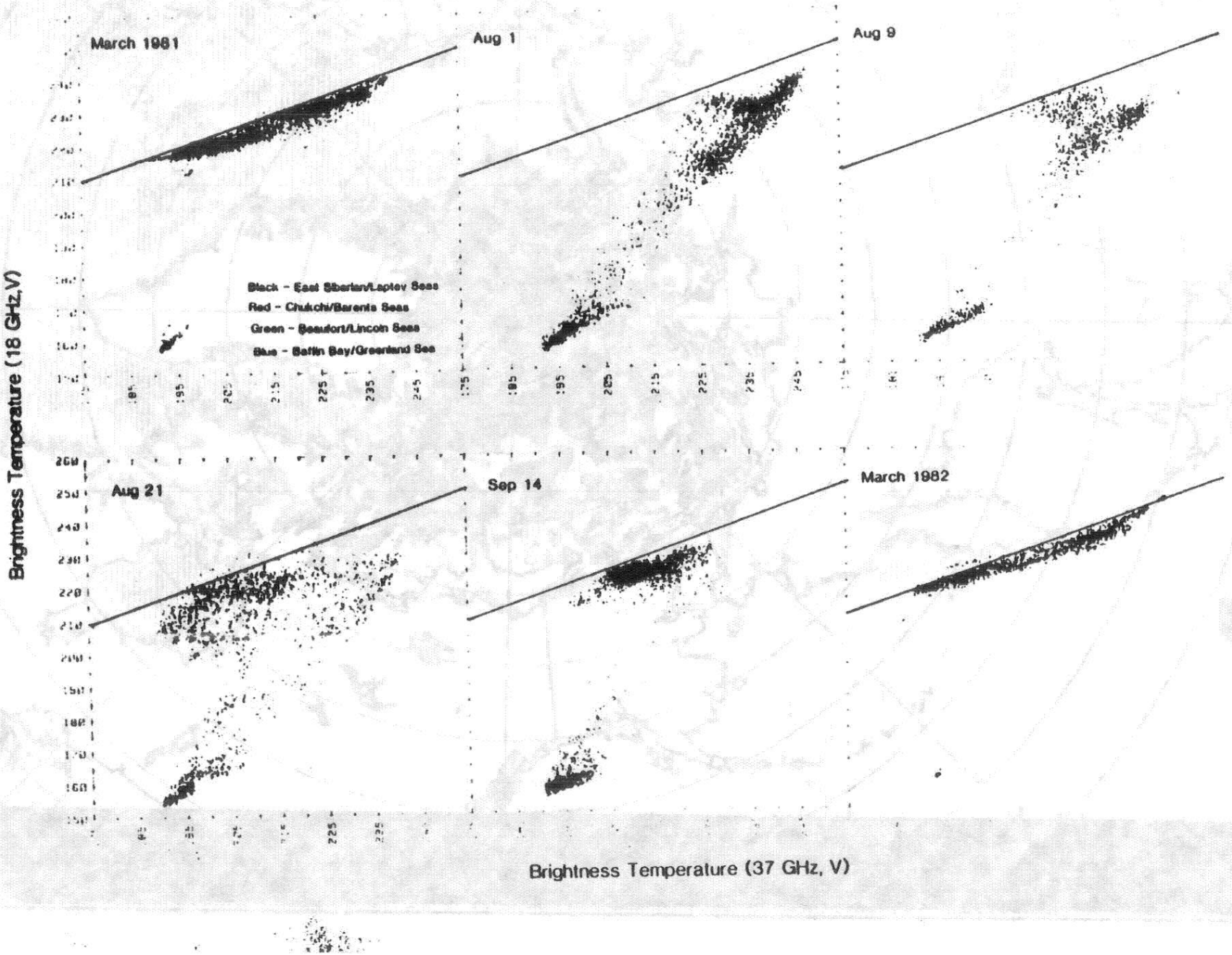


ATMOSPHERIC FILTER

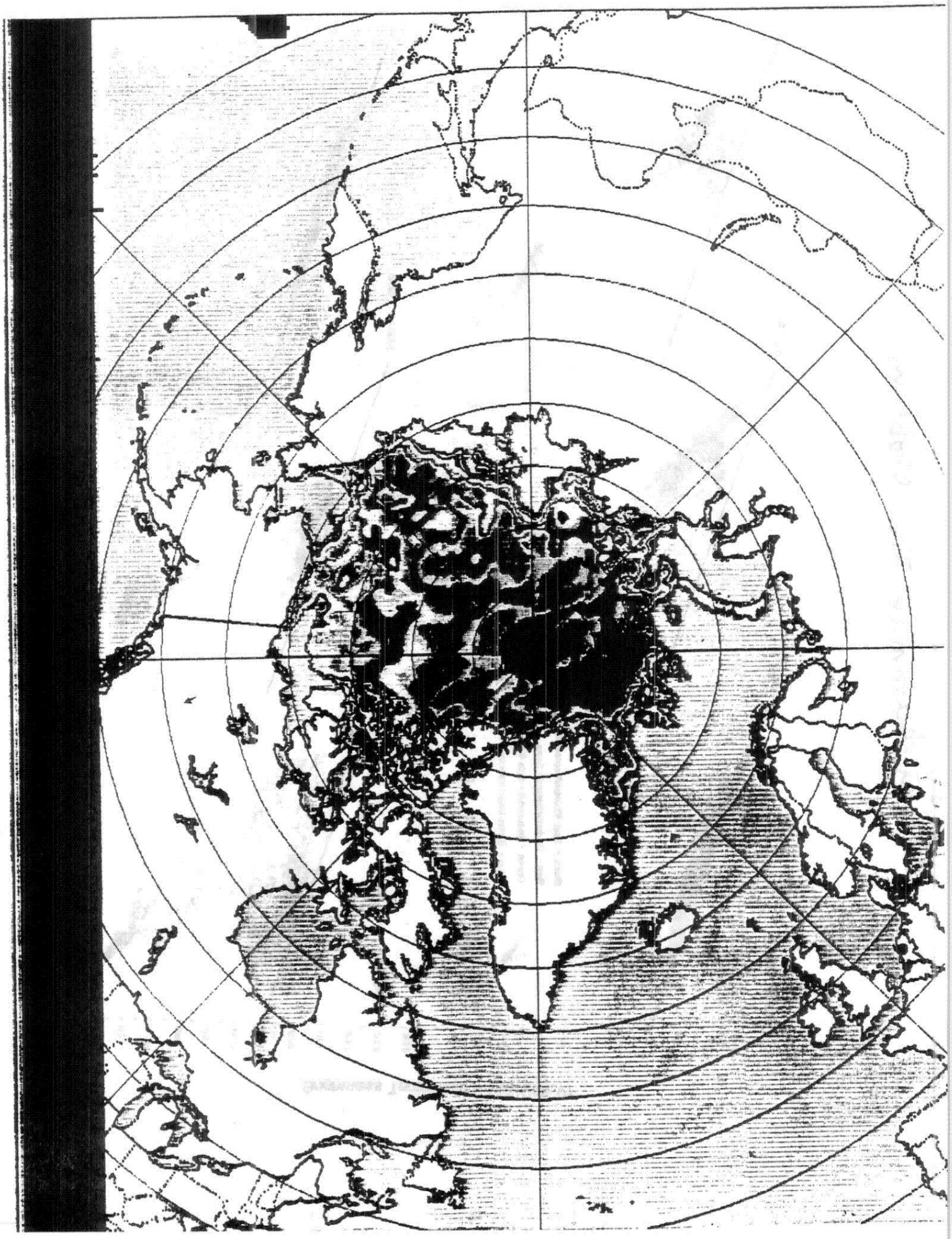
with filter 1 Only



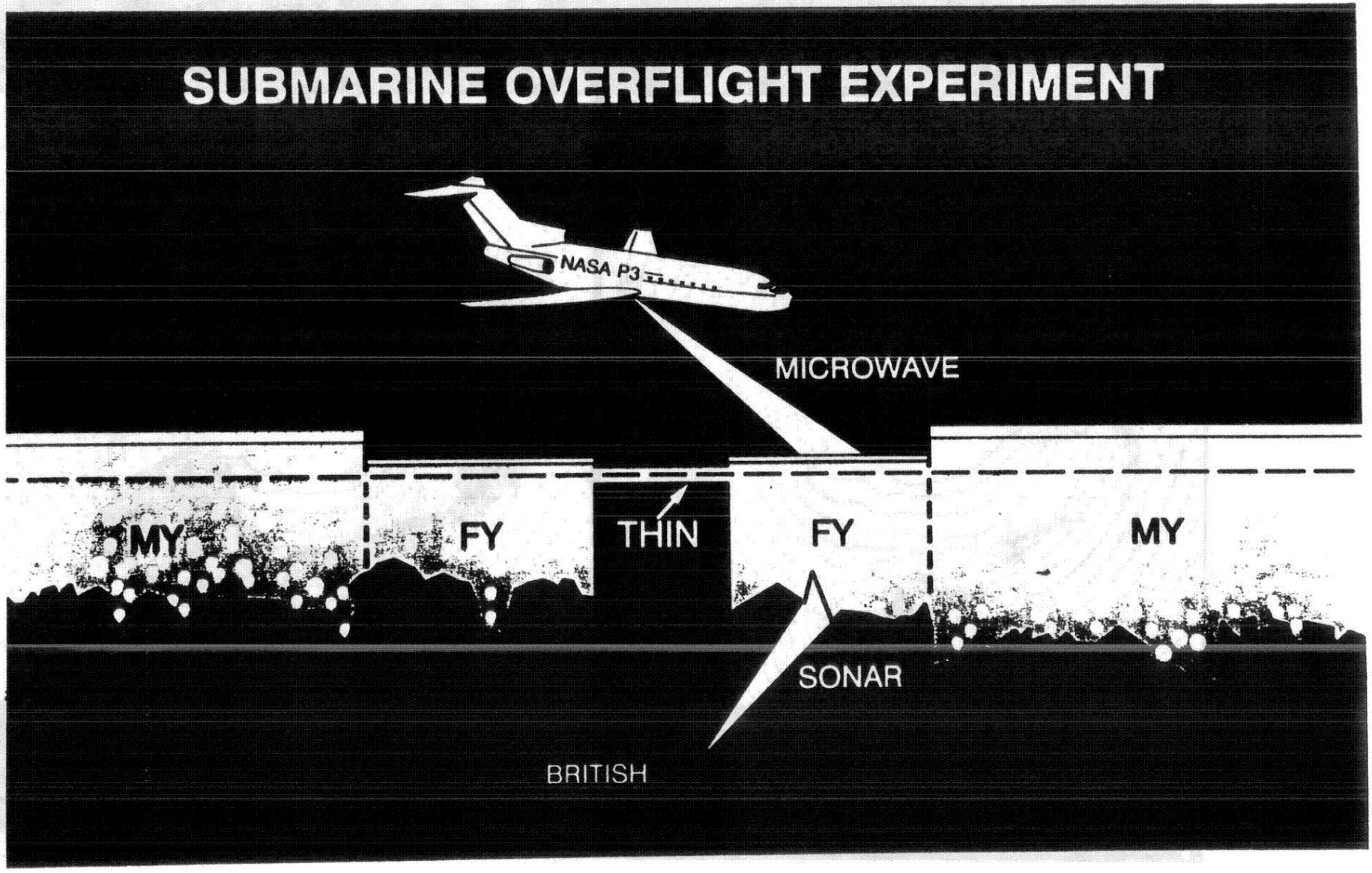
Spring/Summer Ice Problem



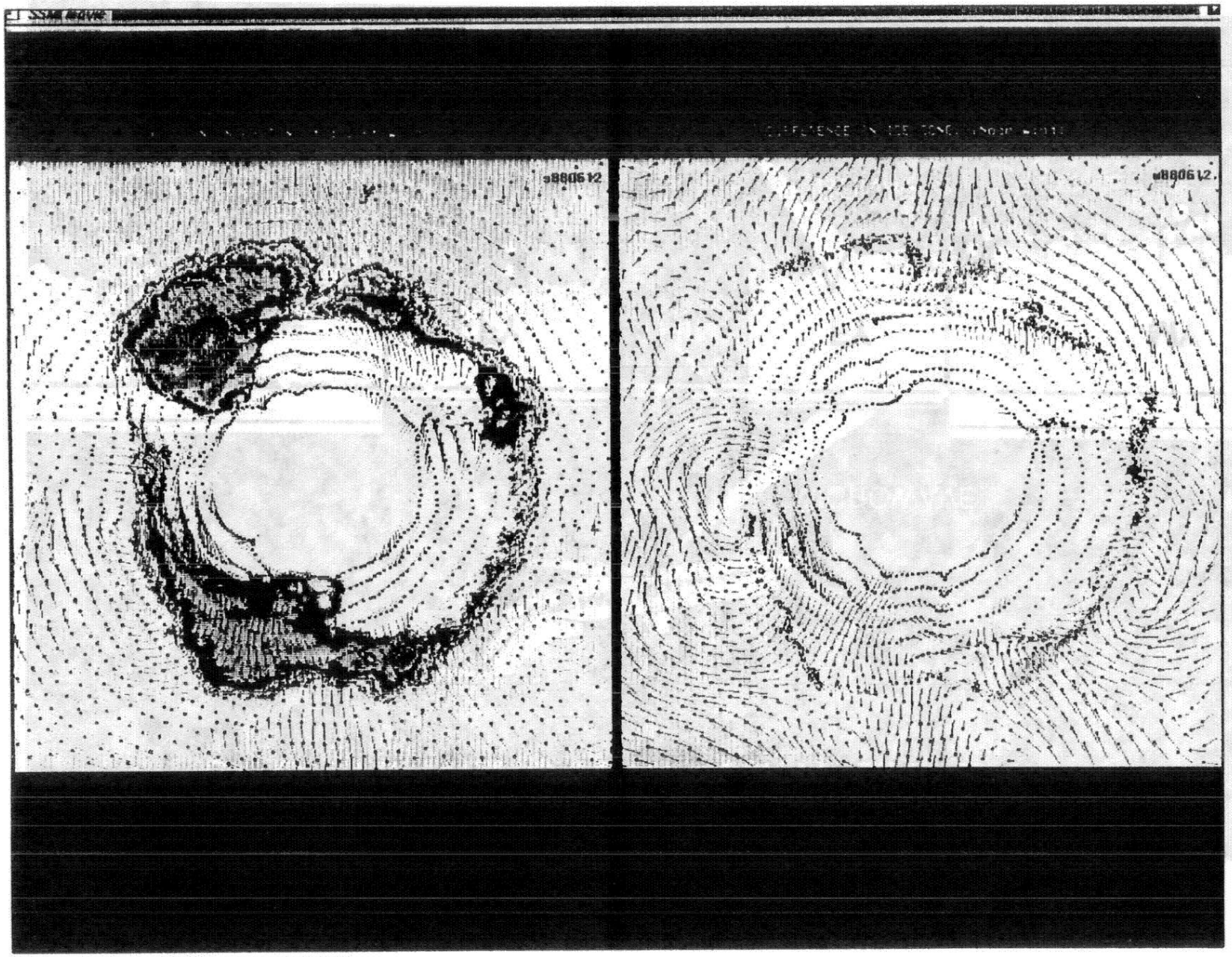
L Atmosphere effect in open water disappears with filter 1 + filter 2



Validation (Aircraft/Submarine Project)

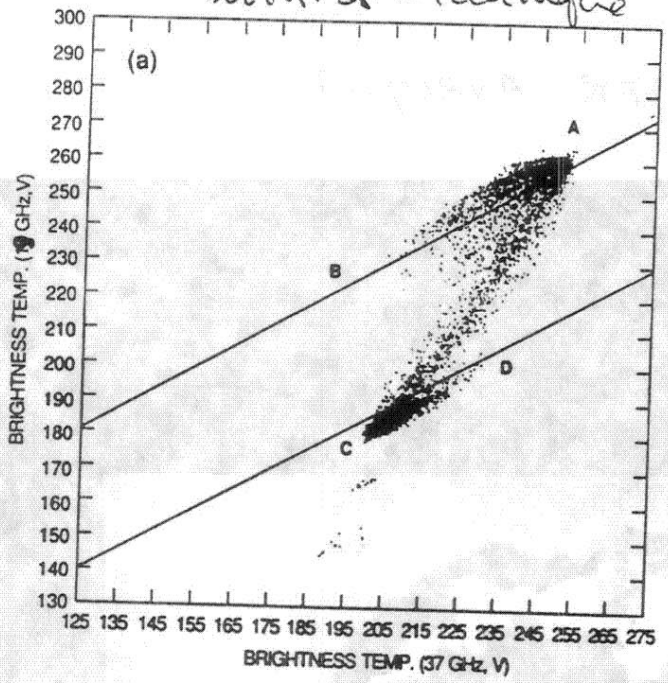


New Ice / Advection Problem

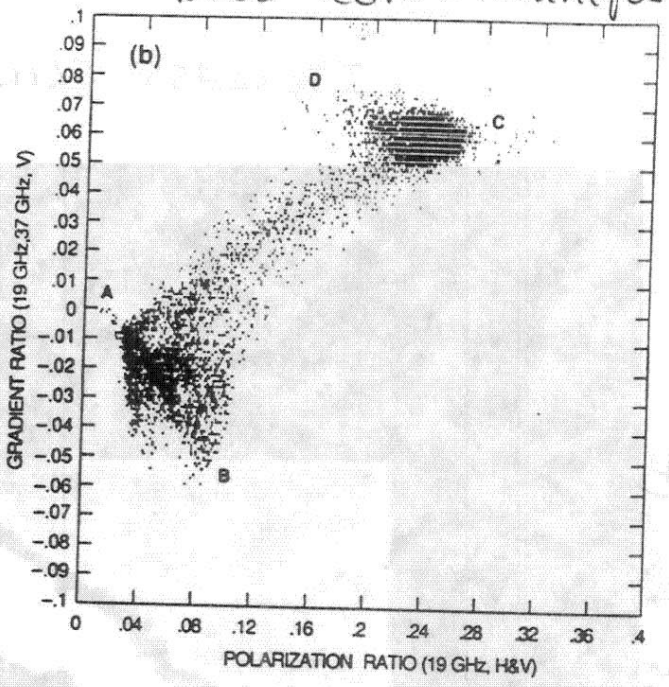


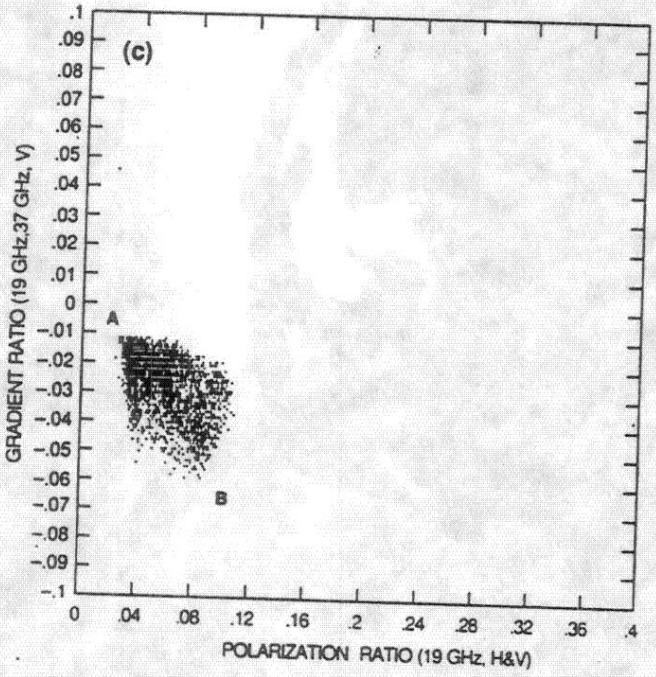
Tie Point for consolidated Ice (AB) needs further validation

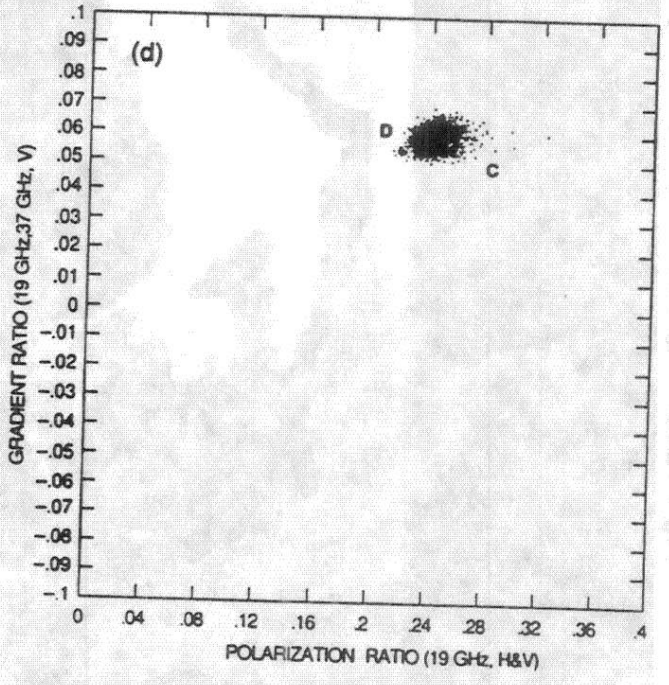
Bootstrap - technique



Nasa team - technique

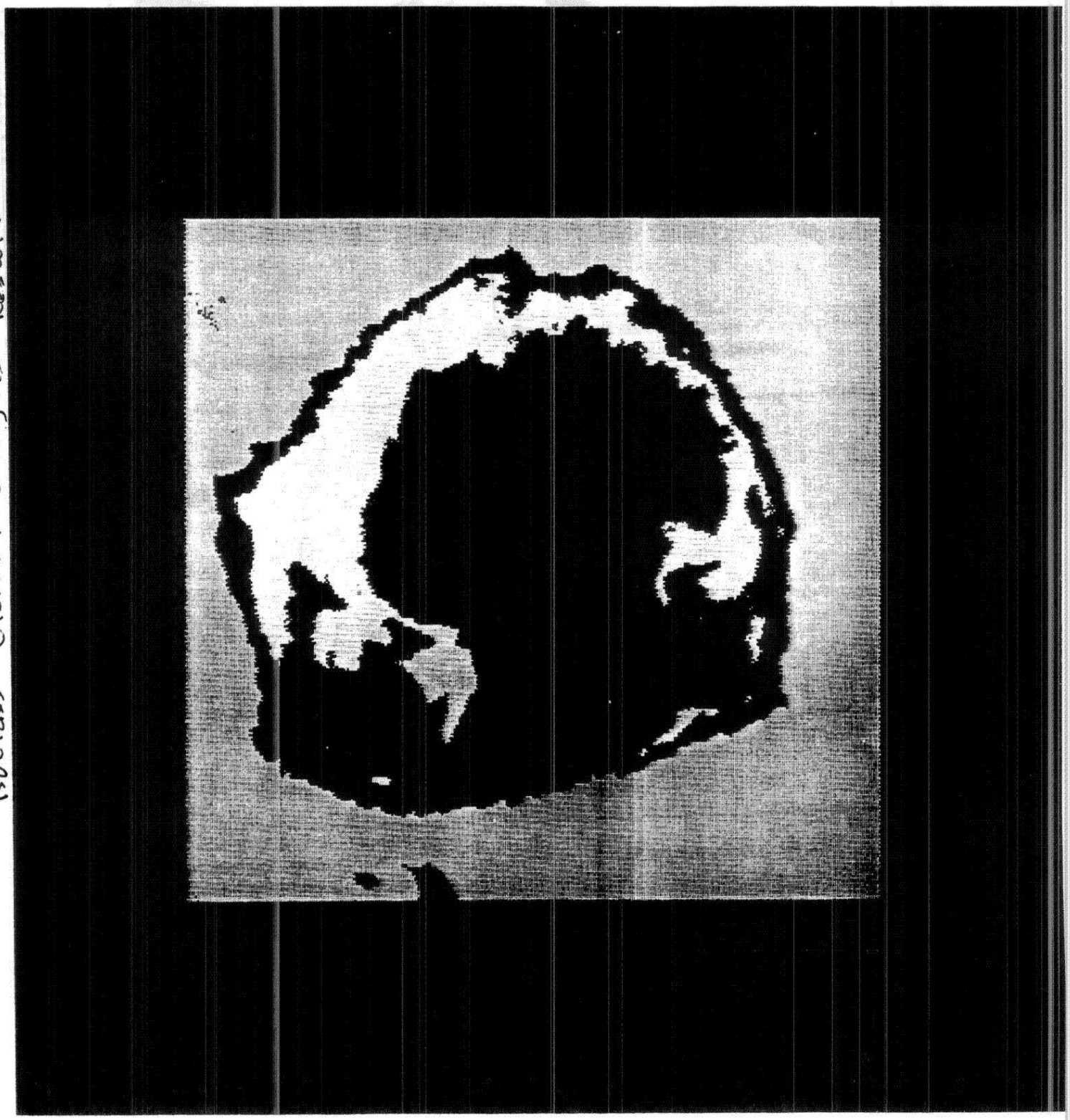






from Comiso et al (1992)

ISOCLASS CLUSTER ANALYSIS



Isoclass Clusster analysis Result

REFERENCES:

Grenfell, T.C., J.C. Comiso, M.A. Lange, H. Eicken, and M.R. Wenshahan, Passive microwave observations of the Weddell Sea, J. Geophys. Res., (Submitted, February 1993)

Comiso, J.C., Satellite remote sensing of the Polar Oceans, J. Mar. Sys., 2, 395-434, 1991.

Comiso, J.C., P. Wadhams, W. Krabill, R. Swift, J. Crawford, and W. Tucker, Top/Bottom multisensor remote sensing of Arctic sea ice, J. Geophy. Res., 96(C2), 2693-2711, 1991.

Comiso, J.C., Arctic Multiyear ice Classification and Summer Ice Cover using Passive Microwave Satellite Data, J. Geophys. Res., 95(C8),13411 -13422,13593-13597, 1990.

Comiso, J. C., T. C. Grenfell, D. L. Bell, M. A. Lange, and S. F. Ackley, Passive Microwave In Situ Observations of Winter Weddell Sea Ice, J. Geophy. Res., 94, 10891-10905, 1989.

Grenfell, T., and J. C. Comiso, Multifrequency Passive Microwave Observations of First Year Sea Ice Grown in a Tank, IEEE Trans. on Geos. and Rem. Sensing, GE-24,826-831,1986.

Comiso, J. C. and C. W. Sullivan, Satellite Microwave and In-Situ Observations of the Weddell Sea Ice Cover and its Marginal Ice Zone, J. Geophys. Res., 91, C8, 9663-9681, 1986.

Comiso, J. C., Characteristics of Winter Sea Ice from Satellite Multispectral Microwave Observations, J. Geophys. Rev., 91, C1, 975-994, 1986.

Comiso, J. C., Remote Sensing of Sea Ice using Multispectral Microwave Satellite Data, in Advances in Remote Sensing Retrieval Methods, ed. by A. Deepak, H. E. Fleming, and M. T. Chahine, A Deepak Publishing, Hampton, Virginia, pp. 349-368, 1985.

Comiso, J. C., S. F. Ackley, and A. L. Gordon, Antarctic Sea Ice Microwave *Signature and their Correlation with In-Situ Ice Observations*, J. Geophys. Res., 89, C1, 662-672,1984.

Comiso, J. C., Sea Ice Microwave Emissivities from Satellite Passive Microwave and Infrared Observations, J. Geophys. Res., 88, C12, 7686-7704, 1983.

Comiso, J. C., and H. J. Zwally, Antarctic Sea Ice Concentrations *Inferred from Nimbus-5 ESMR and LANDSAT imagery*, J. Geophys. Res., 87, C8, 5836-5844, 1982.

NASA BOOKS:

Zwally, H. J., J. C. Comiso, C. L. Parkinson, W. J. Campbell, F. D. Carsey, and P. Gloersen, Antarctic Sea Ice 1973-1976 from Satellite Passive Microwave Observations, NASA Spec. Publ. 459, 1983.

Parkinson, C. L., J. C. Comiso, H. J. Zwally, D. J. Cavalieri, P. Gloersen, and W. J. Campbell, Arctic Sea Ice 1973-1976 from Satellite Passive Microwave Observations, NASA Spec. Publ. 489, 1987.

Gloersen P., W. Campbell, D. Cavalieri, J. Comiso, C. Parkinson, H.J. Zwally, Arctic and Antarctic Sea Ice, 1978-1987: Satellite Passive Microwave Observations and Analysis, NASA Spec. Publ. 511, 1992.

AGU MONOGRAPH CHAPTERS:

Comiso, J.C, T.C. Grenfell, M. Lange, A. Lohanick, R. Moore, and P. Wadhams, "Microwave remote sensing of the Southern Ocean Ice Cover," Chapter 12, Microwave Remote Sensing of Sea Ice, (ed. by Frank Carsey), American Geophysical Union, Washington, D.C., 243-259, 1992.

Wadhams, P. and J.C. Comiso, "The ice thickness distribution inferred using remote sensing techniques," Chapter 21, Microwave Remote Sensing of Sea Ice, (ed. by Frank Carsey), American Geophysical Union, Washington, D.C., 375-383, 1992.

Eppler, D., M.R. Anderson, D.J. Cavalieri, J.C. Comiso, L.D. Farmer, C. Garrity, P. Gloersen, T. Grenfell, M. Hallikainen, A.W. Lohanick, C. Maetzler, R.A. Melloh, I. Rubinstein, C.T. Swift, C. Garrity, "Passive Microwave Signatures of Sea Ice," Chapter 4, Microwave Remote Sensing of Sea Ice, (ed. by Frank Carsey), American Geophysical Union, Washington, D.C., 47-71, 1992.

Steffen, K., D. J. Cavalieri, J. C. Comiso, K. St. Germain, P. Gloersen, J. Key, and I. Rubinstein, "The estimation of geophysical parameters using Passive Microwave Algorithms," Chapter 10, Microwave Remote Sensing of Sea Ice, (ed. by Frank Carsey), American Geophysical Union, Washington, D.C., 201-231, 1992.

Martin, S., K. Steffen, J.C. Comiso, D.J. Cavalieri, M. Drinkwater, B.M. Holt, "Microwave Remote Sensing of Polynyas," Chapter 15, Microwave Remote Sensing of Sea Ice, (ed. by Frank Carsey), American Geophysical Union, Washington, D.C., 303-311, 1992.

Grenfell, T.C, D.J. Cavalieri, J.C. Comiso, M.R. Drinkwater, R.G. Onstott, I. Rubinstein, K. Steffen, I. Rubinstein, D.P. Winebrenner, "Microwave signatures of new and young ice," Chapter 14, Microwave Remote Sensing of Sea Ice, (ed. by Frank Carsey), American Geophysical Union, Washington, D.C., 291-301, 1992.

CONCLUSIONS:

- Main Sources of Errors with Passive Microwave Data are:

  a. New Ice and its unpredictable emissivity.
  b. Too many ice types
  c. Surface Effects: Snow, Wetness, Meltponding.

- The Bootstrap Technique provides a consistent and accurate determination of the global sea ice concentration. Errors, especially those associated with snow, wetness, and roughness are minimined.

- Sea ice type classification can be accurately done if there are at the most only three radiometrically different surfaces. Local and seasonal algorithms would help solve the problem. Neural Net or Isoclass results can be used to identify the regions or ice regimes suitable for local studies.

- Passive Microwave Data can be made More Accurate with the aid of Ancillary Data, including SAR and AVHRR data.

NORSEX-85H Ice Concentration Algorithm for SSM/I

Kjell Kloster, O.M. Johannesen and Stein Sandven
Nansen Environmental and Remote Sensing Center
Solheimsvik, Norway

NORSEX-85H is an extension of the NORSEX algorithm, to take advantage of the improved spatial resolution of the 85 GHz SSM/I channels. The basic algorithm was developed after the NORSEX experiment in the Barent Sea in 1979 for use with SSMR data and published in the J. of Geophys. Research (1983). It computes total ice and the two ice types multiyear ice (MY) and first-year ice (FY), from the two channels 18V and 37V. Only vertical polarization is used since it is less sensitive to surface structure (snow layering, roughness) than the horizontally polarized channels.

The ice emissivities and the atmospheric opacities used in the algorithm were measured during the NORSEX-79 experiment. Ocean water emissivities are theoretical values published by Stogryn (1971). A minor change in the water emissivities is made when SSM/I data are inputted instead of SMMR data.

Brightness temperature at the surface is modelled as the linear combination of the area-fraction of water, FY-ice and MY-ice in the field-of-view. A simple atmospheric model with surface air temperature as parameter is used to convert satellite-observed brightness temperature to surface-observed brightness temperature.

The NORSEX algorithm requries that input brigntness values are adjusted, if necessary to correspond to model values for calm open polar water. This adjustment is made based on a few suitable scenes and thereafter kept unchanged.

A rough estimate of the average surface air-temperature over pack ice (100% ice) is inputted for each scene (found e.g. from seasonal mean values or by automatic ice stations). The NORSEX output are percentages of open water, FY-ice and MY-ice with spatial resolution of approx. 60km for SSM/I (the resolution of 19V).

85H is very sensitive to the difference between water and FY-ice. It is also very sensitive to the atmosphere. It is used to sharpen the ice-water boundary (especially effective at the ice edge) in the following way. 85H is spatially lowpass filtered to the NORSEX resolution of 60km. NORSEX values are then multiplied with the ratio of the 85H signal to the lowpass-filtered 85H signal. This results in an image with a spatial resolution of approx. 20km, given by the 85H signal, and with ice concentraion values given primarily by the NORSEX algorithm.

The algorithm was developed at NERSC by K.Kloster for use under the SIZEX'92 experiments in the Greenland and Barents Sea. The ice edge defined e.g. by the 30% contour line compares favorably with the ice-water boundary seen in near-simultaneous SAR images both under SIZEX'92 and under later experiments.

NERSC, 25.May 93 K.K.

NORSEX-85H SEA ICE ALGORITHM.

Description.

1. Selection of grid.
A suitable grid size, grid resolution and projection is chosen for the 2-dimensional arrays to be used.
For e.g. Svalbard waters, chosen grid parameters may be:
Gridsize in pixels: 256x, 256y.
Projection: Polar stereographic, with centerline along 0E, center pixel at 76N.
Grid (pixel) resolution: 6000m.

2. Read SSMI data to arrays.
Values of brightness temperatures in 18V, 37V and 85H channels are read to three arrays (to the nearest-neighbour gridcell using value geographical position).
Filtering/interpolation distances given below refer to SSMI-data from CNODDS, Monterey.
Output arrays are: 18V, 37V, 85H (brightness temperature arrays).

3. NORSEX ice compute.
For all gridcells with non-empty values , total ice and multiyear ice are computed, using the Norsex algrithm (for details, see under point 6).
Input parameter is: mean surface air temperature in the pack-ice (100%ice).
Input arrays are: 18V and 37V.
Output arrays are: TOT (total ice concentr.) and MY (multiyear ice concentr.).

4. Fill of empty gridcells.
Interpolation is done using distance-weighted average of non-empty gridcells out to a maximum distance, to compute values in empty gridcells.
This is done on the following Input and Output arrays:
TOT (using 18 000m max.dist.)
MY (using 18 000m max.dist.)
85H (using 6 000m max.dist.).

5. Unsharp masking to spatially sharpen total ice.
The 85H array is lowpass-filtered, using the average of all input-gridcells within a distance of 30 000m to compute the output-gridcell value.
TOT array values are multiplied by the ratio of unfiltered 85H to lowpass-filtered 85H values for all gridcells.
Input arrays are: TOT, 85H.
Output array is: TOT85 (sharpened total ice concentration).

6. Description of the NORSEX ice compute routine.

a) Enter mean atm.surf.temp.over 100% ice.
This is the mean temperature over pack-ice in the area of interest.
Use is made of temperature seasonal average, measured by buoys, etc.
E,g,: winter: 230 -250K, summer: 273K.

NORSEX-85H ICE -CONCENTRATION ALGORITHM FOR SSMI.

by

Kjell Kloster, O.M.Johannessen and Stein Sandven,
Nansen Environmental and Remote Sensing Center.

Abstract.

NORSEX-85H is an extension of the NORSEX algorithm, to take advantage of the improved spatial resolution of the 85 GHz SSMI channels.

The basic algorithm was developed after the NORSEX marginal ice zone experiment near Svalbard in 1979 (Norsex Group, Science, 1983) for use with SMMR data (Svendsen et.al., J.of Gephys. Res., 1983). It computes area concentration of total ice and the two ice types: multiyear ice (MY) and first-year ice (FY) from the two channels 18V and 37V. Only vertical (V) polarization is used since it was found to be significantly less sensitive to surface structure (snow layering, snow density, roughness) than horizontal polarization.

The ice emissivities and the atmospheric opacities used in the algorithm were basically measured during the NORSEX'79 experiment. Ocean water emissivities are theoretical values (Strogyn, 1971). Brightness temperature of the surface is modelled as the linear combination of the area-fraction of water, FY-ice and MY-ice in the field-of-view. A simple atmospheric model with surface air temperature as parameter is used to convert satellite-observed brightness temperature to surface-observed brightness temperature.

The NORSEX algorithm requires that input brightness values are adjusted with a few degree K to give 100% water over calm open polar water. These adjustments are made based on a few suitable scenes where the state for the atmosphere and the surface is known, and thereafter kept largely unchanged. Adjustments are different for SMMR and SSMI.

A rough estimate of the average surface air-temperature over pack-ice (100%-ice) is used as input for each scene (found e.g. from seasonal mean values or by automatic stations in the Arctic Ocean Buoy Program). The NORSEX algorithm output is % Water, % FY-ice and % MY-ice with a spatial resolution of approx. 60km for SSMI (the resolution of 19V).

85H is very sensitive to the difference between water and FY-ice. It is also very sensitive to the atmosphere. It is used to sharpen the ice-water boundary (especially effective at the ice edge) in the following way:

85H is spatially lowpass filtered to the 18V/37V algorithm resolution of 60km. Concentration values are then multiplied with the ratio of the 85H-signal to the lowpass-filtered 85H-signal. This results in an image with a spatial resolution of approx. 20km, given by the 85H-signal, and with ice concentration values given primarily by the basic NORSEX algorithm.

The NORSEX-85H algorithm was developed at NERSC (Kloster 1993) for use under the SIZEX'92 experiments in the Greenland and Barents Sea. The ice edge defined by the 30 -50% contour lines compares favorably with the ice - water boundary seen in near-simultaneous SAR images both under SIZEX'92 and under a later experiment, CARDEEP'93.

b) Compute the effective ice-emission temperature.
Interpolate between air temperature and water temperature.

c) Compute the brightness temp. of pure surfaces.
Uses emissivities as given by Norsex (ice) and Strogyn (water).

d) Enter satellite measured brightness temperatures: Tb19V, Tb37V.

e) Adjust the value of satellite measured brightness temperatures.
Adjustments are "tuned" to get ice concentr. near 0% for calm polar waters.

f) Set initial: atmos.surf.temperature,ta and mean surface emissivity, eps.
Do 2 iterations - improving ta and eps: !

g) Interpolate atmos. opacity between give arctic (250K) and subarctic (270K) values (Norsex).
Use the atmosphere temperature, ta as input.

h) Find emitted brightness at the surface by correcting for the atmosphere.
Use standard form of the radiation equation for the atmosphere.

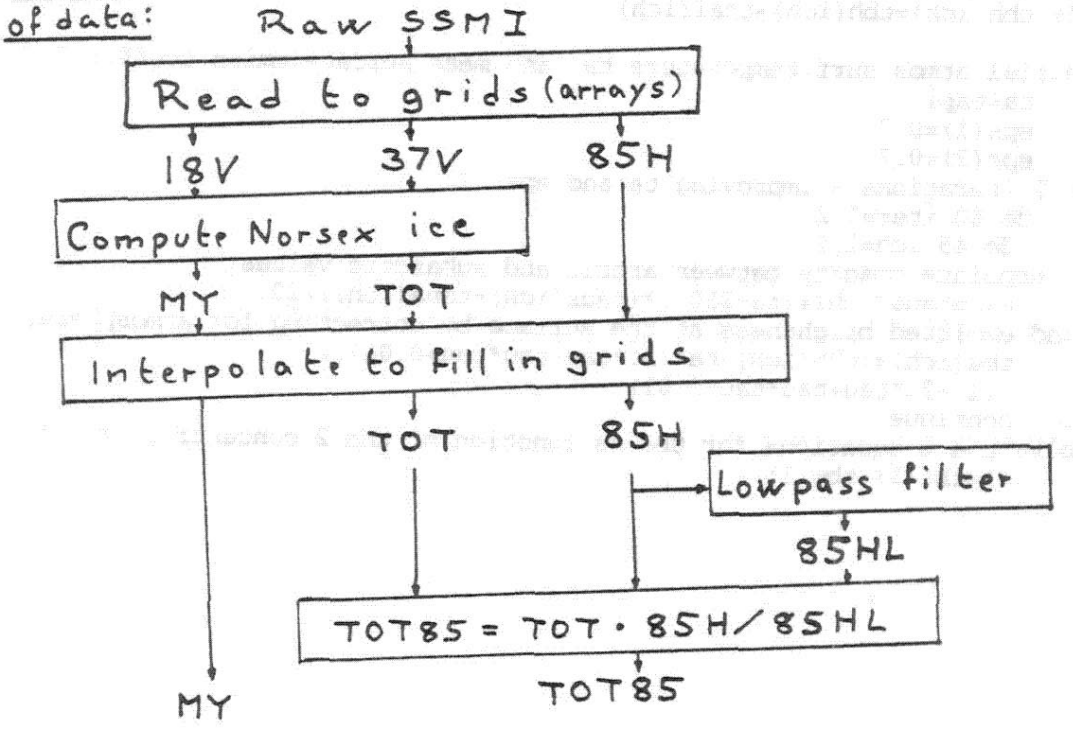
i) Solve the 2 equations for surface-emmitted brightness.
The unknowns are MY and FY ice concentrations: cm, cf.
Compute total ice concentration, ct.

j) Find new surface atm.temp. and surface emissivity values.
Use the computes value of the total ice concentration.

k) Do the next iteration.

l) Write the results.

Flow of data:



Fortran code

```
      program main
c SSMI passive microwave ice compute.
c Norsex algorithm, using SSMI 19V,37V data.
c K.Kloster, Nansen Center (NERSC), E.Griegsv.3a, N-5037 Solheimsvik.
c Last update may.93.
c
c Tb = brightness temperature (2 channels).
c tbh = satellite measured Tb,  tba = surface measured Tb:
      dimension tbh(2), tba(2)
c tbw, tbf, tbm = homogeneous Water, FY-ice and MY-ice surface Tb:
      dimension tbw(2), tbf(2), tbm(2)
c e = emission coefficients of water, FY, MY:
      dimension e(3,2)
c taus, taua = opacity for Subarctic and Arctic winter atmospheres:
      dimension taus(2), taua(2)
c Corrections to satellite measured Tb.
      dimension tcal(2)
c Mean surface emissions:
      dimension eps(2)
c Data from Strogyn (water) and Norsex (ice):
      data e /.621,.95,.80, .712,.95,.65/
c Data from Norsex:
      data taus /.04, .10/
      data taua /.03, .07/
c Data from Greenland -Svalbard waters, January 93:
      data tcal /0.,7./
c
      write(*,*)'Norsex ice algorithm for 19V,37V !'
      write(*,*)'Enter mean atmos.surf.temp.over 100% ice:'
      read(*,*) tapi
      do 43 ich=1,2
c effective ice temperature:
      tice=0.4*tapi+0.6*272.
c brightness of pure surfaces:
       tbw(ich)=e(1,ich)*272.
       tbf(ich)=e(2,ich)*tice
       tbm(ich)=e(3,ich)*tice
   43 continue
   20 continue
      write(*,*)'Enter satellite measured Tb19V, Tb37V:'
      read(*,*) tbh(1),tbh(2)
c meas.Tb adjust:
   48 do 49 ich=1,2
   49 tbh(ich)=tbh(ich)+tcal(ich)
c
c initial atmos.surf.temperature,ta  and mean surface emiss.coeff.:
      ta=tapi
      eps(1)=0.7
      eps(2)=0.7
c do 2 iterations - improving ta and eps: !
      do 60 iter=1,2
       do 45 ich=1,2
c interpolate opacity between arctic and subarctic values:
       tau=taua(ich)+(ta-250.)*(taus(ich)-taua(ich))/20.
c find emmitted brightness at the surface by correcting for atmosphere:
       tba(ich)=(tbh(ich)-ta*(2.*tau-tau*tau+0.01))/
     1  (1.-2.*tau+tau*tau-0.01)
   45  continue
c solve the 2 equations for tba as function of the 2 concentr., cm, cf:
      a11=tbf(1)-tbw(1)
```

```
      a21=tbf(2)-tbw(2)
      a12=tbm(1)-tbw(1)
      a22=tbm(2)-tbw(2)
      c1=tba(1)-tbw(1)
      c2=tba(2)-tbw(2)
      d=a11*a22-a12*a21
      cm=(a11*c2-a21*c1)/d
      cf=(a22*c1-a12*c2)/d
      ct=cf+cm
c improve surface atm.temp from value of ice concentr.:
      ta=272.+(tapi-272.)*ct
      do 65 ich=1,2
   65 eps(ich)=(e(1,ich)*(1.-cm-cf)+e(2,ich)*cf+e(3,ich)*cm)/3.
c next iteration:
   60 continue
c
c write result:
      write(*,13) tba(1),tba(2)
   13 format('surface brightness (deg.K) ='2f5.0)
   70 write(*,14) 100.*ct,100.*cm
   14 format('tot.ice & my-ice (percent) ='2f5.0)
c
      write(*,*)'next compute(1) or exit(2):'
      read(*,*) id
      if(id.eq.2) stop
      go to 20
      end
```

Example of program run.

```
Norsex ice algorithm for 19V,37V !
Enter mean atmos.surf.temp.over 100% ice:
250
Enter satellite measured Tb19V, Tb37V:
178,203                                   Ocean values
surface brightness (deg.K) = 169.  194.
tot.ice & my-ice (percent) =  -1.   -1.
next compute(1) or exit(2):
1
Enter satellite measured Tb19V, Tb37V:
248,240                                   First-year ice values
surface brightness (deg.K) = 248.  246.
tot.ice & my-ice (percent) =  99.    4.
next compute(1) or exit(2):
1
Enter satellite measured Tb19V, Tb37V:
218,188                                   Multiyear ice values
surface brightness (deg.K) = 216.  185.
tot.ice & my-ice (percent) =  96.   79.
next compute(1) or exit(2):
```

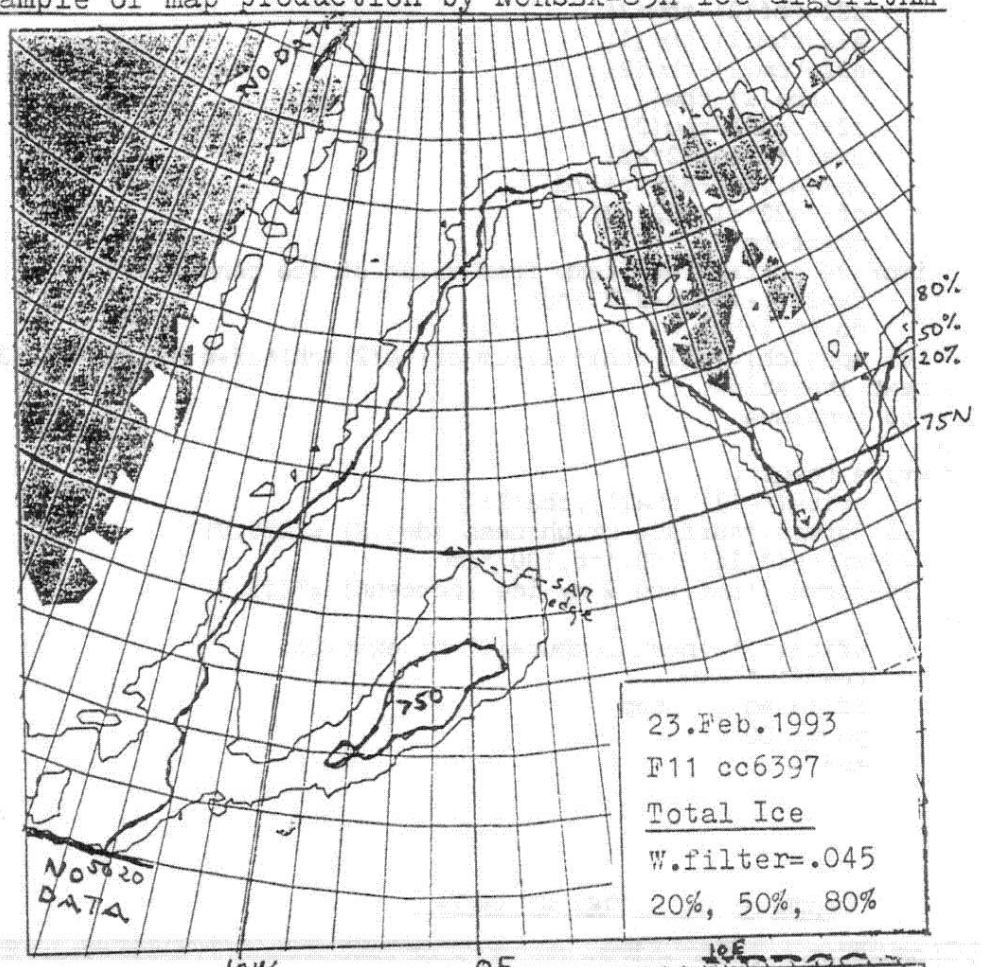
NB

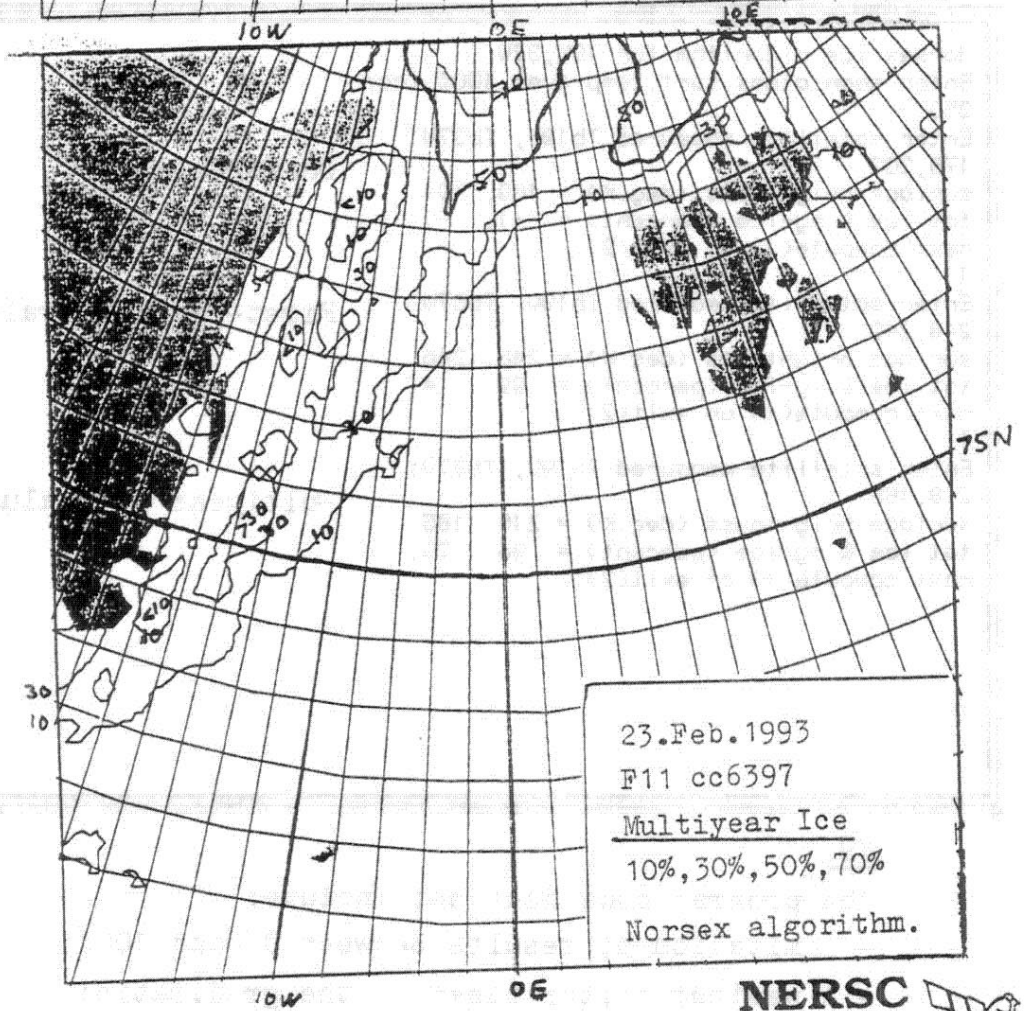
The program code does not include:

- Limitation of results between 0% and 100%
- A weather filter based on the grad.ratio:

  (tbh(2)-tbh(1))/(tbh(2)+tbh(1))

Example of map production by NORSEX-85H ice algorithm





NERSC
Fax. 05-200050
Tlf. 05-297288

SAR for Validating and Improving SSM/I Sea Ice Estimates

Florence Fetterer
Naval Research Laboratory
Remote Sensing Applications Branch
Stennis Space Center, MS 39529-5004
Tel. (601) 688-5456 FAX (601) 688-4149
Omnet: F.Fetterer, Internet: fetterer@snaps.nrlssc.navy.mil

Satellite passive microwave imagery is routinely used to produce Arctic and Antarctic-wide maps of sea ice concentration and percent concentration by ice type. These maps are used for climatological studies as well as for operational ice analysis. The accuracy of algorithms producing ice type concentrations is adversely affected by variability in the emissivity and physical temperature of ice as well as factors such as the presence of snow, frozen melt ponds, young ice, and atmospheric effects. C-band SAR imagery from ERS-1, however, provides excellent discrimination between first year and multi-year ice under any weather conditions in winter. SAR imagery colocated with SSM/I data can therefore be used to validate SSM/I ice type concentration estimates. Furthermore, SSM/I algorithms rely on assumed and "global" brightness temperatures, or tiepoints, for first year ice, multi-year ice, and open water. Although global tiepoints are used in the operational algorithms, the use of regional tiepoints can improve ice type concentration estimates. The measured brightness temperature for any SSM/I channel is the linear combination of the brightness temperature tiepoint of first year, multi-year and open water times the respective concentrations of each surface type in that channel's field of view. SAR provides relatively accurate ice type concentrations and thereby allows us to solve simultaneously for local brightness temperature tiepoints. Another way to obtain local tiepoints is to use SAR to confirm consolidated first year and multi-year ice in the SSM/I field of view. Both methods were applied to a 6-day data set from the Beaufort Sea spanning three weeks in late March, 1992. Compared with SAR, the NASA Team algorithm underestimated the percentage of multi-year ice by about 20%. The use of local tiepoints from SAR improved agreement to within 2-8%. Further research is needed to determine how far in time and space a local tiepoint can reasonably be extrapolated.

SPN SSM/I ALGORITHM SYMPOSIUM
Algorithm Questionnaire

"SAR DERIVED LOCAL TIE POINTS FOR NASA TEAM SEA ICE ALGORITHM"
Florence Fetterer, respondent

Please provide the following essential information about your algorithm(s).

* ALGORITHM DESCRIPTION

- Type (statistical, physical, other)

A method to improve the ice type estimates of the NASA Team algorithm by using local tie points derived with the aid of SAR imagery. (See Fetterer, et al., "Remote Sensing Aids in Sea Ice Analysis," EOS, June 15, 1993.)

- Input required / Output produced

Input: Coregistered SAR and SSM/I 100 km areas
Output: Set of tie points for first- and multi-year ice

- Auxiliary sensor/data base requirements *Data base of geocoded SAR images*

- Major limitations / approximations

See below. Presently works with NASA Team algorithm only. Possibly could be adapted to assist other algorithms.

- Computer resource requirements

All software presently runs on a Sun Sparc2.

* ALGORITHM PERFORMANCE

- Development / test data sets (regional / global / seasonal)

Beaufort Sea, winter, up to about 80 N. Used with very small data set so far (9 images, 9 days).

- Ground truth (accuracy / limitations)

No true ground truth (at SAR resolution)

* ALGORITHM PERFORMANCE (continued)

- Major assumptions of evaluation

SAR correctly identifies the percentage of first- and multi-year ice in a scene. True validation pending; however, believed to be more correct than the SSM/I.

- Strengths / weaknesses

Increases value of both SAR and SSM/I data: SAR has local accuracy but small field of view, SSM/I has large field of view but uncertainty in first- and multi-year results due to real variability in the appropriate tie points.

* ALGORITHM MATURITY

- Operational useage

Could be fully automated for operational use.

- Refinement / additional development

Need to determine if local tiepoints from SAR can be extrapolated in time and space.

- Availability

Remote Sensing Aids in Sea-Ice Analysis

EOS, Transactions, AGU
Vol 74 No 24 15JUN93

Florence Fetterer, Denise Gineris, and Conrad Johnson

Satellite-borne synthetic aperture radar (SAR) is fast becoming an indispensable tool for operational sea-ice analysis. In anticipation of this, the Naval Research Laboratory and the National Oceanic and Atmospheric Administration established a data link between the Alaska SAR Facility (ASF) in Fairbanks and the Navy/NOAA Joint Ice Center in Suitland, Md. The Joint Ice Center is the national center for ice analysis and forecasting. At the NRL Remote Sensing Applications Branch, we are working to ensure that SAR and other satellite data are used to best advantage for ice analysis by putting together appropriate software tools for manipulating images, developing algorithms for automated image analysis, and combining sensor data in ways that increase confidence in the final product, usually an ice type and concentration map. This article gives a brief look at some recent work in each of these areas.

Operationally Available Satellite Data

Ice analysts regularly use data from polar-orbiting satellites. The Defence Meteorological Satellite Program satellites carry the Operational Linescan System (OLS) and the Special Sensor Microwave Imager (SSM/I); the NOAA series of satellites carries the Advanced Very High Resolution Radiometer (AVHRR); and the European Space Agency's ERS-1 has a SAR. Figure 1 shows the Beaufort Sea as seen by four sensors during the LeadEx experiment [*LeadEx Group*, 1993] in March 1992. Figure 1a is an OLS thermal band (10.2–12.8 μm) 2.4-km resolution image. Fine (0.6-km resolution) data are also available. When digital data are enhanced by linear contrast stretching, the limitations of the 8-bit radiometric resolution are apparent. An important feature of OLS imagery is that resolution is maintained across the swath width.

Figure 1b is an AVHRR thermal (10.5–11.5 μm) image. AVHRR data are recorded with 10-bit radiometric resolution. Enhancing AVHRR visible or thermal band imagery often reveals detail in the spatial variation of albedo or temperature indicative of surface ice conditions. Spatial resolution ranges from 1.1 km at sensor nadir to about 6 km at the swath edges. The large patches of first-year (FY) ice north of 72° have a brighter or warmer thermal signature than that of thicker multiyear (MY) ice. Leads appear as bright, linear features. Because of its wide swath (2900 km), frequent coverage, and availability in digital form, AVHRR imagery is the primary satellite data source for ice analysis. While analysts find certain filters and channel ratios useful for enhancing ice features, automated algorithms for parameters such as concentration, type, ice velocity, and lead mapping have limitations that require them to be used selectively rather than routinely [see *Steffen et al.*, 1993]. Resolution too coarse to resolve small areas of open water and the lack of an automatic cloud screening algorithm that works well under all conditions hinder the development of operational algorithms for AVHRR.

The Joint Ice Center uses an ice concentration algorithm for SSM/I [*Hollinger*, 1991] to check concentration and locate the ice edge, particularly when AVHRR imagery is obscured by clouds. The area shown in Figure 1 has close to 100% concentration. Figure 1c shows brightness temperature from the SSM/I 85.5-GHz channel. The resolution of this channel is about 15 km. Although the presence of FY ice is apparent in the image by elevated brightness temperatures, the 85.5-GHz channel is not used in ice-type algorithms because of its sensitivity to atmospheric effects. First-year ice concentration calculated using the NASA Team algorithm [*Cavalieri et al.*, 1984] and displayed as an image shows the same gross features but with some differences presumably caused by the much larger field of view of the other channels used by the algorithm.

Finally, Figure 1d shows the area in a 100-km square, 240-m resolution ERS-1 SAR (C-band VV polarization) scene. Multiyear ice is clearly distinguishable by its bright backscatter signature. A few ridges are discernable in the dark FY ice south of the LeadEx camp. More ridges are visible in the full-(30 m) resolution imagery of the same scene. When compared with the imagery from other satellite sensors, the utility of SAR for assessing ice conditions on a local scale is apparent.

SAR for Ice Analysis

Since March 1992, SAR imagery from ERS-1 has been received on an almost daily basis at the Joint Ice Center. The imagery is displayed and archived in an SAR workstation designed by the Jet Propulsion Laboratory. The workstation runs the same algorithms for ice motion and ice classification as those that create the motion and ice-type products distributed by ASF. To the database management and algorithm functions of the workstation, NRL has added functions designed to make SAR imagery more useful for supporting field operations. These include functions for drawing latitude and longitude grids on imagery, measuring distances on imagery, and a ship-routing tool. In addition to using SAR routinely to spot check the twice-weekly Western Arctic Ice Analysis product, SAR imagery has been used to aid in routing the Coast Guard icebreaker *Polar Star* on a research cruise in the Bering Strait, to guide aircraft to thin ice for deploying sonobuoys through leads, and to fix the location of the pack edge off the often cloudy north slope of Alaska during summer. The position of the multiyear ice edge in the spring is an important predictor of the earliest date barges will be able to resupply the North Slope (C. Bertoia, personal communication, 1993).

With high resolution but a narrow swath, ERS-1 SAR imagery lends itself to manual analysis for support of local operations. RadarSat, with a 500-km swath width mode, will offer a more synoptic view of Arctic ice conditions. The large volume of data from RadarSat will make the use of algorithms for analysis especially attractive. If an analyst can have confidence in an ice-type map produced by an algorithm without checking the image it came from, SAR can be efficiently used to improve the accuracy of the Arctic-wide analysis. We have evaluated the wintertime performance of the ASF algorithm for ERS-1 data [*Kwok et al.*, 1992] by comparing supervised classification (classification using manually selected training sets for each image) to the algorithm's classification for images acquired over a 3-week period in the Beaufort, Chukchi, and East Siberian seas.

Remote Sensing (cont. on page 267)

Florence Fetterer and Conrad Johnson, The Naval Research Laboratory Remote Sensing Applications Branch, Stennis Space Center, MS 39522-5009; Denise Gineris, Sverdrup Technology, Stennis Space Center, MS 39522-5009

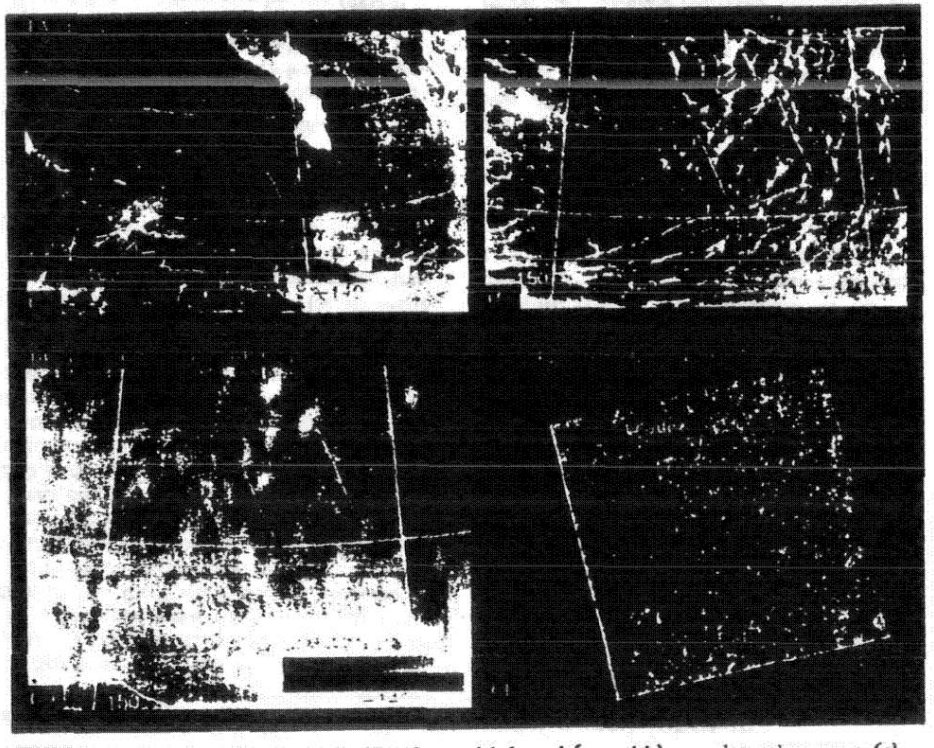


Fig. 1. The Beaufort Sea as viewed by thermal infrared (a and b), passive microwave (c), and active microwave (d) sensors on March 29, 1992. The yellow square was drawn around the SAR image, saved as a geographically referenced NSIPS graphics file, and read onto the other images. The circle marks the location of the LeadEx field experiment.

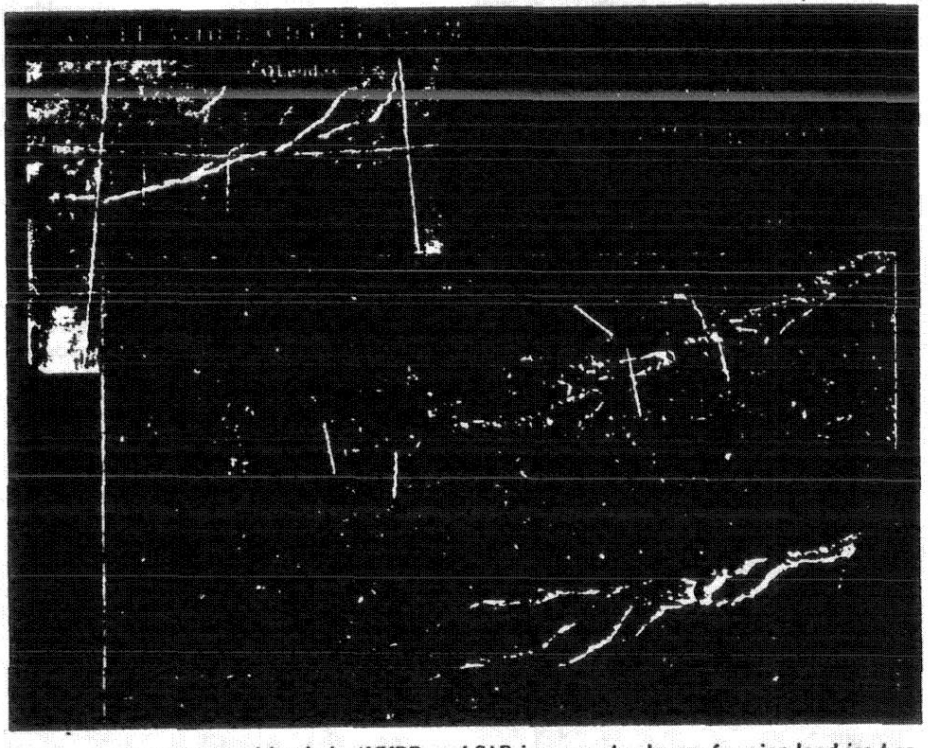


Fig. 2. A view of several leads in AVHRR and SAR imagery. As shown, freezing lead ice has a wide range of backscatter signatures. In this and other examples, the loose association of higher backscatter with thicker ice fails altogether. An NSIPS graphic tool was used to measure the width of the lead in the SAR image. In addition to distance, geographical headings and coordinates can be read off any mapped image. The blue line was saved as an NSIPS graphics file and read onto the AVHRR image. Note that it is shifted off the lead visible in the AVHRR image. This could be because the ice has moved or the geolocation accuracy of AVHRR imagery is poor.

March 1992. The NASA Team algorithm with global tiepoints underestimates the percentage of MY ice by about 20% when compared with SAR. Results using local tiepoints from consolidated ice (type "a") are in better agreement. Results using tiepoints from the mixed ice in Figure 3a (type "b") give improved agreement for the image from which the samples were taken (circled points) but not for images from other days. The method of using mixtures of ice could probably be made more robust by using larger and more widely separated grid elements for independent samples. On an appropriately large scale, however, most of the Beaufort Sea SAR images available at the time of the analysis showed roughly the same 65%–35% mixture of MY and FY ice.

The difference between FY and MY tiepoints is less for tiepoints derived using SAR than for global tiepoints, since the global tiepoints are taken from a multiyear data set's maximum and minimum values, while SAR-derived tiepoints accommodate the presence of other types of ice with intermediate emissivities. This makes the algorithm overly sensitive to input. In summary, these results demonstrate a method that could be automated for operational use of assimilating SAR estimates into SSM/I estimates, but further work is needed to establish the merit of doing so. Certainly SAR imagery makes it easier to track variability in the emissivity of MY ice.



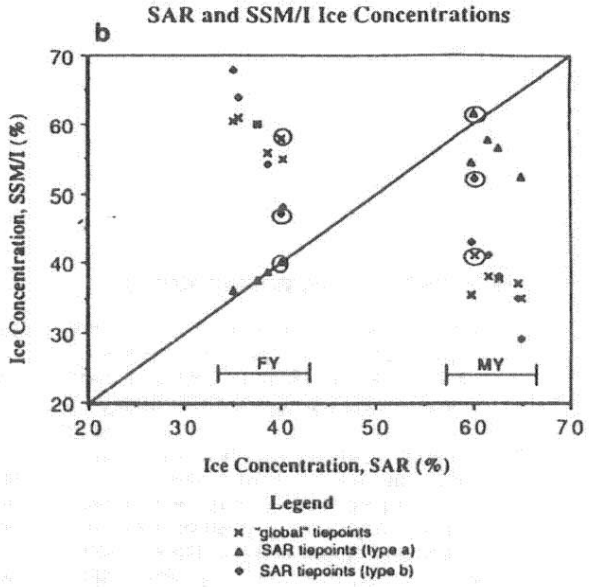


Fig. 3. (a) A SAR image from March 29, 1992, with 25-km SSM/I grid, and (b) ice type concentration estimates from SAR compared with those from SSM/I using standard global tiepoints, tiepoints (type a) derived with the aid of SAR to identify consolidated FY and MY ice, and tiepoints (type b) derived with the aid of the SAR image in (a).

The NRL Satellite Image Processing System

The figures were created using the NRL Satellite Image Processing System (NSIPS). NSIPS is an image-processing and manipulation package developed to visualize and gather information from different satellites in an easy to use environment. A point and click, menu-driven graphical interface lets the user see all available options. With this approach, less time is needed to train and support users. One unique feature of NSIPS is that all images warped to a map projection retain their projection information so that the user can get latitude and longitude as well as data values directly from displayed images. All graphics are referenced by latitude and longitude on warped images by the graphic editor. Graphics drawn on one image can be saved and displayed on another image in a different projection and the graphics will conform to the new projection. The NSIPS package is divided into seven main subsystems: processing (to ingest and warp satellite data); files (to read, convert, display, add grids, add landmasks, add coastlines, and export satellite data); analysis (to examine satellite files on a point or slice basis); display (to add or modify graphics, zoom, modify color tables, build movie loops, cut, paste, plot satellite paths, or display altimeter data on an image); filter and transformations (to apply standard filters to imagery and allow composites of satellite data); image file calculations (to mathematically manipulate an image); and user functions (to allow the user to easily add their own routines to the NSIPS package). All menus have on-line help files. The NSIPS package is currently supported on SUN and Silicon Graphics workstations.

Summary

Since 1961, when photographs from the Television Infrared Observation Satellite (TIROS-II) were used to help route a U.S. Navy transport ship through ice into a Newfoundland harbor [*Massom*, 1991], satellite imagery has been used operationally for ice analysis. While increasingly sophisticated instrumentation in space has been a boon to polar research, operational analysis in the U.S. has not yet benefitted to the same degree. This situation can be redressed through algorithm development. In the past, we developed algorithms for lead statistics and ice motion from AVHRR. Current work on using SAR with SSM/I will continue. Plans include collaboration with investigators at the University of Kansas to refine an expert system for ice classification [*Haverkamp and Tsatsoulis*, 1992]. An expert system is one approach to overcoming the problem of overlapping classes when ice is classified on the basis of backscatter.

To some extent, the information requirements of the operational analyst match those of the scientist studying the polar regions, although the balance between accuracy and timeliness may be struck differently. Algorithms can best help the analyst extract the information content of satellite data if they can run on large data sets to produce an Arctic-wide analysis of known accuracy in near-real time with little or no human intervention. This is a tough requirement and, while working toward it, image-processing tools are making manual analysis quicker and more fruitful.

Acknowledgments

The authors wish to thank John Schmidt, NRL Remote Sensing Applications Branch, and Tim Gremillion, Sverdrup Technology, for technical and programming help, and CDR Brad Smith, Cheryl Bertoia, and Gary Wohl of the Navy/NOAA Joint Ice Center. This work was sponsored by the Chief of Naval Operations under program element 603704N, CDR P. Ranelli, program manager.

References

Cavalieri, D. J., P. Gloersen, and W. J. Campbell, Determination of sea ice parameters with the Nimbus 7 SMMR, *J. Geophys. Res., 89*, 5355, 1984.

Haverkamp, D., and C. Tsatsoulis, The use of an expert system in combination with active and passive microwave data to classify ice, *Proc. Int. Geosci. and Rem. Sens. Symp.*, Houston, Tex., May 26–29, pp. 1625–1627, 1992.

Hollinger, J., *DMSP Special Sensor Microwave/Imager Calibration/Validation Final Report, Vol. II*, Naval Research Laboratory, Washington, D.C., 1991.

Kwok, R., E. Rignot, B. Holt, and R. Onstott, Identification of sea ice types in spaceborne Synthetic Aperture Radar imagery, *J. Geophys. Res., 7*, 2391, 1992.

Massom, R., *Satellite Remote Sensing of Polar Regions, Polar Research Series*, Belhaven Press, London, 307 pp., 1991.

LeadEx Group, The LeadEx experiment, *Eos Trans. AGU, 74*, in press, 1993.

Poe, G. A., Optimum interpolation of imaging microwave radiometer data, *IEEE Trans. Geosci. Remote Sens., 28*, 800, 1990.

Steffen, K, R. Bindschadler, J. Comiso, D. Eppler, F. Fetterer, J. Hawkins, J. Key, D. Rothrock, R. Thomas, and R. Weaver, Snow and ice applications of AVHRR in polar regions, *Ann. Glaciol., 17*, in press, 1993.

Remote Sensing (cont. from page 265)

Results show that the algorithm does well at discriminating between MY and FY ice. The RMS difference between supervised and algorithm classification of MY ice is 7% with a mean difference of 4%.

Since the ice-type algorithm is based on assumed backscatter distributions for each ice type, variability in backscatter may contribute to classification error. The backscatter of MY ice in our data set of sixty-four calibrated images ranged from -12.9 to -6.0 dB with a mean of -10.3 dB. First-year ice was of two types: visibly deformed FY, for which backscatter ranged from -19.4 to -10.9 dB with a mean of -14.7 dB, and smooth FY, for which backscatter ranged from -21.5 to -16.6 dB with a mean of -17.3 dB. A good example of backscatter variability that causes unavoidable misclassification by a backscatter-based algorithm is shown in Figure 2. A large lead has a bright, warm thermal signature in the AVHRR image. In the SAR image, the backscatter signature of freezing lead ice ranges from -16 to -10 dB with wind-roughened water at -3.5 dB.

Merging SAR with SSM/I

While SAR gives excellent local information, SSM/I estimates of ice type and concentration are on a scale more suited to Arctic-wide analysis. Algorithms for ice type and concentration from SSM/I depend on the assumption that the brightness temperature measured by each sensor channel is a linear combination of the brightness temperature of MY ice, FY ice, and open water in the field of view for that frequency, or

$$^{T}B\text{measured} = {}^{C}(FY)\,{}^{T}B(FY) + {}^{C}(MY)\,{}^{T}B(MY) + {}^{C}(OW)\,{}^{T}B(OW)$$

where ^{T}Bmeasured is the measured brightness temperature at a given frequency; C is the concentration of FY, MY, and open water in the field of view for that frequency; and ^{T}B is the brightness temperature "tie point," or the brightness temperature that would be measured by the sensor if only that ice type were in the field of view. Brightness temperatures for these types are usually empirically determined and treated as constants. However, the tiepoints that will give the correct mixture (correct on the basis of ground truth) vary, not only because the emissivity and temperature of each ice type is variable, but also due to factors such as the presence of snow, frozen melt ponds, young ice, and atmospheric effects.

By providing ice-type concentration estimates, SAR can be used to obtain regional rather than hemispheric or "global" tiepoints. This possibility was demonstrated using the SAR image in Figure 3a. SSM/I data from 6 hours earlier were processed to the same projection and shifted to match a coastline for the best possible geolocation. Since data at vastly different resolutions are being compared, *Poe*'s method [1990] was used to obtain optimally interpolated measurements for each channel at approximately 3.5-km spacing. The measurements that fell within each 25-km grid cell on the SAR image were averaged to produce a single TB-measured value for each channel, while the SAR algorithm gives $^{C}(FY)$ and $^{C}(MY)$ for each grid cell. Using the two grid cells shown, the equation above was solved simultaneously for $^{T}B(FY)$ and $^{T}B(MY)$; there is no open water. Another way to obtain local tiepoints is to use SAR to confirm consolidated FY and MY ice in the SSM/I field of view. This was done for FY ice using fast ice north of Alaska and for MY ice at about 77°N.

Figure 3b shows FY and MY concentrations from six SAR images of roughly the same area compared with concentrations from SSM/I for 6 days over 3 weeks in late

Remote Sensing (cont. on page 268)

Session 2

Snow Cover

(Chris Neale, Utah State, Chair)

ENCL(8)

Session 2

Snow Cover

(Chris Neale, Utah State, Chair)

Global Snow Cover Identification Using SSM/I Measurements

Norman C. Grody[1]
Allan Basist[2]

Algorithms are under development for identifying snow cover using SSM/I measurements. Snow and ice coverage is identified by their scattering signature, i.e., when the 22 GHz measurements exceed the 85 GHz measurements. Although this scattering feature is the primary identifier, it must be combined with other discriminates to account for precipitation, deserts, and frozen ground which can also scatter microwave radiation. Furthermore, forested regions and melting snow reduces the scattering effect at 85 GHz. These atmospheric and surface features must be accounted for when generating a global snow cover product.

A classification technique was developed using the 22 and 85 GHz vertically polarized channels to help separate snow cover from deserts and precipitation. In addition, the 19 GHz polarization difference is used to isolate snow cover from frozen ground. Deserts and warm precipitation are identified when the 22 GHz measurement exceeds 257 K. However, cold precipitation is mis-classified as snow when the measurements are below the 257 K threshold. Also, melting snow is mis-classified as rain when the measurements are above the 257 K threshold. As discussed in the presentation, we feel that the scattering measurements obtained from the SSM/T-2 sounding channels may provide a more accurate (also more objective) means of separating precipitation from snow cover.

[1]NOAA/Satellite Research laboratory
5200 Auth Road, Room 712
Camp Springs, MD 20746
301-763-8042

[2]NOAA/Climate Analysis Center
5200 Auth Road, Room 605
Camp Springs, MD 20746
301-763-8227

Identification of Snow Cover Using SSM/I Measurements.

Norman C. Grody and Allan Basist

Norman Grody is with the National Environmental Satellite Data and Information Service (NESDIS) and Allan Basist is with the Climate analysis Center (CAC) of the National Oceanic and Atmospheric Administration (NOAA), Washington, D.C. 20233.

ABSTRACT

Satellite observations of the earth's surface provide information for use in meteorology, hydrology, agriculture, and oceanography. The primary advantage of passive microwave measurements over those in the visible and infrared is their ability to probe through non-precipitating clouds, enabling observations under nearly all-weather conditions. This paper discusses the use of the Special Sensor Microwave Imager (SSM/I) aboard the DMSP satellites to identify snow cover. A procedure is developed to identify snow cover and discriminate between a number of other surface and atmospheric parameters based on the SSM/I measurements.

I. INTRODUCTION

Snowmelt is the major component of the total annual water supply in large parts of the world. The amount of water stored as snow is important in forecasting its affect on the water supply, flooding, irrigation and management of agricultural commodities. Snow cover information is also required to specify the initial state of regional and mesoscale models for numerical weather prediction. In general, repetitive coverage of the areal extent, water equivalent or depth and liquid water content is required on a daily basis.

Measurements of snow coverage from space began in 1966, with the launch of the first polar orbiting satellite to obtain visible images of the earth. Beginning about that time, an operational snow cover product was produced weekly by subjectively analyzing the visible measurements from the NOAA polar orbiting satellites for the latest clear conditions during the week [1]. As a major limitation, the data acquisition is hampered by cloud cover, sometimes at critical times when a snowpack is ripe. Furthermore, information on water equivalent, free water content, and other properties pertinent to accurate runoff predictions are not currently available using visible or infrared measurements.

The primary advantage of passive microwave measurements over those in the visible and infrared is their ability to probe through non-precipitating clouds, providing daily observations. Besides penetrating clouds, the subsurface microwave emission can propagate through various snow depths depending on the frequency, thereby enabling a measure of snow depth. Furthermore, the microwave emission characteristics change dramatically between dry snow and melting snow [2]. The use of microwave data can therefore lead to an analysis of the internal snowpack properties under nearly all-weather conditions.

Snow cover measurements from space using microwave radiometry was first obtained using the Nimbus-E Microwave Spectrometer (NEMS), launched aboard Nimbus-5 on December, 1972. This experimental, nadir viewing instrument had a spatial resolution of 200 km and contained window channels at 22 and 31 GHz to view the surface; it also included three channels within the 60 GHz oxygen band for obtaining temperature soundings. Snow and ice coverage was identified by their scattering signatures, i.e., when the 22 GHz measurements exceeded the 31 GHz measurements [3]. Although more advanced instruments have been developed over the past twenty years (containing more channels with higher spatial resolution and greater area coverage), the same dual frequency approach is used today for snow identification [4,5,6].

The latest, and most advanced instrument is the Special Sensor Microwave Imager (SSM/I), which was developed as part of the Defense Meteorological Satellite program (DMSP) and flown aboard the Air Force Block 5D satellite in 1987 and again in 1991. The SSM/I is a conically scanning radiometer having channels at 19,

22, 37 and 85 GHz [7]. All measurements are obtained with dual polarization except for the 22 GHz channel. The addition of an 85 GHz channel makes the SSM/I unique to previous instruments. This channel has the highest frequency and highest resolution (15 km) ever flown for a microwave radiometer. Due to its high frequency, the 85 GHz channel provides the highest sensitivity for measuring scattering materials such as snow cover and the ice particles formed aloft in the case of precipitation. Both snow cover and precipitation have been identified using the 85 GHz channel in conjunction with the lower frequency measurements [8].

II. CLASSIFICATION TECHNIQUE

As mentioned above, the scattering due to snow cover produces a positive difference between low and high frequency channels. Although this scattering signature is the primary identifier of snow, it must be combined with other discriminates to account for precipitation, deserts and frozen ground, which can also scatter microwave radiation. Furthermore, melting snow removes the snow scattering signature. These atmospheric and surface features must be accounted for when developing a global snow cover product.

A decision tree approach was applied to identify snow cover and precipitation using the vertically polarized SSM/I measurements at 22 and 85 GHz as the primary classifiers [8]. Revisions to the decision tree are needed to account for frozen ground and some ice covered surfaces. As before, only antenna temperatures shall be used. However, the previous study convolved the 85 GHz measurements to the 19 GHz resolution to minimize the effects of different spatial resolution when using multifrequency algorithms, whereas the full resolution measurements are used here. As such, some of the parameters involving the 85 GHz measurements will be different from that cited in the original paper [8].

Low loss scattering materials such as ice particles are often identified by the condition T22v > T85v, where T22v and T85v denotes the vertically polarized antenna temperatures at the respective frequencies. Figure 1 shows the regions where T22v > T85v for February 1992; based on SSM/I measurements from the F-11 satellite. Note that over land, snow and ice cover, precipitation, deserts and frozen ground display the scattering signature. However, over oceans the condition T22v > T85v only identifies aged sea ice. A more refined parameter called a scattering index must be used to identify the scattering due to precipitation over oceans [8]. Since we are only interested in land surfaces, it is unnecessary to use the scattering index approach for identifying scattering materials, and need only consider the difference between the low and high frequency channels, i.e., T22v > T85v.

A. Precipitation Signature

Both precipitation and snow cover contain ice particles which scatter the upwelling radiation. The density and size of the ice particles is often smallest for precipitation, resulting in smaller scattering effects (higher low-frequency measurements) than for snow cover. Even in the absence of scattering, the low frequency emission arising from below the ice layer is higher for precipitation conditions than for frozen ground. Based on these observations, precipitation (also deserts) can be separated from snow cover by requiring the 22 GHz measurements to be less than a given threshold (i.e., T22v < 257 K). An additional relationship, given by T85v < 168 + .49*T22v, is used to account for intense rain events which reduces the 22 GHz measurements below 257 K due scattering by large ice particles. These results, as well as other conditions discussed here, are based on numerous comparisons of the SSM/I measurements with surface observations of daily snow cover and rainfall observations over the U.S. Also used for comparison is the globally produced weekly composite snow cover charts derived from satellite imagery.

B. Frozen Ground Signature

Figure 2 is a schematic diagram, showing the location of the various geophysical parameters in the space formed by the 22 and 85 GHz measurements. The largest geographical regions containing snow cover are bound by the three line segments discussed above, i.e., T22v = T85v, T22v = 257 and T85v = 168 + .49*T22v. However, as indicated in Figure 2, the small triangular area formed by the lines T22v = T85v, T22v = 257 and T85v = 240 can contain frozen ground as well as snow cover. Since frozen ground often occurs adjacent to snow cover, the misclassification of frozen ground as snow cover would result in an extension of snow covered regions. Also, measurements within areas of the Tibetan Plateau reside in this triangular space, suggesting the possibility of frozen ground for this anomalous region. These ambiguities due to frozen ground are removed by considering all measurements within the triangle as snow-free except when T19v-T37v > 7.

C. Subsurface Ice Signature

The third and final signature to be discussed is that observed over Greenland and Antarctica. As indicated in Figure 1, at lower elevations these surfaces display a non-scatterer signature (i.e., T22v < T85v), although they contain deep snow cover above a glacial subsurface. In fact, the polarization and frequency spectrum of the antenna temperature measurements resemble a water surface. I initially thought we were observing melting ice (in February) but believe that subsurface ice layering effects are more reasonable. For lack of a better understanding we have designated this area in Figure 2 as substratified ice; it is

formed by the lines T22v = T85v, T85v = 240, T22v= -344+2.3*T85v.

Note that the measurement space occupied by these geographical regions is quite large, although it does not overlap any other features such as wet ground. It should also be mentioned that the parts of Greenland and Antarctica exhibiting snow-scattering signatures lie in the snow designated area of Figure 2.

III. CONCLUSIONS

This paper presents a method using the vertically polarized antenna temperatures from the SSM/I to identify snow cover. Snow cover is currently being produced daily as an experimental product using the method described above and summarized in Figure 2. Figure 3 shows the monthly averaged product for February 1992, and should be compared with the unclassified scattering signature shown in Figure 2. Note how the classification procedure eliminates much of the desert areas, precipitation and frozen ground surfaces. Preliminary comparisons with surface data and visible satellite imagery suggests that the SSM/I product is capable of identification most of the significant snowfall (> 1 inch). However, further investigations are needed to consider issues such as melting snow and snow around forested areas which are presently undetected by our analysis. Finally, we hope to eventually develop a means of deriving snow depth as well as areal extent from the SSM/I.

REFERENCES

[1] Matson, C.F. Ropelewski, and M.S. Varnadore, "An atlas of satellite-derived northern hemispheric snow cover frequency," Washington D.C., U.S. Department of Commerce, 1986.

[2] R. Hoffer, and C. Matzler, "Investigations of snow parameters by radiometry in the 3 to 60 mm wavelength region," J. Geophys. Res., 85, 453-460, 1980.

[3] K.F. Kunzi, A.D. Fisher, D.H. Staelin, and J.W. Waters, "Snow and ice surfaces measured by the Nimbus 5 microwave spectrometer," J. Geophys. Res., 881, 4965-4980, 1976.

[4] K.F. Kunzi, S. Patil, and H. Rott, "Snow-cover parameters retrieved from Nimbus-7 Scanning Multichannel Microwave Radiometer (SMMR) data," Rev. Geophys. Space Phys., 22, 452-467, 1984.

[5] J.L. Foster, D.K. Hall, and A.T.C. Chang, "An overview of passive microwave snow research and results," Rev. Geophys. Space Phys., 22, 195-207, 1984.

[6] R.R.Ferraro, N.C. Grody, and J.A. Kogut, "Classification of geophysical parameters using passive microwave satellite measurements," IEEE Trans. Geosci. Remote Sensing, GE-24, 1008-1013, 1986.

[7] J.R. Hollinger, B. Lo, G. Poe, R. Savage and J. Pierce, "Special Sensor Microwave/ Imager User's Guide," 120 pp., Naval Research Laboratory, Washington, D.C, 1987.

[8] N.C. Grody, "Classification of snowcover and precipitation using the special sensor microwave imager," J. Geophys. Res.,

96, 7423-7435, 1991.

Figure Legends:

Figure 1. The hatched areas show the regions where the 22 GHz average measurements are greater than the 85 GHz vertically polarized SSM/I measurements for February, 1992. The mean difference is below 5 K for frozen ground, less than 15 K for deserts, and up to 60 K and more for precipitation, snow and ice covered surfaces.

Figure 2. Schematic diagram showing the different parameters occupying the space defined by the 22 and 85 GHz, vertically polarized antenna temperatures. The region within the solid boundary is used to indentify snow cover.

Figure 3. The hatched areas show the regions of snow cover for February 1992 using the classification procedure based on Figure 2.



FIG 1 FIGURE 1.

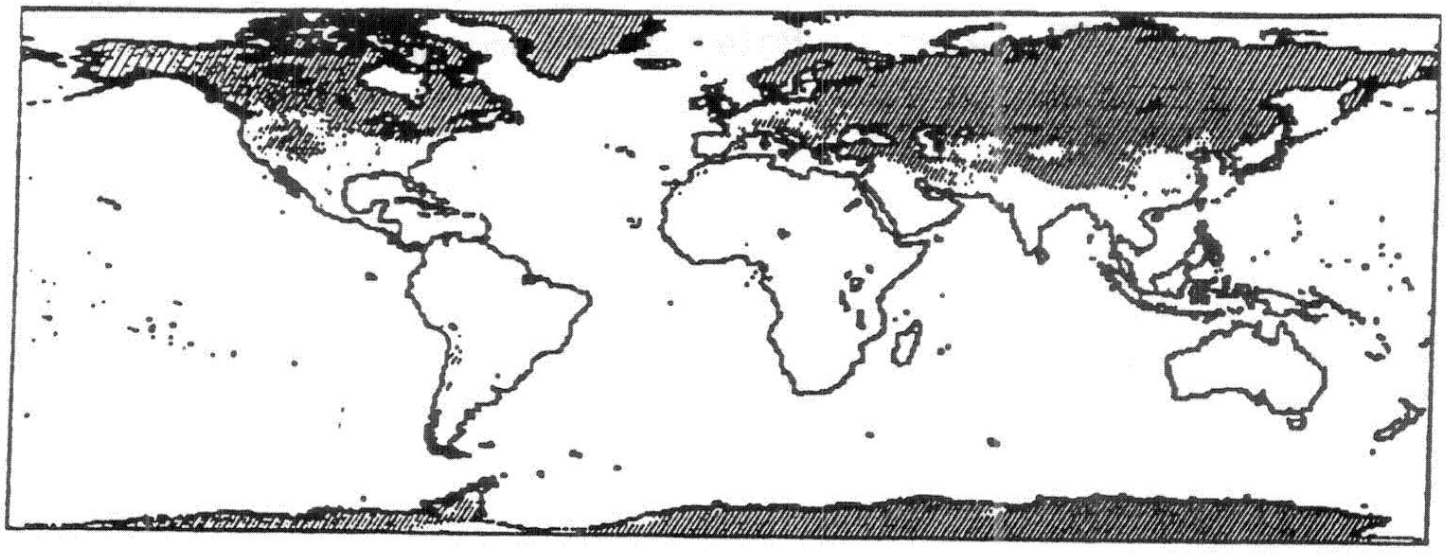
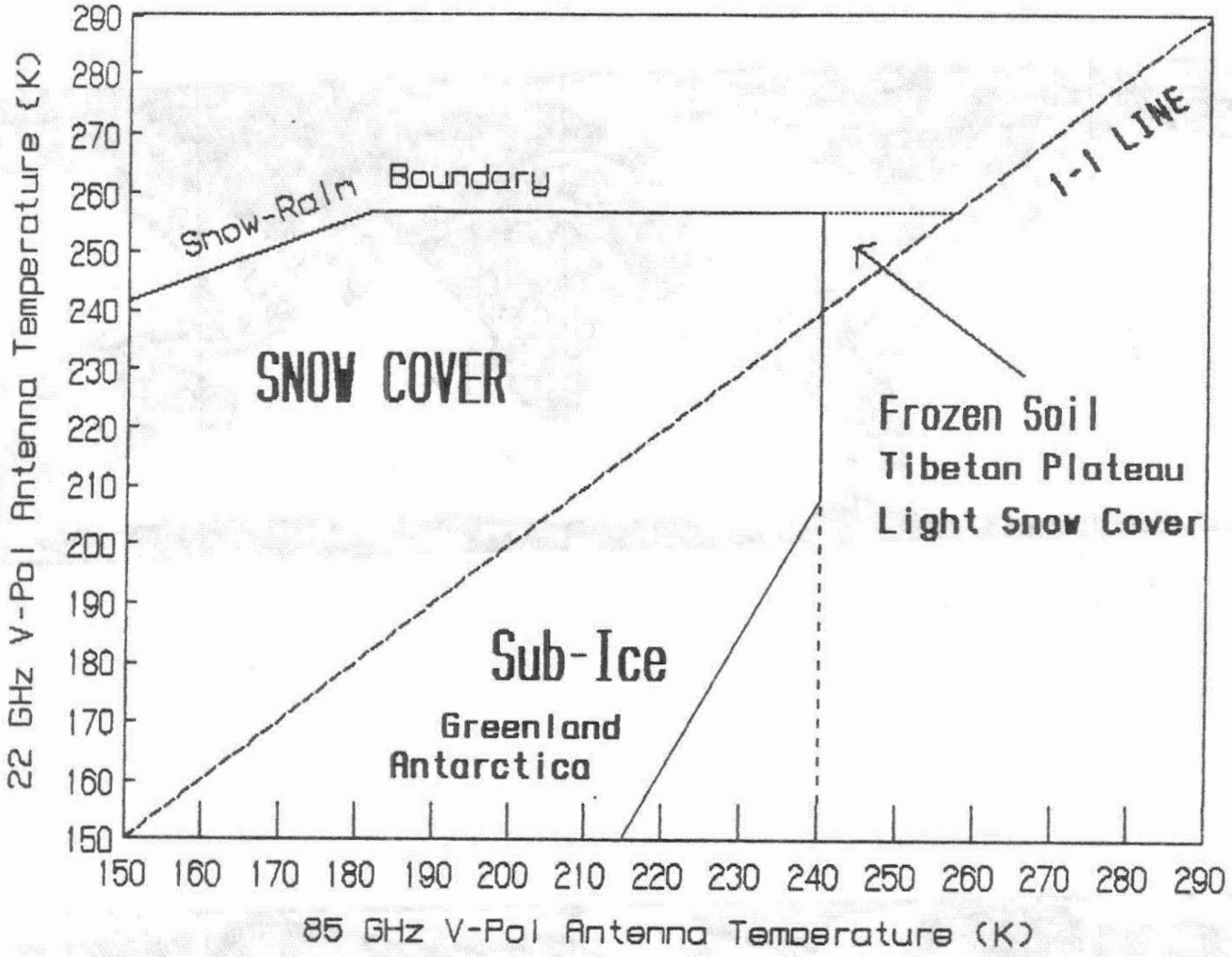


FIGURE 3.

SNOW COVER IDENTIFICATION



DEVELOPMENT AND OPERATIONAL APPLICATION OF A CANADIAN SNOW WATER EQUIVALENT ALGORITHM USING SSM/I DATA

A.E. Walker and B.E. Goodison
Climate Research Branch Canadian Climate Centre
4905 Dufferin Street Downsview, Ontario, M3H 514
Phone: (416)739-4357 Fax: (416 739-5700

An ongoing Canadian Climate Centre (CCC) research program has focussed on the development and testing of algorithms for the determination of snow cover particularly snow water equivalent ISWET from passive microwave satellite data for the open prairie region of Western Canada. Although the original algorithms were derived from airborne data (passive microwave and gamma) testing and validation has continued with the launch of SSM/1 radiometers on U. S. DMSP satellites since June 1987. The SWE algorithm that has been applied to SSM/I data uses a 37 and 19 GHz vertically polarized brightness temperatures gradient. Comparisons between between SSM\1 derived SWE values and ground snow survey measurements have shown that the regional patterns of snow distribution from both data sources agree very well, with average values generally with 10mm of each other.

Access to SSM/I data in near real-time via the Civilian Navy/NUAA Oceanic Data Distribution System (CNODDS) has provided the capability to generate snow products within hours after data acquisition. Since the 1988/89 winter season, maps depicting current SWE conditions have been produced on a weekly basis during the winter months (December to April) using near real-time SSM/I data. These maps are distributed by fax machine to several water resource agencies for their use in monitoring snow conditions, planning for ground surveys, and preparing run-off forecasts. These users are also an important source of validation by providing feedback on the representativeness of the SWE information presented on the maps and identifying problem areas which may require further research.

This paper will outline the development of the Canadian SSM/I SWE algorithm and describe recent enhancements which have resulted from research into the problem areas identified during the algorithm validation process. One example is a wet snow indicator which overcomes the problem off discriminating wet snow from snow-free land. Although this algorithm is currently only valid for the open prairie region, algorithm development research has been initiated for other landscape regions of Canada. Ongoing and future research efforts will be presented, which focus on improving the capability to retrieve representative SWE information from SSM/I data.

Disclosure Statement: the authors (Anne E. Walker and Barry E. Goodison) of the paper give permission for the public dissemination of the abstract and any associated supporting material.

SPN SSM/I ALGORITHM SYMPOSIUM
Algorithm Questionnaire

"SNOW WATER EQUIVALENT ALGORITHM"
Anne Walker and B. E. Goodison, respondents

Please provide the following essential information about your algorithm(s).

* ALGORITHM DESCRIPTION

- Type (statistical, physical, other)

Statistical (linear regression using airborne experimental data sets).

- Input required / Output produced

Input: Brightness temperatures from 19 GHz (v-pol); 37 GHz (v-pol); (and 37 GHz (h-pol) for wet snow)
Output: Snow water equivalent in mm

- Auxiliary sensor/data base requirements *None*

- Major limitations / approximations

Only validated for open prairie region of Canada

- Computer resource requirements *Very modest; e. g. , a personal computer*

* ALGORITHM PERFORMANCE

- Development / test data sets (regional / global / seasonal)

Developed using aircraft observations over Canadian prairie, tested using SMMR and SSM/I data sets over same area. Currently being tested for Northern Hemisphere at NOAA Snow and Ice Data Center.

- Ground truth (accuracy / limitations)

Sources of ground truth: snow courses, airborne GAMMA. Accuracy within 10 - 20 mm (comparison of amounts and spatial patterns).

- Major assumptions of evaluation

Must take into account limitations of comparing point-based ground measurements (irregular distribution spatially) with SSM/I derived snow water equivalent for 25 km footprint.

* ALGORITHM PERFORMANCE (continued)

- Strengths / weaknesses

Most reliable under cold, dry winter snow conditions; zero values produced under wet snow conditions. Underestimation in vegetated areas.

* ALGORITHM MATURITY

- Operational useage

Snow water equivalent maps, using near real-time data from CNODDS, are produced weekly every winter from December to April and FAX'd to users

- Refinement / additional development

Using 37 GHz polarization difference, develop wet snow indicator (yes/no) to discriminate wet snow areas from snow free land.

- Availability

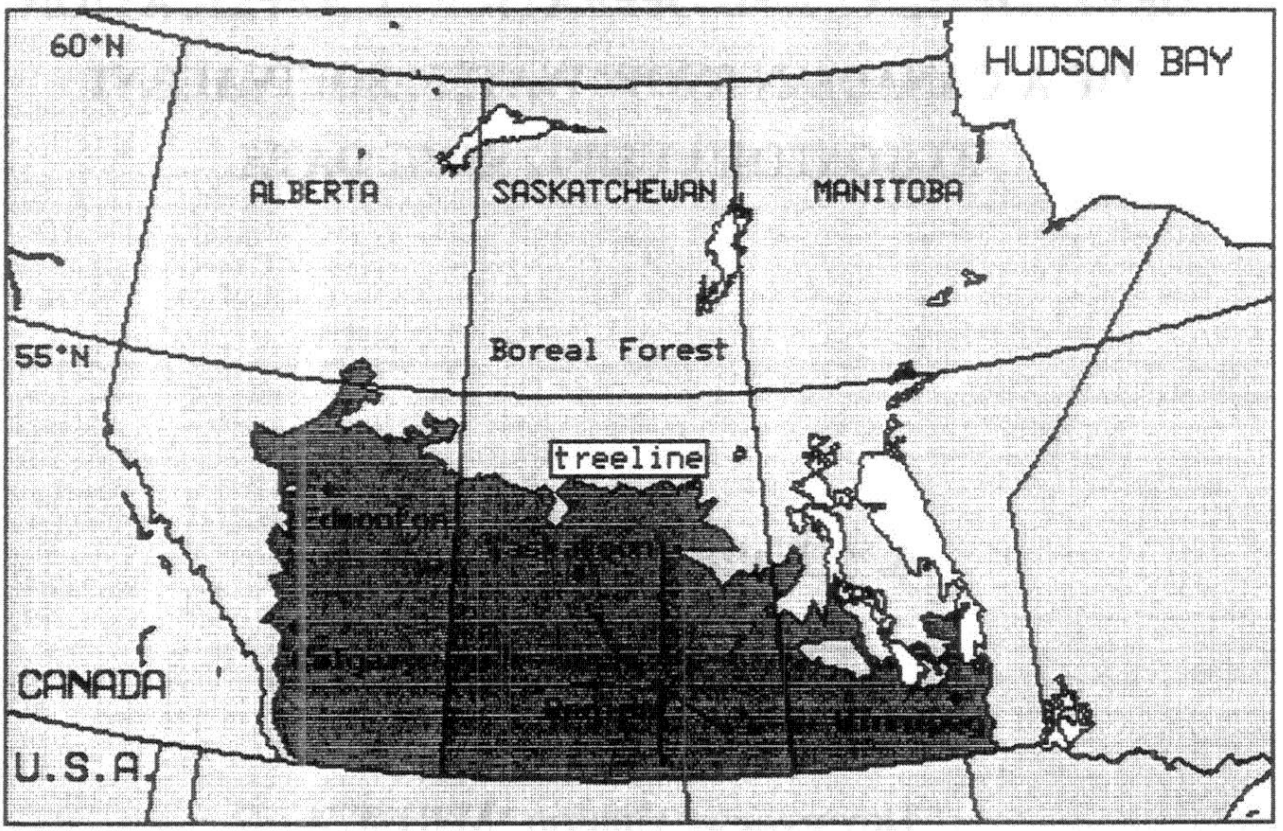
Algorithm is available upon request. Snow water equivalent products are available from private company (Ph. D. Associates, Inc.).

DEVELOPMENT AND OPERATIONAL APPLICATION OF A CANADIAN SNOW WATER EQUIVALENT ALGORITHM USING SSM/I DATA

A.E. Walker and B.E. Goodison

Climate Research Branch
Canadian Climate Centre
4905 Dufferin Street
Downsview, Ontario M3H 5T4
CANADA

THE CANADIAN PRAIRIE REGION
PASSIVE MICROWAVE SNOW COVER RESEARCH STUDY AREA



CANADIAN PRAIRIE REGION - SNOW COVER DETERMINATION USING PASSIVE MICROWAVE DATA

BACKGROUND

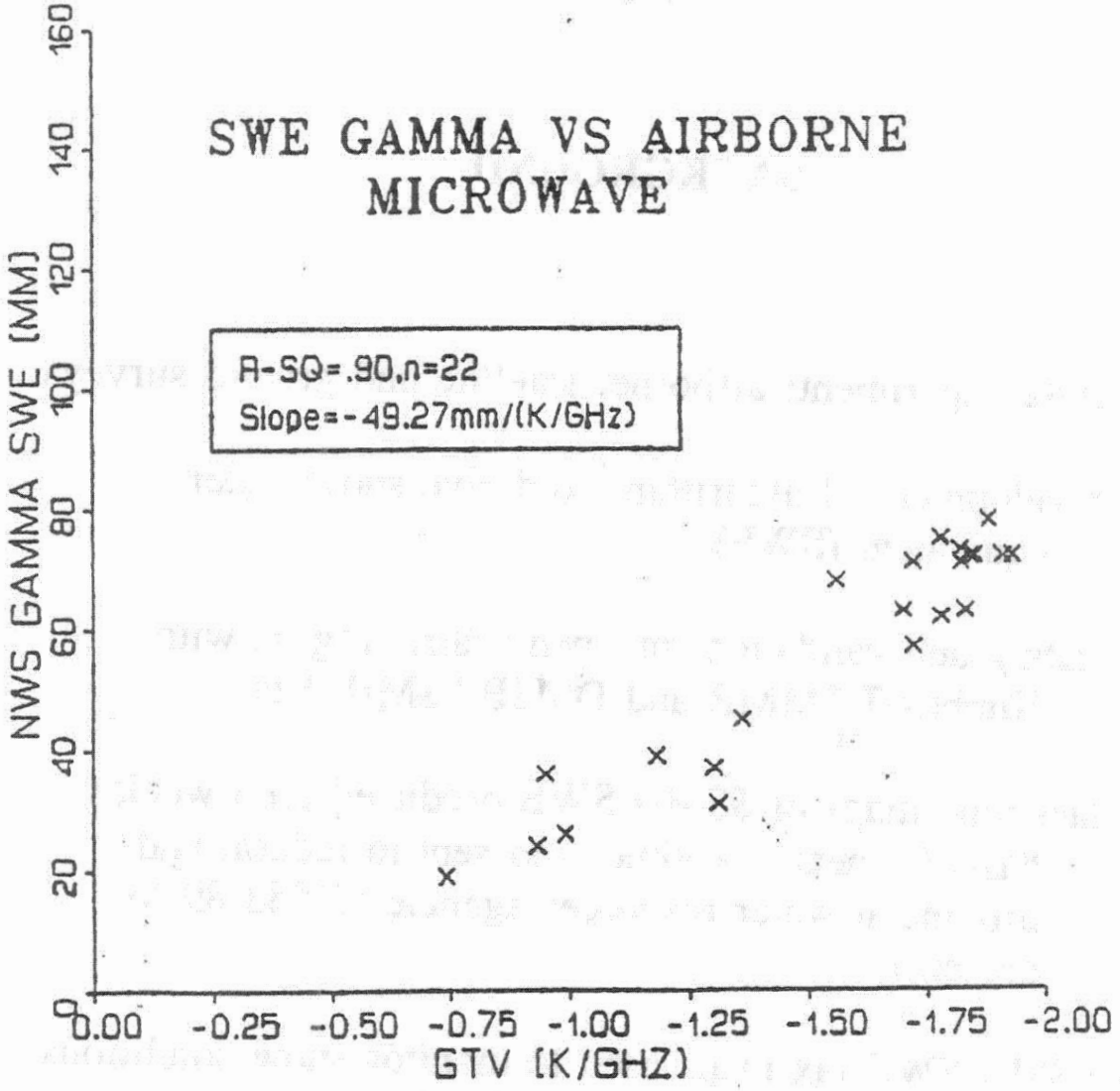
- 1982 experiment: airborne, satellite and ground surveys

- development of algorithms to derive snow water equivalent (SWE)

- testing and validation for open prairie region with Nimbus-7 SMMR and DMSP SSM/I data

- facsimile maps of SSM/I SWE produced on a weekly basis (in near real-time) and sent to federal and provincial water resources agencies (1988/89 to present)

- SSM/I SWE fax maps used to monitor snow conditions throughout winter season, plan for ground surveys, and prepare runoff forecasts


SWE GAMMA VS AIRBORNE MICROWAVE
R-SQ=.90,n=22
Slope=-49.27mm/(K/GHz)
NWS GAMMA SWE (MM)
0
20
40
60
80
100
120
140
160
0.00
-0.25
-0.50
-0.75
-1.00
-1.25
-1.50
-1.75
-2.00
GTV (K/GHZ)

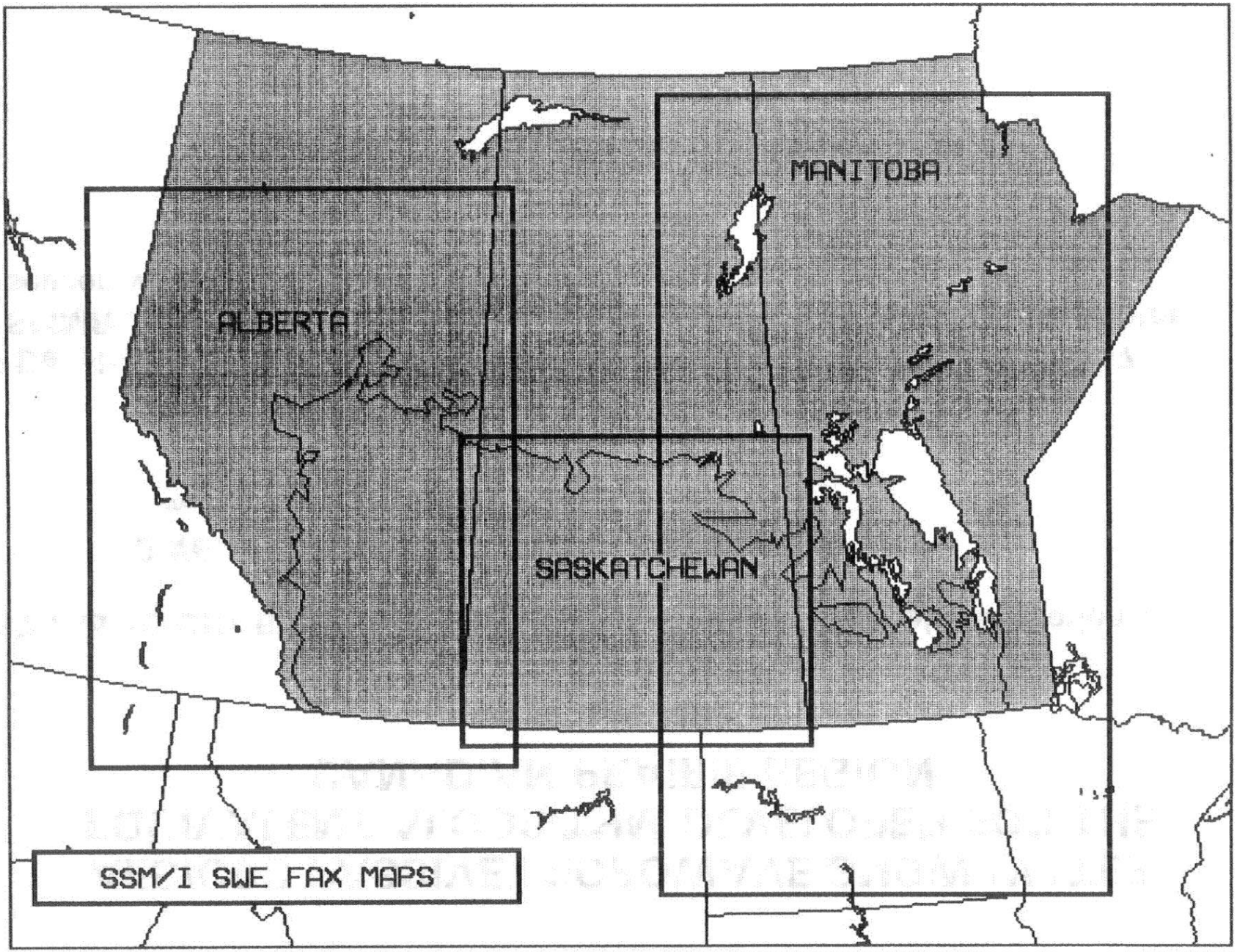
AES/CCC PASSIVE MICROWAVE SNOW WATER EQUIVALENT ALGORITHM DEVELOPED FOR THE CANADIAN PRAIRIE REGION

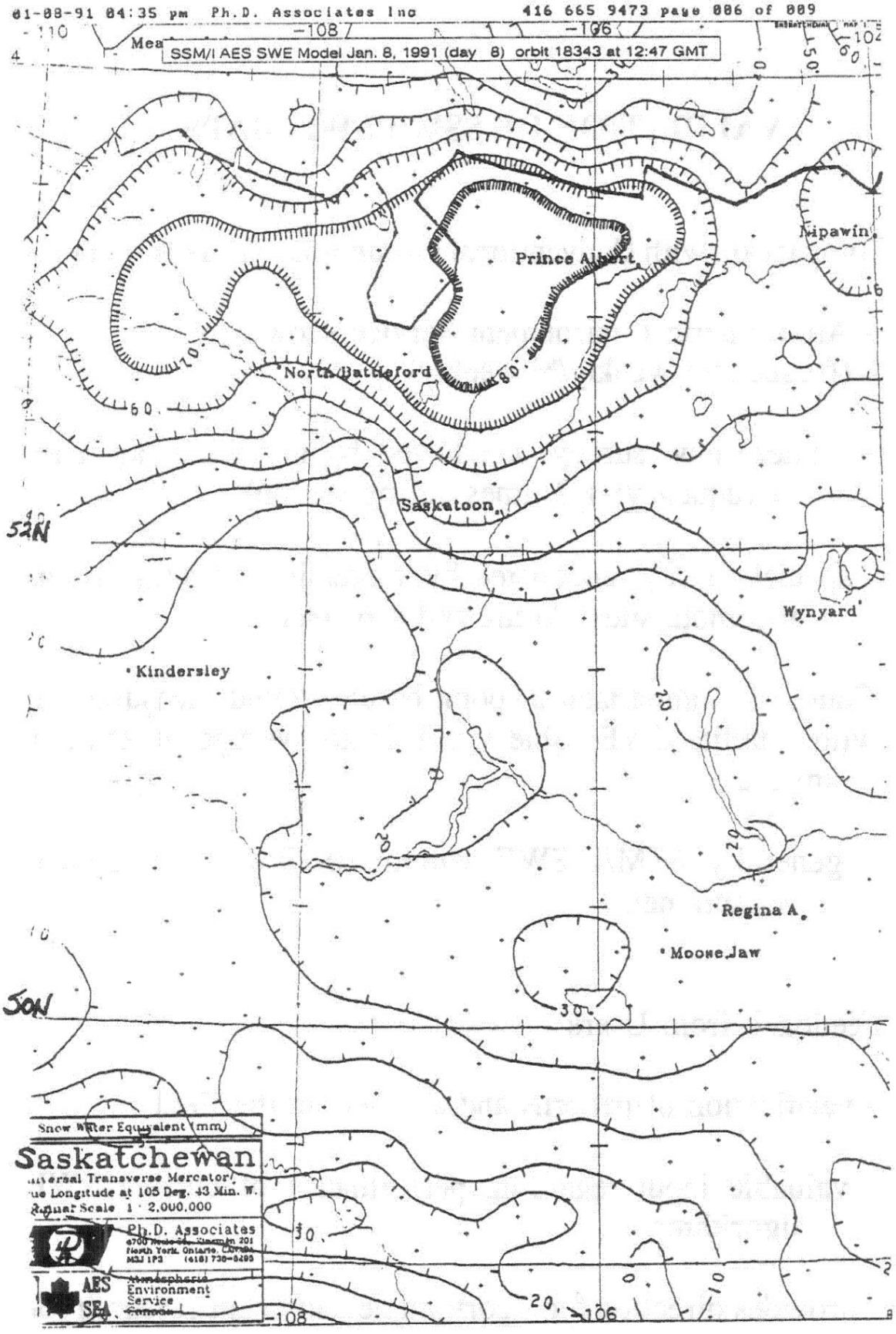
37 and 19 GHz Brightness Temperature Gradient (Vertical Polarization):

$$SWE = -20.7 - 49.27 (V37 - V19) / 18.0$$

(mm)

***Developed from intensive airborne studies and tested using Nimbus-7 SMMR and DMSP SSM/I data. Used operationally since 1988/89 winter season with near real-time SSM/I data.**


MANITOBA
ALBERTA
SASKATCHEWAN
SSM/I SWE FAX MAPS



↑ FOREST

OPEN PRAIRIE ↓

OPERATIONAL SSM/I SWE MAP PRODUCT

SOUTHERN SASKATCHEWAN

VALIDATION OF SSM/I SWE MAPS

(1) Comparison with Conventional Ground-based Measurements

- Atmospheric Environment Service snow course (frequency: weekly/bi-weekly)

- winter snow surveys conducted by provincial agencies (frequency: 1-2 times during season)

- special surveys conducted by university research groups at remote sites (Arctic and sub-Arctic)

Caution: comparison of point-based ground measurement with satellite SWE value which is an average of 25km x 25km area

- generally SSM/I SWE within 10-20 mm of ground measurements

(2) Feedback from Users

- verification of patterns and amounts in the field

- valuable input regarding performance of current SWE algorithms

- provides direction for algorithm development research for improved, more representative SWE retrievals from SSM/I data

FACTORS WHICH AFFECT THE PERFORMANCE OF CURRENT SSM/I SWE ALGORITHMS

FOCUS OF CURRENT RESEARCH

(1) Vegetation (Forest) Cover

- results in an underestimation of SWE

(2) Wet (Melting) Snow

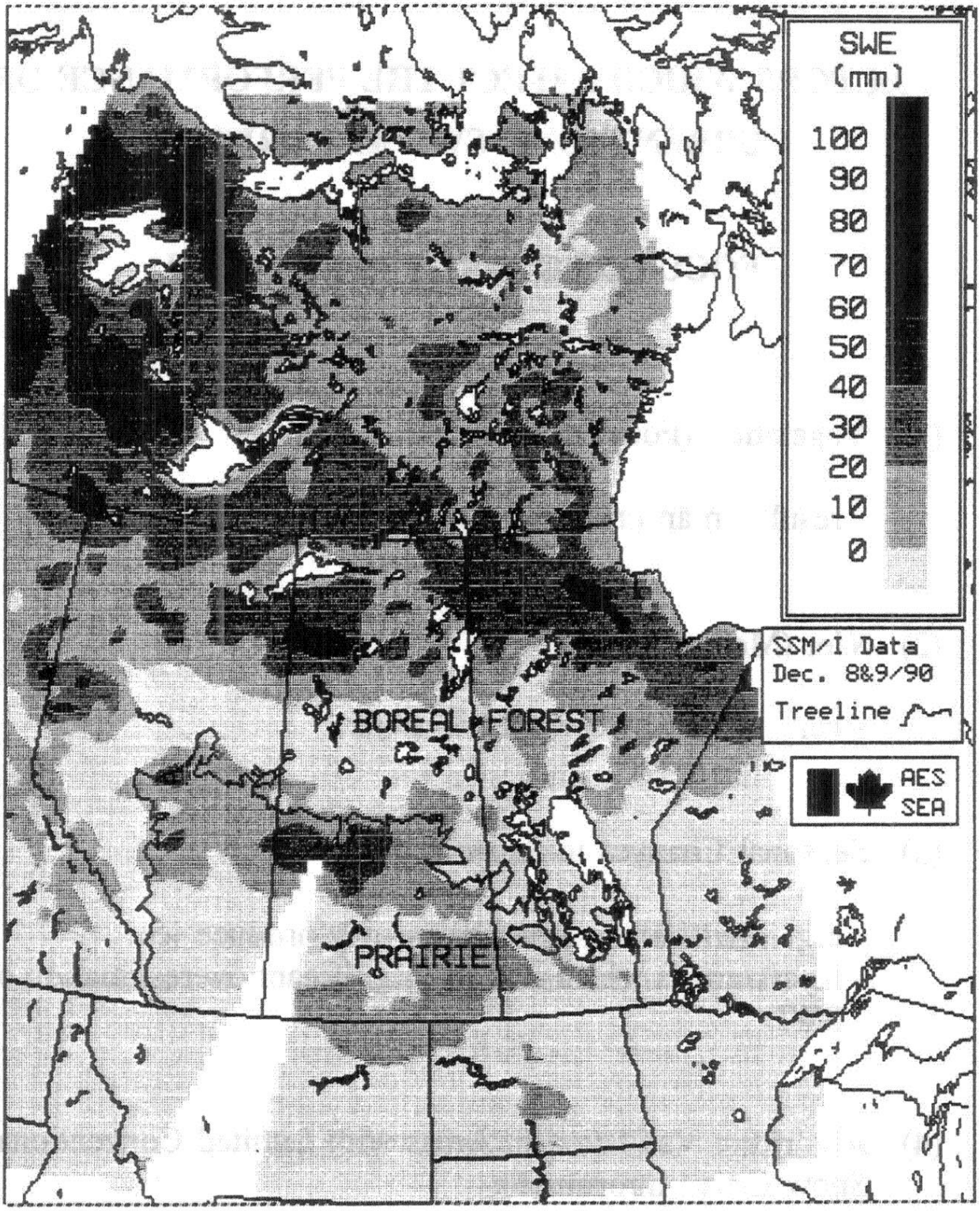
- very low or zero values of SWE

(3) Seasonal Changes in Snowpack Structure

- e.g., melt/refreeze processes may produce ice layers/crusts which result in significant overestimation of SWE

(4) Algorithm Validation in Areas with Limited Conventional Snow Cover Information

- e.g., Arctic and sub-Arctic regions of Canada


SWE
(mm)
100
90
80
70
60
50
40
30
20
10
0
SSM/I Data
Dec. 8&9/90
Treeline
AES
SEA
BOREAL FOREST
PRAIRIE

PROBLEM: WET SNOW

- presence of liquid water within snowpack alters microwave emission characteristics

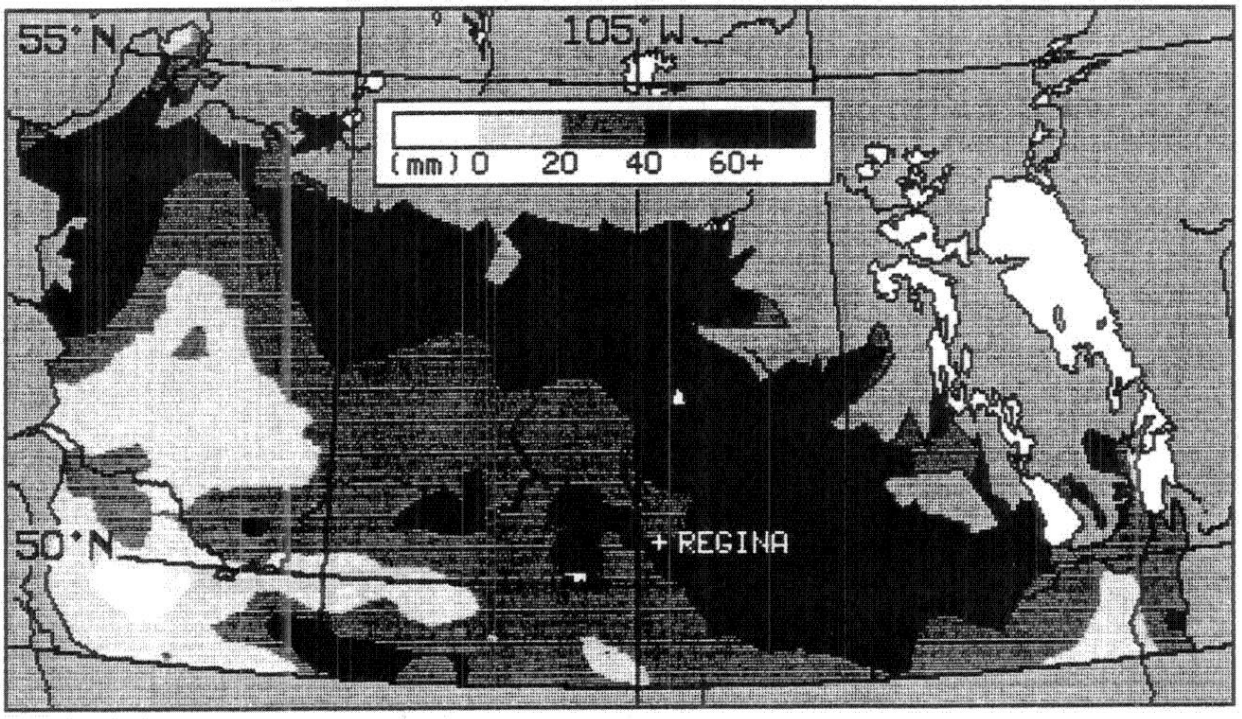
- increase in observed microwave brightness temperatures results in "zero" SWE values using SSM/I algorithm

- areas of wet snow are falsely depicted as areas of snow-free land

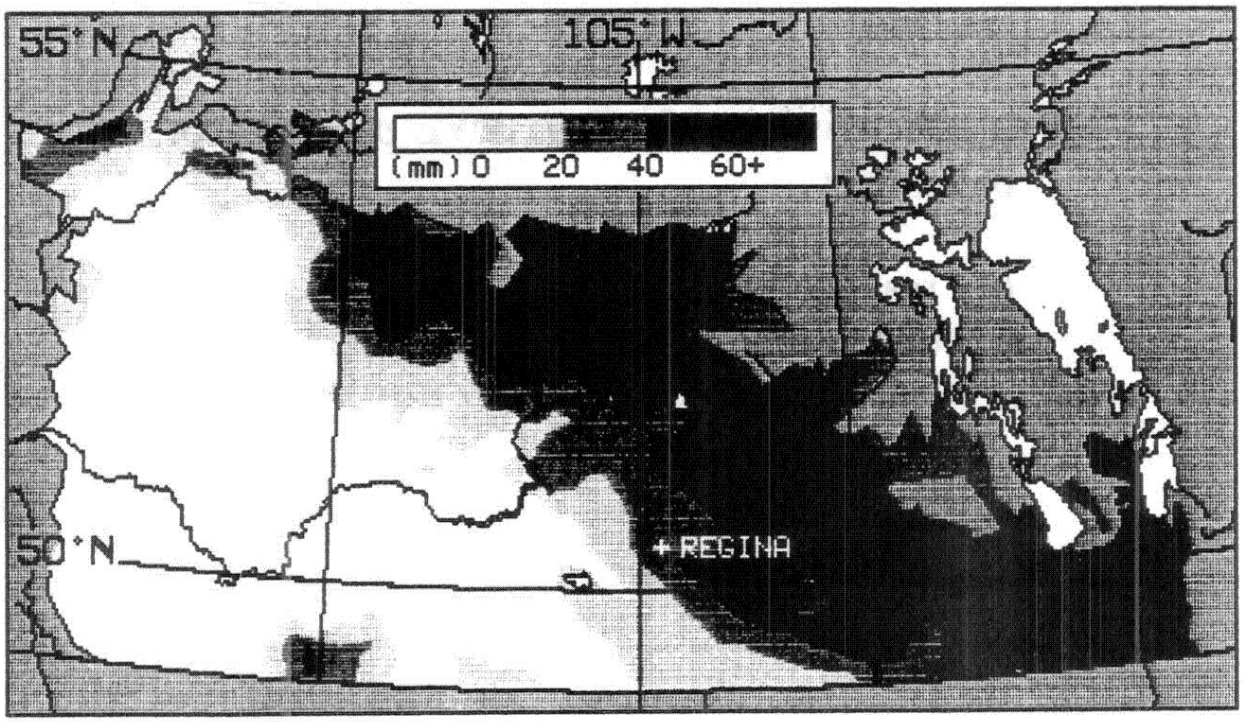
- limits effective use of SSM/I SWE products for providing:

  (i) real-time information to users
  (ii) climate time-series analyses

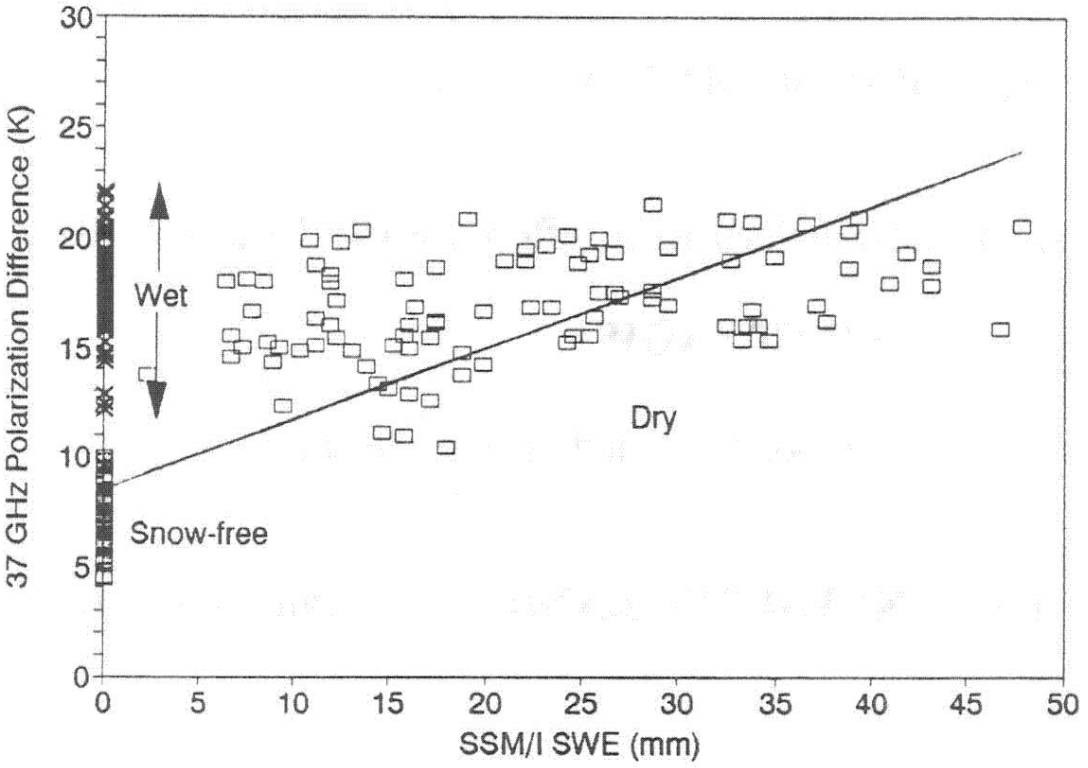
SSM/I SNOW WATER EQUIVALENT JANUARY 31, 1991



SSM/I SNOW WATER EQUIVALENT FEBRUARY 2, 1991



SSM/I WET SNOW ANALYSIS
DAYS 31 & 33/91



SSM/I WET SNOW INDICATOR:

Applied when SSM/I SWE = ZERO

If 37 GHz polarization difference (V37-H37) $\geq$ 10.0:

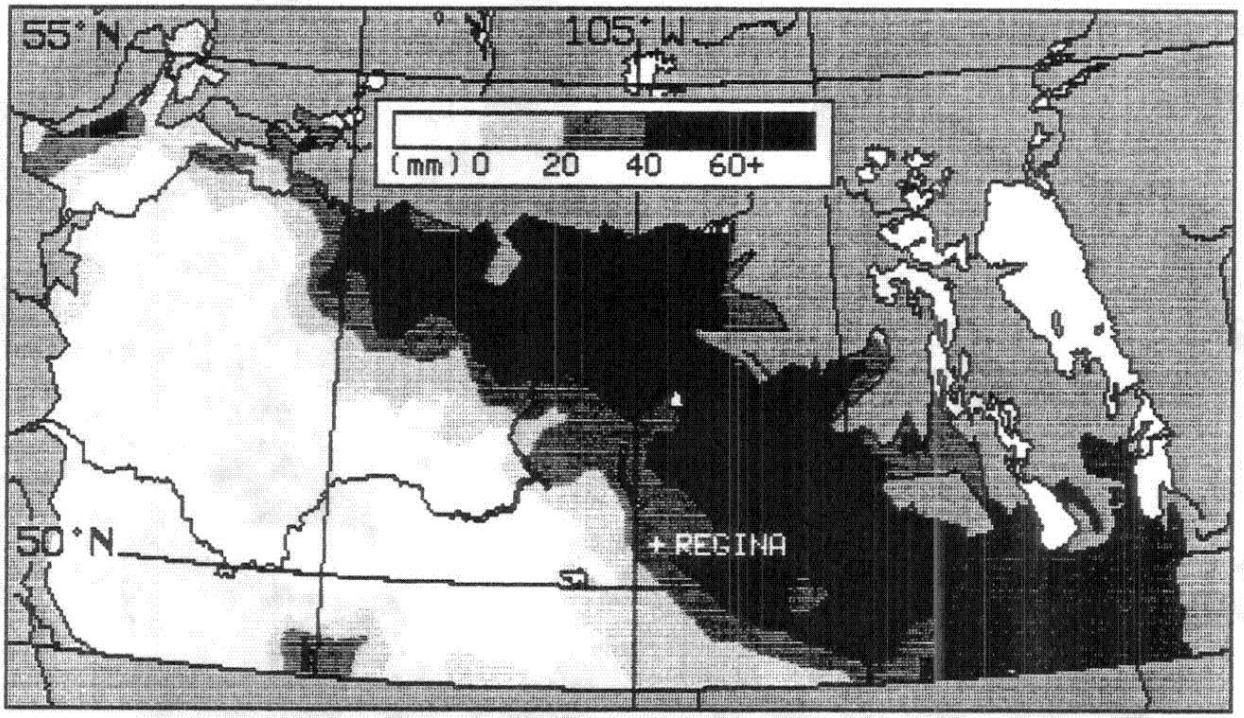
then **WET SNOW**

$\Rightarrow$ Symbol is plotted at pixel location

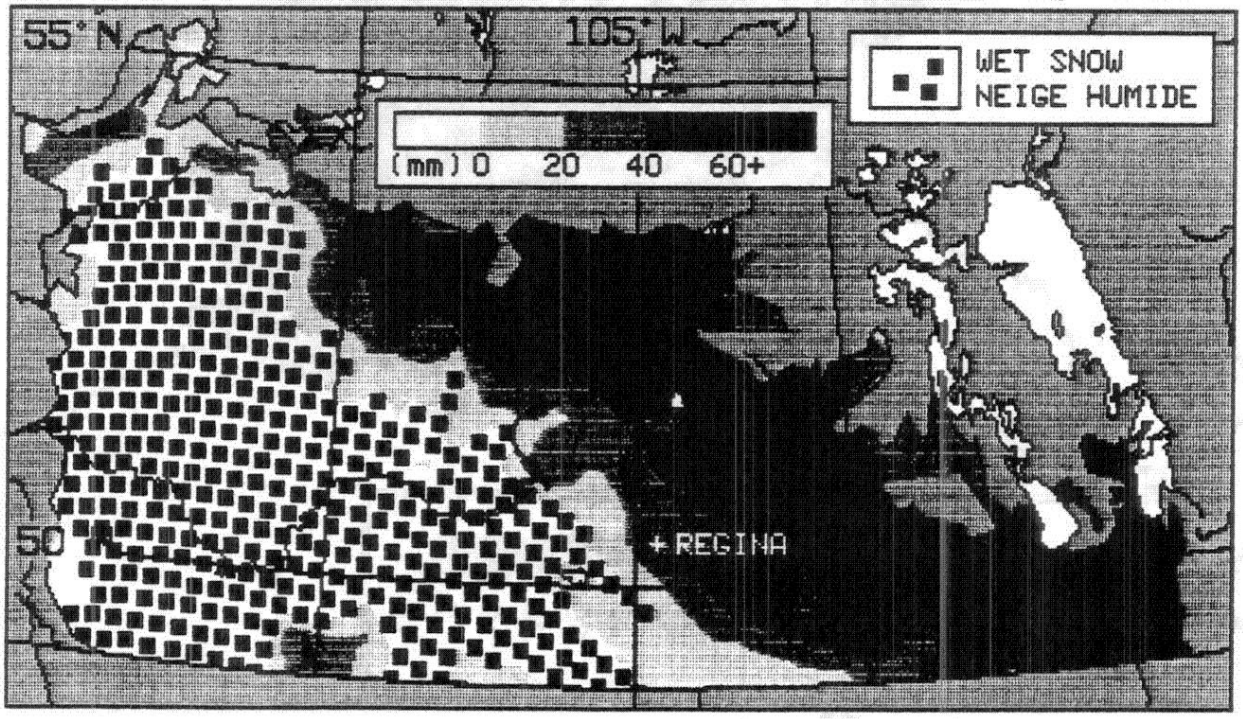
Else, **SNOW-FREE LAND** $\Rightarrow$ No symbol plotted

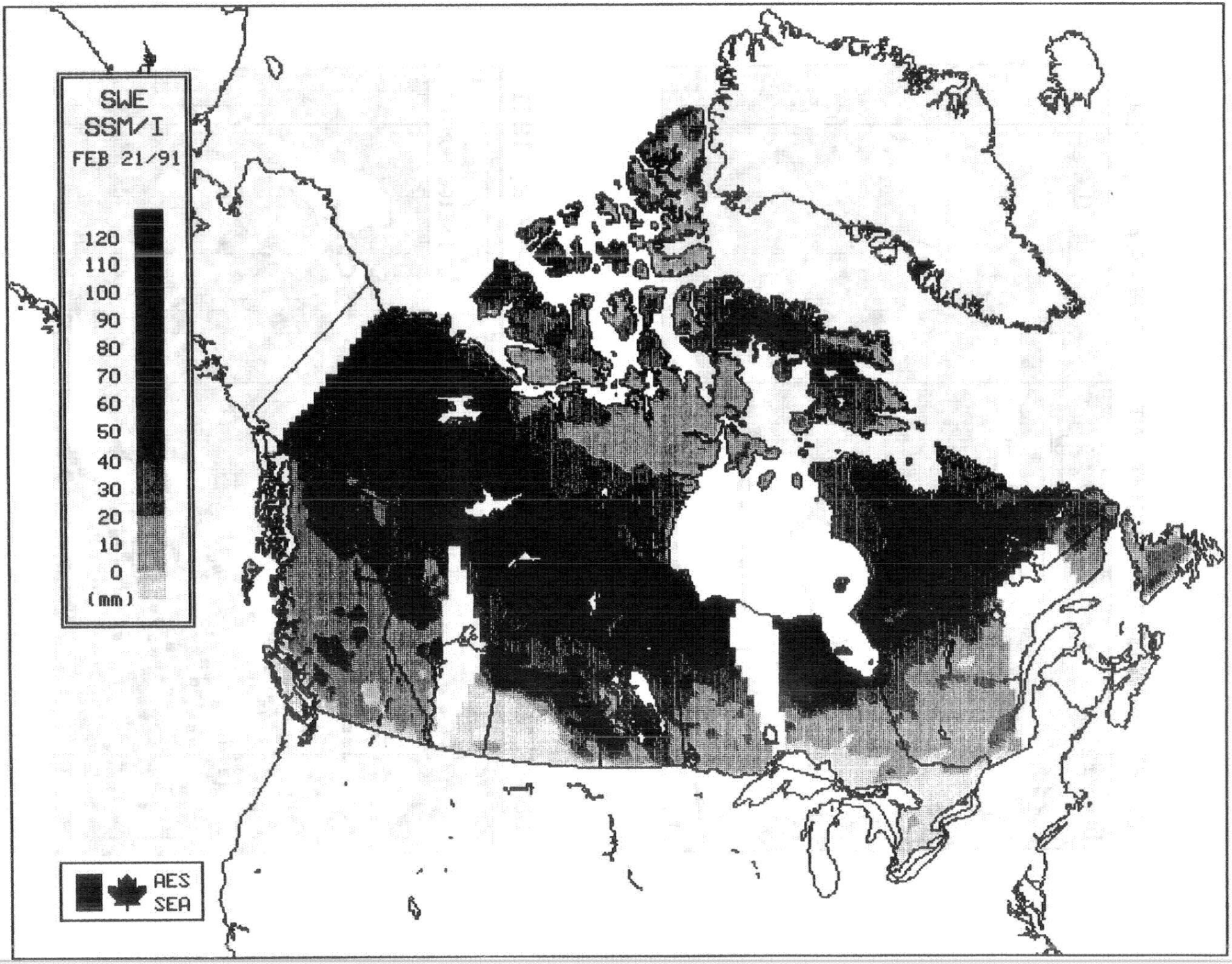
Note: Testing and validation of the wet snow indicator has been limited to the open prairie region of Canada; may also be applicable to other regions of similar terrain and vegetative characteristics.

SSM/I SNOW WATER EQUIVALENT FEBRUARY 2, 1991



SSM/I SNOW WATER EQUIVALENT FEBRUARY 2, 1991




SWE
SSM/I
FEB 21/91
120
110
100
90
80
70
60
50
40
30
20
10
0
(mm)
AES
SEA

AES/CCC RESEARCH DIRECTION

PASSIVE MICROWAVE SNOW COVER APPLICATIONS

- Canadian Prairies SSM/I SWE Fax Map Program
  - will continue as long as access to near real-time SSM/I data from CNODDS

- CRYSYS - Cryospheric System to Monitor Global Change in Canada
  - Canadian project within NASA's Earth Observing System (EOS) program (P.I. - Dr. B. Goodison)
  - Snow cover component - development of algorithms for other landscape regions (e.g. boreal forest, sub-Arctic and Arctic) using SSM/I data
  - research in preparation for launch of EOS MIMR

- Development of a Ground-based Microwave Radiometer System
  - cooperative research project involving government (federal and provincial), university and private sector
  - 3-channel dual-polarization radiometer
  - snow cover and soil moisture applications
  - study microwave signatures for specific snow cover conditions (including vegetation effects)
  - objective: improved, reliable algorithms for use with current and future satellite sensors

CANADIAN CLIMATE CENTRE SSM/I SNOW COVER RESEARCH WORK

REFERENCES

Goodison, B.E., 1989: Determination of areal snow water equivalent on the Canadian Prairies using passive microwave satellite data. IGARSS '89: Remote Sensing, an Economic Tool for the Nineties. July 10-14, 1989, Vancouver, B.C. IEEE No. 89CH2768-0, Vol. 3, 1243-1246.

Goodison, B.E., A.E. Walker and F.W. Thirkettle, 1990: Determination of snow water equivalent on the Canadian Prairies using near real-time passive microwave data. Proc. Workshop on Applications of Remote Sensing in Hydrology, Saskatoon, February 13-14, 1990, 297-316.

Goodison,B.E., A.E. Walker and F.W. Thirkettle, 1990: Determination of snow cover on the Canadian Prairies using passive microwave data. Proc. Int. Symp. on Remote Sensing and Water Resources. Enschede, The Netherlands, Aug. 20-24, 1990, 127-136.

Thirkettle, F., A.Walker, B.Goodison and D. Graham, 1991: Canadian Prairie snow cover maps from near real-time passive microwave data: From satellite to user information. Proc. 14th Canadian Remote Sensing Symp., Calgary, Alberta, May 6-10, 1991, 172-177.

Walker, A.E. and B.E.Goodison, 1991: Monitoring snow cover in the boreal forest region of the Canadian Prairies using passive microwave data. Proc. 14th Canadian Remote Sensing Symp., Calgary, Alberta, May 6-10, 1991, 296-299.

Walker, A.E. and B.E. Goodison, 1992: Discrimination of a wet snowcover using passive microwave satellite data. Proc. of the International Symposium on Remote Sensing of Snow and Ice, International Glaciological Society, May 17-22, 1992, Boulder, Colorado, Annals of Glaciology, Vol.17 (in press).

Goodison, B.E, and A.E. Walker, 1992: Use of snow cover derived from satellite passive microwave data as an indicator of climate change. Proceedings of the International Symposium on Remote Sensing of Snow and Ice, International Glaciological Society, May 17-22, 1992, Boulder, Colorado, Annals of Glaciology, Vol.17 (in press) .

Goodison B.E. and A.E. Walker, 1993: Canadian development and use of snow cover information from passive microwave satellite data, Proc. EAS/NASA International Workshop on Passive Microwave Remote Sensing Research Related to Land-Atmosphere Interactions, St. Lary, France, January 11-15, 1993 (in press).

Walker, A.E. and B.E. Goodison, 1993: Passive microwave derived snow cover for hydrological and climatological applications in northern regions. Proc. of the Ninth International Northern Research Basins Symposium/Workshop, Whitehorse, Yukon Territory, August 14-22, 1992, p. 575-588.

Validation Data Sets for SSM/I Derived Snow Cover Products

Richard Armstrong and Molly Hardman
CIRES/NSIDC CB 449
University of Colorado
Boulder, CO 80309

The National Snow and Ice Data Center (NSIDC) has distributed DMSP Special Sensor Microwave Imager (SSM/I) brightness temperature grids for the Polar Regions on CD-ROM beginning in July of 1987. In order to expand this product to include snow covered regions, the area of coverage will become global. Based on recommendations from the SSM/I Products Working Team (SPWT), the Equal Area SSM/I Earth Grid (EASE-Grid) is being developed. (Version 0.0 was distributed on CD-ROM for evaluation during the last quarter of 1992.) The SPWT was formed in 1989 by NASA Headquarters and focusses on solving problems associated with the extraction of land surface information (primarily vegetation, soils, and snow cover) from SSM/I data. The intent of the EASE-Grid concept is to provide the general user with a data structure (i.e. interpolation from swath coordinates to fixed earth grid, projection and gridding scheme) which is easier to use than swath format, yet maximizes the radiometric integrity of the original temperature values, provides high spatial and temporal precision, and involves no averaging of the swath data.

In order to provide a standard environment in which to validate algorithm output, it is necessary to produce baseline reference data sets using other, more direct, methods of measurement. In the case of snow depth and snow water equivalent, validation data are typically obtained from surface point measurements at various weather and climate reporting stations worldwide. The spatial density of these reporting stations varies greatly from one region to another. Where point (vector) measurements are applied to validate grid cell (raster) data, methods have typically been subjective or qualitative in nature. Visual comparisons are made between a few images with results presented in tabular form. In order to make quantitative comparisons between SSM/I algorithm output and surface measurements, it is first necessary to apply a method which will interpolate between the point measurements and the area-integrated SSM/I value. NSIDC is developing such a technique using EASE-Grid format. Once the two data sets are in the same grid scheme, digital image subtraction techniques are used to make comparisons. NSIDC has compiled a validation data set of surface station measurements for the northern hemisphere winter of 1988-1989 using specific data from the United States, Canada, and the former Soviet Union, as well as data from WMO for the remaining regions. Results from the statistical methods currently being applied in the analysis are presented. These include the development of time-series images representing the mean, maximum, and minimum differences between the validation data and the algorithm output. Ancillary data sets (e.g. vegetation, surface temperature, digital elevation) are applied to assist in determining why certain regions typically provide reasonable results in contrast to regions where large differences between algorithm output and validation occur.

SPN SSM/I ALGORITHM SYMPOSIUM
Algorithm Questionnaire

"SNOW COVER ALGORITHM INTERCOMPARISONS"
Richard Armstrong, respondent

Please provide the following essential information about your algorithm(s).

* ALGORITHM DESCRIPTION

- Type (statistical, physical, other) *Statistical and decision tree*

NOAA Snow and Ice Data Center (NSIDC) will test the following algorithms against a standard earth-gridded snow depth data set:

1. *Grody - NOAA*
2. *Goodison - Canadian Climate Centre*
3. *DMSP Cal / Val*
4. *Nagler - Univ. of Innsbruck, Austria*

Preliminary results should be available by autumn, 1993.

- Input required / Output produced

Input: Typically frequency and polarization differences from all channels to satisfy all four algorithms listed above
Output: Snow cover / depth

- Auxiliary sensor/data base requirements

None for now, but we propose visible spectrum input in future enhancements

- Major limitations / approximations

Problems with resolution, wet snow, dense vegetation

- Computer resource requirements *Workstation or 486 PC*

* ALGORITHM PERFORMANCE

- Development / test data sets (regional / global / seasonal)

Global EASE-Grid data sts will be available from NASA SSM/I Pathfinder within about one year for July 1987 - November 1988.

- Ground truth (accuracy / limitations)

Regional EASE-Grid snow depth and water equivalent data sets currently under development at NSIDC.

* ALGORITHM PERFORMANCE (continued)

- Major assumptions of evaluation

Accurate (reasonable) interpolation from point measurements to the area integration of the SSM/I cell

- Strengths / weaknesses

Excellent all weather snow extent - poor to good estimate of depth or water equivalent, depending on region.

* ALGORITHM MATURITY

- Operational useage

Currently successful at regional scale (Goodison/Walker, Canada) and soon to be evaluated at global scale (Armstrong)

- Refinement / additional development

Include 85 GHz to monitor better shallow snow (Nagler/ Armstrong). Integrate SSM/I and OLS (NSIDC).

- Availability

All algorithms, and data, are available upon request.

Validation Data Sets for SSM/I Derived Snow Cover Products

Richard Armstrong and
Molly Hardman
NSIDC/WDC-A Glaciology
University of Colorado, Boulder

SPN SSM/I Algorithm Symposium
June 8-10, 1993
Monterey, CA

SSM/I DATA FOR SNOW COVER/CLIMATE RESEARCH

PRIMARY OBJECTIVES:

I. Produce a Prototype Snow Cover Climatology for first 5 Years of SSM/I

- A. Assess the Utility of the Data Set;
  1. Study of Surface Energy Budgets and the Hydrologic Cycle of the Cryosphere
  2. Input to Earth Systems Models
  3. Potential Role of Snow and Ice in Global Change Detection

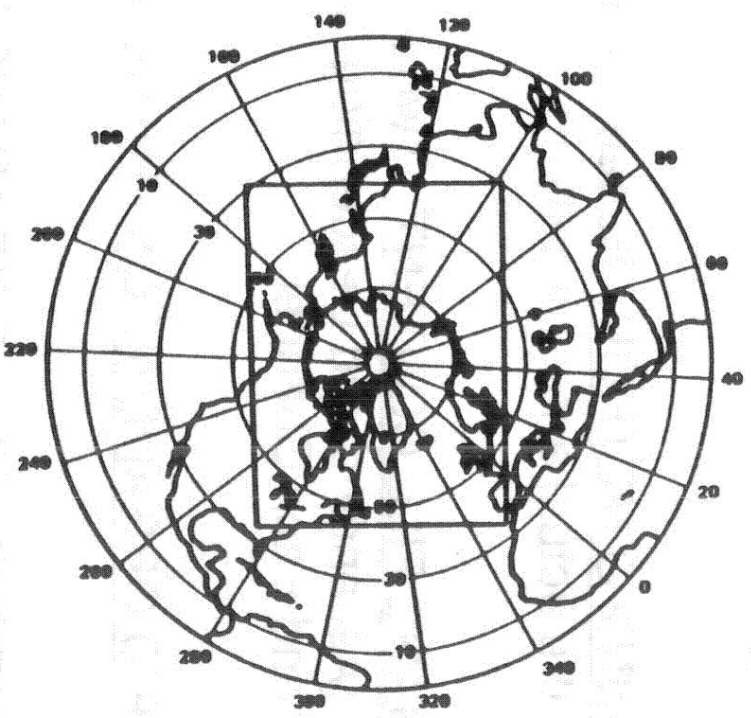
II. Produce, Archive, Distribute Data Products

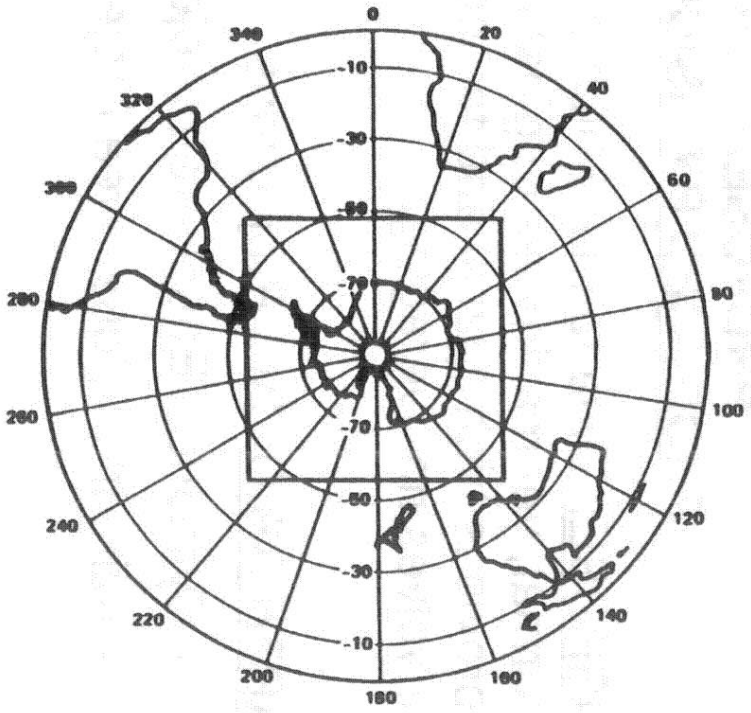
- A. Develop Optimal Format for Global Data
- B. Test Existing Algorithms

III. Establish and Coordinate Activities of SSM/I Land Products Working Team (SPWT)

SNOW AND ICE DATA CENTER

SSM/I GRIDS





EQUAL AREA SSM/I EARTH (EASE) GRID

PROPOSED VERSION 1.0

PRODUCED BY NSIDC AND SPWT

PURPOSE: Data format which is easier to use than swath format, yet maximizes original radiometric integrity, provides high spatial and temporal precision, and involves no averaging.

EARTH GRID: Two Projections

- Cylindrical Equal Area Projection
- Azimuthal Equal Area Projection

Cell Size: - 25.0 km for all channels; 12.5 km for 85 GHz V and H

BINNING METHOD: Based on coefficients derived from the actual antenna pattern

IMAGE FILE CONTENT: Two Files (Arrays) for Each Day (Ascending and Descending Orbits) for Each Projection and Each Channel

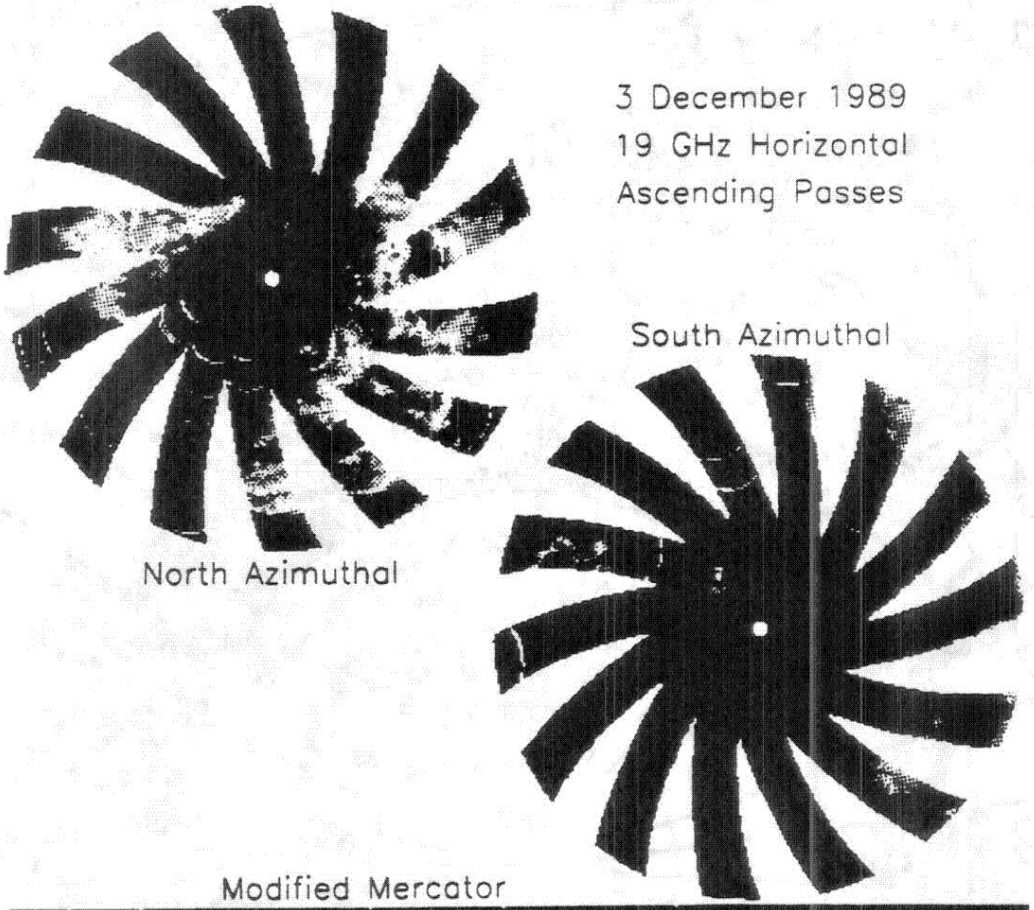
GRID ORGANIZATION: Row/Column, Band Sequential

COORDINATE & GRID TRANSFORMATIONS: No Special Tools Required, Array Files are Both I,J and Lat./Lon.

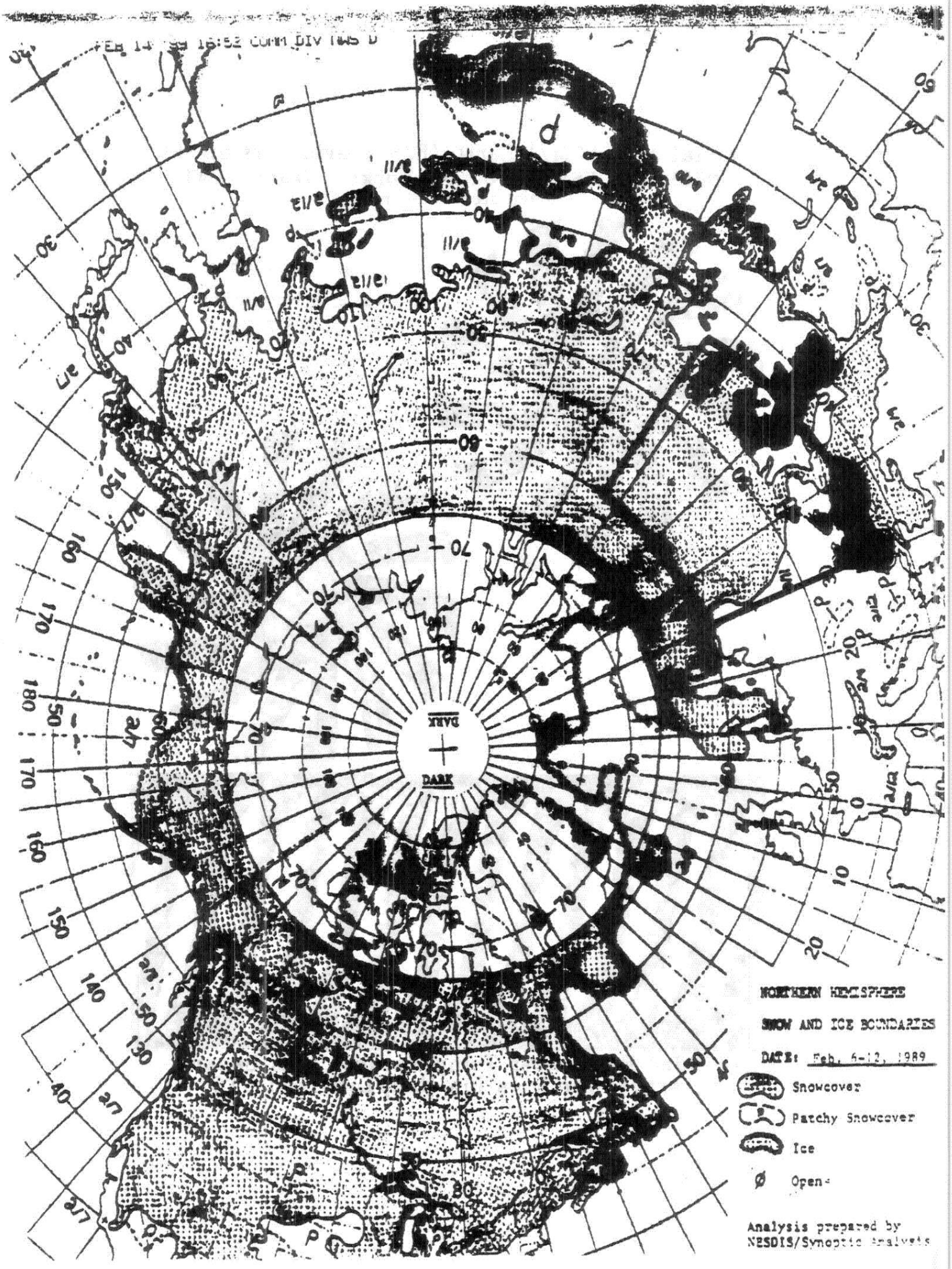
Equal Area SSM/I Earth (EASE) Grid Version 0.0

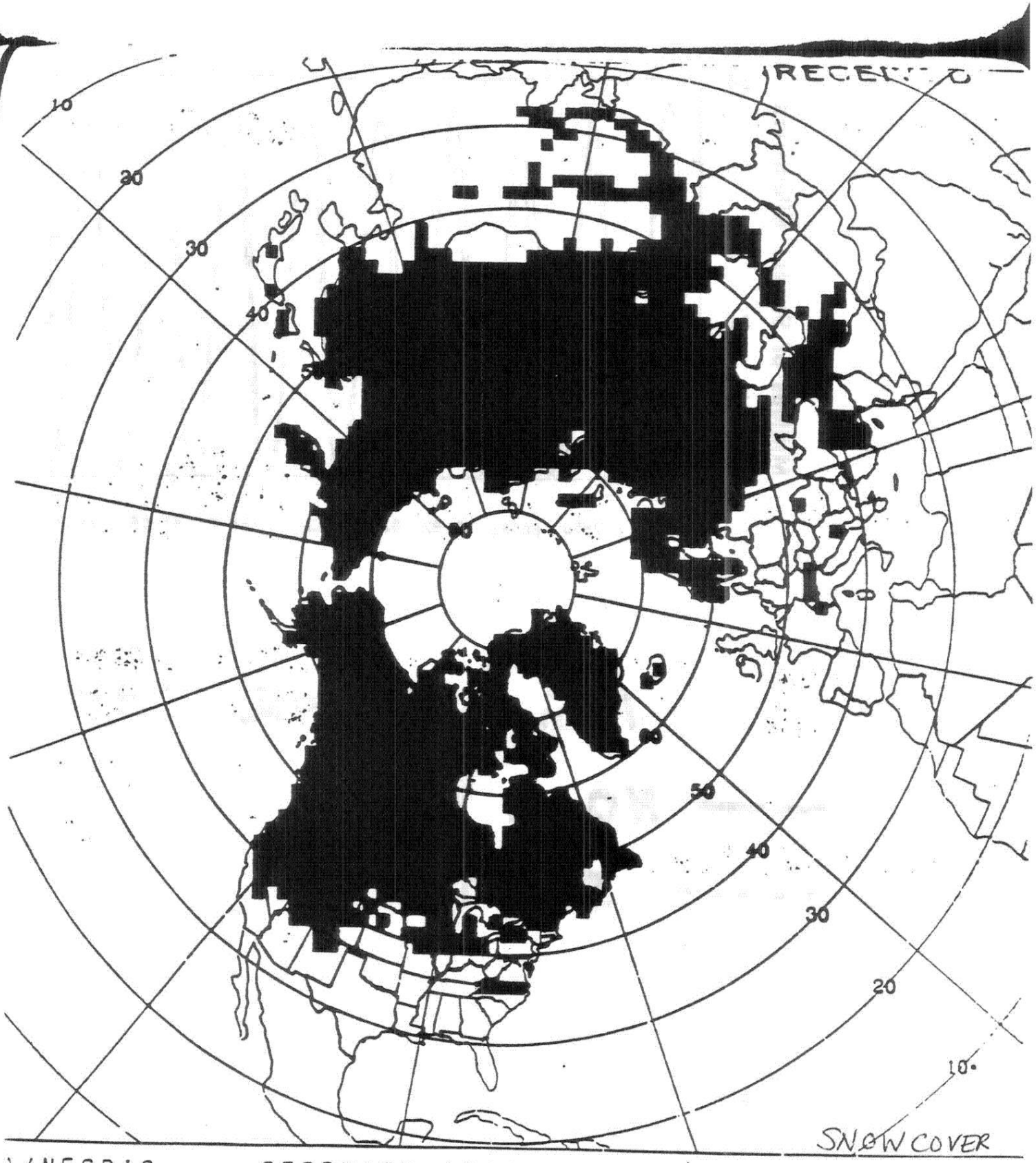
NSIDC and SSM/I Products Working Team (SPWT)

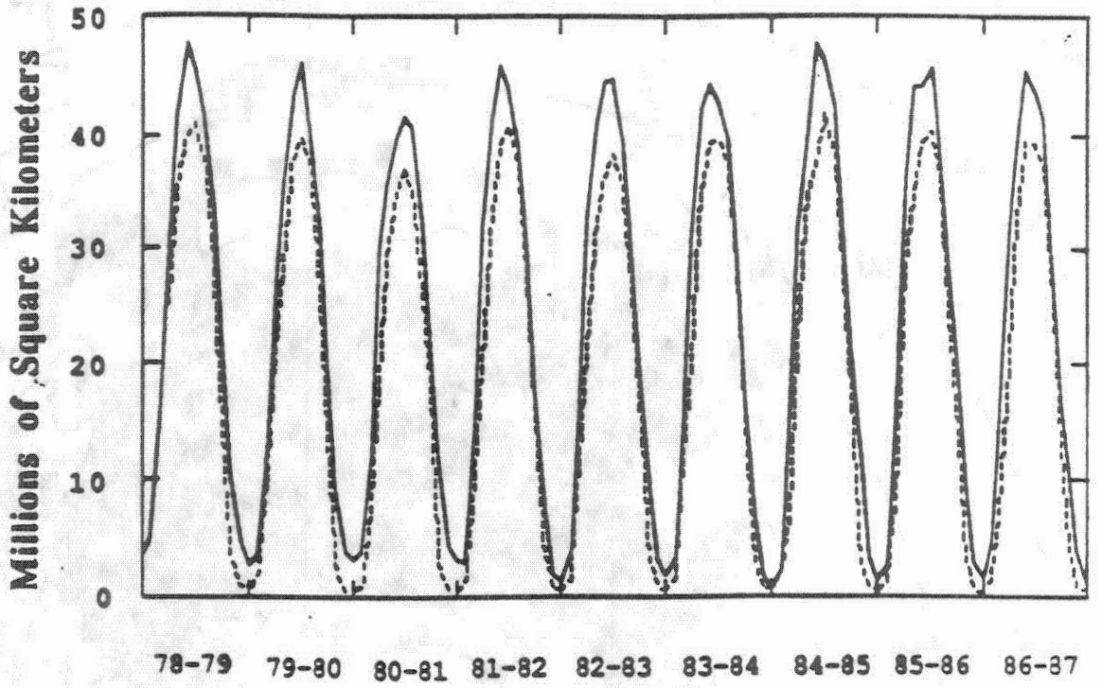
Distributed October 1992



Gridded Brightness Temperatures with Separate Arrays for Location (Lat/Lon) and UTC


NORTHERN HEMISPHERE
SNOW AND ICE BOUNDARIES
DATE: Feb. 6-12, 1989
Snowcover
Patchy Snowcover
Ice
Open
Analysis prepared by
NESDIS/Synoptic Analysis
DARK
DARK


RECEIVED
10
20
30
40
50
40
30
20
10
SNOW COVER
A/NESDIS FEBRUARY 1989 MONTHLY MEAN



Robinson 1992

Figure 10

—— NOAA Visible

- - - - SMMR

SNOW COVER DATA FROM HYDROMETEOROLOGICAL STATIONS IN THE FSU

A. STATION DATA

STATION NAME, NUMBER, LOCATION

SITE (OPEN, FORESTED, BUILDINGS)

MEAN DEPTH (CM) FOR DAYS 1-10, 11-20, 21-30/31)

DAYS OF MONTH WITH SNOW COVER

B. TRANSECT DATA (1-2 KM SNOW COURSE)

(1-6 TRANSECTS NEAR STATION, APPROX. EACH 10 DAYS)

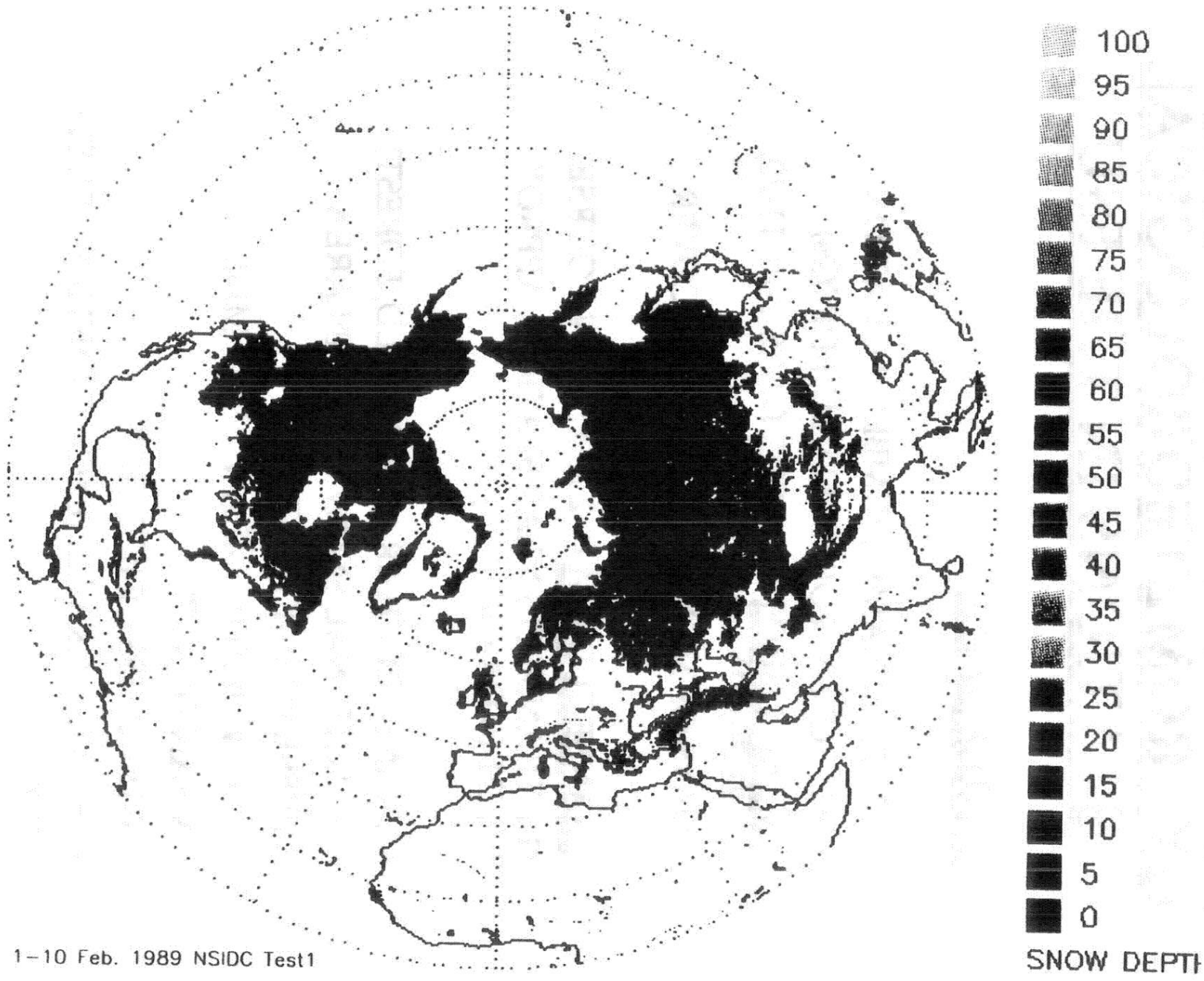
- TRANSECT CHARACTER (FIELD, FOREST)
- FRACTIONAL SNOW COVER IN AREA
- PRESENCE OF ICE CRUST

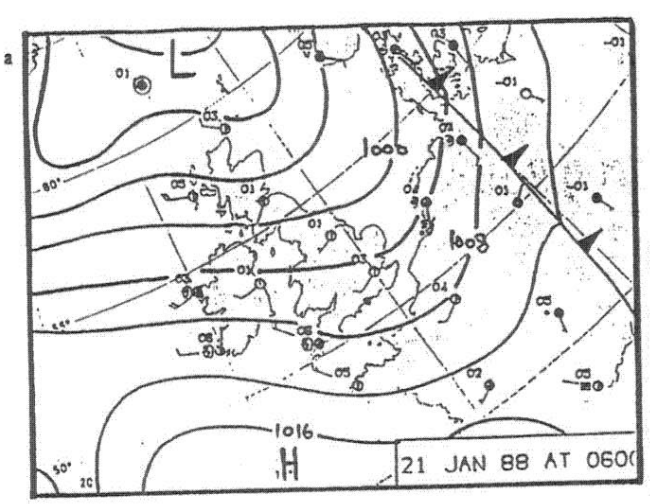
  SNOW DEPTH - MEAN, MAX., MIN.
- MEAN DENSITY

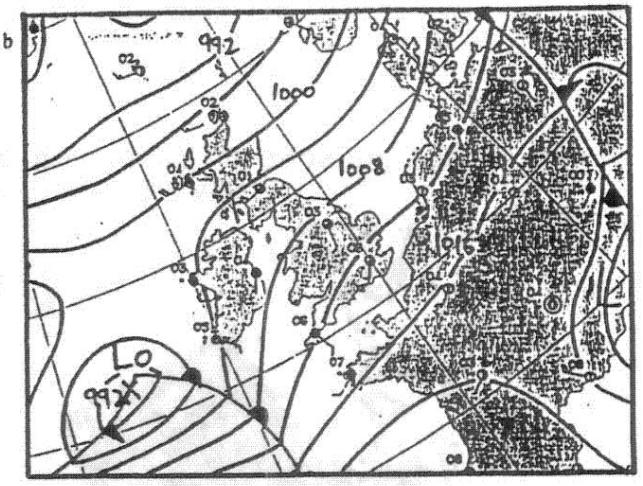
  THICKNESS OF ICE CRUST
- SNOW PACK W.E. (EXCLUDING ICE CRUST)

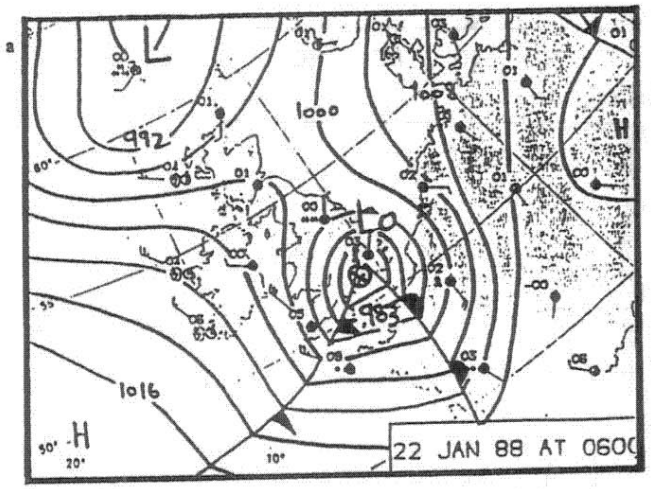
  TOTAL W.E.
- CHARACTER OF SNOW SURFACE
- CHARACTER OF SNOW COVER

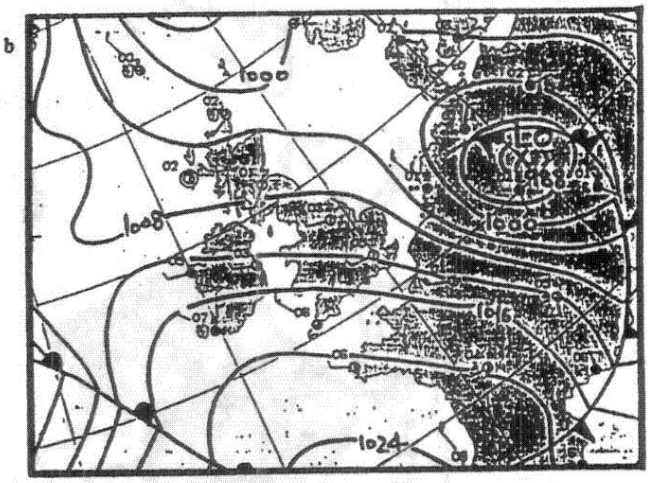
SJR 6/93

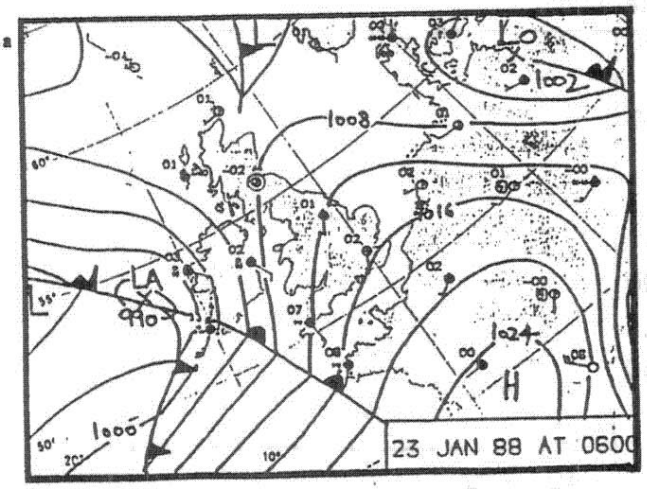

100
95
90
85
80
75
70
65
60
55
50
45
40
35
30
25
20
15
10
5
0
SNOW DEPTH
1-10 Feb. 1989 NSIDC Test1

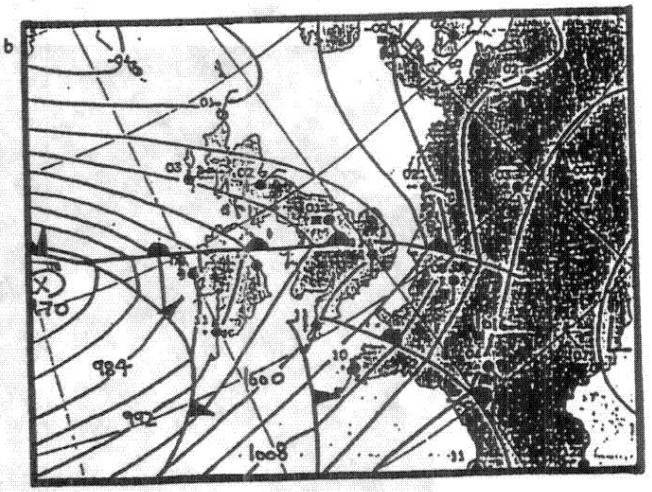

a
L
1000
1008
1016
H
21 JAN 88 AT 060


b
992
1000
1008
1016
LO
992


a
L
992
1000
LO
988
1016
H
22 JAN 88 AT 060

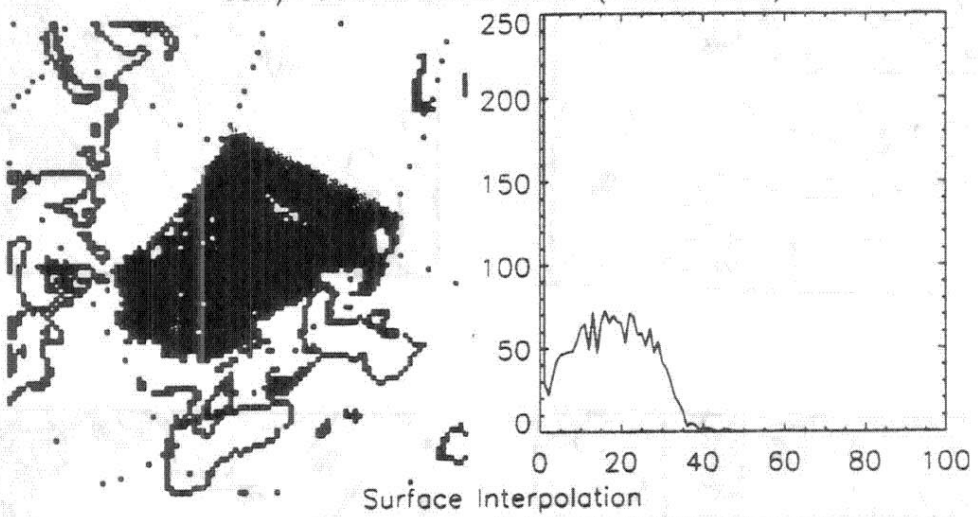

b
1000
LO
1008
1016
1024


a
LO
1002
1008
1016
LA
990
1024
H
1000
23 JAN 88 AT 060

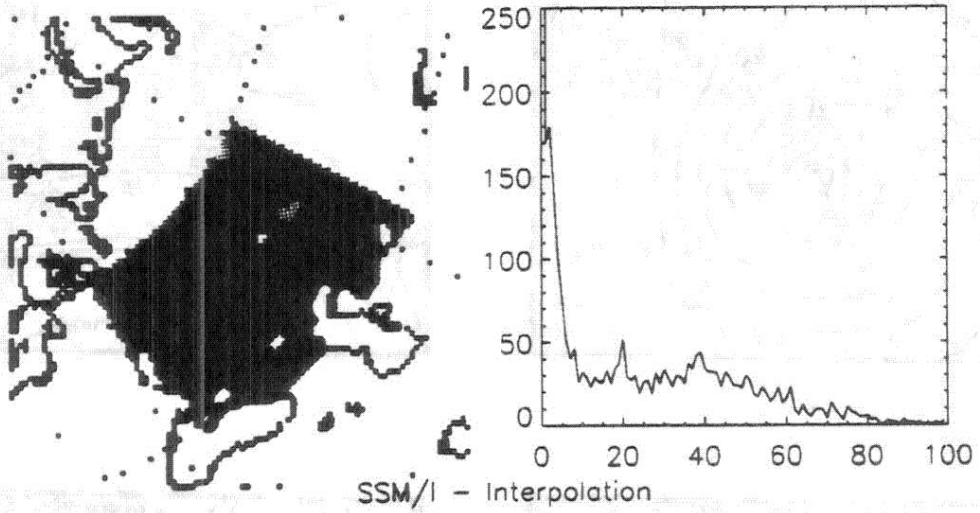

b
984
992
1000
1008

Comparisons of Satellite & Surface Measurements – 890210

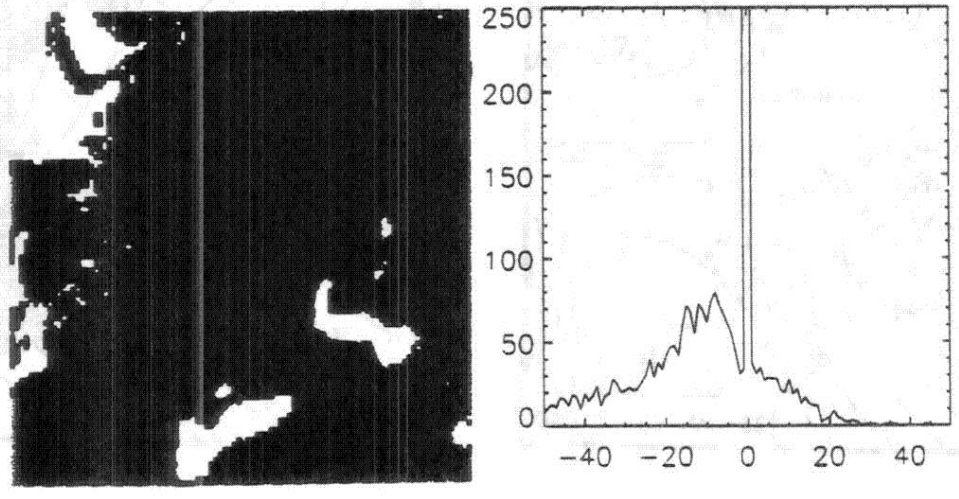
SSM/I Derived Snow Cover (NSIDC Test1)



Surface Interpolation



SSM/I – Interpolation



Improvements to SSM/I Techniques and Algorithms in areas of Sand, Sea Ice, Snow and Frozen Ground

by
E.C, Barrett, R.J. Kelly, D.A. Kilham and D.R. Kniveton
(Remote Sensing Unit, University of Bristol, Bristol, UK),
C. Durbin
(Royal Navy)
and
J.C. Scott
(UK Defence Research Agency)

Interest in the DMSP SSM/I instrument and its practical applications in environmental mapping and monitoring has been high in the Remote Sensing Unit, University of Bristol, UK since the early days of F8. Since then a wide-ranging research programme has been developed, aided by active links with NASA, NOAA and NRL in the USA, and by the meteorological Office, the National Rivers Authority, and particularly by the Defence Research Agency in the UK. The areas of primary concern in Lee Bristol work programme have included areas not researched in detail by other SSM/I scientific colleagues, involving principally the UK and neighbouring areas of the eastern North Atlantic plus parts of Africa and Australia.

In this paper results from a number of tests of SSM/I-based techniques and algorithms will be presented, all of which are thought significant nor applications elsewhere. Amongst them are recognitions of the need to modify existing SSM/I deconvolution/remapping methods and ice analysis algorithms for effective operational performance, new findings on the usefulness of overland snow area/depth/water equivalence algorithms, and details of newly-developed routines to help differentiate between rain and surface scatterers especially in region of sand (bare soil) and frozen ground.

Applications of these and other improved SSM/I techniques and algorithms will soon be made by the Royal Navy both globally and regionally, the latter in relation to data obtained directly from DMSP satellites by the new UK Ministry of Defence DMSP reception facility now under construction and expected to become operational before the end of 1993.

Improvements to SSM/I Techniques & Algorithms for Evaluations of Snow, Sea Ice, and Rainfall in Areas of Sand/Bare Soil

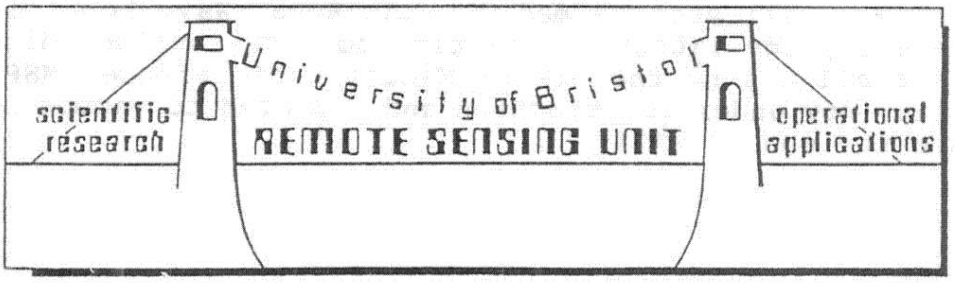
by

E.C. Barrett, R.J. Kelly, D.A. Kilham & D.R. Kniveton,
(Remote Sensing Unit, University of Bristol, Bristol, UK)

C. Durbin
(Royal Navy)

and

J.C. Scott
(UK Defence Research Agency)



CONTENTS

1. SSM/I Snow Cover and SWE Monitoring over the UK:

   - SSM/I deconvolution and remapping;

   - snow detection and evaluation.

2. SSM/I Sea Ice Detection and Algorithm Validation over the Eastern Greenland Sea.

3. SSM/I Rainfall Measurement in Areas of Sand/Bare Soil.

1. SSM/I Snow Cover Monitoring over the UK

Key issues involve:

- Scale of UK drainage basins.
- Type(s) of UK snow.
- Rapidity of snow event changes.

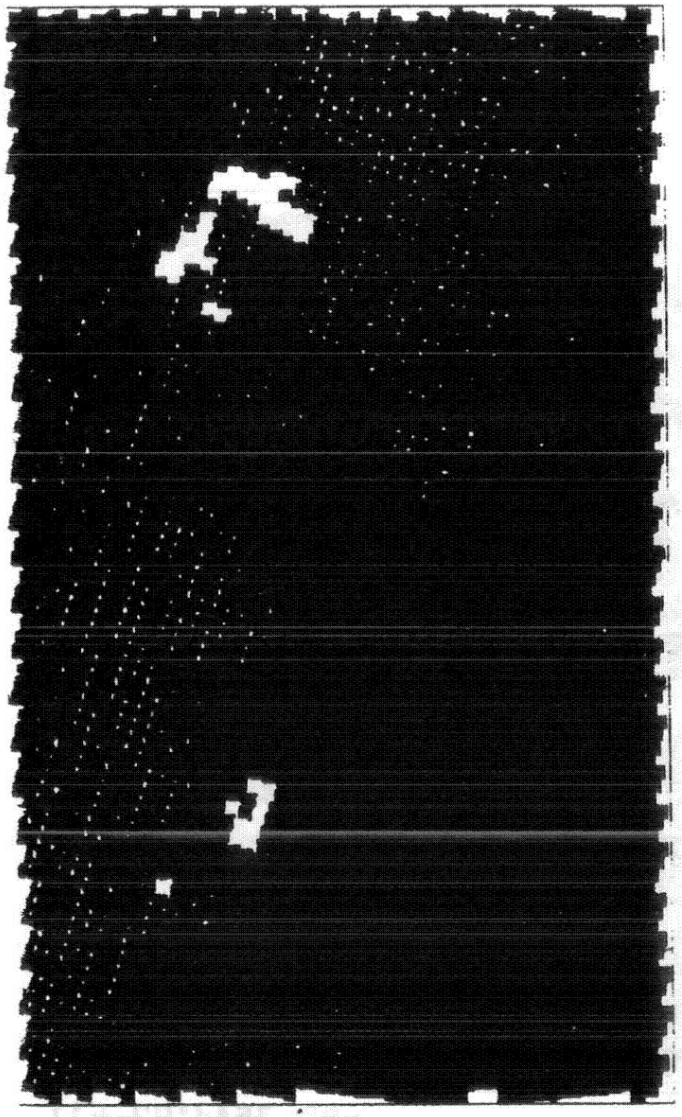
Related activities included:

- Implementation of Poe (1990) routine.
- Identification of Poe problem.
- Solution of Poe problem.
- Snow area and SWE technique implementation/development.

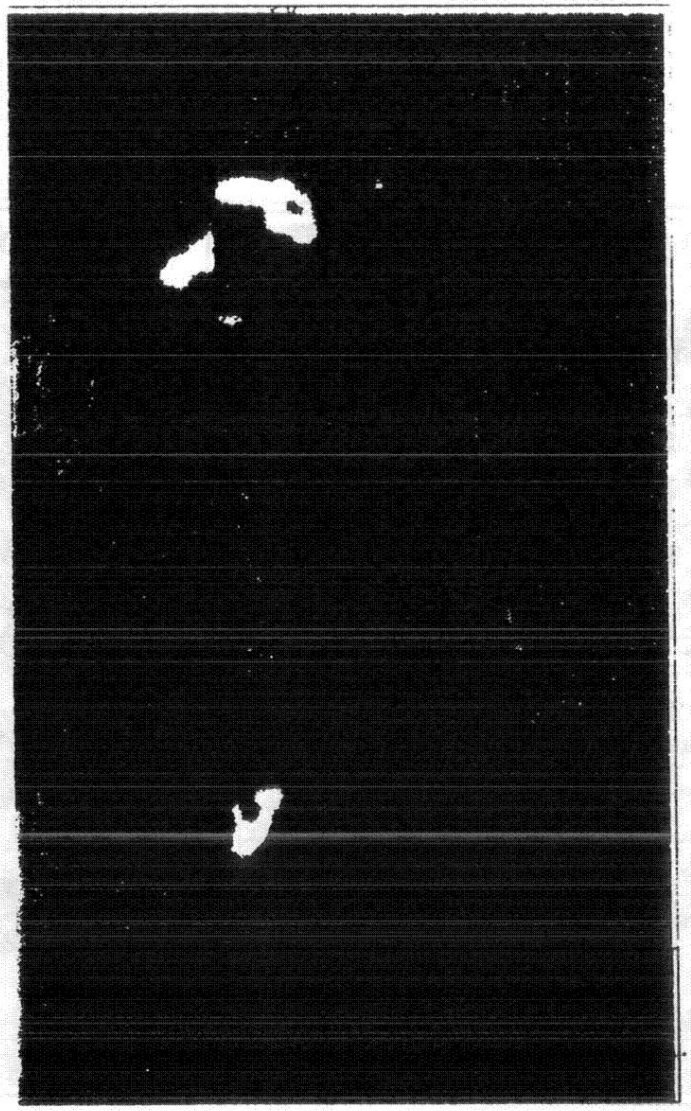
Key findings:

- Different remapping required for F11 et seq vs. F8.
- Different snow depth calibration curves for different regions.
- Use of DTM improves snow distribution patterns.

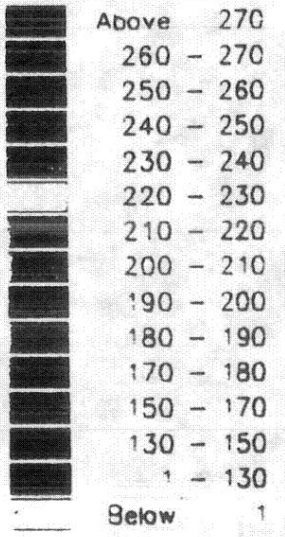
Improved SSM/I Data Processing by Poe Technique

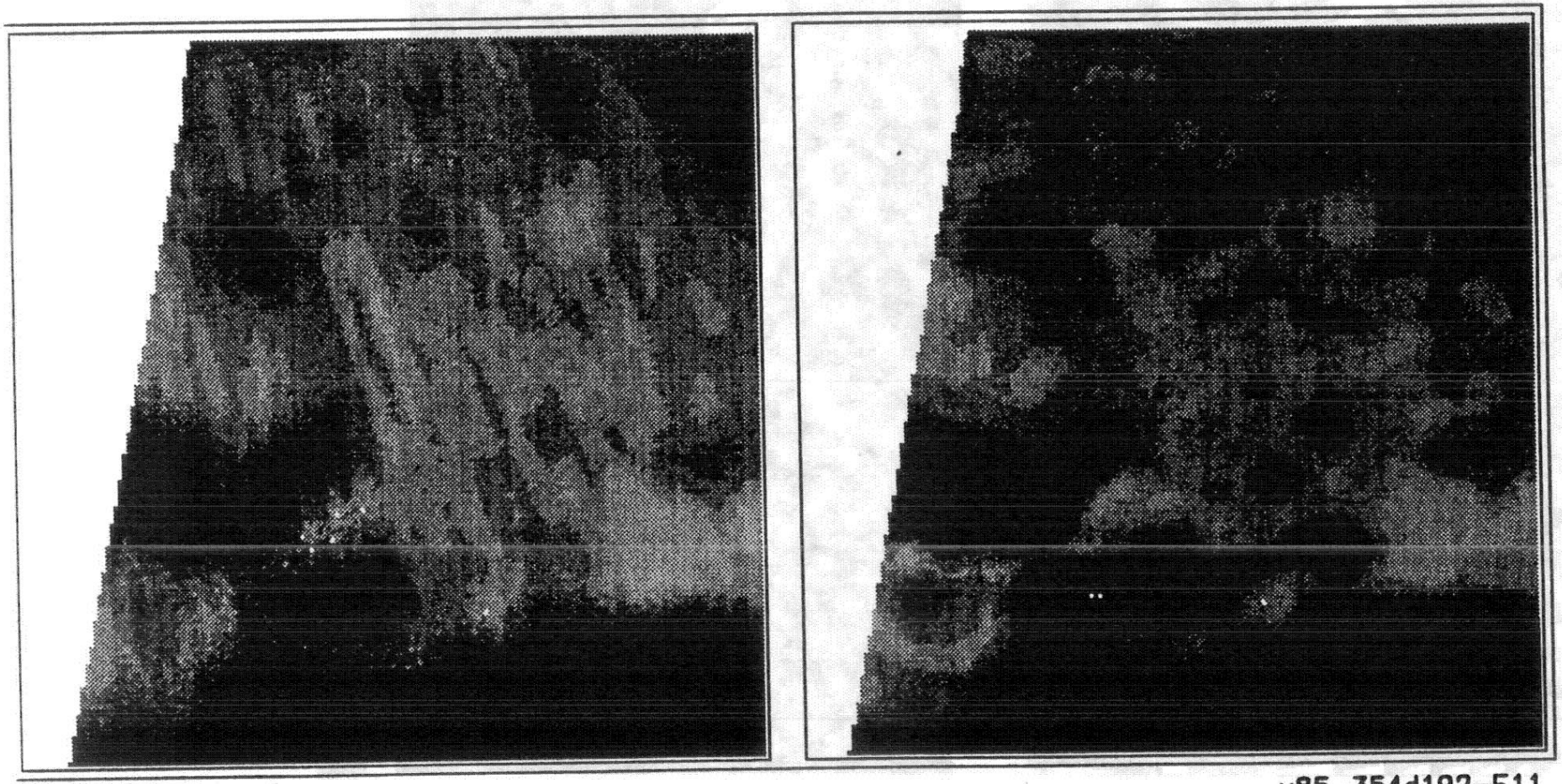


Nearest neighbour interpolation



Poe technique interpolation





v85–354d192–F8

v85–354d192–F11





s354d1_F8_v85.dat

s354d1_F11_v85

R. Kelly 1

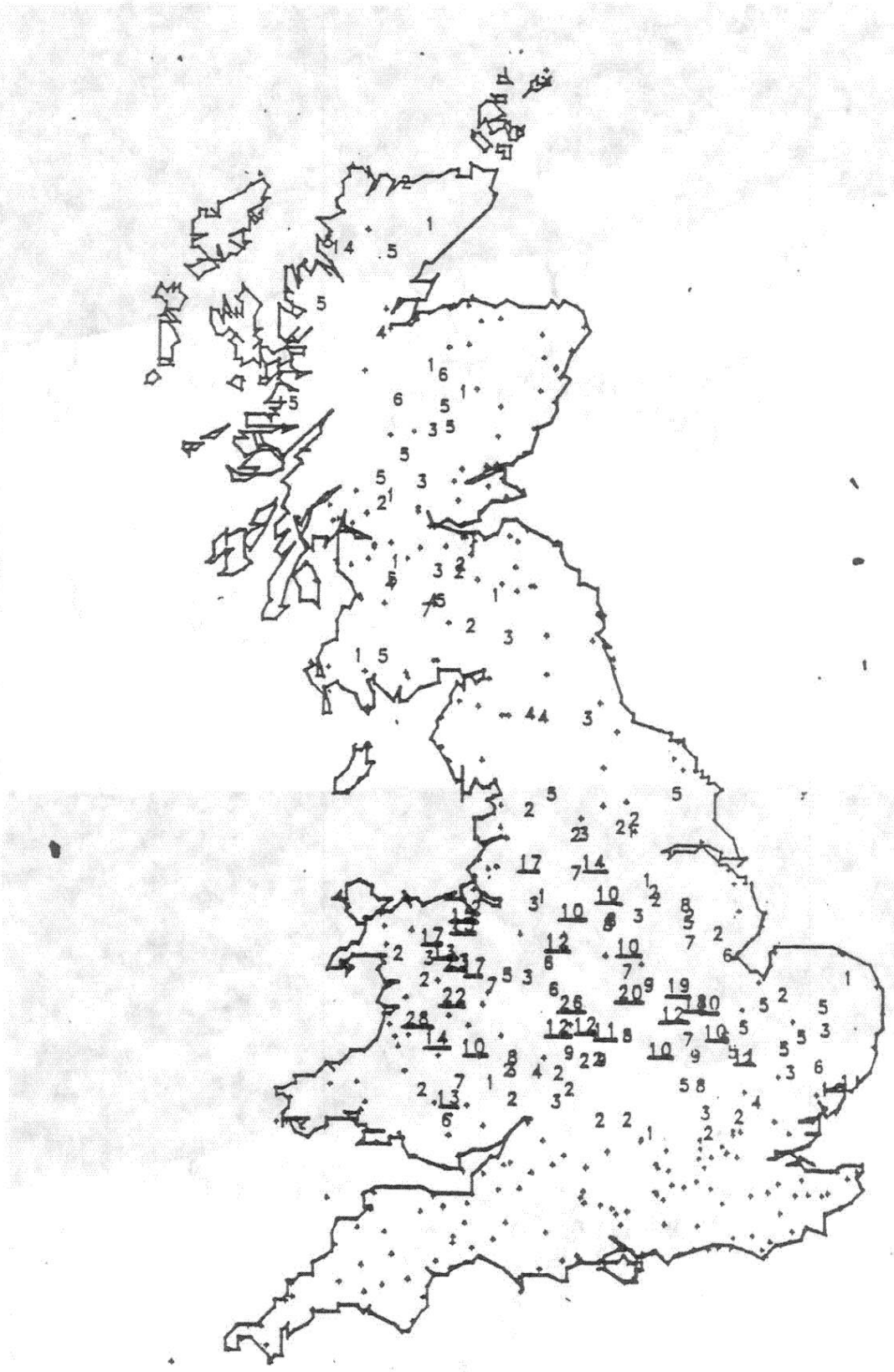
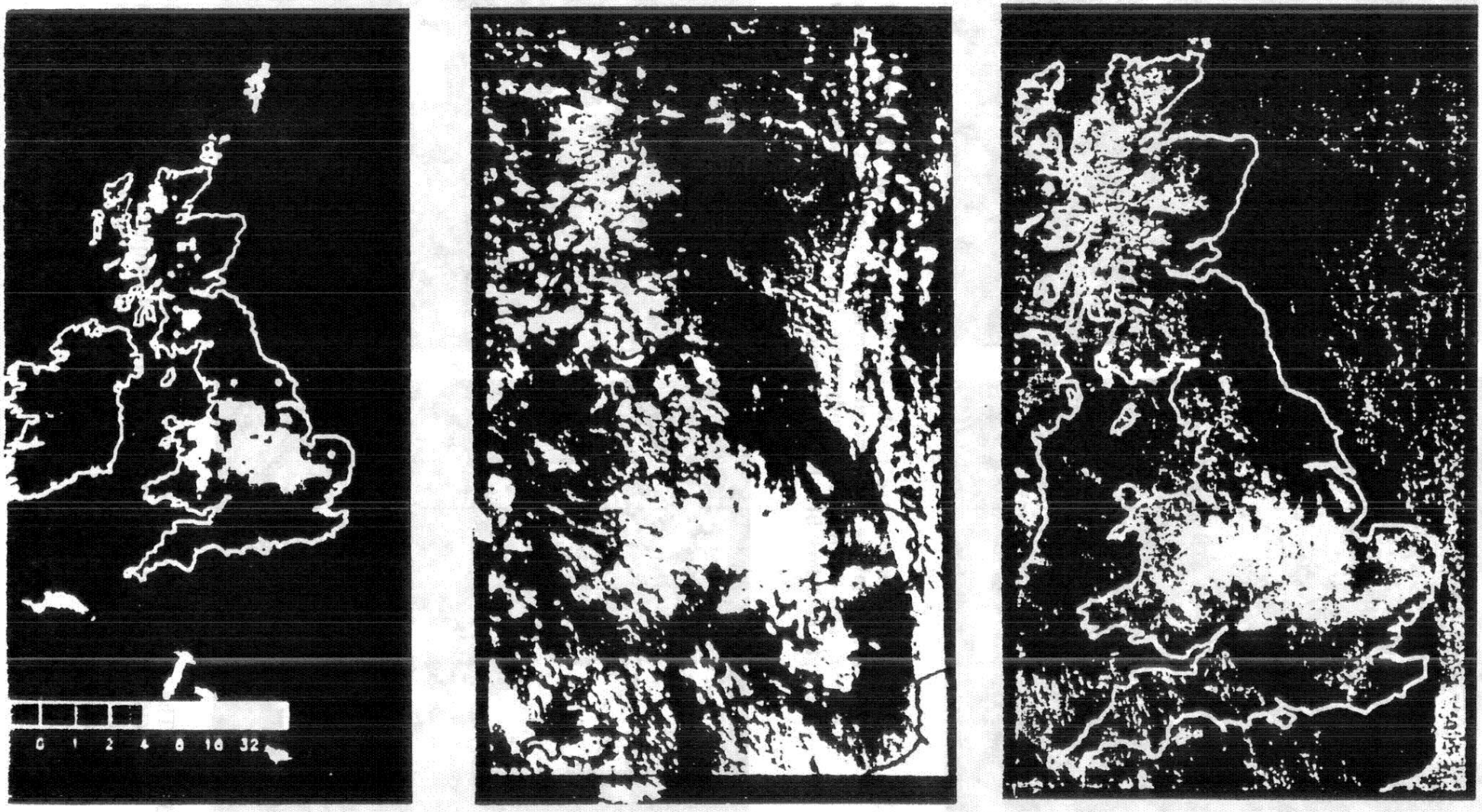


Figure 3.5. Surface-reported snow depths at 0900Z on 22 January 1988 compiled from nearly 600 station reports (depths greater than 9 cm are underlined).



(a) (b) (c)

Plate 3.4. (a) Surface-reported snow depths at 0900Z, 22 January 1988, interpolated from nearly 600 station reports; (b) the visible image from the AVHRR (at 1522Z); and (c) the AVHRR unsupervised snow classification.

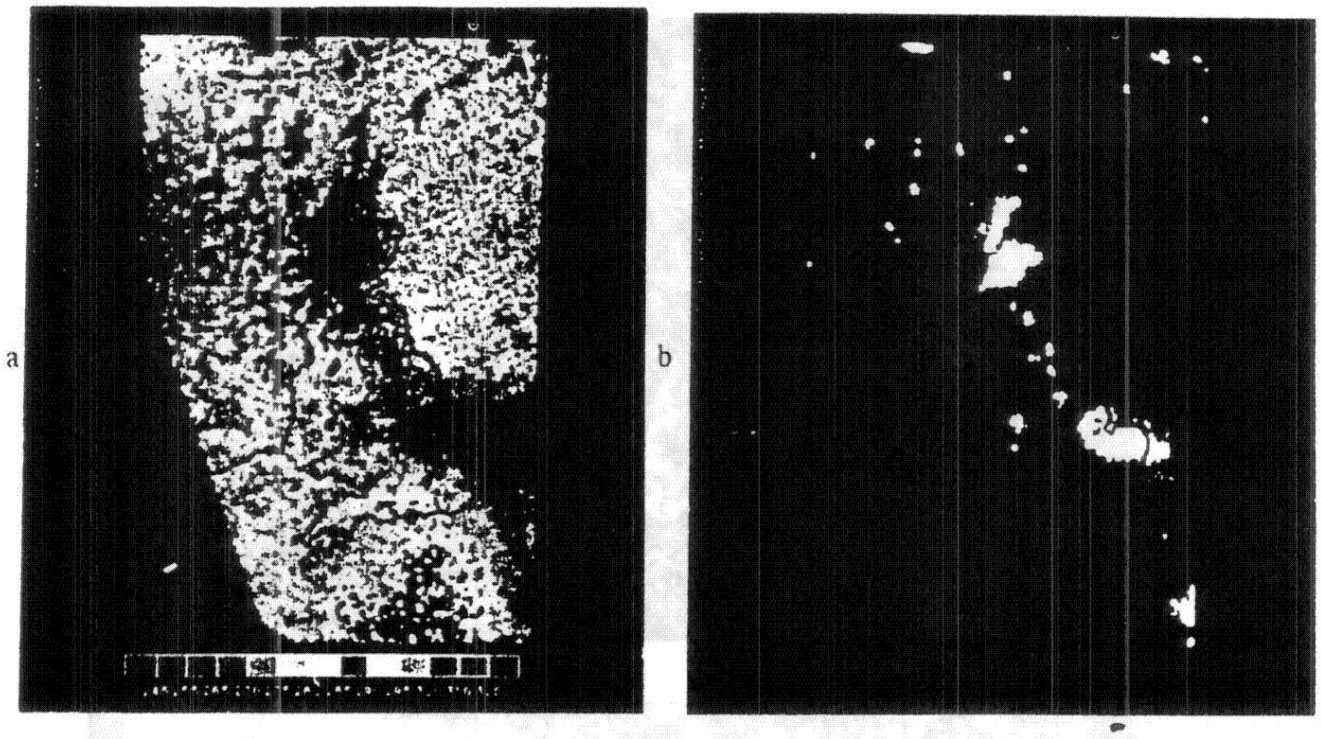


Plate 3.9. The passive microwave results for the morning of 22 January 1988 (0535Z), for (a) the polarization corrected temperatures (scale in degrees Kelvin); and (b) the Fiore/Grody technique, where white indicates snow, and light and dark blue indicates rain.

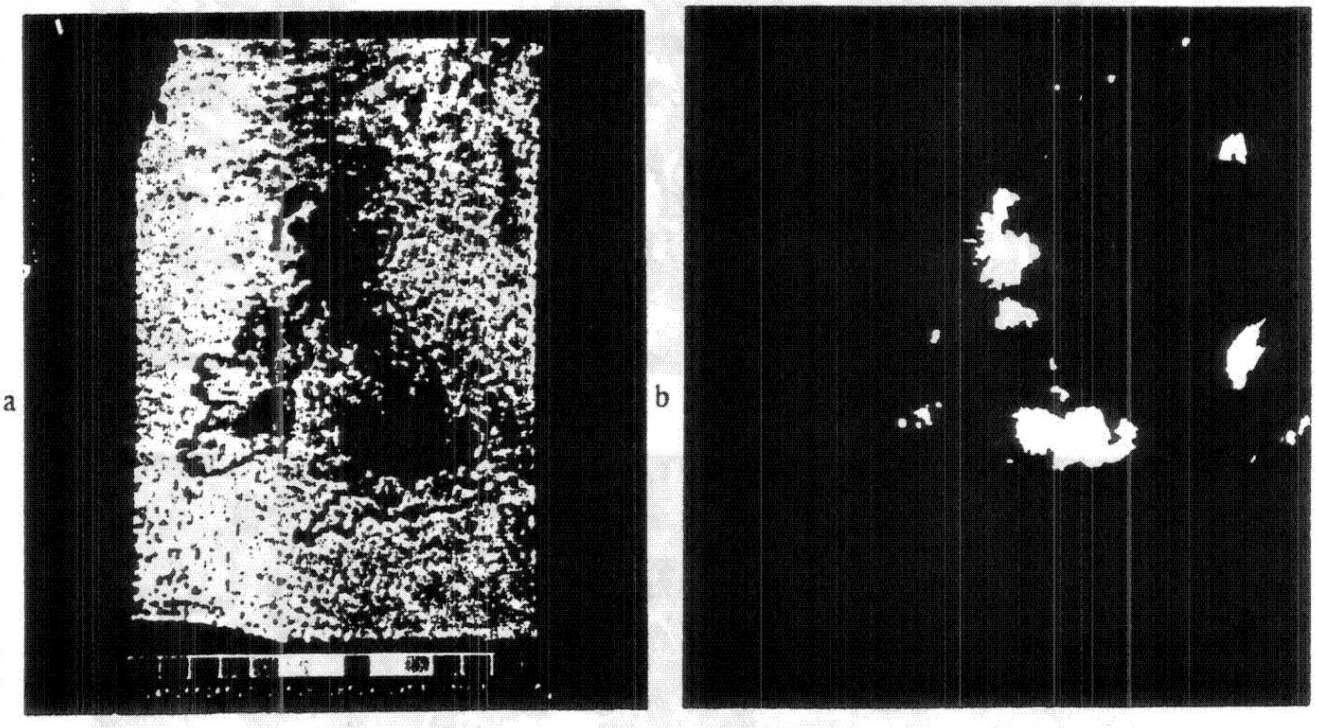
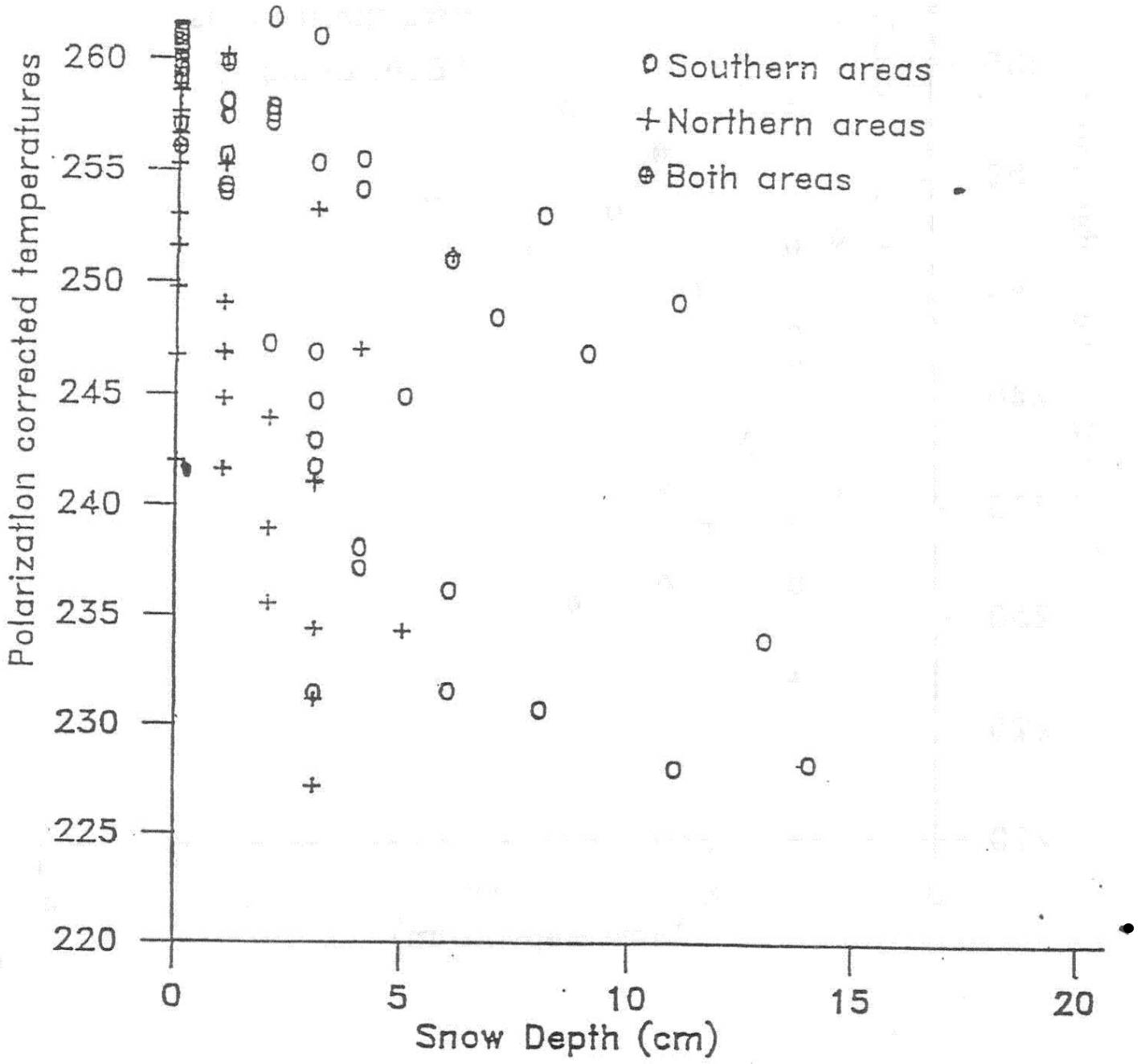


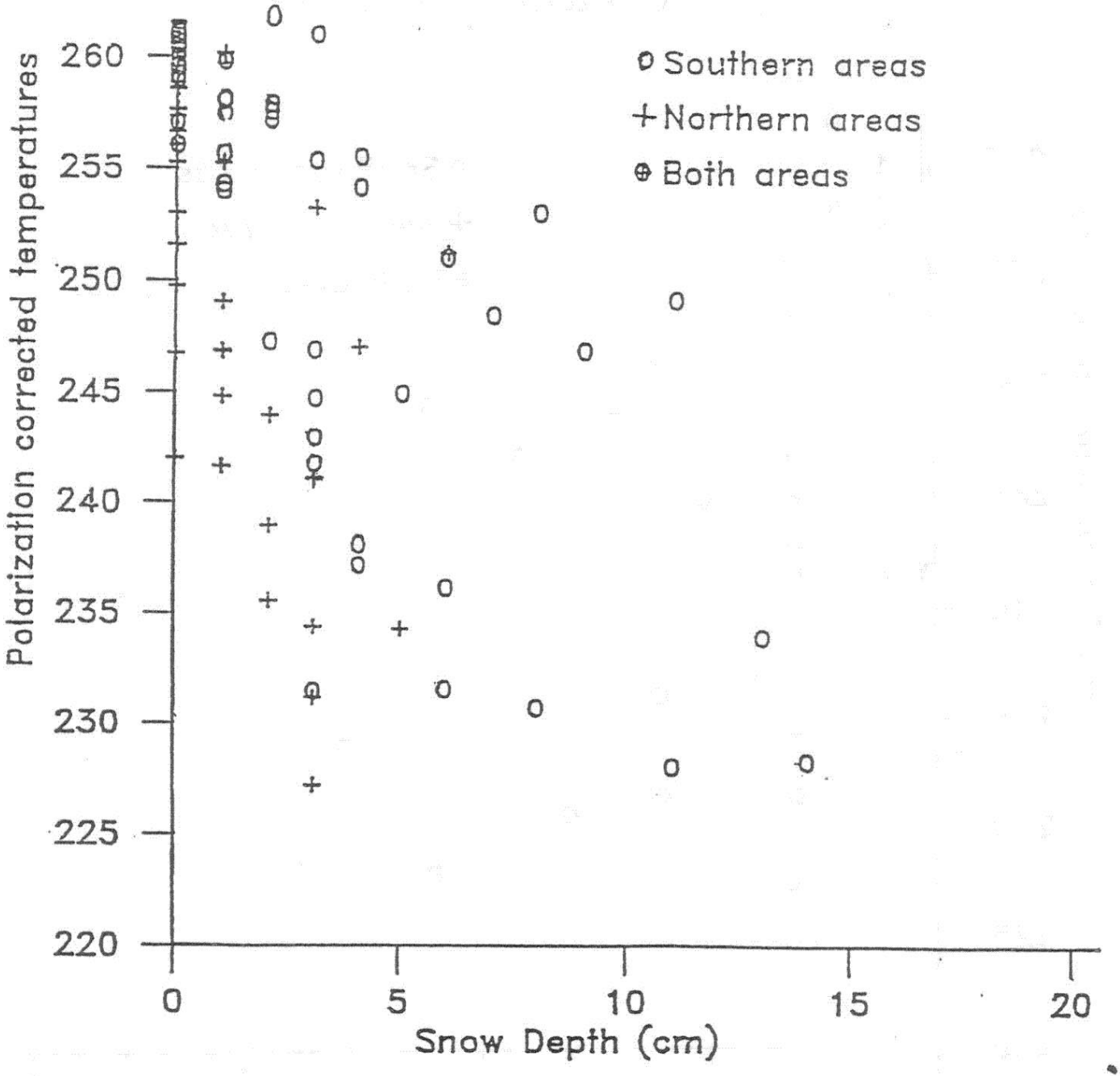
Plate 3.10. The passive microwave results for the evening of 22 January 1988 (1916Z), for (a) the polarization corrected temperatures (scale in degrees Kelvin); and (b) the Fiore/Grody technique, where white indicates snow, and light and dark blue indicates rain.

PCTs vs. Snow Depth
(22 Jan. 1988)

POLARIZATION CORRECTED TEMPERATURE



REPRODUCED AT GOVERNMENT EXPENSE



REPRODUCED AT GOVERNMENT EXPENSE

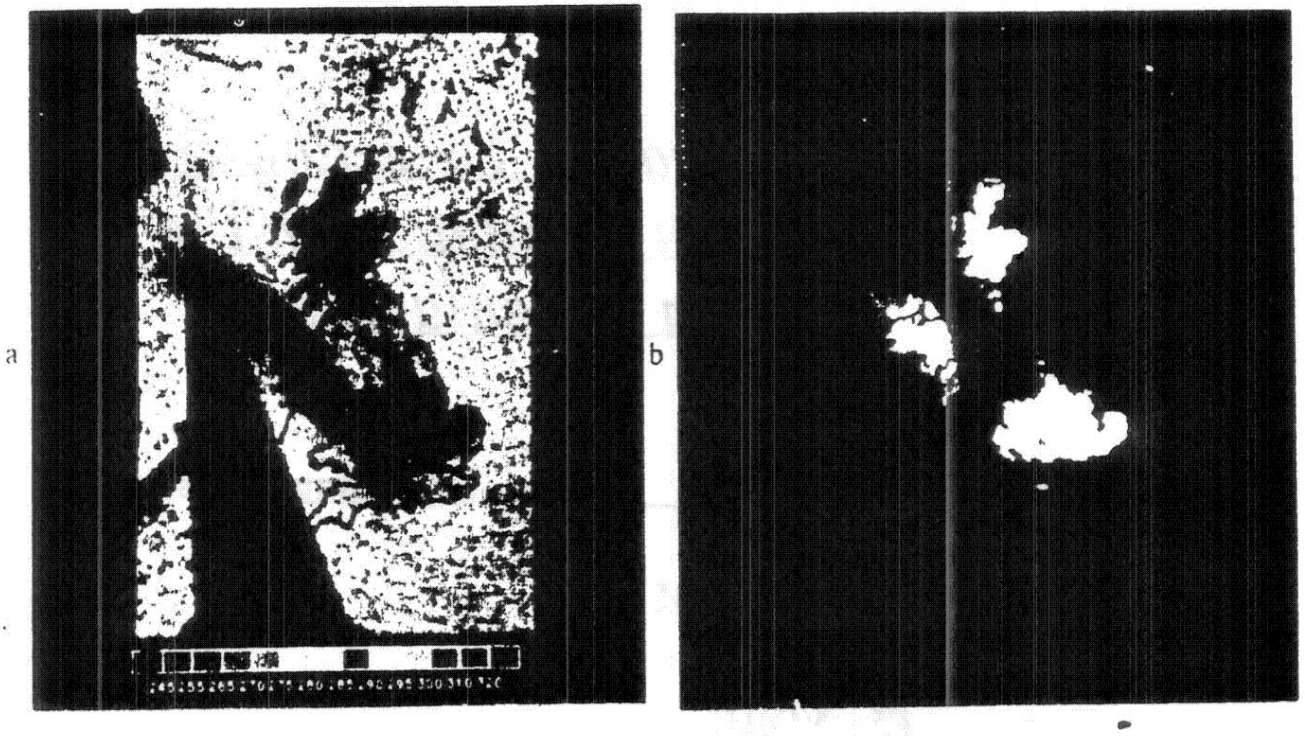


Plate 3.11. The passive microwave results for the morning of 23 January 1988 (0509Z), for (a) the polarization corrected temperatures (scale in degrees Kelvin); and (b) the Fiore/Grody technique, where white indicates snow, and light and dark blue indicates rain.

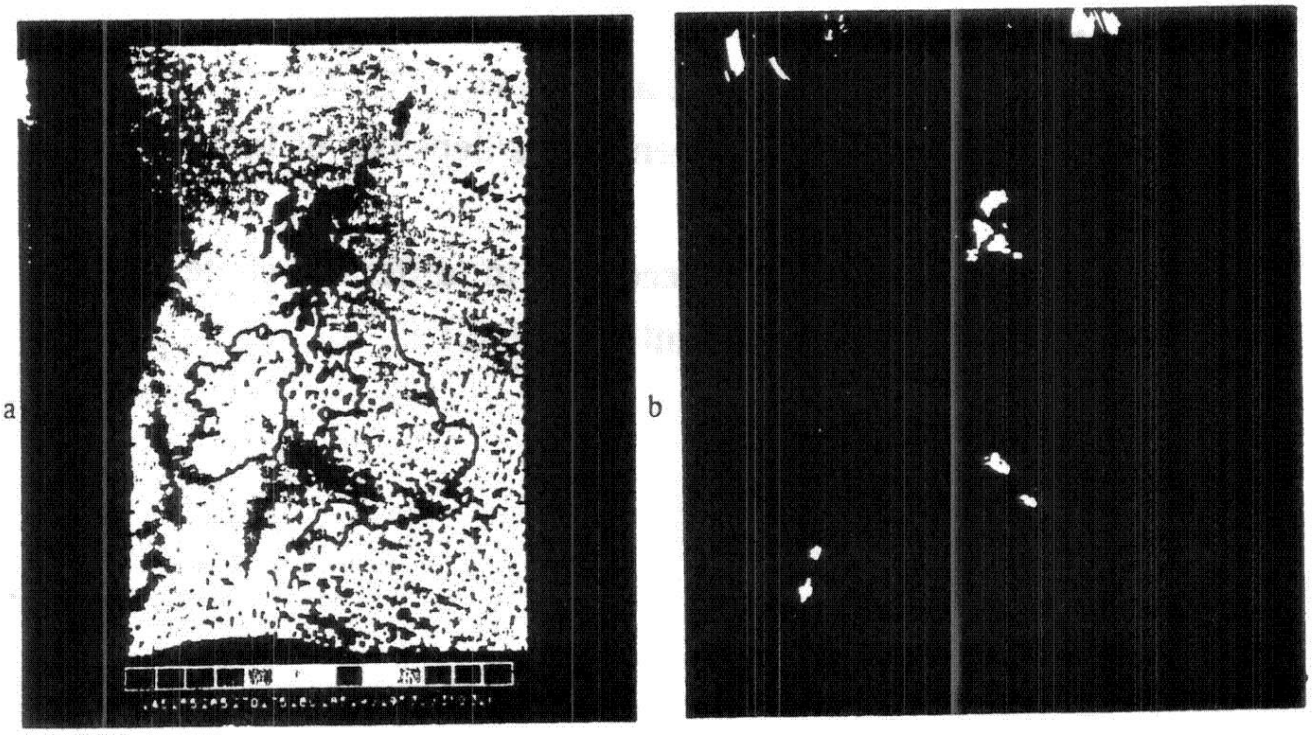


Plate 3.12. The passive microwave results for the evening of 23 January 1988 (1904Z), for (a) the polarization corrected temperatures (scale in degrees Kelvin); and (b) the Fiore/Grody technique, where white indicates snow, and light and dark blue indicates rain.

2. SSM/I Sea Ice Detection & Algorithm Validation in the Eastern Greenland Sea

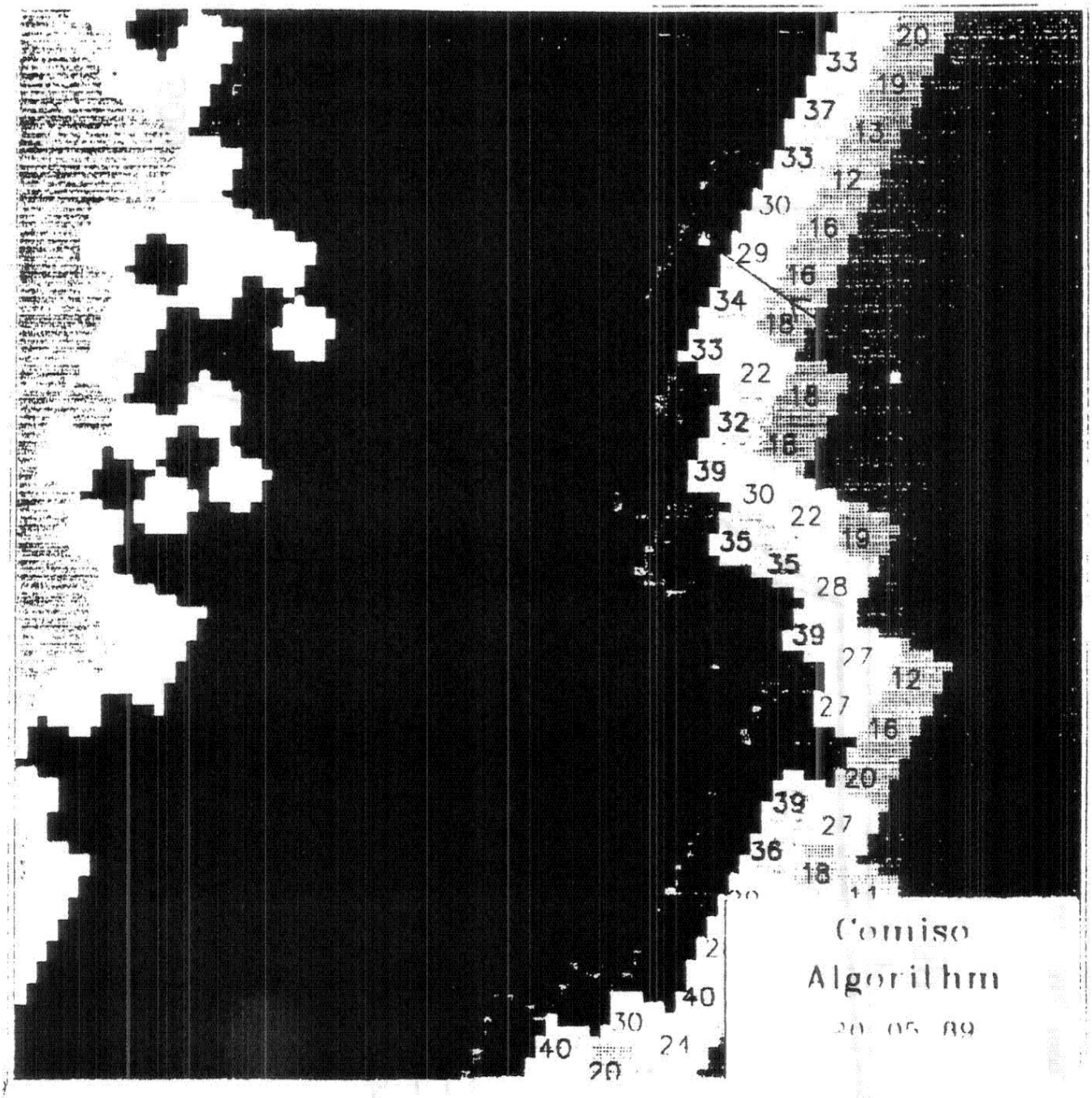
Application of different existing algorithms to selected cases.

* (NASA - TEAM
* Cavalieri *et al.*
* AES1 YORK
* AES2).

Validation using surface data sets.

Conclusions that different algorithms:

- provided different types/densities of information; and
- were more successful in different contexts (ice edge, ice concentration etc.)



KEY (? ice ... ed ... stream)

90	100
80	90
70	80
60	70
50	60
40	50
30	40
20	30
10	20
0	10

Figure 3.9 Start and end locations of sonar transect marked in yellow

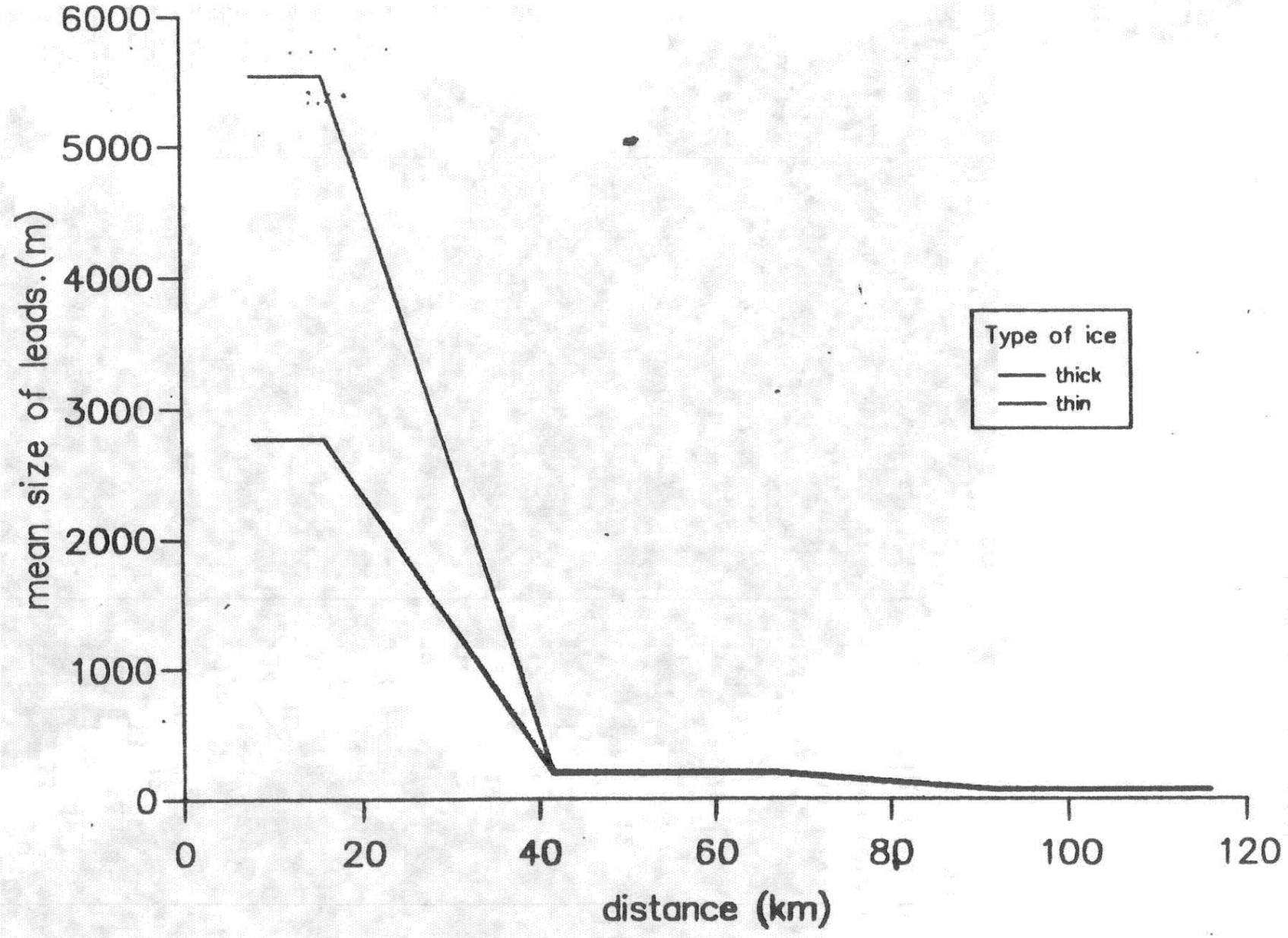


Figure 3.10 Mean size of leads and polynyas as derived from sonar data for transect on 20 May 1989.

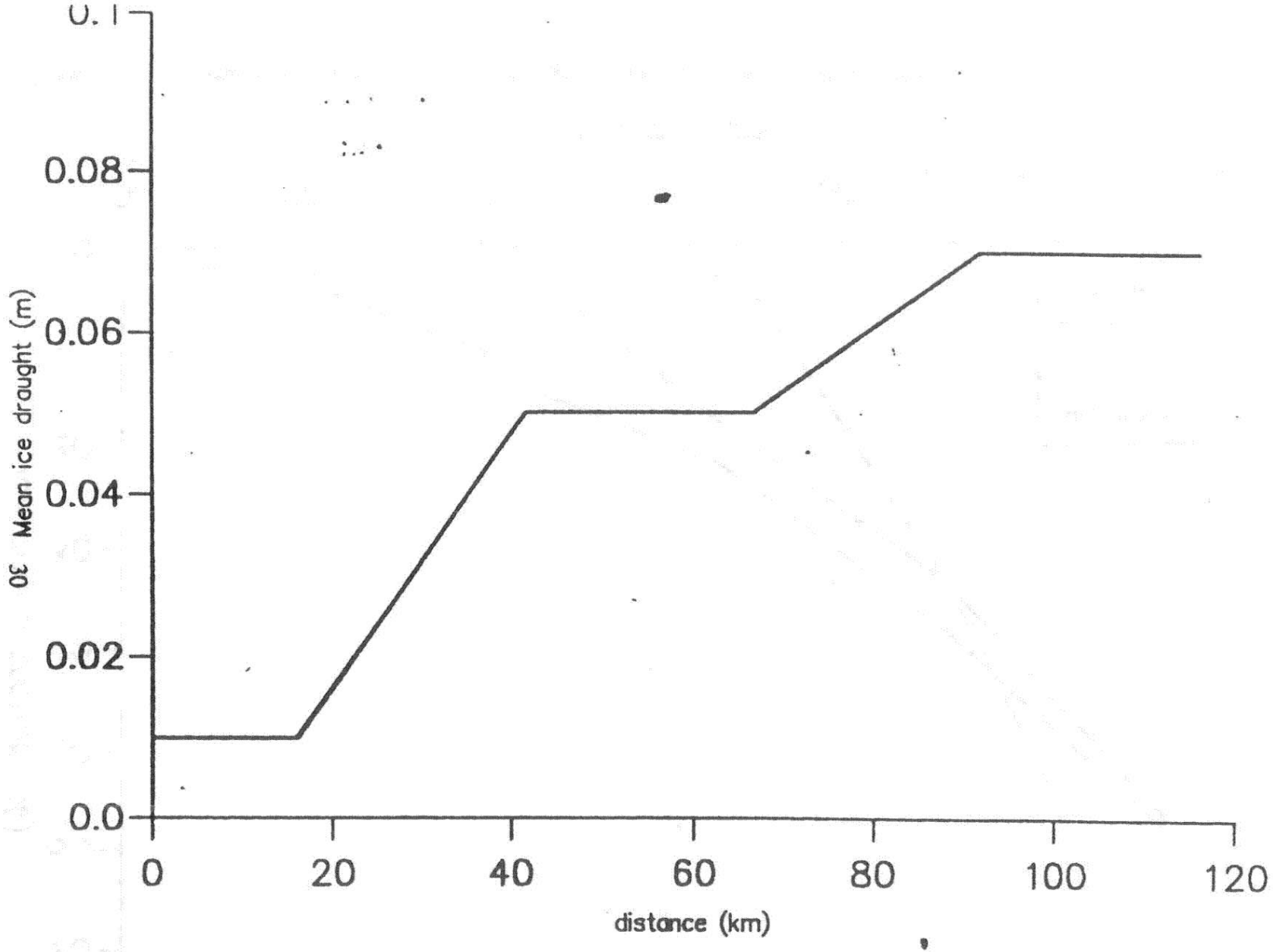


Figure 3.11 Mean ice draught as derived from sonar data for 20 May 1989.

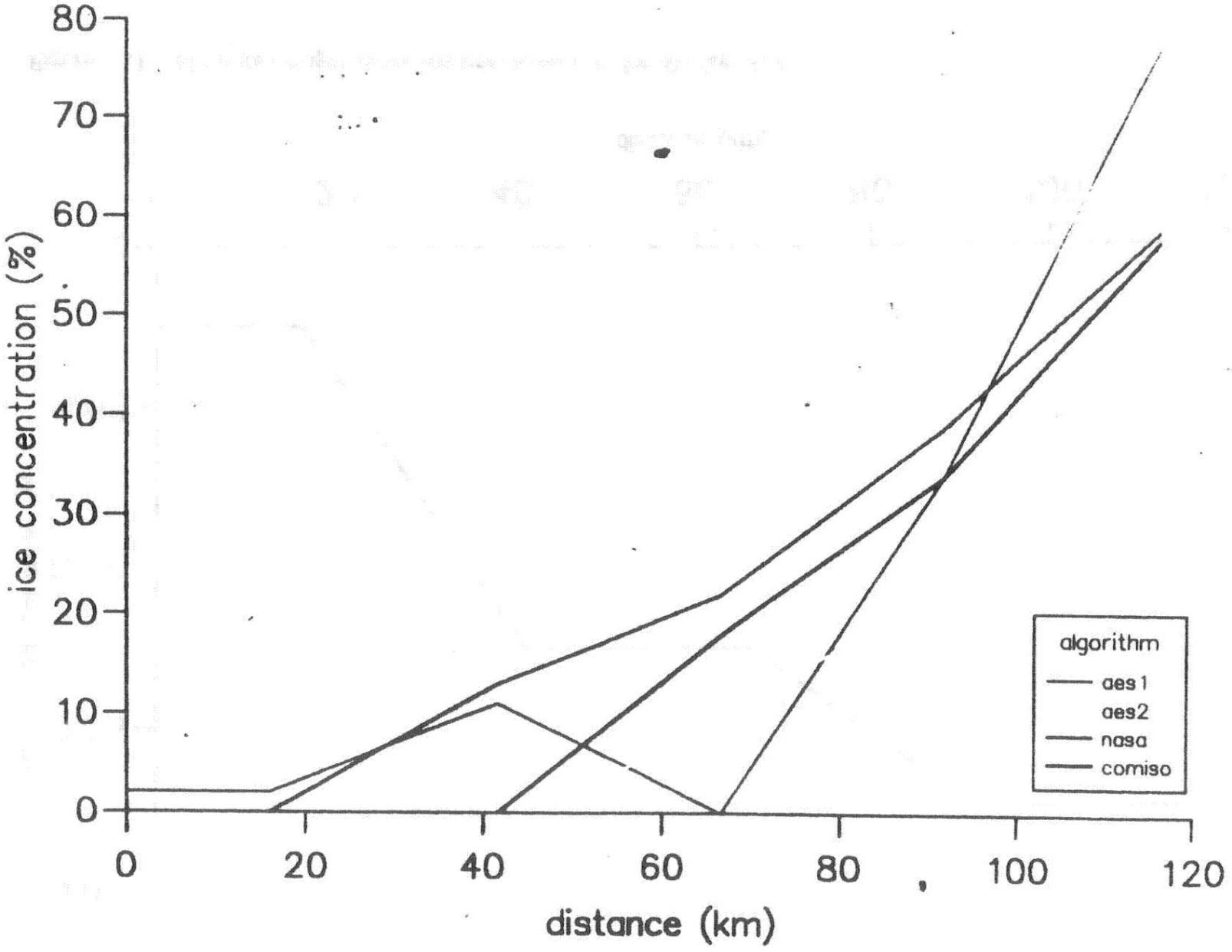


Figure 3.12 Percentage ice concentration along transect for each algorithm on 20 May 1989.

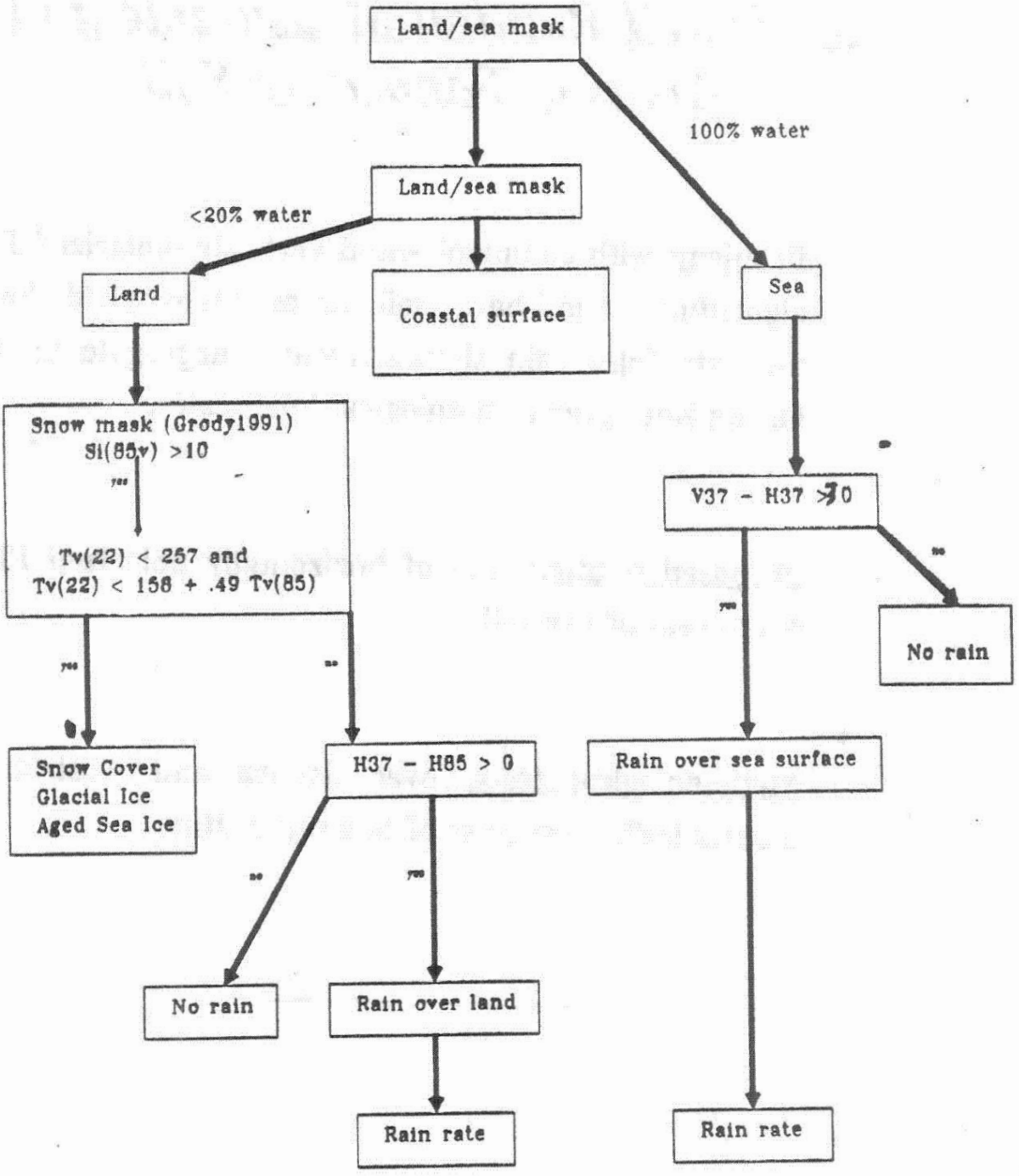
3. SSM/I Rainfall Measurement in Areas of Sand/Bare Soil

- Problem: with commonly-used vertically-polarized FD algorithms, sand/bare soil areas often yield low-intensity false rain signals....which aggregate up to large values over climatological time scales.

- Proposed solution: use of horizontally polarized FDs over areas of dry soil.

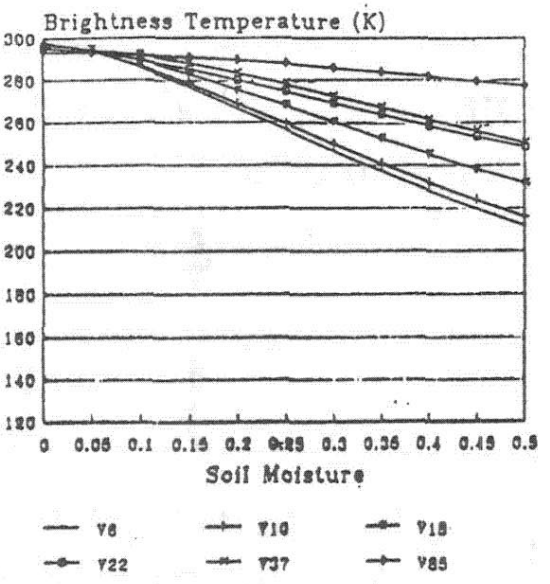
- Methodological tests: over Sahara and Australian deserts indicate success of this sub-routine.

BRISTOL GLOBAL RAINFALL ALGORITHM

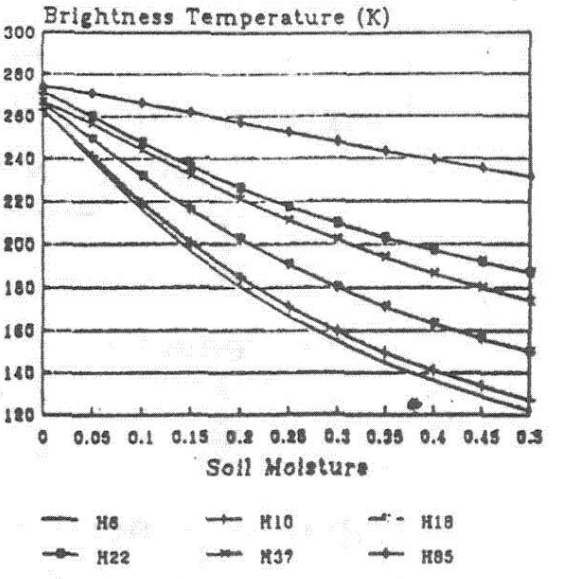


*Note:SI(85v)=F−Tv(85v), where F=A+BTv(19v)+CTv(22)+DTv(22)**2*

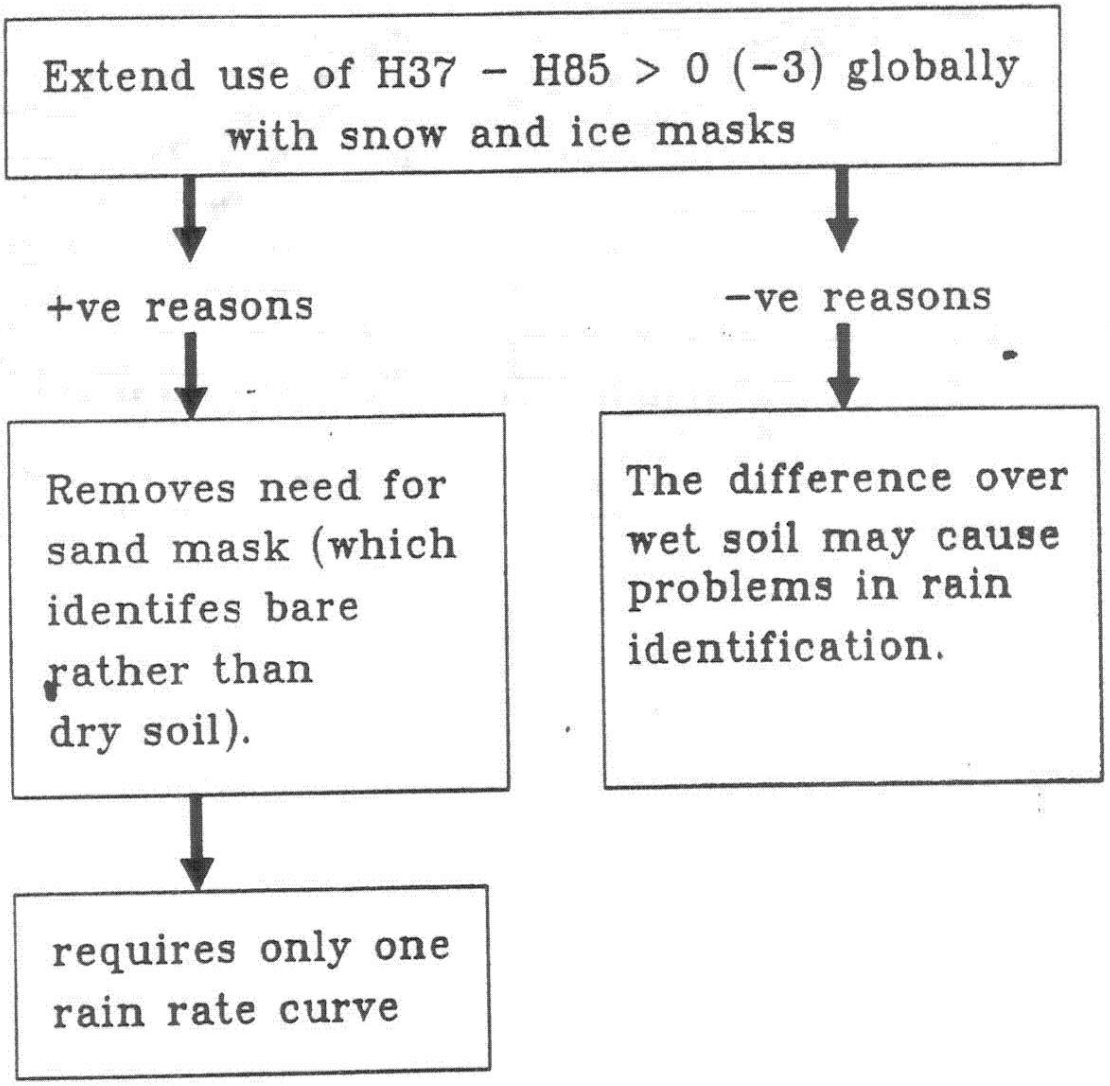
a) vertical T_B



b) horizontal T_B



Horizontal freqency difference algorithm



Conclusions

Snow

- Different remapping required for F11 et seq vs. F8.
- Use of 85 GHz for snow "veneer".
- Different snow depth calibration curves for different regions.
- Use of DTM improves snow distribution patterns.

Sea Ice

Different algorithms:

- provide different types/densities of information.
- were more successful in different contexts (ice edge, ice concentrations).

Sand/Bare Soil

- Hierarchical approach is flexible and adaptable.
- implement horizontally polarized FDA over areas of dry soil.

June 8, 1993

Comments from Ed Josberger Ice@UPS.EDU
U.S. Geological Survey
University of Puget Sound
Tacoma WA 98416 206-593-6516

With regard to snow water equivalent determinations: I would like to emphasize the importance of grain size on the T_b's. This factor was barely touched on in the snow discussions but it is most important. It may account for the inability to produce global algorithms, as well as ~~the~~ generating inter annual variations. The grain size variations are very pronounced in deeper mountainous snow packs where depth hoar forms. These large grains, ~5mm, ~~grain~~ can comprise a major fraction of the snow pack.

I would urge all snow/SSMI research efforts to collect vertical profiles of grain size and type, density, ~~and~~ temperature and stratigraphy. My own snow interests have focused on the Upper Colorado River Basin, particularly the mountainous areas. I have an 8 year data set of snow pack properties that overlaps the SSMR and SSM/I observations. Analysis of the Satellite data, grain size data, and SCS Snotel data sets shows a strong difference in microwave emissions between the mountains of Colorado

and Wyoming the is the result of differences in the average grain size from each area.

Session 3

Land Parameters

(Chris Neale, Utah State, Chair)

ENCL(9)

Session 3

Land Parameters

(Chris Neale, Utah State, Chair)

Surface Soil Moisture Retrievals with SSM/I: Empirical and Physically-Based Approaches

C. M. U. Neale and G. Vassiliades[1]

Previous work on surface moisture retrievals using brightness temperatures from the SSM/I conducted during the SSM/I calibration/validation effort have shown that surface moisture can be sensed but that the accuracy of the retrievals depends on numerous factors. There is considerable noise in the SSM/I signatures overland due to the large footprint size and heterogenous nature of the land surface with respect to vegetation cover, presence of water bodies and surface roughness. The short wavelengths of the SSM/I result in a small surface penetration or sensing depth as well as decreased sensitivity to surface moisture with the presence of a vegetation cover of relatively low densities. Retrievals of moisture from footprints with high vegetation densities are physically impossible at these wavelengths.

The presentation will summarize the methodology in developing the existing empirically-based algorithms and show examples of their performance. In addition, a new method of retrieving surface moisture and temperature based on the inversion of a radiative transfer model (RTM) for the SSM/I microwave frequencies will also be presented. The model and inversion techniques will be described and examples of retrievals using this physically-based approach will be shown. In this method, some of the sub-footprint variability in surface emissivities are taken into account in order to increase retrieval accuracies.

---

1 Associate Professor and Graduate Student, respectively, Dept. of Biological and Irrigation Engineering, Utah State University, Logan, Utah 84322-4105

SPN SSM/I ALGORITHM SYMPOSIUM
Algorithm Questionnaire

"SURFACE MOISTURE ALGORITHM"
Christopher Neale, respondent

Please provide the following essential information about your algorithm(s).

* ALGORITHM DESCRIPTION

- Type (statistical, physical, other) *Statistical and physical algorithms*

- Input required / Output produced

Input: (statistical) Brightness temperatures from four lower frequency channels
(physical) Brightness temperatures from all seven channels
Output: (statistical) Retrieves surface moisture as a depth of water
(physical) Retrieves surface soil moisture as a volumetric content

- Auxiliary sensor/data base requirements

(Statistical) Dynamic data base for surface classification and running averages of polarization differences of 19GHz and 37GHz.
(Physical) Database of surface characteristics

- Major limitations / approximations

(Statistical) Noisy, but simple.
(Physical) Complicated, need to know surface physical parameters

- Computer resource requirements

(Statistical) Large disk space
(Physical) Fast workstation with large disk space

* ALGORITHM PERFORMANCE

- Development / test data sets (regional / global / seasonal)

Regional, central plains of U.S. due to availability of good database (dense network of weather stations)

- Ground truth (accuracy / limitations)

Quality contol of NOAA climatological data

- Major assumptions of evaluation

- Strengths / weaknesses

(Statistical) Dynamic data base needs to be implemented for algorithms to work properly.

* **ALGORITHM MATURITY**

- Operational useage

(Statistical) Current DMSP algorithm; however, the dynamic data base has not been implemented.

- Refinement / additional development

(Statistical) Need global dynamic data base of surface type, average polarization differences.

- Availability

Physical algorithm is in development and not ready for distribution.

SSM/I Scene Classification

Richard C. Savage
Hughes Aircraft Co.
16800 E. CentreTech Pkwy
Aurora, CO 80011

Classification of the multispectral scene observed by the SSM/I is a fundamental step in the assignment of environmental meaning, that is, an environmental data record (EDR). Early processing logic incorporated *ad hoc* binary categorization rules (IF...THEN); these have been greatly improved by later investigators, such as Neale (1988) and Grody (1991). For example, it is obviously important to distinguish snow-covered ground from areas of precipitation. There are also advantages in an approach based on continuous multispectral functions, such as eigenvalue/vector analysis, which preserve more subtleties of temporal change and difference. This approach has been incorporated in the version of SSM/I processing used with the WetNet data and the Seasonal Surface Type Database at AF Global Weather Central. Categorization can be imposed after classification as needed.

SPN SSM/I ALGORITHM SYMPOSIUM
Algorithm Questionnaire

"HUGHES SURFACE CLASSIFICATION ALGORITHM"
Richard Savage, respondent

Please provide the following essential information about your algorithm(s).

* ALGORITHM DESCRIPTION

- Type (statistical, physical, other) *Statistical*

- Input required / Output produced

  Input: SSM/I brightness temperatures
  Output: Classification discriminants and 23 surface type categories

- Auxiliary sensor/data base requirements *None*

- Major limitations / approximations

  Only three of six discriminant values used (could be improved). Ground truth limited, but can be improved.

- Computer resource requirements *Minimal*

* ALGORITHM PERFORMANCE

- Development / test data sets (regional / global / seasonal)

  Global, all season.

- Ground truth (accuracy / limitations)

  Largely Matthews' land classification data base (NCAR).

- Major assumptions of evaluation

  Objective mathematical analysis technique (eigenfunction); simple computer logic.

- Strengths / weaknesses

  Lack of adequate ground truth.

* ALGORITHM MATURITY

- Operational useage

  Under evaluation at AFGWC.

- Refinement / additional development

  Time series analysis beginning.

- Availability

  Code and documentation at AFGWC and NASA Wetnet.

SSM/I Scene Classification

HUGHES

Richard Savage
John Heinrichs
08 Jun 93

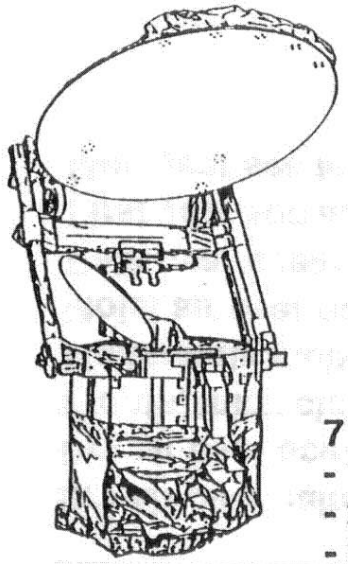
General Description

HUGHES

- Fully SSM/I-based surface type classifier
- Can recognize 23 categories
- Developed for Air Force operational use
- Implemented for WetNet PS/2

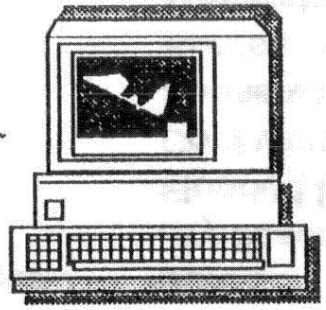
Classification Process

HUGHES



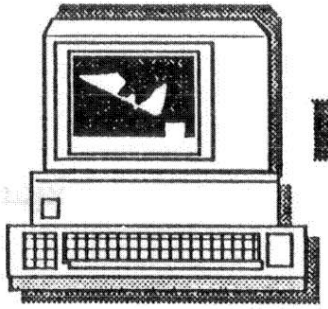
SSM/I

7 Channels
- 19 GHz V, H
- 22 GHz V
- 37 GHz V, H
- 85 GHz V, H



Calculate Discriminants

3 Discriminant Scores



Lookup Table

Surface Type

290-568G003.1

Categories Recognized

HUGHES

Ocean Categories

Dry air over calm ocean
Dry air over ocean
Fronts, thick clouds over ocean
Moderately moist air over ocean
Moist air over ocean
Rain over ocean
First year sea ice
Multiyear sea ice

Land Categories

Snow
Deep snow
Glacial snow
Bare soil
Dry desert
Flooded land/land-water mix
Cold vegetation
Dense vegetation
Sparse vegetation
Moderate vegetation
Rain over land
Wet desert

Other Categories

Coast
Unknown

HUGHES

Classifier derivation

Truth Data

HUGHES

- Used to build training data set of matching SSM/I brightness temperature vectors and a priori classifications
- Obtained from both fixed and variable sources
  - Matthews land use/cultivation intensity database
  - Climatic Analysis Center product communications system (temperature and precipitation data, weather and crop summaries)
  - Snow cover charts from National Snow and Ice Data Center in Boulder, CO
  - USDA crop summaries

Discriminant Analysis - Theory

HUGHES

- Let
  - M = number of categories
  - N_k = number of training data powers for Category k
  - $\underline{I}_k$ = average brightness temperature vector for Category k
  - $\underline{I}$ = overall average brightness temperature vector
- Calculate

  A = among groups sums of squares and cross products (SSCP) matrix

  $$= \sum_{k=1}^{M} \sum_{i=1}^{N} (\underline{I}_k - \underline{I})\ (\underline{I}_k - \underline{I})^T$$

  W = within groups SSCP

  $$= \sum_{k=1}^{M} \sum_{i=1}^{N} (\underline{T}_k(i) - \underline{I}_k)\ (\underline{T}_k(i) - \underline{I}_k)^T$$

- Take right eigenvectors of the matrix $W^{-1}A$. These define transformation from brightness temperature space to discriminant space

Discriminant Analysis - Results

HUGHES

- Analysis performed separately for land and ocean points
- 85 GHz vertical polarization not included
- Percentage of variance explained:

	D1	D2	D3	D4	D5	D6
Land	39.97	34.50	15.02	6.63	3.11	0.77
Ocean	65.36	21.99	8.77	2.32	1.51	0.05

- Decision to use only 3 discriminants
- Sensitive to phenomena

	D1	D2	D3
Land	Snow	Soil Moisture	Vegetation
Ocean	Sea ice Cloud Water	Atmospheric Water Vapor	Multiyear Sea Ice Precipitation

Cluster Analysis

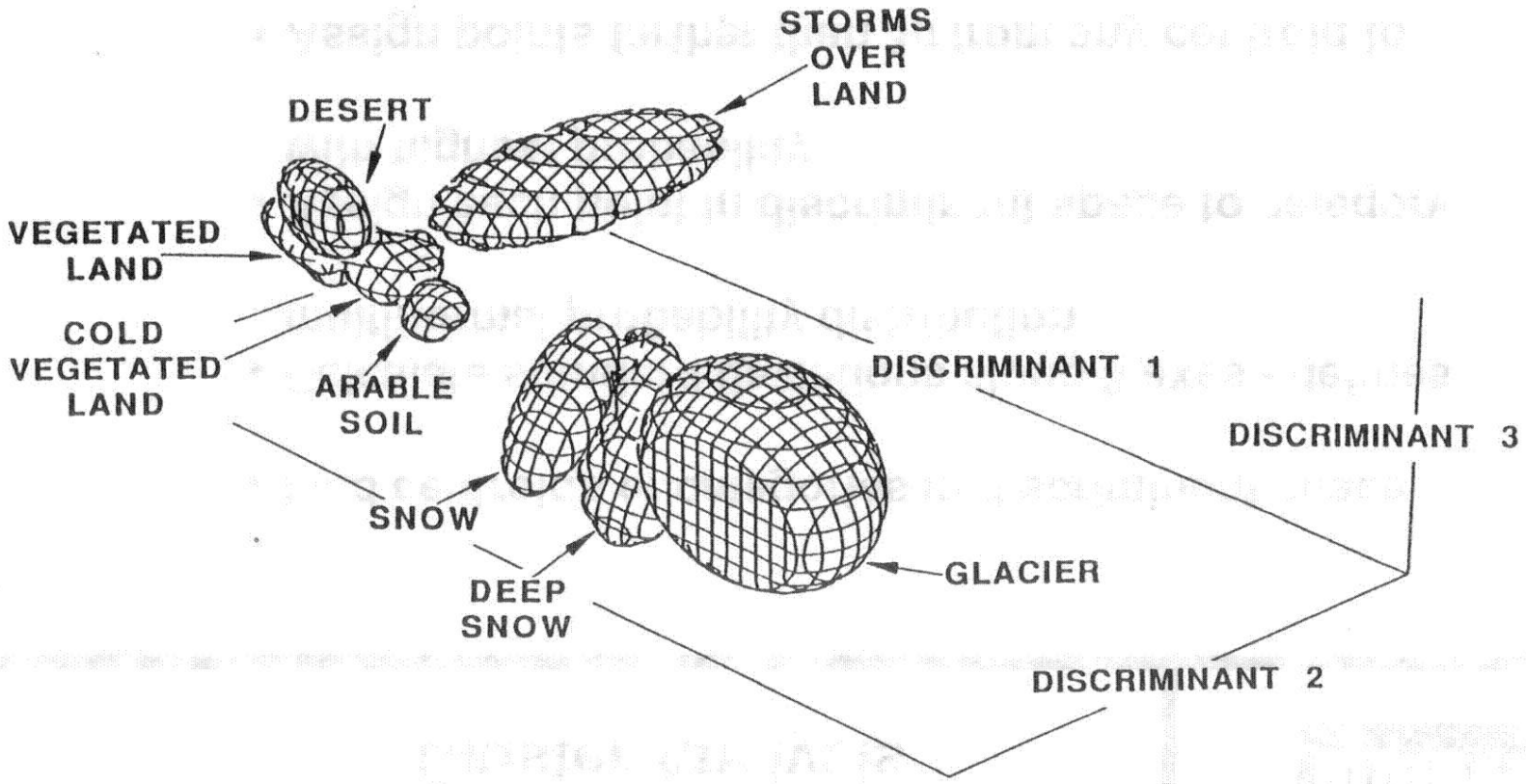
HUGHES

- Find centroids of categories in discriminant space
- Calculate standard deviations along 3 axes - defines multinormal probability distribution
- Assign each point in discriminant space to category with highest probability
- Assign points farther than 3σ from any centroid to "unknown"

Discriminant Space for Land

HUGHES

- 3 Standard Deviations Surface for Training Data

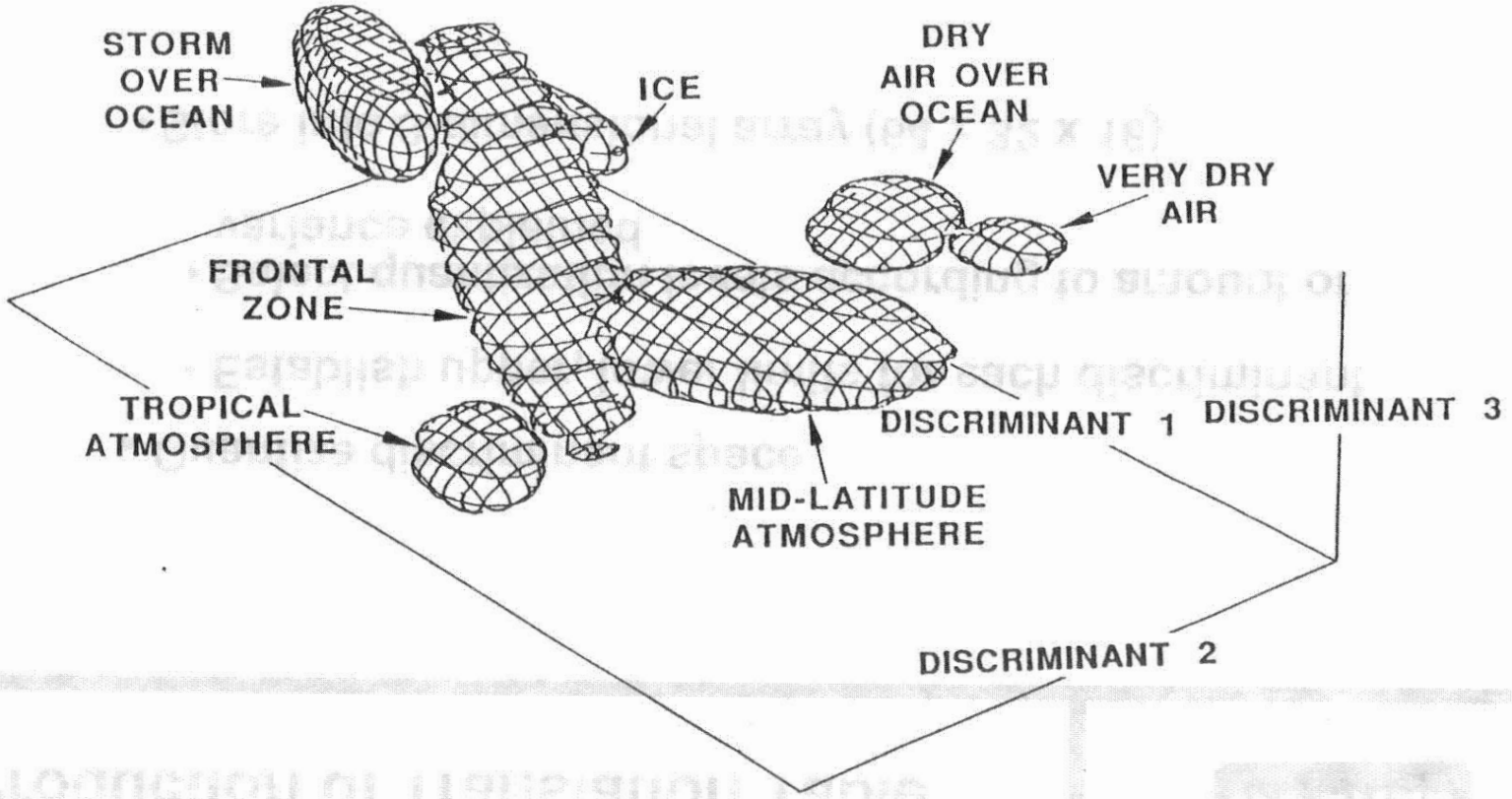


290-568G011.1

Discriminant Space for Ocean

HUGHES

- 3 Standard Deviations Surface for Training Data



290-568G012.1

Production of Translation Table

HUGHES

- Quantize discriminant space
  - Establish upper, lower limits for each discriminant
  - Select quantization levels according to amount of variance explained
- Store into 3-dimensional array (64 x 32 x 16)

Classification Results

HUGHES

- Classification requires only calculation of 3 linear combinations and one reference into translation table
- 1 to 2% unknown
- Verified by examination of time series, playback of training data
- Ambiguities:
  - Flooded soil/desert
  - Bare soil/melting snow
  - Snow/wet desert

A STATISTICAL SURFACE TYPE CLASSIFIER FOR SSM/I DATA

J. F. Heinrichs
A. J. Koscielny
R. C. Savage

Hughes Aircraft Company
Colorado Engineering Laboratories
16800 East CentreTech Parkway
Aurora, CO 80011

This work was performed under USAF contract FO4701-87-C-0016.

1. INTRODUCTION

Classification of surface types is a problem of general interest in remote sensing. The SSM/I (Special Sensor Microwave Imager), built by Hughes Aircraft Company and flown aboard DMSP (Defense Meteorological Satellite Program) platforms, with its ability to penetrate clouds to the surface below, as well as its rapid global coverage, offers a new source of information for surface categorization. The SSM/I is a passive microwave radiometer with seven channels: 19.35 GHz (vertical and horizontal polarizations), 22.235 GHz (vertical only), 37.0 GHz (vertical and horizontal), and 85.5 GHz (vertical and horizontal). It has demonstrated the capability to generate a number of useful surface products, including snow water content, soil moisture, ice concentration, and surface temperature.

A requirement exists for an operational surface type classifier, both to support the estimation of environmental parameters and to provide a historical record of changes in surface characteristics. The desired classifier must be accurate, fast (minimal number of computations per point), robust (resistant to data errors, mixed pixels, and unusual surface types), and easily understood and maintained by the data user. These considerations militate against a complicated system of discrete logic statements of the IF...THEN...ELSE type (distinguishing some categories with such approaches requires that almost all of the conditions be checked).

The basis for our classifier is a training data set, assembled from manually categorized SSM/I observations made between 1987 and 1989. A discriminant analysis was performed, which reduced the number of variables from the seven SSM/I brightness temperatures to three discriminant scores. Bounded regions in the space defined by the discriminants were established for each surface type, with all points outside these regions typed as "unknown". The space was quantized to yield a simple lookup table for translating discriminant scores to surface types. The method has been implemented in operational software and demonstrated to be both accurate and efficient.

2. TRAINING DATA

The first step in development of our classifier was to assemble a training data set of matching SSM/I brightness temperature vectors and surface types.

SSM/I data was obtained from two primary sources. First, FNOC (the Fleet Numerical Oceanography Center) at Monterey, CA regularly archives full resolution SSM/I data in the DEF (Data Exchange Format). Second, AFGWC (Air Force Global Weather Central) at Omaha, NE supplied us with a large number of "snapshots" of their global polar stereographic gridded SSM/I database. In all cases, the data used were SDRs (Sensor Data Records), which contain geolocated, calibrated, and antenna pattern corrected brightness temperatures. In order to produce the most useful classifier, we restricted our training data to the period prior to failure of the 85 GHz vertically polarized channel (although, as described below, the algorithm finally implemented does not use this channel). Images of the data sets were examined and those with excessive data dropouts and gain variations were excluded.

The absence of any single available data set capable of providing adequate "ground truth" information on surface type precluded automated assembly of the training data set. Instead, several sources of a priori classification were examined and each training data point was assigned manually to a particular category. Our primary sources of surface type information included:

a. The Matthews land use/cultivation intensity data base (Matthews, 1983), which provides global coverage with one degree resolution. This is a static data base and thus does not reflect seasonal changes in snow cover, sea ice, or vegetation.

b. The Climatic Analysis Center Product Communications System (CAC-PCS), which offers dialup access to a global data set of temperature and precipitation data, as well as weather and crop summaries.

c. Snow cover charts from the National Snow and Ice Data Center (NSIDC) in Boulder, CO.

Candidate training data subsets were built from these sources and the matching SSM/I brightness temperatures. Computation of basic statistical measures and examination of histograms and scatter plots allowed the candidate data points to be edited and odd or misclassified data removed prior to incorporation in the training data set. The final data set contained the time, latitude, longitude, surface elevation, the seven SSM/I brightness temperatures, and the assigned surface type for each point. Table 1 lists the surface types selected and the number of training data points for each category. It should be pointed out that the names given to the categories are descriptive rather than rigorously defined and serve mainly to simplify discussion.

3. ANALYSIS METHOD

Previous work by Koscielny and Savage (1989) demonstrated that principal components analysis revealed significant information about the nature of the surface and suggested the use of discriminant analysis for surface categorization. We proceeded in this direction, basing our approach on the method of Cooley and Lohnes (1971). In this method, the among-group and within-group SSCP (sums of squares and cross-products) matrices are calculated over the training data set. The right eigenvectors of the matrix obtained by multiplying the inverse of the within-group SSCP by the among-group SSCP are taken, and represent the linear combinations of the original brightness temperatures that best separate the data into the pre-defined classes. Tables 2 and 3 list, for land and water respectively, the coefficients of the eigenvectors, along with a measure of the discrimination ability of each. These figures are from the most recent analysis, which was used for the operational implementation and excluded the 85 GHz vertically polarized channel. Note that the first three eigenvectors together account for over 96% of the discrimination information for ocean and over 89% for land. Using just these three enabled us to simplify the analysis and produce a faster classifier, while preserving almost all of the information in the original brightness temperature vectors.

Figures 1 to 3 are images made by calculating the three discriminants at each point in the Northern hemisphere (using a data set from January 3, 1989). Although the discriminants have statistical meaning in that they explain the variance in the training data set, their physical meaning is often difficult to assess. However, we feel that it is instructive to discuss how the discriminants differ in sensitivity to certain phenomena. It should also be noted that the discriminant analysis is done separately for land and water, and that the images are composites of both. The meaning of a particular discriminant value over land is completely different for a water point. Discriminant 1, for example, seems to respond well to cloud water content and air mass discontinuities over oceans whereas, over land, it seems to indicate the presence of snow (seen in northern North America and Siberia). Discriminant 1 is also capable of identifying the presence of sea ice, but does not distinguish between first year and multiyear ice. Discriminant 2 seems to respond (over land) to soil moisture. Note the dark areas corresponding to the Sahara and Gobi deserts. It is more difficult to interpret discriminant 2 over water, but our best guess is that atmospheric water vapor is the primary influence. Discriminant 3 responds very well to vegetation over land (notice the lush vegetation on the southern slope of the Himalayas and along the Mississippi river floodplain) and precipitation over water (the rain bands along fronts are picked out distinctly). In addition, discriminant 3 appears to distinguish between multiyear ice (which is very dark in the image) and other sea ice (which is indistinguishable from the ocean background.

The space defined by these three discriminants was then partitioned, so that each point was assigned a unique surface type or a value indicating "unknown". The centroid (in discriminant space) of the training data points belonging to each category was determined. The training data were assumed to have a multinormal distribution around the centroid, and the 3x3 covariance matrix defining the distribution for each category was calculated. For each point in discriminant space, the probability of belonging to each class was determined using a trivariate normal pdf (probability density function) calculated by the method of Afifi and Azen (1972). Each point was then assigned to the class with the highest probability. Points not within a specified number of standard deviations of any centroid were typed "unknown". A value of 3.5 was chosen to give a probability of 0.0005 of classifying a point as unknown. The isosurfaces for probability defined by this limit are ellipsoids, as described by Tatsuoka (1973).

To facilitate use of a simple lookup (translation) table to find the surface types and confidence factors for measured SSM/I temperature vectors, the rectilinear region of discriminant space containing all of the ellipsoids was determined and quantized. The level of quantization was determined by the desire to have the smallest category contain several bins. Furthermore, as the variance of the discriminants differed, the quantization of the three axes should differ as well. Finally, the memory available for the translation tables in the computer system on which the classifier was to be used operationally was severely limited. These considerations led us to a translation table size of 64x32x16. Two translation tables are required (one each for land and ocean).

Finally, to reduce the total amount of stored historical information required by the operational implementation, we developed a method to estimate the significance of a change in surface characteristics. A set of change thresholds (one for each surface type) was obtained by calculating the square root of the trace of the covariance matrix (in discriminant space) taken over the training data belonging to that type. The process updating the historical database is executed every day, and the current set of discriminants is compared with the most recent previous discriminants and stored if and only if (a) the new discriminants map to a different surface type or (b) they map to the same surface type, but the Euclidean distance between the old and new discriminants exceeds the change threshold.

Tables 4 (land) and 5 (ocean) list, for each surface type, the coordinates of the centroid in discriminant space, the three standard deviations defining the probability distribution around the centroid, and the change threshold.

4. RESULTS

The analysis described above yielded a classifier requiring calculation of only three linear combinations (for a total of 21

additions and 21 multiplications) and one access into the appropriate translation table for each point. Examination of surface type images formed by classifying the AFGWC gridded data sets yielded very few gross misclassifications, and the number of points typed "unknown" was generally about 1-2 percent. A time series of these images during 1988 was produced, and temporal variations were observed to correspond closely with actual physical changes. Some category pairs were found to be noticeably, but not severely, ambiguous (flooded soil/desert, bare soil/melting snow).

The software implementation of the classifier, along with associated support code to maintain a historical database, was successfully tested on the target computer system (a UNISYS 1100 at AFGWC) in April 1990, with final delivery and operational implementation scheduled for August. As the software is used, and the historical record grows, we intend to further verify the accuracy of classification by using more recently available "truth" data sets, such as the AVHRR NDVI (Normalized Difference Vegetation Index) data on CD-ROM for the 1988 growing season (available from the U.S. Geological Survey).

5. CONCLUSION

Our research has demonstrated, firstly, that SSM/I data is very effective for surface categorization and, secondly, that a statistical classifier of the form herein described is both accurate and efficient, well-suited for both research and operational needs.

We intend to further develop our approach to classification with the goal of being able to make progressively finer distinctions. In particular, as part of the WetNet system, we will be conducting an investigation into measurement of plant health (stress) with SSM/I data. This work will build upon the classification strategy described above, and we will make the algorithms and associated software available to the research community via WetNet.

6. ACKNOWLEDGEMENTS

The statistical analysis portion of classifier development was performed on a VAX 8600. Display and analysis of images was done on a Sun 3 using IDL (Interactive Data Language), developed by Research Systems, Inc. of Boulder, CO.

We wish to thank the Defense Meteorological Satellite Program Office for their support, as well as Ms. Sue Glassner of FNOC and Capt. Tom Hamill of AFGWC for their assistance in making SSM/I data available to us.

7. BIBLIOGRAPHY

Afifi, A. A. , and S. P. Azen, 1972: Statistical Analysis, Academic Press, New York.

Cooley, W. W., and P. R. Lohnes, 1971: Multivariate Data Analysis, John Wiley, New York.

Koscielny, A. J., and R. C. Savage, 1989: A Color Composite Display for SSM/I Imagery, presented at the Fifth Conference on Interactive Information Systems for Meteorology, Oceanography, and Hydrology, held by the American Meteorological Society, January 30 - February 3, 1989, Anaheim, CA.

Matthews, E. 1983: Global Vegetation and Land Use: New High-Resolution Data Bases for Climatic Studies, J. Clim. and App. Met. 22, pp. 474-487.

Tatsuoka, M. H., 1971: Multivariate Analysis, John Wiley, New York.

Table 1

Contents of training data set

Type	Description	# Data
1	Dry air over calm ocean	467
2	Dry air over ocean	491
3	Fronts, thick clouds over ocean	703
4	Moderately moist air over ocean	500
5	Moist air over ocean	141
6	Rain over ocean	376
7	Snow covered land	864
8	Deep snow	603
10	Glacial snow	363
12	First year sea ice	805
13	Multiyear sea ice	583
14	Arable soil	240
15	Desert (dry surface)	1446
16	Flooded land/land-water mix	336
18	Cold vegetation	429
19	Dense vegetation	444
20	Sparse vegetation	385
21	Moderate vegetation	371
22	Rain over land	276
23	Desert (wet surface)	456

Table 2

Results of Discriminant Analysis for Land

Eigenvector coefficients

#	19V	19H	22V	37V	37H	85H	Percent Trace
1	-0.01410	0.00557	0.04355	-0.00899	-0.00491	0.01714	39.97
2	-0.07081	0.06036	0.02723	-0.00201	0.00946	-0.02294	34.50
3	0.14542	0.00873	-0.13984	0.05689	-0.01545	-0.03886	15.02
4	-0.23123	-0.02802	0.26179	0.01533	0.04534	-0.05949	6.63
5	-0.13957	0.07857	0.24038	-0.04106	-0.14666	0.02918	3.11
6	0.26904	-0.29103	0.11481	-0.45873	0.38759	0.00009	0.77

Table 3

Results of Discriminant Analysis for Ocean

Eigenvector coefficients

#	19V	19H	22V	37V	37H	85H	Percent Trace
1	0.07139	-0.02779	-0.01337	-0.05460	0.04003	0.00250	65.36
2	-0.03664	-0.02142	0.06026	-0.03921	0.03917	0.00785	21.99
3	-0.12149	0.01953	0.03141	0.13087	0.00235	-0.05135	8.77
4	0.07796	0.06499	-0.14753	0.15073	-0.13501	0.06957	2.32
5	0.03462	-0.02297	0.08729	0.04404	-0.04796	-0.04993	1.51
6	0.53788	-0.34961	-0.04264	-0.31222	0.21929	0.01388	0.05

Figure 1

Image of Discriminant 1 - January 3, 1989



Figure 2

Image of Discriminant 2 - January 3, 1989



Figure 3

Image of Discriminant 3 - January 3, 1989



Table 4

Parameters Defining Land Surface Types
in Discriminant Space

Surface Type	Centroids DS1	DS2	DS3	Standard Deviations DS1	DS2	DS3	Change Threshold
7	32.87	18.07	8.82	3.869	1.958	0.720	4.4
8	28.20	19.87	8.95	4.374	2.202	1.216	5.0
10	18.23	9.53	7.78	5.202	2.757	1.549	6.1
14	43.72	18.25	7.72	3.651	1.770	1.011	4.2
15	47.29	12.72	10.23	3.317	1.170	0.747	3.6
16	46.79	15.47	4.90	4.630	1.641	1.411	5.1
18	44.99	20.04	7.59	1.254	0.714	0.576	1.6
19	49.47	20.61	7.40	0.997	0.489	0.517	1.2
20	49.74	17.15	9.16	3.064	1.152	0.723	3.4
21	49.33	19.63	8.58	1.161	0.522	0.532	1.4
22	35.50	25.56	11.40	2.921	1.579	1.079	3.5
23	43.75	12.88	7.63	2.602	1.540	0.703	3.1

Note: Surface type numbers are from Table 1

Table 5

Parameters Defining Ocean Surface Types
in Discriminant Space

Surface Type	Centroids DS1	DS2	DS3	Standard Deviations DS1	DS2	DS3	Change Threshold
1	6.43	4.53	9.05	1.823	1.312	0.460	2.3
2	11.72	6.79	8.04	2.198	1.607	0.593	2.8
3	22.73	18.94	6.94	5.330	3.433	1.568	6.5
4	11.94	12.71	6.49	2.256	2.408	0.557	3.3
5	14.03	18.18	5.83	1.331	0.682	0.396	1.5
6	40.28	16.69	10.93	6.519	4.137	1.218	7.8
12	40.97	7.88	7.91	2.466	1.251	0.824	2.9
13	40.61	6.40	5.55	2.566	1.409	1.627	3.3

Note: Surface type numbers are from Table 1

Recent Dabbling

HUGHES

- No funded activity
- Small McBASI program for WETNET magneto-optical disks (attached)
  - Specify LAT/LON (HARP-coded)
  - Feed MOs into PS/2
  - Create files of sequential data
- Sample follows

```
1 REM  ************************************************************
3 REM  This program extracts all of the SSM/I data on a WetNet MO
4 REM  disk that covers a single point identified by latitude and
5 REM  longitude
6 REM  ************************************************************
7 REM  (C) 1993  Hughes Aircraft Company
8 REM  All rights reserved
9 REM  ************************************************************
10 REM
20 REM  Find the first SSM/I pass
30 REM
40 G = 1
50 N1 = 2000 + 30*(G-1)
55 KEYIN "LWU DEL TEMPLW"
60 KEYIN "LWU MAKE TEMPLW"
70 KEYIN "DF ";N1;" 1 BAND=1 DEV=F TEMPLW"
75 OPEN "TEMPLW",10
80 INPUT @10,A$
90 CLOSE 10
95 IF LEN(A$)<>4 GOTO 200
100 G = G + 1
110 IF G<40 GOTO 50
120 STOP
200 REM
201 REM  When first pass is found, start looking for passes that cover
202 REM  the desired point
203 REM
205 D = 1
207 O = 1
210 N = N1+ 30*(d-1) + (o-1)
230 KEYIN "LWU DEL TEMPLW"
240 KEYIN "LWU MAKE TEMPLW"
250 KEYIN "DF ";N;" 1 EC 41.14 96.39 BAND=1 DEV=F TEMPLW"
260 OPEN "TEMPLW",10
270 INPUT @10,A$
280 CLOSE 10
290 IF LEN(A$)=4 GOTO 450
300 REM
301 REM  If this is a good pass, load all 7 SSM/I channels into
302 REM  successive frames
303 REM
310 KEYIN "DF ";N;" 2 EC 41.14 96.39 BAND=2"
320 KEYIN "DF ";N+15;" 3 EC 41.14 96.39 BAND=3"
330 KEYIN "DF ";N+15;" 4 EC 41.14 96.39 BAND=4"
340 KEYIN "DF ";N+15;" 5 EC 41.14 96.39 BAND=5"
350 KEYIN "DF ";N+15;" 6 EC 41.14 96.39 BAND=6"
360 KEYIN "DF ";N+15;" 7 EC 41.14 96.39 BAND=7"
370 KEYIN "LA ";N
380 Q = 1
381 REM
382 REM  Move the cursor over the desired point and capture the value
383 REM
390 KEYIN "SF ";Q
400 KEYIN "PC E 41.14 96.39"
410 KEYIN "E"
420 KEYIN "D"
430 Q = Q + 1
440 IF Q<8 GOTO 390
450 o = o + 1
460 if o<16 goto 210
470 d = d + 1
480 if d<30 goto 207
490 keyin "P"
500 stop
```

HUGHES

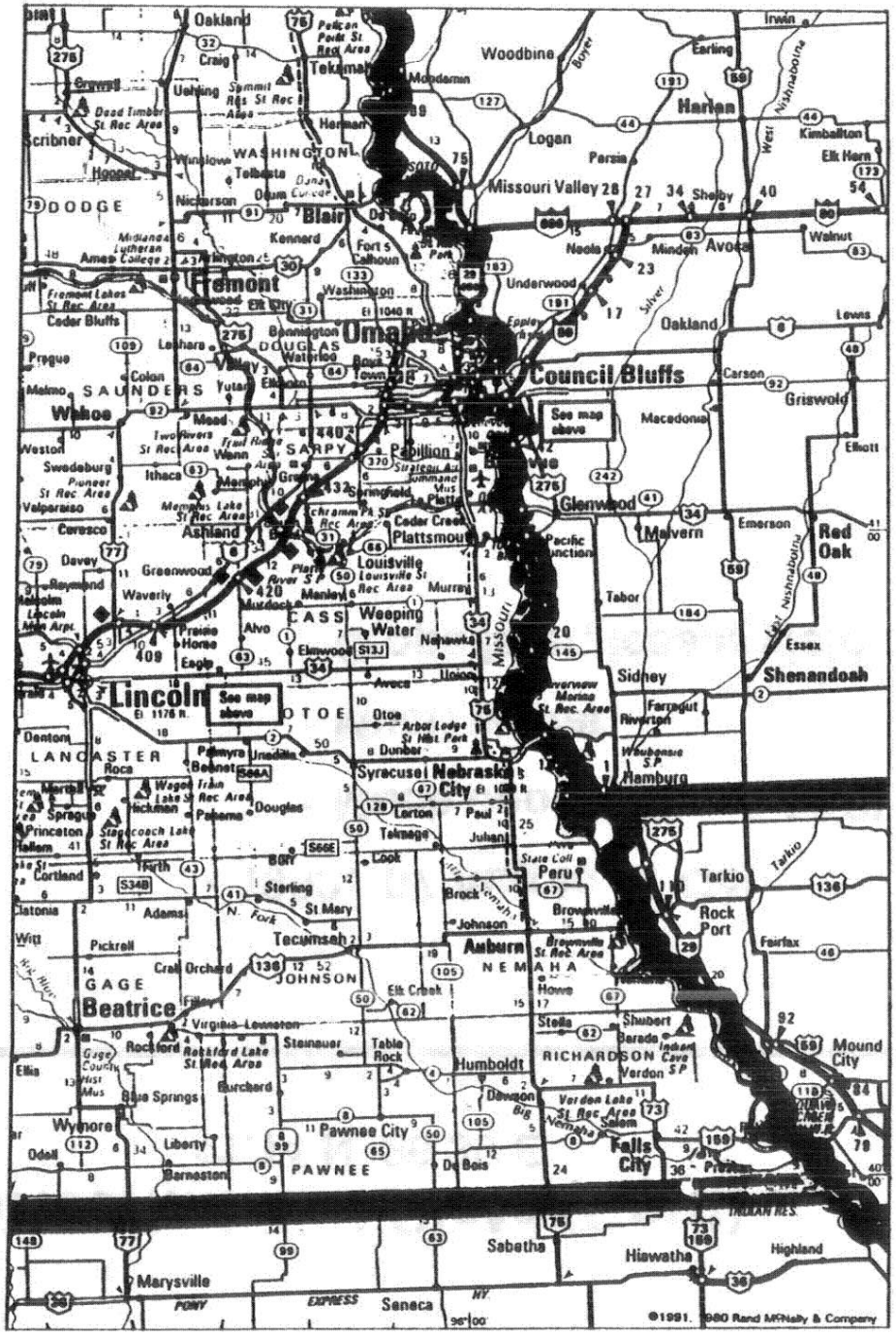
MO Data Extraction

Discriminant Plots

41.14 N, 96.39 E

HUGHES

- Location
  - Sarpy County, NE
  - East of I-80, North of Platte River
  - Rolling, partly wooded farm country
- 1988: 01 Feb to 14 Feb
  - Mixture of surface types
  - Snow (7) + arable soil (14)
- 1987: 08 Aug to 16 Nov
  - Widespread rain approximately 24 Aug (not snow)
  - Moderate vegetation, becoming arable soil
  - Precipitation events through period
  - Diurnal variations in DS1
  - "Watching the corn grow"



293-155P011.1

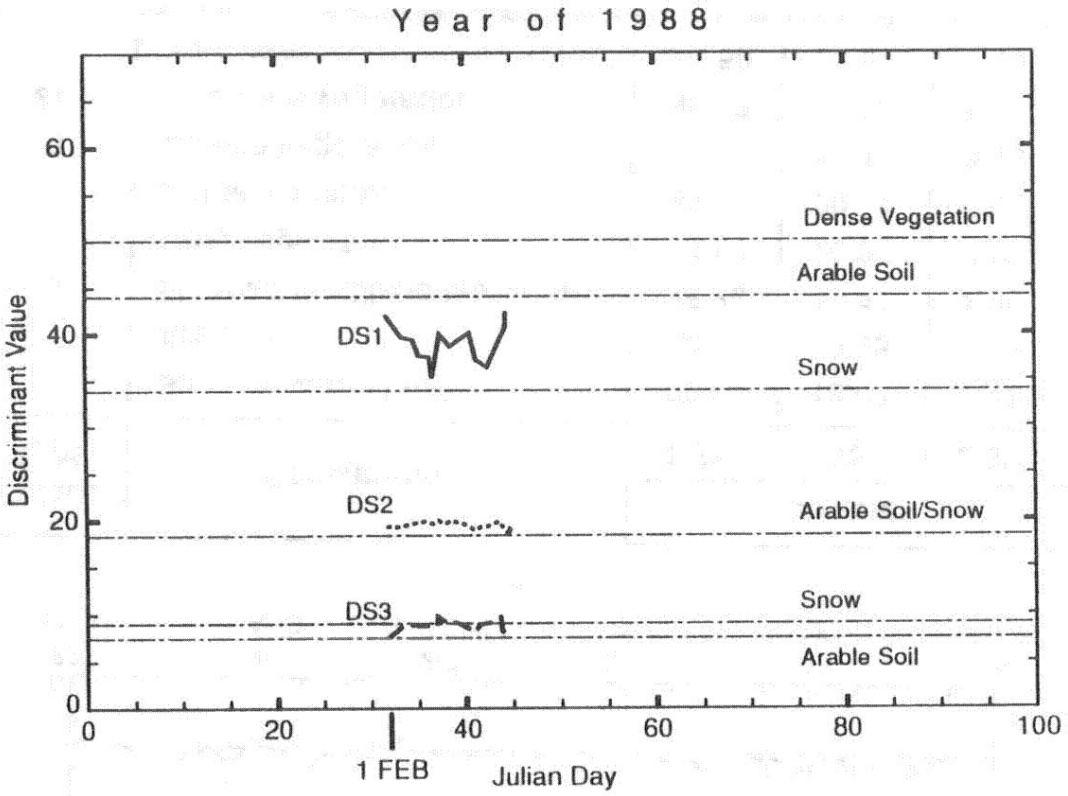
HUGHES

Data Area

Discriminant Plots (Cont)
41.14 N, 96.39 E

HUGHES

- 1992: 07 Aug to 11 Oct
  - Much cooler (Pinatubo?)
  - Much wetter
  - Crops later, lesser yield

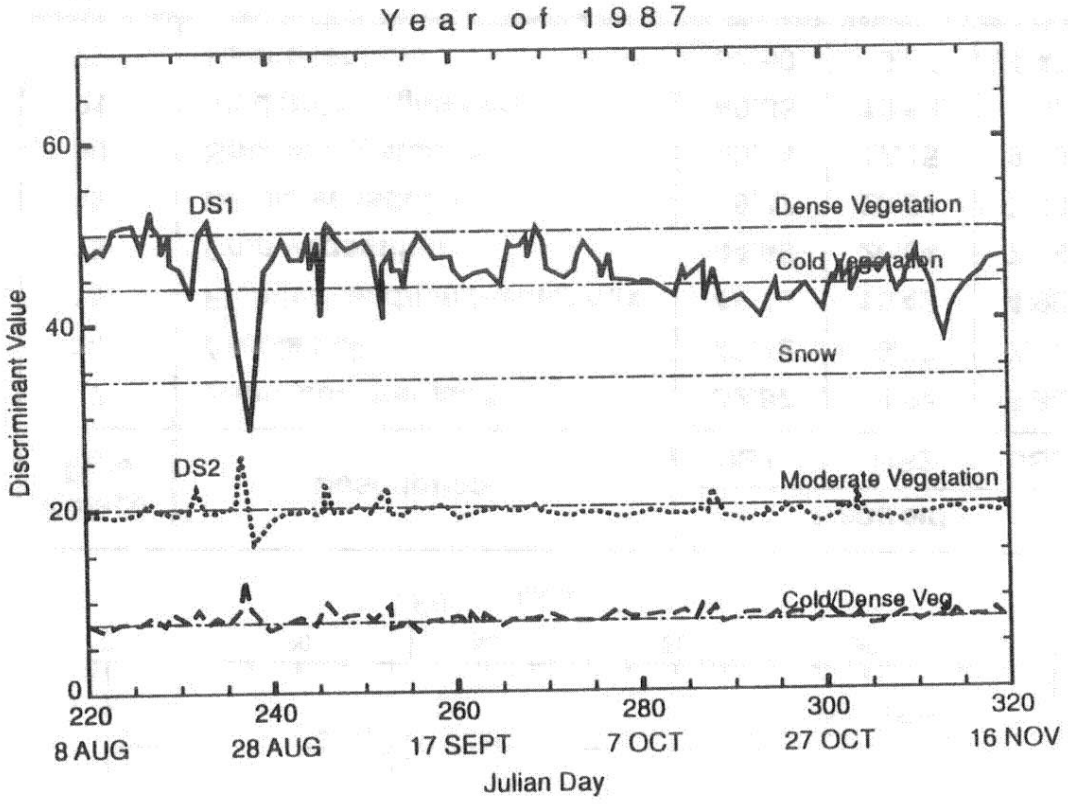


Suface Type	Description	Centroids		
		DS1	DS2	DS3
7	Snow covered land	32.87	18.07	8.82
14	Arable soil	43.72	18.25	7.72
16	Flooded land/land-water mix	46.79	15.47	4.90
18	Cold vegetation	44.99	20.04	7.59
19	Dense vegetation	49.47	20.61	7.40
20	Sparse vegetation	49.74	17.15	9.16
21	Moderate vegetation	49.33	19.63	8.58
22	Rain over land	35.50	25.56	11.40

293-155P009.2

HUGHES

1988 Classification Data

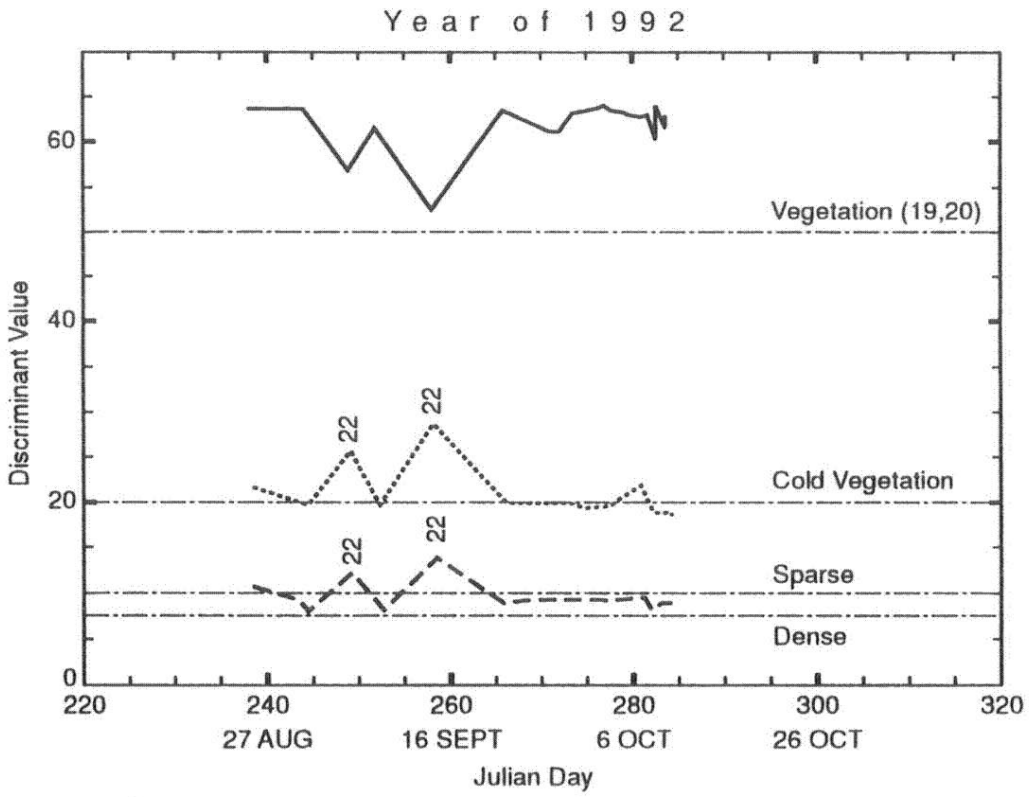


Suface Type	Description	Centroids		
		DS1	DS2	DS3
7	Snow covered land	32.87	18.07	8.82
14	Arable soil	43.72	18.25	7.72
16	Flooded land/land-water mix	46.79	15.47	4.90
18	Cold vegetation	44.99	20.04	7.59
19	Dense vegetation	49.47	20.61	7.40
20	Sparse vegetation	49.74	17.15	9.16
21	Moderate vegetation	49.33	19.63	8.58
22	Rain over land	35.50	25.56	11.40

293-155P008.2

HUGHES

1987 Classification Data



Suface Type	Description	Centroids		
		DS1	DS2	DS3
7	Snow covered land	32.87	18.07	8.82
14	Arable soil	43.72	18.25	7.72
16	Flooded land/land-water mix	46.79	15.47	4.90
18	Cold vegetation	44.99	20.04	7.59
19	Dense vegetation	49.47	20.61	7.40
20	Sparse vegetation	49.74	17.15	9.16
21	Moderate vegetation	49.33	19.63	8.58
22	Rain over land	35.50	25.56	11.40

293-155P007.2

HUGHES

1992 Classification Data

AFGWC SSM/I Applications: Thunderstorm and Wet Desert Discrimination during Desert Storm, and Tropical Cyclone Analyses

Charles R. Holliday
Air Force Global Weather Central
Offutt AFB, NE

Meteorologists at AFGWC apply their interpretative skills to satellite imagery to develop operational applications of satellite data for tactical users. Data interpretation is enhanced through the use of new visualization software on both Sun workstations and the VAX-based Satellite Data Handling System. This paper describes two major applications of SSM/I data at AFGWC. The methods described have been applied more recently to support Operations Restore Hope and Southern Watch.

During Operation Desert Storm, AFGWC utilized the Special Sensor Microwave/Imager (SSM/I) to augment DMSP visual and infrared surveillance of the Mid-east region. In particular, the microwave data provided additional capabilities for reconnaissance of thunderstorms, especially at nighttime when high cirrus clouds obscured convective activity in infrared imagery. The SSM/I soil moisture and surface type parameters were also used for trafficability information across the desert. In fact, using the visible/IR observations, real-time adjustments of the SSM/I soil moisture algorithm were made to improve the algorithm's accuracy in the recognition of wet desert.

The SSM/I data are also used extensively for tropical storm tracking and analyses. The standard product is a bulletin sent to the Joint Typhoon Warning Center at Guam which identifies storm position and gale wind ($>$ 30 kts) radius. Normally the bulletin is based on the DMSP visible/IR and microwave data; however, the "see through" capability of the microwave sensor is relied upon when the storm eye is covered by a cirrus shield. In these high wind speed, high liquid water regions, the SSM/I wind speed algorithm is adjusted to correct a negative bias between the SSM/I and observed wind speeds.

Session 4

Cloud Liquid Water
Column Water Vapor
Surface Wind Speed

(John Alihouse, NOAA/NESDIS, Chair)

ENCL(10)

Session 4

Cloud Liquid Water

Column Water Vapor

Surface Wind Speed

(John Allroues, NOAA/NESDIS, Chair)

SSM/I Algorithms for the Estimation of Column Water Vapor

Grant W. Petty
Dept. of Earth and Atmospheric Sciences
Purdue University
West Lafayette, IN

A statistical algorithm for globally estimating column water vapor over the ocean has been developed based on a derivative of the Alishouse et al. raob/SSM/I matchup data set. In the revised training data set, the original raob water vapor estimates were retained, but new SSM/I brightness temperatures were selected using a technique designed to identify and eliminate island-contaminated pixels. All uncontaminated pixels within a 50 km radius and 2 hours of each raob sounding were incorporated in the final training data set, which consists of a total of 599 raob estimates of column water vapor and 6132 SSM/I pixels.

The new algorithm uses a linear combination of functions of the form log(300-Tb). The brightness temperatures Tb are supplied by the 19V, 22V, and 37H channels.

All water vapor algorithms known to the author were applied to the raob data set in order evaluate their comparative performance. Most other algorithms exhibited noticeable biases; these biases, however, could be corrected by fitting a cubic polynomial to the residuals. Once the biases were removed, rms differences between SSM/I estimates and raob estimates ranged from 2.63 kg/m^2 for the Cal/Val algorithm to 3.15 kg/m^2 for the Wentz algorithm. Our new algorithm yielded a somewhat improved rms difference of 2.58 kg/m^2. This value must be treated with caution, however, since the training data set and the validation data set are not independent; further validation is therefore still necessary.

A theoretical analysis of selected algorithms was also undertaken. Among other things, it appears that the new global regression algorithm is significantly less susceptible to liquid water crosstalk and other sources of contamination than the current Cal/Val algorithm.

SPN SSM/I ALGORITHM SYMPOSIUM
Algorithm Questionnaire

"WATER VAPOR ALGORITHM"
Grant Petty, respondent

Please provide the following essential information about your algorithm(s).

* ALGORITHM DESCRIPTION

- Type (statistical, physical, other) *Statistical*

- Input required / Output produced

  Input: Brightness Temperatures from 19 GHz (v-pol); 22 GHz (v-pol) 37 GHz (h- pol);
  Output: Column water vapor

- Auxiliary sensor/data base requirements *None*

- Major limitations / approximations *Over ocean only*

- Computer resource requirements *Minimal*

* ALGORITHM PERFORMANCE

- Development / test data sets (regional / global / seasonal)

  Global

- Ground truth (accuracy / limitations)

  Quality controlled raob estimates of precipitable water

- Major assumptions of evaluation

- Strengths / weaknesses

Improved linearity and reduced liquid water crosstalk as compared with Cal/Val algorithm; rms errors comparable or slightly better than Cal/Val.

* ALGORITHM MATURITY

- Operational useage

  Used in research mode for approximately one year at limited number of university labs.

- Refinement / additional development

  Requires additional validation against independent data set.

- Availability

  Algorithm is available upon request.

WATER VAPOR ALGORITHM EVALUATION CRITERIA

- RMS differences from raobs
- Linearity of response / presence of systematic biases
- Theoretical crosstalk sensitivity and noise sensitivity

Petty Water Vapor Algorithm

Integrated water vapor [kg m^{-2}] is estimated using

$$V = 174.1 + 4.638 \ln(300 - T_{19V}) - 61.76 \ln(300 - T_{22V}) + 19.58 \ln(300 - T_{37H}). \quad (1)$$

V is flagged as precipitation contaminated and discarded if $T_{19V} - T_{19H} > 15$ K (preliminary criterion; subject to revision).

Modified Wind Speed Algorithm

Original Cal/Val (Goodberlet et al. 1989) wind speed algorithm:

$$U' = 1.0969 T_{19V} - 0.4555 T_{22V} - 1.76 T_{37V} + 0.7860 T_{37H} + 147.9 \quad (2)$$

Petty water vapor correction:

$$U = U' - 2.130 + 0.2198 V - 0.4008 \times 10^{-2} V^2, \quad (3)$$

where U has units of [m s^{-1}] and V is computed from (1).

Improved criteria for detecting liquid water/rain contamination of retrieved wind speeds are still under development.

RESULTS OF INITIAL WATER VAPOR ALGORITHM INTERCOMPARISON

N = 599 Raobs
6132 SSM/I pixels processed -> average of 10 pixels per raob

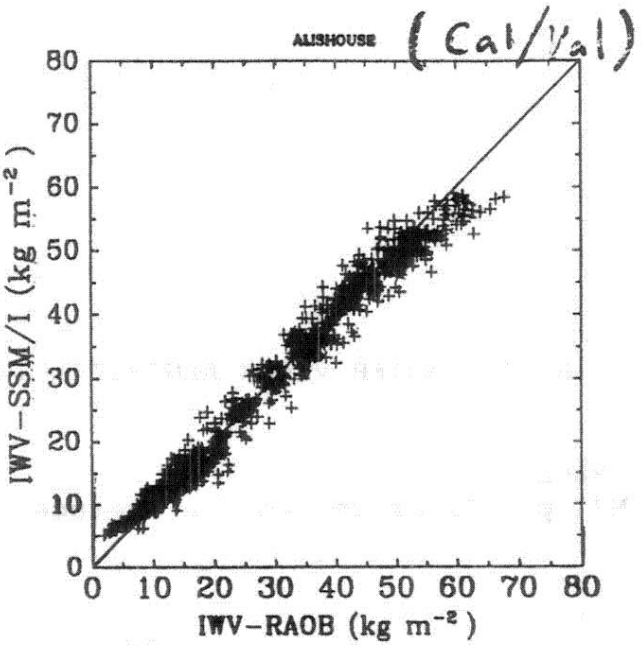
Before correction:

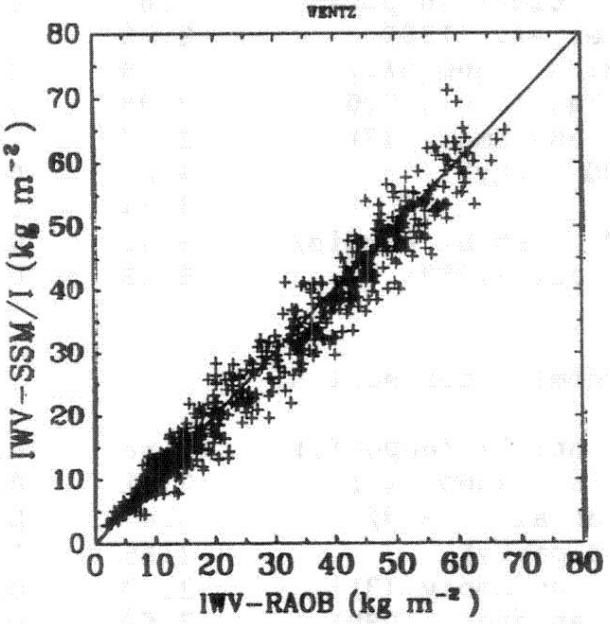
	RMS	r	RMS Fract. (%)
*Petty statistical (unpubl.)	2.61	0.989	12.7
*Alishouse et al. (1989)	2.76	0.988	17.9
Petty physical (unpubl.)	2.88	0.988	19.7
*Petty and Katsaros (1990)	2.98	0.985	17.7
Schluessel and Emory (3)	3.07	0.986	17.4
(unpubl. 3d party)	3.27	0.987	12.7
Wentz	3.44	0.981	14.5
Lojou (1990 - Ph.D. thesis)	5.05	0.985	34.4
Tjemkes et al. (1990)	6.03	0.946	31.4

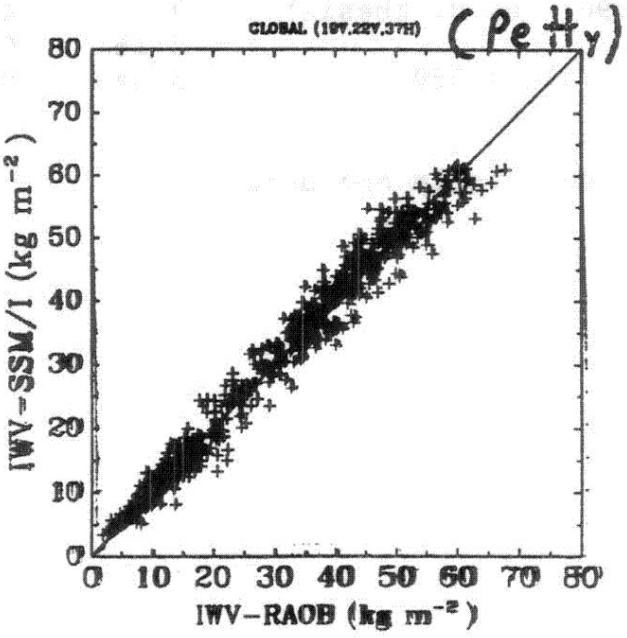
After cubic polynomial correction:

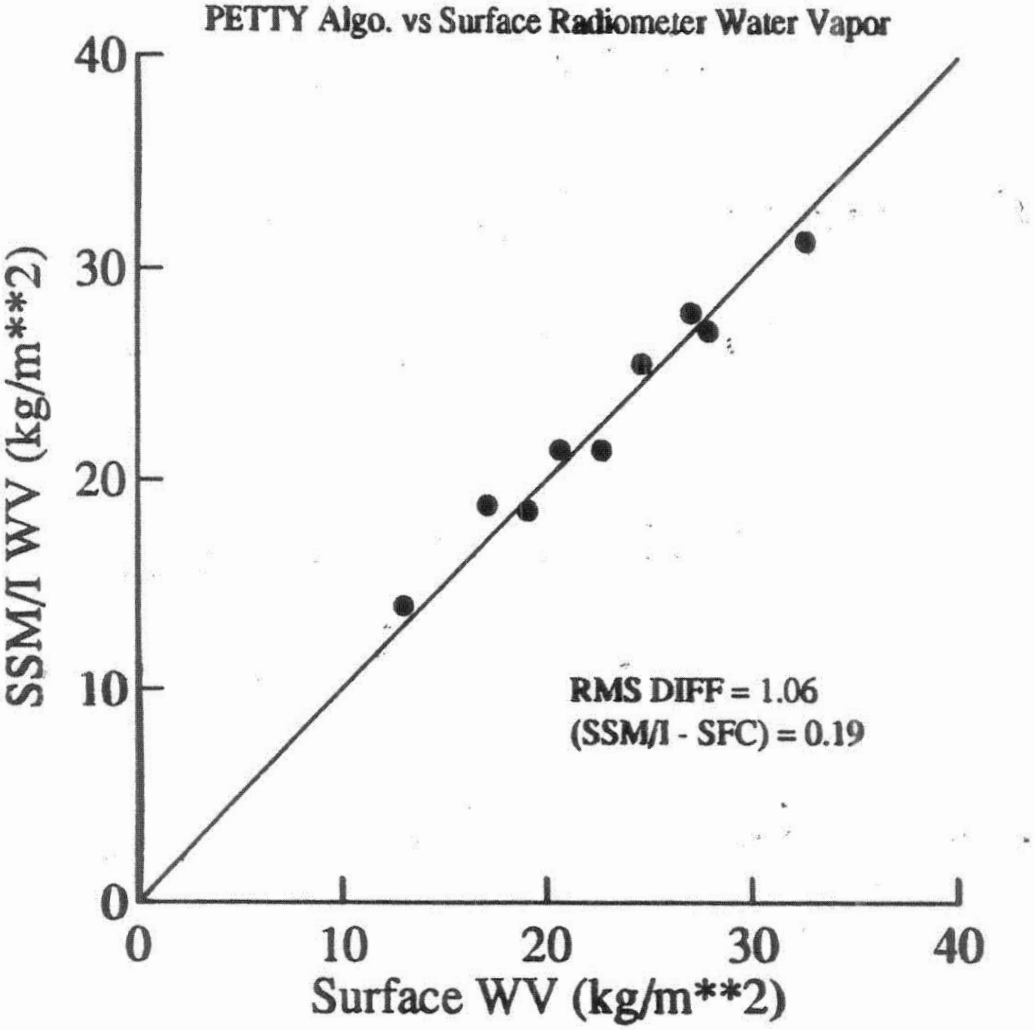
*Petty statistical (unpubl.)	2.58	0.989	11.9
Petty physical (unpubl.)	2.61	0.988	11.4
*Alishouse et al. (1989)	2.63	0.988	13.3
(unpubl. 3d party)	2.65	0.988	12.0
Schluessel and Emory (3)	2.68	0.988	12.4
*Petty and Katsaros (1990)	2.69	0.988	13.9
Lojou (1990 - Ph.D. thesis)	2.71	0.988	13.5
Wentz	3.16	0.983	15.1
Tjemkes et al. (1990)	5.54	0.947	26.2

*Raob data set not independent


ALISHOUSE
(Cal/Val)
IWV-SSM/I (kg m^{-2})
IWV-RAOB (kg m^{-2})
0
10
20
30
40
50
60
70
80


WENTZ
IWV-SSM/I (kg m^{-2})
IWV-RAOB (kg m^{-2})
0
10
20
30
40
50
60
70
80


GLOBAL (19V,22V,37H)
(Petty)
IWV-SSM/I (kg m^{-2})
IWV-RAOB (kg m^{-2})
0
10
20
30
40
50
60
70
80


PETTY Algo. vs Surface Radiometer Water Vapor
SSM/I WV (kg/m**2)
Surface WV (kg/m**2)
0
10
20
30
40
RMS DIFF = 1.06
(SSM/I - SFC) = 0.19

SSM/I Algorithms for the Estimation of Column Cloud Water

Grant W. Petty
Dept. of Earth and Atmospheric Sciences
Purdue University
West Lafayette, IN

All known over-ocean cloud liquid water algorithms for the SSM/I, including two developed by the author, have undergone a preliminary theoretical and empirical evaluation. For the theoretical evaluation, an analytic brightness temperature model was used to evaluate the relative sensitivity of each algorithm to cross-talk from various sources. For the empirical evaluation, we examined the behavior of each algorithm when it was applied to known cloud-free SSM/I brightness temperatures. We are also in the process of examining the SSM/I retrievals in the vicinity of San Nicolas Is., during July 1987, when an upward-looking microwave radiometer provided some measure of surface "truth." The latter comparisons are not yet complete, but we expect to be able to present preliminary findings at the Symposium.

From our experiments with the cloud-free data, we find that the Cal/Val liquid water algorithm exhibits a significant water vapor-dependent bias, with liquid water overestimates of up to 2 kg/m^2 possible in a moist tropical atmosphere. Our own algorithms and the Wentz algorithm exhibit no such bias; however, the latter algorithm appears to exhibit somewhat higher "background" noise (i.e., rms deviations from zero in the cloud free data set), as compared with our own 85.5 GHz liquid water algorithm.

SPN SSM/I ALGORITHM SYMPOSIUM
Algorithm Questionnaire

"CLOUD LIQUID WATER
Grant Petty, respondent

Please provide the following essential information about your algorithm(s).

* ALGORITHM DESCRIPTION

- Type (statistical, physical, other)

Statistical component predicts clear-sky polarization difference; physical component estimates cloud water from polarization reduction

- Input required / Output produced

Input: SSM/I Brightness Temperatures; water vapor and wind speed from Petty algorithms
Output: column cloud water in non-precipitating clouds over ocean

- Auxiliary sensor/data base requirements

Depending on accuracy requirements: sea surface temperature from climatology or other estimate of cloud temperature

- Major limitations / approximations

No cloud water algorithm will give reliable results in precipitation. However, the normalized polarization, P_{37}, generated as an intermediate product in LW_{37} algorithm gives an excellent qualitative discrimination between rain/no rain over water. This requires special handling of wind speed estimates used as input to the algorithm, since this estimate will usually be contaminated - can either cap value or interpolate spatially from uncontaminated areas.

- Computer resource requirements

Modest, apart from possible need for sea surface temperature look-up table or some other means to provide independent estimates of cloud temperature.

* ALGORITHM PERFORMANCE

- Development / test data sets (regional / global / seasonal) *Global algorithm*

* ALGORITHM PERFORMANCE (continued)

- Ground truth (accuracy / limitations)

Limited ground truth available for CLW in clouds - San Nicolas Island radiometer gives partial verification. Large data base of cloud free SSM/I pixels validates estimates of zero cloud water.

- Major assumptions of evaluation

Algorithm should return zero value of cloud water in cloud free areas. Theory should provide reliable basis for calibration in clouds.

- Strengths / weaknesses

Low base noise level; good background compensation; insignificant water vapor crosstalk.

* ALGORITHM MATURITY

- Operational useage

Used in research mode in at least two university labs; may be in use elsewhere as well but not feedback to date

- Refinement / additional development

Minor refinement of coefficients possible, though practical impact will be small.

- Availability

Algorithm is available upon request.

Petty 37 GHz Liquid Water Algorithm

Normalized 37 GHz polarization is computed as

$$P_{37} = \frac{T_{37V} - T_{37H}}{78.76 - 0.9901U - 0.3347V}, \tag{4}$$

where U and V are determined from wind speed and water vapor algorithms given on previous page. (Note: Eq. 4 is preliminary and may be modified slightly prior to final publication.)

The 37 GHz-derived liquid water [kg m^{-2}] is then

$$LW_{37} = \left(\frac{-\cos\theta}{\alpha\kappa_e}\right)\ln(P_{37}), \tag{5}$$

where θ is the SSM/I viewing angle (nominally 53.1°),

$$\alpha = 2.185, \tag{6}$$

$$\kappa_e = \exp(-1.35 - 0.0234T_C - 1.22\times10^{-4}T_C^2 + 5.48\times10^{-6}T_C^3), \tag{7}$$

and T_C is estimated cloud temperature in degrees Celsius. If T_C cannot be specified based on independent information, then can estimate "reasonable" T_C using

$$T_C = \frac{T_S}{2}, \tag{8}$$

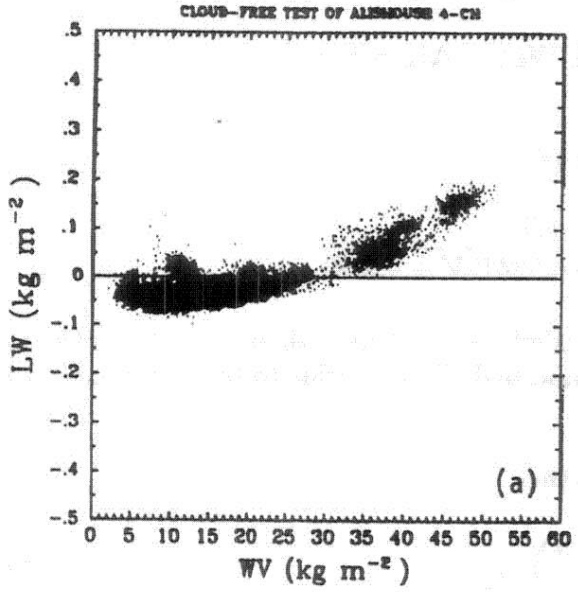
where T_S is sea surface temperature in degrees Celsius.

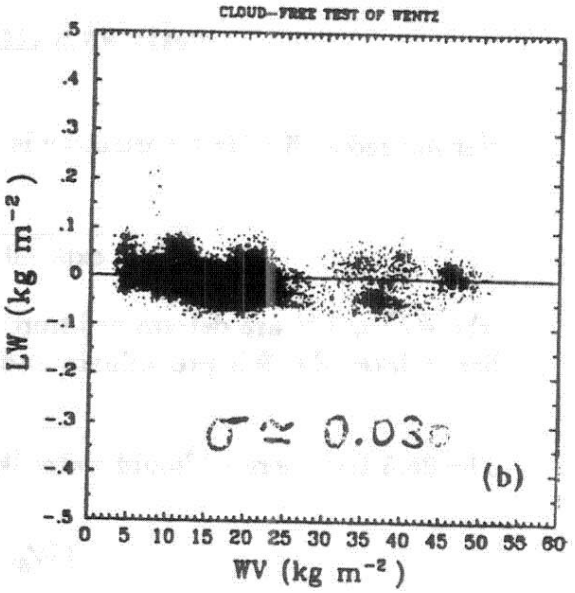
This algorithm is the preferred liquid water algorithm for use wherever there is very high water vapor content (e.g., in the tropics), dense, spatially inhomogeneous clouds, and/or possible light precipitation. Quantitative values probably unreliable when more than very light rain is present.

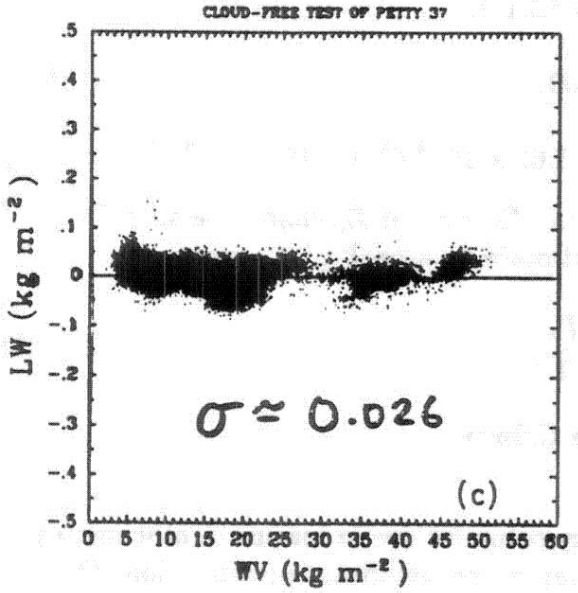
LIQUID WATER ALGORITHM EVALUATION CRITERIA

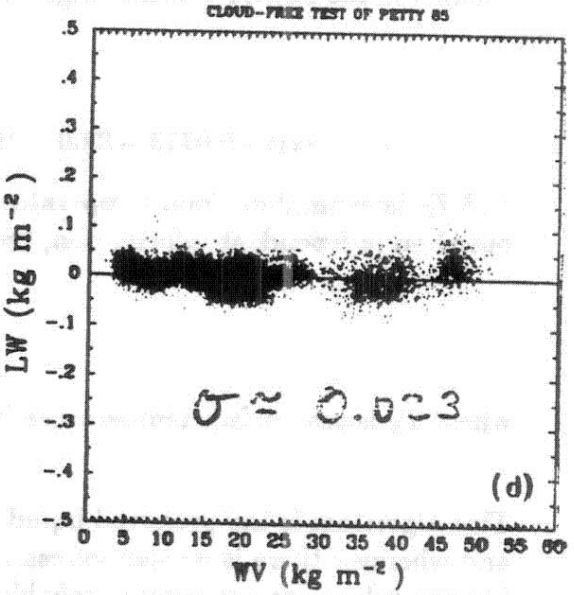
- Ability to correctly retrieve "zero" in the absence of clouds
- Correct magnitudes in the presence of clouds
- Cross-talk, noise, linearity, etc.

cal/Val


CLOUD-FREE TEST OF ALISHOUSE 4-CH
LW (kg m^{-2})
WV (kg m^{-2})
(a)


CLOUD-FREE TEST OF WENTZ
LW (kg m^{-2})
WV (kg m^{-2})
σ ≃ 0.03
(b)


CLOUD-FREE TEST OF PETTY 37
LW (kg m^{-2})
WV (kg m^{-2})
σ ≃ 0.026
(c)


CLOUD-FREE TEST OF PETTY 85
LW (kg m^{-2})
WV (kg m^{-2})
σ ≃ 0.023
(d)

Petty 85.5 GHz Liquid Water Algorithm

Normalized 85.5 GHz polarization is computed as

$$P_{85} = \frac{T_{85V} - T_{85H}}{\exp(-0.02167U - 0.02412V + 4.379)}, \tag{9}$$

where U and V are determined from wind speed and water vapor algorithms given earlier. (Note: Eq. 9 is preliminary and may be modified slightly prior to final publication.)

The 85.5 GHz-derived liquid water [kg m^{-2}] is then

$$LW_{85} = \left(\frac{-\cos\theta}{\alpha\kappa_e}\right)\ln(P_{85}), \tag{10}$$

where θ is the SSM/I viewing angle (nominally 53.1°),

$$\alpha = 2.09, \tag{11}$$

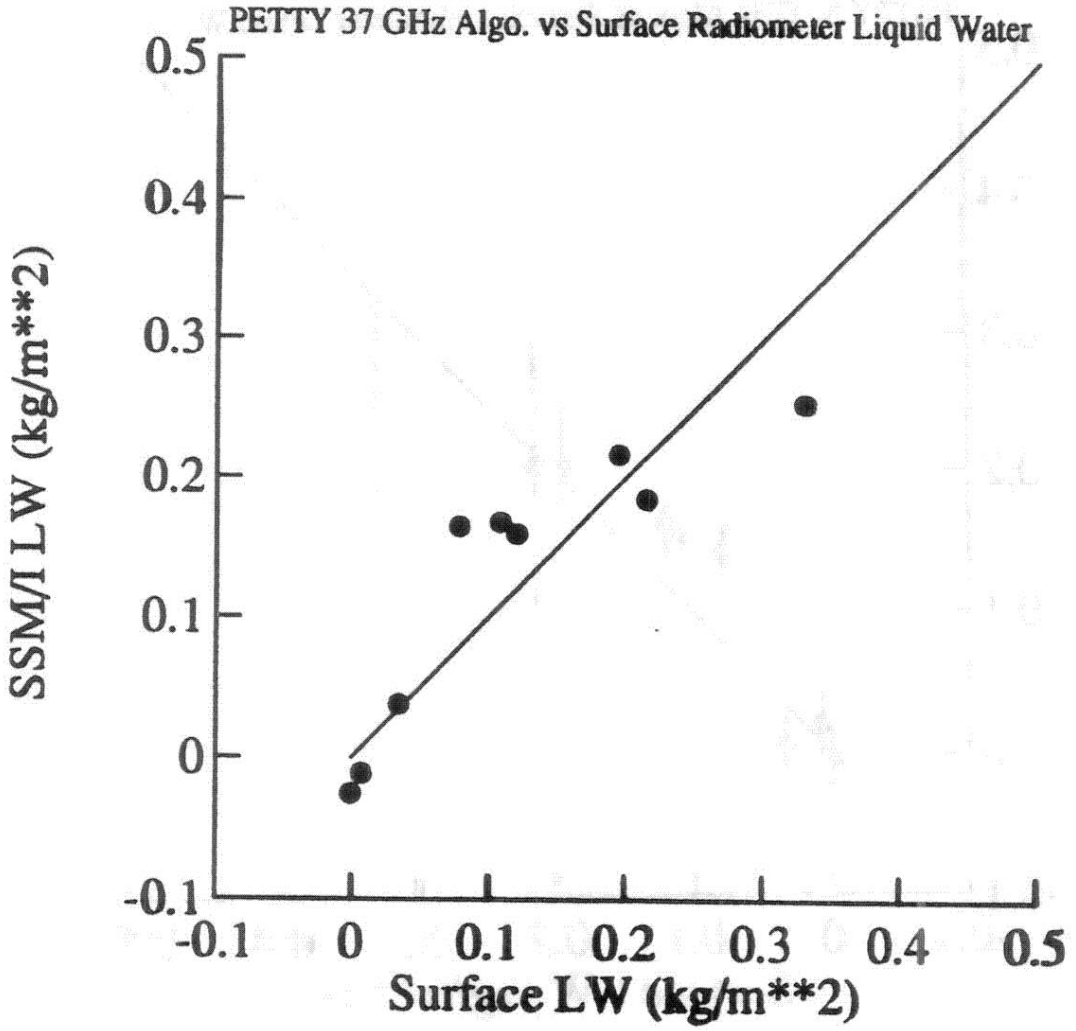
$$\kappa_e = \exp(-0.0713 - 8.00\times10^{-3}T_C - 1.62\times10^{-4}T_C^2 + 1.18\times10^{-6}T_C^3), \tag{12}$$

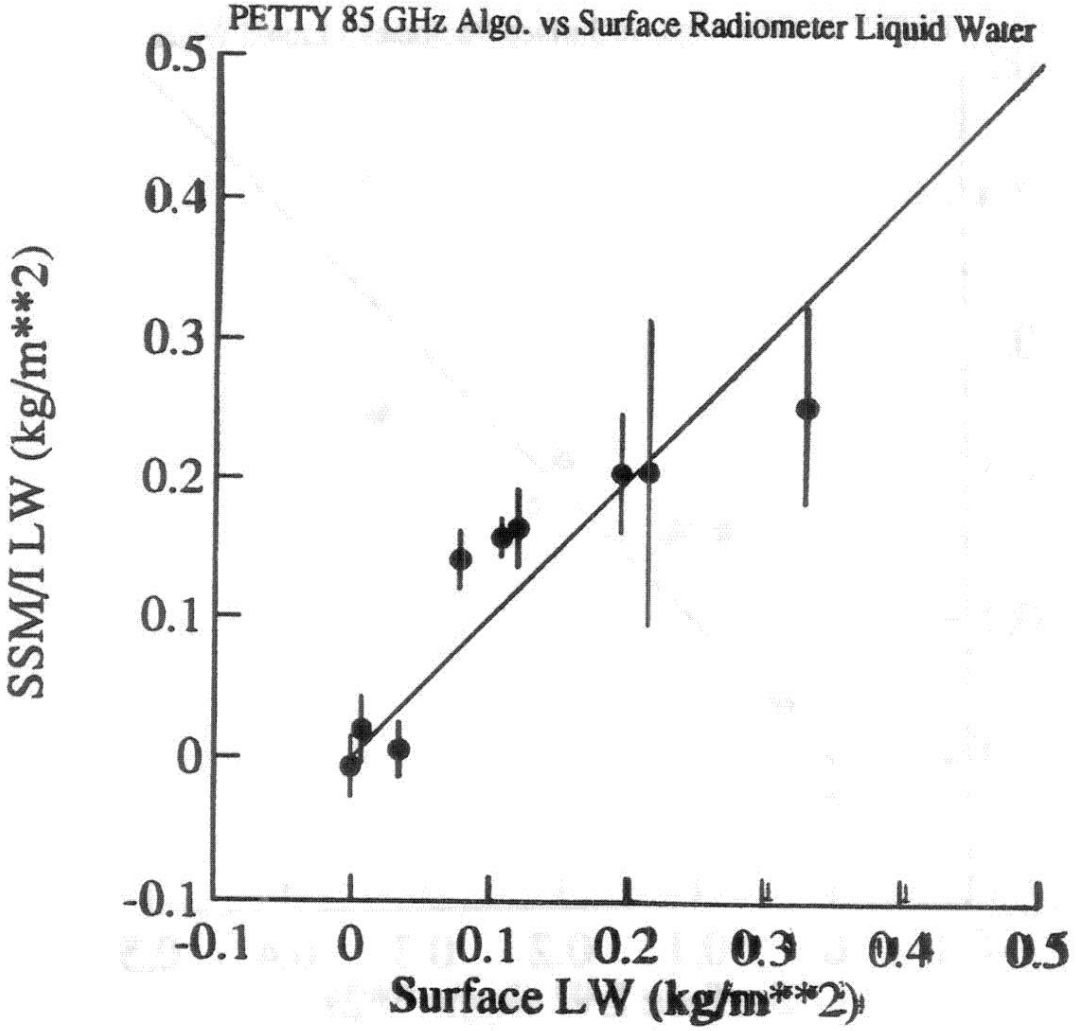
and T_C is estimated cloud temperature in degrees Celsius. If T_C cannot be specified based on independent information, then can estimate "reasonable" T_C using

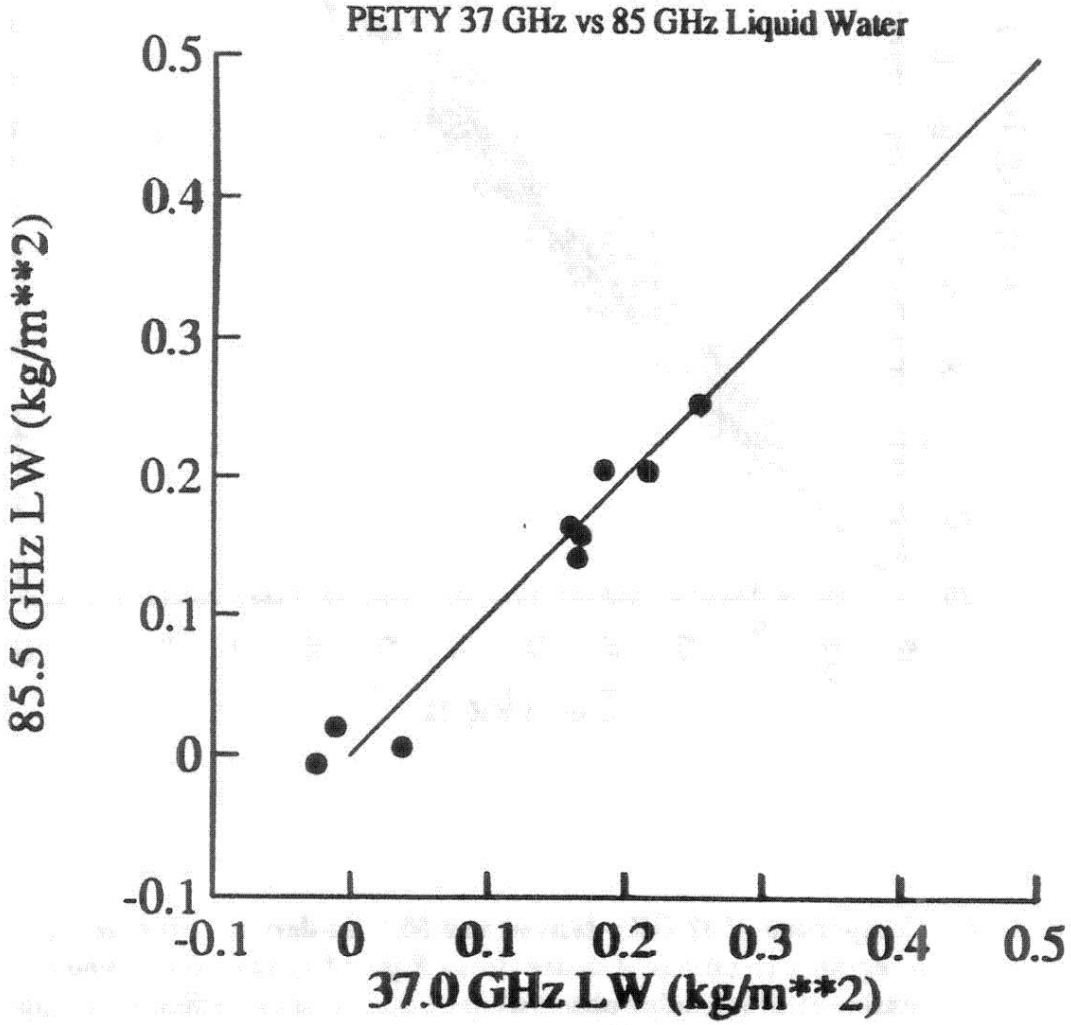
$$T_C = \frac{T_S}{2}, \tag{13}$$

where T_S is sea surface temperature in degrees Celsius.

This algorithm is the preferred liquid water algorithm for use in marine stratocumulus and wherever there is neither excessive water vapor nor significant precipitation. Quantitative values are probably unreliable when dense convective clouds are present, or when more than drizzle-intensity precipitation is present. In moist tropical atmospheres, estimates will be noisier than those retrieved using the 37 GHz channels.


PETTY 37 GHz Algo. vs Surface Radiometer Liquid Water
SSM/I LW (kg/m**2)
0.5
0.4
0.3
0.2
0.1
0
-0.1
-0.1
0
0.1
0.2
0.3
0.4
0.5
Surface LW (kg/m**2)


PETTY 85 GHz Algo. vs Surface Radiometer Liquid Water
SSM/I LW (kg/m**2)
0.5
0.4
0.3
0.2
0.1
0
-0.1
-0.1
0
0.1
0.2
0.3
0.4
0.5
Surface LW (kg/m**2)


PETTY 37 GHz vs 85 GHz Liquid Water
85.5 GHz LW (kg/m**2)
37.0 GHz LW (kg/m**2)
0.5
0.4
0.3
0.2
0.1
0
-0.1
-0.1
0
0.1
0.2
0.3
0.4
0.5

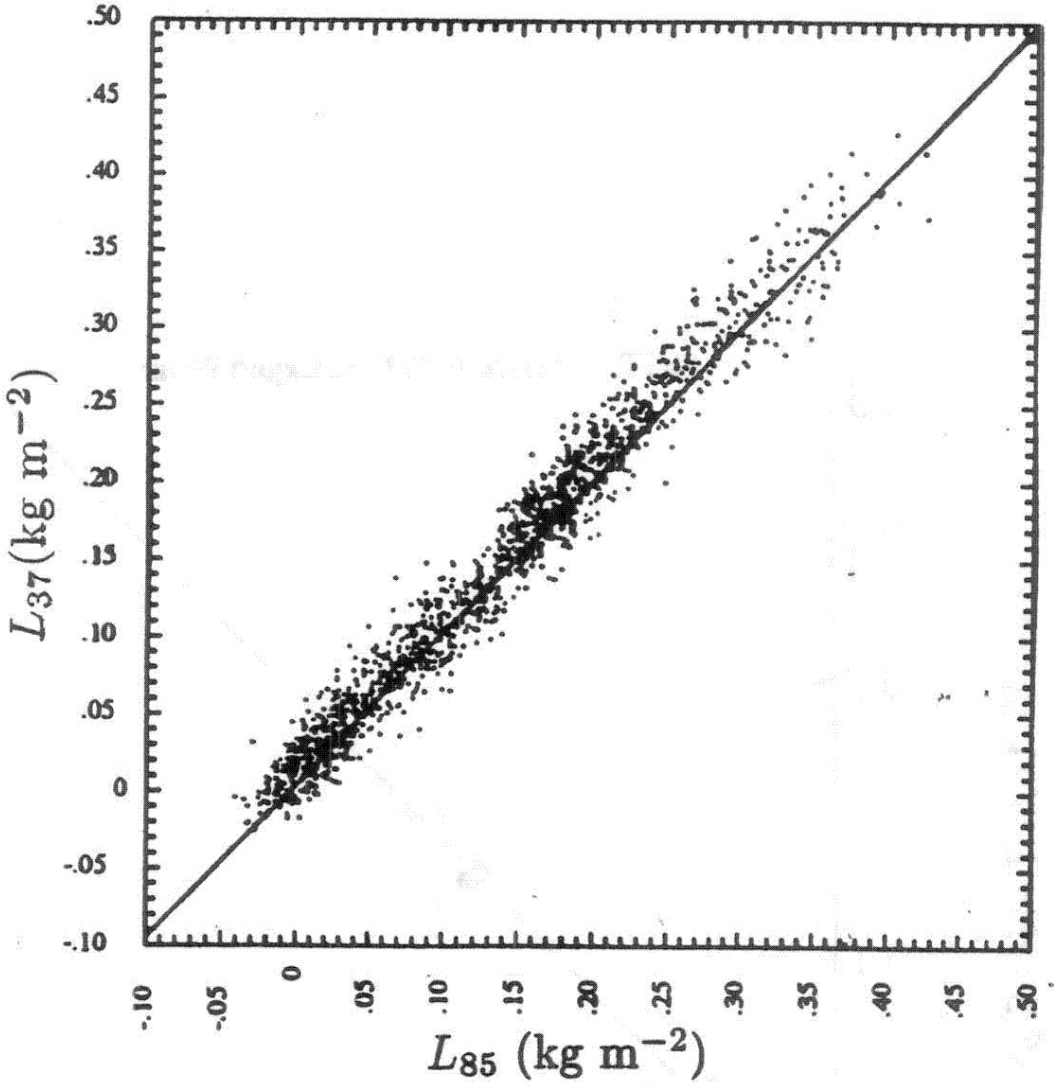


Fig. 12.2 **Comparison of 37 GHz-derived and 85 GHz-derived estimates of integrated cloud liquid water (from Eqs. 12.7, 12.8) for a region of marine stratocumulus observed near the coast of California during three successive SSM/I passes.**

From Petty (1990)

PRELIMINARY CONCLUSIONS
(pending availability of independent validation data)

- New water vapor algorithm exhibits improved linearity, crosstalk and noise sensitivity vs. Cal/Val algorithm; significantly improved rms errors vs. Wentz algorithm

- New liquid water algorithms exhibit much less water vapor crosstalk than Cal/Val algorithm and reduced background noise level relative to Wentz algorithm

- Independent 37 GHz and 85 GHz estimates of liquid water consistent with one another; some unexplained disagreement with surface based liquid water

Interannual Variation of Cloud Liquid Water Content Derived from SSM/I Observations

Ute Hargens, Clemens Simmer, and Eberhard Ruprecht

Institut für Meereskunde
an der Christian-Albrechts-Universität Kiel
Dürsternbrooker Weg 20, D-2300 Kiel 1, Germany

A method is developed to infer cloud liquid water path (LWP) over the ocean from passive microwave measurements of SSM/I. The algorithm is based on simulated satellite observations. They are calculated with a radiative transfer model applied to about 3000 radiosonde ascents over the Atlantic Ocean. Since radiosonde observations do not contain direct information about cloud water and ice, these parameters are parameterized based on relative humidity and temperature.

A multiple linear regression is applied to the simulated radiances and the calculated LWP to derive the algorithm. The estimated retrieval accuracy is 0.03 kg/m^2 including instrumental noise. Validation of the LWP-algorithm was pursued through a comparison with measurements of a ground-based 33GHz microwave radiometer on board the R.V. Poseidon during the Internation Cirrus Experiment 1989 in the North Sea. The liquid water path values agree within the range of uncertainty caused by the different sampling characteristics of the observing systems. The algorithm is applied to SSM/I observations over the Atlantic Ocean. Mean monthly distribution of LWP is calculated for many months and for different years. The striking feature is the very large interannual variability in almost all regions of the Atlantic Ocean.

Such variability demonstrates that a comparison between actual monthly values and results from climate models should be carried out with caution. There are, however, differences between our results and those of the climate model ECHAM-T42 of the Max-Planck-Institut, Hamburg, which are too large to be explained by the interannual variability.

SPN SSM/I ALGORITHM SYMPOSIUM
Algorithm Questionnaire

"CLOUD LIQUID WATER
Clemens Simmer, respondent

Please provide the following essential information about your algorithm(s).

* ALGORITHM DESCRIPTION

- Type (statistical, physical, other) *Statistical*

- Input required / Output produced

  Input: SSM/I Brightness Temperatures (from Wentz tapes)
  Output: Cloud liquid water path in kg / m^2

- Auxiliary sensor/data base requirements *None*

- Major limitations / approximations

  Reliable up to 0.5 kg / m^2 ; set higher LWP values (derived) to 0.5

- Computer resource requirements [none mentioned]

* ALGORITHM PERFORMANCE

- Development / test data sets (regional / global / seasonal)

3000 radiosondes over the Atlantic Ocean, only ship observations (no island stations); 70 radiosondes over the North Sea for model calibration; three weeks (Sept - Oct 89) of Meteosat data over the North Sea to identify cloud free areas to test the LWP = 0 limit

- Ground truth (accuracy / limitations)

  None available for LWP

- Major assumptions of evaluation

- Strengths / weaknesses

  *The algorithm is **global**, but unreliable above 0.5 kg / m^2*

* ALGORITHM MATURITY

- Operational useage

Producing monthly mean maps within a project of the German Ministry of Science and Technology to relate cloud optical depth to cloud liquid water content.

- Refinement / additional development

(In work) Include stratiform cloud types, partial cloud cover and three-dimensional effects in profiles

- Availability

Interannual Variation of Cloud Liquid Water Content

Derived from SSM/I Observations

Ute Karstens, Clemens Simmer, and Eberhard Ruprecht

Institut für Meereskunde
an der Christian-Albrechts-Universität Kiel
Düsternbrooker Weg 20, D-2300 Kiel 1, Germany

1. Algorithm Development
   - general procedure
   - radiative transfer model
   - cloud water analysis
   - regression analysis
2. Algorithm Verification
   - model calibration
   - comparison with ground-based measurements
   - detection of cloud-free areas
3. Results
   - monthly means for October 1987-91
   - mean and variability October 1987-91
4. Discussion and Conclusion
   - applications (climate model)
   - improvements

Algorithm-Development

SYNOPS
V_o, SST

Radiosonde Ascents
p(z), T(z), RH(z)

Cloud Analysis
LWC

Radiative Transfer Simulations

vertical Integration

simulated
Brightness Temperatures
$T_{Bs}(\nu,\theta,z)$

Cloud Water Path
LWP

Multiple Linear Regression Analysis

measured
Brightness Temperatures
$T_B(\nu,\theta,z)$

Corrections due to
Differences between
Model and Satellite

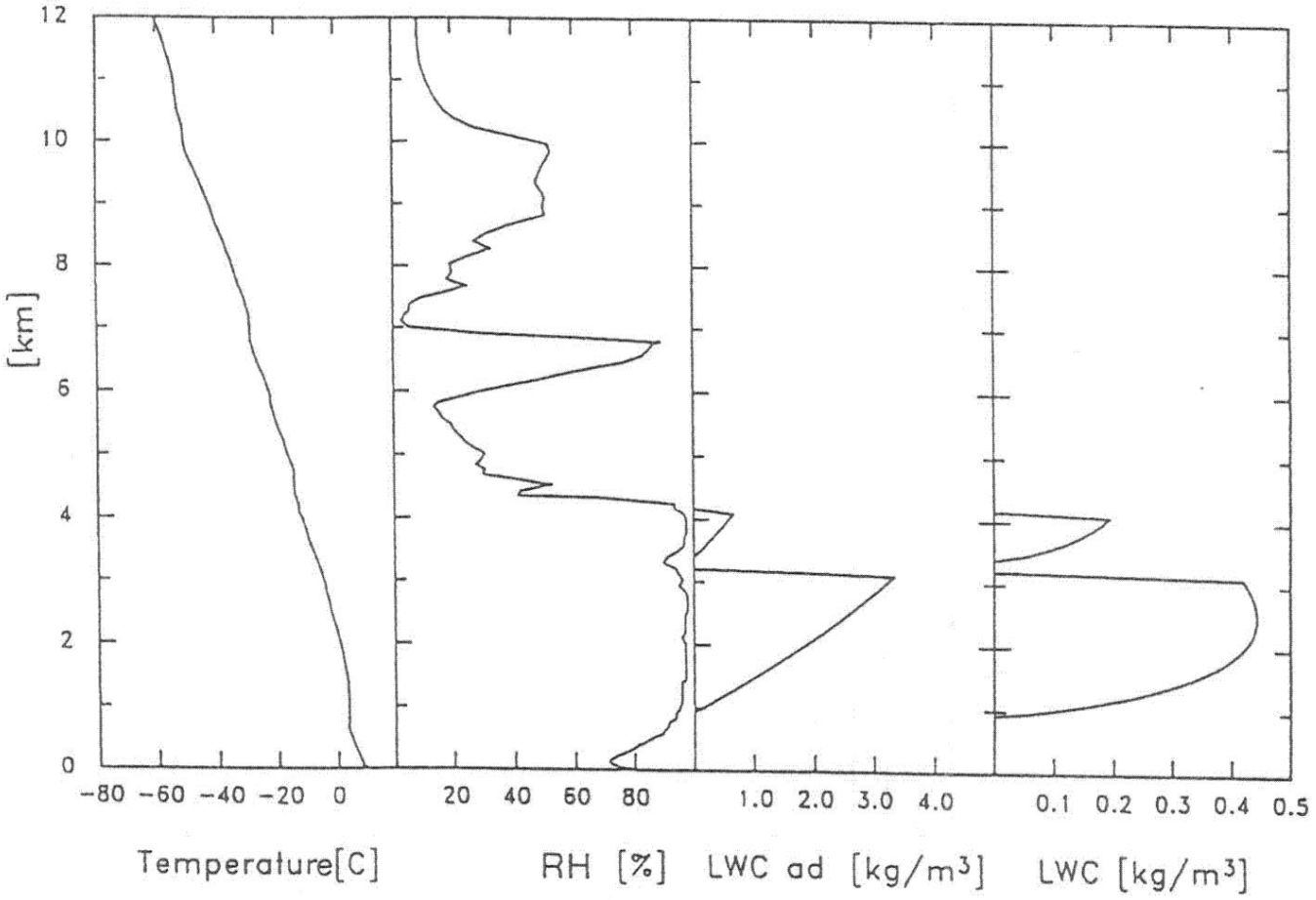
Algorithm

retrieved
Cloud Liquid Water Path
LWP

Radiosonde Ascent over the North Sea

October 11, 1989, 1800 UT

- cloud water analysis -

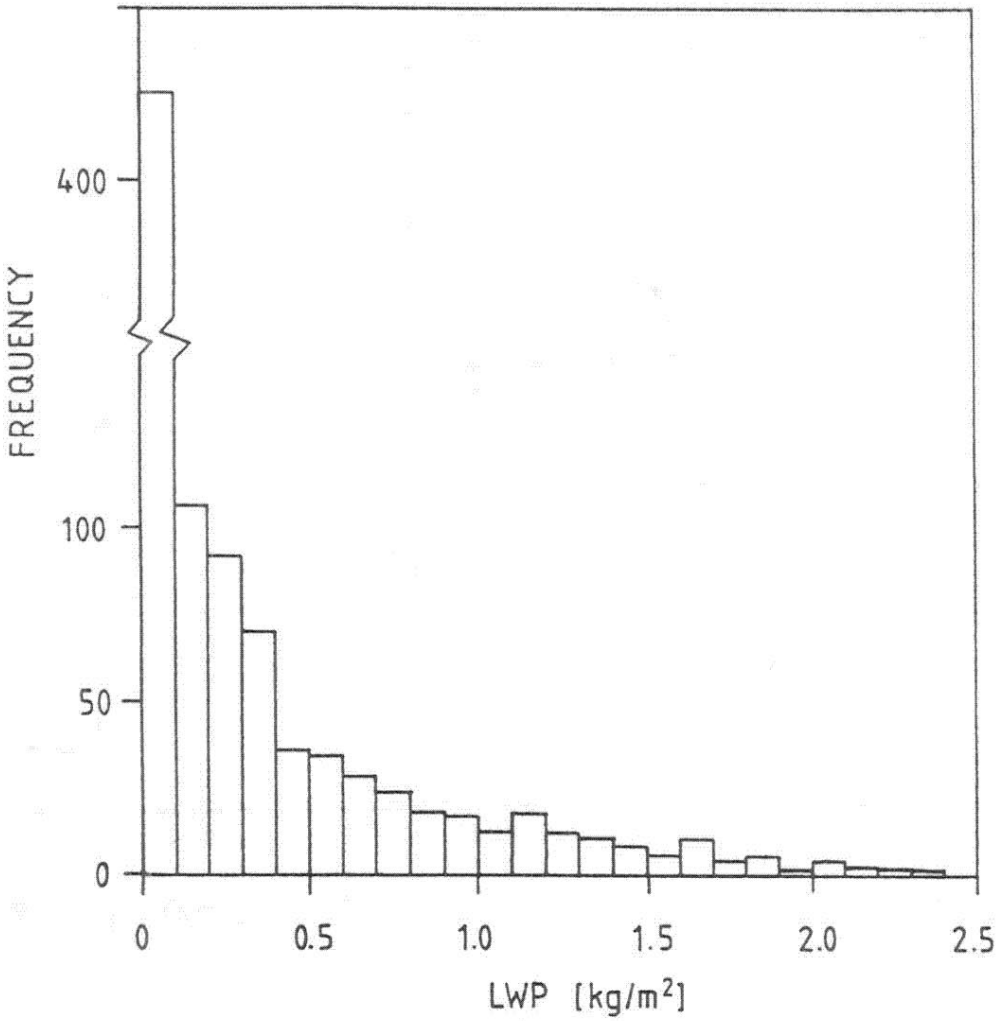


$$LWC_{ad} = \int_{z_o}^{h} \varrho(z) \frac{c_p}{L} (\Gamma_d - \Gamma_s) dz$$

$$LWC = LWC_{ad} \cdot (1.239 - 0.145 \ln(h - z_o))$$

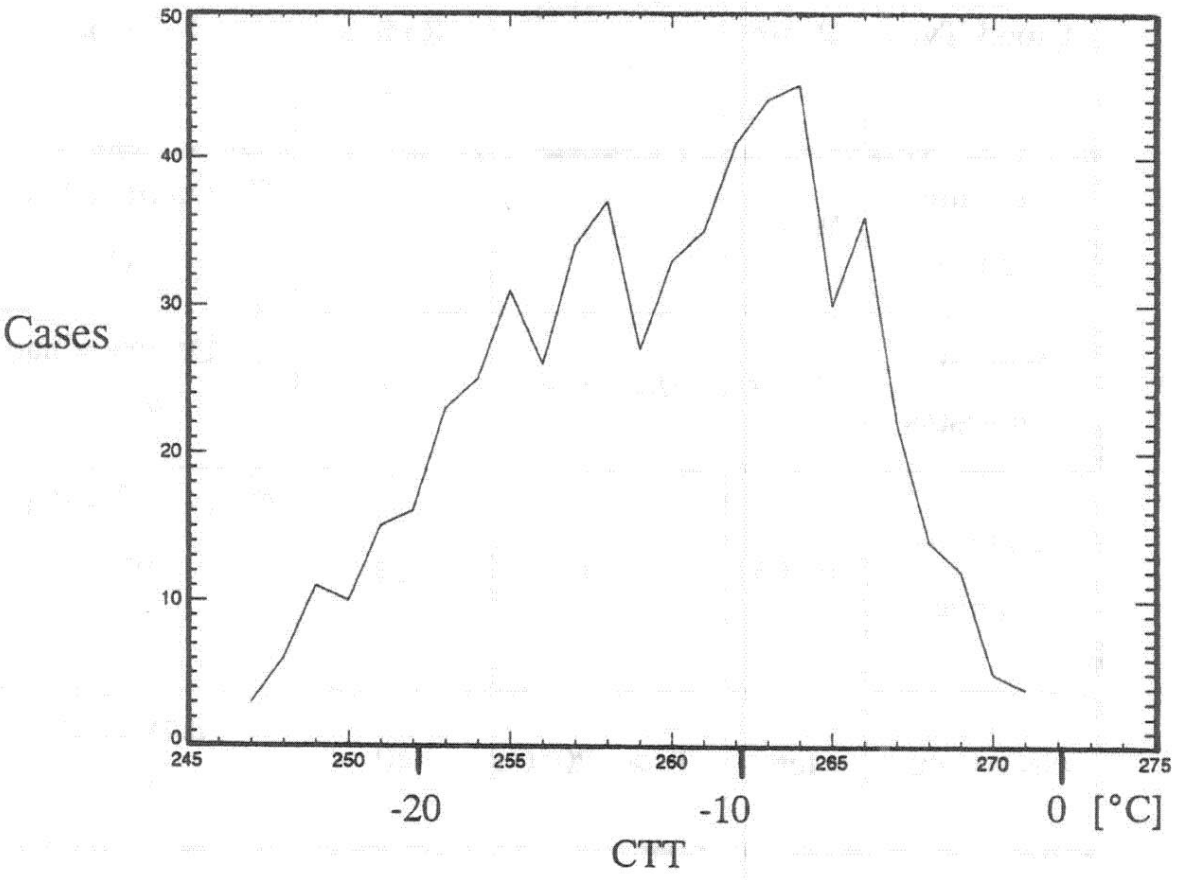
adiabatic liquid water path	LWP_{ad}	= 4.35 kg/m^2
modified adiabatic LWP	LWP	= 0.91 kg/m^2

Frequency Distribution
of
Modified Adiabatic Liquid Water Path



~ 2000 Radiosonde Ascents over the
North Atlantic Ocean
during
First GARP Global Experiment (FGGE)
March - October 1979

Frequency Distribution of
Analyzed Water-Cloud Top-Temperatures (CTT)
from Radiosonds Ascents

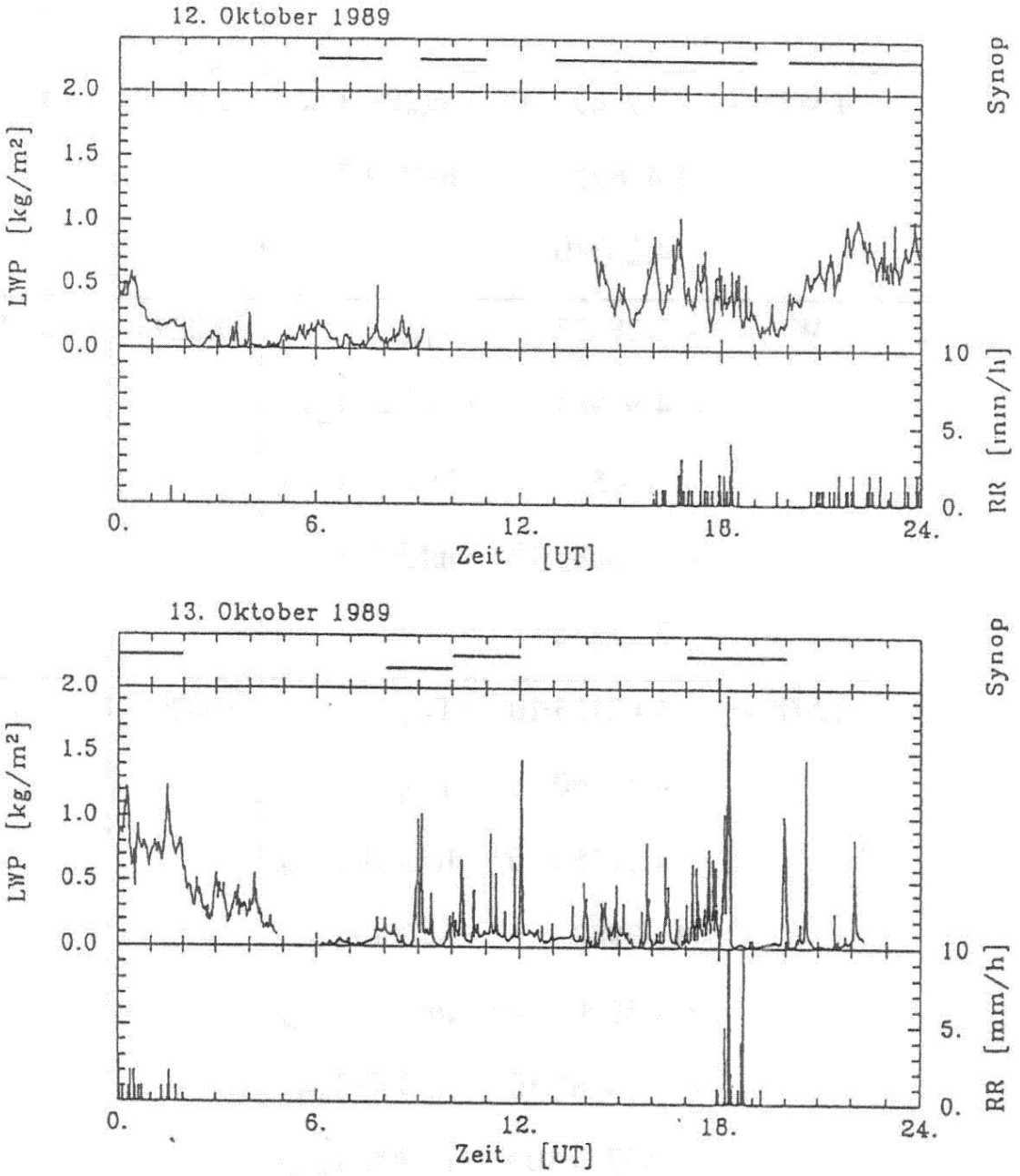


~ 2000 Radiosonde Ascents over the
North Atlantic Ocean during
First GARP Global Experiment (FGGE)
March - October 1979

Cloud Drop Spectra for Radiative Transfer Simulations

Cloud Type	Phase	LWC-Range g/m^3	Mode Radius μm	Reference
cumulus humilis	Water	< 0.2	4	C1 Deirmendjian, 1969
cumulus congestus	Water	0.2 - 0.4	6	C5 Deirmendjian, 1975
cumulo-nimbus	Water	> 0.4	20	C6 Deirmendjian, 1975
cirrostratus	Ice	T > -20°C	40	Ulaby et al., 1981

Cloud Liquid Water Path from Ground-Based Microwave Radiometry and Rainfall Events during ICE'89



——— Rain fall according to synoptic observations

LWP-Algorithms

	LWP [kg/m^2]	RMS [kg/m^2]	BIAS [kg/m^2] (LWP=0)
1	$LWP = +3.99635\cdot10^{-1}\cdot\ln(289-T_{22V}) - 1.40692\cdot\ln(280-T_{37V}) + 4.29930$	0.0287	-0.004
2	$LWP = +2.28522\cdot T_{19V} + 4.92984\cdot10^{-1}\cdot\ln(280-T_{22V}) - 1.85055\cdot\ln(280-T_{37V}) + 4.33686\cdot10^{-1}\cdot\ln(280-T_{37H}) + 3.23216$	0.0296	-0.010
3	$LWP = +1.02133\cdot10^{-3}\cdot T_{19V} + 4.69790\cdot10^{-5}\cdot T_{19H} + 4.32159\cdot10^{-1}\cdot\ln(280-T_{22V}) - 1.73982\cdot\ln(280-T_{37V}) + 4.50602\cdot10^{-1}\cdot\ln(280-T_{37H}) + 1.34987\cdot10^{-1}\cdot\ln(300-T_{85V}) - 1.50254\cdot10^{-1}\cdot\ln(300-T_{85H}) + 3.31623$	0.0296	-0.019

Mean Differences between SSM/I-Measurements and Radiative Transfer Simulations

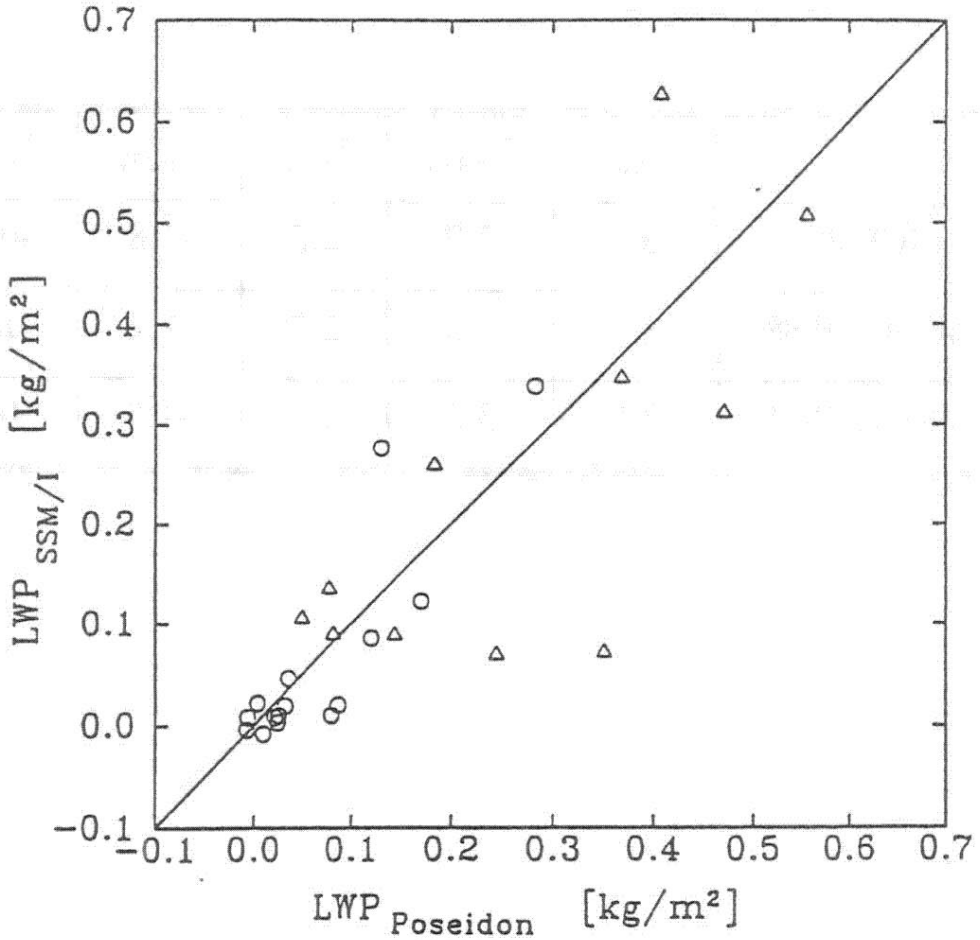
	$T_{B,19V}$	$T_{B,19H}$	$T_{B,22V}$	$T_{B,37V}$	$T_{B,37H}$
ICE'89	3.3	2.7	2.3	-1.8	-0.9
Wentz, 1988	2.0	2.3	2.7	-1.2	0.7
Wentz, 1991	2.0	3.5	1.3	-1.6	-0.2

Cloud Liquid Water Path derived from

Satellite ($LWP_{SSM/I}$)

and from

Ground-Based Microwave Radiometry ($LWP_{Poseidon}$)



International Cirrus Experiment (ICE)

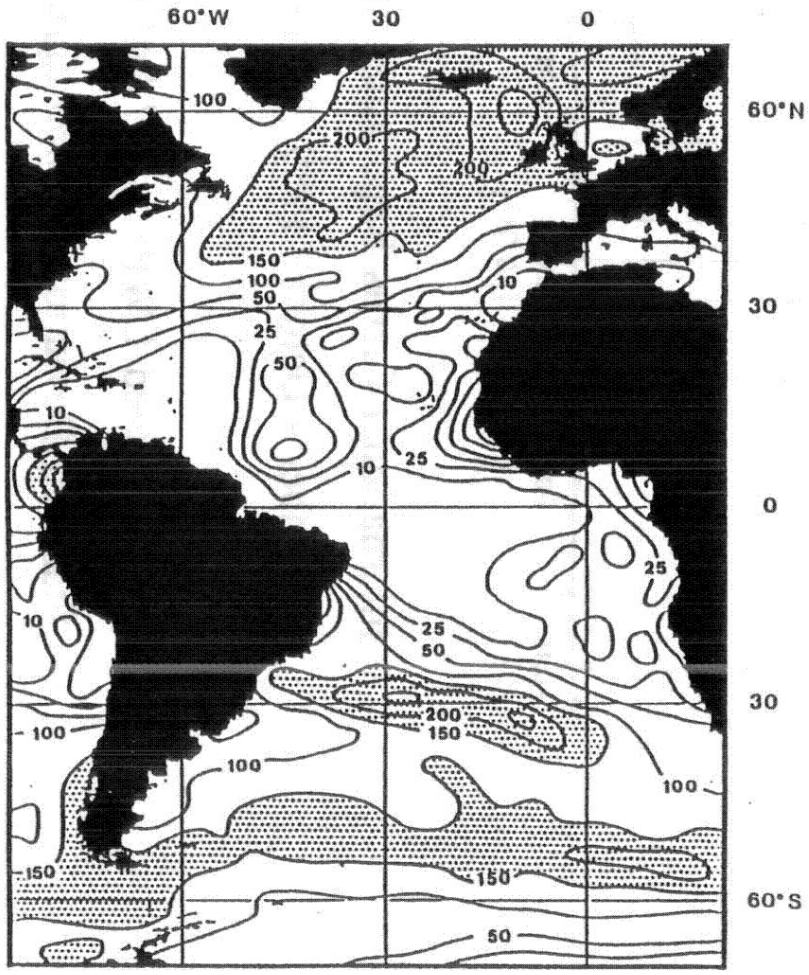
September-October 1989 (North Sea)

○ homogeneous clouds: RMS = 0.048 kg/m² BIAS = 0.003 kg/m²

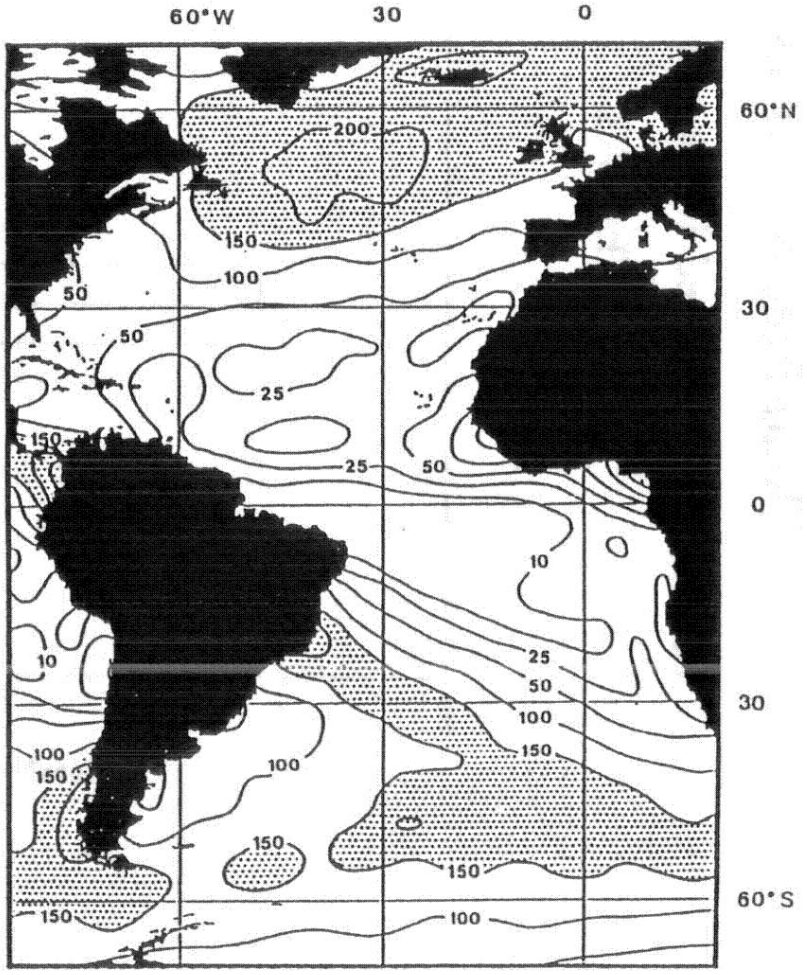
△ scattered clouds: RMS = 0.126 kg/m² BIAS = 0.028 kg/m²

Climate Model ECHAM-T42 (LWP in g/m^2)

10 years run with prescribed SST and ice-cover from 1979 - 1988



October 1987

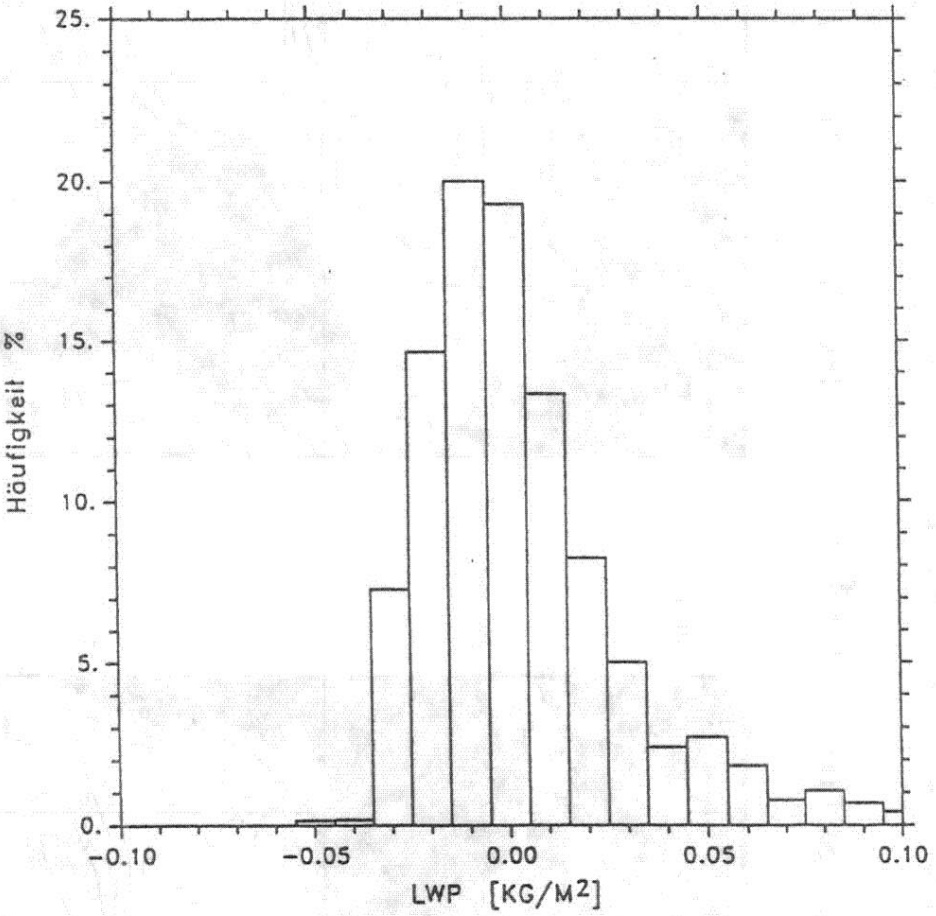


10-year mean October

Cloud-Free Situations

detected by co-located IR-measurements

from METEOSAT



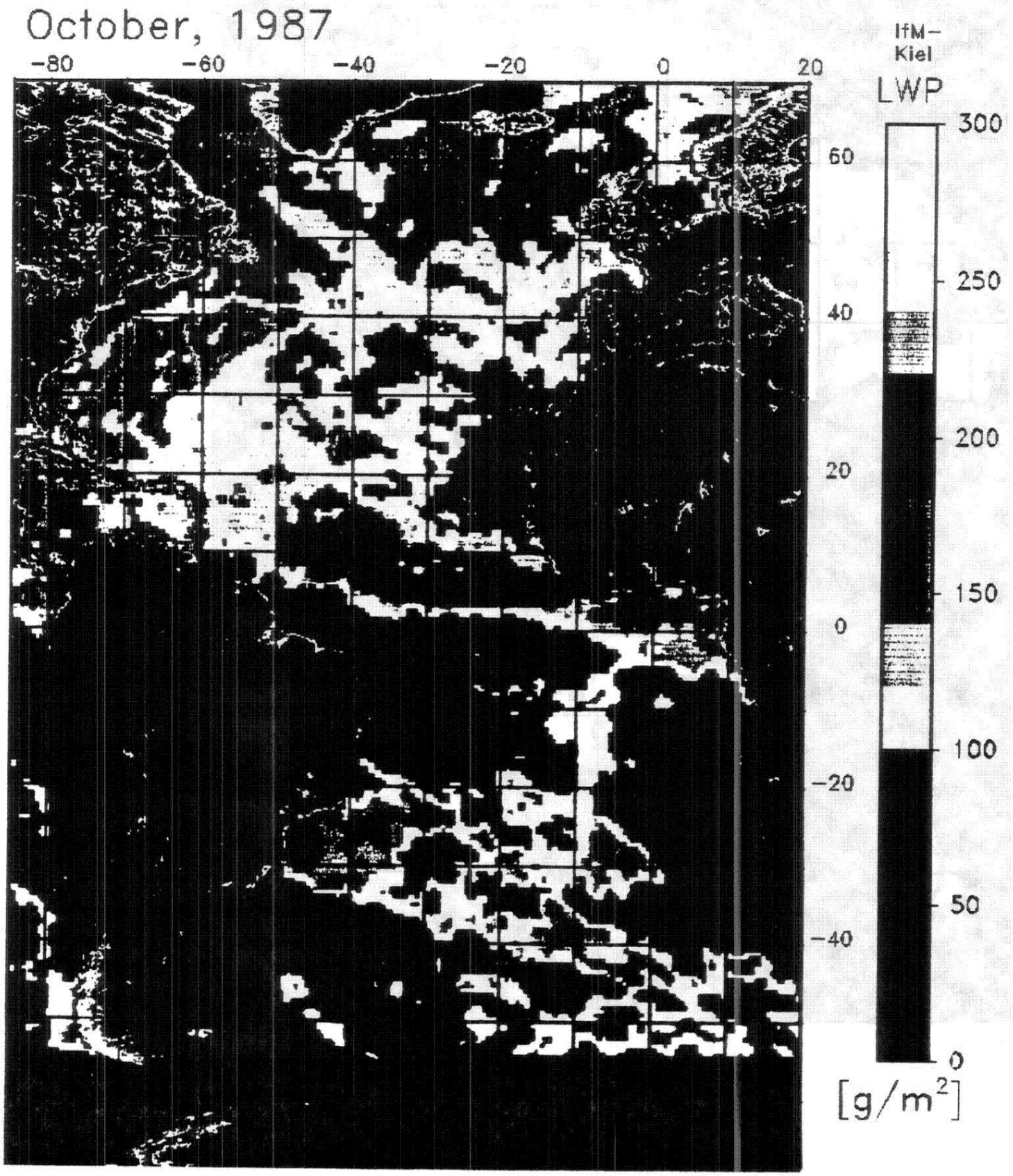
International Cirrus Experiment (ICE)

September - October 1989 (North Sea)

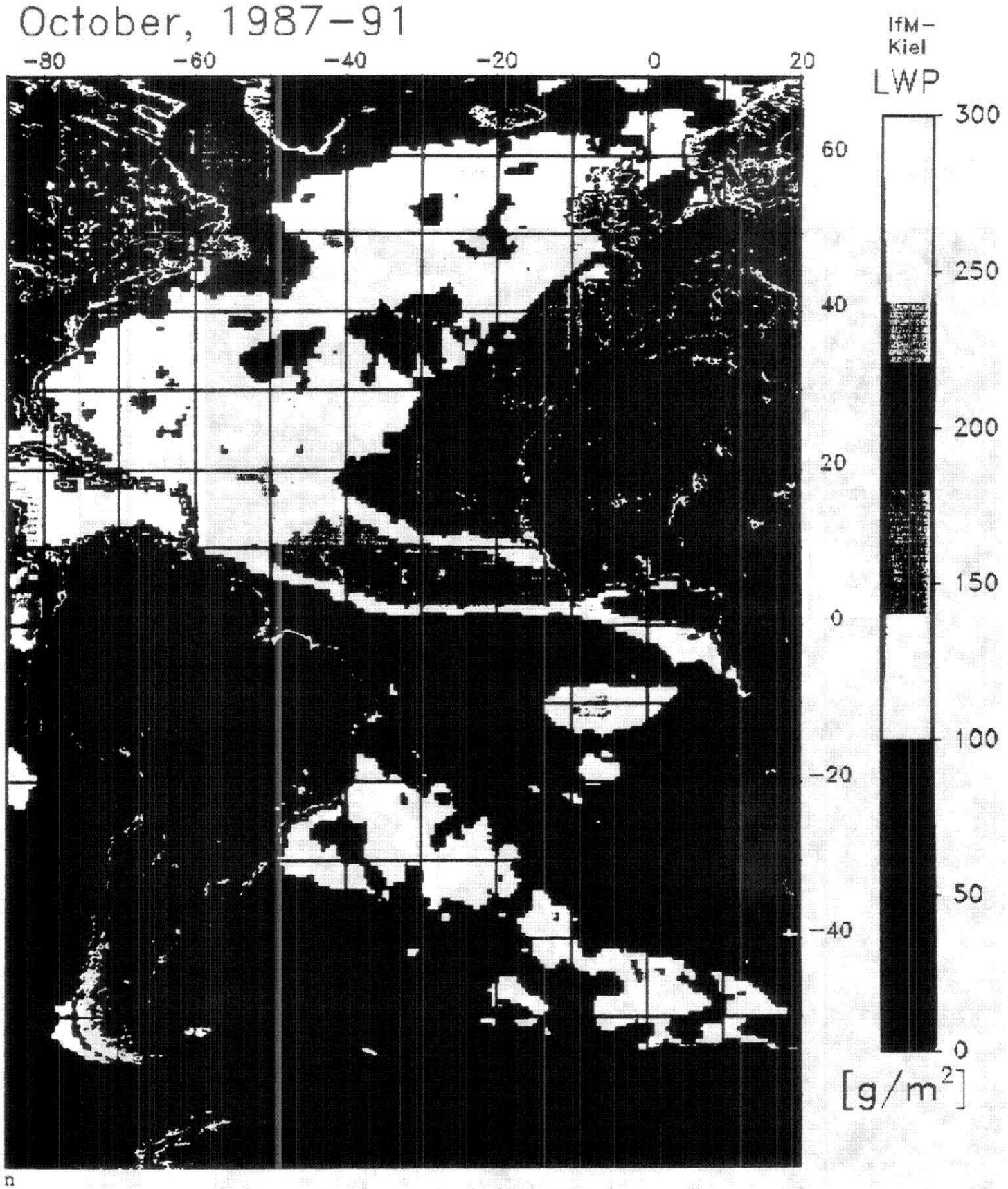
Mean derived LWP: 0.007 kg/m^2

Standard Deviation: 0.035 kg/m^2

[SIMMER]


October, 1987
-80
-60
-40
-20
0
20
60
40
20
0
-20
-40
IfM-
Kiel
LWP
300
250
200
150
100
50
0
[g/m²]

[SIMMER]


October, 1987–91
−80
−60
−40
−20
0
20
60
40
20
0
−20
−40
IfM–
Kiel
LWP
300
250
200
150
100
50
0
[g/m²]

n

Intercomparison of SSM/I Integrated Water Vapor Algorithms

Charles L. Norris
Scripps Institution of Oceanography
University of California, San Diego
San Diego, CA 92093-0224
(619) 530-0341
cnorris@ucsd.edu

Precipitable water (PW) measurements from the Special Sensor Microwave / Imager (SSM/I) are a source of information which is not readily available from other sources. The spatial and temporal sampling frequency of the SSM/I makes it ideal for gathering PW information over the global oceans where traditional measurements are impossible. Several PW algorithms based on the SSM/I exist in the published literature, but the question of the relative performance of the different algorithms has been unanswered. This investigation addresses this question by comparing several SSM/I PW algorithms with each other and with a large set of radiosonde soundings.

Three SSM/I PW algorithms from the current literature were tested; the algorithm by Alishouse et al (1990), the algorithm by Wentz (1986) and the algorithm by Schluessel and Emery (1990). Overall, the algorithms agreed well with one another and with radiosondes, but significant differences between the algorithms were observed which could potentially effect subsequent analyses. These differences are discussed in detail.

References
==========

Alishouse, J. C., S. A. Snyder, J. Vongsathorn and R. R. Ferraro, Determination of Oceanic Total Precipitable Water From the SSM/I, IEEE Transactions on Geoscience and Remote Sensing, 23, 811-816, 1990.

Wentz, F. J. New algorithms for microwave measurements of ocean winds: Applications to SEASAT and Special Sensor Microwave / Imager, J. Geophys. Res., 91, 2289-2307, 1986.

Schluessel, P., and W. J. Emery, Atmospheric water vapour over oceans from SSM/I measurements, Int. J. Remote Sensing, 11, 753-766, 1990.

Scripps Institution
of Oceanography

Comparison of SSM/I Precipitable Water With Radiosondes and Atmospheric Analyses

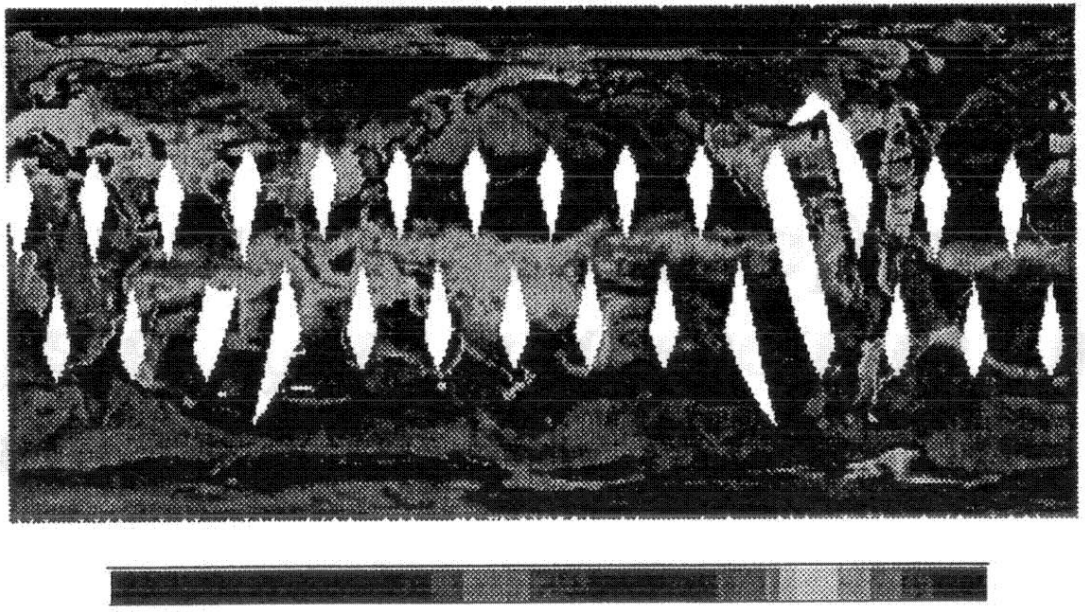
Chuck Norris

Scripps Institution of Oceanography

Scripps Institution
of Oceanography

SSM/I Global Coverage Pattern

February 1988, 22 GHz Brightness Temperature



100 200 300

Brightness Temperature (Kelvins)

Scripps Institution
of Oceanography

SSM/I PW Algorithms

- Three SSM/I PW algorithms were selected for evaluation.
- Wentz - iterative solution of a parameterized radiative transfer equation
- Alishouse et al - equation based on regression analyses with PW from radiosondes
- Schlüssel and Emery - equation based on regression analyses with PW from an atmospheric radiative transfer model

Scripps Institution
of Oceanography

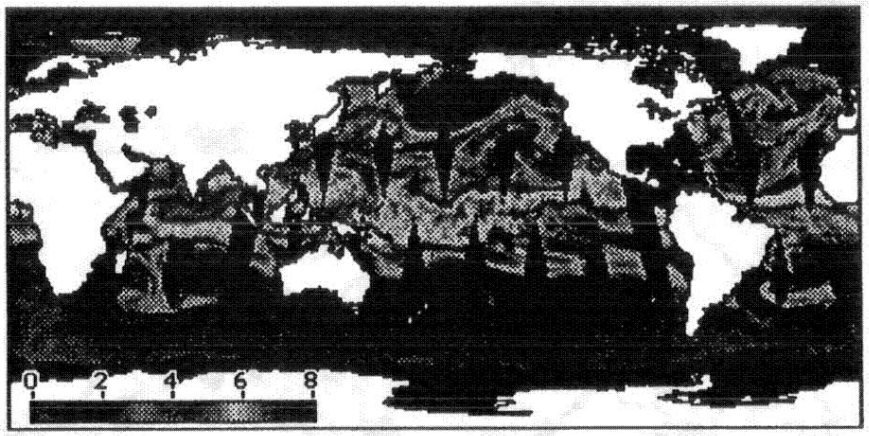
Algorithm Descriptions

- **Wentz**
  - $AX = B$
    - A is a 3x3 matrix of partial derivatives
    - X is a 3 element vector of unknowns (PW, LW, WIND)
    - B is a 3 element vector of the difference between the observed T_B and the values computed for the radiative transfer equation
    - Iterate until change in X is < 1%
- **Alishouse**
  - $PW = a_0 + a_1 T_{19V} + a_2 T_{22V} + a_3 T_{37V} + a_4 T^2_{22v}$
- **Schlüssel**
  - $PW = a_0 + a_1 \ln(280 - T_{22V}) + a2 (T_{37V} - T^{0.8}_{85V})$

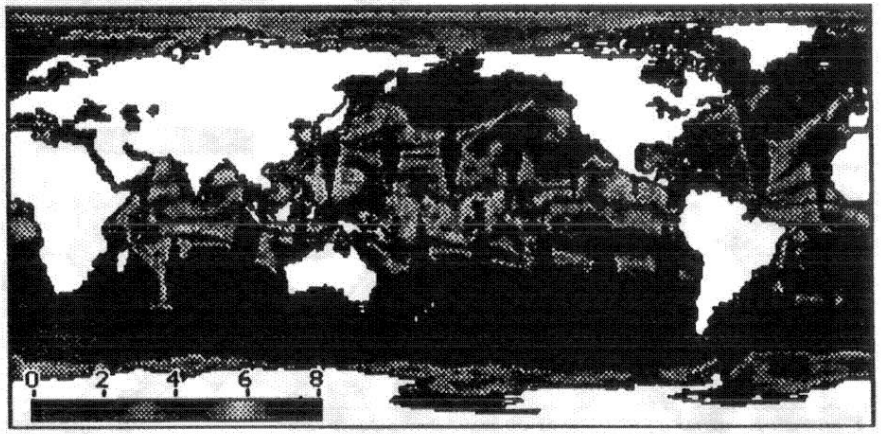
Scripps Institution
of Oceanography

Sample Day (July 14, 1987)

Wentz



Schlüssel



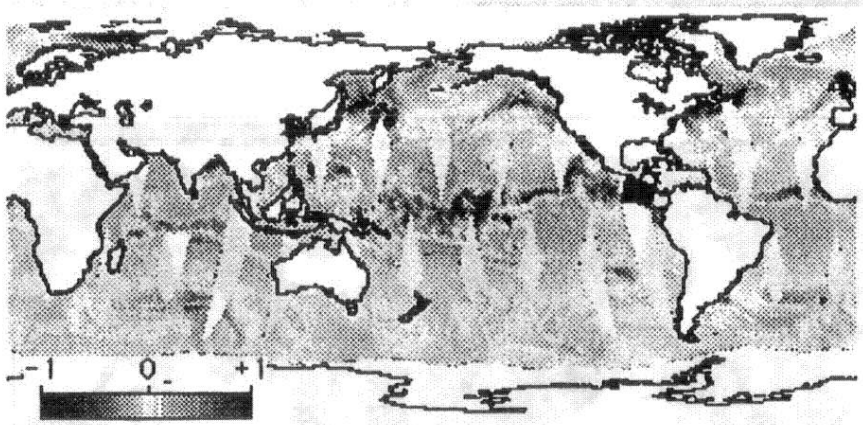
Alishouse



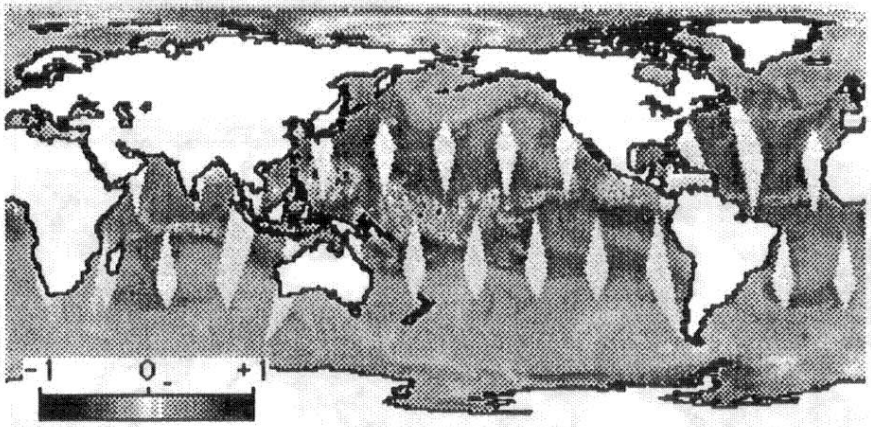
Scripps Institution
of Oceanography

Sample Day (July 14, 1987)

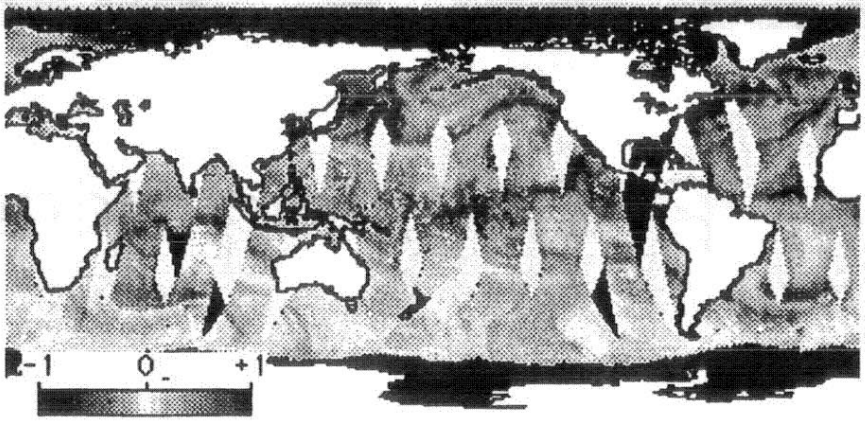
Alishouse - Wentz



Alishouse - Schlüssel



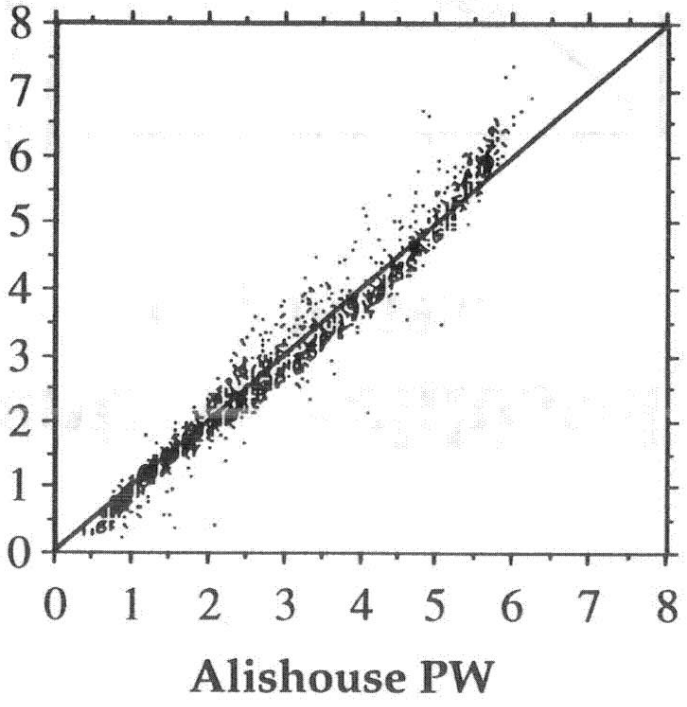
Wentz - Schlüssel



Scripps Institution
of Oceanography

Wentz vs Alishouse PW

July 10, 1987

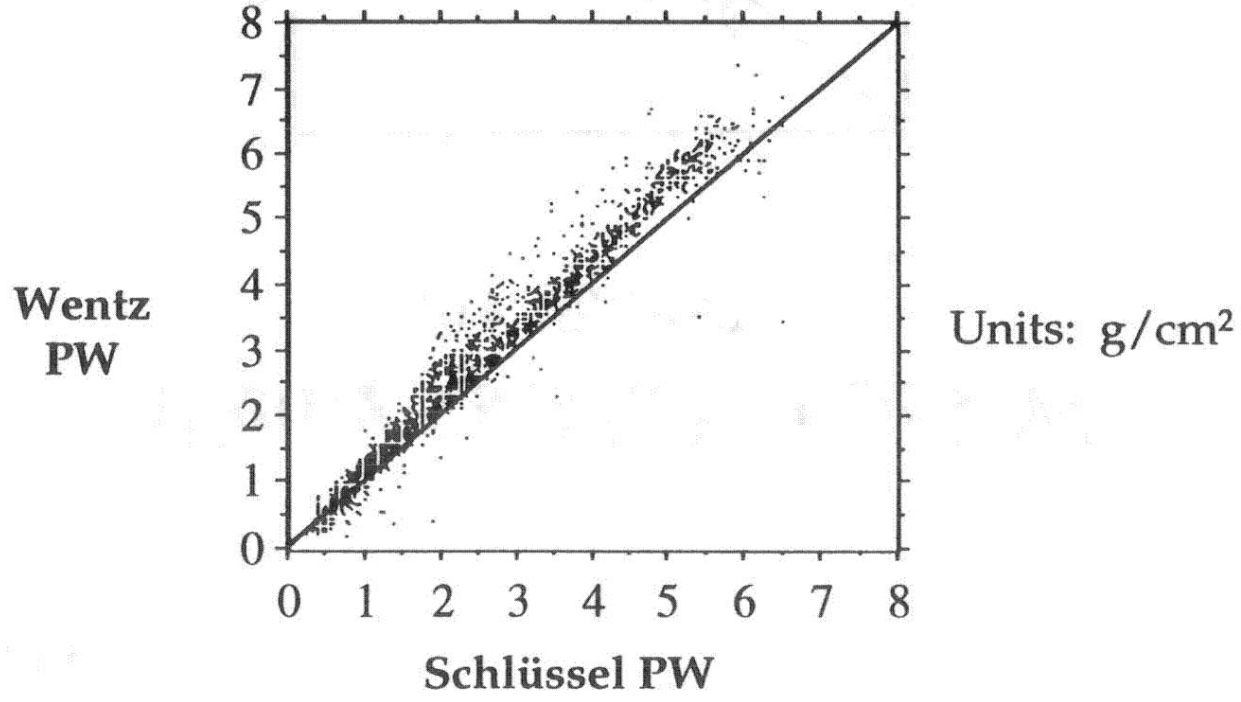


Units: g/cm^2

Scripps Institution
of Oceanography

Wentz vs Schlüssel PW

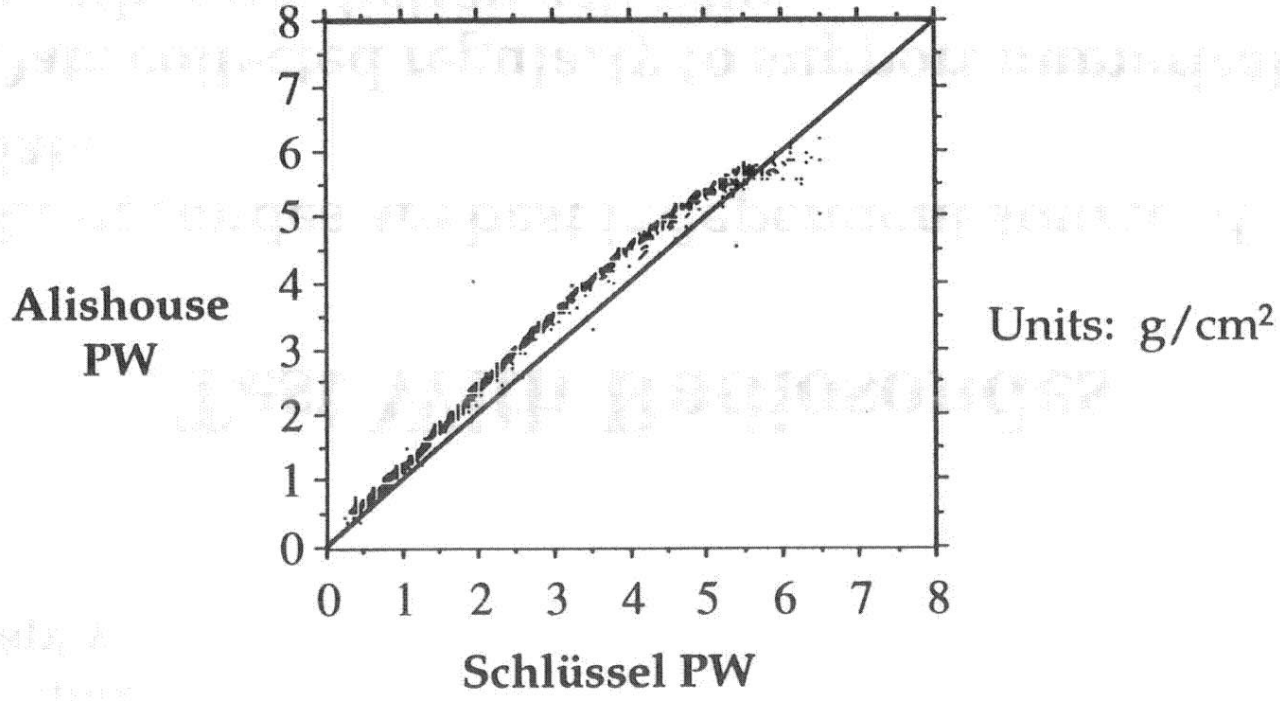
July 10, 1987



Scripps Institution
of Oceanography

Alishouse vs Schlüssel PW

July 10, 1987



Scripps Institution
of Oceanography

Test With Radiosondes

- Radiosondes are best independent source of data
- Data collected regularly to support numerical weather prediction activities
- Can give very precise measure of total precipitable water

Scripps Institution
of Oceanography

Problems with Radiosondes

- Human error
- Time lag in T and RH
- Hysteresis in RH sensor (it remembers moisture)
- Historical problems with RH below 20%
- Not necessarily representative of bulk air properties

Scripps Institution
of Oceanography

Ideal Radiosonde Dataset

- Many sites
- Broad spatial coverage
- Exact measurement of PW

Reality

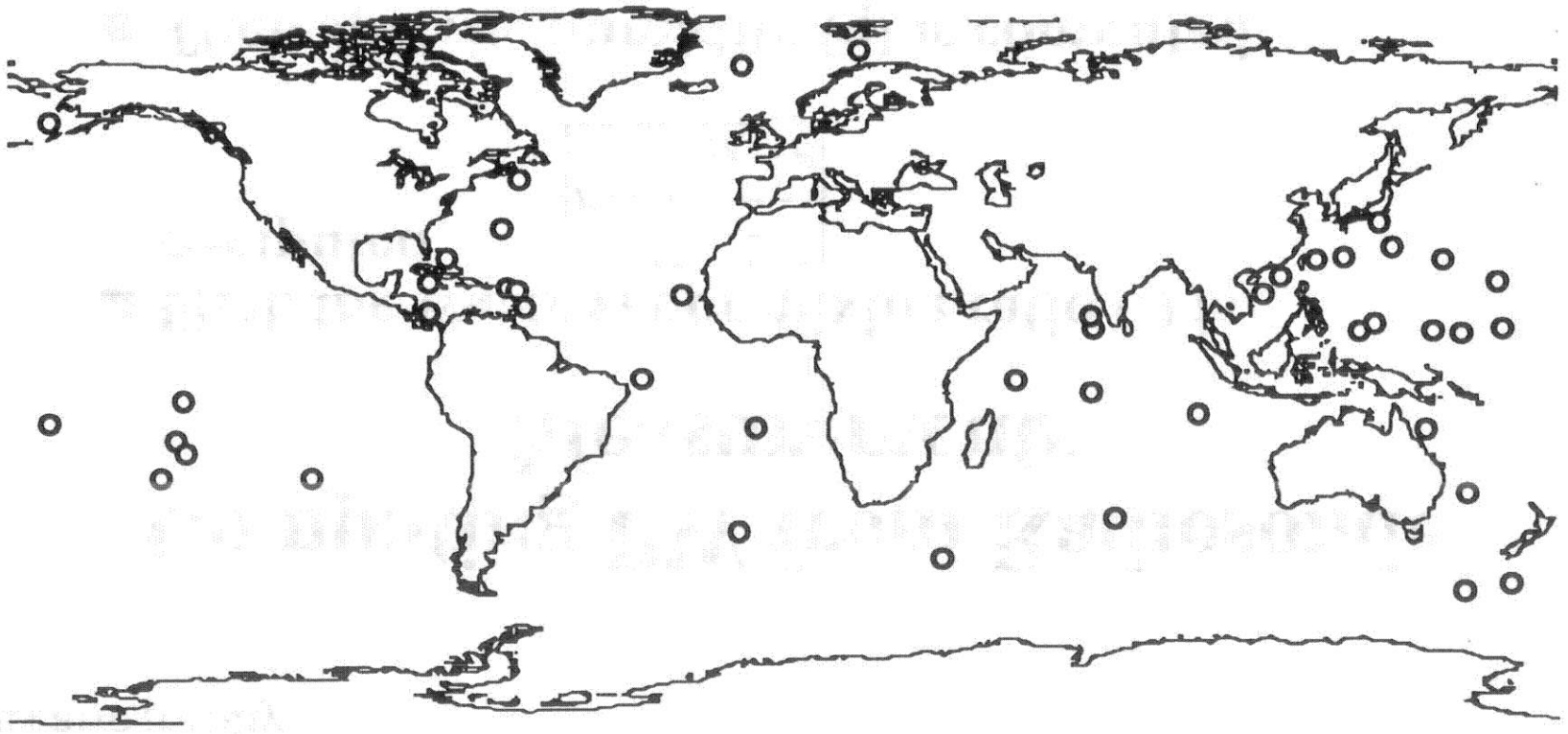
- **Few suitable sites available**
  - **Since SSM/I PW algorithms do not work over land, land contamination must be controlled..**
- **Limited spatial sampling**
- **Inexact measurement, particularly those run by third-world countries.**

Compromises

- **Be as generous as possible with site selection**
  - **Makes total number of samples larger**
  - **Lets us sample the widest possible assortment of atmospheric conditions**
- **Count on sheer size of dataset to beat down errors**
- **Since same dataset is used for all algorithms, errors are the same for all**

Scripps Institution
of Oceanography

Selected Radiosonde Locations



Scripps Institution
of Oceanography

Computing PW from Radiosonde Measurements

- First, the water vapor mixing ratio (r) is computed

$$r = \varepsilon \frac{e}{p - e}$$

- Then specific humidity (q) is computed

$$q = \frac{r}{1 + r}$$

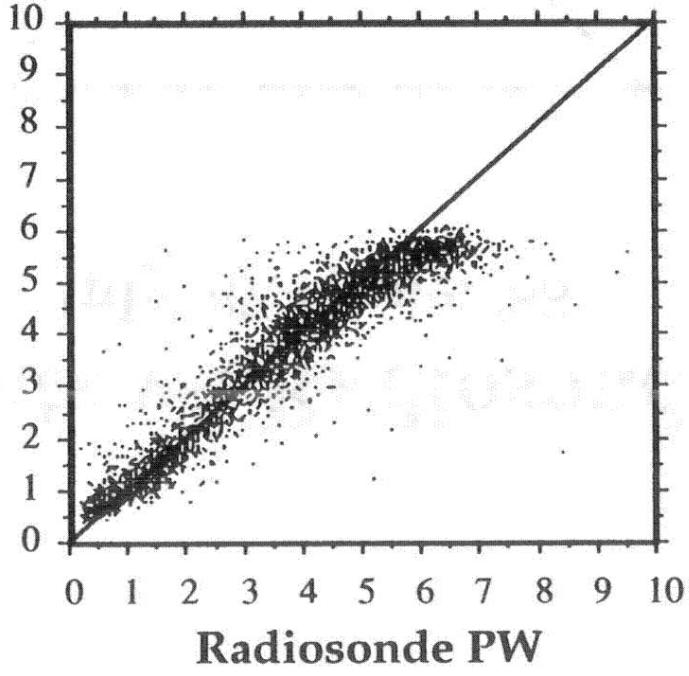
- Integrating q with respect to pressure over the atmospheric column gives us PW

$$PW = \frac{1}{g} \int_{p_0}^{0} q dp$$

Scripps Institution
of Oceanography

Alishouse vs. Radiosonde PW

July '87 - June, '88

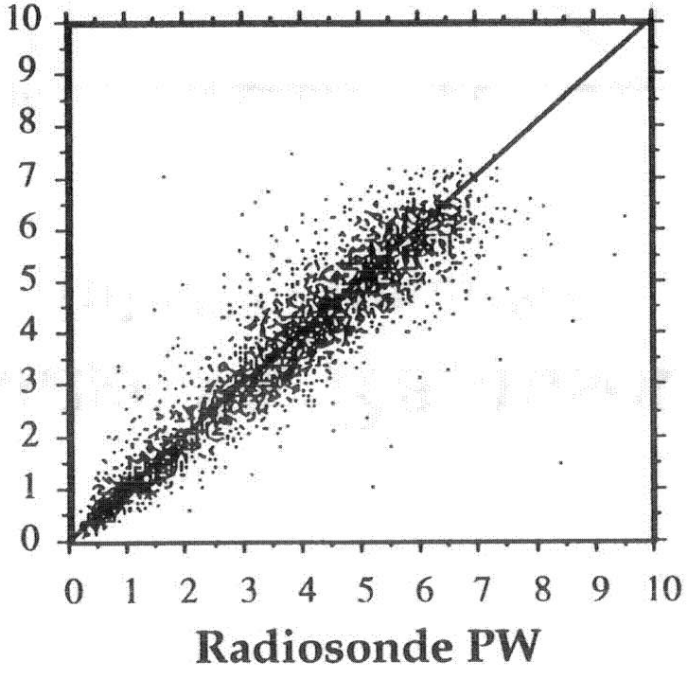


Units: g/cm^2

Scripps Institution
of Oceanography

Wentz vs. Radiosonde PW

July '87 - June, '88

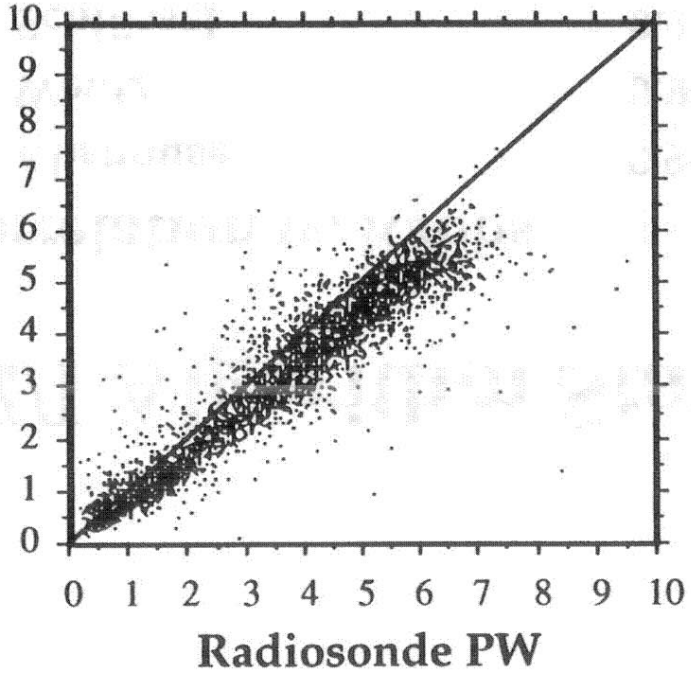


Units: g/cm^2

Scripps Institution
of Oceanography

Schlüssel vs. Radiosonde PW

July '87 - June, '88



Units: g/cm^2

Scripps Institution
of Oceanography

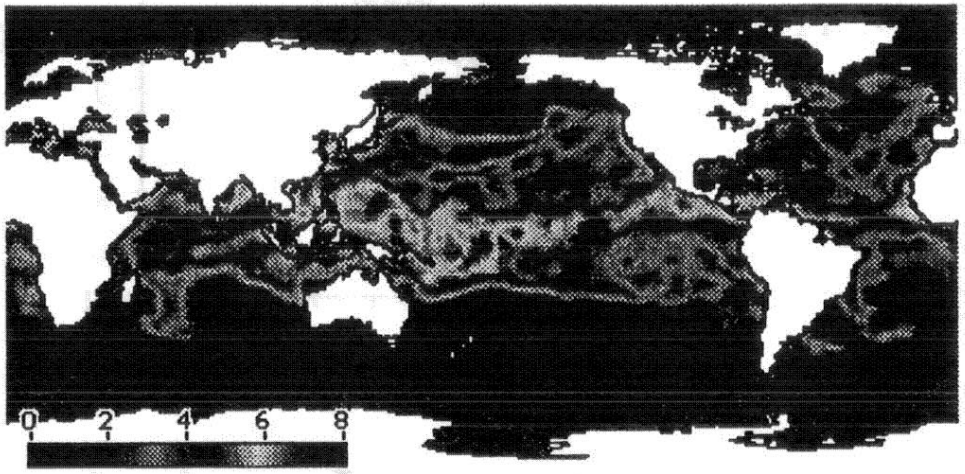
SSM/I Algorithm Statistics

- **Correlation w. Raobs**
  - Alishouse 0.9652
  - Wentz 0.9613
  - Schlüssel 0.9668
- **Slope of Best-Fitting Line**
  - Alishouse 0.8890
  - Wentz 0.9538
  - Schlüssel 0.8703
- **RMS of Residuals (g cm^{-2})**
  - Alishouse 0.4864
  - Wentz 0.5088
  - Schlüssel 0.6171

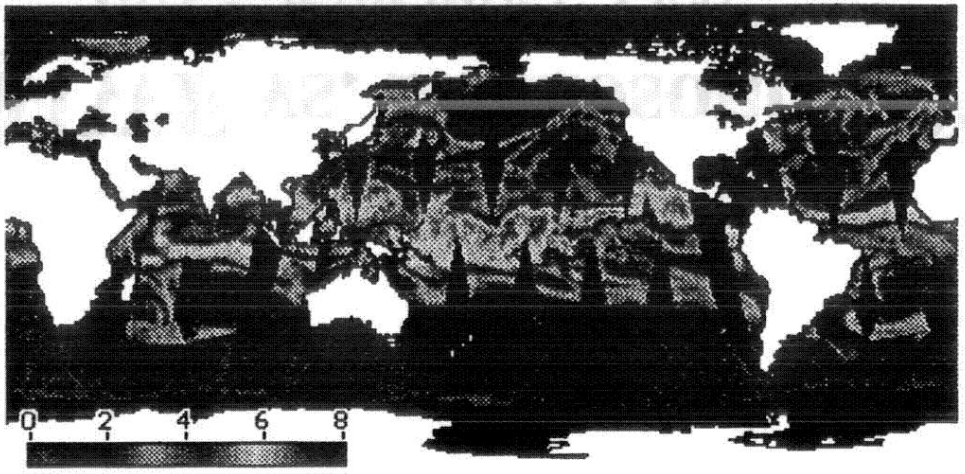
Scripps Institution
of Oceanography

ECMWF Analysis vs SSM/I PW

ECMWF



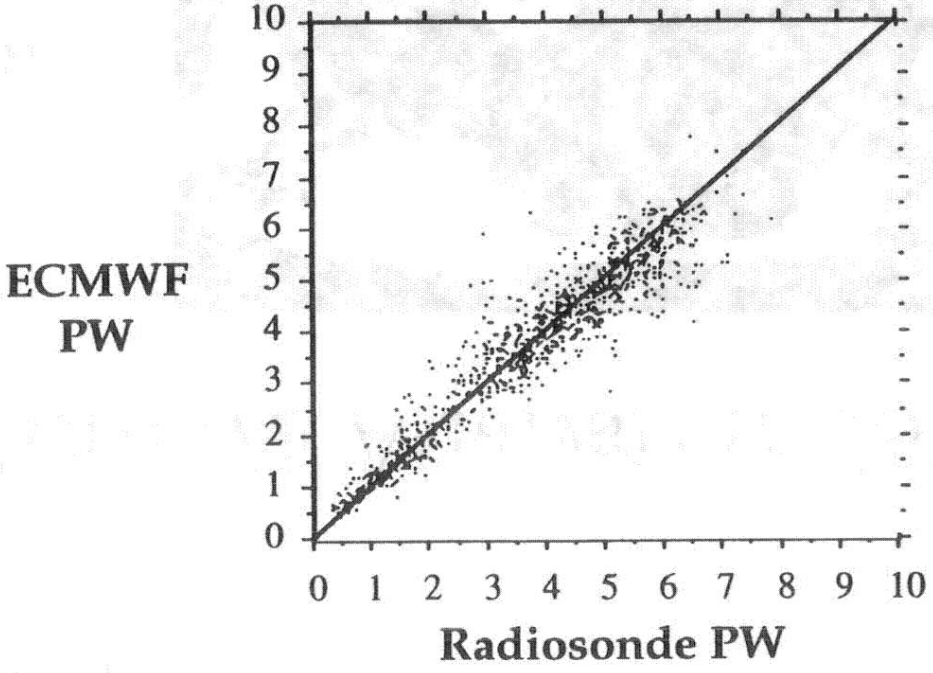
Wentz



Scripps Institution
of Oceanography

ECMWF vs. Radiosonde PW

July - September, 1988



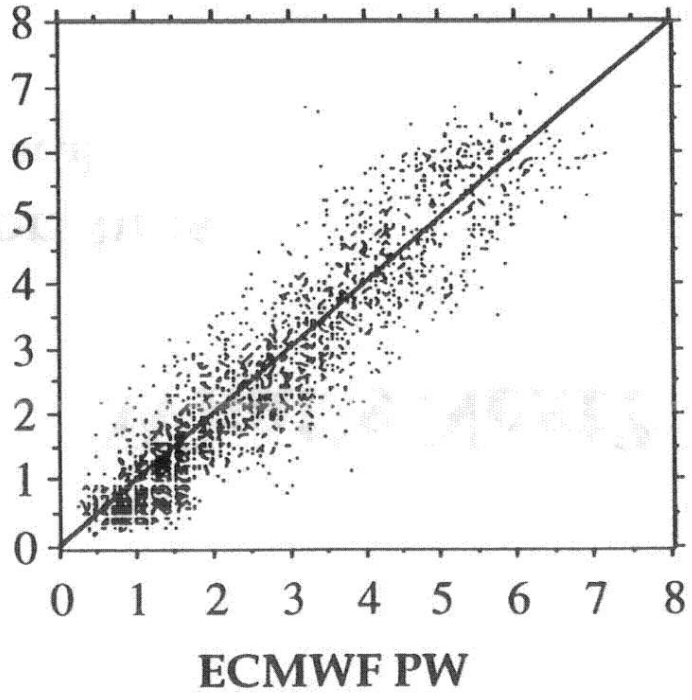
r = 0.969

Units: g/cm^2

Scripps Institution
of Oceanography

Wentz vs ECMWF PW

July 10, 1987



r = 0.872

Units: g/cm²

Scripps Institution
of Oceanography

What's Next?

- **More Algorithms**
  - Tjemkes, et al
  - Petty
  - others?
- **Bigger comparison dataset**
  - Longer time period
- **Better raobs QC**

Consistency of Retrieved Wind Speed and Cloud Water Over Ocean EDRs from Coincident F8 and F11 Data

Jorge V. Geaga and Don J. Rudy
The Aerospace Corporation

Abstract.

Coincident F8 and F11 microwave data were collected and analyzed in preparation for a proposed experiment to tilt the F8 satellite and acquire passive microwave data at higher incidence angles. The distributions of the retrieved windspeed and cloud water over ocean EDRs, for areas with spatially and temporally coincident ocean coverage, are quite similar for both satellites. Surface ground truth data measurements were not available for comparison. Pixel to pixel comparisons between the two satellites were not performed.

Introduction.

Users of weather forecasting data have expressed the desire for a capability to obtain contiguous equatorial coverage with the Block 6 microwave imager, particularly as a requirement for detecting and tracking tropical storms. Shown in Figure 1 is the Special Sensor Microwave/Imager (SSM/I) scan geometry. The SSM/I rotates continuously about an axis parallel to the local spacecraft vertical. The antenna beams define cone surfaces which from an altitude of 833 km make an angle of 53.1 degrees at the earth's surface.

At the present DMSP satellite orbital altitude, one method for achieving the necessary coverage is to increase the incidence angle at the surface from the current 53.1 to approximately 69 degrees. Shown in Figure 2 is the coverage of the SSMIS sensor (assuming a 143.2 degree scan) and shown in Figure 3 is the coverage for an incidence angle of 68.43 degrees [Glac 90a]. A widened swath will enable contiguous coverage at the equator. Concern has been expressed [Glac 90a] on the effects that changes in the phenomenology (e.g. proximity to Brewster angle) would have on the environmental data retrieval. An experiment was proposed [Glac 90b] to pitch the F8 satellite

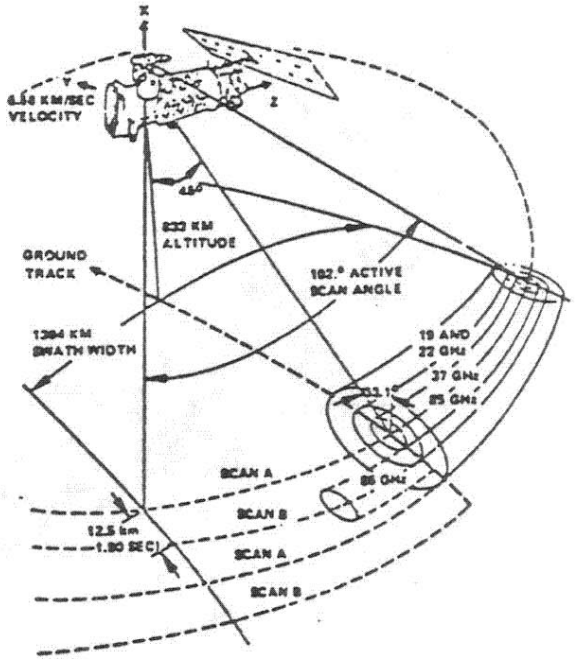


Figure 1: SSM/I Scan Geometry

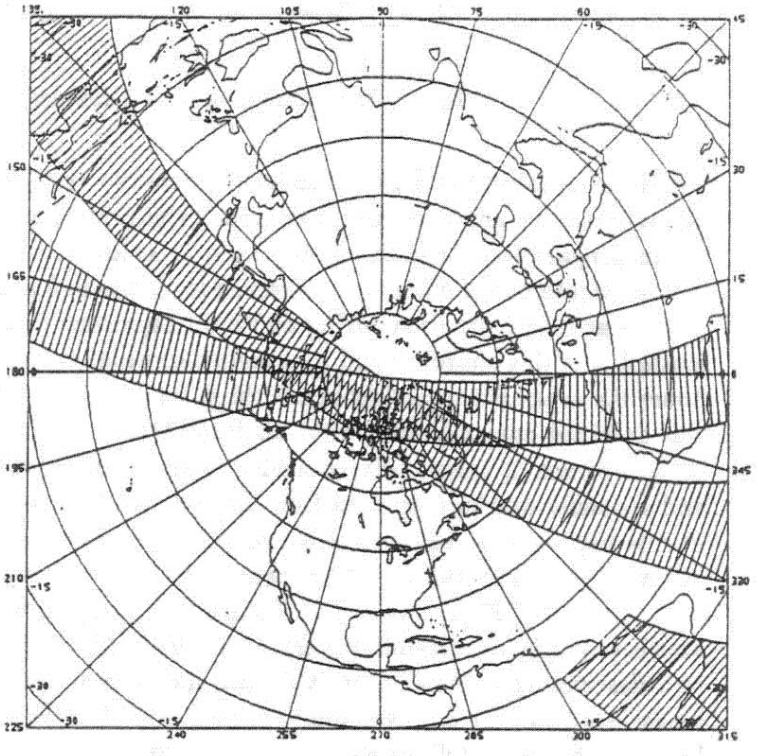


Figure 2: Coverage at 53.1 degrees

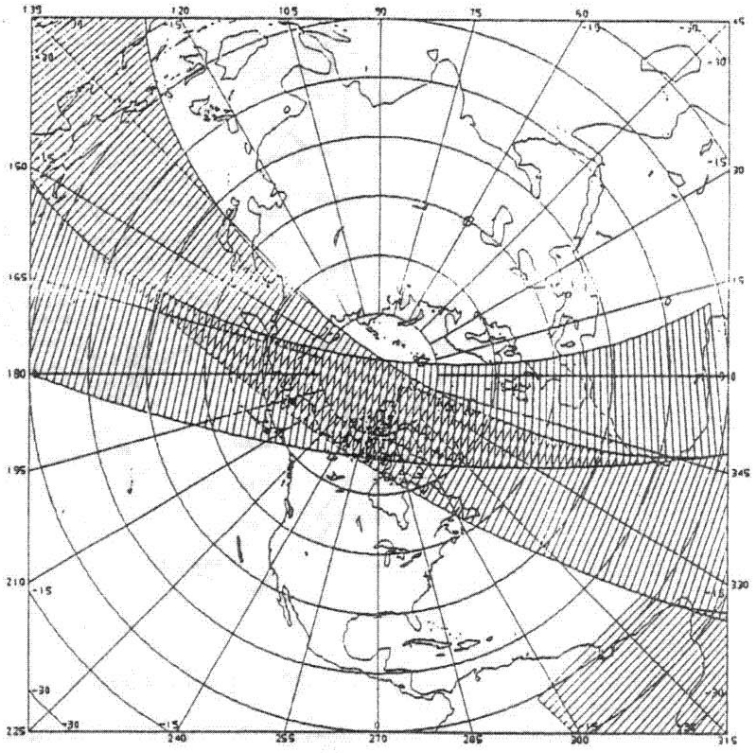


Figure 3: Coverage at 68.43 degrees

to obtain data at the higher incidence angles to test the effects that the larger incidence angles would have on environment information retrieval.

In preparation for such an experiment, studies have been undertaken to investigate use of coincident coverage from the F10 and F11 satellites to provide ground truth data during an F8 tilt experiment. In order to evaluate feasibility of this approach and to establish some level of consistency between "*over the ocean retrievals*" from the three satellites, passive microwave data was archived over a 48 hr period on June 26-27, 1992. Results of analysis on a segment of temporally coincident (within 30 minutes of each other) and spatially overlapping data from the F8 and F11 satellites are reported in this paper. The region covered ranges in latitude from 25N to 50N and in longitude from -162 to -150 degrees. Brightness temperatures from the 37V channel of F8 are shown in Figure 4 in the overlap region. The F8 satellite was in an ascending part of its orbit while the F11 satellite was in a descending part of its orbit during the coverage of this area. Ground measurements were not available for this study. A pixel to pixel comparison between the two satellites was not attempted.

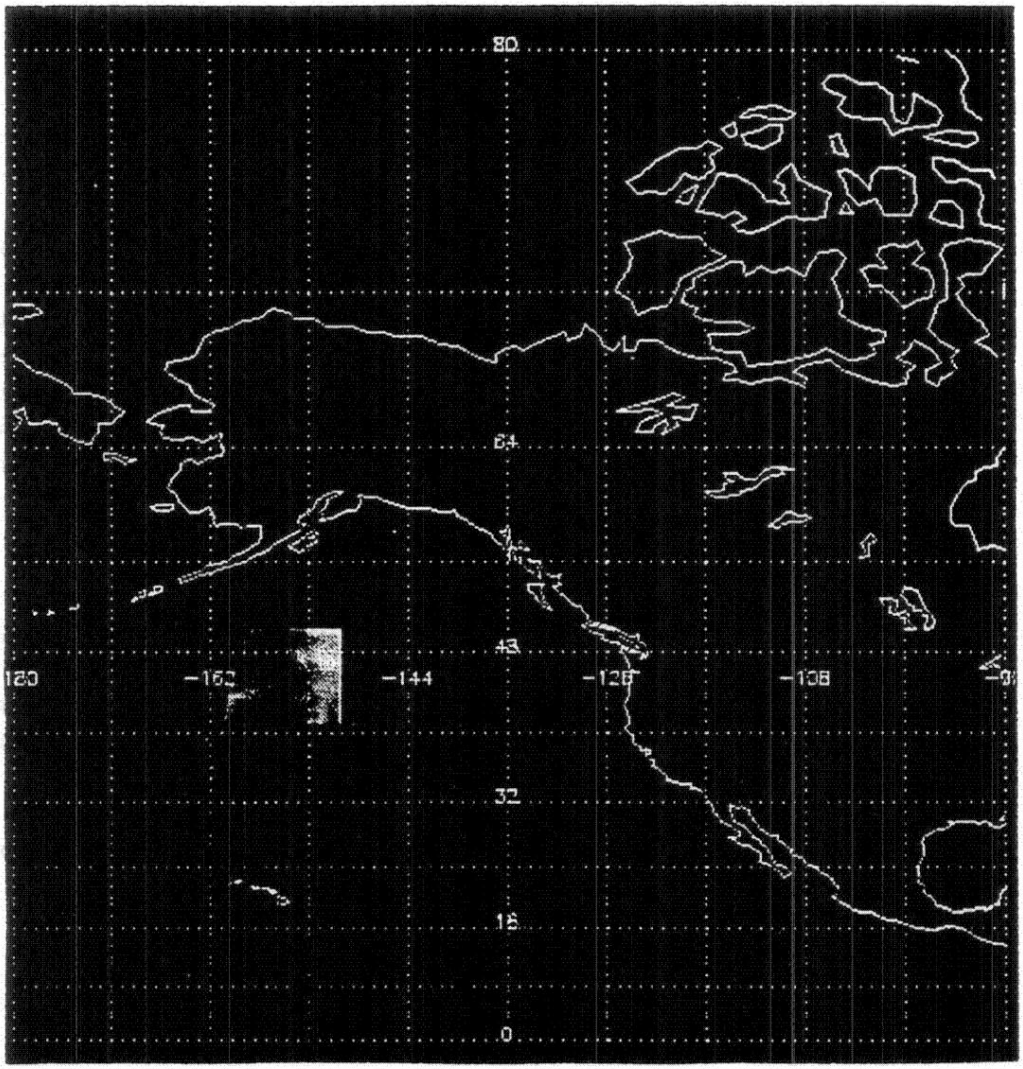


Figure 4: F8 37V Channel in the Overlap Region

Microwave Data

The data requested and recorded at AFGWC in Omaha were the five low resolution channels 19V, 19H, 22V, 37V, and 37H. Brightness temperature profiles in coincident areas were quite similar for the F8 and F11 satellites. Problems were encountered in establishing coincident F10 data. The brightness temperatures recorded for the 19V and 22V channels in the region shown in Figure 4 are shown in Figure 5 for F8 and F11 (as a function of latitude). The magnitude and spreads in brightness temperatures are quite consistent and similar for the 19H, 19V, 37H, and 37V channels. The 22V channel response is noticeably different. A large spread of temperatures is found at latitudes above 40N. This is also evident from the 37V channel of F8 in Figure 4.

Environmental Data Retrieval

The SSM/I windspeed retrievals are valid over open ocean (54 nautical miles from land) for a height of 19.5 meters above the water surface. Errors in windspeed retrieval are induced by atmospheric losses. Surface windspeed signatures are altered by atmospheric emissivity or attenuated by scattering from rain or ice.

Wind speed and cloud water over ocean retrievals were made in the overlap area shown in Figure 4. The expression for wind speed is [Good 90]

$$\begin{aligned} WS(m/s) &= 147.90 + 1.0969T_{B19V} - 0.4555T_{B22V} \\ &\quad -1.7600T_{B37V} + 0.7860T_{B37H}. \end{aligned}$$

The cloud water over ocean retrieval is defined by

$$\begin{aligned} CWOO(Kg/m^2) &= -2.83818 + .0084333T_{B19H} - .0075959T_{B22V} \\ &\quad +.020131T_{B37V} - .0053066T_{B37H}. \end{aligned}$$

The coefficients used for the cloud water over ocean retrieval are from [Holl 91]. The CALVAL coefficients were not utilized in this retrieval since the 85H channel in F8 has failed.

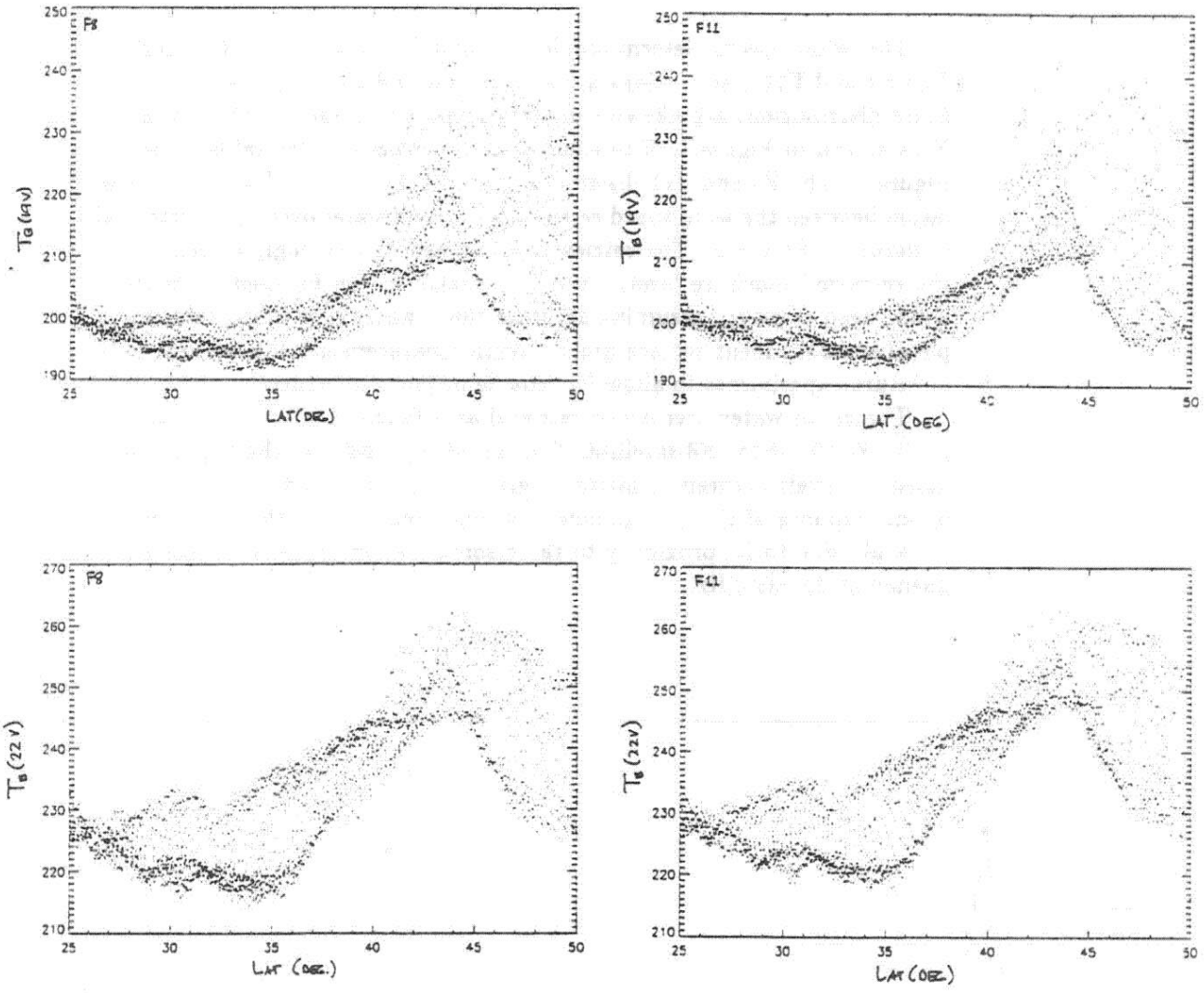


Figure 5: 19V and 22V Brightness Temperatures for F8 and F11

Results.

The wind speeds determined for F8 and F11 are shown in Figure 6. The F8 and F11 distributions are similar. The F8 and F11 T_{B19V} temperature distributions are likewise similar except for an estimated shift of 0.8 K as shown in Figure 7. The cloud water over ocean retrieval is shown in Figure 8. The F8 and F11 distributions are again quite similar. The correlation between the wind speed retrieval and cloud water over ocean retrieval is shown in Figure 9. The retrieved windspeeds are strongly correlated to the retrieved moisture levels. Such a correlation can be used to improve wind speed retrieval, assuming accurate cloud water over ocean retrieval is possible. Coincident surface ground truth measurements will be necessary in future experiments to allow for reliable physical inferences.

The cloud water over ocean retrieval as a function of latitude is shown in Figure 10 for the F8 satellite. This figure suggests that the higher cloud moisture levels occured at latitudes greater than 40N. The noticeably different response of the 22V channel (as compared to the other channels) is probably due to its proximity to the resonant water vapor absorption frequency at 22.235 GHz.

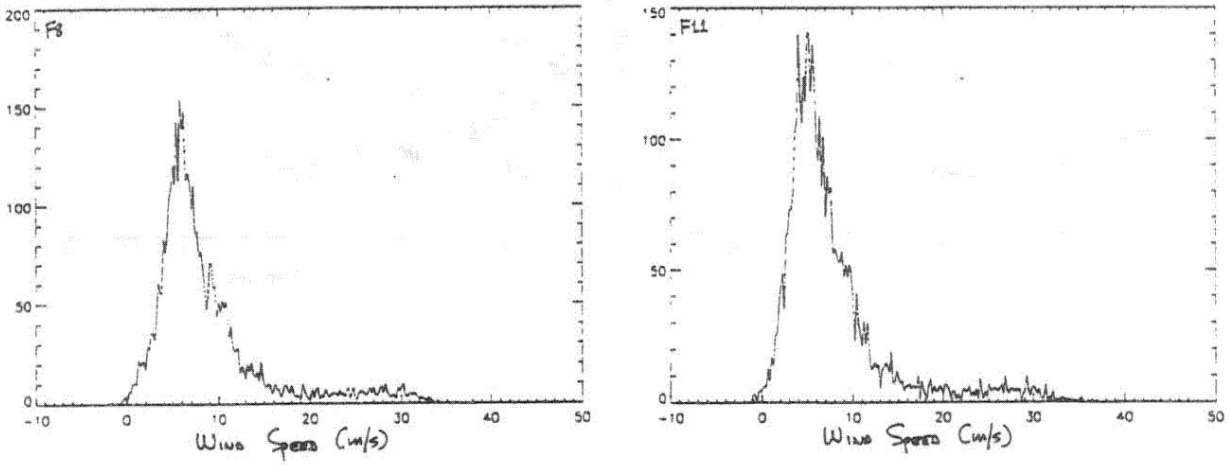


Figure 6: Wind Speed

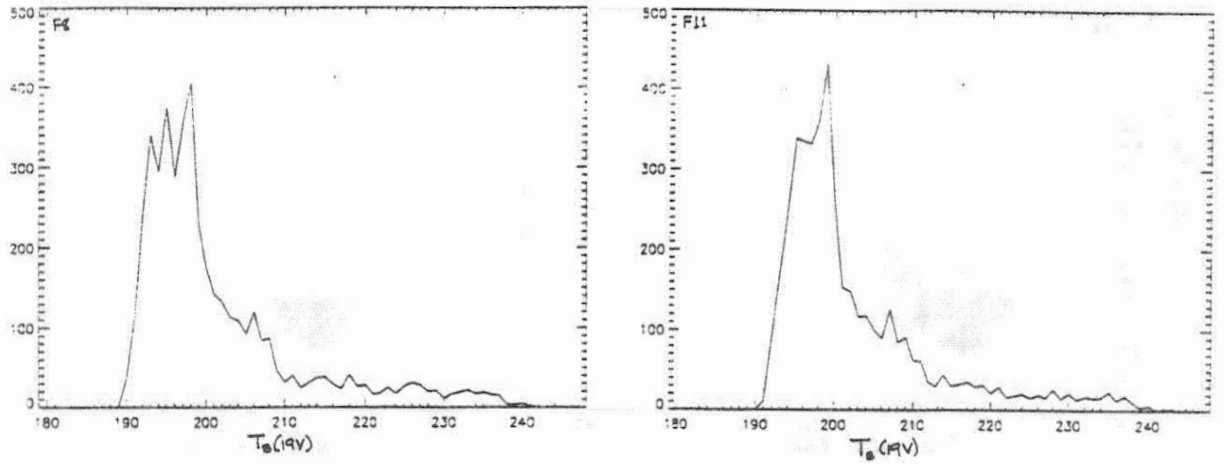


Figure 7: T_{B19V} Distributions

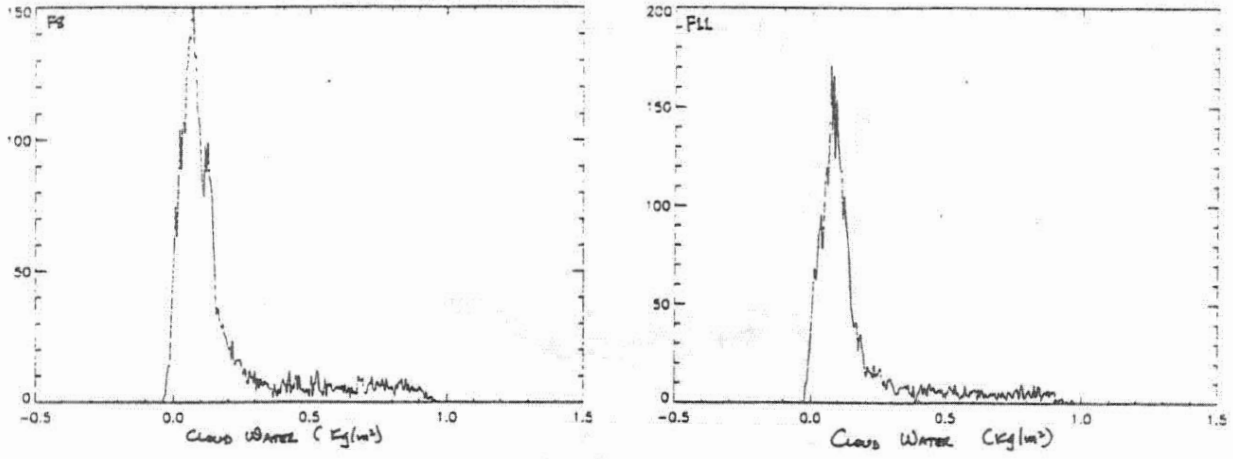


Figure 8: Cloud Water Over Ocean

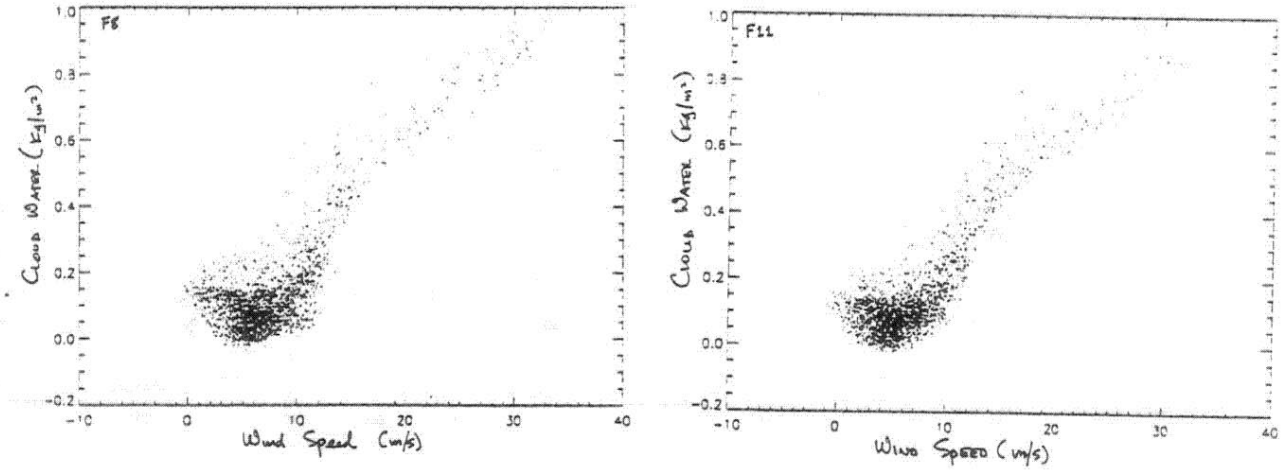


Figure 9: Cloud Water Over Ocean Correlation with Wind Speed

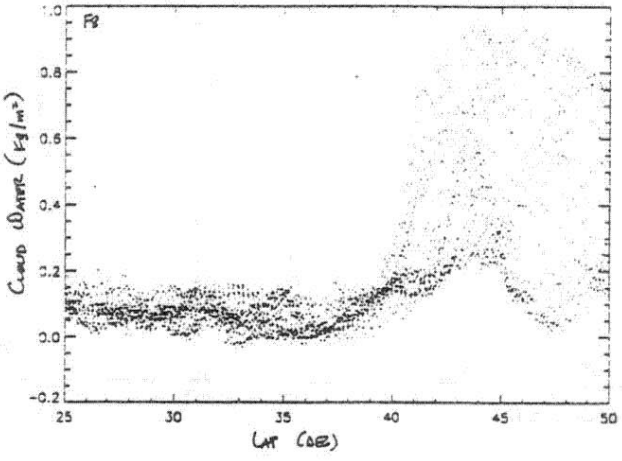


Figure 10: F8 Cloud Water Over Ocean

Based on the results of the studies, we believe that coincident F10 and F11 coverage will provide useful ground truth for the F8 tilt experiment.

References

[Glac 90a] Glackin,D.L., Gasster, S.D., Pihos, G.G, "*Microwave Imager Sounder Incidence Angle Limitations*", unpublished Aerospace Report (March 90).

[Glac 90b] Glackin,D.L., Pihos, G.G., and Gasster, S.D., "*F-8 Tilt Proposal*", Aerospace Memorandum (Sept. 90).

[Good 90] Goodberlet, M., Swift, C.T., Wilkerson, J. "*Ocean Surface Wind Speed Measurements of the Special Sensor Microwave/Imager (SSM/I)*", IEEE Trans. Geo. Rem. Sens., Vol 28, pgs. 823-828 (1990).

[Holl 91] Hollinger, J., Private Communication.

STATUS REPORT OF NASA/NOAA SSMI/I PATHFINDER EFFORT

Christopher M. U. Neale
Associate Professor
Dept. Biological and Irrigation Eng.
Utah State University

Status Report of the NASA/NOAA SSM/I Pathfinder Effort

Christopher M. U. Neale[1]

The SSM/I Pathfinder Science Working Group (SWG) was formed in late March 1993. It consists of researchers and program administrators from NASA, NOAA and researchers from Universities and Private entities. The committee has met twice, with the first meeting being held on April 20-21, 1993, in Tallahassee, Florida, and the second meeting being held on October 21-22, 1993 in Annapolis, Maryland. In order to expedite the decision making process on several issues, the SWG was divided into sub-committees, each with responsibility for a certain area or algorithms and products: (1) Operations, Data Access and Services Sub-Committee, (2) Ocean Parameters Sub-Committee, Precipitation Algorithms Sub-Committee, (4) Snow and Ice Products and (5) Over-land Parameters. The presentation will summarize the decisions of the SWG with respect to data sets, distribution media, format, operational considerations, algorithms and products to be released.

---

1 Chairperson of the SSM/I Pathfinder Science Working Group and Associate Professor, Dept. of Biological and Irrigation Engineering, Utah State University, Logan, Utah 84322-4105

PATHFINDER PROGRAM

- NASA / NOAA sponsored program
- Provide high quality satellite sensor datasets for the scientific community
- Pathfinder efforts:
  - AVHRR
  - GOES
  - TOVS
  - SSM/I
- Science Working Groups

  Provide advice on:
  - Technical issues
  - Data distribution, media, formats
  - Products and algorithms

SSM/I PATHFINDER
SCIENCE WORKING GROUP

BOB ADLER	NASA/GSFC
RICHARD ARMSTRONG	NOAA/NSIDC
BUD BOOTH	NOAA/NESDIS
BASKER CHOUDHURY	NASA
JAMES DODGE	NASA HQ
RALPH FERRARO	NOAA/NESDIS
STEVE GOODMAN	NASA/MSFC
TOM GREENWALD	CSU
JOHN JANOWIAK	NOAA
JIM HOLLINGER	NRL
MARTHA MAIDEN	NASA
CHRISTOPHER NEALE	USU
ENI NJOKU	NASA
KEN MITCHELL	NOAA
GEORGE OHRING	NOAA
GRANT PETTY	PURDUE U.
RICHARD SAVAGE	HUGHES AIRCRAFT CO
ROY SPENCER	NASA/MSFC
PAM TAYLOR	NOAA/NESDIS
CAL SWIFT	U. MASS
FRANK WENTZ	REMOTE SENSING SYS.
MIKE GOODMAN	NASA/MSFC

SWG SUB-COMMITTEES

1. **OPERATIONS, DATA ACCESS AND SERVICES**

   CHAIR: PAM TAYLOR

   BUD BOOTH, JAMES DODGE, JOHN JANOWIAK, MARTHA MAIDEN, GEORGE OHRING, MIKE GOODMAN

2. **PRECIPITATION ALGORITHMS**

   CHAIR: GRANT PETTY

   BOB ADLER, RALPH FERRARO, STEVE GOODMAN ROY SPENCER

3. **OCEAN PARAMETERS**

   CHAIR: FRANK WENTZ

   TOM GREENWALD, JIM HOLLINGER, KEN MITCHELL CAL SWIFT

4. **SNOW AND ICE**

   CHAIR: RICHARD ARMSTRONG

5. **OVER LAND PARAMETERS**

   CHAIR: CHRISTOPHER NEALE

   BASKAR CHOUDHURY, ENI NJOKU, RICHARD SAVAGE

Water vapor:

* **Five algorithms were considered (Alishouse et al., Petty and Kastsaros, Schluessel and Emery, Tjemkes et al. and Wentz.**

* **Initial Recommendation: Alishouse et al. and Wentz**

* **Final Recommendation: Wentz**

Wind Algorithms:

* **Five algorithms were considered (Bates, Goodberlet, Swift and Wilkerson, Schluessel and Luthardt, Smith and Wentz.**

  Initial Recommendation: Goodberlet et al. and Wentz

* **Additional Studies were conducted comparing Wentz and Goodberlet wind algorithms.**

* **Final Recommendation: Pending decision by sub-comittee**

Liquid Water:

* **Three algorithms were considered (Alishouse) et al., Petty and Katsaros and Wentz.**

* **Initial Recommendation: Wentz and Petty**

* FINAL RECOMMENDATION: WENTZ

SNOW AND ICE PRODUCTS

* Snow extent and edge is well documented

* Snow water equivalent algorithms are site specific

* Sea-ice:

  Three algorithms (Cavalieri and Gloerson, Comiso and Ramsier et al.)

* Ice age is difficult to do and existing algorithms need improvement

PRECIPITATION ALGORITHMS:

* Rain / no-rain on a swath basis or rain frequency on a monthly basis (gridded)

* Rain rate retrievals on a swath basis and monthly rain totals on a gridded basis.

* Distinguish between stratiform and convective warm and cold cloud rain, hydrometeor profiles

* Seven algorithms were examined (Spencer et al., Adler and Negri, Grody, Kummerow et al., Olson et al., Petty and Katsaros, Wilheit et al.)

Final recommendations:

Adler et al. algorithm for Benchmark dataset until results of PIP and other ongoing inter-comparisons are known

- to proceed with generation of global rainfall products despite immaturity of existing algorithms

[redacted] LAND ALGORITHMS:

* Land surface type classification (Hughes, Grody and Neale et al.)
* Surface Moisture (Neale et. al)
* Land surface temperature (McFarland et. al)
* Other potential products:

- Fraction of cover, biomass
- Seasonal inundation
- Microwave vegetation index

FINAL RECOMENDATIONS: PENDING

SSM/I SCIENCE WORKING GROUP STUDIES

1. COMPARISON OF APC SCHEMES, STUDY OF GEOLOCATION

NRL: David Spangler and Jim Hollinger

2. COMPARISON OF WENTZ AND GOODBERLET WIND SPEED ALGORITHMS

Grant Petty

3. COMPARISON OF SEA ICE ALGORITHMS

NRL and Joint Ice Center

- GEOLOCATION
  - COMPARED DAY 274 FOR 1987, 1989, 1990, 1991. (PRIOR TO FNOC'S FINAL GEOLOCATION CORRECTION)
  - COMPARED DAY 343 FOR 1991. (AFTER FNOC'S FINAL GEOLOCATION CORRECTION)
  - MEAN GEOLOCATION DIFFERENCES VARIED FROM 8 - 16 KM FOR THE FIRST 4 COMPARISONS.
  - MEAN GEOLOCATION DIFFERENCE OF 3.5 KM FOR THE LAST COMPARISON.

Comparison of Wentz and FNOC SSM/I Data

- Antenna Temperatures
  - Compared day 274 for 1987, 1989, 1990, 1991
  - FNOC antenna temperatures stored to 0.01 K.
  - Wentz antenna temperatures stored to 0.1 K.
  - Wentz antenna temperatures agree with FNOC ± 0.05 K with expected uniform distribution.
  - All channels compare equally well for all years.
- Brightness Temperatures
  - Compared day 274 for 1987
  - Wentz brightness temperatures generally agree with FNOC, mean difference < 0.1 K.
  - The one exception is the 22V, mean difference of almost 0.3 K.
  - The average difference varies for each point along the scan for the low 5 channels (19, 22, and 37 GHz) due to Wentz in scan correction.
  - The 22 GHz channel differs with latitude apparently due to a different cross-pole correction.

FINDINGS AND RECOMMENDATIONS

On Data Sets:

* Time Period: Aug 1, 1987 through November 30, 1988

* Therefore the SSM/I instrument on the DMSP F8 would primarily be used

* Based on the scientific needs of the research community four levels of SSM/I data and products are being proposed:

1. Full resolution SSM/I Antenna Temperatures

   - Swath format

   - Allows for reprocessing of the data for different APC, calibration and geo-location schemes

   - Based on results of NRL study, Wentz APC scheme was recommended

   - Metadata: APC, calibration algorithms

   - Media/Format: Exabyte 8mm cartridges, in HDF

   - Processing center: Marshall Space Flight Center

2. SSM/I Brightness Temperatures

- **Calculated from Ta's and recommended APC**
- **Format: Gridded at 10, 20 and 40 km resolution**
  Browse at 40 km
- **Metadata: APC used, gridding scheme**
- **Processing center: NSIDC**

3. SSM/I Products

Full temporal resolution:

- Ocean, atmospheric and over-land products will be recommended
- Based on full resolution Tb's
- Metadata: APC scheme used, documentation on algorithms, interpolation scheme and maybe some ancillary data
- Media/Format: CD-ROMS using HDF FOR GRIDDED PRODUCTS
  8 mm CARTRIDGES USING HDF FOR FULL RESOLUTION
- Processing center: MSFC for full resolution data
  NSIDC for gridded products

Temporal Averaging:

- daily, pentad, weekly, monthly
- gridded and full resolution

ON PRODUCTS AND ALGORITHMS:

* Issues:

  - Empirical vs. Physically based algorithms
  - Site specific of global
  - Validation
  - MATURE
  - PUBLISHED
  - CONSENSUS

Ocean Parameters:

  * Wind speed and direction
  * Water vapor
  * Liquid water

A Comparison of SSM/I Algorithms for the Estimation of Surface Wind

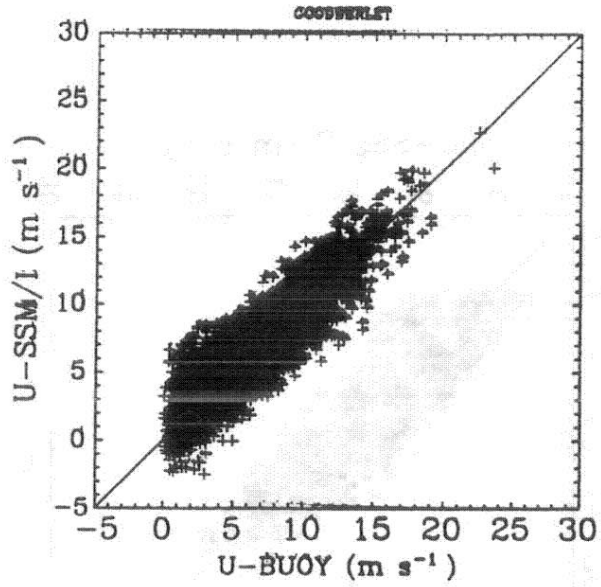
Grant W. Petty
Dept. of Earth and Atmospheric Sciences
Purdue University
West Lafayette, IN

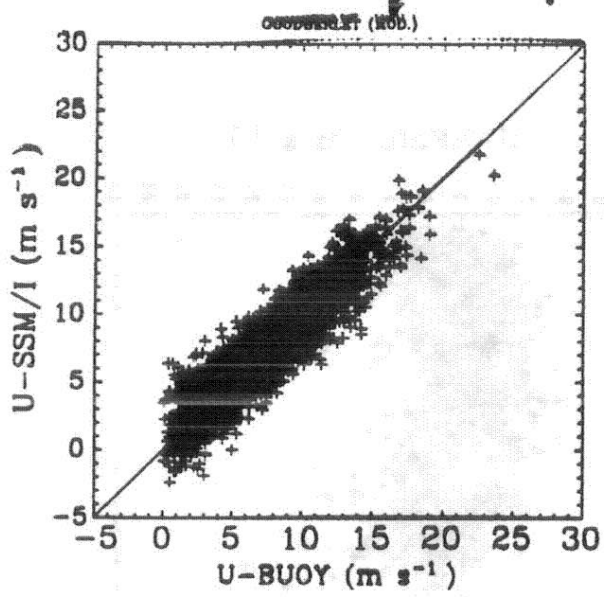
Using a quality-controlled derivative of the buoy/SSMI matchup data set developed by Goodberlet et al. (1989), we have undertaken an independent comparison of the Goodberlet et al. and Wentz wind speed algorithms. Among other things, we find that the Goodberlet statistical algorithm exhibits superior rms errors (1.75 m/s) relative to the Wentz algorithm (1.95 m/s) but that it also exhibits a pronounced water vapor-dependent bias. By applying a correction which is quadratic in SSMI-retrieved water vapor, it is possible to remove most of the bias and to improve the rms error of the Goodberlet algorithm to 1.56 m/s.

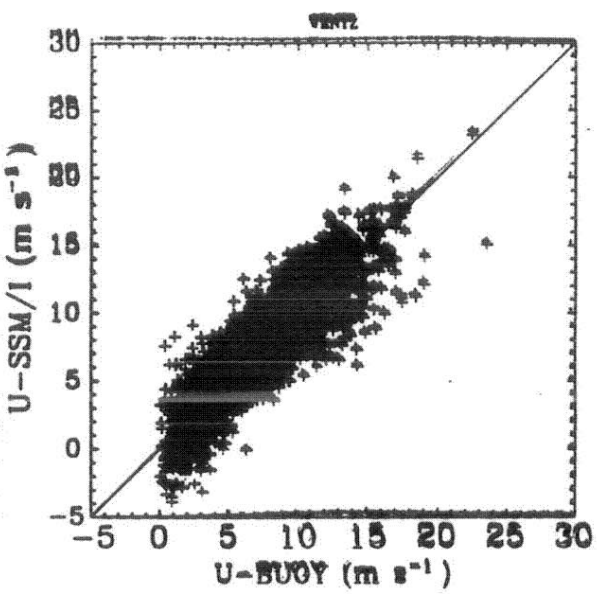
The validation data set does not include wind speeds significantly above 20 m/s (about 40 kts). However, it appears that wind speed estimates from the Wentz and Goodberlet et al. algorithms significantly diverge at higher wind speeds, with a projected difference of 4 m/s in the vicinity of 30 m/s. As yet, we have no basis for determining which estimates are more accurate under these conditions.

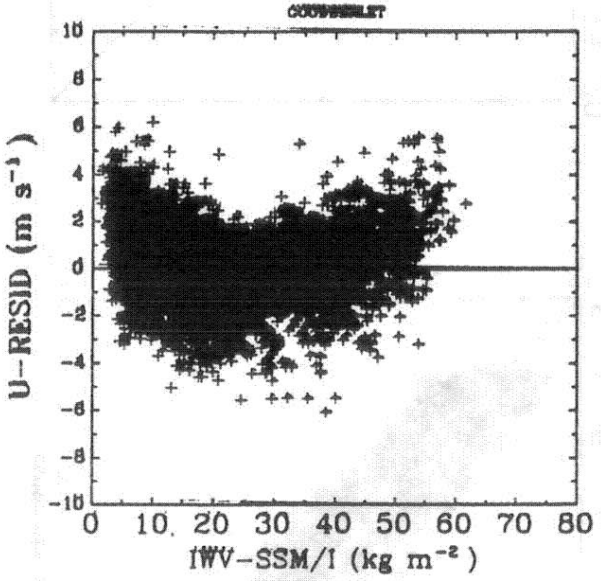
We also examined the dependence of the residuals (SSMI minus buoy wind speeds) on the presence of precipitation and/or heavy liquid water and found that both algorithms show similar deterioration in the presence of rain. Although rain-induced biases can be subtracted, the resulting standard deviation of the residuals remains comparable to or larger than the natural variability of surface wind speed; hence, such corrections would appear to be of little value.

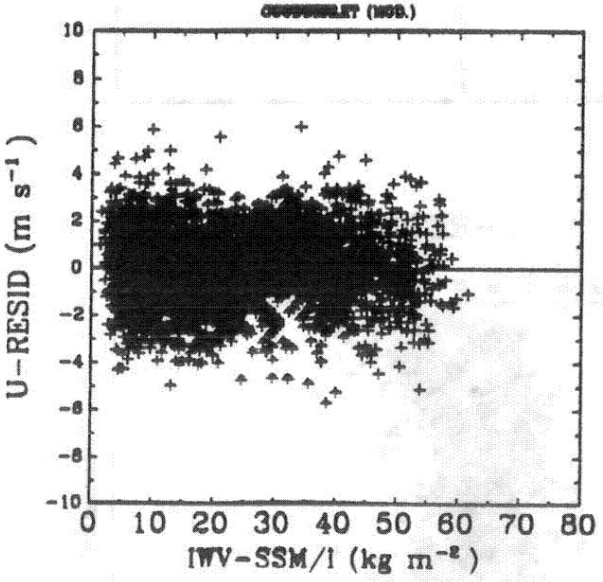
The Goodberlet et al. criteria for identifying precipitation-contaminated wind speed estimates do not satisfactorily discriminate between brightness temperature effects due precipitation and those due to combinations of high water vapor content and high surface wind speed. It is therefore recommended that replacements for the Goodberlet precipitation flags be developed which are referenced to the SSM/I-retrieved liquid water content rather than to thresholded brightness temperatures.

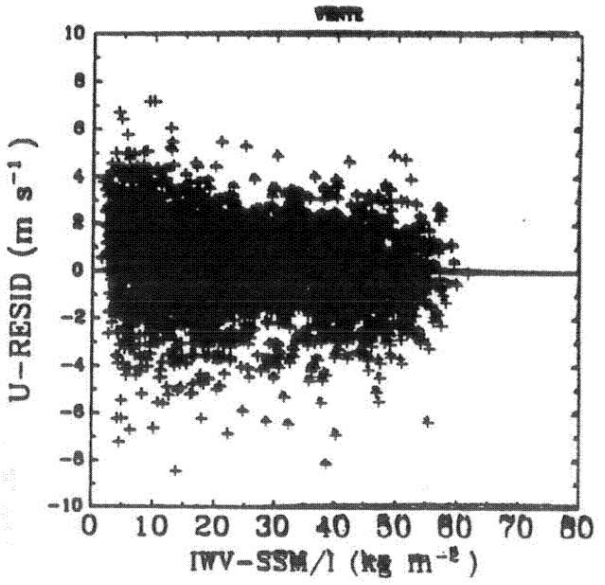

GOODBERLET
U-SSM/I (m s^{-1})
U-BUOY (m s^{-1})

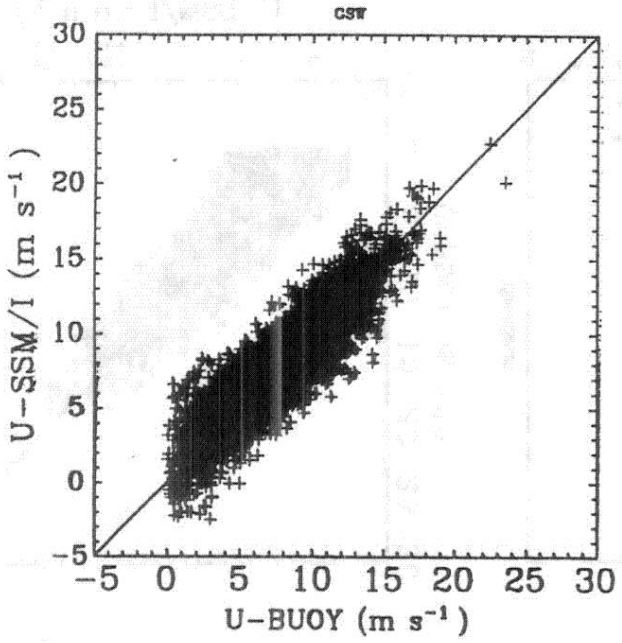

Petty
GOODBERLET (MOD.)
U-SSM/I (m s^{-1})
U-BUOY (m s^{-1})

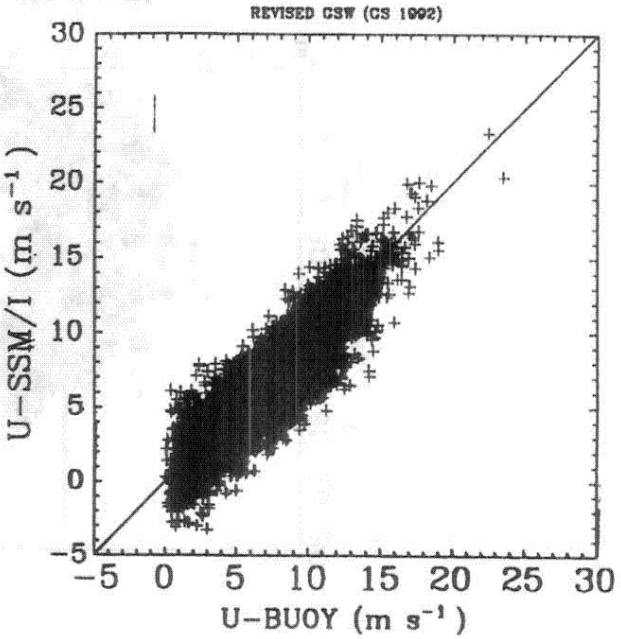

WENTZ
U-SSM/I (m s^{-1})
U-BUOY (m s^{-1})

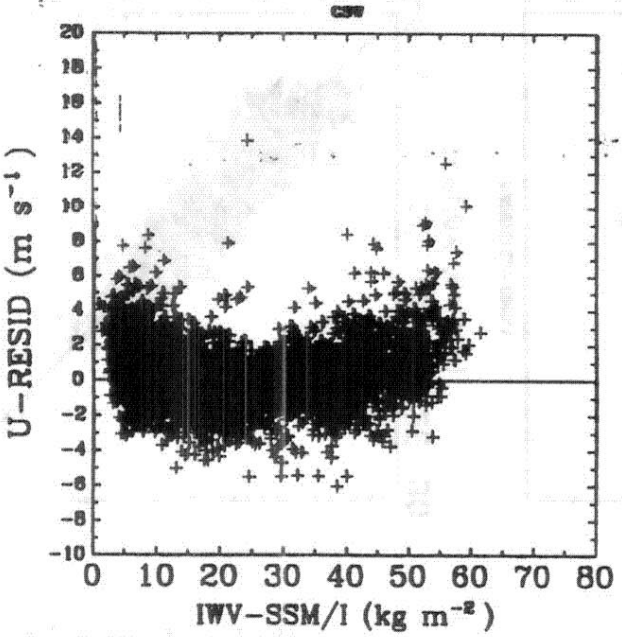

GOODBERLET
U-RESID (m s^{-1})
IWV-SSM/I (kg m^{-2})

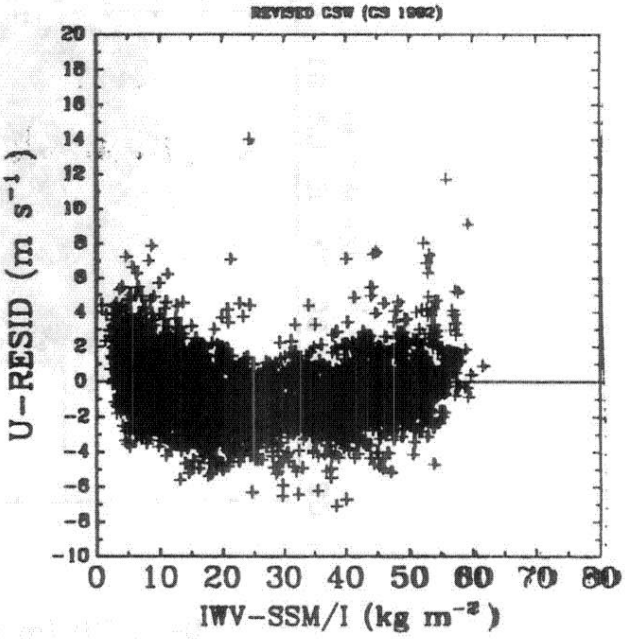

GOODBERLET (MOD.)
U-RESID (m s^{-1})
IWV-SSM/I (kg m^{-2})


WENTZ
U-RESID (m s^{-1})
IWV-SSM/I (kg m^{-2})


CSW
U-SSM/I (m s^{-1})
U-BUOY (m s^{-1})


REVISED CSW (CS 1992)
U-SSM/I (m s^{-1})
U-BUOY (m s^{-1})


CSW
U-RESID (m s^{-1})
IWV-SSM/I (kg m^{-2})


REVISED CSW (CS 1992)
U-RESID (m s^{-1})
IWV-SSM/I (kg m^{-2})

RESULTS OF INITIAL WIND SPEED ALGORITHM INTERCOMPARISON

N = 2741 Buoy/SSMI pairs (objectively screened for heavy cloud/rain)

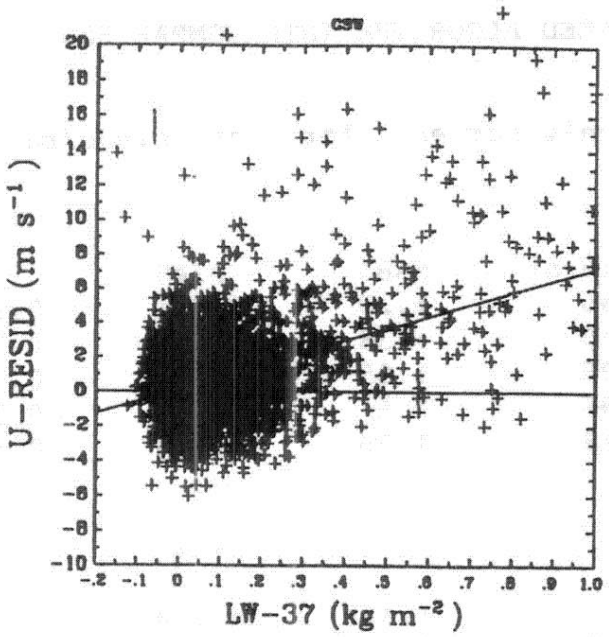
Without correction:

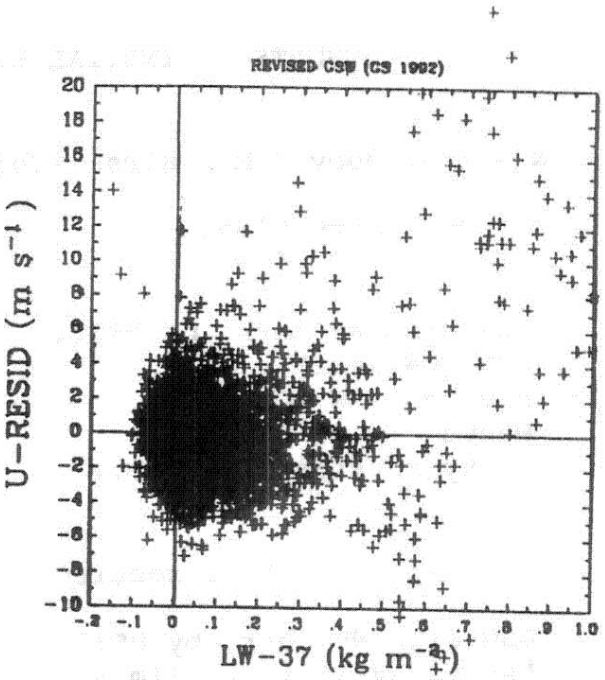
	RMS (m/s)	MABS	BIAS	r
* GSW with WV corr. by PETTY	1.56	1.23	0.001	0.901
* GSW (Cal/Val)	1.75	1.38	0.085	0.882
* Revised GSW (GS 1992)	1.95	1.55	-0.698	0.879
Wentz	1.96	1.54	0.325	0.861
Petty physical (prelim.)	2.18	1.76	-1.384	0.882

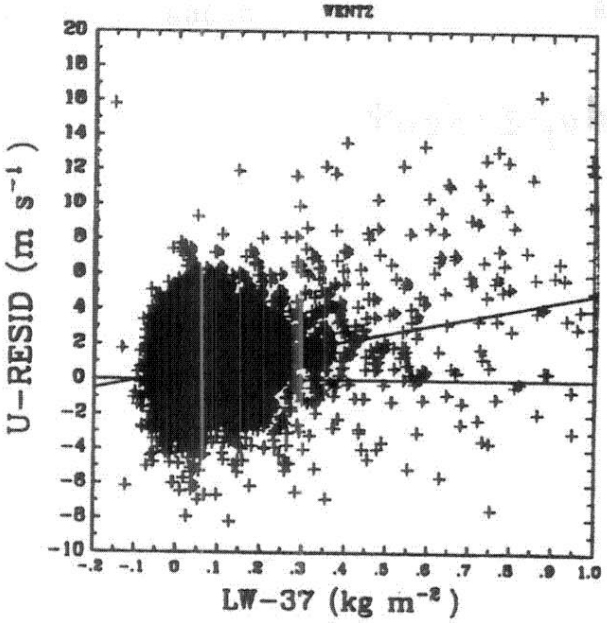
With linear bias correction:

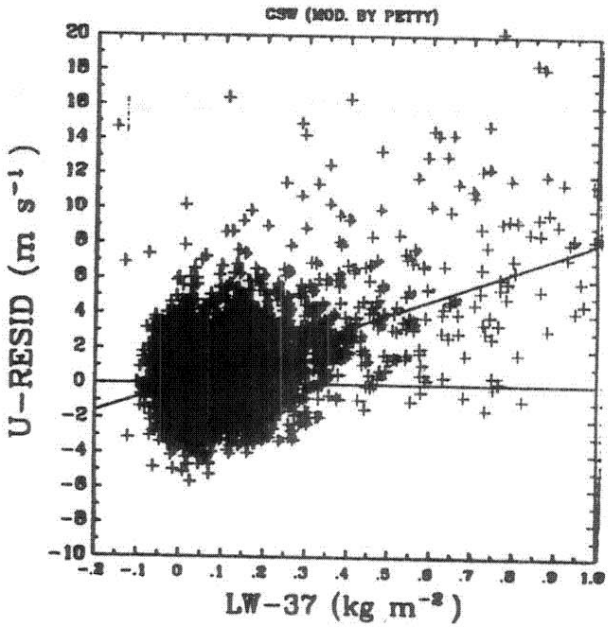
* GSW with WV corr. by PETTY	1.52	1.18	0.000	0.901
Petty physical (prelim.)	1.65	1.29	0.000	0.882
* GSW (Cal/Val)	1.65	1.29	0.000	0.882
* Revised GSW (GS 1992)	1.67	1.30	0.000	0.879
Wentz	1.78	1.35	0.000	0.861

* comparison data not independent


CSW
U-RESID (m s^{-1})
LW-37 (kg m^{-2})


REVISED CSW (CS 1992)
U-RESID (m s^{-1})
LW-37 (kg m^{-2})


WENTZ
U-RESID (m s^{-1})
LW-37 (kg m^{-2})


CSW (MOD. BY PETTY)
U-RESID (m s^{-1})
LW-37 (kg m^{-2})

RANDOM NOISE SENSITIVITY ANALYSIS

CASE 1 = (COOL)

Theta=53.0 WV=15.0 P =1013.0 Hv=1.6 ta=284.0 gamma=5.4 sst=284.0 u= 9.00 lw=0.100 zcld= 1.20

	Wind Speed (m/s)		Water vapor (kg/m**2)			Liquid Water (kg/m**2)		
	UW	UG	WVW	WVP	WVA	LWW	LW37	LW85
T19V	0.0	1.097	0.0	-0.4103E-01	-0.1486	0.0	-0.2347E-01	-0.8585E-02
T19H	0.0	0.0	0.0	0.0	0.0	0.0	0.0	0.0
T22V	0.0	-0.4555	0.7484	0.6508	0.7113	-0.8504E-02	0.5124E-02	-0.2257E-02
T37V	-2.170	-1.760	-0.1117	0.0	-0.3695	0.3768E-01	0.1272E-01	0.1438E-01
T37H	1.099	0.7860	-0.1606	-0.1339	0.0	-0.4448E-02	0.9018E-02	-0.5192E-02
T85V	0.0	0.0	0.0	0.0	0.0	0.0	0.0	-0.1145E-01
T85H	0.0	0.0	0.0	0.0	0.0	0.0	0.0	0.1185E-01
NET	2.432	2.264	0.7736	0.6657	0.8152	0.3888E-01	0.2864E-01	0.2417E-01

CASE 2 = (TEMPERATE)

Theta=53.0 WV=35.0 P =1013.0 Hv=1.7 ta=298.0 gamma=5.7 sst=298.0 u= 7.00 lw=0.100 zcld= 2.00

	Wind Speed (m/s)		Water vapor (kg/m**2)			Liquid Water (kg/m**2)		
	UW	UG	WVW	WVP	WVA	LWW	LW37	LW85
T19V	0.0	1.097	0.0	-0.4813E-01	-0.1486	0.0	-0.2523E-01	-0.8519E-02
T19H	0.0	0.0	0.0	0.0	0.0	0.0	0.0	0.0
T22V	0.0	-0.4555	0.9826	0.9611	1.091	-0.1117E-01	0.3132E-02	-0.5108E-02
T37V	-2.000	-1.760	-0.7972E-01	0.0	-0.3695	0.3272E-01	0.1422E-01	0.1438E-01
T37H	1.068	0.7860	-0.1639	-0.1461	0.0	-0.2720E-02	0.9244E-02	-0.5079E-02
T85V	0.0	0.0	0.0	0.0	0.0	0.0	0.0	-0.1741E-01
T85H	0.0	0.0	0.0	0.0	0.0	0.0	0.0	0.1835E-01
NET	2.267	2.264	0.9994	0.9733	1.161	0.3468E-01	0.3056E-01	0.3116E-01

CASE 3 = (TROPICAL)

Theta=53.0 WV=55.0 P =1013.0 Hv=2.3 ta=301.0 gamma=5.7 sst=301.0 u= 5.00 lw=0.100 zcld= 2.40

	Wind Speed (m/s)		Water vapor (kg/m**2)			Liquid Water (kg/m**2)		
	UW	UG	WVW	WVP	WVA	LWW	LW37	LW85
T19V	0.0	1.097	0.0	-0.5554E-01	-0.1486	0.0	-0.2802E-01	-0.8492E-02
T19H	0.0	0.0	0.0	0.0	0.0	0.0	0.0	0.0
T22V	0.0	-0.4555	1.433	1.386	1.335	-0.1629E-01	-0.1575E-03	-0.9016E-02
T37V	-2.127	-1.760	0.1858E-02	0.0	-0.3695	0.3555E-01	0.1618E-01	0.1438E-01
T37H	1.128	0.7860	-0.1866	-0.1635	0.0	-0.1472E-02	0.1003E-01	-0.4920E-02
T85V	0.0	0.0	0.0	0.0	0.0	0.0	0.0	-0.2623E-01
T85H	0.0	0.0	0.0	0.0	0.0	0.0	0.0	0.2844E-01
NET	2.408	2.264	1.446	1.397	1.393	0.3913E-01	0.3388E-01	0.4336E-01

Went Col/Val Went Petty Col/Va Went 37 GH 85 GH Petty Petty

**** CROSSTALK ANALYSIS ****

CASE 1 = (COOL)

Theta=53.0 WV=15.0 P =1013.0 Hv=1.6 ta=284.0 gamma=5.4 sst=284.0 u= 9.00 lw=0.100 zcld= 0.60

	UW	UG	UGM	WVW	WVP	WVA	LWW	LW37	LW85	
dtheta = 0.2	0.01	-0.41	-0.38	-0.03	0.23	0.07	-0.001	-0.004	-0.002	VIEWING ANGLE
ethet = 0.1	0.44	0.00	0.00	-0.15	0.00	0.00	-0.006	0.000	0.000	VIEW.ANG. ERR.
dwv = 10.0	-0.23	0.77	1.45	9.04	7.32	7.16	0.055	0.065	0.041	WATER VAPOR
dhwv = 0.3	0.07	-0.38	-0.33	0.41	0.36	0.46	-0.015	-0.002	-0.007	WV SCALE HT.
du = 5.0	5.16	5.73	5.80	0.45	0.55	0.77	0.014	0.042	0.010	WIND SPEED
dalw = 0.2	-0.80	0.11	0.11	-0.13	-0.05	-1.14	0.287	0.232	0.210	LIQ WATER
dzcld = 1.2	0.20	0.23	0.23	0.00	0.00	-0.05	0.014	0.013	0.005	CLD HEIGHT
dsst = 4.0	0.26	-0.09	0.02	0.08	0.91	0.94	-0.032	-0.034	-0.018	SFC TMP
esst = 1.0	0.16	0.00	0.00	-0.23	0.00	0.00	0.000	0.000	0.000	SST ERR,
ta-sst = 4.0	-0.58	-0.66	-0.59	0.68	0.59	0.59	-0.014	-0.011	-0.004	AIR-SEA DIFF
dgam = 0.4	0.22	0.22	0.21	-0.15	-0.13	-0.10	-0.001	0.000	-0.001	LAPSE RATE
dp = 12.0	0.03	0.16	0.14	-0.18	-0.16	-0.20	0.009	0.005	0.002	SFC PRES.
CROSSTALK IND	1.19	1.22	1.68	0.99	1.31	1.84	0.071	0.087	0.047	

CASE 2 = (TEMPERATE)

Theta=53.0 WV=35.0 P =1013.0 Hv=1.7 ta=298.0 gamma=5.7 sst=298.0 u= 7.00 lw=0.100 zcld= 1.00

	UW	UG	UGM	WVW	WVP	WVA	LWW	LW37	LW85	
dtheta = 0.2	0.00	-0.37	-0.39	-0.06	0.31	0.17	-0.001	-0.005	-0.003	VIEWING ANGLE
ethet = 0.1	0.40	0.00	0.00	-0.20	0.00	0.00	-0.005	0.000	0.000	VIEW.ANG. ERR.
dwv = 10.0	-0.25	1.42	0.80	8.27	7.60	7.41	0.068	0.044	0.036	WATER VAPOR
dhwv = 0.2	0.11	-0.41	-0.44	0.60	0.58	0.77	-0.025	-0.008	-0.014	WV SCALE HT.
du = 5.0	5.02	5.79	5.75	0.47	0.65	1.04	0.030	0.042	0.017	WIND SPEED
dalw = 0.2	-0.50	-0.44	-0.43	-0.21	-0.13	-0.84	0.210	0.182	0.166	LIQ WATER
dzcld = 2.0	0.27	0.24	0.25	-0.07	-0.07	-0.11	0.018	0.018	0.010	CLD HEIGHT
dsst = 2.5	0.15	-0.49	-0.58	0.19	1.66	1.61	-0.024	-0.025	-0.022	SFC TMP
esst = 1.0	0.49	0.00	0.00	-0.62	0.00	0.00	-0.004	0.000	0.000	SST ERR,
ta-sst = 2.5	-0.41	-0.54	-0.60	1.11	1.06	1.14	-0.017	-0.011	-0.012	AIR-SEA DIFF
dgam = 0.3	0.17	0.22	0.23	-0.30	-0.29	-0.30	0.001	0.000	0.001	LAPSE RATE
dp = 6.3	0.01	0.12	0.13	-0.21	-0.20	-0.25	0.007	0.003	0.002	SFC PRES.
CROSSTALK IND	1.01	1.78	1.41	1.57	2.21	2.54	0.086	0.070	0.050	

CASE 3 = (TROPICAL)

Theta=53.0 WV=55.0 P =1013.0 Hv=2.3 ta=301.0 gamma=5.7 sst=301.0 u= 5.00 lw=0.100 zcld= 1.20

	UW	UG	UGM	WVW	WVP	WVA	LWW	LW37	LW85	
dtheta = 0.2	0.01	-0.29	-0.36	-0.11	0.34	0.16	0.000	-0.005	-0.003	VIEWING ANGLE
ethet = 0.1	0.39	0.00	0.00	-0.25	0.00	0.00	-0.004	0.000	0.000	VIEW.ANG. ERR.
dwv = 10.0	-0.23	2.17	0.68	7.13	6.36	4.93	0.078	0.019	0.039	WATER VAPOR
dhwv = 0.2	0.18	-0.32	-0.40	0.41	0.40	0.54	-0.030	-0.012	-0.016	WV SCALE HT.
du = 5.0	5.46	5.18	5.20	-0.41	-0.13	0.35	0.016	0.040	0.030	WIND SPEED
dalw = 0.2	-0.52	-0.19	-0.11	-0.41	-0.38	-1.06	0.200	0.165	0.149	LIQ WATER
dzcld = 2.4	0.35	0.33	0.37	-0.18	-0.17	-0.19	0.021	0.019	0.011	CLD HEIGHT
dsst = 1.3	0.12	-0.38	-0.71	0.18	1.54	1.32	-0.018	-0.019	-0.020	SFC TMP
esst = 1.0	0.63	0.00	0.00	-1.08	0.00	0.00	-0.004	0.000	0.000	SST ERR,
ta-sst = 1.3	-0.30	-0.38	-0.62	1.22	1.13	1.05	-0.016	-0.010	-0.013	AIR-SEA DIFF
dgam = 0.2	0.15	0.21	0.32	-0.54	-0.50	-0.45	0.003	0.001	0.003	LAPSE RATE
dp = 5.2	0.01	0.12	0.17	-0.27	-0.26	-0.27	0.007	0.003	0.003	SFC PRES.
CROSSTALK IND	1.07	2.32	1.39	1.93	2.11	2.17	0.091	0.054	0.058	

ABSOLUTE RETRIEVAL VALUES

U	UW	UG	UGM	WV	WVW	WVP	WVA	LW	LWW	LW37	LW85
9.00	9.66	9.05	9.01	15.00	13.69	12.23	12.43	0.100	0.147	0.155	0.173
7.00	8.21	6.60	7.33	35.00	32.11	33.74	33.95	0.100	0.104	0.123	0.138
5.00	6.07	6.26	4.45	55.00	50.68	53.34	52.36	0.100	0.118	0.102	0.103

PRELIMINARY CONCLUSIONS
(pending availability of more independent data)

- Cal/Val algorithm gives best RMS error of unmodified algorithms, but significant non-linear water vapor dependent bias

- Significant improvement in RMS errors with subtraction of bias (1.56 m/s)

- Wentz retrievals unbiased but noisy

- Revised Goodberlet and Swift (1992) algorithm still shows water vapor bias; poorer RMS errors outside of heavy cloud

- Precipitation / cloud flags in Cal/Val algorithm unreliable

SSM/I Wind Speed Retrieval Using Neural Networks

By

A. Stogryn

Aerojet Electronic Systems Division, Azusa, California

ABSTRACT

Two fully connected, feed forward neural networks with two neurodes in the hidden layer have been developed by Stogryn, Butler, and Bartolac[1] for wind speed retrievals using SSM/I brightness temperatures. For clear sky conditions, the rms wind speed retrieval error is 1.41 m/sec. A second network, designed for use under adverse weather conditions yielded an rms wind retrieval error of 2.39 m/sec. The latter value represents a factor of more than two improvements over the alternate algorithms that were examined for non-clear conditions.

(1) Paper submitted to Journal of Geophysical Research.

SPN SSM/I ALGORITHM SYMPOSIUM
Algorithm Questionnaire

"SURFACE WIND SPEED ALGORITHM"
Alex Stogryn, respondent

Please provide the following essential information about your algorithm(s).

* ALGORITHM DESCRIPTION

- Type (statistical, physical, other) *Neural network*

- Input required / Output produced

Input: Brightness temperatures from 19 GHz (v-pol); 22 GHz (v-pol) 37 GHz (v- and h-pol);
Output: Ocean surface wind speed

- Auxiliary sensor/data base requirements *None*

- Major limitations / approximations

Will not be usable under medium/heavy rain or very heavy cloud conditions.

- Computer resource requirements *Minimal*

* ALGORITHM PERFORMANCE

- Development / test data sets (regional / global / seasonal)

Used original Cal/Val SSM/I - Buoy data set

- Ground truth (accuracy / limitations)

Better coverage of tropical areas would be desireable. Need better representation of high (> 20 m/s) wind speeds in data base.

- Major assumptions of evaluation

Assume that SSM/I - buoy data set was truly representative of global conditions.

Strengths / weaknesses

Simple computer logic.

* ALGORITHM MATURITY

- Operational useage

Ready for use.

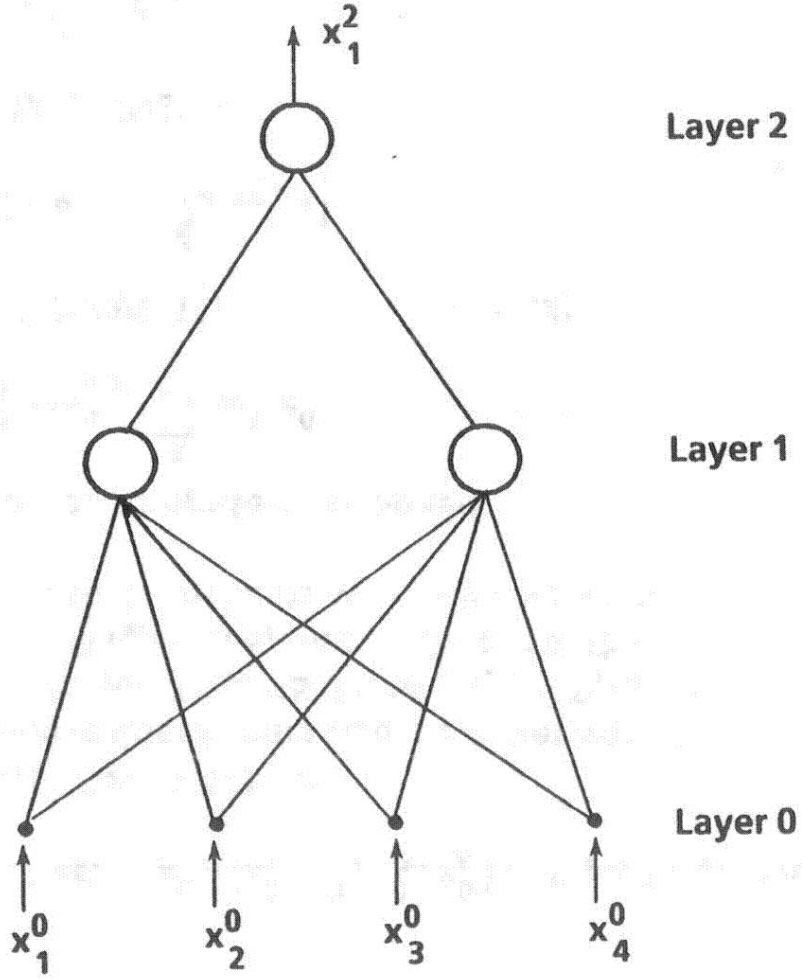
- Refinement / additional development

Much larger data set for validation and/or additonal training of neural networks would be desireable.

- Availability

Algorithm is available upon request.

Architecture Of Neural Networks Used For Wind Speed Retrieval



Neural Network Wind Speed Computation

1. Input Vector $x^0 = (x_1^0, x_2^0, x_3^0, x_4^0) = (T_{19V}, T_{22V}, T_{37V}, T_{37H})$

2. If $(T_{37V} - T_{37H} > 50)$ Then
   Choose Coefficients w, α, β For Network 1
   Else If $((T_{37V} - T_{37H} \leq 50)$ And $(T_{19V} \leq T_{37V})$ And
   $(T_{19H} < 185)$ And $(T_{37H} < 210)$ Then
   Choose Coefficients w, α, β For Network 2
   Else
   Do Not Compute Wind Speed

3. $NET_i^1 = w_{i\,o}^1 + \sum_{j=1}^{4} w_{i\,j}^1 x_j^0 \qquad (i = 1,2)$

   $x_i^1 = TANH\,(NET_i^1) \qquad (i = 1,2)$

   $NET_1^2 = w_{10}^2 + \sum_{j=1}^{2} w_{1\,j}^2 x_j^1$

   $x_1^2 = TANH\,(NET_1^2)$

   $w = \alpha\, x_1^2 + \beta$

593-1175x

Coefficients For Neural Networks

Coefficient	Network 1	Network 2
w_{10}^1	$.51201 \times 10^1$	$-.45894 \times 10^1$
w_{20}^1	$-.85913 \times 10^1$	$-.23821 \times 10^1$
w_{11}^1	$-.45846 \times 10^{-1}$	$.29969 \times 10^{-1}$
w_{21}^1	$-.20847 \times 10^{-2}$	$-.10475 \times 10^0$
w_{12}^1	$.12842 \times 10^{-1}$	$-.55465 \times 10^{-2}$
w_{22}^1	$.38434 \times 10^{-2}$	$.32067 \times 10^{-1}$
w_{13}^1	$.55038 \times 10^{-2}$	$.59813 \times 10^{-3}$
w_{23}^1	$.52710 \times 10^{-1}$	$.95475 \times 10^{-1}$
w_{14}^1	$-.30396 \times 10^{-2}$	$-.49660 \times 10^{-2}$
w_{24}^1	$-.22575 \times 10^{-1}$	$-.30870 \times 10^{-1}$
w_{10}^2	$-.11263 \times 10^1$	$-.80492 \times 10^0$
w_{11}^2	$-.98683 \times 10^0$	$-.18955 \times 10^1$
w_{12}^2	$-.15381 \times 10^1$	$-.11758 \times 10^1$
α	$.22777 \times 10^2$	$.20761 \times 10^2$
β	$.13333 \times 10^2$	$-.45291 \times 10^0$

593-1176x

Retrieval Performance (m/sec) Of Wind Speed Algorithms For $T_{37V} - T_{37H} > 50K$

Model	Bias	rms Error
Neural Net	0.1	1.41
GSW	0.3	1.98
SL	0.4	1.97
Wentz	0.0	1.68

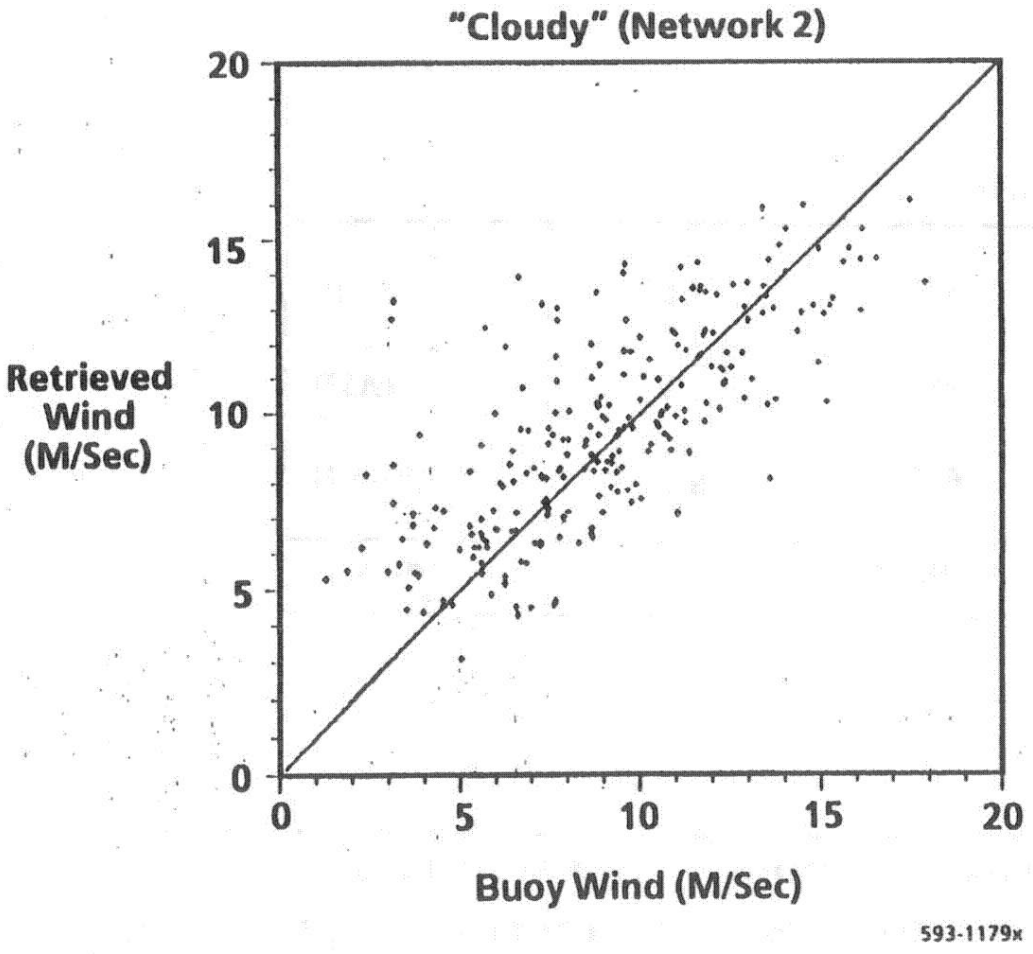
593-1177x

Retrieval Performance (m/sec) Of Wind Speed Algorithms For "Cloudy" Cases

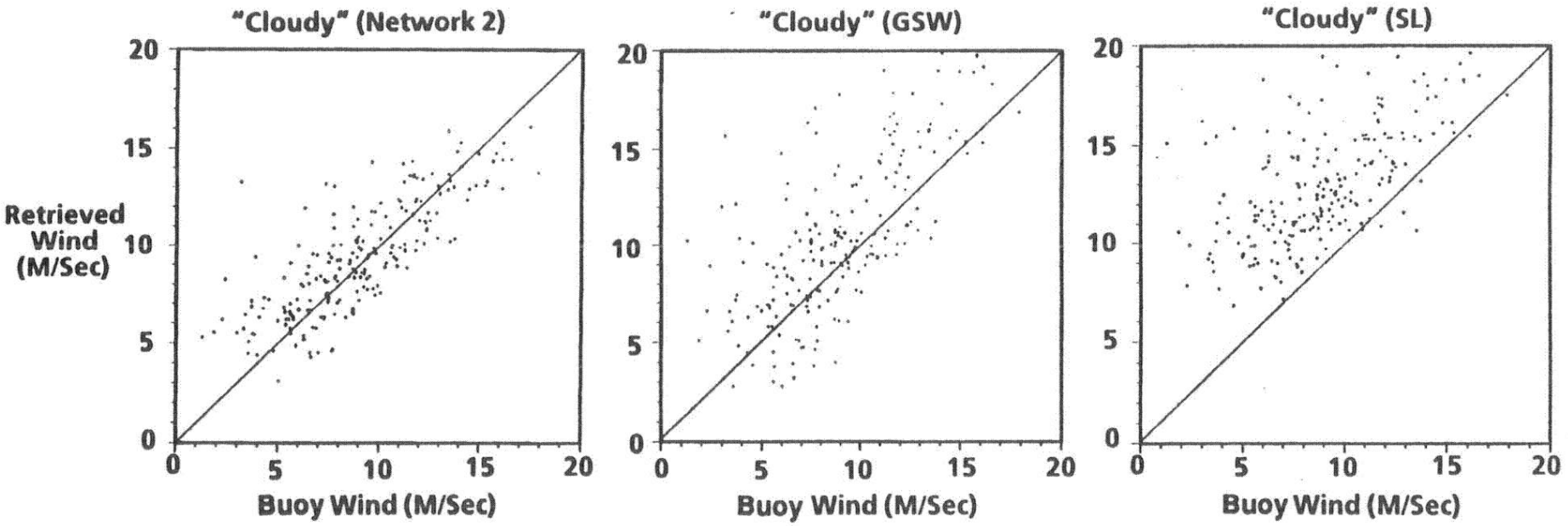
Model	Bias	rms Error
Neural Net	0.5	2.39
GSW	1.8	8.76
SL	4.5	5.69

593-1178x

Retrieved vs. Buoy Winds Using Neural Network For "Cloudy" Cases



Comparison Of Neural Network, GSW, And SL Algorithms For "Cloudy" Cases Restricted To $T_{37V} - T_{37H} > 35K$



Session 5

Precipitation

(Gene Poe, NRL, Chair)

ENCL(11)

Session 5

Precipitation

(Gene Poe, NRL, Chair)

Global Rain Rate Retrievals Using SSM/I Scattering and Emission Algorithms

Ralph R. Ferraro[1]
Norman C. Grody[1]
Gerard F. Marks[2]
Sheldon J. Kusselson[3]

Two types of rain algorithms have been developed and evaluated by the National Oceanic and Atmospheric Administration (NOAA), National Environmental Satellite, Data, and Information Service (NESDIS). The first is an improvement to the Grody Scattering Index (i.e., JGR-1991) which has been developed at the NOAA/Satellite Research Laboratory for the retrieval of global (e.g., land/water, all latitudes) rain rates. The algorithm consists of separate components over land and water and identifies the scattering signal of rain at 85 GHz from all other surface types. The second algorithm is an ocean only algorithm which is based upon the retrieval of liquid water at 19 GHz. Both algorithms have been calibrated against near co-incident measurements of ground-based radar data from sites in the United States, Japan, and the United Kingdom. Because global applicability is desired, the minimum retrieved rain rate is on the order of 1-2 mm/hr; any lower rain rate will introduce false signatures globally.

Comparisons of both algorithms with independent data from radar, rain gauge, and operational IR estimates generated by the NESDIS Synoptic Analysis Branch will be presented for a variety of storm systems. In addition, comparisons against the present "Cal/Val" rain algorithm will be shown. Finally, error statistics of all algorithms will be presented.

[1] NOAA/Satellite Research Laboratory
5200 Auth Road, Room 712
Camp Springs, MD 20746
301-763-8042

[2] S M Systems and Research Corporation
4201 Northview Drive, Suite 301
Bowie, MD 20716

[3] NESDIS/Synoptic Applications Branch
5200 Auth Road, Room 401
Camp Springs, MD 20746

Global Rain Rate Retrievals Using SSM/I Scattering and Emission Algorithms

Ralph R. Ferraro
Norman C. Grody

NOAA/Satellite Research Laboratory

Gerard F. Marks

S M Systems and Research Corp.

Sheldon J. Kussleson

NOAA/NESDIS Synoptic Analysis Branch

NOAA Scattering Algorithms

Utilizes the scattering properties of ice particles in rain layer to infer regions of rain.

Uses screening logic to separate other scattering surfaces.

Scattering Index (SI) for land and water; water SI is also sensitive to emission signal of rain.

SI(L)=[451.88-.44Tb(19v)-1.775Tb(22v)+.00574Tb(22v)^2]-Tb(85v)
SI(W)=[-174.38+.72Tb(19v)+2.439Tb(22v)-.00504Tb(22v)^2]-Tb(85v)

If SI>10K, then rain is present. Convert to Rain Rate via relationships with coincident radar.

Land: RR(mm/hr) = -2.71 + 0.362*SI(L)
Ocean: RR(mm/hr) = -1.05 + 0.149*SI(W)

NOAA Emission Algorithms

Valid over ocean only, these algorithms retrieve total liquid water content of clouds and rain.

Cloud liquid water (Q), can be derived using **any** of the SSM/I frequencies, although 19 and 37 GHz are best suited.

Varying cloud and sensor properties generally result in different values for Q19 and Q37 for the same footprint.

Q to rain rate relationships derived from radar matchups.

Retrieve rain if Q>0.4 mm:

$$RR(mm/hr) = -0.25 + 2.66*Q19$$
$$RR(mm/hr) = -0.17 + 0.31*Q37 + 5.50*Q37^2$$

A few words on verification....

There are 4 ways to verify the SSM/I rain algorithms, each of which contain **unique** information on the algorithm performance:

1. Rain/no-rain (instantaneous)

2. Rain rate (instantaneous)

3. Global rain fields - look for false signatures/noise

4. Monthly rain estimates - look for global rainfall distributions
   look for persistent errors (screening checks)

Co-incident radar data for instantaneous rain rate calibration/validation

1. AMeDAS - Japan

2. FRONTIERS - U.K.

3. RADAP-II - Tampa, FL

"Bin" data by 1 mm/hr categories and generate average SSM/I value

Statistics for Cal/Val and SI(LW)

Statistics vs. radar data (linear fit: SSM/I = A*RADAR + B)

		Cal/Val			NOAA SI(LW)				
Radar	**Surface**	**A**	**B**	**Corr.**	**A**	**B**	**Corr.**	**#obs**	**RR Range**
AMeDAS	Land	0.09	0.84	0.92	0.84	1.09	0.93	1269	0-17 mm/hr
Frontiers	Land	0.06	1.02	0.80	0.98	-1.04	0.94	1526	0-7
AMeDAS	Ocean	0.31	0.70	0.85	0.88	1.06	0.90	6400	0-15
Frontiers	Ocean	0.15	1.33	0.85	0.80	1.09	0.93	734	0-4
RADAP	Ocean	0.16	1.75	0.77	0.30	5.10	0.67	479	0-12

Intercorrelations (linear fit: Cal/Val = A*NOAA SI + B)

Radar	**Surface**	**A**	**B**	**Corr.**
AMeDAS	Land	0.10	0.74	0.99
Frontiers	Land	0.07	1.01	0.94
AMeDAS	Ocean	0.33	0.40	0.95
Frontiers	Ocean	0.20	1.09	0.98
RADAP	Ocean	0.35	0.25	0.60

Summary

Cal/Val algorithm:

1. Rain rates too low over land (at least a factor of 5) and ocean (at least a factor of 3).

2. Highly sensitive to mid-high latitude ocean rain

3. Screening logic does not allow for mid-high latitude, cold season land retrievals.

NOAA algorithms:

1. Q37 most similar to cal/val high-latitude ocean rain.

2. SI(LW) **best overall algorithm for global rain retrievals**; may underestimate oceanic high-latitude rains.

3. Screening logic allows for retrievals **over all land, independent of latitude**.

Recommendations

Three options for improvements to current rain algorithm:

1. Leave Cal/Val as is, but make improvements for:
   a. more retrievals over land
   b. increase/improve calibration to generate higher rain rates

2. Implement NOAA SI(LW).

3. Blended algorithm:
   a. NOAA SI(L) over land.
   b. Take maximum of SI(W) and Cal/Val over ocean.
   [**note**: results from AIP/2 (8/93) may help answer high-latitude rain issue.]

Review abstract for
Shared Processing Network SSM/I Algorithm Symposium
FNOC, Monterey, CA, 8-10 June, 1993

PRECIPITATION ESTIMATION FROM SSM/I DATA WITH THE GODDARD SCATTERING ALGORITHM

G.J. Huffman
USRA, Laboratory for Atmospheres, Goddard Space Flight Center
R.F. Adler
Laboratory for Atmospheres, Goddard Space Flight Center

The Goddard Scattering Algorithm (GSCAT) provides fine-scale global estimates of instantaneous precipitation rate from SSM/I data. A preprocessing module applies quality-control screening logic to the SSM/I data. The first step of GSCAT is to use all SSM/I channels in various empirical relationships to mask off non-precipitating areas. Some pixels are marked "ambiguous," indicating uncertainty about whether they represent (cold) surface conditions or precipitation. Second, the precipitation rate is estimated for non-masked pixels from the horizontally polarized 85.5 GHz T_a according to a numerical model-based regression equation. The masking and rainrate relationships are varied according to the underlying surface type. Finally, ambiguous pixels are accepted or deleted. Scene-by-scene acceptance can be done subjectively or by simple neighborhood comparison. Acceptance for pentads and months is done by setting an empirical threshold on fractional coverage of ambiguous and "cold surface" pixels.

Validation against the Global Precipitation Climatology Centre raingage analyses (monthly 2.5°x2.5° grids over/near land) has been carried out for July 1987 to June 1988. GSCAT is competitive with the analyses and better than rainrates inferred from infrared data with the Arkin GPI technique (tropics and subtropics only). Preliminary validation for the same period against the Morrissey Pacific atoll data indicates rough parity with the GPI in that area. The main uncertainty in GSCAT is the inability to detect warm rain.

SPN SSM/I ALGORITHM SYMPOSIUM
Algorithm Questionnaire

"GSCAT2 (Goddard Scattering Algorithm, Version 2)"
Rain Rate Algorithm (Adler, Huffman, Negri)
George Huffman, respondent

Please provide the following essential information about your algorithm(s).

* ALGORITHM DESCRIPTION

- Type (statistical, physical, other) *Statistical precipitation estimator*

- Input required / Output produced

Input: Antenna Temperatures from 19 GHz (v- and h-pol); 22 GHz (v-pol) 37 GHz (v- and h-pol); 85 Ghz (h-pol)
Output: Instantaneous rainrate and certainty flags in scan-orbit coordinates, or 0.5 by 0.5 degree lat-lon grid

- Auxiliary sensor/data base requirements

Surface type data base, currently Wentz-CIA coast-thickened coast

- Major limitations / approximations

Rainrate (after masking) is only a simple linear function of T(85GHz; h-pol), and this function is different for each of land, ocean, coast surface types.

- Computer resource requirements

About 10 CPU minutes/day on a Silicon Graphics, Inc. 4D310S with 8mm tape input and 64 mB RAM, to go from Remote Sensing Systems archive tapes to the listed output (plus other).

* ALGORITHM PERFORMANCE

- Development / test data sets (regional / global / seasonal)

AIP1 (regional monthly) and AIP2 (regional swaths; in progress); Morrissey atoll data (West Pacific monthly); GPCC (global, monthly, mostly land) rain gauge data

- Ground truth (accuracy / limitations)

Radar doesn't actually measure rain and Z-R calibration equation is questionable. AIP1 radars are not always turned on, at least one AIP2 radar is "wet". Rain gauge data do

not provide uniform coverage and they "undercatch" rain, particularly in windy or snow conditions

- Major assumptions of evaluation

Mostly interested in monthly results and mostly forced to validate data on 2.5 by 2.5 deg lat-lon boxes

- Strengths / weaknesses

Monthly results competitive with other precipitation estimates from SSM/I; realistic amplitude in many features, such as ICTZ; reasonable correlation with verification on monthly scale, given sampling limitations

Algorithm can not retrieve precipitaion over frozen, cold, wet ground, ice, ice pack, and some land/water interfaces; can't recognize or correctly handle shallow, "orographic" and "warm" rain; perhaps is underestimating precipitation in polar waters

* ALGORITHM MATURITY

- Operational useage

Run for three years of SSM/I data by Remote Sensing Systems and two years of data in-house

- Refinement / additional development

Looking at: 1) behavior in high polar oceans; 2) shift to using brightness temperatures instead of antenna temperatures; 3) verification against GPCC and NWP model

- Availability

Algorithm is available upon request. Implemented "as is" by F. Wentz of Remote Sensing Systems and NASA/MSFC Pathfinder group; code is large, but "clean".

Precipitation Estimation from SSM/I Data with the Goddard Scattering Algorithm

George J. Huffman (USRA) and Robert F. Adler
NASA/GSFC Code 912

1. Introduction

GSCAT (the Goddard Scattering Algorithm)

- was developed on F8 T_a
- with missing T_a(86v)
- for global fine-grid monthly precip estimates.

Method: In the original scan-orbit coordinate system

1. screen for non-precipitating pixels with all channels, and
2. apply simple T_a(86h)-rainrate regression relations from a numerical model.

2. Preprocessing

1. Apply quality control to all channels:
   - missing
   - bad orbit segments
   - unphysical temperatures
   - jumps in scan-average values

2. Bilinearly interpolate low-res channels to T(86) res

3. Find navigation-based surface type flag
   - guarantee consistancy between lat/lon and flag
   - Wentz sfc plus CIA coast; coast thickened to 75 km

3. Screening Non-precipitating Pixels

Many of the tests are adapted from prior work:

- Adler/Negri "cold ocean" test (water)
  86h > 37h
  37h < 185

- Grody "light precip" test (water)
  22v < 255
  22v < 158 + .49 * 86h

- Grody "desert sand polarization" test (land)
  19v - 19h > 20

- Adler/Negri "not-coast" test (coast)
  86h - 37h < -10

- Adler/Negri "coast" test (coast)
  sd (86h) > 10
  cr_cor (37h,86h) > .5
  slope (37h,86h) < 1.2

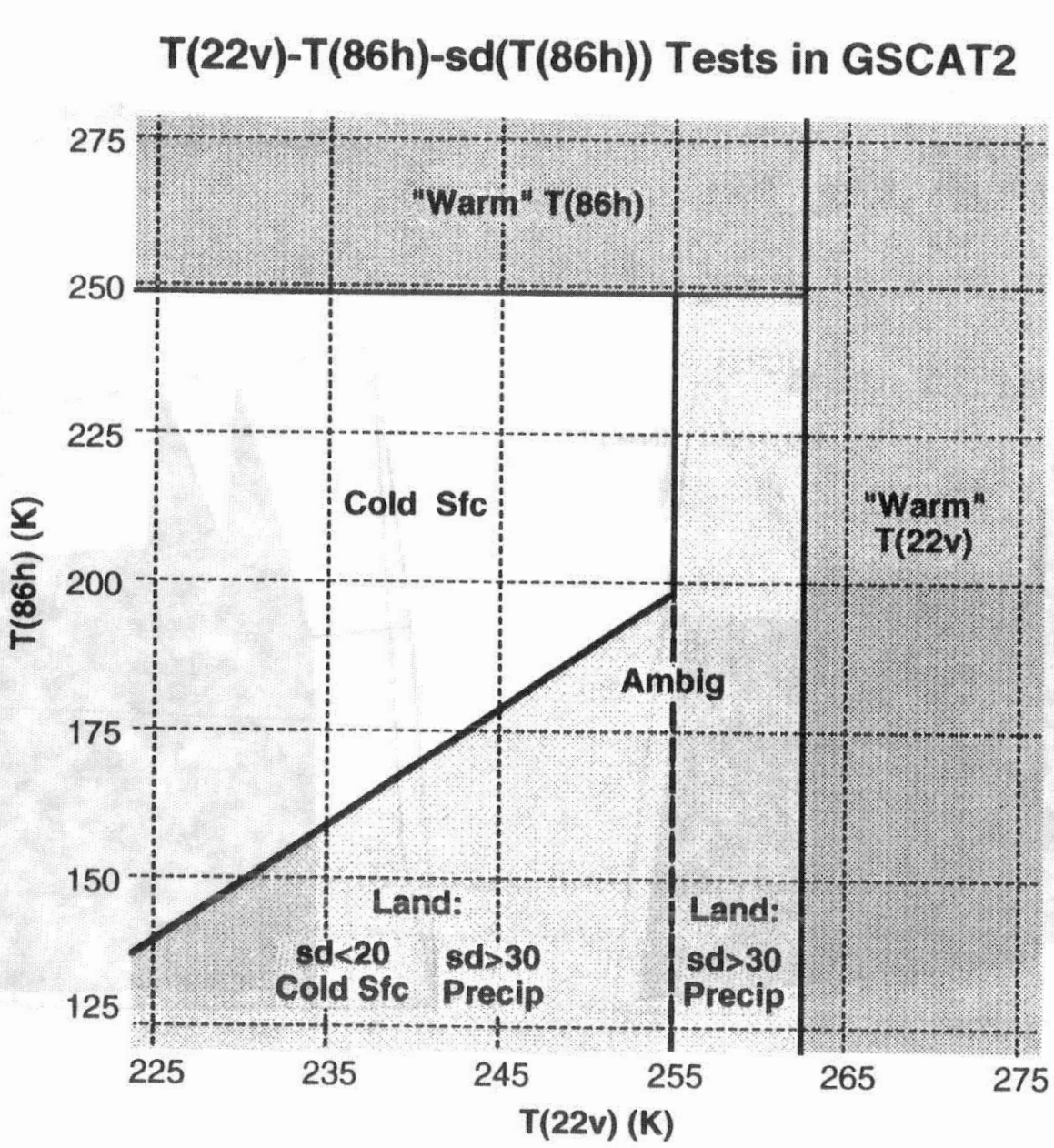
Other tests are grouped in a "22/86 wedding cake":

- Channel value combinations that sometimes represent precip and sometimes represent cold surface are classified as "ambiguous."

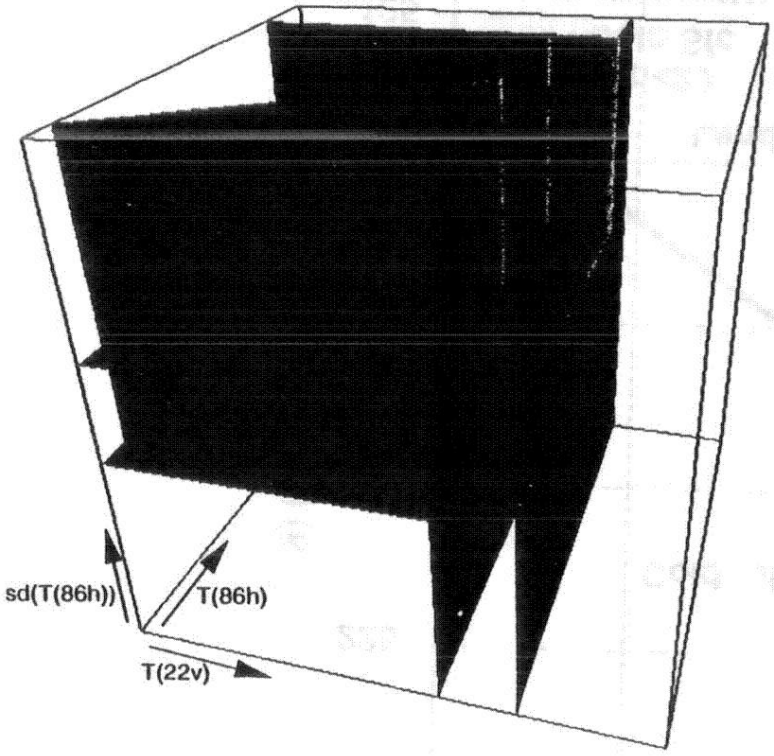
- The rainrate on these pixels is computed, but marked for possible deletion.

- The "ambiguous" range is trimmed over land sfc type by noting that
  1. "high" sd (86h) is always convection, and
  2. "low" sd (86h) at low 22v is cold surface.

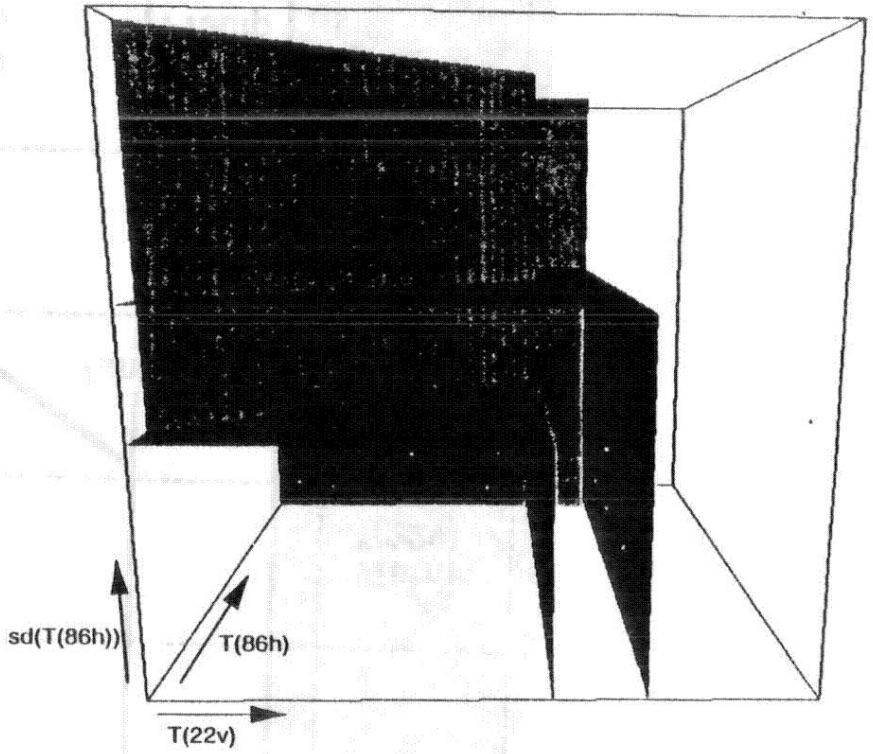
- Tests on sd (86h) are only done over land sfc type, since background fluctuations are large over other sfc types.


T(22v)-T(86h)-sd(T(86h)) Tests in GSCAT2
"Warm" T(86h)
Cold Sfc
"Warm"
T(22v)
Ambig
Land:
sd<20
Cold Sfc
sd>30
Precip
Land:
sd>30
Precip
T(86h) (K)
275
250
225
200
175
150
125
225
235
245
255
265
275
T(22v) (K)

REPRODUCED AT GOVERNMENT EXPENSE



T(22v) – T(86h) – sd(T(86h)) Tests in GSCAT2, Perspective 1



T(22v) – T(86h) – sd(T(86h)) Tests in GSCAT2, Perspective 2

REPRODUCED AT GOVERNMENT EXPENSE

The heart of GSCAT is implemented as a decision tree.

The decision tree is in two layers:

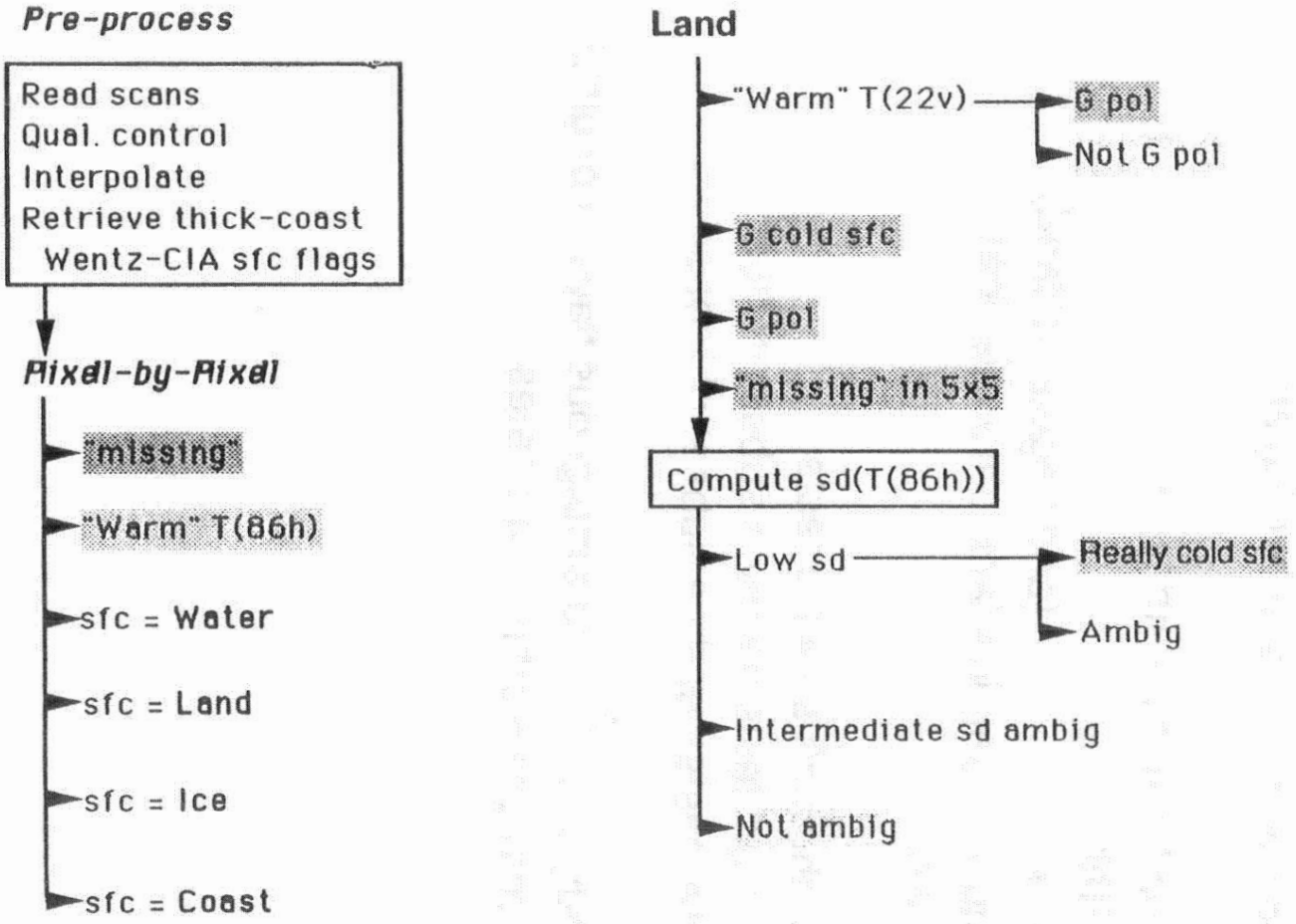
1. (mostly) sort by sfc type
   water
   land (and vegetated land)
   possible sea ice (and perennial ice)
   coast

2. run through specific tests
   "water" tests nearly a subset of "ice"
   "ice" tests nearly a subset of "coast"

The output is "$\hat{T}$" and ambiguous flags in original (high-res) scan-orbit coordinates.

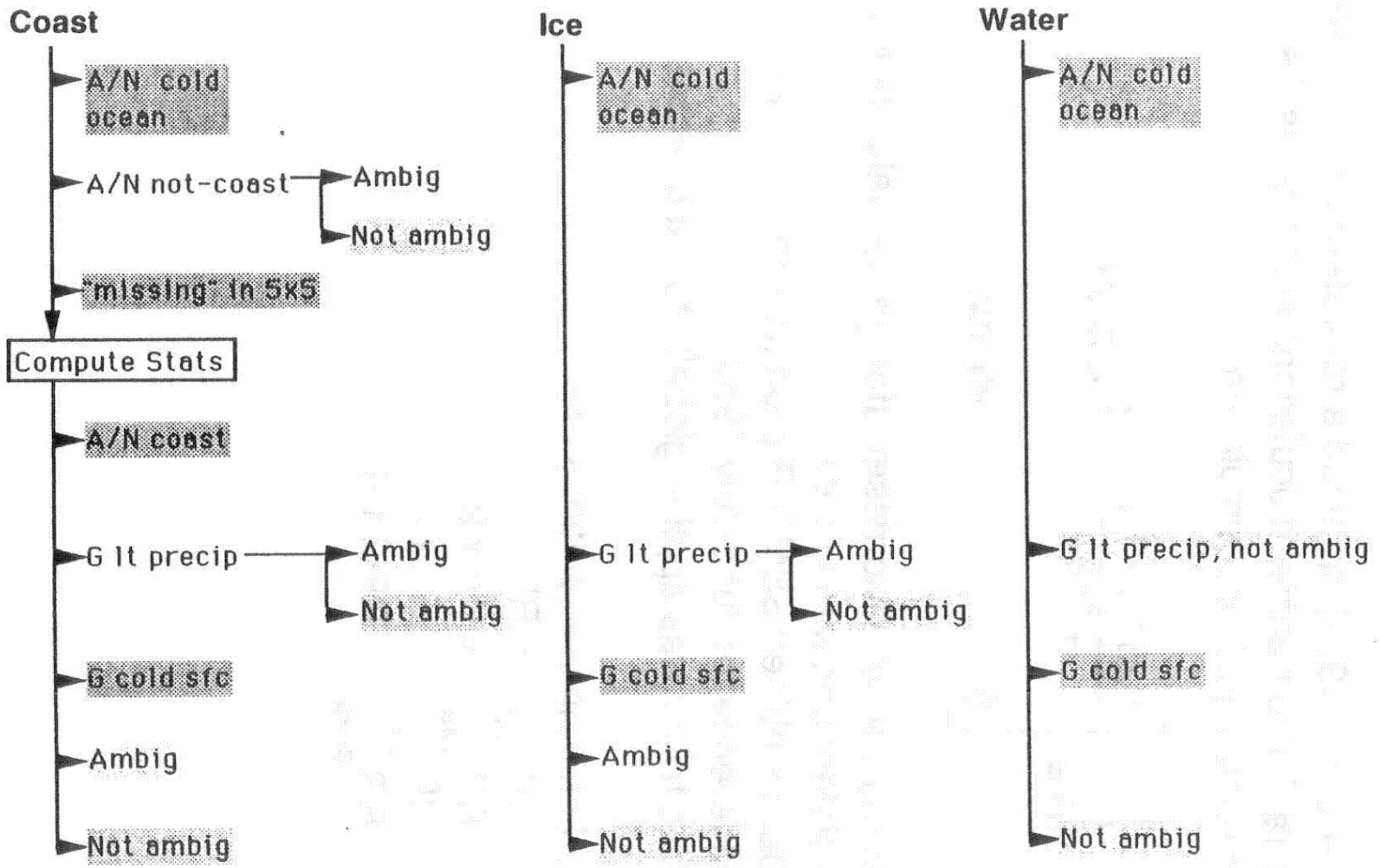
REPRODUCED AT GOVERNMENT EXPENSE

Goddard Scattering Algorithm, Version 2



REPRODUCED AT GOVERNMENT EXPENSE

GSCAT2, cont.



REPRODUCED AT GOVERNMENT EXPENSE

4. Scattering Estimates of Precip

Adler et al. (1991) deduced a rainrate-microwave relation in a radiative transfer calculations with the results of a numerical squall line simulation:

$$RR = \begin{cases} \dfrac{(251.0 - \uparrow T)}{4.188} & \uparrow T < 247K \\ 0 & \text{otherwise} \end{cases}$$

Comparison with Morrissey atoll gauge data showed consistent underestimates:

- Our combined SSM/I-IR product showed a factor of 2.0 difference for June-July 1989.
- This factor was applied globally to water areas.

The final rainrate relations are:

$$RR_{land} = RR$$
$$RR_{water} = RR \times 2$$
$$RR_{ice} = RR \times 2$$
$$RR_{coast} = RR \times 1.5$$

REPRODUCED AT GOVERNMENT EXPENSE

5. Examples and Validation

Hurricane Hugo

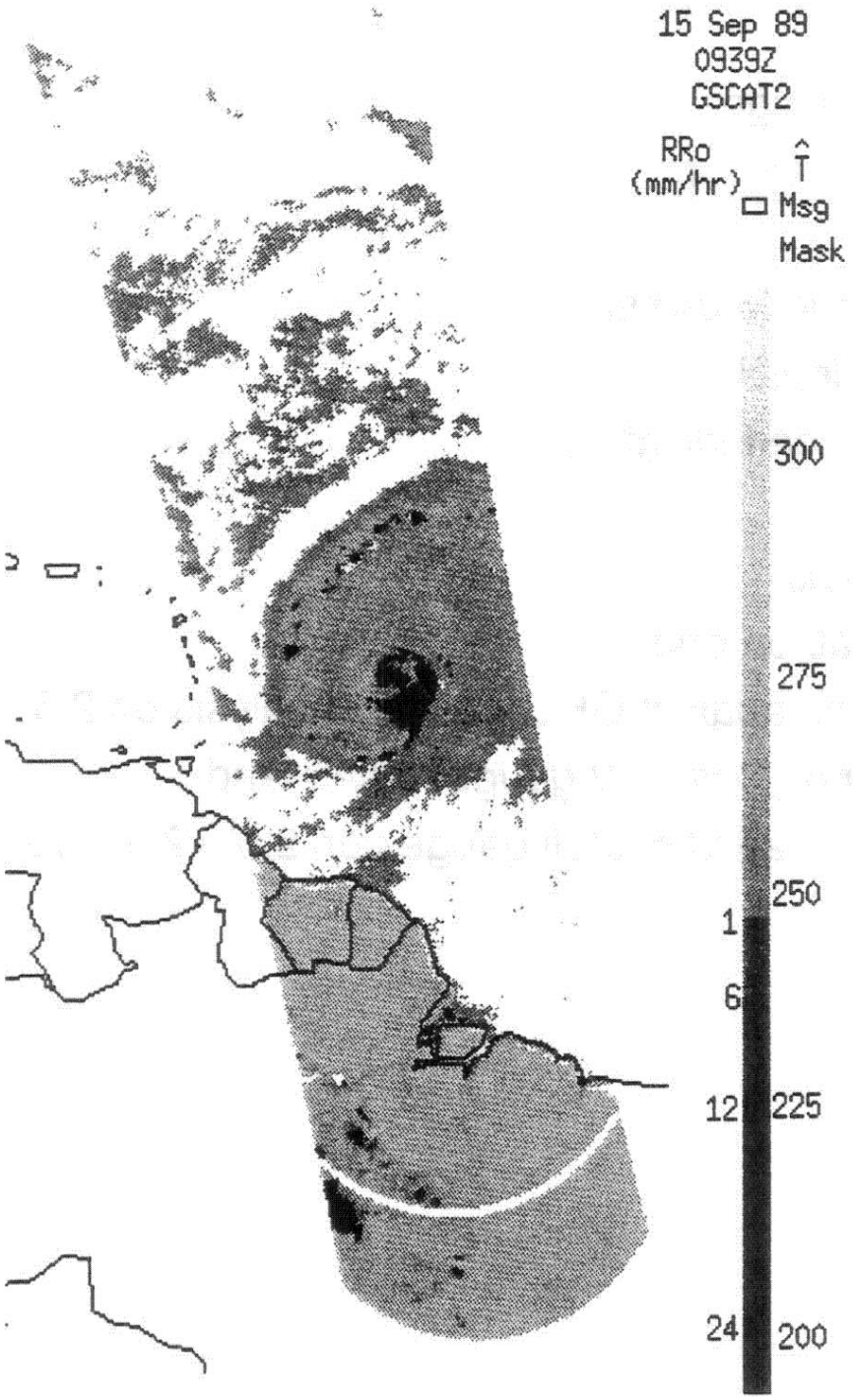
- Precip depiction

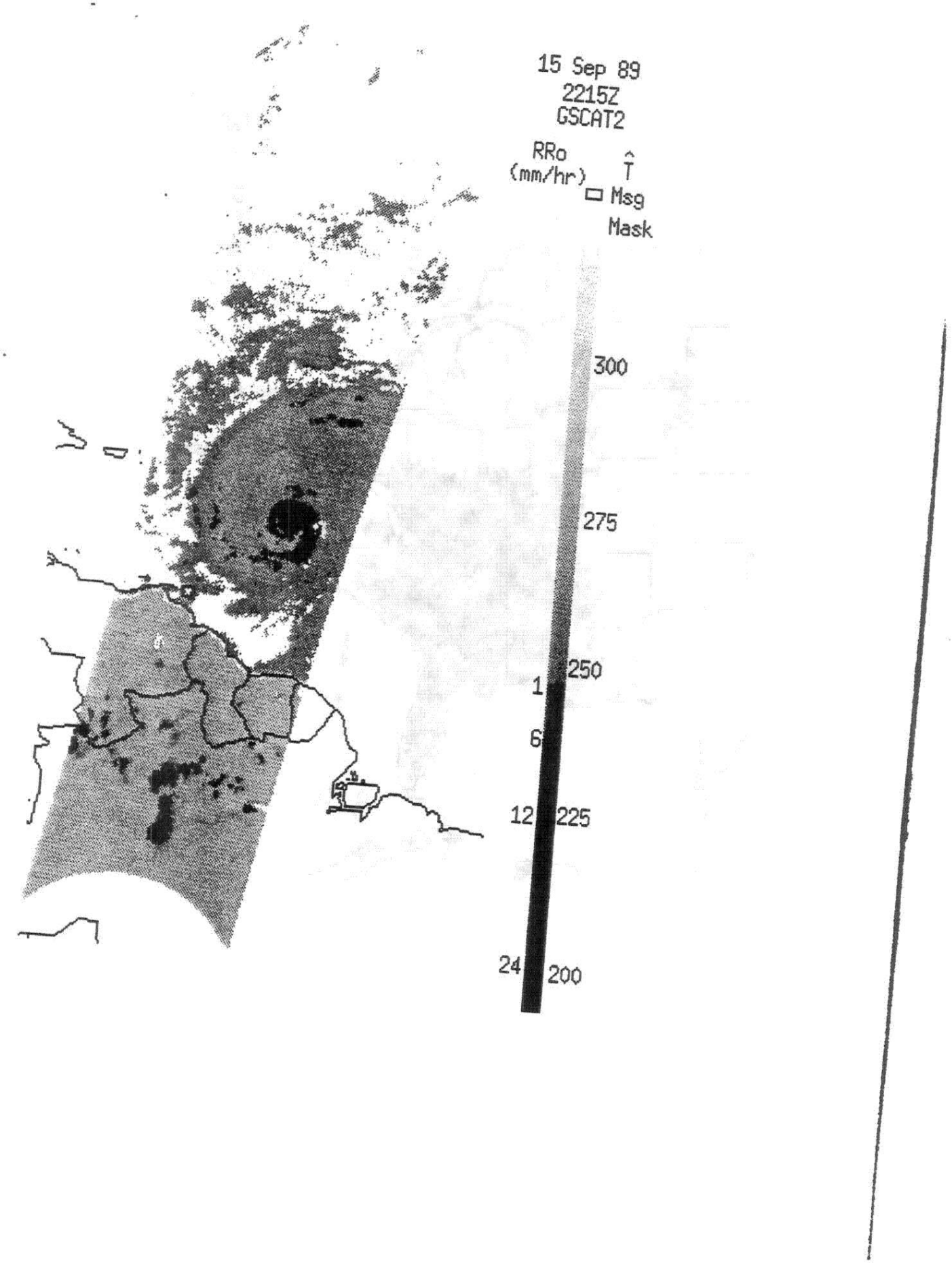
Rain band in Midwest

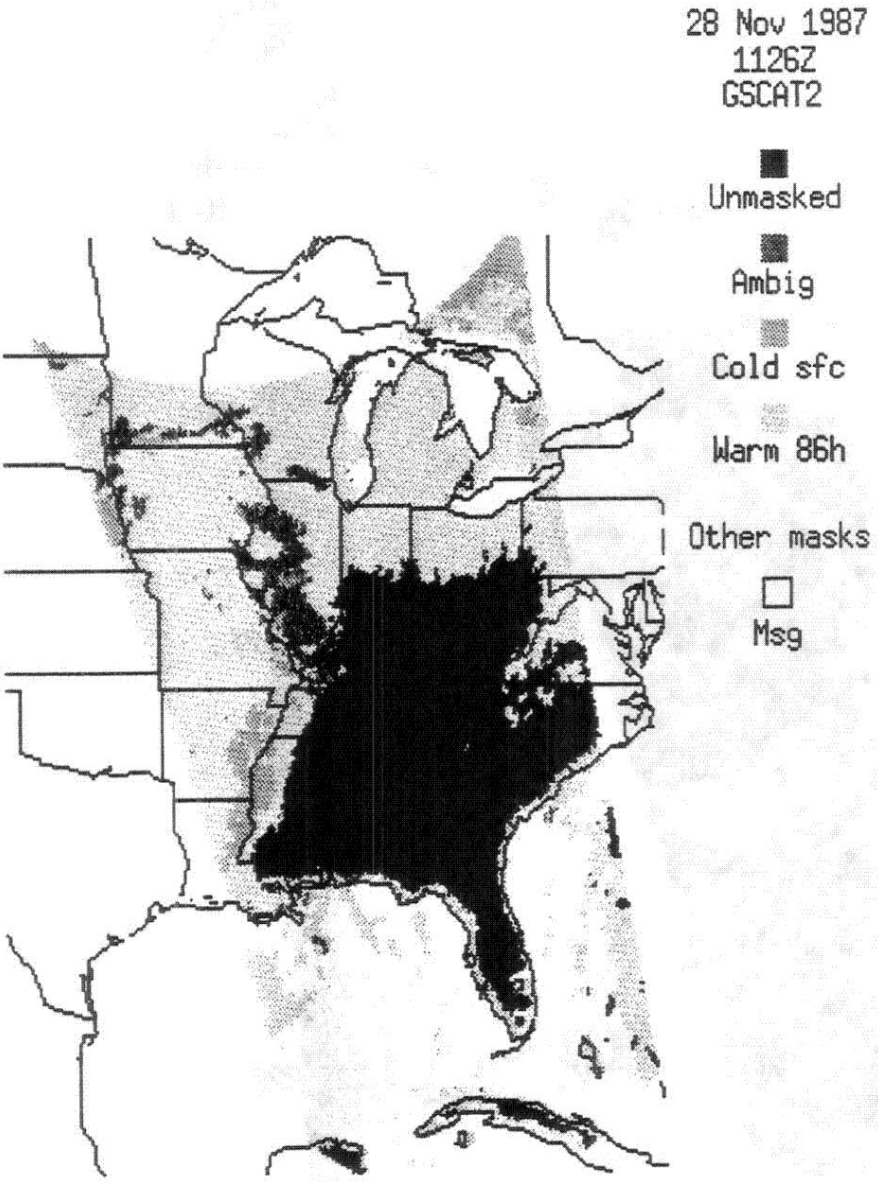
- Precip depiction
- Confidence indicators

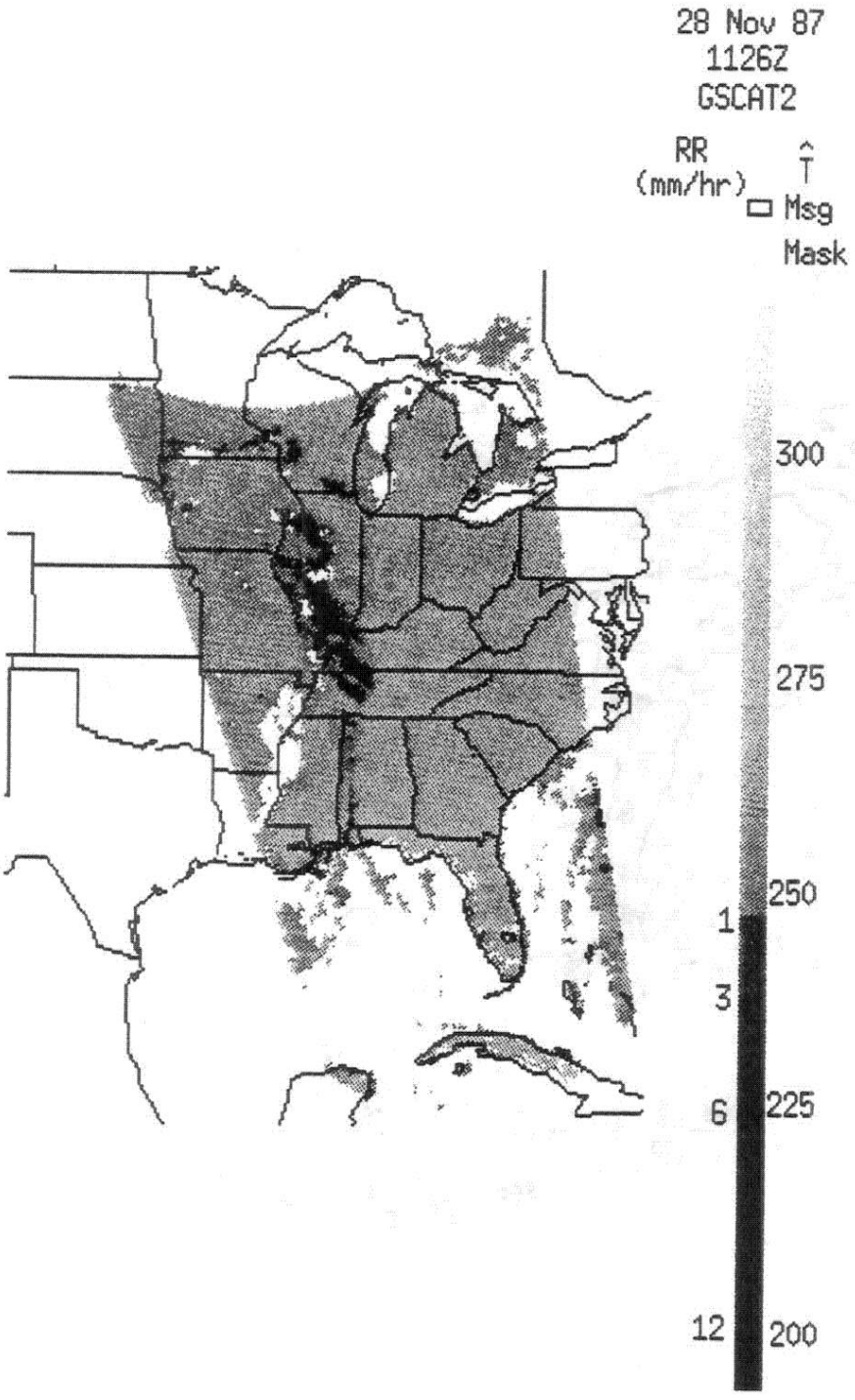
Global Maps

- .5°x.5° lat/lon grid
- Validation against GPCC gauge analysis on 2.5° x2.5° grid (at least 2 gauges) over land
- Validation against atoll gauges on 2.5° x2.5° over ocean

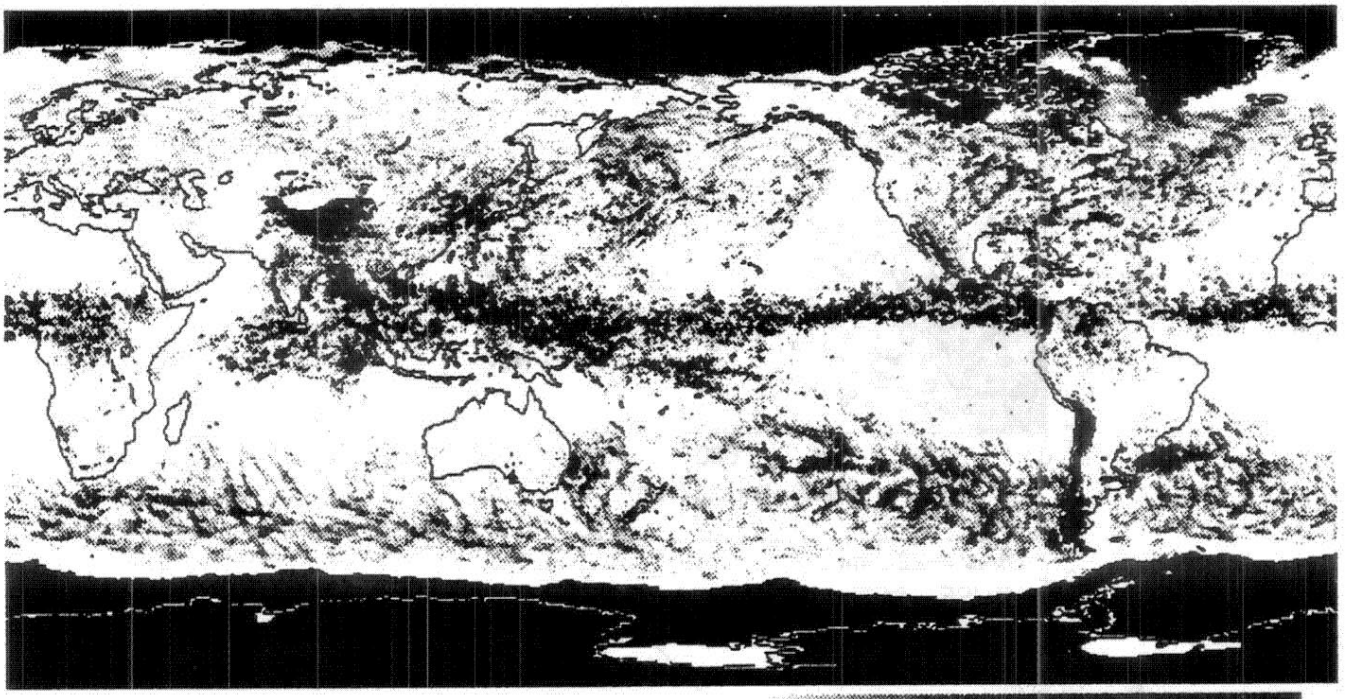

15 Sep 89
0939Z
GSCAT2
RRo
(mm/hr)
T
Msg
Mask
300
275
250
1
6
12
225
24
200


15 Sep 89
2215Z
GSCAT2
RRo
(mm/hr)
T̂
Msg
Mask
300
275
250
225
200
1
6
12
24


28 Nov 1987
1126Z
GSCAT2
Unmasked
Ambig
Cold sfc
Warm 86h
Other masks
Msg

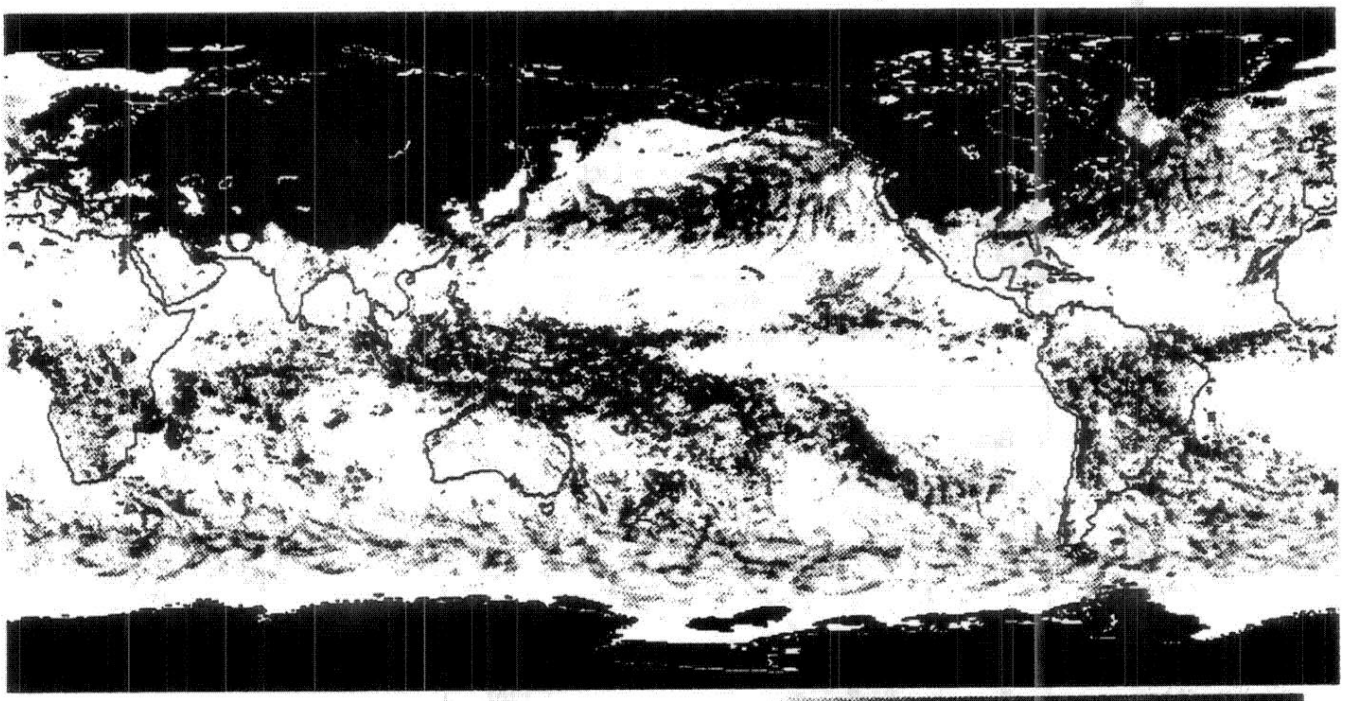

28 Nov 87
1126Z
GSCAT2
RR
(mm/hr)
Msg
Mask
300
275
250
1
3
6
225
12
200


US DEPT OF COMMERCE
NOAA/NWS/NMC WASHINGTON
1135Z SAT 28 NOV 1987 RADAR SUMMARY
SD



GSCAT2 microwave pcp .5x.5 (mm) Aug 1987

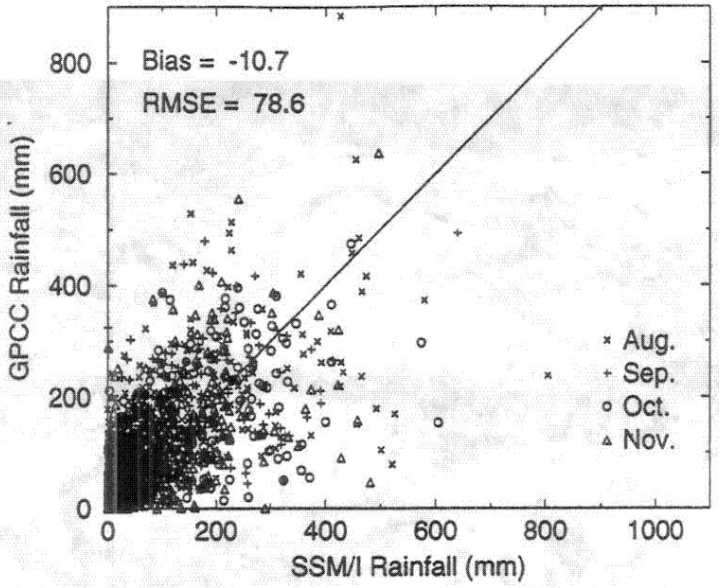
0 100 200 300 400 500+



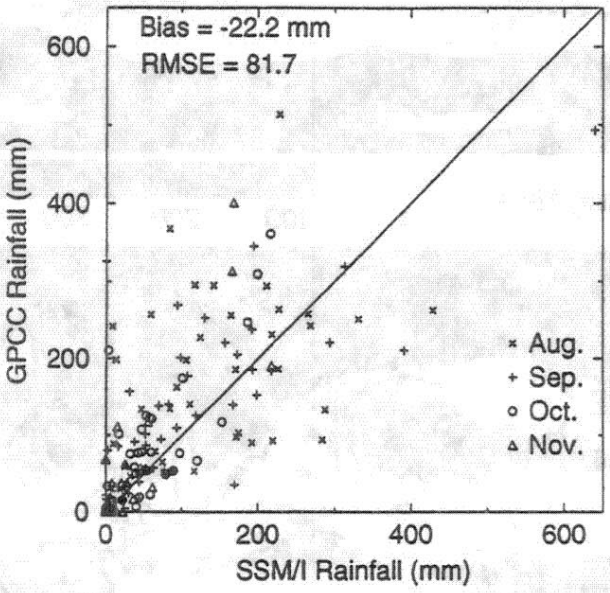
GSCAT2 microwave pcp .5x.5 (mm) Feb 1988

0 100 200 300 400 500+

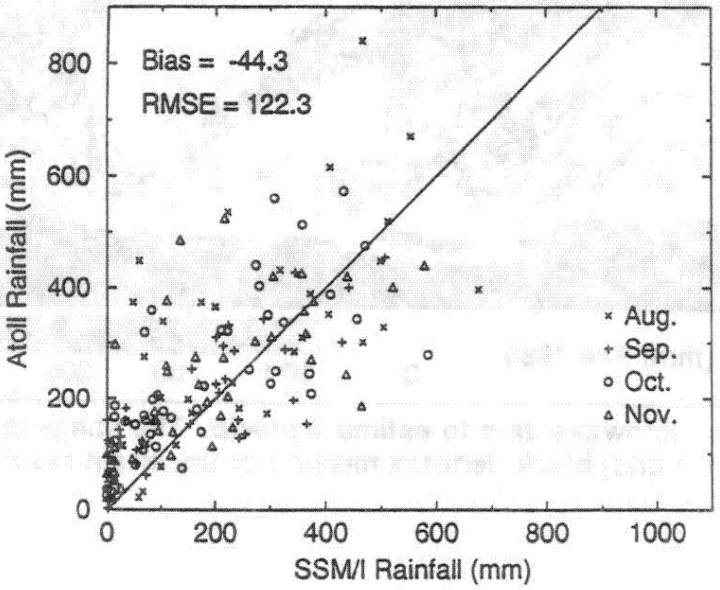
GSCAT2 uses high-res SSM/I microwave data to estimate precip. The image is an average for a month on a 0.5°x0.5° lat/lon grid; black denotes missing or uncertain results.



40°S to 40°N



Tropical Africa



Atolls

6. Comments on Confidence

"Cold sfc" pixels are assigned zero precip rate, but it's really just "not large," so they are considered unreliable for most uses.

"Ambig" pixels either have the computed precip or are artifacts.

Cold sfc and ambig pixels can be controlled in time-averages by deleting boxes with "too many." Empirically, the cutoff is

- ~40% for pentads, and
- ~20% for months.

Hypothesis: In individual swaths, many ambiguous pixels can be categorized as cold sfc or precip by comparison with surrounding pixels.

There is no marker for shallow orographic and warm rain.

It is possible that GSCAT2 incorrectly represents polar ocean conditions.

7. Summary

The Goddard Scattering Algorithm has been developed for global, monthly precip estimates.

All SSM/I channels are quality-controlled and used to mask off non-precipitating areas.

At remaining pixels we apply a simple relation to 86h to deduce precip rate. The relation is based on radiative calculations for a numerically modelled squall line, with adjustment for ocean areas based on monthly gauges.

Monthly results are competitive with other SSM/I-based techniques. Instantaneous results are physically reasonable.

Cold land and ice prevent useful retrievals.

Shallow orographic and warm rain are not detectible with the scattering approach.

Measures of uncertainty are being developed.

An Intercomparison of the Navy Cal/Val and SSM/I Pathfinder Precipitation Algorithms

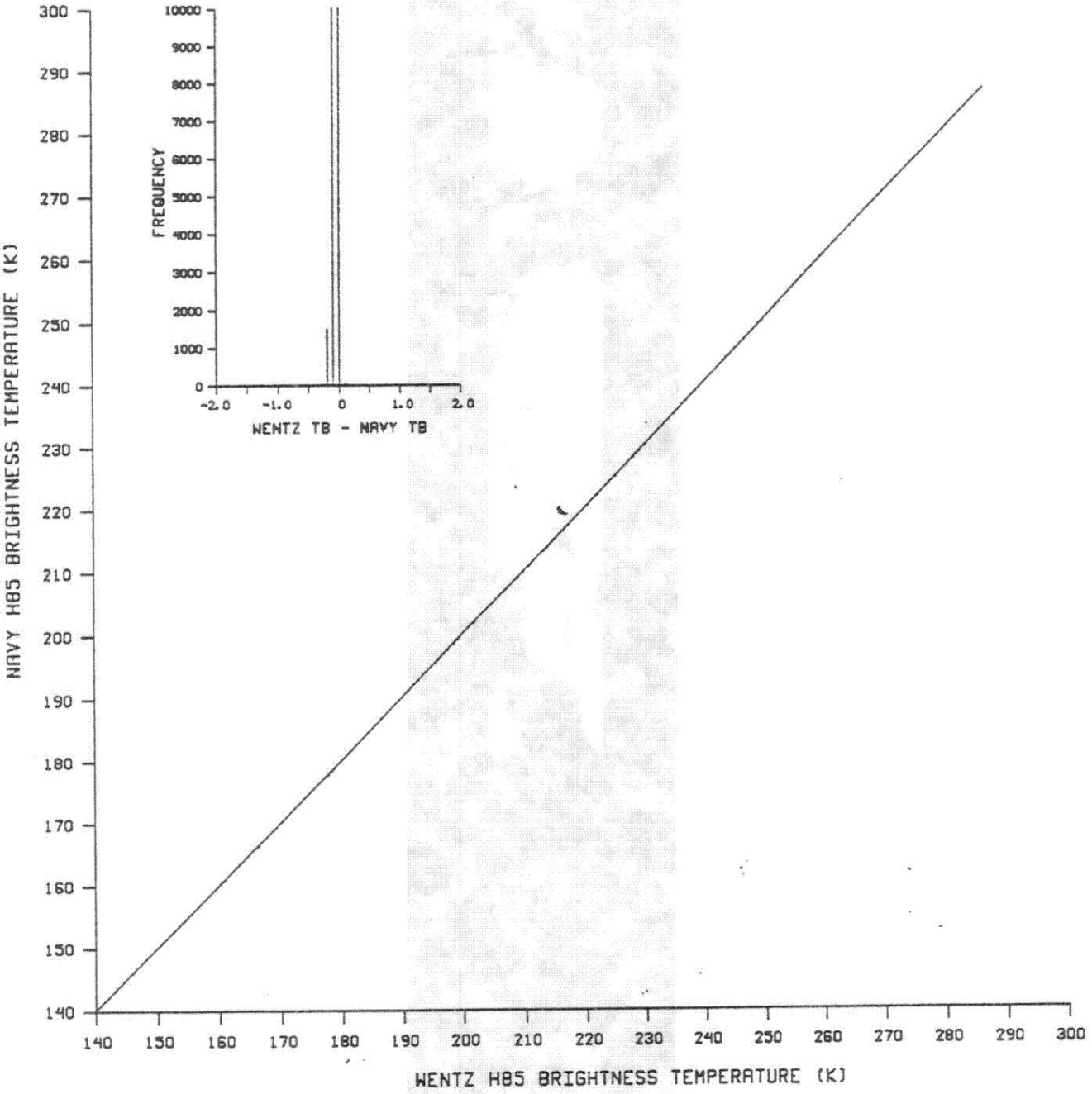
Steven J. Goodman[1], Frank J. LaFontaine[1,2] George J. Huffman[3,4] and Robert F. Adler[4]
[1]NASA/Marshall Space Flight Center, Huntsville, AL 35812
[2]Institute for Global Change Research and Education (IGCRE)
[3]Universities Space Research Association
[4]NASA/GSFC, Laboratory for Atmospheres, Greenbelt, MD 20771

ABSTRACT

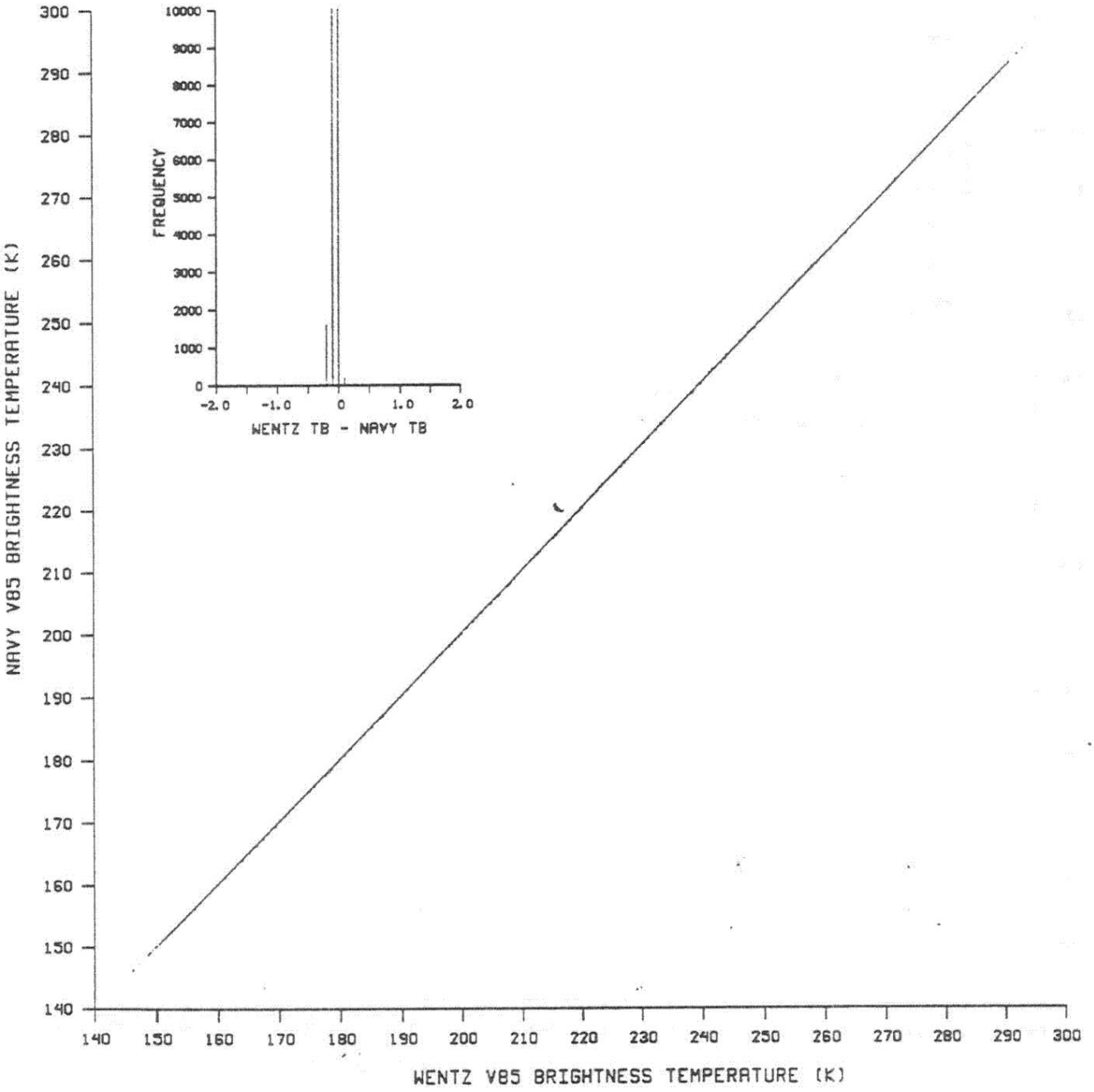
Algorithm evaluation and verification under varying environmental conditions (tropical vs extra-tropical, land vs ocean, winter vs summer) is an important component of the process to improve existing operational algorithms. A community consensus SSM/I precipitation algorithm, desired by global change science investigations (e.g., the SSM/I Pathfinder) and operational users, has been difficult to achieve, in part, because of limited opportunities for independent validation and intercomparison. Open access to the SSM/I data base has permitted algorithm intercomparisons via the WMO Algorithm Intercomparison Projects (AIPs) and the NASA WETNET project. These projects provide a forum to intercompare a number of SSM/I precipitation algorithms from various authors. Wentz format tapes serve as the primary source for the antenna/brightness temperature (Ta/Tb) or sensor/environmental data record (SDR/EDR) data base for WETNET and Pathfinder. In this paper we compare the Cal/Val algorithm also implemented from the Wentz tapes for the period 1987,-1988 with the Pathfinder algorithm also implemented from Wentz tapes. In addition, we do not find any statistically significant differences between the Cal/Val algorithm estimates as computed from either the Wentz or Navy brightness temperatures.


WENTZ H37 BRIGHTNESS TEMPERATURE 16 AUG 1987 -- REV 806 -- ASCENDING
SOUTH
NORTH

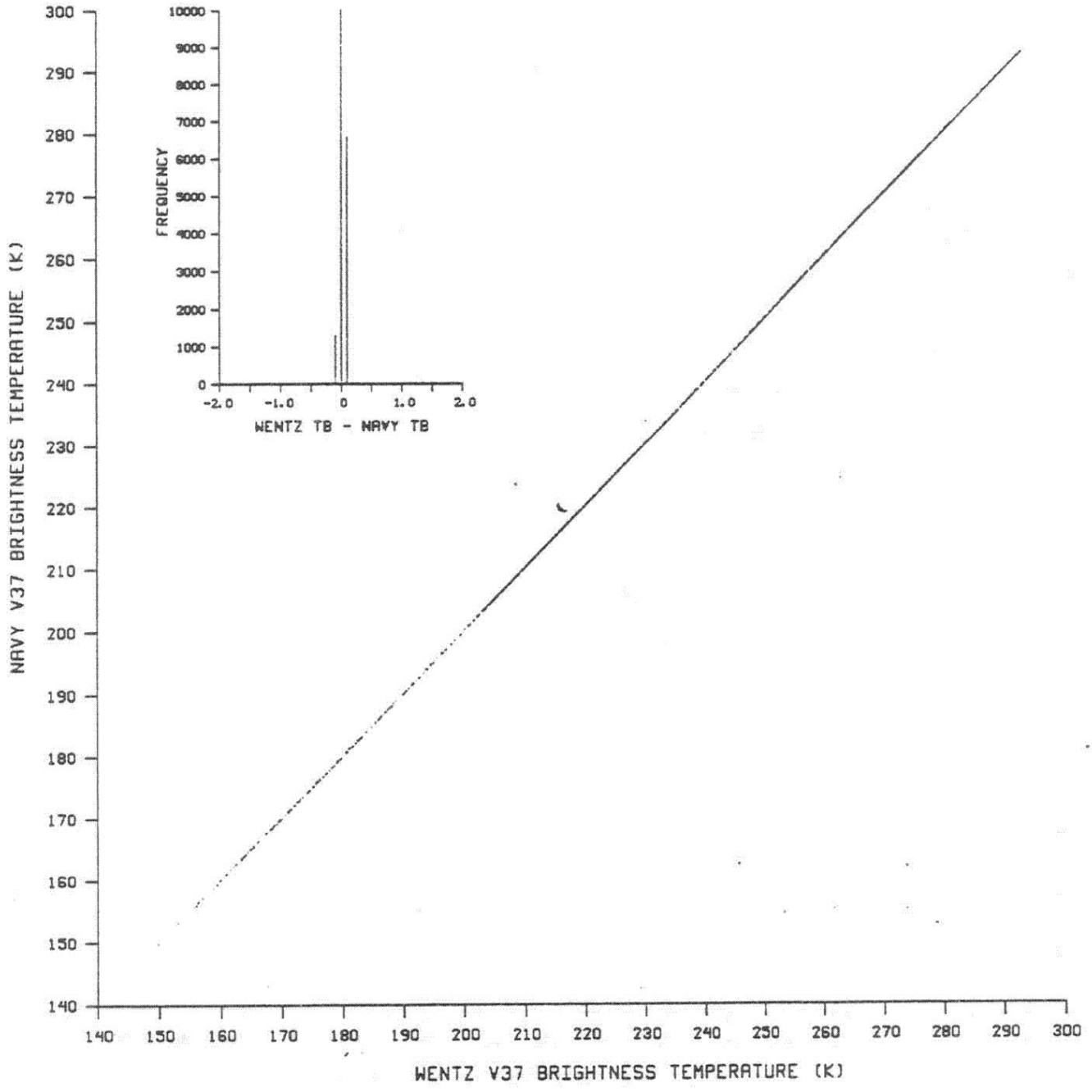
SCATTERPLOT OF WENTZ VS NAVY(CAL/VAL) H85 BRIGHTNESS TEMPERATURES
FOR 16 AUG 1987 -- REV 806 (ASCENDING) -- LAND/OCEAN DATA
WITH FREQUENCY GRAPH OF THE TB DIFFERENCES (inset)



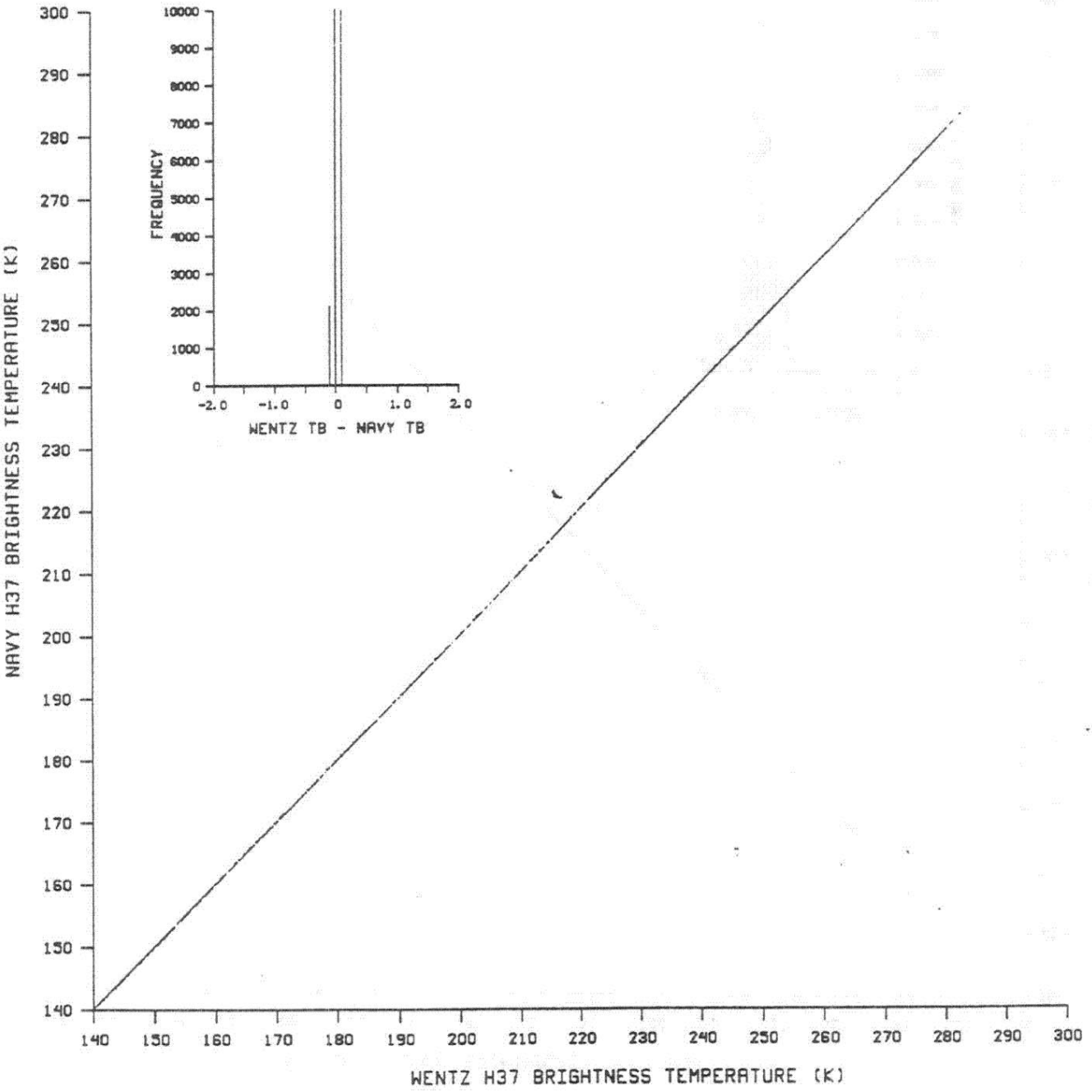
SCATTERPLOT OF WENTZ VS NAVY(CAL/VAL) V85 BRIGHTNESS TEMPERATURES
FOR 16 AUG 1987 -- REV 806 (ASCENDING) -- LAND/OCEAN DATA
WITH FREQUENCY GRAPH OF THE TB DIFFERENCES (inset)



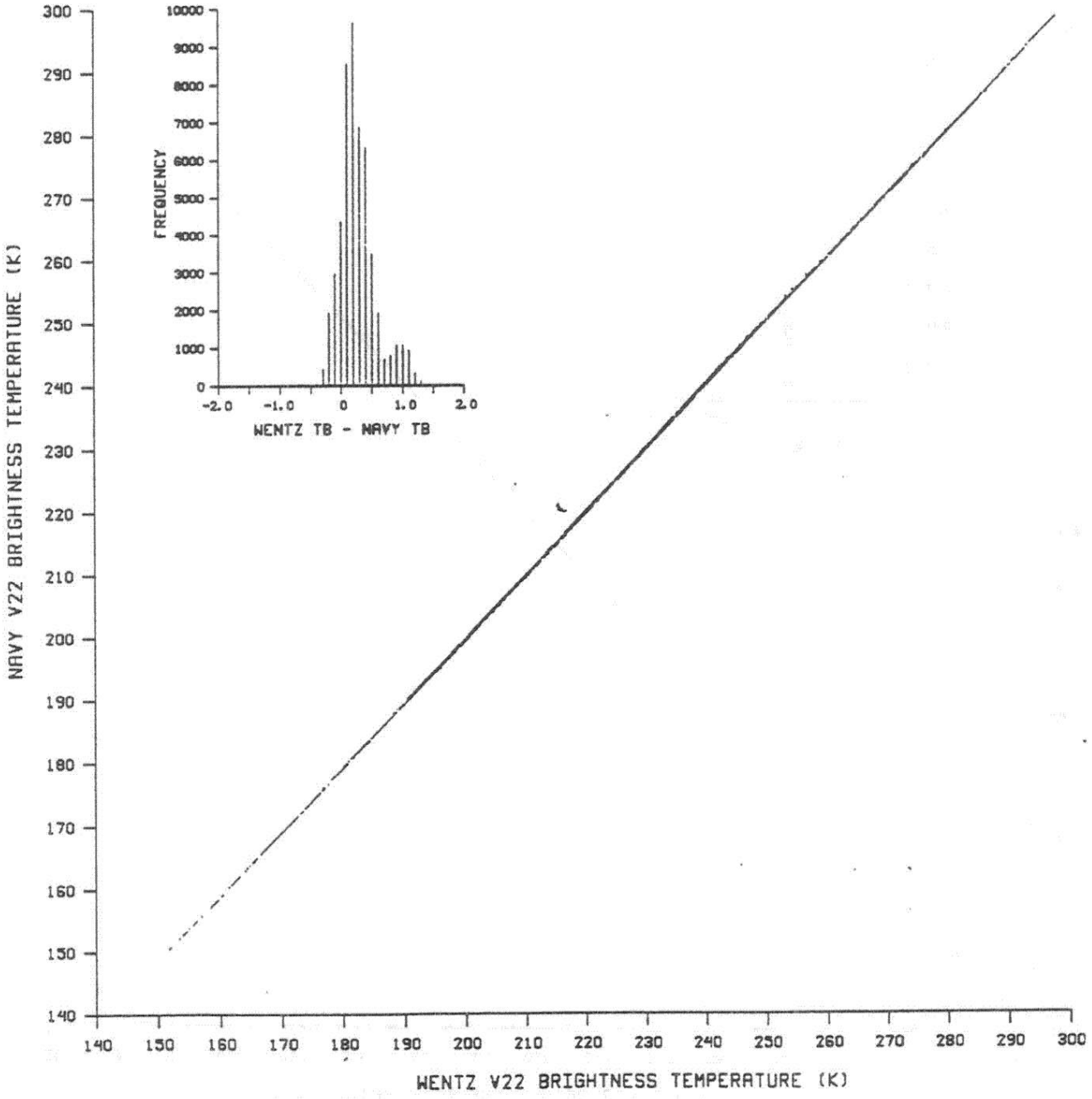
SCATTERPLOT OF WENTZ VS NAVY(CAL/VAL) V37 BRIGHTNESS TEMPERATURES
FOR 16 AUG 1987 -- REV 806 (ASCENDING) -- LAND/OCEAN DATA
WITH FREQUENCY GRAPH OF THE TB DIFFERENCES (inset)



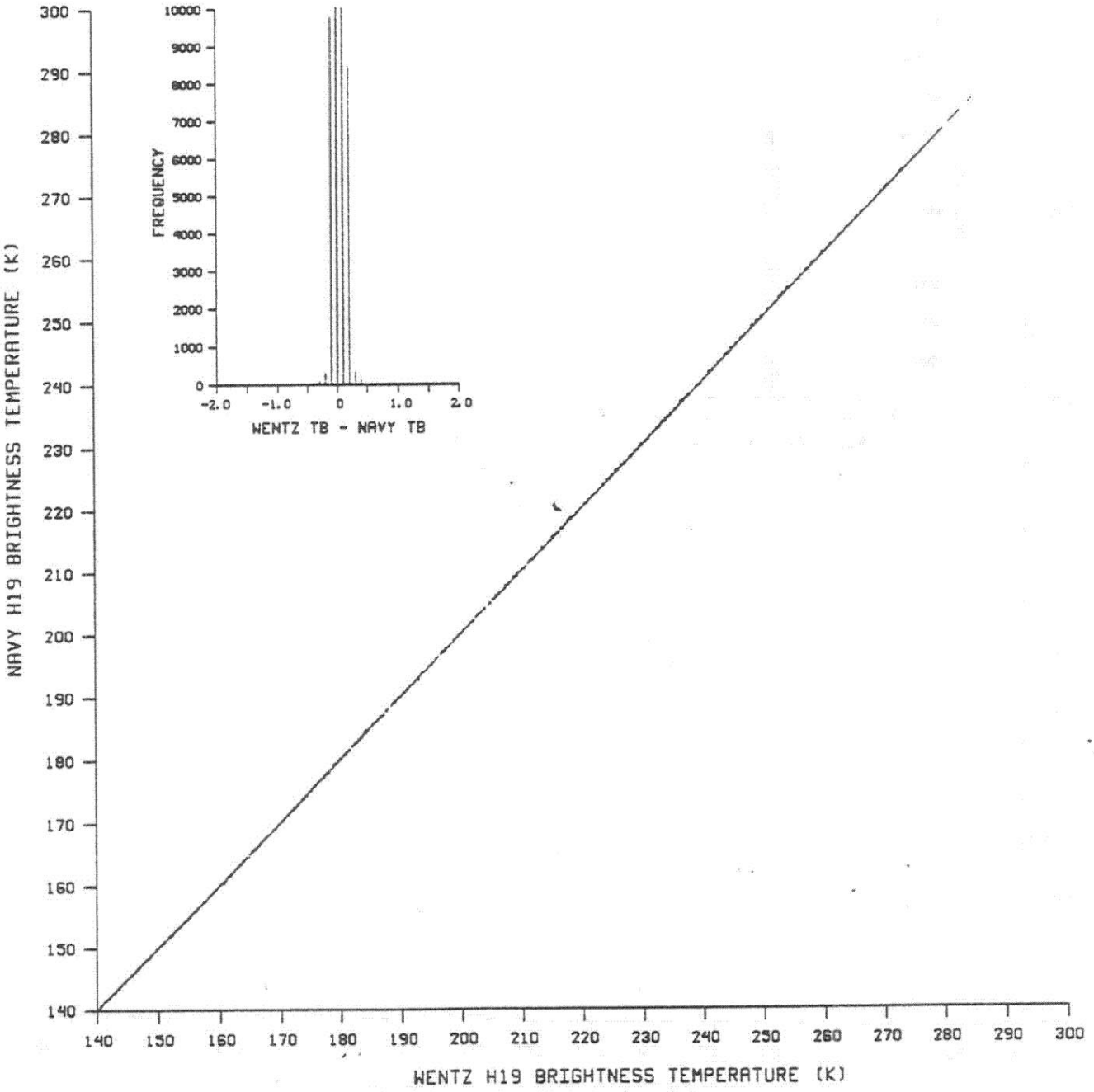
SCATTERPLOT OF WENTZ VS NAVY(CAL/VAL) H37 BRIGHTNESS TEMPERATURES
FOR 16 AUG 1987 -- REV 806 (ASCENDING) -- LAND/OCEAN DATA
WITH FREQUENCY GRAPH OF THE TB DIFFERENCES (inset)



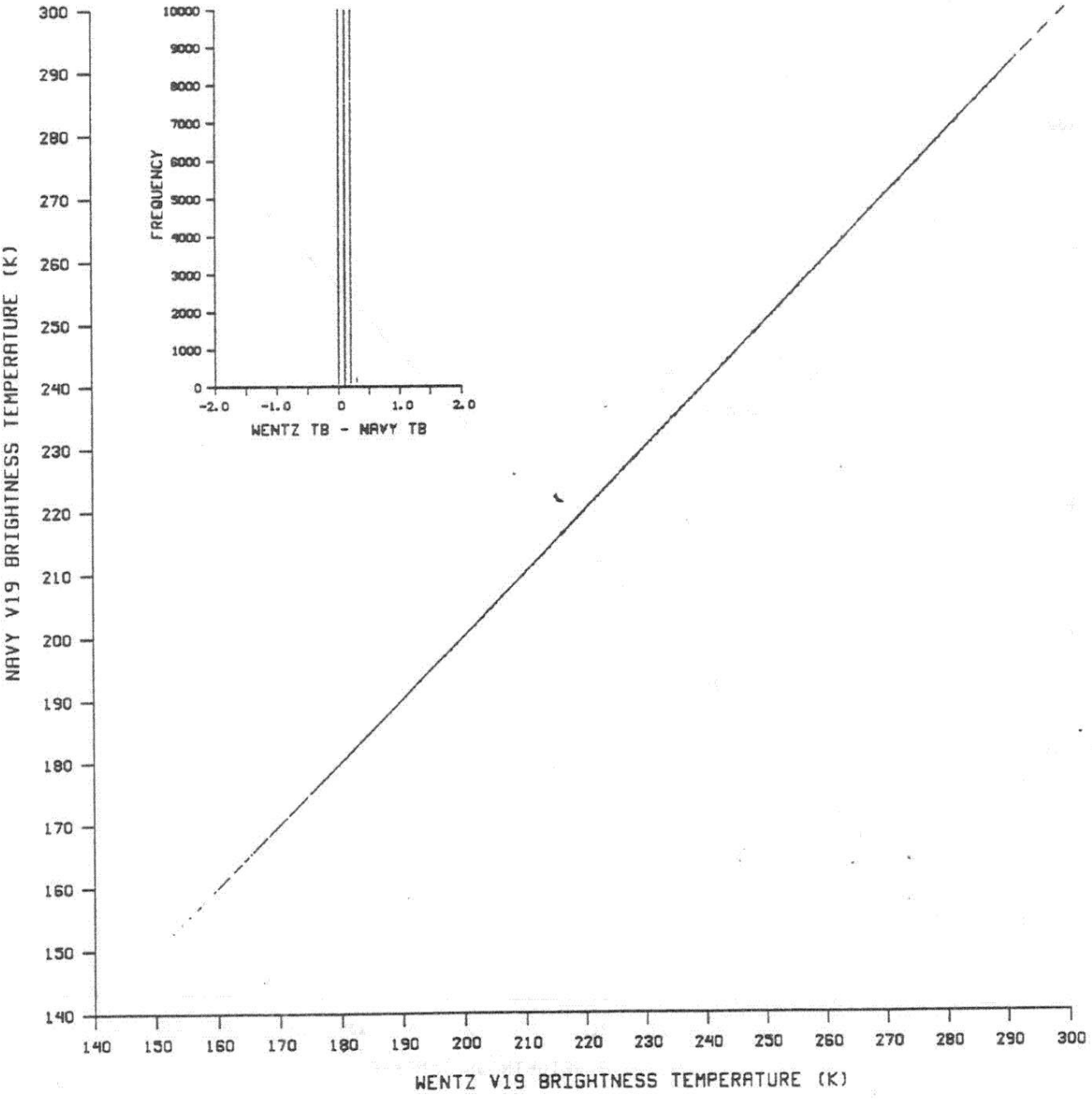
SCATTERPLOT OF WENTZ VS NAVY(CAL/VAL) V22 BRIGHTNESS TEMPERATURES
FOR 16 AUG 1987 -- REV 806 (ASCENDING) -- LAND/OCEAN DATA
WITH FREQUENCY GRAPH OF THE TB DIFFERENCES (inset)



SCATTERPLOT OF WENTZ VS NAVY(CAL/VAL) H19 BRIGHTNESS TEMPERATURES
FOR 16 AUG 1987 -- REV 806 (ASCENDING) -- LAND/OCEAN DATA
WITH FREQUENCY GRAPH OF THE TB DIFFERENCES (inset)



SCATTERPLOT OF WENTZ VS NAVY(CAL/VAL) V19 BRIGHTNESS TEMPERATURES
FOR 16 AUG 1987 -- REV 806 (ASCENDING) -- LAND/OCEAN DATA
WITH FREQUENCY GRAPH OF THE TB DIFFERENCES (inset)



μ_1 μ_2

"T" TEST RESULTS WENTZ VS NAVY(CAL/VAL) BRIGHTNESS TEMPERATURES
FOR 16 AUG 1987 -- REV 806 (ASCENDING) -- LAND/OCEAN DATA

CHANNEL	SAMPLES	VARIANCE	"T" VALUE
V85	206336	1367.820 W (1368.549 N)	-0.6859
H85	206336	1841.778 W (1842.617 N)	-0.5898
V37	51584	1556.662 W (1555.971 N)	0.0420
H37	51584	3135.277 W (3132.478 N)	0.0523
V22	51584	1615.425 W (1633.603 N)	1.0993
V19	51584	2022.507 W (2017.476 N)	0.3891
H19	51584	4271.739 W (4261.811 N)	0.1134

FOR ∞ D.O.F. AT A CONFIDENCE LEVEL OF .95 --- ALPHA = 1.645

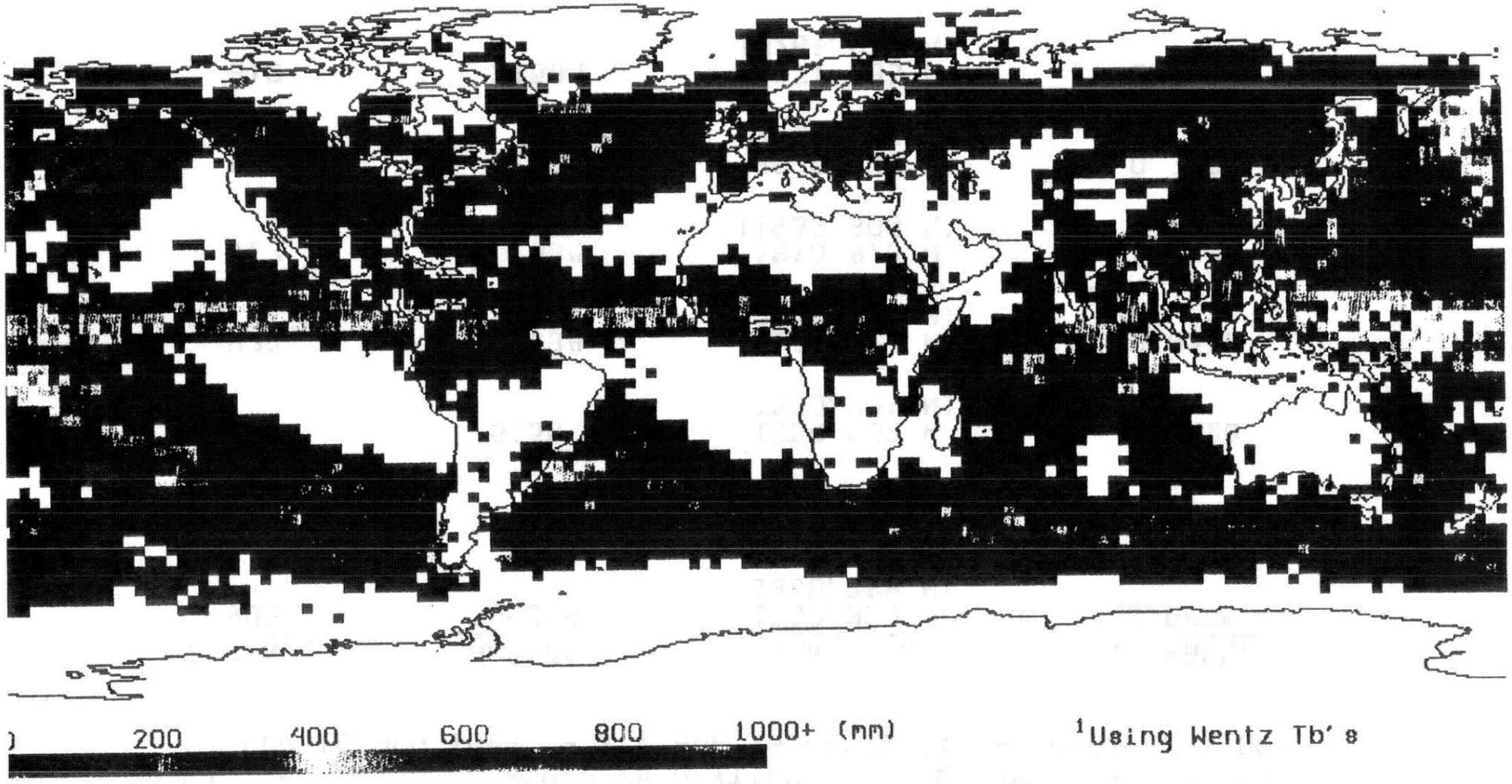
$t_{\alpha/2} = 1.960$

$H_0: \mu_1 - \mu_2 = 0$

$H_1: \mu_1 - \mu_2 \neq 0$

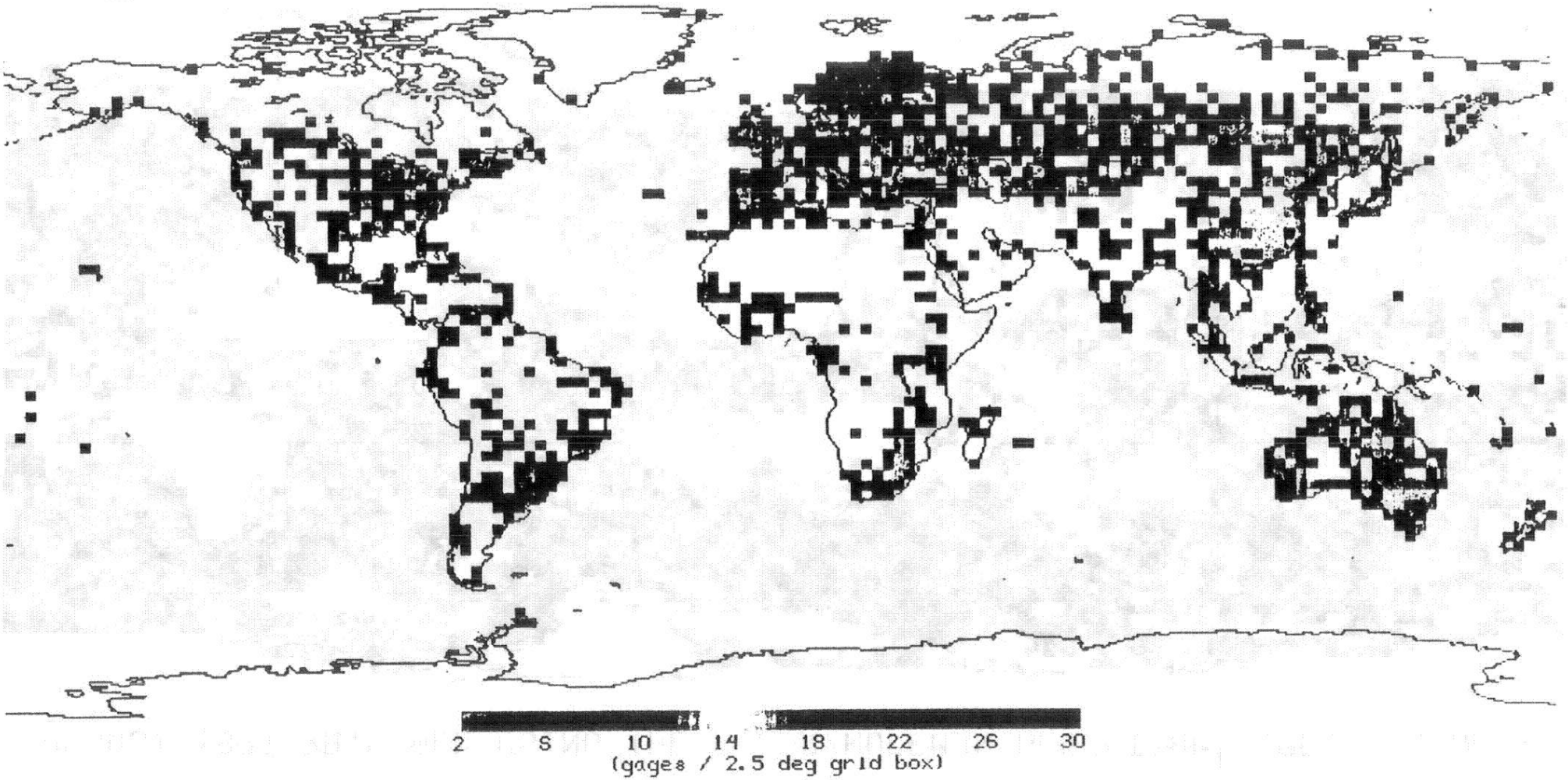
Rej. H_0 $\begin{cases} t < -t_{\alpha/2} \\ t > t_{\alpha/2} \end{cases}$

AUGUST 1987 RAINFALL USING THE NAVY(CAL/VAL) ALGORITHM[1] (RES=2.5 DEG)

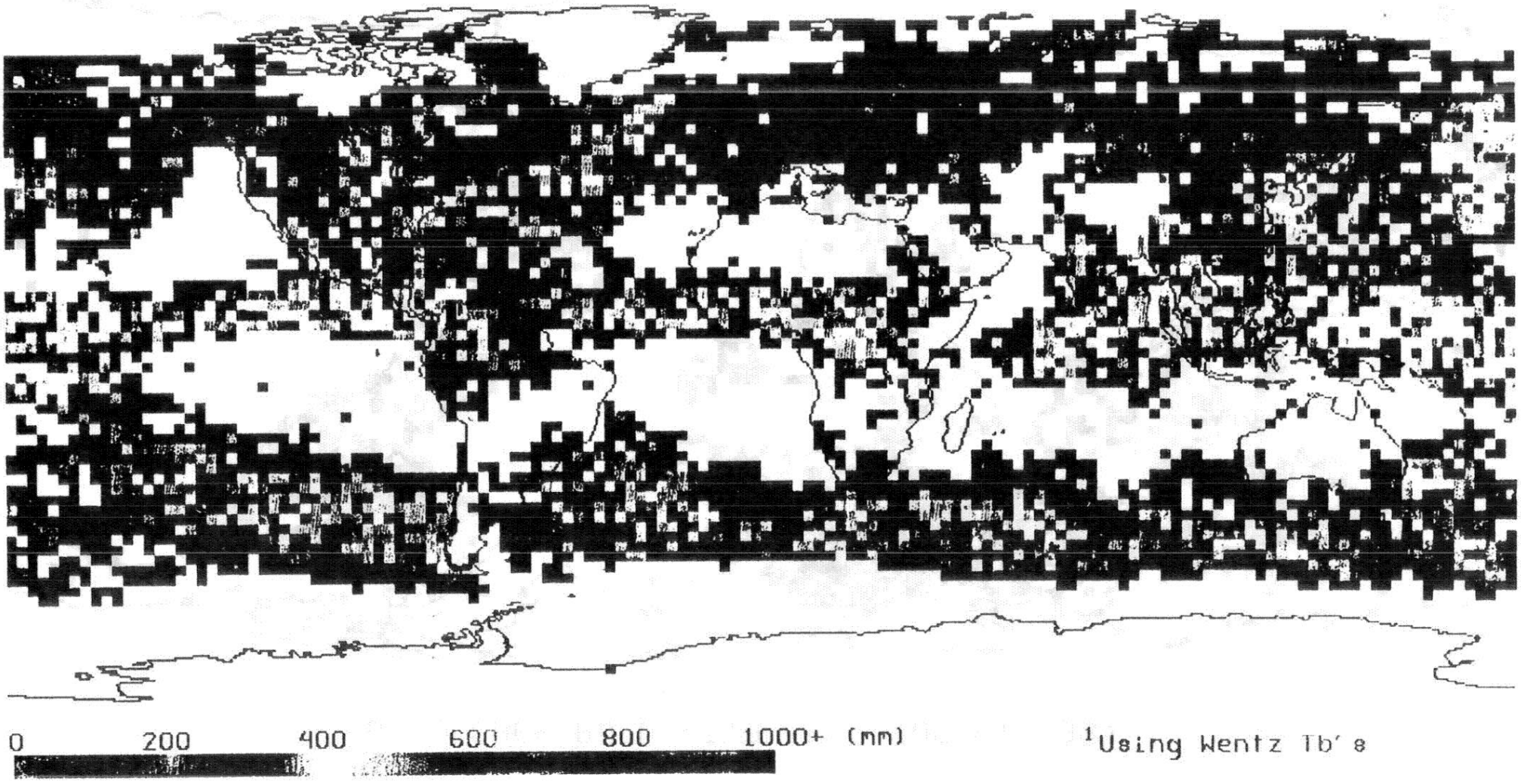


[1]Using Wentz Tb's

GPCC GAGE POPULATION FOR AUGUST 1987

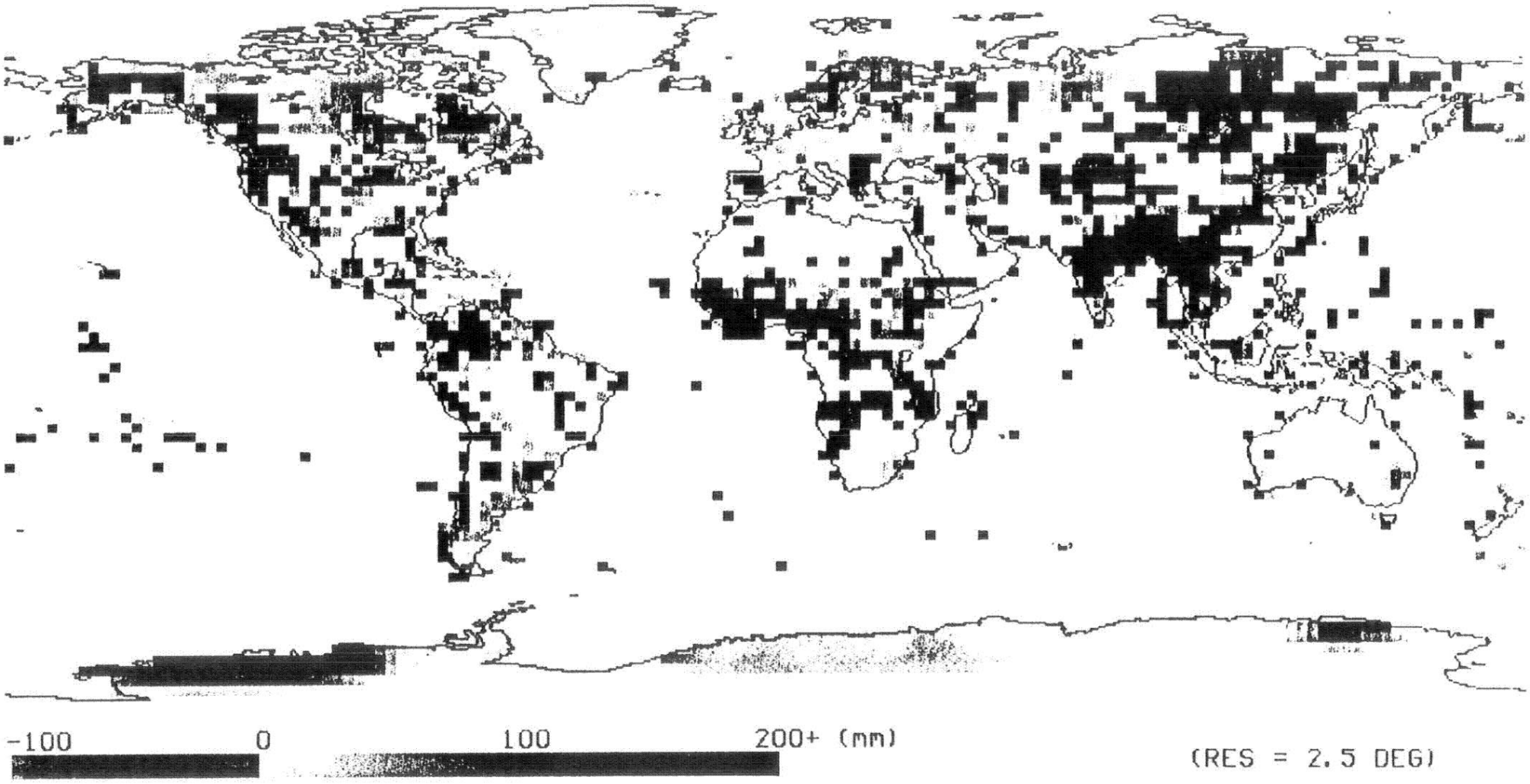


AUGUST 1987 RAINFALL USING THE ADLER/HUFFMAN ALGORITHM[1] (RES=2.5 DEG)



[1]Using Wentz Tb's

AUGUST 1987 RAINFALL DIFFERENCE GPCC/INTERPOLATED - NAVY(CAL/VAL)



ISSUES AND CONCERNS
SPN SSM/I Algorithm Symposium

Date: 06-09-93

Author(s): Steven Goodman / NASA

General **1. What is the problem?** Provide subject, scope and illustration if necessary.

Re: Snow, Ice, Precip. algorithms

When applied globally, problems & errors in performance need to be better documented so research community can attack issues.

- Need to better exploit multi-sensor approaches.

Specific: Cal/Val Precip underestimates at higher rain rate

Issue: 1 - screening ⇒ Hughes D-Metrix for rain/no-rain can be improved under varying surface conditions

Issue 2- Calibration - Regression model based on lower rain rate data base.

2. How did we get here? What do we know about the problem? How long has it existed? What brought the problem into being? What are the effects of the problems we see now or in the future?

Problem appears to be due to training data set - small sample from Darwin, Aust & Kwaja
Also. radar ground truth data in error/no vertical info, Use ERS-1
Methodology is pretty sound - physical/statistical. Might improve performance by
Again comparing with more "truth" data
WETNET PIP-2 will provide the data base.

Multi-sensor → screening atmos. correction blended geo/polar sats fo

ISSUES AND CONCERNS
SPN SSM/I Algorithm Symposium

3. Where do we want to come out? Specify goal in terms of complete, acceptable or compromise solution(s). What are the criteria for an acceptable solution?

Acceptable soln - Redo regression model with PIP-2 data base

Criteria - Compare existing performance with others submitted for PIP-2, Reduced BIAS; limits more specific on "truth" data Keep data base on performance problem areas

4. Which is the best solution? Consider drawbacks and implementation.

5. Agreement and plan for action:

Some Evaluations of SSM/I Retrieved Fields in Tropical and Extra-tropical Cyclones

Simon W. Chang, Randall J. Alliss* and Glenn Sandlin

Naval Research Laboratory, Washington DC 20375
*North Carolina State University, Raleigh NC 27695

In an attempt to validate the SSM/I algorithms in NRL CAL/VAL reports, the SSM/I retrieved rain rates, marine surface wind speeds and integrated water vapor (IWV) of Hurricanes Florence (1988) and Hugo (1989) and the ERICA IOP 4 (1989) extra-tropical marine cyclone were examined. Land-based raingage measurements, ship and buoy reports, and numerical model results were used for comparisons. Significant results were presented here.

For Hurricane Hugo, there was a timely SSM/I overpass just prior to Hugo's landfall in south Carolina. Assuming the rainfall rates remained stead over a period of four hours after the overpass, accumulated rainfall amounts over land were computed by moving the retrieved rainrate distribution along the storm's track. A comparison with the objectively analyzed four hour rainfall amount measured by a raingage network in Georgia, North and South Carolinas was made. The SSM/I and raingage amounts were amazingly similar. For example, both fields showed heavy precipitation along the SC coast with a maximum of 80 mm, reducing inland to 5 mm in southern NC. In Charleston, SC, where Hugo made land fall nearby, the 4 h rainfall amount was 89 mm by SSM/I retrieval and 87 mm by raingage analysis.

The SSM/I retrieved marine surface winds (with flags 0 and 1) in Florence were compared with in situ buoy observations and an objectively analyzed wind field enhanced by Omega dropsondes deplored by NOAA P-3's. It is found that the SSM/I winds were stronger than the buoy reports but weaker than the analysis enhanced by dropsonde observations.

The SSM/I retrieved marine surface winds (with flag 0) in ERICA IOP 4 storm were compared ship reports. It was found that the SSM/I winds were lower than ship reports in areas of rapid wind shifts and changing synoptic conditions. The retrieved winds compared well with ship reports in southern latitudes where the weather pattern was steady. The retrieved IWV was shown to be useful in locating surface fronts--high IWV gradients were found to the north of the warm front and to the west of the cold front. The retrieved IWV amount was approximately 5 mm higher than the model produced IWV amount in general.

Some Evaluations of SSM/I Retrieved Fields in Tropical and Extra-tropical Cyclones

Simon W. Chang, Randall J. Alliss* and Glenn Sandlin

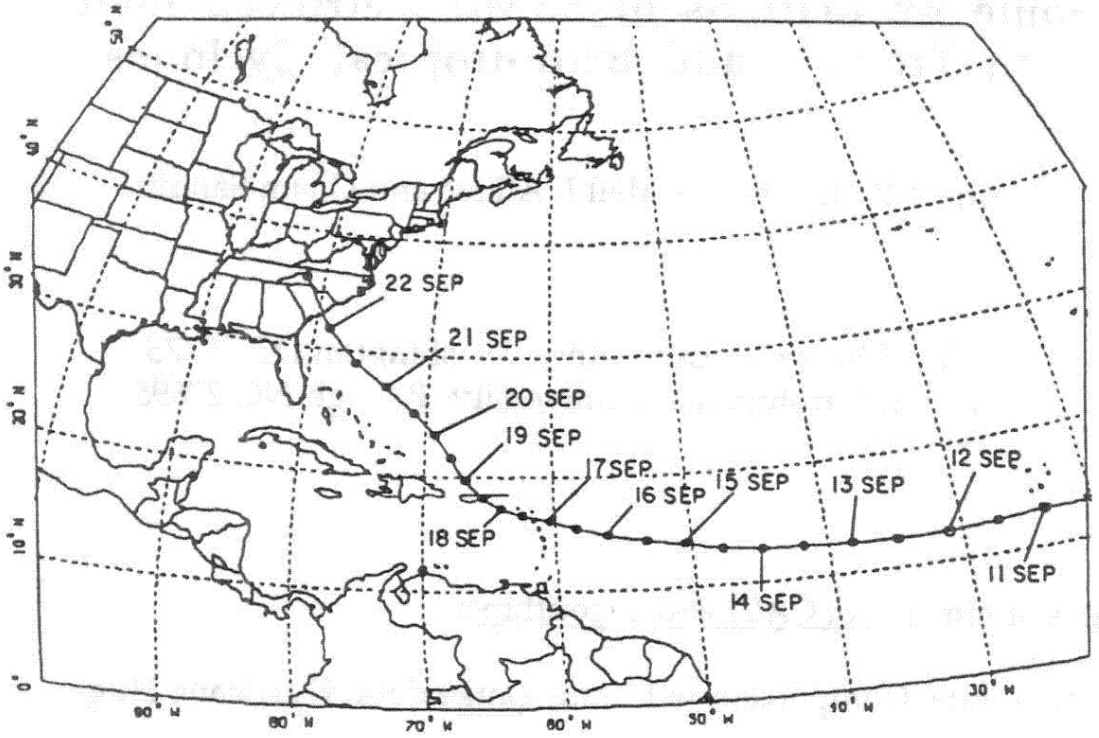
Naval Research Laboratory, Washington DC 20375
*North Carolina State University, Raleigh NC 27695

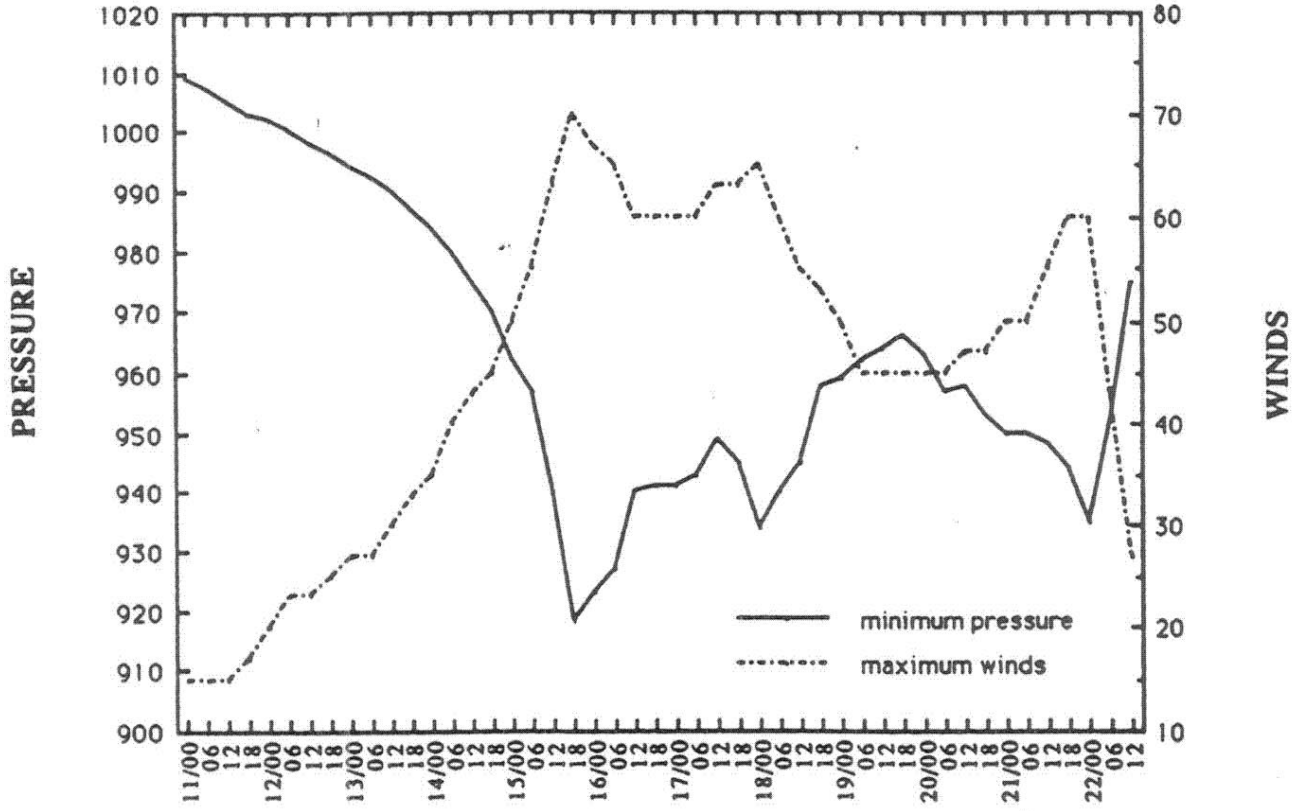
An examination of CAL/VAL algorithms:

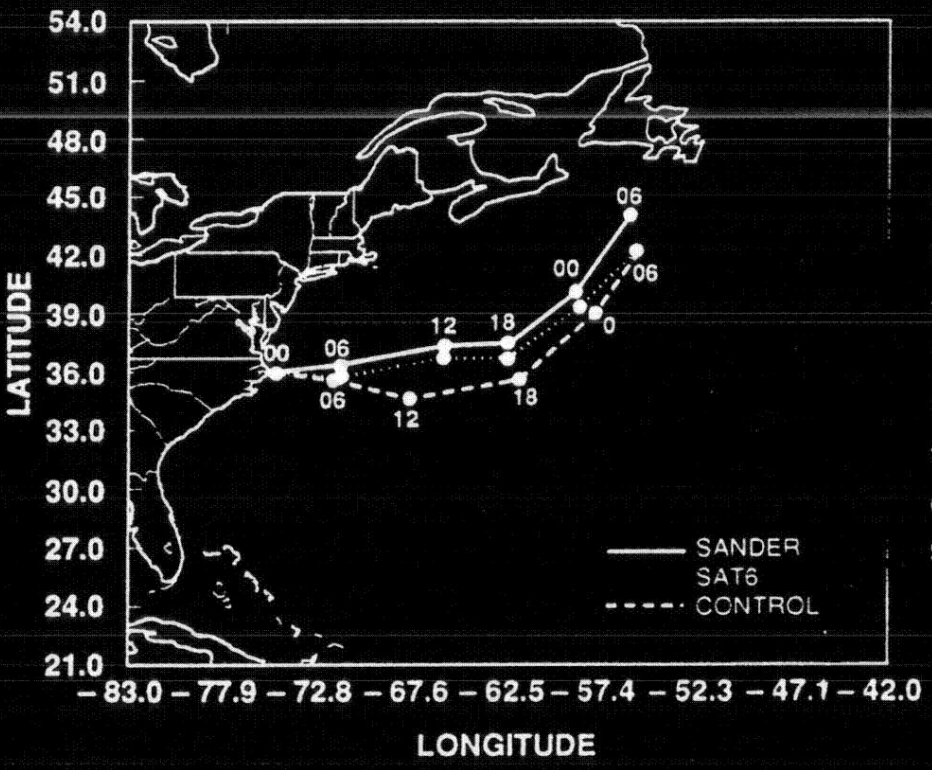
1. Rain rate: Comparison with rain gauge data, Hurricane Hugo.

2. Marine surface winds: Ship and buoy reports, ERICA IOP 4.

3. Integrated water vapor: Objective analysis and limited-area model prediction, ERICA IOP 4.


22 SEP
21 SEP
20 SEP
19 SEP
17SEP
16 SEP
15 SEP
13 SEP
12 SEP
18 SEP
14 SEP
11 SEP


PRESSURE
WINDS
minimum pressure
maximum winds



The assimilation of SSM/I rainfall rates also improved the prediction of the location of the marine cyclone. Figure shows the locations of the low pressure centers at 6 h interval as in Sander's analysis (solid line), the standard NRL model prediction (dashed line), and the NRL model with SSM I rainfall rates (SAT6, dotted line).

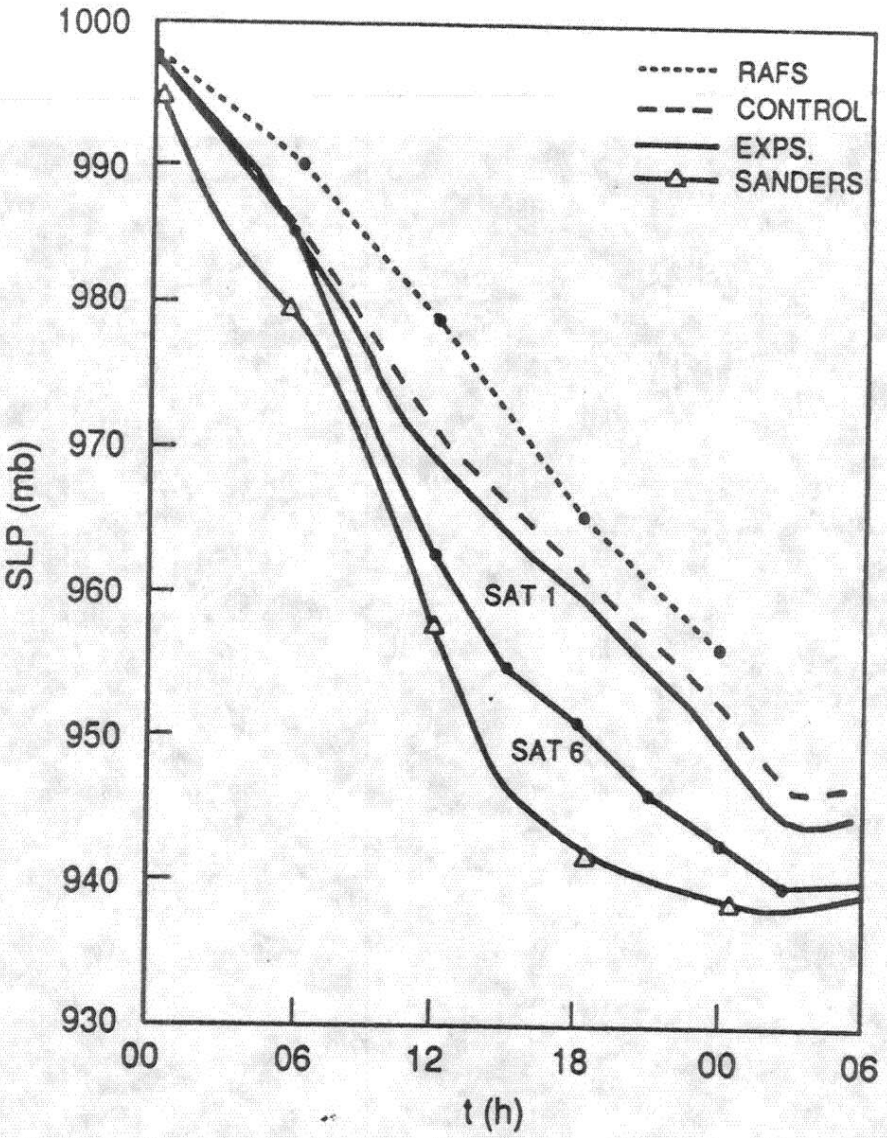
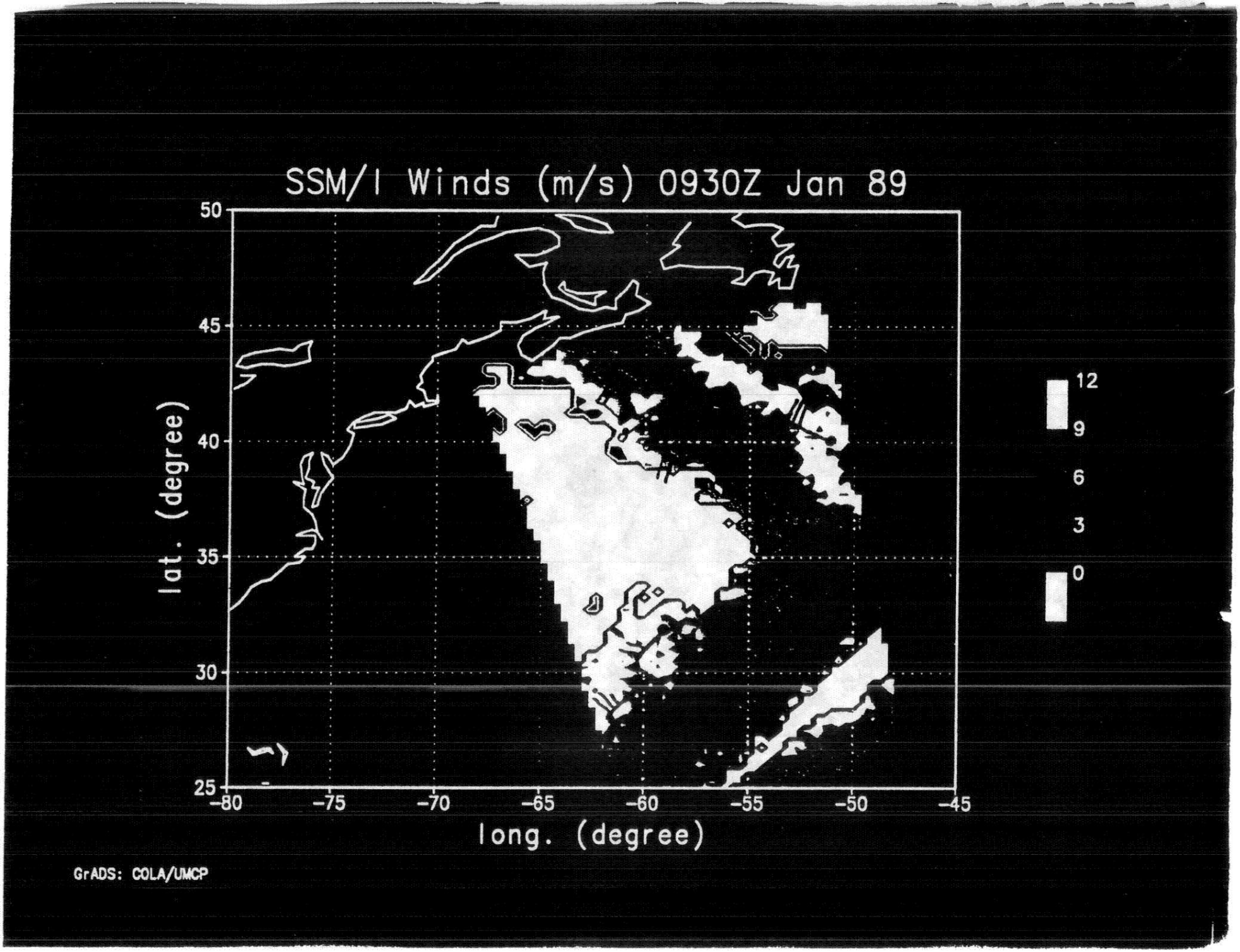
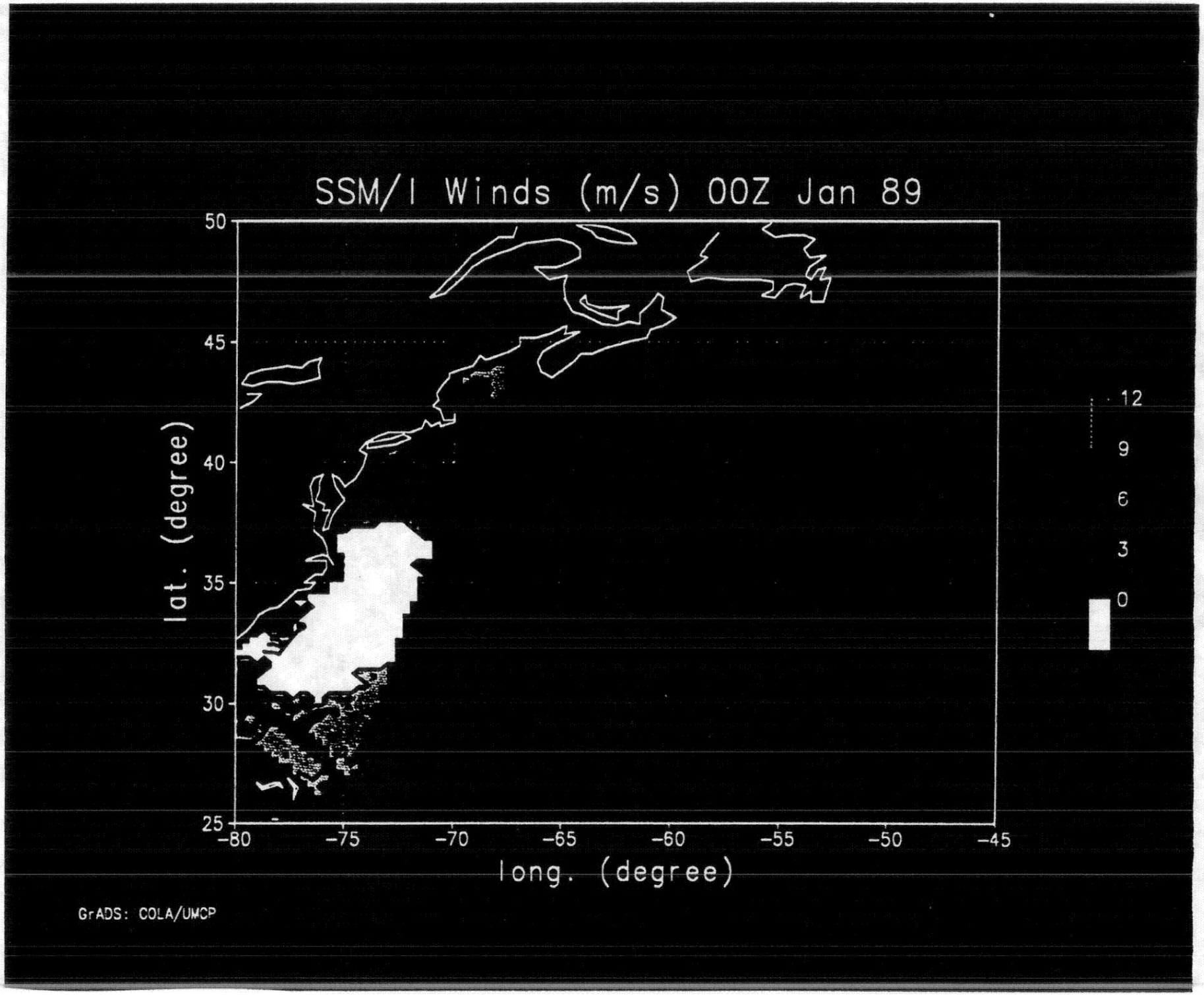
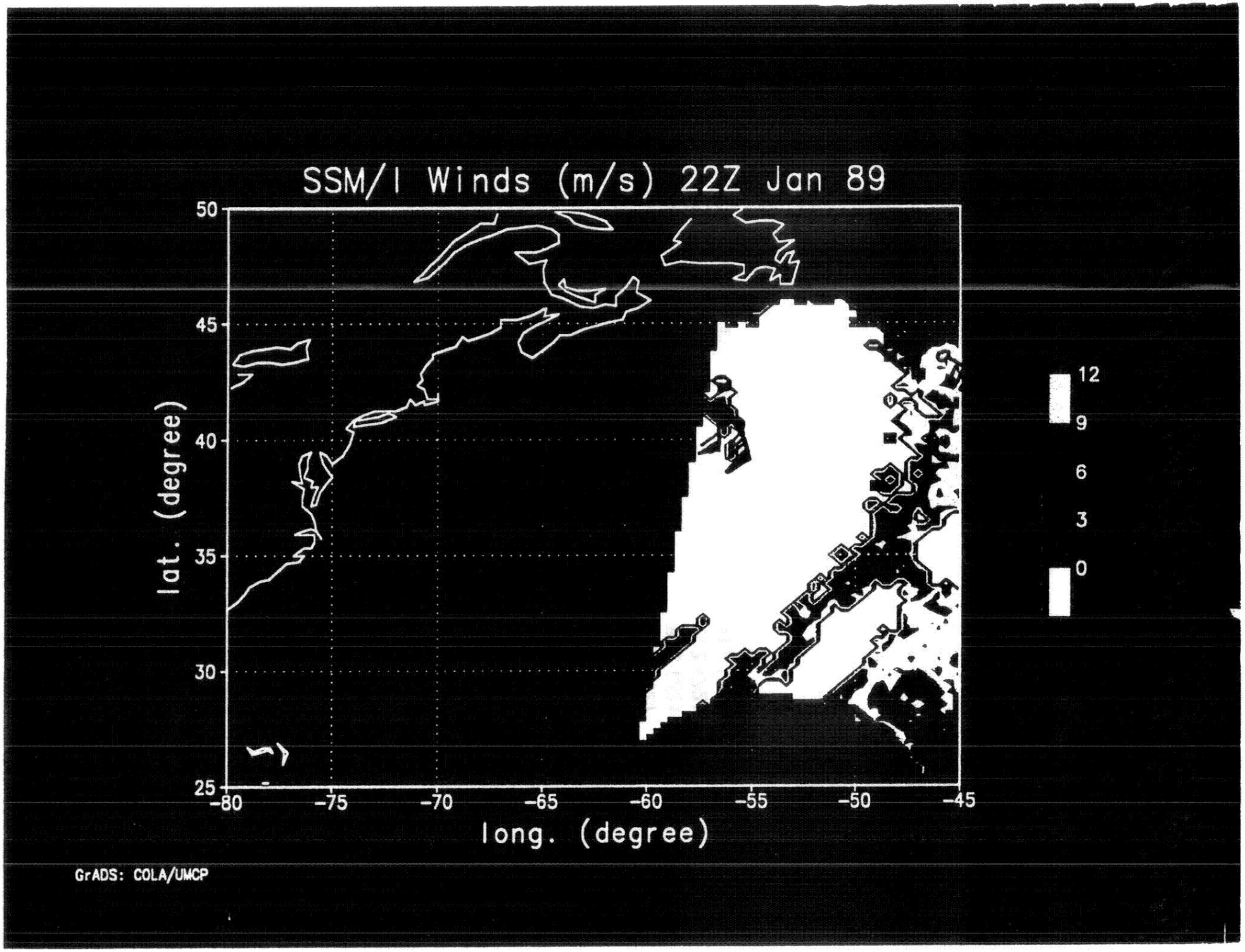


Fig. 11. Time evolution of the central SLP of the explosive cyclone for the RAFS analyses (dotted), NRL model (no sat, dashed), assimilation experiments SAT1 and SAT6 (solid lines), and Sander's analysis (triangle) from 00 UTC January 4 to 06 UTC January 5, 1989. Other assimilation experiment results lie between the two solid lines.


SSM/I Winds (m/s) 0930Z Jan 89
50
45
40
35
30
25
lat. (degree)
-80
-75
-70
-65
-60
-55
-50
-45
long. (degree)
12
9
6
3
0
GrADS: COLA/UMCP

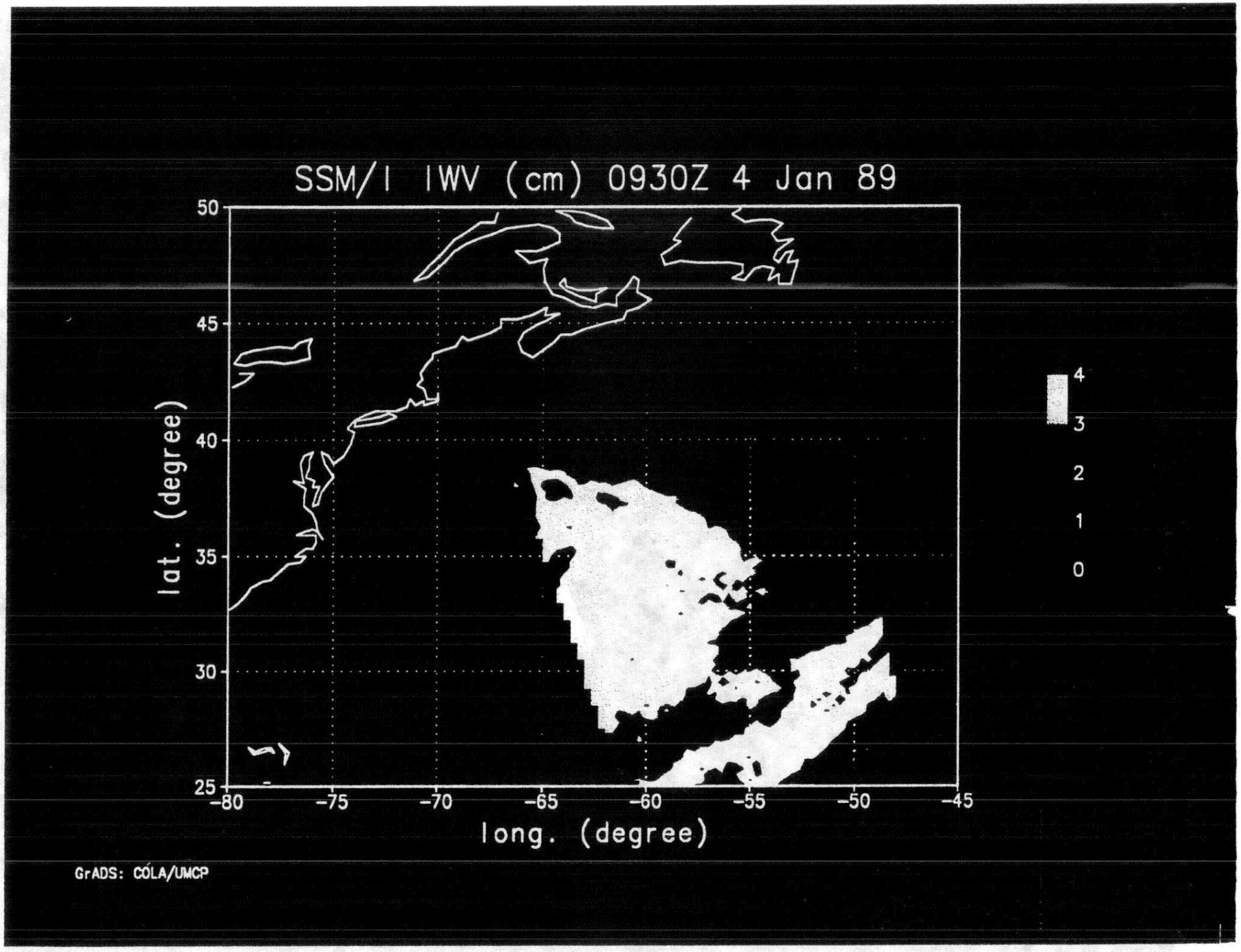

SSM/I Winds (m/s) 00Z Jan 89
50
45
40
35
30
25
lat. (degree)
-80
-75
-70
-65
-60
-55
-50
-45
long. (degree)
12
9
6
3
0
GrADS: COLA/UMCP

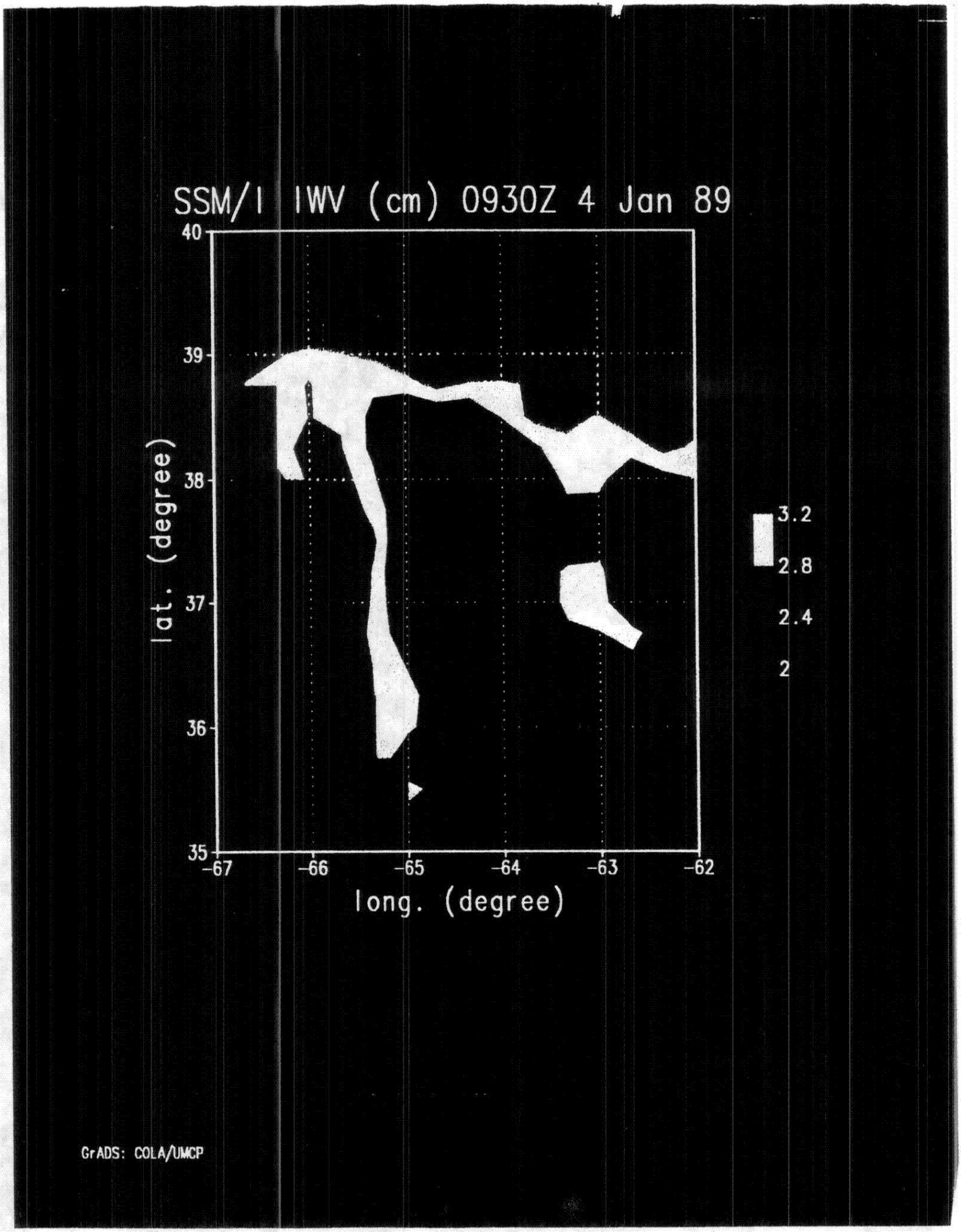

SSM/I Winds (m/s) 22Z Jan 89
50
45
40
35
30
25
lat. (degree)
-80
-75
-70
-65
-60
-55
-50
-45
long. (degree)
12
9
6
3
0
GrADS: COLA/UMCP

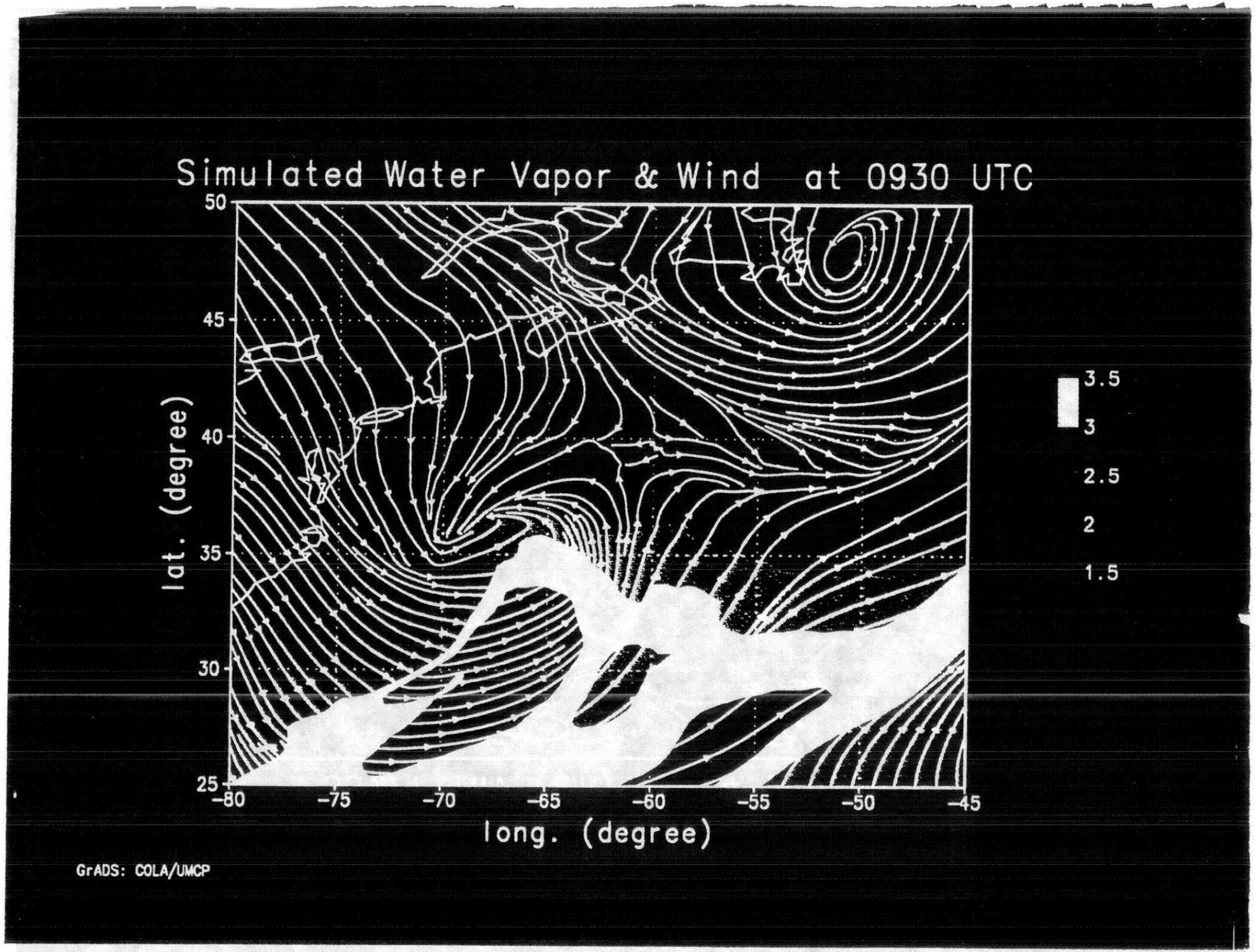
Marine Surface Wind Speeds (m/s)

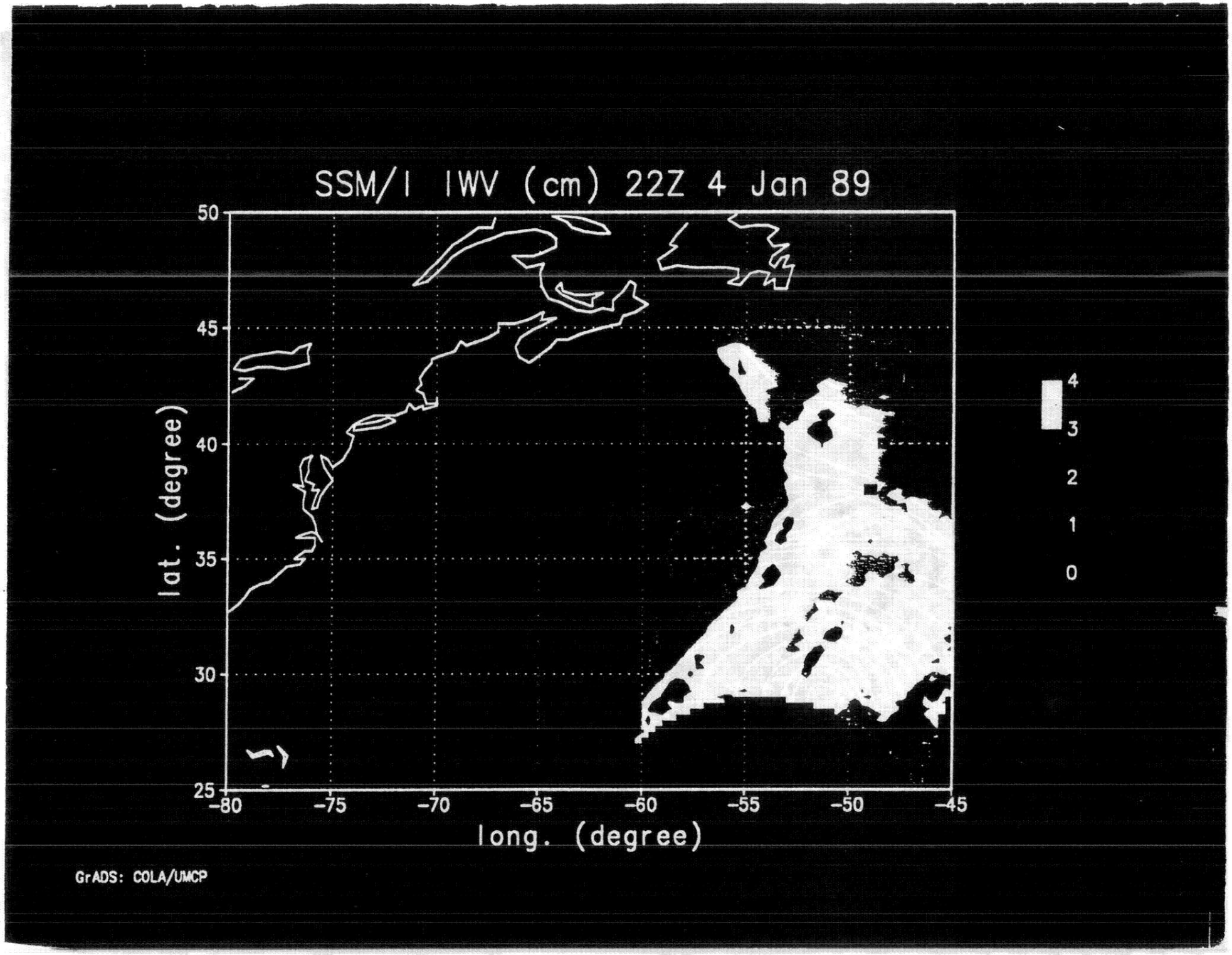
(4-5 Jan. 1989)

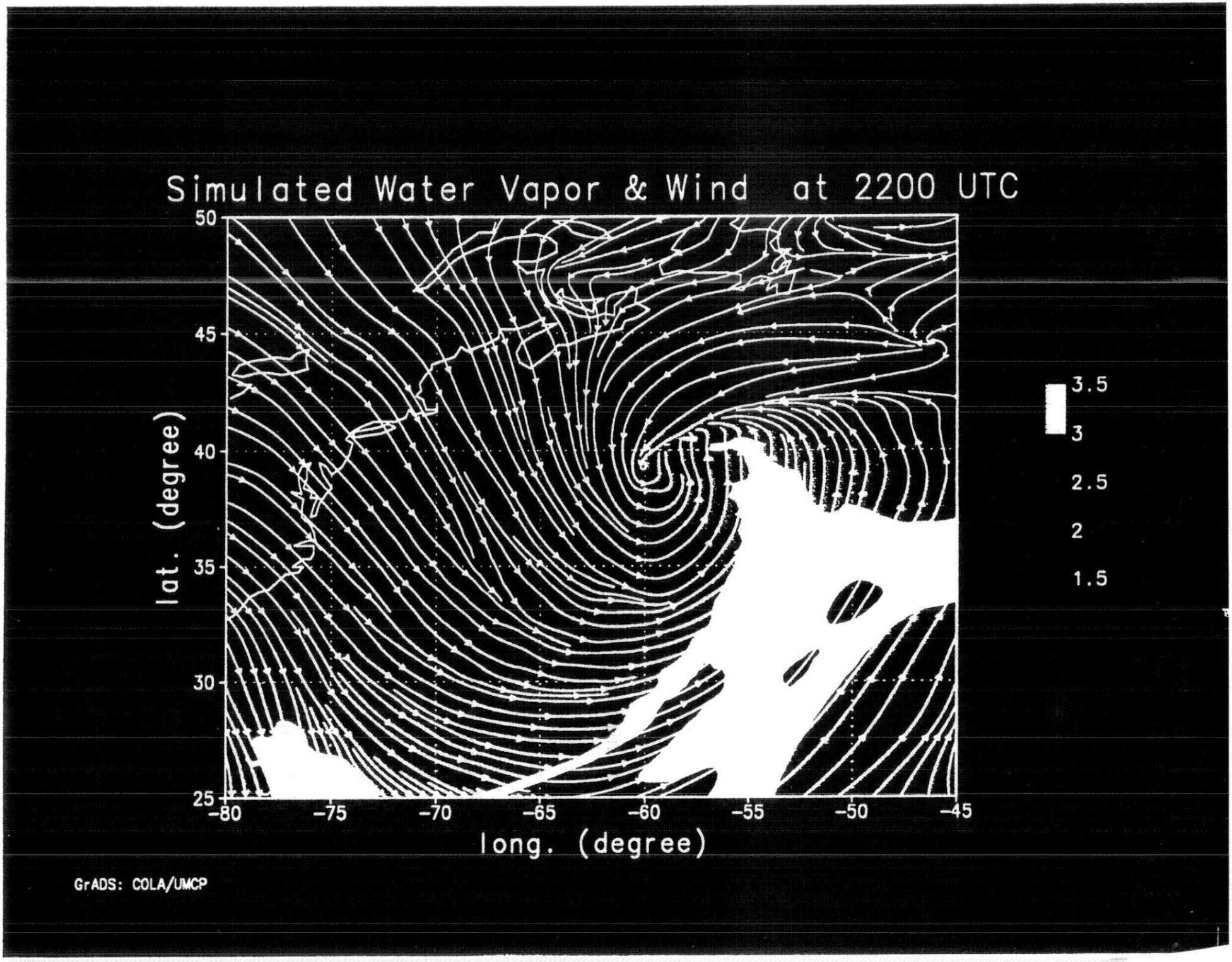
Ship or Buoy Report (UTC)	SSM/I (UTC)
2.5 (00)	0-3 (00)
5.0 (00)	3-6 (00)
5.0 (00)	3-6 (00)
17.5 (00) WRGL	>12 (00)
10 (00)	6-9 (00)
12.5 (00)	9-12 (00)
15.0 (06)	12-15 (0930)
12.5 (06)	9-12 (0930)
10.0 (12)	6-9 (0930)
5.0 (12)	6-9 (0930)
10.0 (06)	6-9 (0930)
5.0 (12)	3-6 (0930)
10.0 (06)	3-6 (0930)
10 (06)	9-12 (0930)
12.5 (12)	9-12 (0930)
7.5 (06)	6-9 (0930)
7.5 (00)	6-9 (22)
5.0 (18)	0-3 (22)
40.0 (18)	>12 (22)
30.0 (18)	>12 (22)


SSM/I IWV (cm) 0930Z 4 Jan 89
50
45
40
35
30
25
lat. (degree)
-80
-75
-70
-65
-60
-55
-50
-45
long. (degree)
4
3
2
1
0
GrADS: COLA/UMCP


SSM/I IWV (cm) 0930Z 4 Jan 89
40
39
38
37
36
35
lat. (degree)
-67
-66
-65
-64
-63
-62
long. (degree)
3.2
2.8
2.4
2
GrADS: COLA/UMCP


Simulated Water Vapor & Wind at 0930 UTC
50
45
40
35
30
25
lat. (degree)
-80
-75
-70
-65
-60
-55
-50
-45
long. (degree)
3.5
3
2.5
2
1.5
GrADS: COLA/UMCP


SSM/I IWV (cm) 22Z 4 Jan 89
50
45
40
35
30
25
lat. (degree)
-80
-75
-70
-65
-60
-55
-50
-45
long. (degree)
4
3
2
1
0
GrADS: COLA/UMCP


Simulated Water Vapor & Wind at 2200 UTC
50
45
40
35
30
25
lat. (degree)
-80
-75
-70
-65
-60
-55
-50
-45
long. (degree)
3.5
3
2.5
2
1.5
GrADS: COLA/UMCP

SUMMARY

Rain Rate:

CAL/VAL Vol. 1 algorithm produces rain rate close to rain gauge analysis. (Vol. 2 retrieval--a factor of four smaller.)
When assimilated into numerical prediction models, produces better forecasts.

Wind:

Hampered by cloud cover.
Otherwise retrieves values with expected errors.
Lower values over regions with fast shifting of synoptic conditions.

Vapor:

Good spatial distribution, gradients and details.
5 Kg m^{-2} (0.5 cm) higher than objectively analyzed moisture field.

ON THE USE OF SSM/I DATA IN THE SHORT-TERM PREDICTION OF MARITIME PRECIPITATION

Roland E. Nagle

Computer Sciences Corp.
Monterey, California

ABSTRACT

Maritime precipitation derived from SSM/I data using several different algorithms are shown including a modified version of the Petty-Katsaros algorithm. These data are input to a numerical model which allows the diagnosed precipitation areas to be remapped to later periods in time (location). The model is based on the relationship between hydrometeors and the mid-troposphere relative vorticity and uses the phase velocity of the atmospheric short wavelength systems as derived from the long wavelength component of the 1000-500mb thickness field as the displacement current. The initial precipitation areas are remapped to later positions via the use of a quasi-Lagrangian coarse mesh integration algorithm. Examples of the individual fields used in the procedure are shown and the results are illustrated in the form of animated sequences of twenty-four hour forecasts of SSM/I rain rate and net water vapor content. Forecasts are verified against the corresponding patterns which existed at the forecast verification time.

Global Rainfall Monitoring: the WetNet Precipitation Intercomparison Project (PIP-1): Results and Reflections

by

Eric C. Barrett, Chris Kidd & Dominic Kniveton
(Remote Sensing Unit, University of Bristol, Bristol, UK) and
Michael G. Goodman & Brian Motta
(Marshall Space Flight Center, Huntsville, AL)

NASA's WetNet Project involves scientists from some 40 institutes in North America, Europe, Asia and Australia. Its practical work programme is centred on a number of Working Groups, the largest of which is the Precipitation Working Group, chaired by E.C. Barrett. The PrecipWG has organized two algorithm intercomparison projects, PIP-1 which has a global climatological emphasis, and PIP-2 which is case-study and meteorologically orientated.

PIP-1 participants were invited to submit SSM/I-based rainfall estimates for the months of August, September, October and November 1987, for global arrays with a 1/2° grid square resolution, and for selected latitude and longitude profiles. Results from a number of other sources were selected for comparative purposes, including some based on data from other satellite sensors (the GPI, using geostationary infrared, and the Spencer algorithm using the NOAA MSU), and from ground observing systems (the continental raingauge data set of the GPCC, and the Pacific atoll rain gauge data set of Morrissey).

Processing of the resulting algorithm outputs frown approximately 20 different laboratories was planned by RSU, Bristol, and performed by MSFC, Huntsville. Results are to be presented at a special PIP-1 Results Workshop in Bristol UK from 10-12 May 1993. A summary of the key findings will be presented in this paper, along with a series of related reflections, and recommendations for future precipitation algorithm design, development, calibration and verification. Part of the future programme of NetWet PrecipWG is to specify "community algorithms" in this field. Scenarios for this to be accomplished will be described and discussed.

Global Rainfall Monitoring: the WetNet Precipitation Intercomparison Project (PIP-1)

by

Eric C. Barrett, Chris Kidd & Dominic Kniveton
(Remote Sensing Unit, University of Bristol, UK)

and

Michael Goodman & Brian Motta
(Marshall Space Flight Center, Huntsville, AL)

CONTENTS

* PIP-1: the plan
* PIP-1: preliminary results
* PIP-1: follow-on proposals

WetNet

is .. ..

".... a pilot program .... designed to enhanee scientific analysis and encourage an interdisciplinary approach to research problems ..... A key element of the project is cooperative research among teams of scientists."

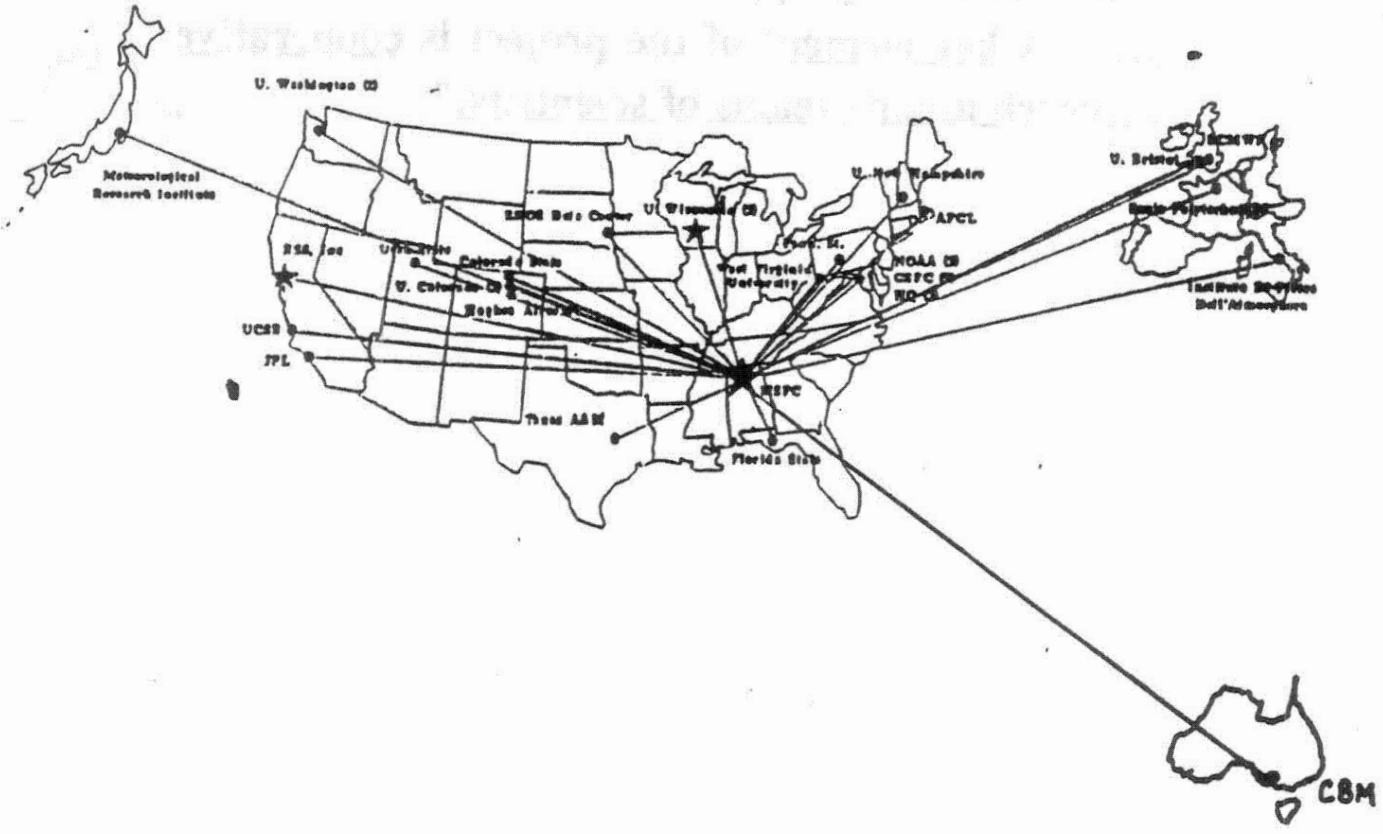
WetNet

is .. ..

".... a pilot program .... designed to enhance scientific analysis and encourage an interdisciplinary approach to research problems ..... A <u>key element</u> of the project is <u>cooperative research among teams of scientists.</u>"

but problems with Ci and layd Str. clouds

Figure 1


U. Washington
Meteorological Research Institute
U. Wisconsin
APCL
NOAA
UCSD
JPL
MSFC
Texas A&M
Florida State
CSM

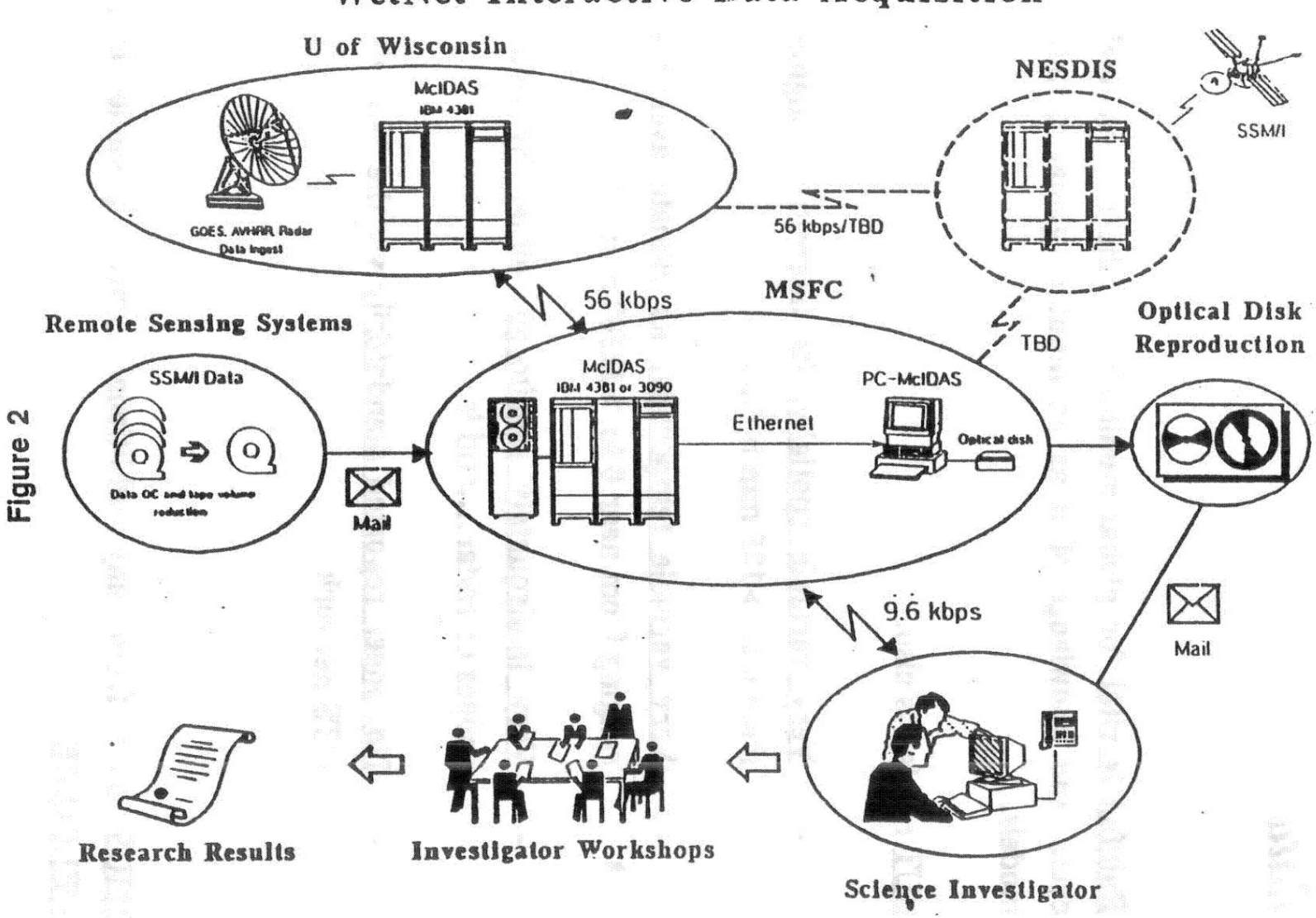

WetNet Interactive Data Acquisition
U of Wisconsin
McIDAS
IBM 4381
GOES, AVHRR Radar
Data Ingest
NESDIS
SSM/I
56 kbps/TBD
56 kbps
MSFC
TBD
Remote Sensing Systems
Optical Disk
Reproduction
SSM/I Data
McIDAS
IBM 4381 or 3090
PC-McIDAS
Ethernet
Optical disk
Data QC and tape volume reduction
Mail
9.6 kbps
Mail
Research Results
Investigator Workshops
Science Investigator

Figure 2

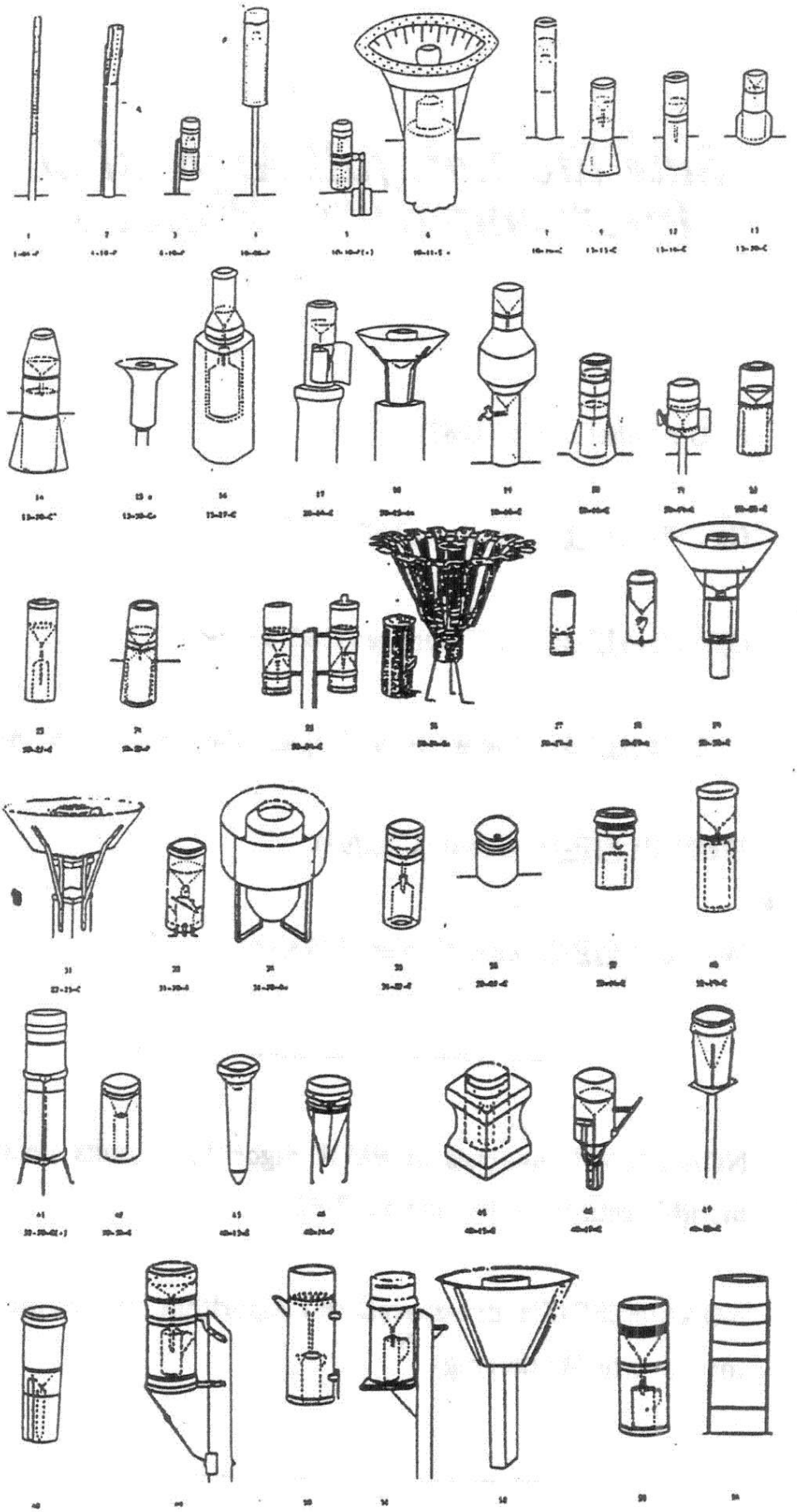
RAINFALL: the need for improved data

Rainfall is vital for global monitoring of the hydrological cycle, and knowledge of it as an input to global climate models.

BUT rainfall is also:

- **Very variable spatially, its intensities ranging from 0 to >125 mm h^{-1}....**
- **Very variable temporally, its climate averages ranging from near 0 to >12500 mm y^{-1}....**
- **Very inadequately monitored, either by rain-gauges or radar....and is**
- **No longer reported mandatorily via the WMO's GTS network.**

THUS data from any additional source possible is WELCOME!



Typen der nationalen Standardniederschlagsmesser weltweit, nach der Grösse der Auffangöffnung eingeordnet. Nach Sevruk und Klemm (1989).

RAIN GAUGES

Satellite Rainfall Algorithm Intercomparison Projects

* FAO's Sahel Study (1987).

* GPCP's AIP-1: Japan (1990). ✓

* GPCP's AIP-2: NW Europe (1992/93). ✓

* GPCP's AIP-3: the western Tropical Pacific (in planning).

* WetNet's PIP-1: global (1992/93). ✓

* WetNet's PIP-2: case studies (1993/94).

---

* NOAA/NWS's analysis of PMW algorithm results providing monthly estimates through 1987-92.

* NOAA/NESDIS's pre-operational algorithm intercomparison for Climate Monitoring.

Satellite Rainfall Algorithm Intercomparison Projects

* FAO's Sahel Study (1987).

* GPCP's AIP-1: Japan (1990). ✓

* GPCP's AIP-2: NW Europe (1992/93). ✓

* GPCP's AIP-3: the western Tropical Pacific (in planning).

* WetNet's PIP-1: global (1992/93). ✓

* WetNet's PIP-2: case studies (1993/94).

---

* NOAA/NWS's analysis of PMW algorithm results providing monthly estimates through 1987-92.

* NOAA/NESDIS's pre-operational algorithm intercomparison for Climate Monitoring.

PIP-1 plan

Objectives

1. To demonstrate, test and intercompare techniques for global monthly rainfall monitoring by SSM/I

2. To "validate" SSM/I rainfall monitoring techniques through comparisons with other data sets

3. To gain insights into rainfall algorithms and radiative processes through studies of their differences in terms of the specific assumptions, strengths and weaknesses of each

4. To pave the way for subsequent PIPS, and the use of SSM/I rainfall algorithms operationally, even through development of "community algorithms"?

5. To confirm to the wider scientific community the importance of the WetNet-style interdisciplinary and multilaboratory activities

PIP-1 Management

A Steering Committee has been set up for PIP-1, involving

- **Jim Dodge (NASA-HQ)**
- **Eric Barrett (Univ. Bristol)**
- **Mike Goodman (NASA - MSFC)**
- **John Janowiak (NOAA - NESDIS)**
- **Eric Smith (FSU, Tallahassee)**

In RSU Bristol, PIP-1 results will be generated by a team including Eric Barrett, Michael Beaumont, Chris Kidd and Dominic Kniveton.

PIP-1 Data Sets

I ANALYSIS:

1. WetNet SSM/I (F8) data for August through November 1987 as provided by MSFC on optical disks

2. The global coastline mask as distributed on ODs by MSFC

II INTERCOMPARISON/VALIDATION (to be distributed to participants after receipt of their initial results) ~ a total of 16 algorithm outputs from 12 laboratories (in USA, UK, Germany, Italy & Japan)

1. GPI IR monthly rainfall products

2. ECMWF global model estimated monthly rainfall products

3. Spencer's MSU monthly rainfall products

4. Adler's combined GPI/SSM/I monthly rainfall products

5. GPCC global continental raingauge data set for 1987

6. Morrissey's Pacific Atoll raingauge data set

PIP-1 Deliverables

Digital products for Aug - Nov 1987 to include as many as possible of the following:

1. Global arrays of estimated total monthly rainfall for ½° grid squares (origin 180°W, 90°S), plus histograms of estimated monthly rainfall for land, oceans, and land plus oceans.

2. Estimated instantaneous rain rates for time-latitude and time-longitude displays, for each day from JD213-334 (ascending and descending passes separately), also at ½° resolutions.

Results to be delivered initially to MSFC on floppy disks, for extraction of further statistics, and subsequent assessment by RSU, Bristol.

PIP-1 Schedule

1. November 1991: invitations to participate

2. January 1992: receipt of final elements of PIP-1 data sets

3. January - July 1992: generation of results by participating laboratories

4. 31 July 1992: deadline for deliverables to MSFC

5. August - September 1992: generation of supplementary statistics by MSFC, and supply of "validation" data sets to labs

6. October - March 1993: preparation of PIP-1 intercomparison results by RSU

7. ~~13 - 14 April~~ 10 - 12 May 1993: discussion/review meeting in Bristol UK

8. After April 1993: publication of individual and overall results

Analysis of Deliverables

Images, graphs and statistics will be prepared as follows:

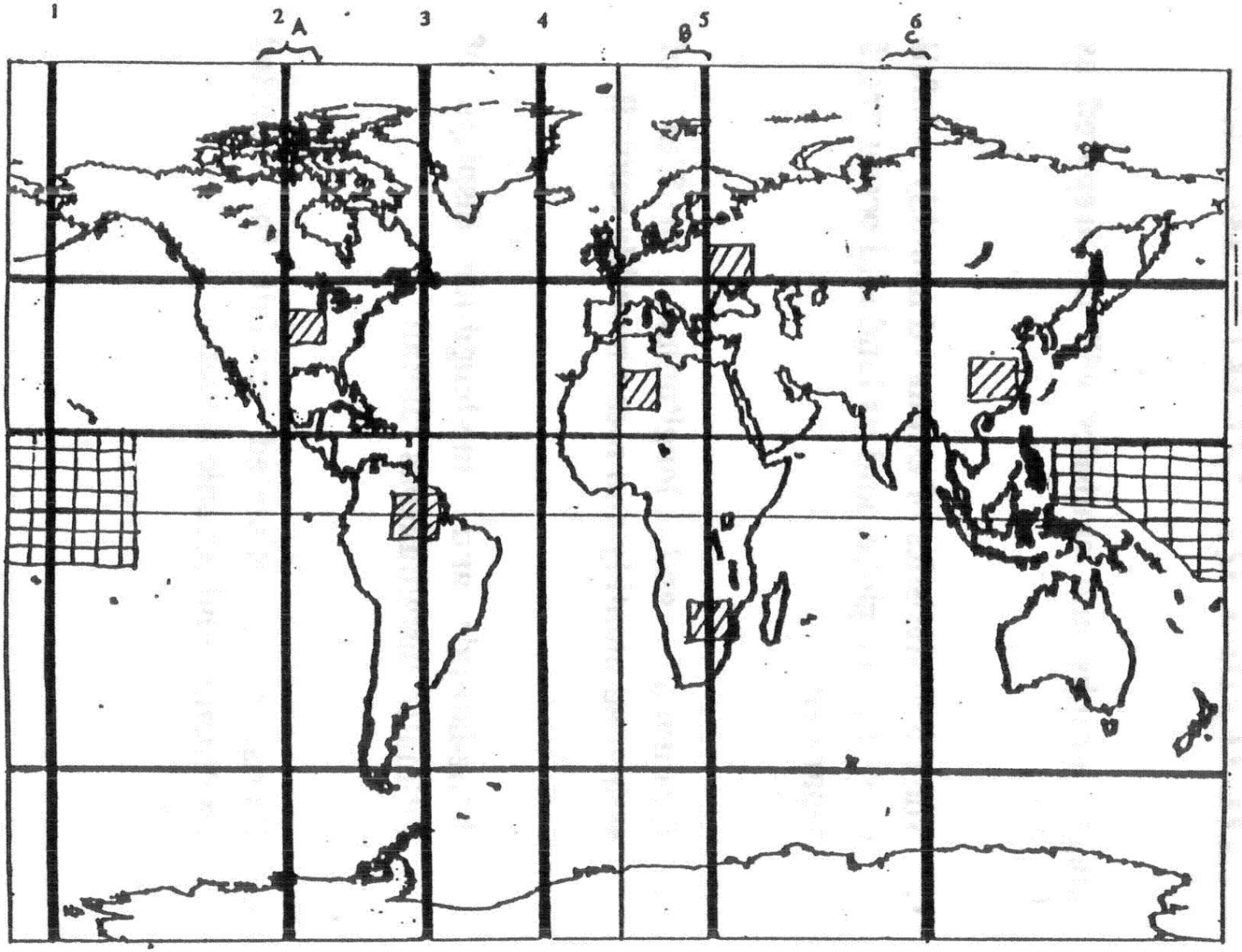
1. **Maps and statistics of estimated monthly rainfall totals for the globe, and its land and ocean areas separately**

2. **Latitudinal and longitudinal profiles of estimated monthly and mean monthly rainfall**

3. **Time-latitude and time-longitude displays of estimated instantaneous rainfall**

4. **Statistics of estimated rainfall for selected continental and oceanic regions**

Figure 1: Half degree sections of interest.



PIP-1 Results: some relevant points

* Originally scheduled to be finalized by mid-April, some processing of statistics is still being completed.

* A preliminary review of results was undertaken at the PIP-1 Results Workshop, Bristol, UK from 10-12 May 1993.

* A period of "results digestion" is now under way: opinions on the "best" algorithm(s) will be sent to ECB from PrecipWG Members by 15 July.

* "Digested results" will be prepared for publication in a Special PIP-1 Edition of *"Remote Sensing Review"* - contents to be approved in Logan, Utah in September (WetNet Plenary) and published in December 1993.

* Composite ("community") algorithms will be sought based on PIP-1 results.

Fig. 3. Sites of stations with precipitation data received via GTS (CLIMAT and SYNOP reports) in August 1987.

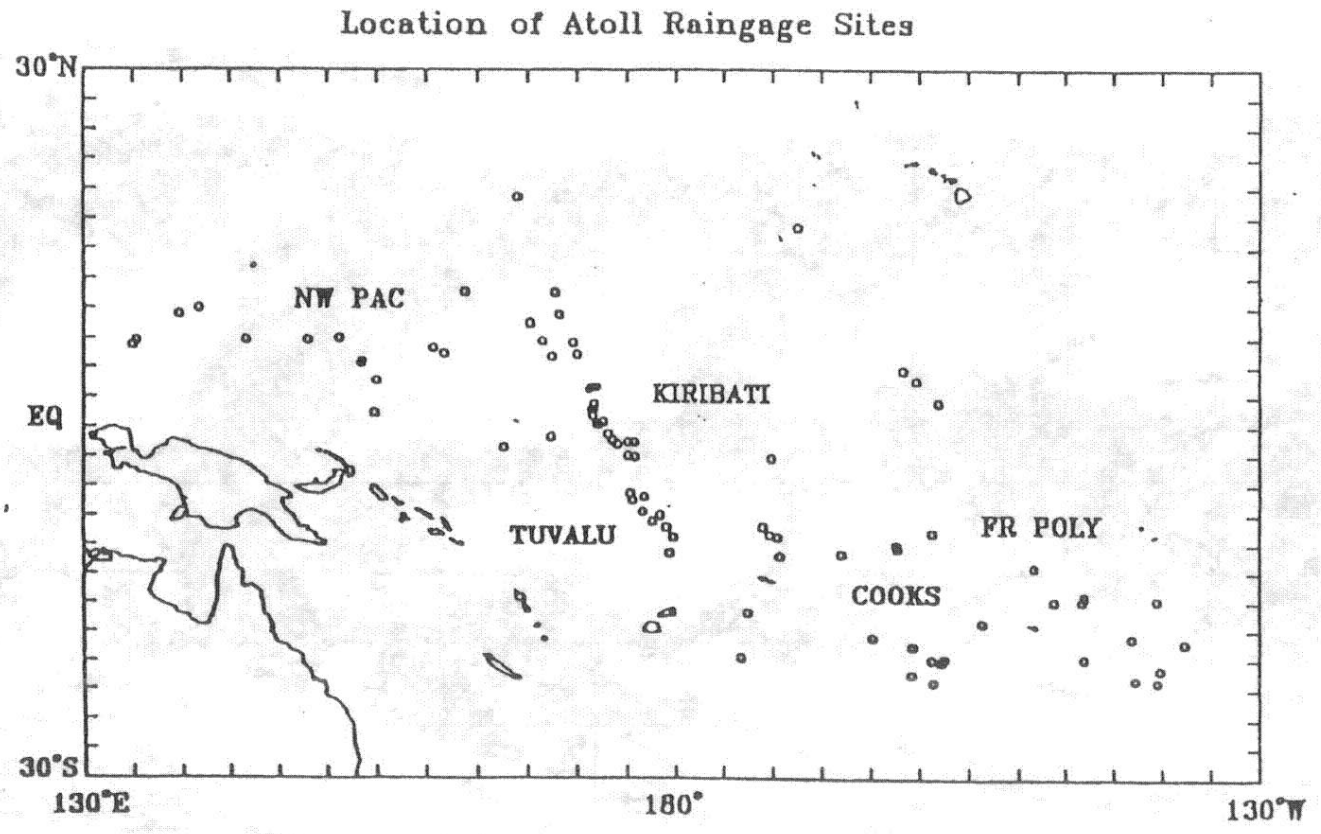
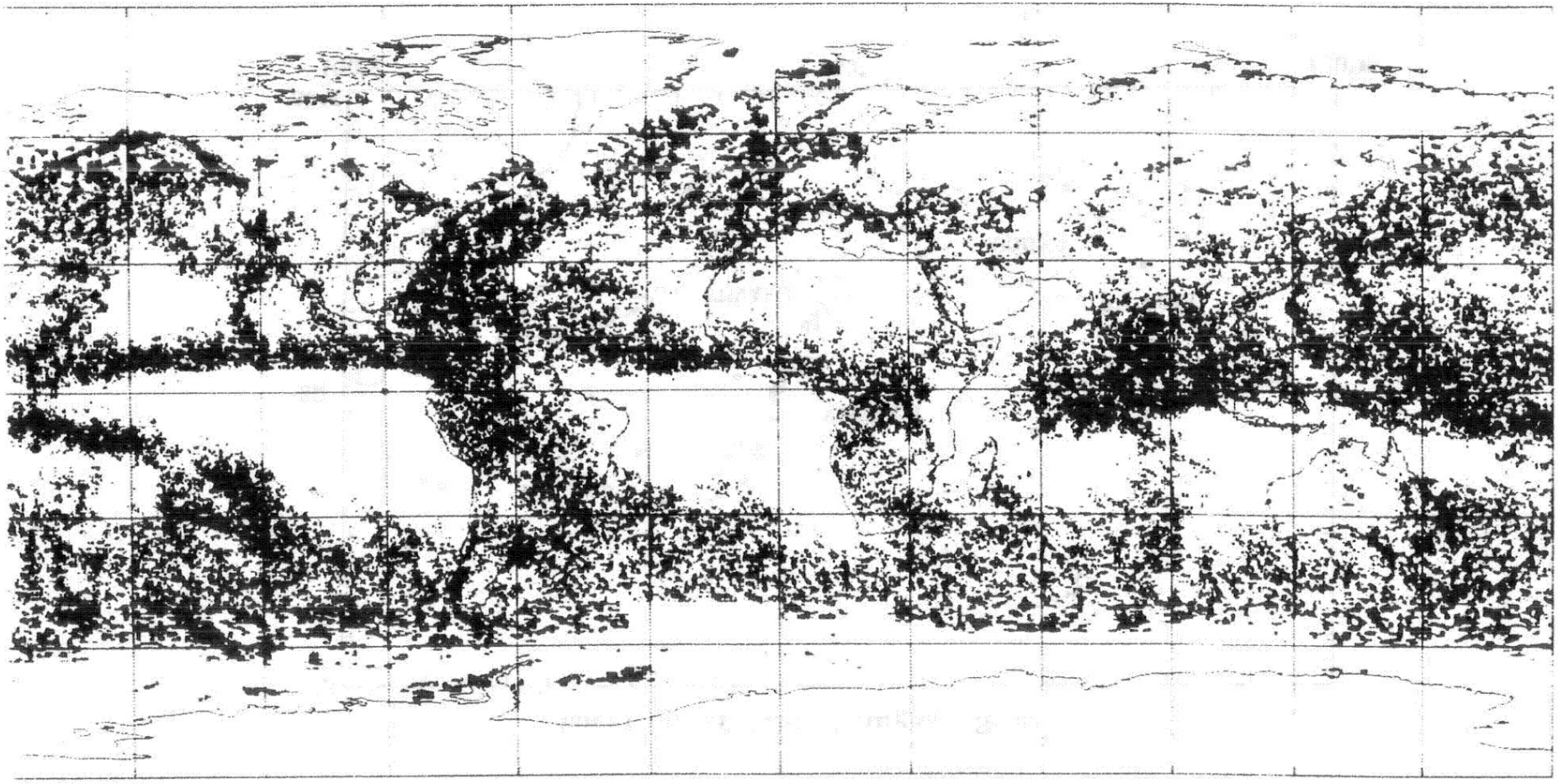
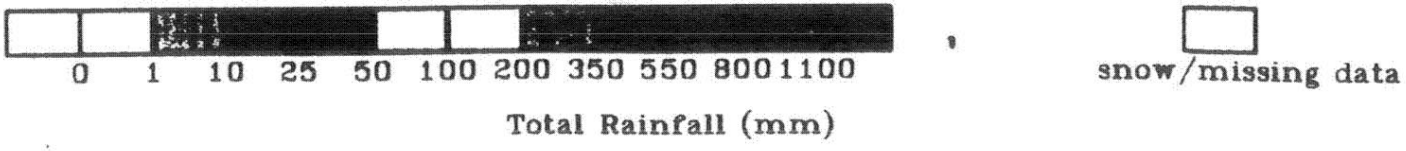


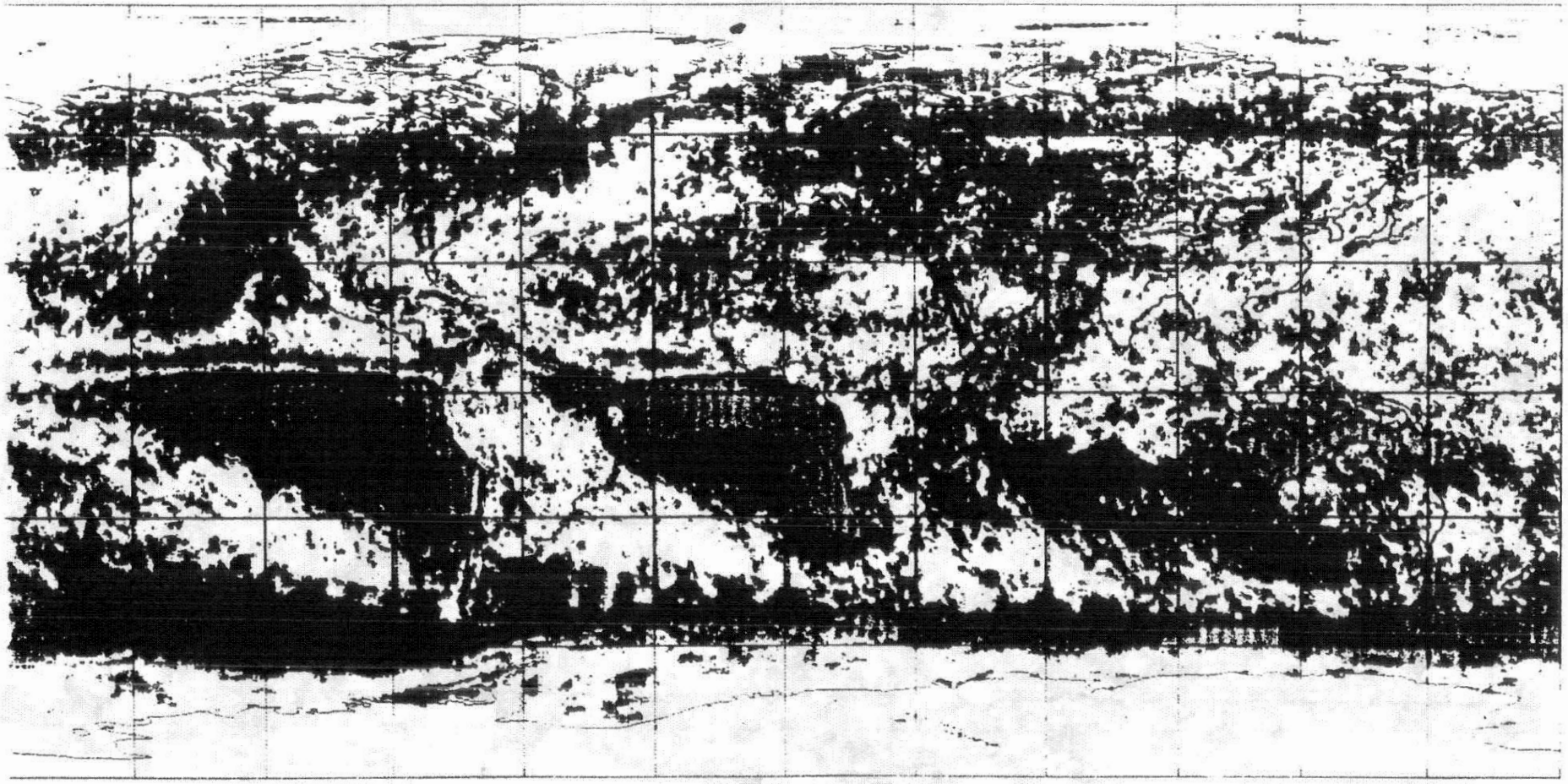
Figure 1 Distribution of Pacific atoll raingage stations.

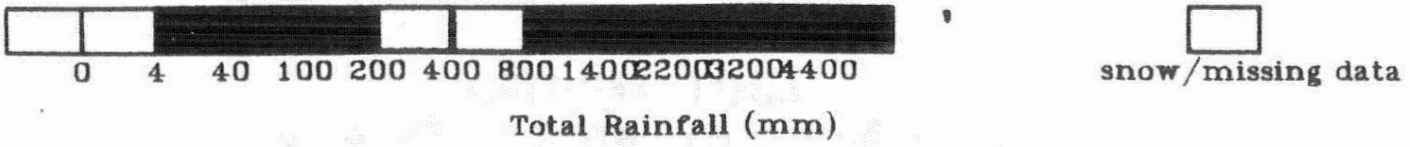
Adler (ADL)
October 1987



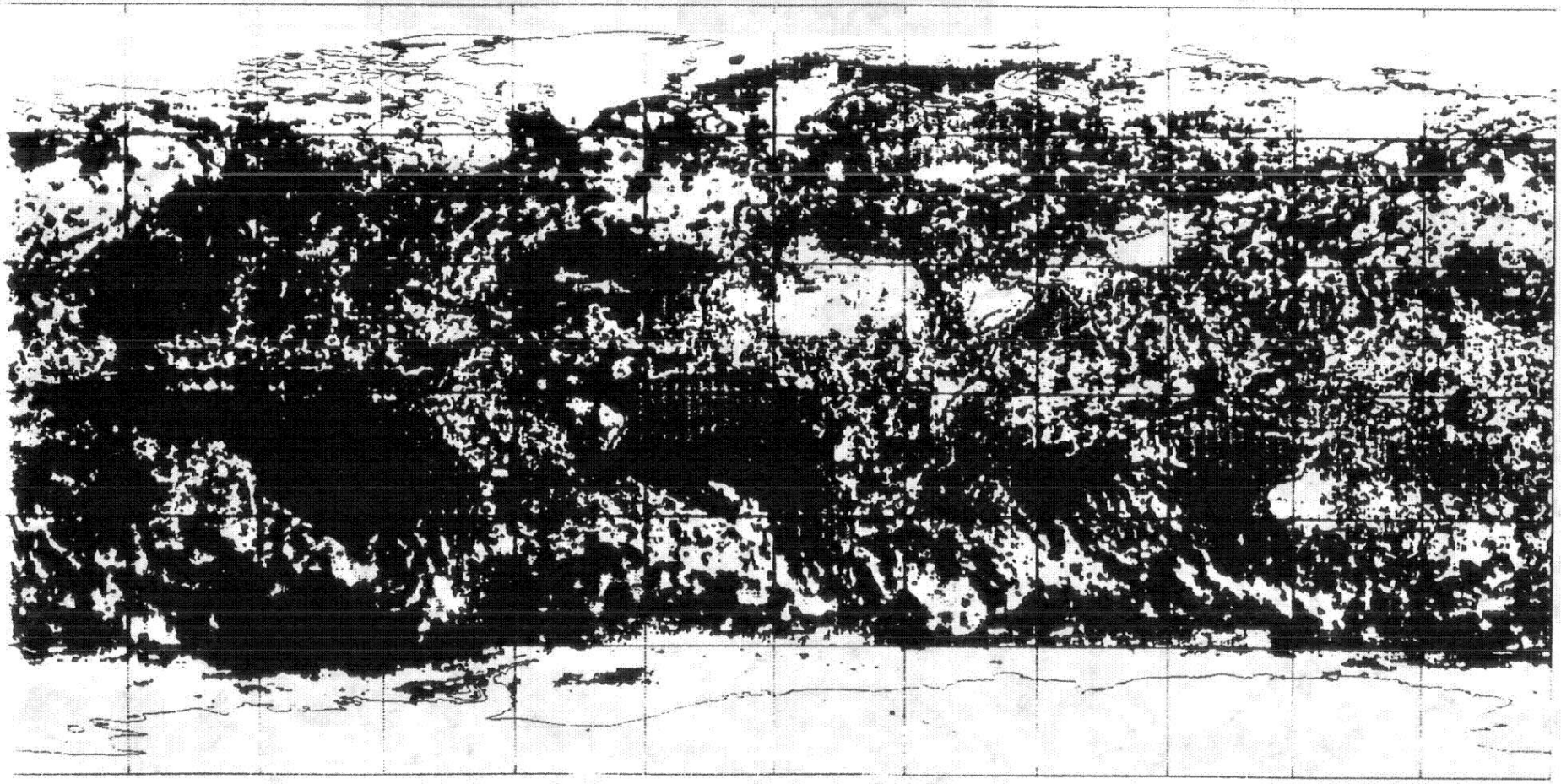


Average values (0.5 degrees)
Aug–Nov 1987





Average values (0.5 degrees)
October 1987

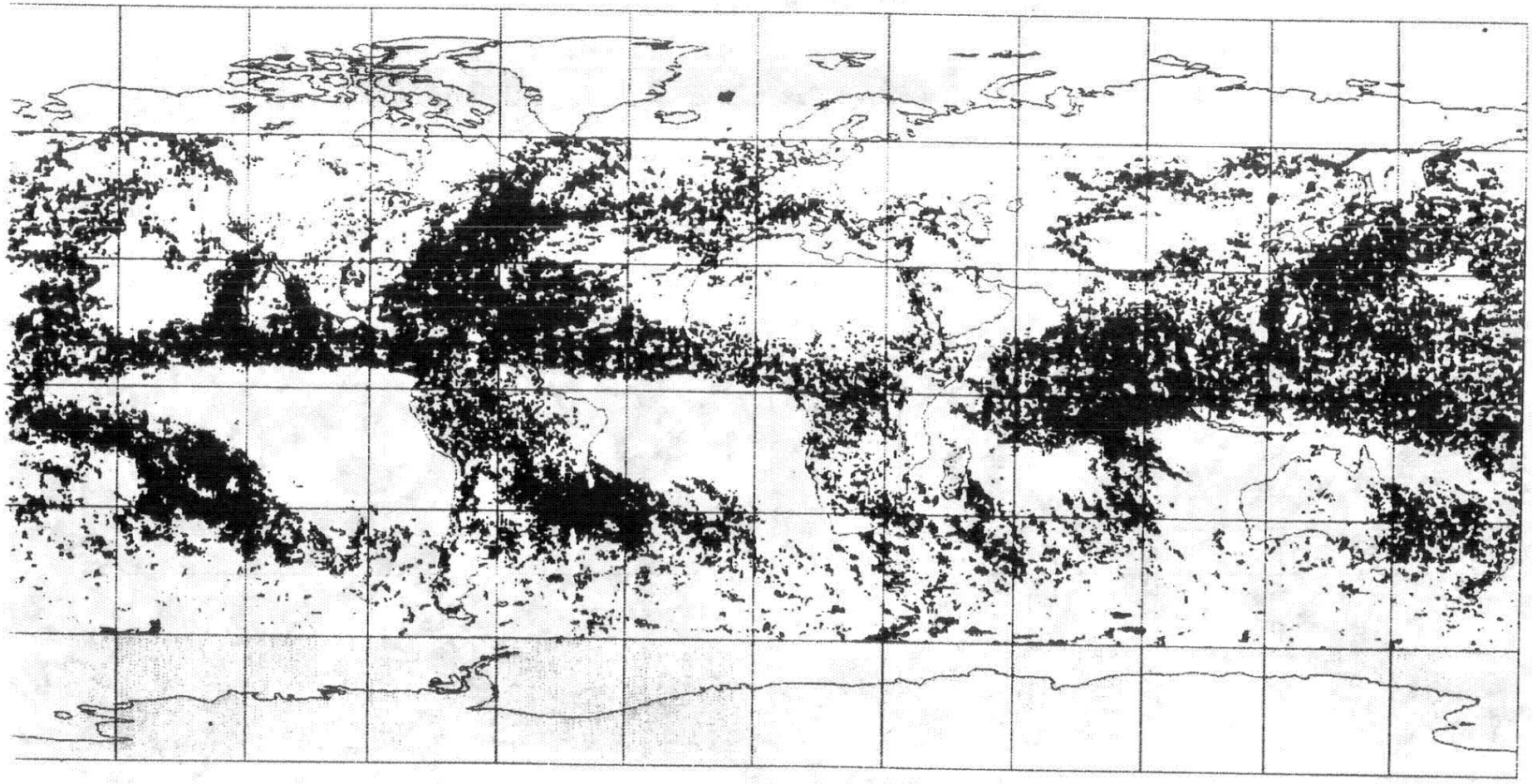


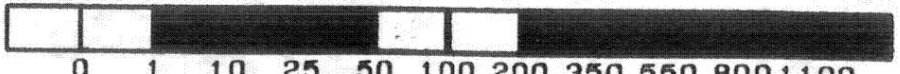
0 1 10 25 50 100 200 350 550 800 1100

Total Rainfall (mm)

snow/missing data

Smith(1) (SMI)
October 1987



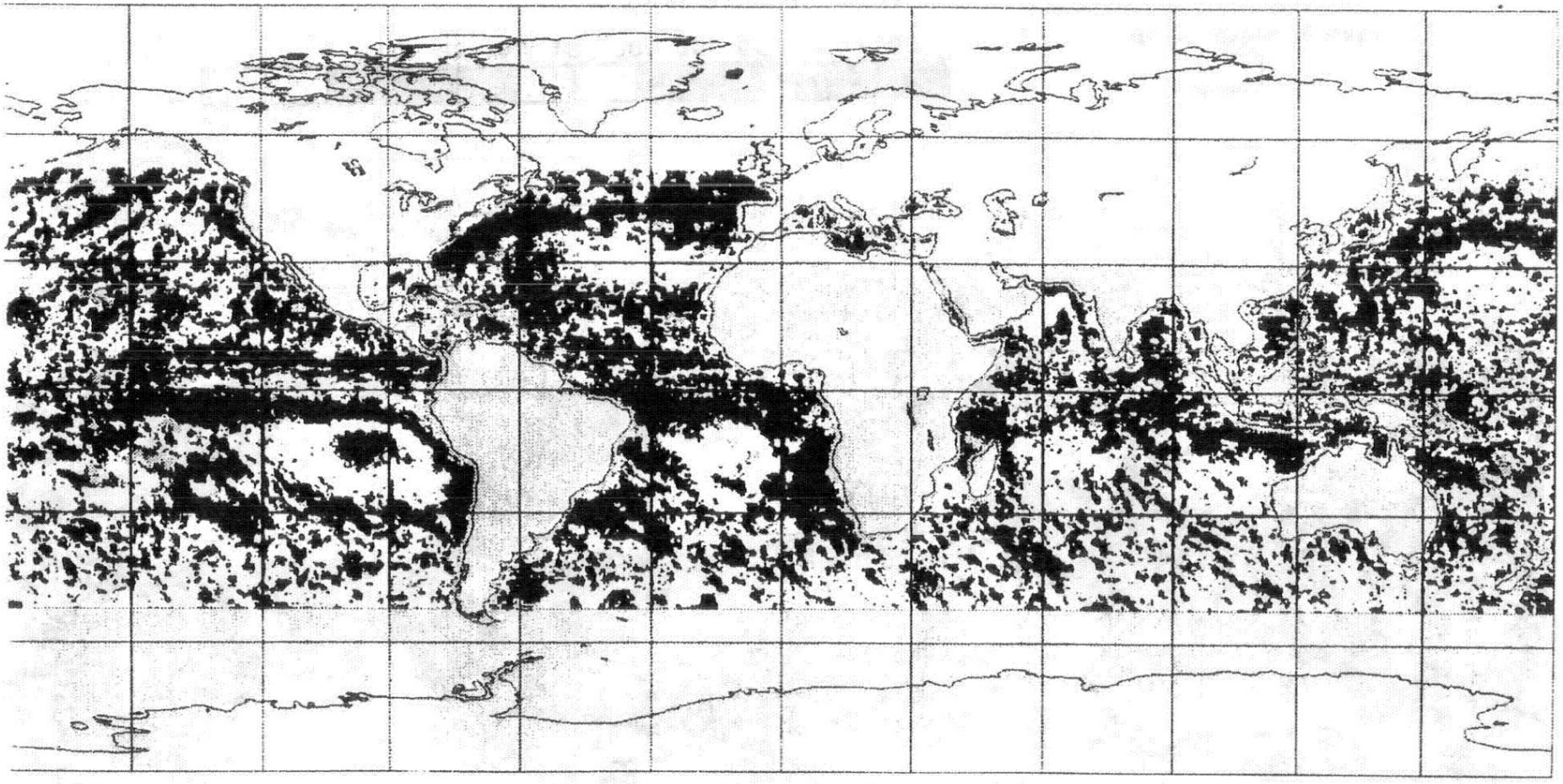


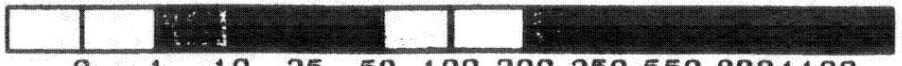
Total Rainfall (mm)



snow/missing data

Wilheit (WIL)
October 1987



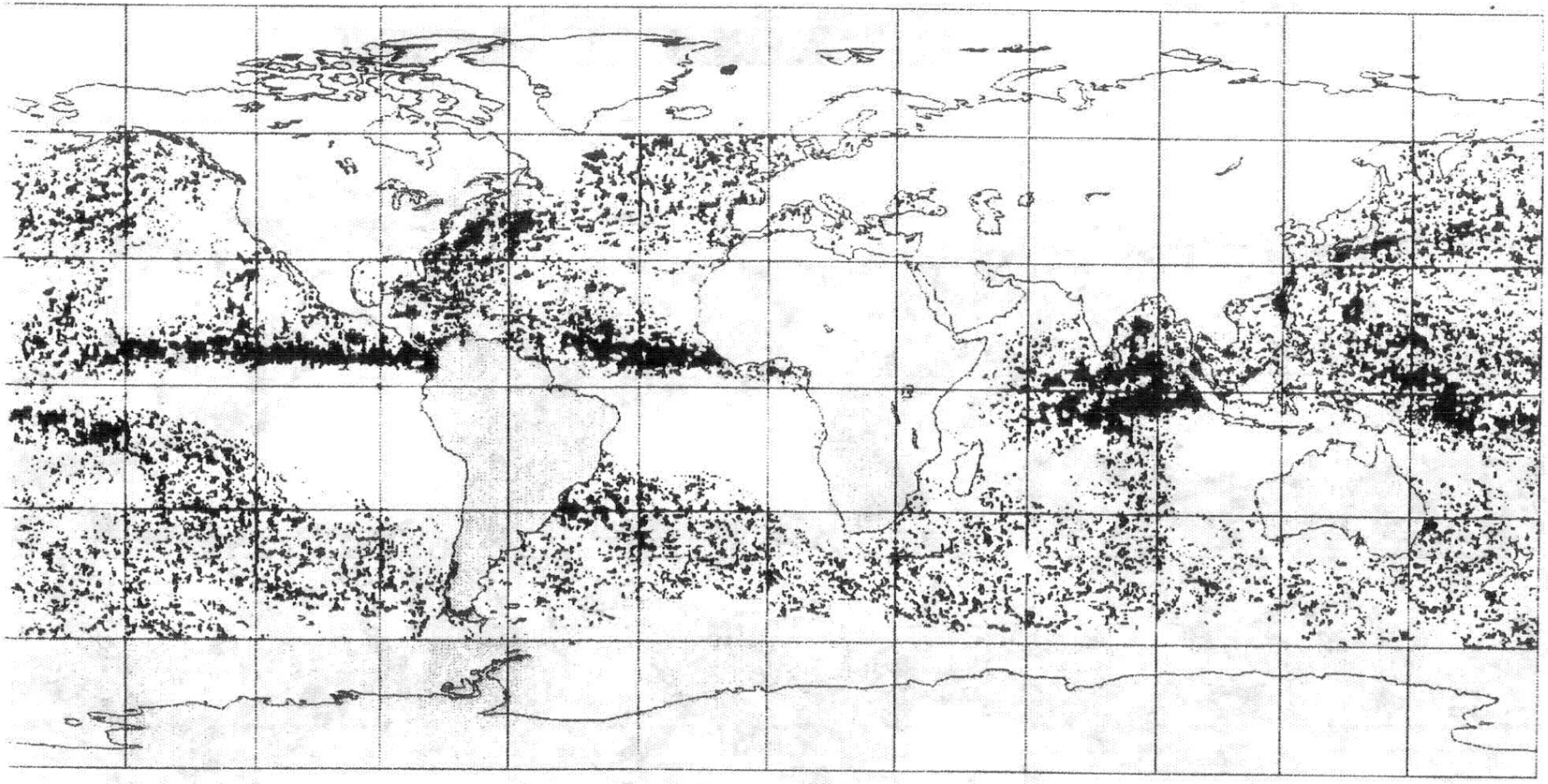


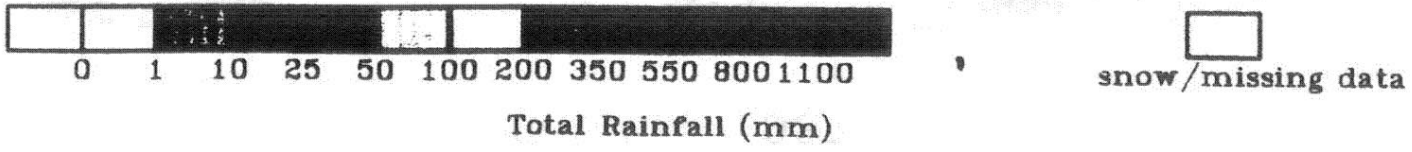
Total Rainfall (mm)



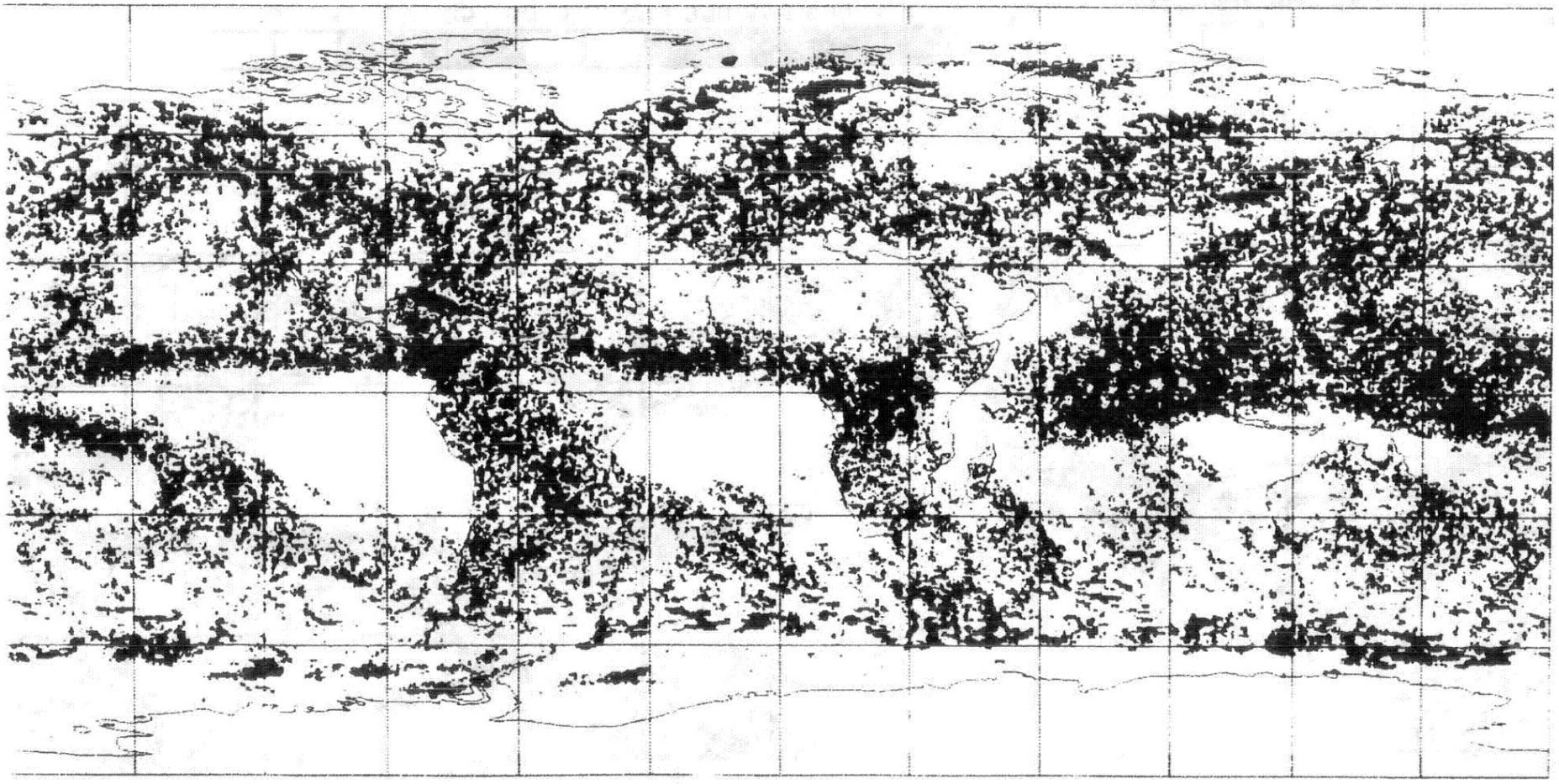
snow/missing data

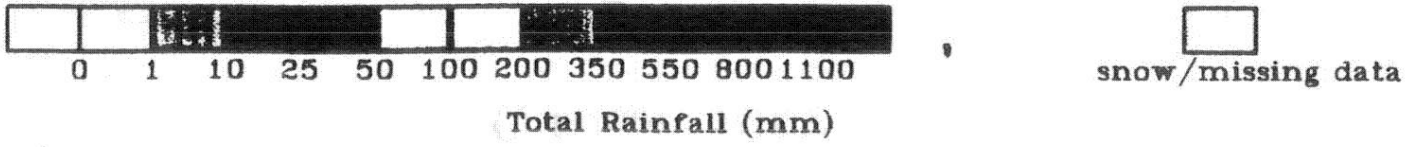
Berg (BER)
October 1987



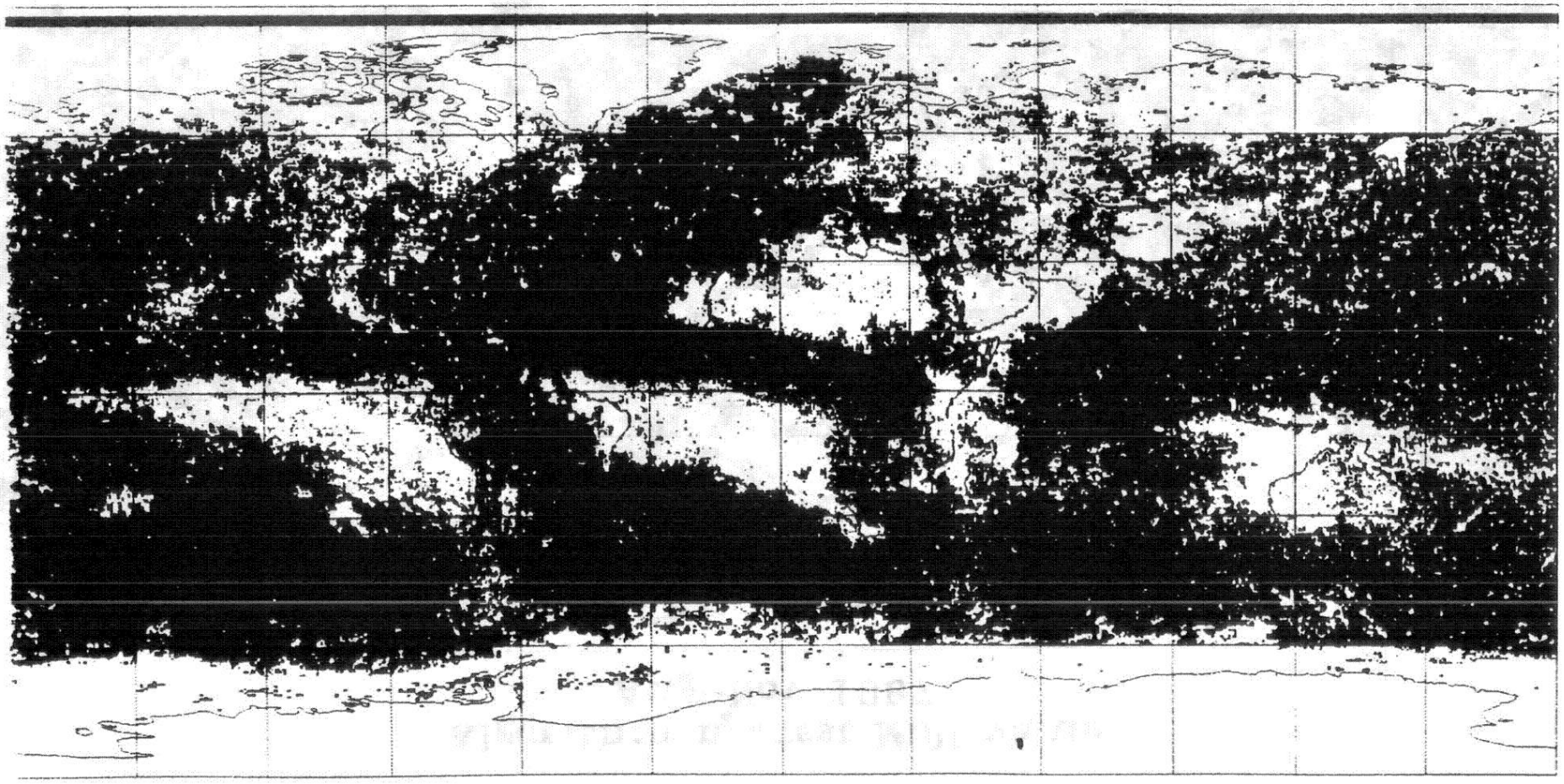


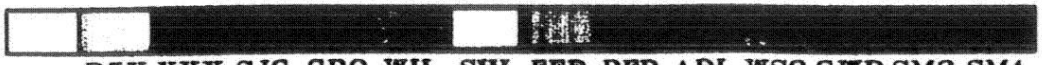
Grody (GRO)
October 1987





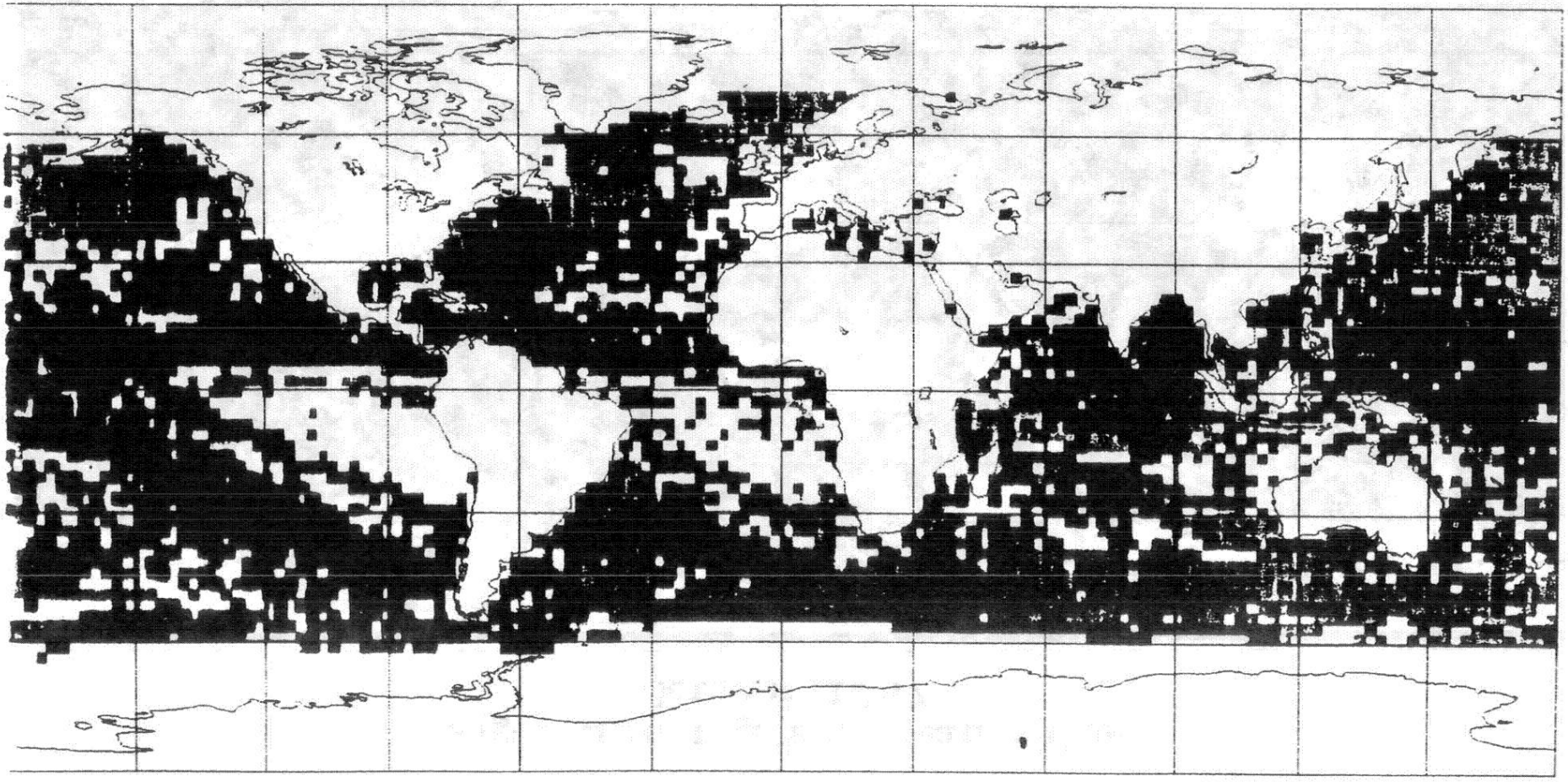
Algorithm nearest mean value
October 1987

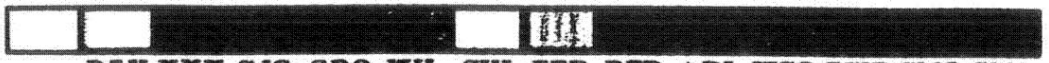




D5K XXX SJG GRO WIL SHI FER BER ADL WSO GWP SM2 SM1

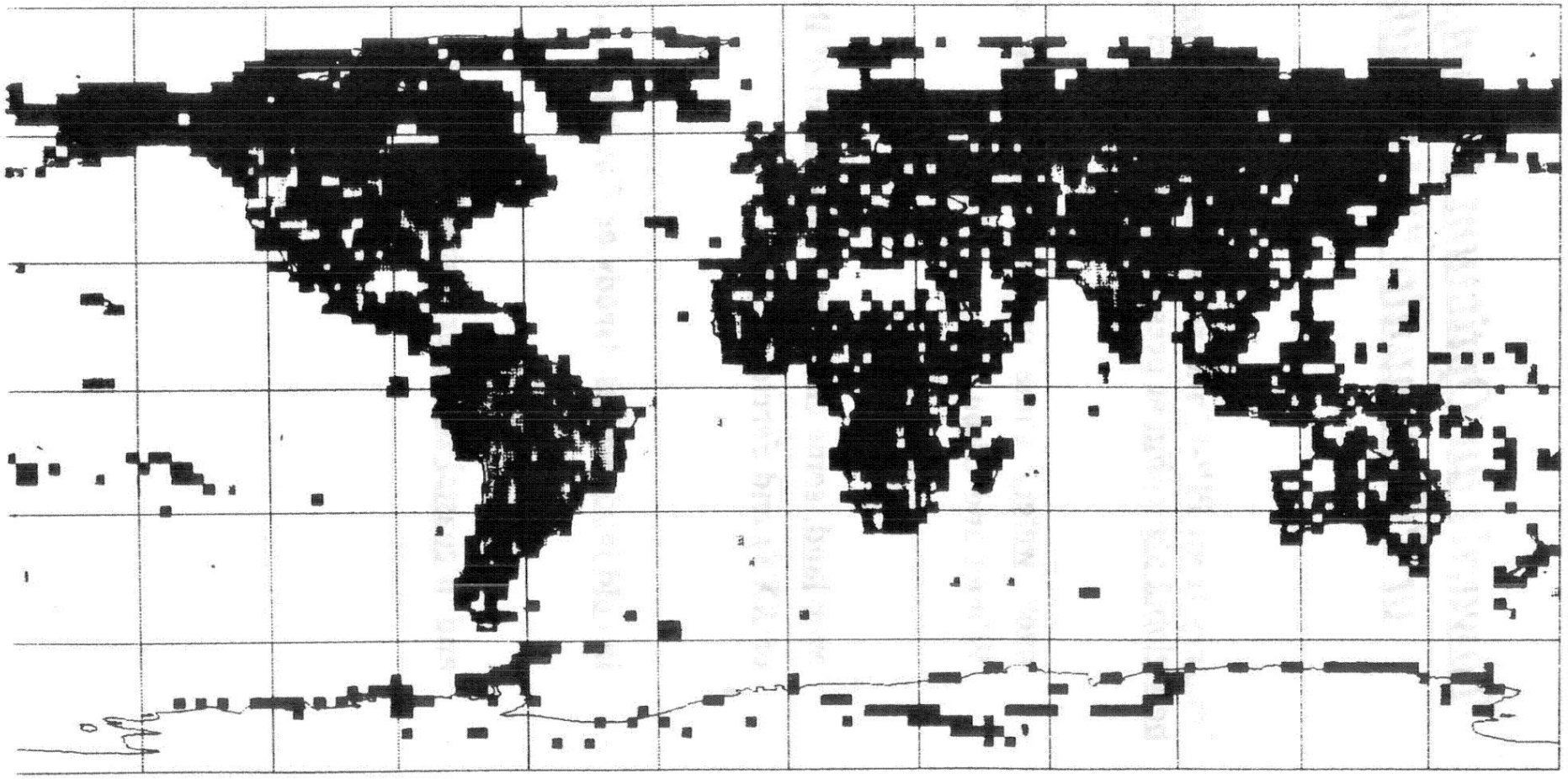
Algorithm nearest MSU value
Aug–Nov 1987





D5K XXX SJG GRO WIL SHI FER BER ADL WSO GWP SM2 SM1

Algorithm nearest GPCC value
Aug–Nov 1987





D5K XXX SJG GRO WIL SHI FER BER ADL WSO GWP SM2 SM1

Towards an Optimum ("Composite" or "Community") Algorithm

Imagery from PIP-1, and related statistics, suggest that the best global algorithm at present would be constructed from:

- **over water, some combination of Grody, Smith, Wilheit and Olson....?**

- **over land, some choice or combination of Bristol (D5K or XXX) and Ferriday....?**

- **in cold land regions, Grody or Goodman....?**

- **and in coastal zones, probably Adler....?**

However:

- a programme of PIP-1 results permutations now beginning in RSU should be more conclusive than mere "eyeballing"....

- most algorithms seem to have done best in the (types of) regions for which they were calibrated....

- further "composite algorithm" development should be encouraged (2 or 3 groups of laboratories?)....

- standard calibration AND validation data sets should be used for evaluation in subsequent global intercomparsons....

- more uniform approaches should be sought (through more purely "physical" rather than more pragmatic "empirical" approaches?) - but will take longer (a decade??) to out-perform the more immediately "pragmatic" possibilities....

Session 6

Future Directions

(Marie Colton, FNOC, Chair)

ENCL(12)

Session 6

Future Directions

(Marie Colton, FNOC, Chair)

DMSP BLOCK 6 F8 TILT EXPERIMENT: A STATUS REPORT

Samuel D. Gasster
Radar & Signal Systems Department

David L. Glackin
DMSP Directorate

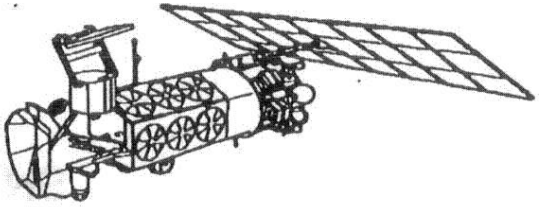
Don J. Rudy
Sensing & Exploitation Department

all at The Aerospace Corporation
2350 East El Segundo Blvd.
El Segundo, CA
90245-4691

The F8 Tilt Experiment was proposed in response to trade studies performed for the microwave imager during Phase I of the DMSP Block 6 Concept Studies. These studies indicated that in order to achieve the DMSP Block 6 goal of contiguous swaths at the equator for the microwave imager, it would be necessary to increase the earth incidence angle (EIA), the spacecraft orbital altitude (over the current 833 km), or a combination of both. Increased orbital altitude introduces several systems concerns, including an increase in the natural radiation environment and the need for a large sensor aperture to maintain resolution. On the other hand, increased EIA introduces several major concerns regarding remote sensing physics and phenomenology. These include increased atmospheric attenuation, decreased ocean emissivity for horizontal polarization, decreased sensitivity in the vertical polarization channels due to Brewster angle effects, and several other effects as well. In addition, geophysical parameter retrieval techniques may require nonlinear algorithms at the higher EIA, and existing models for predicting brightness temperatures may not be adequate.

In 1990 the Operation Line Scanner (OLS) on F8 failed but the SSM/I remained operational (currently both 85 GHz channels are not operating on F8). The possibility of rotating the spacecraft about its pitch axis to achieve an increased EIA from the F8 SSM/I was therefore considered. The present paper reviews the status of the F8 Tilt Experiment test and analysis plans.

DMSP BLOCK 6
F8 TILT EXPERIMENT:
A STATUS REPORT



DR. SAMUEL D. GASSTER
RADAR & SIGNAL SYSTEMS DEPARTMENT
DR. DON J. RUDY
SENSING & EXPLOITATION DEPARTMENT
DAVID L. GLACKIN
DMSP DIRECTORATE
THE AEROSPACE CORPORATION

JUNE 9, 1993

OUTLINE

- INTRODUCTION
- TILT EXPERIMENT TEST PLAN
- TILT EXPERIMENT ANALYSIS PLAN
- CONCLUSIONS

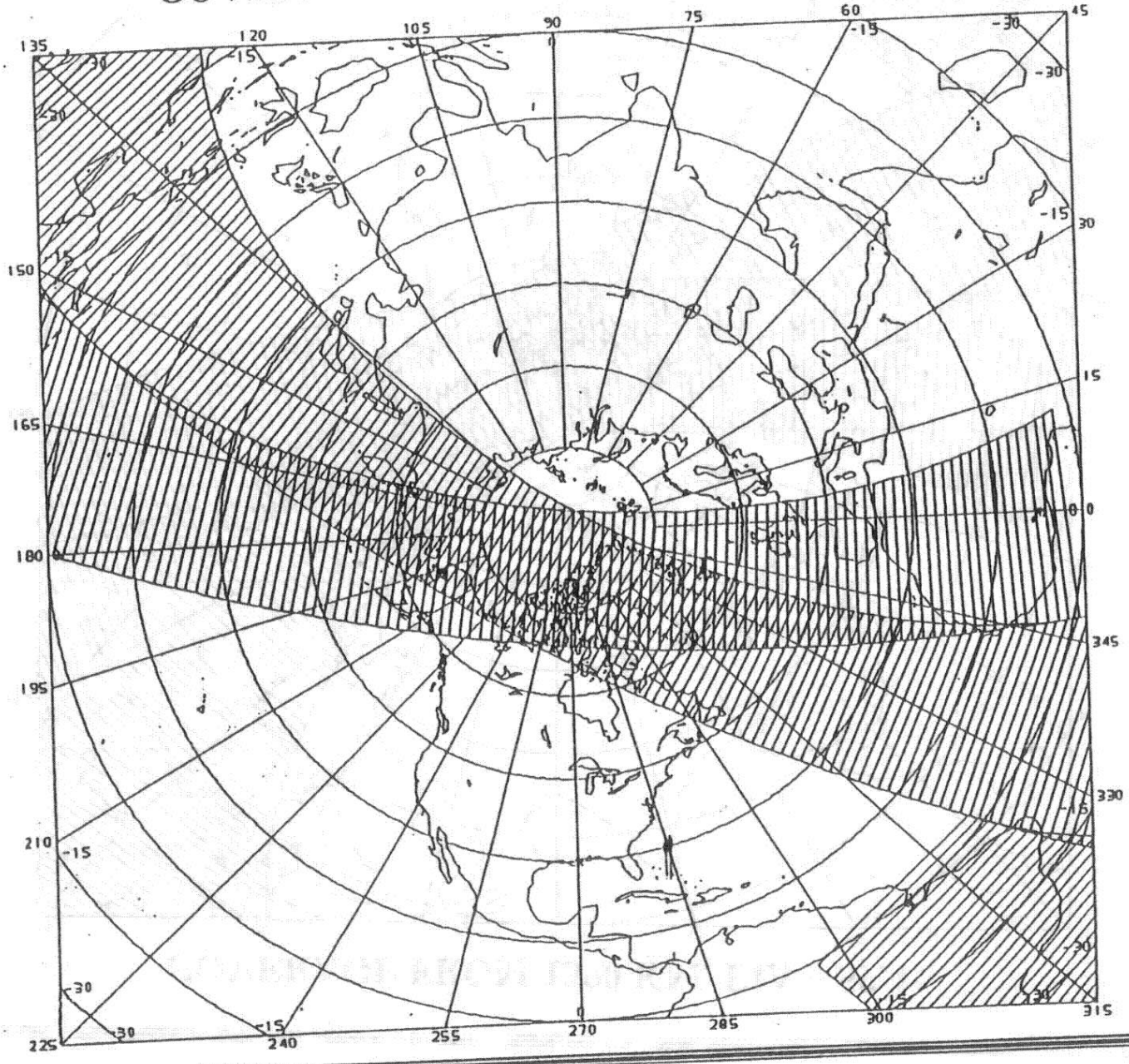
INTRODUCTION

- MOTIVATION
  - DMSP DOES NOT PROVIDE CONTIGUOUS EQUATORIAL COVERAGE
    - » 5D-2 SSM/I H = 833 km, EIA = 53.1°, ACTIVE SCAN = 102°, SWATH = 1395 km
    - » 5D-3 SSM/IS, ACTIVE SCAN = 143°, SWATH = 1700 km, 62% EQUATORIAL COVERAGE
  - USERS AT JOINT TYPHOON WARNING CENTER DESIRE CONTIGUOUS COVERAGE
  - DMSP BLOCK 6 HAS A GOAL OF CONTIGUOUS EQUATORIAL COVERAGE
- APPROACHES TO INCREASE SWATH AND ACHIEVE CONTIGUOUS EQUATORIAL COVERAGE
  - INCREASE SATELLITE ALTITUDE
  - INCREASE MICROWAVE IMAGER EARTH INCIDENCE ANGLE (EIA)
  - COMBINATION OF BOTH
- CONCERNS ASSOCIATED WITH EACH APPROACH
  - HIGHER ALTITUDE
    - » INCREASE IN NATURAL RADIATION
    - » LARGE SENSOR APERTURE REQUIRED TO MAINTAIN SPATIAL RESOLUTION
  - HIGHER EIA
    - » INCREASED ATMOSPHERIC PATH
    - » DECREASE IN ε_H for the OCEAN
    - » DECREASED SENSITIVITY IN V-POLARIZATION CHANNELS DUE TO BREWSTER ANGLE EFFECTS
    - » INCREASED IMPACT OF CLOUD INHOMOGENEITIES

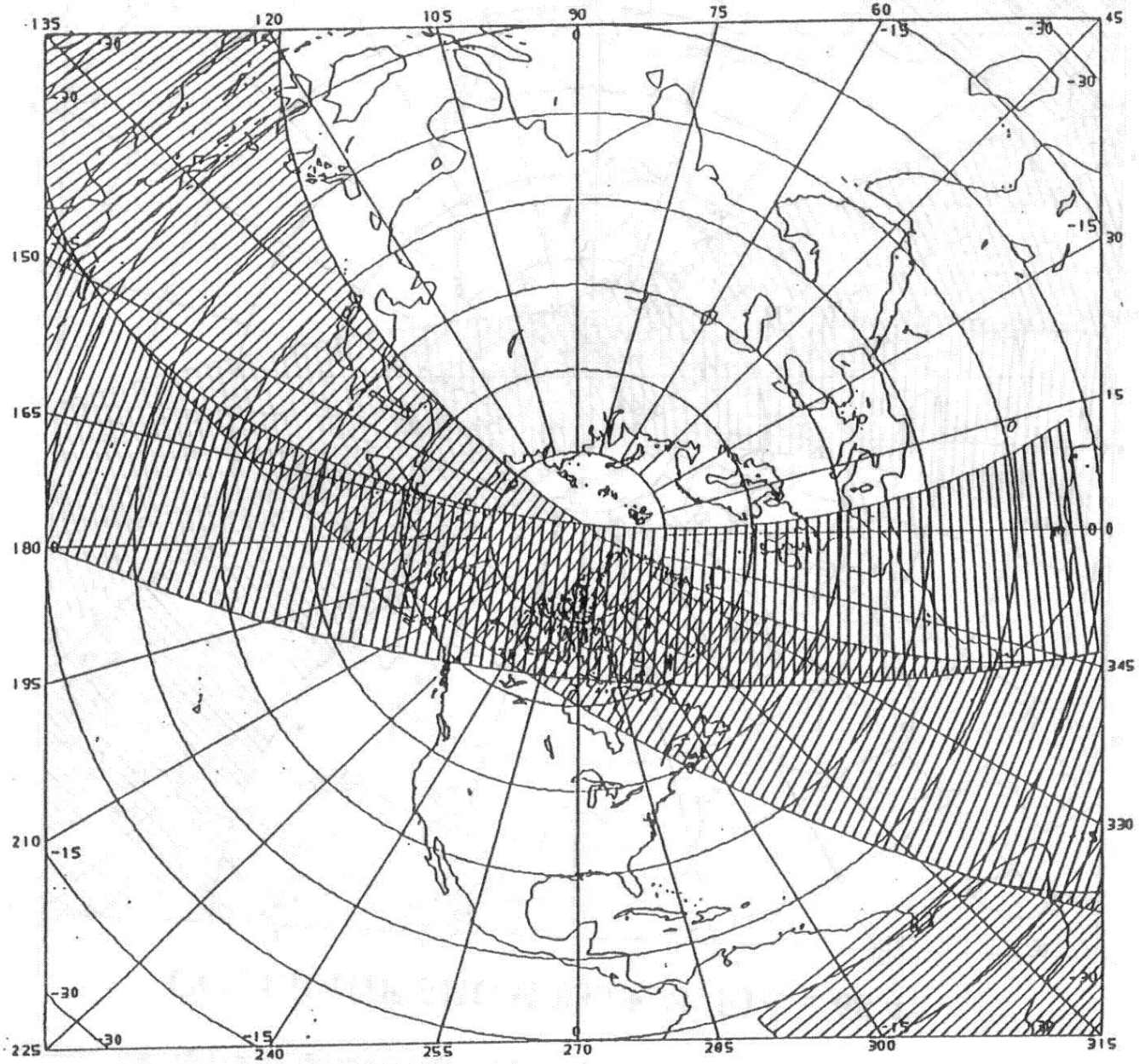
INTRODUCTION (contd)

- CONCERNS OVER LACK OF MEASUREMENTS AT HIGH EIA MOTIVATED TWO EXPERIMENTS
  - NRL TOWER TEST USING SSM/I SIMULATOR
  - DMSP 5D-2 F8 SATELLITE TILT EXPERIMENT
- F8 TILT EXPERIMENT
  - OLS ON F8 S/C FAILED IN 1990
  - SSM/I STILL OPERATIONAL (19, 22, 37 GHz CHANNELS ONLY, 85 GHz DEAD)
  - PROPOSAL TO PITCH S/C TO INCREASE SSM/I EIA MADE BY AEROSPACE CORPORATION

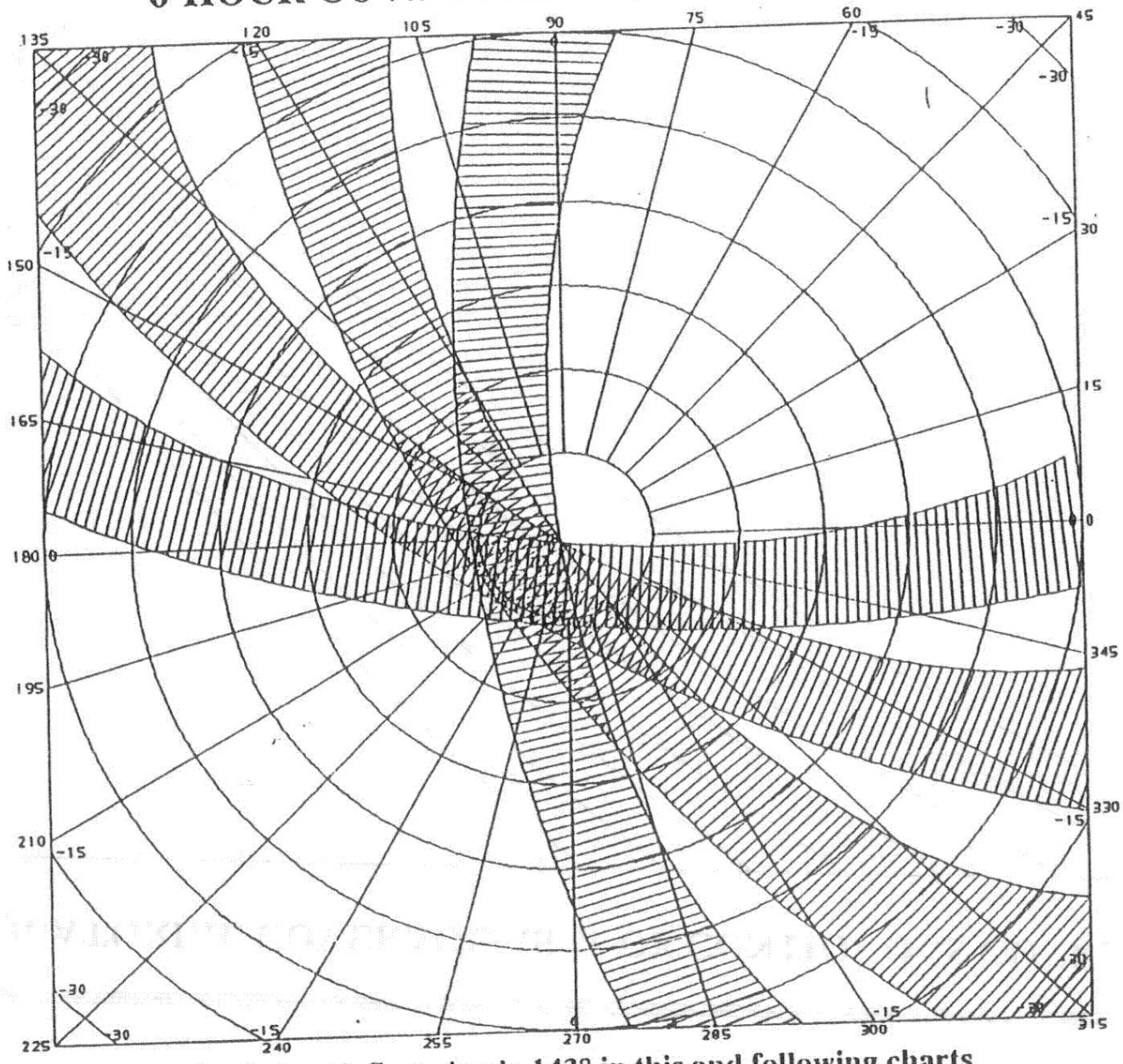
COVERAGE FROM 833 KM, EIA = 68.4°



COVERAGE FROM 1390 KM, EIA = 59.4°

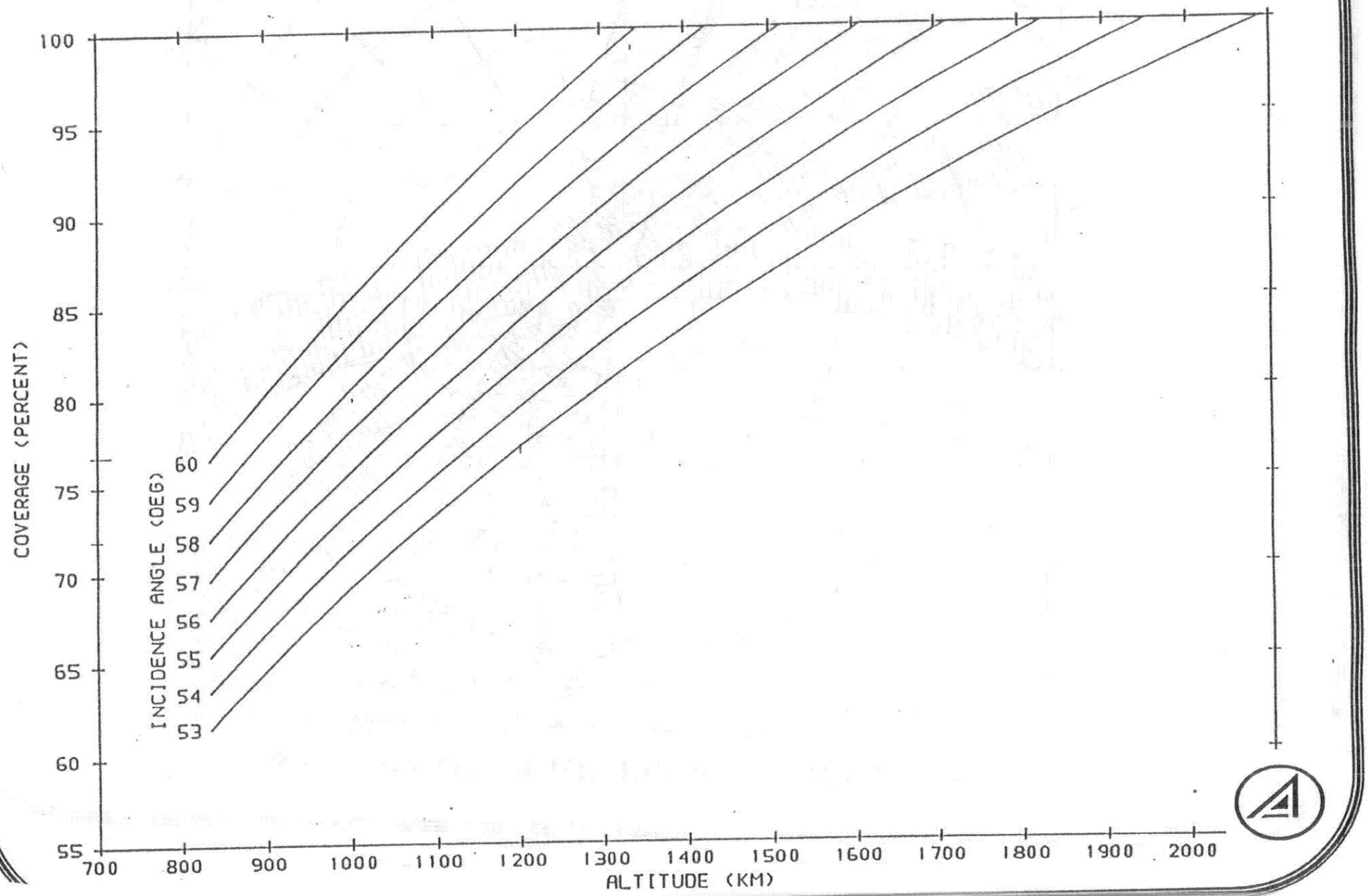


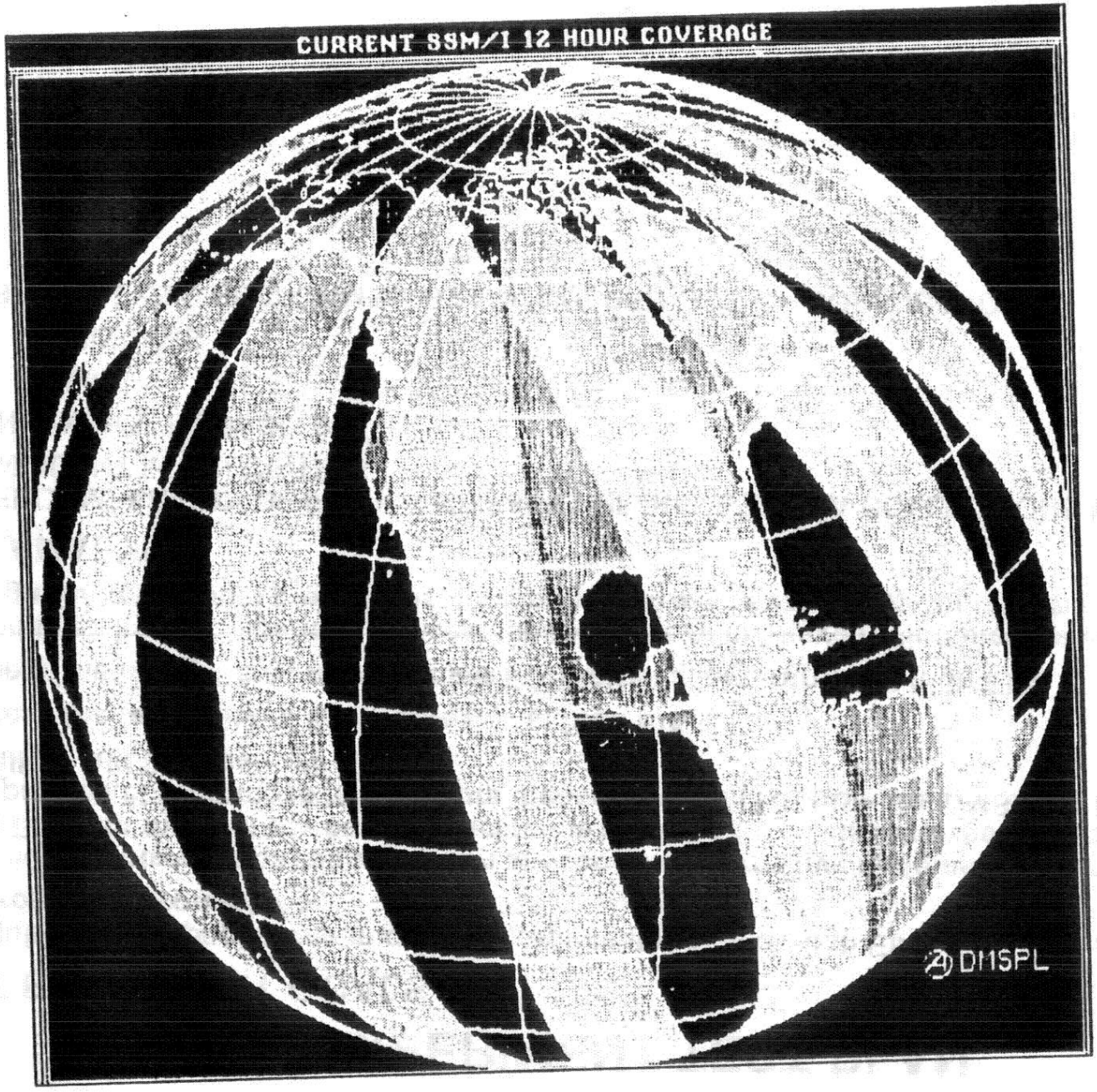
6-HOUR COVERAGE FROM 833 KM, EIA=53°



Active Azimuth Scan Angle 143° in this and following charts

EQUATORIAL COVERAGE AS % OF CONTIGUOUS COVERAGE





1093-93 S39

TILT EXPERIMENT TEST PLAN

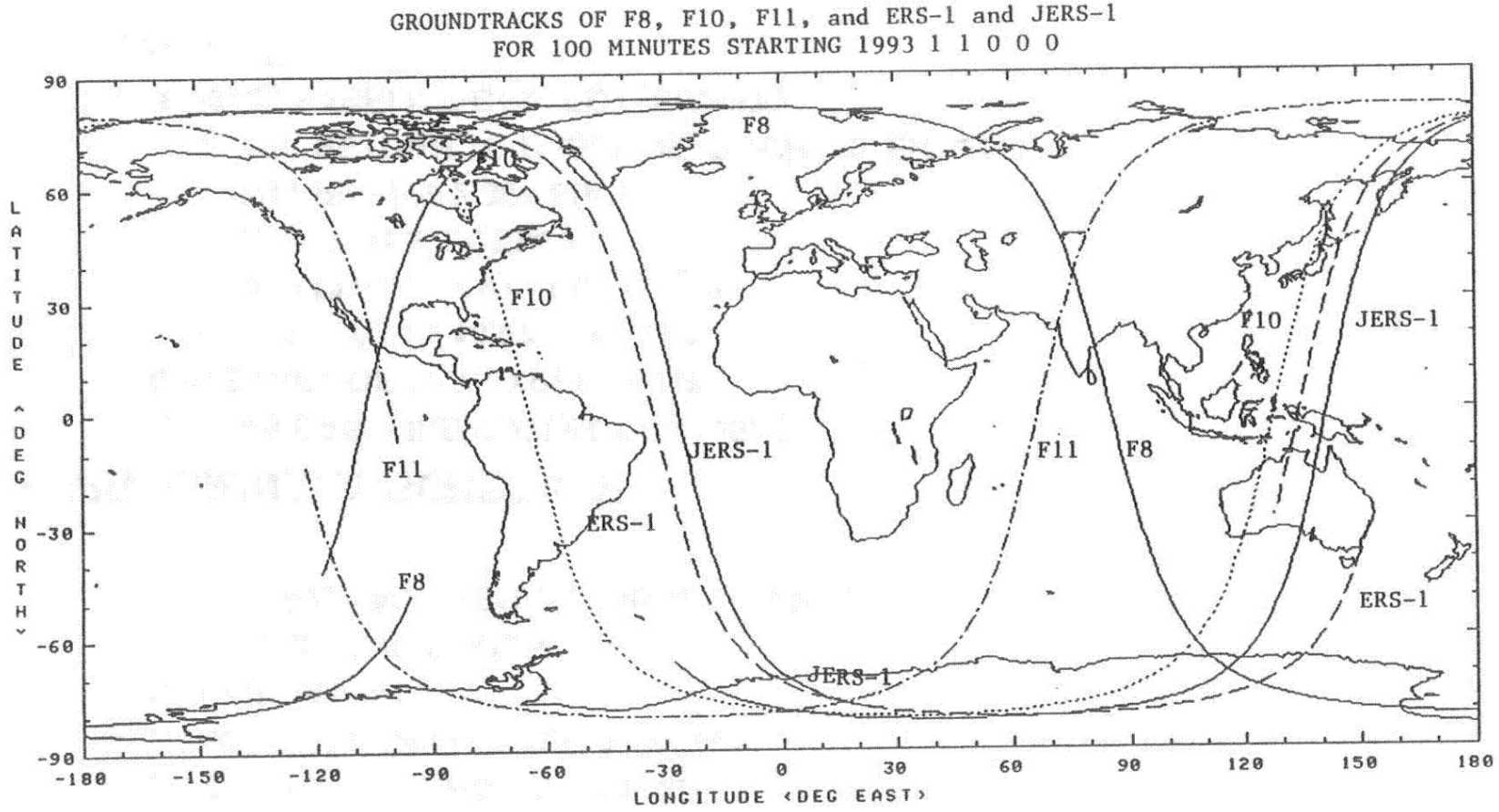
- F8 TILT EXPERIMENT GOALS
  - Acquire actual spaceborne microwave radiometer data at high EIA (≤70°) over a range of environmental conditions.
  - Provide an inter-comparison between spaceborne microwave radiometer measurements at high EIA with those at the nominal incidence angle of 53°. This involves the inter-comparison of brightness temperature measurements (TB) from the DMSP F8, F10 and F11 satellites and their derived EDR's.
  - Assess the feasibility of EDR retrievals at high EIA.
  - Assess the need, if any, for nonlinear EDR retrieval algorithms at high EIA.
  - Provide an inter-comparison between spaceborne microwave radiometer measurements (T_B) at high EIA and model predictions, in conjunction with available ground truth observations.
- ORBIT ANALYSIS
  - INTERCOMPARISON OF F8/F10 AND F8/F11 REQUIRES DATA COLLECTIONS WHICH ARE COINCIDENT IN SPACE/TIME
  - COINCIDENCE DEFINED BY
    - 30 km
    - 30 MINUTES
  - ORBIT ANALYSIS PERFORMED TO LOCATE PERIODS OF COINCIDENCE

TILT EXPERIMENT TEST PLAN (contd)

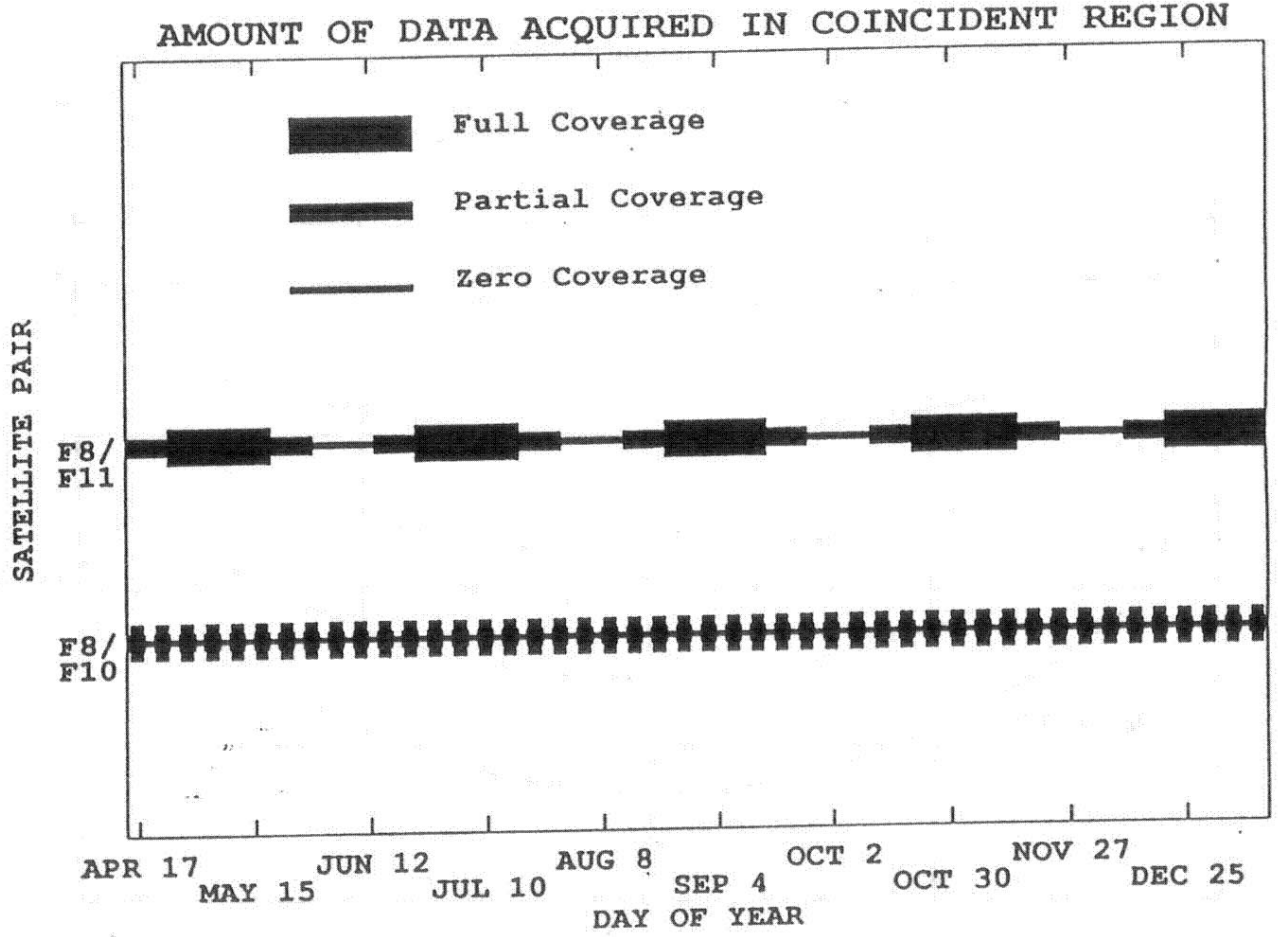
- DATA COLLECTION
  - SSM/I PRIMARY DATA TO BE COLLECTED
  - SSM/I DATA COLLECTED AT FNOC
  - OTHER DATA COLLECTED AT AFGWC
  - OTHER DATA
    - » BUOY AND RAOBS
    - » SSM/T1 AND SSM/T2 SOUNDER DATA

- PRELIMINARY SCHEDULE
  - 6/23–25 BASELINE COLLECT (EIA=53°)
  - 6/25 START OF TILT EXPERIMENT
    - » 6/29 PITCH = 10.67°, EIA = 69°
    - » 6/30 PITCH = 7.97°, EIA = 64.5°
    - » 7/9 PITCH = 5.°, EIA = 60°
    - » 7/11 PITCH = 2.88°, EIA = 57°
    - » 7/12 RETURN TO BASELINE, PITCH = 0, EIA = 53°
  - ~~6/23–25~~ 5 BASELINE COLLECT (EIA=53°)

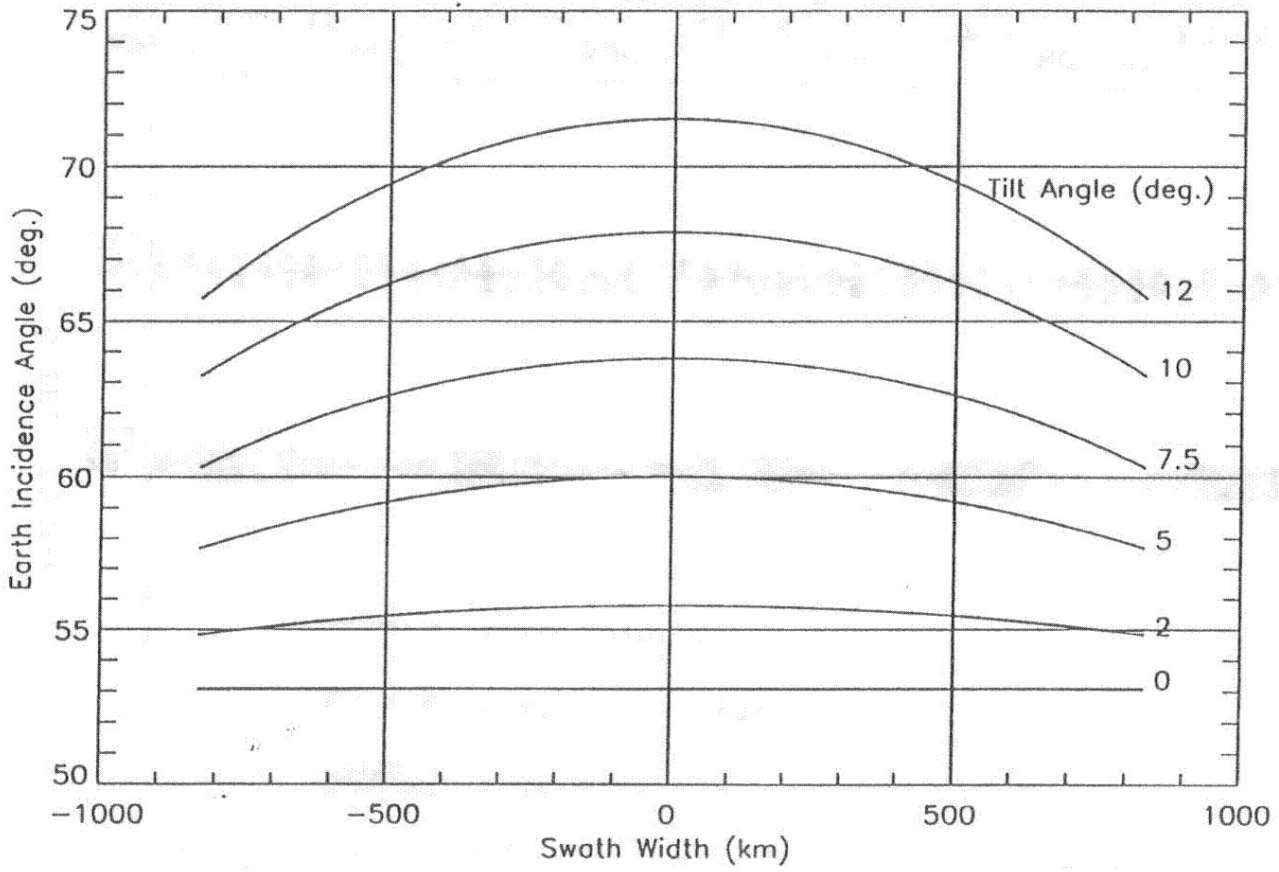
7/12 - 7/13 ^


GROUNDTRACKS OF F8, F10, F11, and ERS-1 and JERS-1
FOR 100 MINUTES STARTING 1993 1 1 0 0 0
LATITUDE <DEG NORTH>
LONGITUDE <DEG EAST>
90
60
30
0
-30
-60
-90
-180
-150
-120
-90
-60
-30
0
30
60
90
120
150
180
F8
F10
F10
F10
F11
F11
F8
JERS-1
JERS-1
JERS-1
JERS-1
ERS-1
ERS-1
ERS-1
F8

COINCIDENCE WINDOWS



EIA AS A FUNCTION OF PITCH AND SWATH



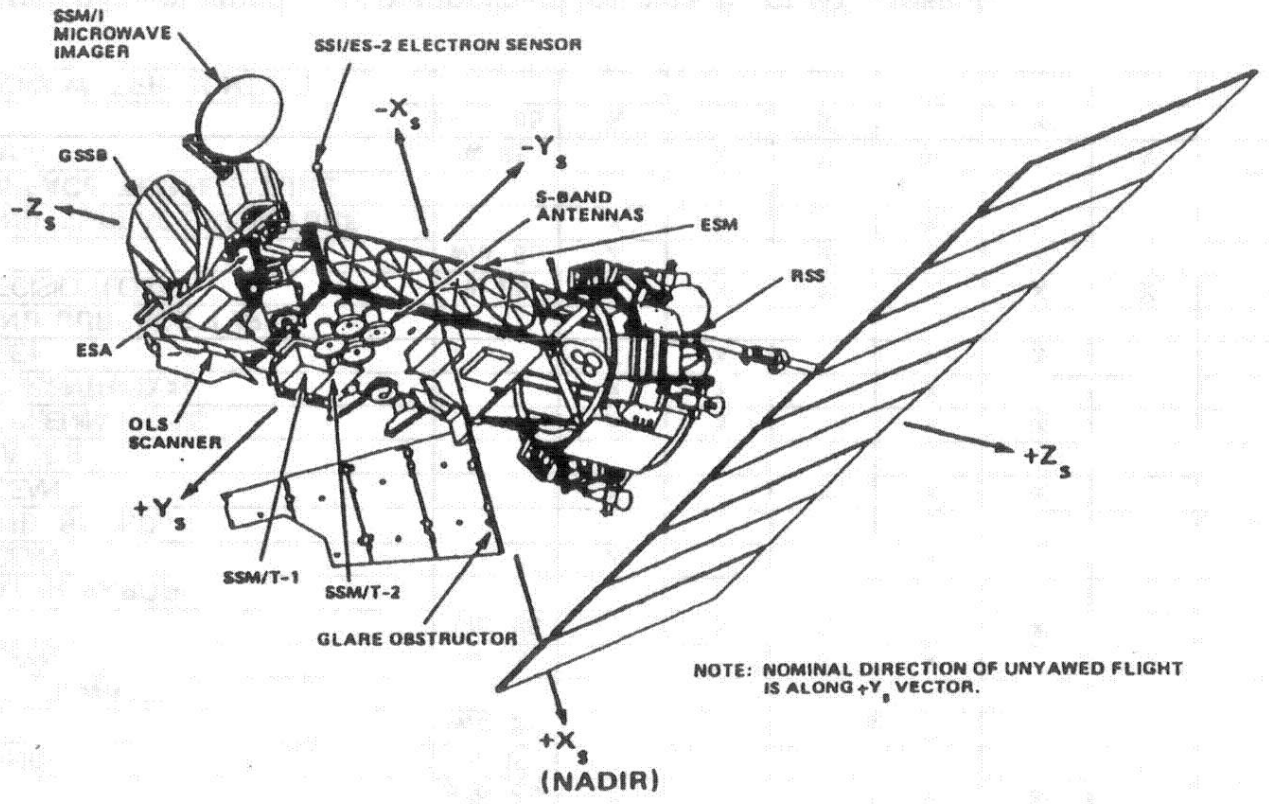
SSM/I ENVIRONMENTAL RETRIEVAL ALGORITHM CHANNEL USAGE

ENVIRONMENTAL RETREIVAL ALGORITHM		CHANNEL USAGE						
		19 V	19 H	22 V	37 V	37 H	85 V	85 H
RAIN RATE								
SCREENING LOGIC	w 85	X	X		X	X	X	X
	w/o 85	X	X		X	X		
OCEAN	w 85	X		X	X		X	X
	w/o 85	X			X	X		
LAND	w 85						X	X
	w/o 85	X			X			
CLOUD WATER								
OCEAN	w 85		X	X	X		X	
	w/o 85		X	X	X	X		
WATER VAPOR								
OCEAN		X		X	X			
WIND SPEED								
OCEAN		X		X	X	X		
SEA ICE								
SCREENING LOGIC		X	X		X	X		
CONCENTRATION		X	X		X	X		
AGE†		X	X		X	X		
LAND SURFACE TYPES								
DECISION LOGIC	w 85	X	X	X	X	X	X	X
	w/o 85	X	X	X	X	X		
LAND SURFACE MOISTURE		X	X		X	X		
SURFACE TEMPERATURE								
LAND	w 85		X	X	X		X	
	w/o 85	X	X	X		X		
SNOW WATER CONTENT					X			

† Age concentration is not found, only predominant ice type, FY or MY, present.

There is no CLOUD AMOUNT algorithm; none was found which worked. There is no LIQUID WATER algorithm; originally this was meant to include all hydrometers greater than 100 microns (i.e., rain drops) whereas CLOUD WATER included only particles smaller than 100 microns (i.e., clouds) [7,8,9].

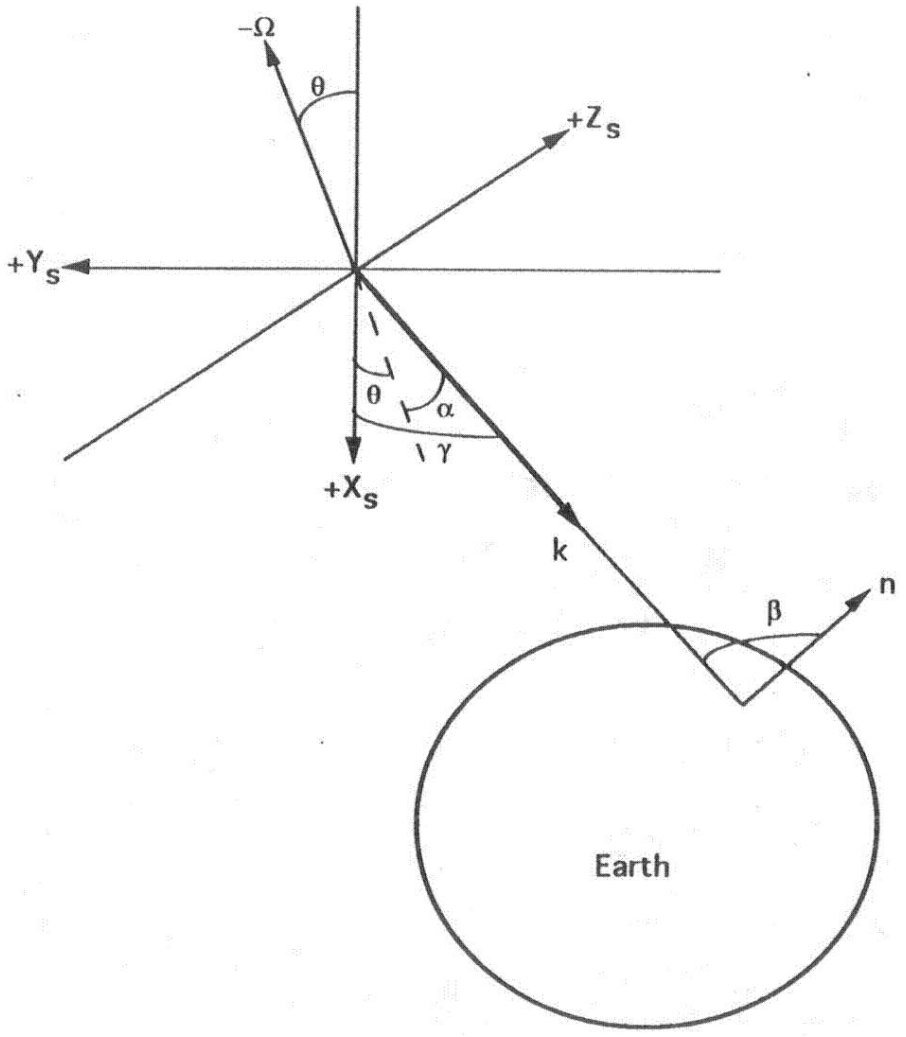
DMSP S/C BODY FIXED AXES



NOTE: THIS FIGURE SHOWS THE 5D–3 S/C WITH THE SSM/I. THE GEOMETRY DOES CORRESPOND TO THE 5D–2 F8 S/C WITH THE ACTIVE PORTION OF THE SSM/I SCAN IN THE $-Y_S$ DIRECTION. THE PITCH AXIS IS THE $+Z_S$ AXIS.

TILT GEOMETRY

Pitch Angle	EIA
0.0°	53°
–10.674°	69°
–7.967°	64.5°
–4.999°	60°
–2.875°	57°
0.0°	53°



$X_s Y_s Z_s$ – s/c reference coordinate system

α = SSM/I cone angle (45°)

θ = pitch angle, $+Z_s$ is the pitch axis

γ = SSM/I look angle

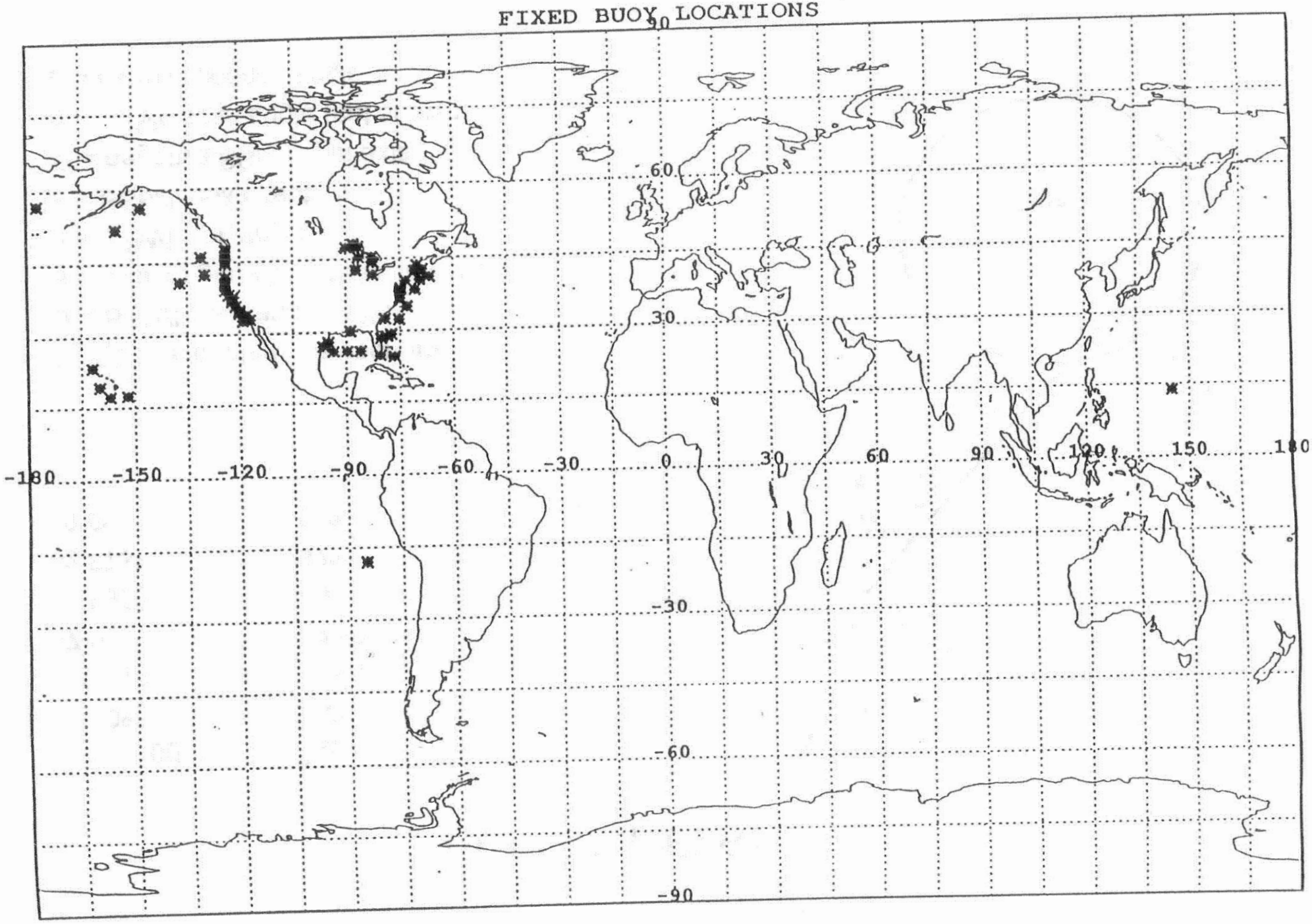
k = SSM/I look direction

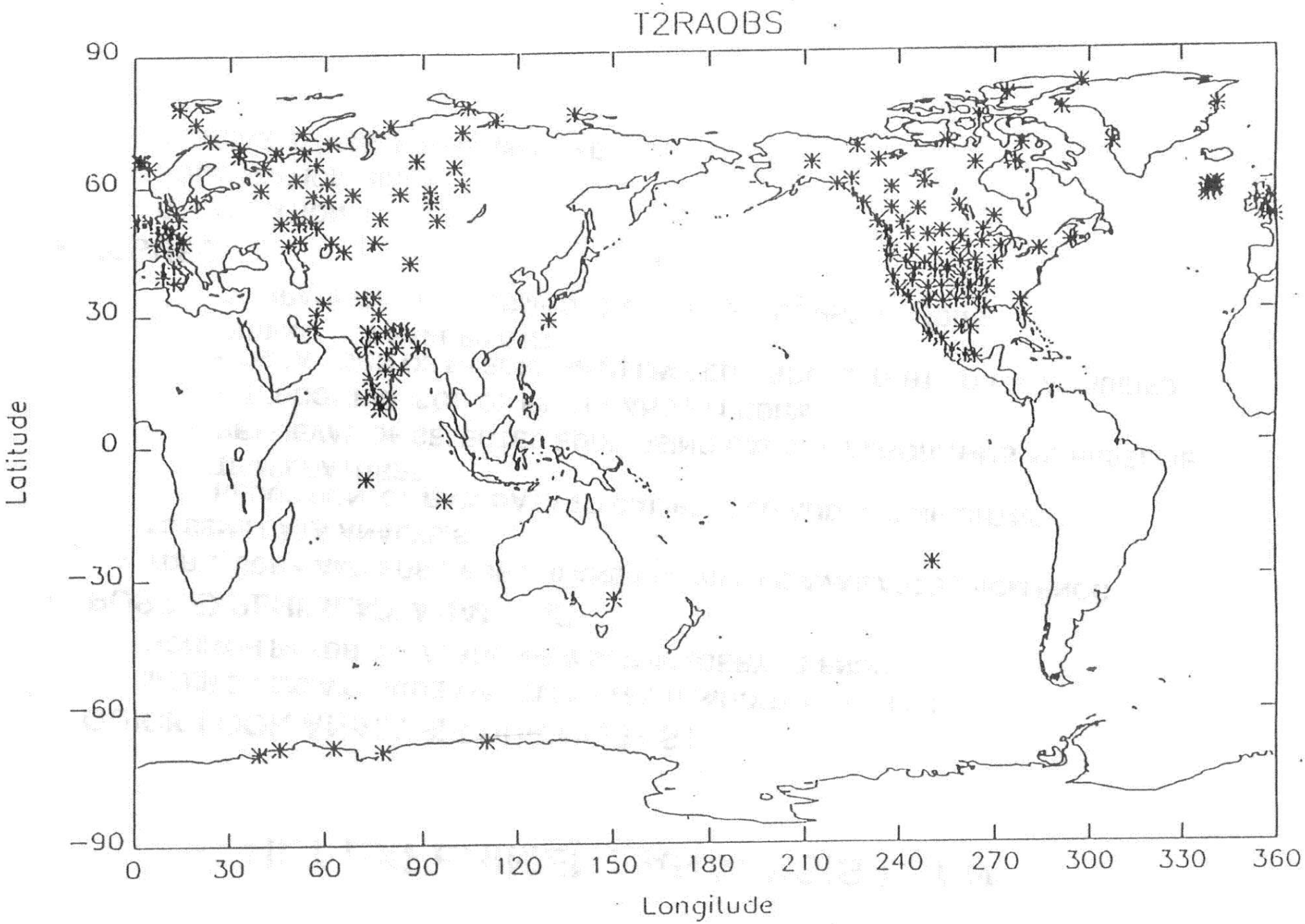
Ω = negative SSM/I spin axis

ϕ = SSM/I scan angle (not shown)

β = earth incidence angle

FIXED BUOY LOCATIONS




T2RAOBS
90
60
30
0
−30
−60
−90
Latitude
0
30
60
90
120
150
180
210
240
270
300
330
360
Longitude

TILT EXPERIMENT ANALYSIS PLAN

- QUICK LOOK ANALYSIS DURING TEST
  - MONITOR S/C ATTITUDE VIA TELEMETRY READOUT AT AFGWC
  - MONITOR F8 TDR DATA, AND VIEW SDR IMAGERY AT FNOC
- POST EXPERIMENT ANALYSIS
  - TDR's, SDR's AND EDR's FOR F10 AND F11 WILL BE AVAILABLE FROM FNOC
  - F8 SSM/I DATA ANALYSIS
    - » REDUCTION OF RAW DATA TO CALIBRATED AND APC BRIGHTNESS TEMPERATURES
    - » RETRIEVAL OF SELECTED EDR's USING CAL/VAL ALGORITHMS AS BASELINE
    - » INTERCOMPARISON OF F8, F10, AND F11 EDR's
    - » COMPARISON OF F8 EDR's WITH LIMITED GROUND TRUTH DATA ACQUIRED DURING TILT EXPERIMENT
    - » COMPARISON OF F8 SSM/I DATA WITH MODEL PREDICTIONS
- ISSUES
  - GEOLOCATION
  - POLARIZATION MIXING
  - INCREASED SSM/I FOOTPRINT SIZE

KEY PERSONNEL AND ORGANIZATIONS

- Defense Meteorological Satellite Program (DMSP) SPO
  - Capt. Juan Vasquez - Project Officer
  - LCDR Randy Tompkins - Navy Liaison
  - LCOL Ed Arrance - AWS Liaison
- The Aerospace Corporation
  - Ed Miller - Project Coordinator
  - Samuel Gasster - Analysis Team Leader
  - David Glackin - Phenomenology
- Fleet Numerical Oceanography Center (FNOC)
  - Marie Colton - SSM/I Data Collection/Processing
- Naval Research Laboratory (NRL)
  - Gene Poe - SSM/I Data Processing
  - Jim Hollinger - SSM/I Data Processing
- SPAWAR
  - CDR Leslie Burgess - Navy DMSP Project Officer
- AFGWC
  - Capt. Jeff Malan - Operations
- Martin Marietta Astro-Space
  - Rich Czyzewski, John Stetson, Bob Taddei

CONCLUSIONS

- F8 TILT EXPERIMENT PROVIDES A UNIQUE OPPORTUNITY TO COLLECT HIGH EIA MICROWAVE DATA FROM AN ORBITING S/C
- POTENTIAL TO ASSESS ABILITY TO RETRIEVE SOME ENVIRONMENTAL PARAMETERS FROM HIGH EIA DATA
- POTENTIAL TO IMPROVE MICROWAVE RADIATIVE TRANSFER MODELS AT HIGH EIA IN COMBINATION WITH NRL TOWER TEST RESULTS
- DATA WILL BE GENERALLY AVAILABLE

REFERENCES

1. D. L. Glackin and S. D. Gasster, Microwave Imager Sounder Incidence Angle Limitations, The Aerospace Corporation, IOC 5224-90-036 (March 8, 1990).
2. D. L. Glackin, S. D. Gasster and J. V. Geaga, DMSP Block 6 Microwave Incidence Angle Investigation, Proc. Specialist Meeting on Microwave Radiometry and Remote Sensing Applications, Boulder, CO, Ed R. Westwater, Chairman (Jan. 14-16, 1992).
3. Specifications for the DMSP Block 6, Attachment 4 to Contract #F04701-91-C-0068, 4 Volumes (July 9, 1991).
4. D. L. Glackin, G. G. Pihos and S. D. Gasster, F-8 Tilt Proposal, The Aerospace Corporation, IOC 5224-90-161 (Sept. 5,1990).
5. V. Olson, Risk Reduction of Block 6 Microwave Sensors, The Aerospace Corporation, IOC (July 20,1990).
6. L. A. Rose, et al., NRL Microwave Tower Measurements, Preliminary Report and Data on the December 1991 Measurements, Naval Research Laboratory (June 18, 1992). L. A. Rose, et al., NRL Microwave Tower Measurements, June 1992 Measurements, Naval Research Laboratory (October 15, 1992).
7. DMSP Special Sensor Microwave/Imager, Calibration/Validation, Vol. I and II, DMSP SSM/I Cal/Val Team, J. Hollinger, coordinator, Naval Research Laboratory, Washington, DC (1989).
8. V. Noble, Block 6 Microwave Radiometers: 55° Cone Angle, NRL Memo 8310-578 and enclosure (15 November 1989).
9. J. Hollinger, Naval Research Laboratory, private communication (1993).
10. S. D. Gasster, et al., DMSP Block 6 F8 Tilt Experiment Data Analysis Plan (DRAFT), The Aerospace Corporation (1993).
11. E. A. Meindl and G. D. Hamilton, Programs of the National Data Buoy Center, Bull. AMS, **73(7)**, 985-993 (1992).
12. R. G. Taddei, Minutes of F8 Tilt Experiment TIM, 22 March 1993 , Martin Marietta Astro Space, Princeton, New Jersey (April 5, 1993).
13. Dr. C.-C. Chao, The Aerospace Corporation, private communication (1992).
14. Standard Formats for Weather Data Exchange Among Automated Weather Information Systems, FCM-S2-1982, US Dept. of Commerce, NOAA (1982). Note that the latest version of this report is FCM-S2-1990.
15. Don Boucher, The Aerospace Corporation, private communication (1993).

A Review of the SSMIS Imaging Algorithms

William Kreiss, Gene Poe* and Alex Stogryn
Aerojet Electronic Systems Division
Azusa, CA

The DMSP Special Sensor Microwave Imager/Sounder (SSMIS) is the follow-on microwave instrument to the current temperature and humidity sounders, SSM/T-1 and SSM/T-2, and the microwave imager SSM/I. As such the SSMIS contains the same channel frequencies as the SSM/I (except 85.5GHz is replaced by 91.65GHz), the same conical scan geometry with corresponding beam resolutions and sampling intervals (12.5 km at 91.65 GHz and 25 km at 19.35, 22.235 GHz and 37 GHZ) and a larger swath width (1700 km). In addition, the radiometer sensitivities have been improved with the SSMIS (0.33K at 19.35 and 22.235 GHz and 0.19K at 37 GHz for SSMIS compared with SSMI 0.45K at 19.35 GHz, 0.73K at 22.235 GHz and 0.37 K at 37 GHz). The imaging parameter requirements for the SSMIS are esssentially the same as the SSM/I as defined in the DMSP SSM/I Cal/Val Final Report. In view of the improvements in the radiometer sensitivities (and antenna beam efficiencies) and the additional infromation provided by high resolution imagery (15 km) at 150 and 183 (+/- 1, +/-3 and +/- 7 GHz) it is expected that the accuracies of the SSMIS EDRs will exceed those of SSM/I.

The retrieval algorithms currently incorporated in the SSMIS gournd processing take advantage of the heritage of the comprehensive DMSP SSM/I Cal/Val program coordinated by the Naval Research Laboratory with a team of scientists and sensor experts as well as the numerous reports and publications of researchers of SSM/I data since its first launch in June 1987. For the most part the SSMIS imaging retrieval algorithms are patterned after the recommendations of the DMSP SSM/I Cal/Val with the following enhancements. First, the University of York has developed an enhancement of the SSM/I sea ice algorithm which is discussed in a separate paper in this symposium. Second, the work of Spencer and Grody has been used to construct a rain flag algorithm that takes advantage of the higher spatial resolution of the dual polarized 91.65 GHz data in conjunction with channel comparisons at the lower frequencies to remove ambiguities over cold or snow covered surfaces. In addition, the information content of the higher resolution 150 and 183 GHz humidity sounding channels has been included in the rain flag. Third, the most recent correction to the SSM/I Cal/Val ocean wind speed algorithm has benn included to improve retrievals under adverse weather conditions. Fourth, the work of Kunzi and Chang has been incorporated in the development of the snow water equivalent algorithm. Finally, the sea ice edge and snow pack boundary algorithms employ the efficient edge detection Sobel operators. This paper summarizes the descriptions and expected performances of the SSMIS retrieval algorithms for the imaging parameters.

It is expected that improvements in these algorithms will be available before and after the launch of the SSMIS. The design of the SSMIS ground processing software is sufficiently modular that these improvements may be incorporated easily when desired.

*now at Naval Research Laboratory, Passive Microwave Section